INDIAN AGRICULTURAL
RESEARCH INSTITUTE, NEW DELHI.

18878

I. A. R. I. 6.
MGIPC—S4—10 AR—21-6-49—1,000.

PROCEEDINGS

OF THE

ROYAL SOCIETY OF LONDON

SERIES A—MATHEMATICAL AND PHYSICAL SCIENCES

VOL CLXIII

LONDON
Printed and published for the Royal Society
By the Cambridge University Press

22 December 1937

PRINTED IN GREAT BRITAIN BY
WALTER LEWIS, M.A.
AT THE CAMBRIDGE UNIVERSITY PRESS

CONTENTS

SERIES A VOL CLXIII

No. A 912—5 November 1937

PAGE

The Glide of Single Crystals of Sodium and Potassium. By E. N. da C. Andrade, F.R.S. and L. C. Tsien. (Plates 1, 2) 1

Preparation of Single Crystal Wires of Metals of High Melting Point. By E. N. da C. Andrade, F.R.S. (Plate 3) 16

The Glide of Single Crystals of Molybdenum. By L. C. Tsien and Y. S. Chow. (Plates 4, 5) 19

Slip Bands on Mercury Single Crystals. By K. M. Greenland. (Plates 6, 7) 28

The Critical Shear Stress of Mercury Single Crystals. By K. M. Greenland. (Plate 8) 34

Critical Phenomena in Gases—I. By J. E. Lennard-Jones, F.R.S. and A. F. Devonshire 53

Reaction Kinetics in Films. The Hydrolysis of Long-Chain Esters. By A. E. Alexander and E. K. Rideal, F.R.S. 70

Nitrogen Oxides in Internal Combustion Engine Gases. By T. K. Hanson and A. G. Egerton, F.R.S. 90

The Interaction of Atoms and Molecules with Solid Surfaces. X—The Activation of Adsorbed Atoms by Metallic Electrons. By J. E. Lennard-Jones, F.R.S. and E. T. Goodwin 101

The Interaction of Atoms and Molecules with Solid Surfaces. XI—The Dispersal of Energy from an Activated Link. By J. E. Lennard-Jones, F.R.S. 127

The Interaction of Atoms and Molecules with Solid Surfaces. XII—Critical Phenomena in a Two-Dimensional Gas. By A. F. Devonshire . 132

A Comparison of the Absorption Spectra of some Typical Unsymmetrical Cyanine Dyes. By B. Beilenson, N. I. Fisher and F. M. Hamer . 138

No. A 913—19 November 1937

PAGE

The Emission of the Latent Energy due to previous Cold Working when a Metal is Heated. By H. Quinney and G. I. Taylor, F.R.S. . . . 157

Spontaneous Emulsification, and Reactions Overshooting Equilibrium. By J. W. McBain, F.R.S. and Ts-Ming Woo. (Plates 9–12) . . . 182

A Comment on the Paper by Sten von Friesen "On the Values of Fundamental Atomic Constants". By J. S. E. Townsend, F.R.S. . . . 188

The Variation with Temperature of the Thermal Conductivity and the X-ray Structure of some Micas. I—The Thermal Conductivity up to 600° C. By R. W. Powell and E. Griffiths, F.R.S. 189

The Variation with Temperature of the Thermal Conductivity and the X-ray Structure of some Micas. II—The X-ray Examination of the Structure. By W. A. Wood. (Plates 13–15) 199

The Formation and Structure of Polymers of the Insoluble Cross-Linked Type. By R. G. W. Norrish, F.R.S. and E. F. Brookman . . . 205

Photochemical Reactions in the Fluorite Region. II—Photochemical Decomposition of Formaldehyde Vapour. By R. G. W. Norrish, F.R.S. and W. A. Noyes, Jr. 221

Thermal Radiation and Absorption in the Upper Atmosphere. By G. H. Godfrey and W. L. Price 228

The Size-Grading of Sand by Wind. By R. A. Bagnold 250

The Angular Distribution of Protons Projected by Fast Neutrons. By P. I. Dee and C. W. Gilbert. (Plate 16) 265

The Nature of the Interaction between Neutron and Proton from Scattering Experiments. By H. S. W. Massey and R. A. Buckingham 281

Electrosmosis between Plane Parallel Walls produced by High-Frequency Alternating Currents. By L. Rosenhead and J. C. P. Miller (with note by J. J. Bikerman) 298

The Glide of Single Crystals of Sodium and Potassium

By E. N. da C. Andrade, F.R.S. and L. C. Tsien, B.Sc.

Physics Laboratory, University College, London

(*Received* 22 *June* 1937)

[Plates 1, 2]

1—Introduction

The data on the glide of elements of single crystals are particularly scarce for metals of the cubic body-centred form, only tungsten (Goucher 1924), α-iron (Taylor and Elam 1926; Gough 1928; Fahrenhorst and Schmid 1932) and β-brass (Taylor 1928; Elam 1936) having been so far investigated. Metals of this crystal structure are, however, of particular interest, since, while the glide direction for the pure metals is, according to most workers, always the most closely packed, i.e. the [111] direction, the glide plane is not, as it generally* is in other structures, the most closely packed plane. In general, with these body-centred cubic crystals there is a certain indefiniteness about the glide plane. For α-iron, according to Taylor and Elam, slip does not, except for particular orientations of the shear stress with respect to the crystallographic axes, occur on any particular crystallographic plane, but rather in rod-like elements. According to the later work of Elam, while the slip bands sometimes agree with the (110) plane, they do not in general do so, nor is [111] invariably the glide direction. Gough resolves his deformation into slip on pairs of planes: Fahrenhorst and Schmid decide for the (123) plane as "most probable" but their experiments do not definitely establish this plane. In the case of β-brass Elam decides that no simple crystallographic distortion can explain all the results, and extends this conclusion to α-iron. The question is, then, a complicated one.

Our results with sodium and potassium show a simpler state of things, and have led to the conclusion that slipping does here take place in the [111] direction, and on, or very near to, a crystallographic plane, the (123) plane, but it must be pointed out that our method of manufacture of single crystal rods led, for some reason not yet fully clear, to crystals in which the [111] direction was generally near to a plane containing the axis. As regards twinning the results are inconclusive. A further limitation of the generality of our results is that, so far, on account of difficulties of manipulation at low temperatures, the measurements have been carried out at one temperature only. It is hoped, however, in the future, to extend the work to other temperatures.

---

* For other structures than the body-centred cube the most closely packed planes are always glide planes, but at higher temperatures other planes can in certain cases function. For instance, in the case of magnesium, above 225°C., (1011) and (1012) act as glide planes, as well as the most closely packed, viz. (0001), planes (Schmid 1931).

2—PREPARATION OF THE CRYSTALS

Except in a few preliminary experiments the sodium used for the crystals was prepared by distillation from a specimen supplied by Messrs. Hopkin and Williams. The apparatus used is shown in fig. 1. Some 60 g. of sodium, freshly cut from a lump, were quickly introduced into the tube A, and the whole system evacuated with a hyvac pump. The sodium was then melted by an electrical furnace surrounding A: at a temperature

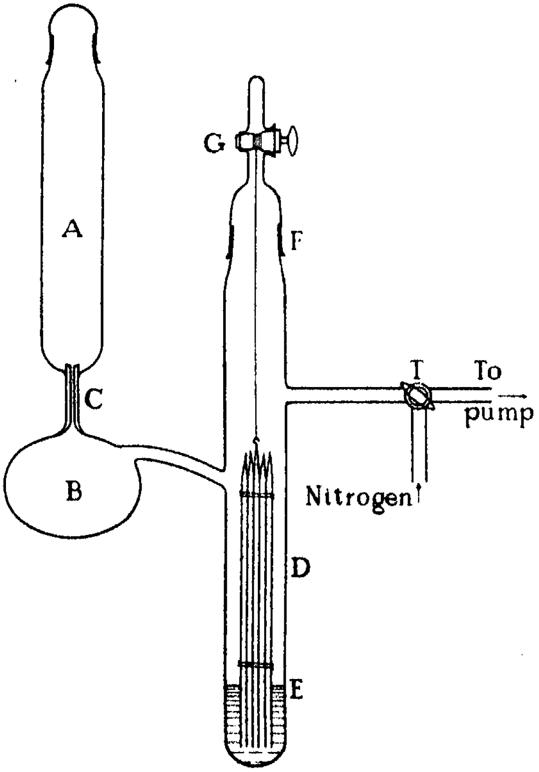

FIG. 1

of about 200° C. the molten metal broke through the crust of oxide, and passed through the capillary tube *C*, which acted as a filter, into *B*, from which it was distilled over into *DE* where it was maintained in a molten state by a furnace provided with a long mica window, for observation. Two specimens of distilled sodium, as used for growing the crystals, were submitted to Messrs. Hilger for spectrochemical analysis. The report pronounced the metal to be of great purity; calcium, silicon and bismuth being present to the extent of less than 1 part in 10^6, while potassium, the chief impurity, did not amount to more than 1 part in 10^4. The distillation *in vacuo* assured that there should be no dissolved gas in the metal.

The sodium was filled into tubes, of about 2 mm. internal diameter and 13 cm. length. They were cleansed with chromic acid, caustic soda and running water, and then dried *in vacuo* at about 200° C. A little apiezon oil (*A* or *B*) was then introduced, and the tubes left to drain, in a vertical position, so that a film of oil was left on the wall. Without this oil film the sodium was liable to stick to the clean glass very firmly: to secure the best thickness of oil film was a matter of experience. The tubes were then drawn off to a fine point at one end, the solid glass being made into a little hook, for convenient suspension. A bundle of some fifteen such tubes, open ends down, was hung in *DE*, by a fine platinum wire, to a grooved tap *G*. When sufficient sodium had been distilled into *DE* the tubes were lowered, by turning *G*, until the open ends were well below the liquid metal, and a little nitrogen was then allowed to enter through *T*, which forced the metal into the tubes. The metal was allowed to solidify, nitrogen again introduced until atmospheric pressure was reached, the apparatus opened at *F* and the tubes removed. Before the metal solidified the lower ends of the tubes had been arranged to be just under the surface *E*, which enabled the break to be made easily. The metal at the open ends of the tubes quickly became protected by a coat of oxide.

The sodium rod was converted into a single crystal by slowly lowering the tube, pointed end first, out of a jacket maintained at a temperature of 100° C., i.e. about 2° C. above the melting-point of the metal. This was done by hanging the tube to a wheel turned by clockwork, which gave a rate of lowering of about 2 mm./min. The crystals are very easily prepared: in fact the rod was sometimes a single crystal before this treatment, and a good crystal 1·5 cm. in diameter and 3·5 cm. long was once prepared simply by heating at 100° C. for 2 hr. After the oil film treatment had been adopted the crystal could always be removed from the tube by gently pressing it out with a steel rod. It is possible that the oil also helps in the formation of the single crystals, for in preliminary experiments, when the metal was distilled into an unoiled tube, the rod was often polycrystalline. This may have been due to minute irregularities on the glass wall acting as starting points for crystallization, irregularities which are masked or modified by the oil film.

The single crystals of potassium were prepared in exactly the same way.

3—MANIPULATION OF THE CRYSTALS

The crystals had to be stretched, preferably by a known amount, to develop the slip planes. The difficulties are two: first, the ease with which the metal oxidizes, and secondly, its softness. To enable the crystal to be extended, examined with ease from all directions and photographed if necessary, the apparatus shown in fig. 2 was constructed.

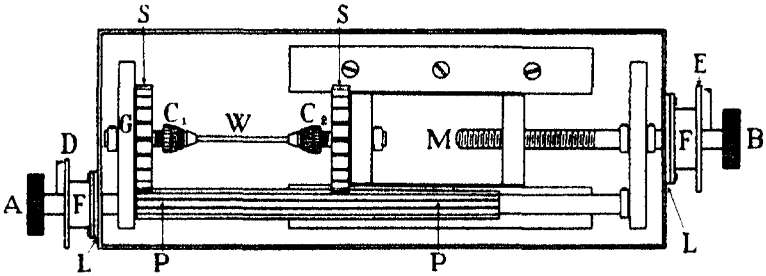

FIG. 2

A brass bath (21 × 8 × 6 cm.), seen from above in the figure, carried pin chucks C_1 and C_2, the former being secured to a plate *G* rigidly fixed to the bottom plate, while the latter was attached to a slide *M*, which could be traversed by a screw, turned by the head *B*. The movement of the slide was measured on the graduated circle *E*. The pin chucks were mounted on the supporting plates so as to turn freely about a longitudinal axis, a rotation being effected by spur wheels *S*, *S*, engaging with a long pinion *PP*. By this device the wire *W* could be turned about its longitudinal axis without deformation, whatever the extension, the angle being given by the reading on a graduated circle *D*. Escape of the liquid from the bath was prevented by stuffing boxes *F*, *F*, and lead disks *L*, *L*.

The choice of a suitable liquid for the bath gave some trouble, since nearly all liquids apparently took up enough moisture to react with sodium. Chemically pure paraffin oil was finally adopted, which had stood in contact with clean sodium wire, and as an additional precaution sodium wire, frequently renewed, was kept in the bath itself. To prevent air coming into contact with the oil, the bath, which was filled to the top, was closed by a plate of glass, sealed with adhesive tape. In spite of all these precautions a thin film of oxide, which was perceptible in half an hour, slowly formed on the crystal. With practice the crystal could be properly mounted in 10 min., and photographed while still bright. For the photography a travelling microscope with a 40 mm. Beck apochromatic objective was used. The angle made with the wire axis by the glide planes could be visually measured, if necessary, by a rotating head, carrying the eyepiece.

For the X-ray photography the crystal had to be protected by a solid layer of some kind. The thick grease known as apiezon *L* was found to be suitable: it was heated to about 55° C., and the crystal, drained for about 10 sec. after removal from the oil-bath, was plunged into it, and quickly removed. In this way a thin, uniform, waxy layer was formed, which effectively shielded the crystal and was quite transparent enough to enable the surface markings to be seen. This latter condition was necessary, to enable the glide planes to be fixed relative to the X-ray beam, and so identified crystallographically.

4—DETERMINATION OF THE GLIDE ELEMENTS

The glide elements were determined by the Laue method of crystal analysis. The source of the heterogeneous beam of X-rays was a Shearer tube, with copper target, run at 40 kV and about 5 mA. The cathode was cooled by an insulated syphon system, so disposed that the convection caused by the local heating circulated the water. The window was of lithium, about 1 mm. thick, the absorption of which is extremely low (Clay 1934). The beam was limited by passage through a hole 0·7 mm. diameter, and the photographic plate, normal to the original X-ray beam, was 3 cm. from the wire axis.

The glide planes having been developed by slight extension the crystal was arranged with its axis vertical and rotated in azimuth until the normal to the glide plane lay in the plane through the wire axis and the horizontal beam of X-rays.

The method of identification of the glide plane and glide direction was based on the use of standard stereographic projection diagrams, prepared for the body-centred crystal with the X-ray beam travelling along various simple zone axes. The spots obtained in the photographic plate were transferred to a stereographic diagram with a primitive circle of 5 cm. radius, and the pole of the glide plane, obtained by direct angular measurement of the visible traces, was transferred to the same diagram. With any satisfactory photograph a number of strong spots could be found which, in the projection diagram, lay on a great circle. The diagram was then rotated, by calculation, about the diameter of this great circle so as to bring the great circle into coincidence with the primitive circle. If the diameter of the great circle is a simple zone axis, the diagram so obtained will correspond to one of the standard projection figures, and the various planes, and consequently the pole of the glide plane, can then be identified.

A typical photograph, with twenty-six Laue spots (only eighteen of which are visible in the reproduction), taken with sodium, is shown in fig. 3, Plate 2 and the corresponding stereographic projection, with glide plane and glide direction inserted, in fig. 4. It is clear that the intense spots

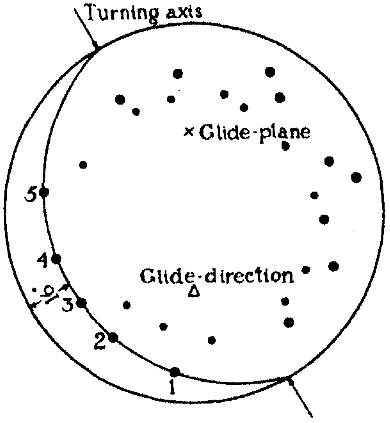

Fig. 4—Stereographic Projection of Laue spots.

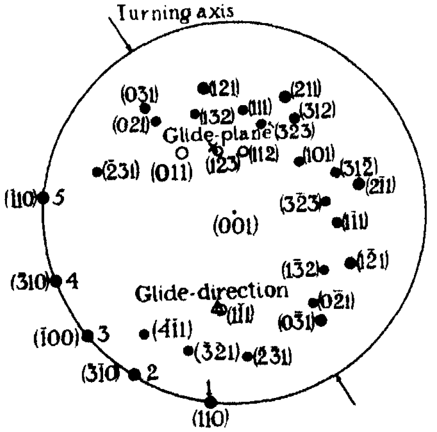

Fig. 5—Rotation of Fig. 4 about axis, giving standard figure for X-rays travelling along zone axis (001). The black discs represent spots actually on the photograph: the open circles mark the position of important planes not so represented.

1, 2, 3, 4 and 5 lie on a great circle, whose axis is marked. Rotation about this axis gives fig. 5, in which these spots lie on the primitive circle. This figure agrees with the standard figure for the X-ray beam travelling along the zone axis (001). It will be seen that the glide plane very nearly coincides with (123) and the glide direction with [111].

In fig. 6 the open circles represent the results of eleven independent determinations of the glide plane, with sodium, shown on a large scale, the fragment of the stereographic diagram corresponding to a primitive circle of 7·5 cm. radius. The centre of gravity of these eleven determinations falls almost exactly on the pole of the (123) plane, which is therefore taken to be the glide plane.

Fig. 7 represents, in a similar way, the results on the glide plane obtained with potassium. Once more the departures from the (123) plane are small, and the centre of gravity of the six determinations falls exceedingly close to the (123) plane.

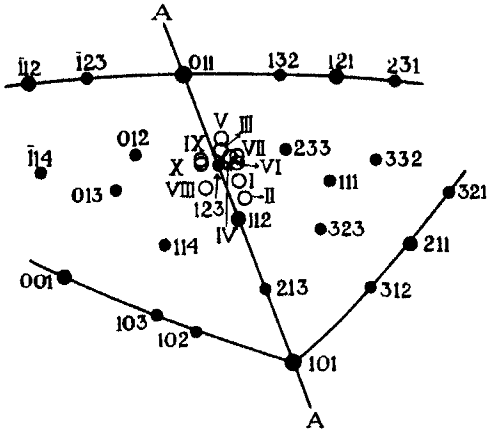

FIG. 6—Glide plane of Na single crystal. Radius of primitive circle = 7·5 cm.

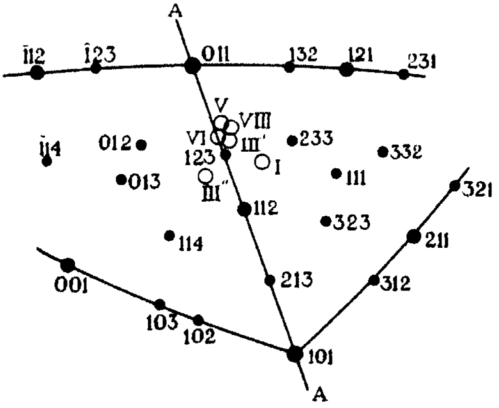

FIG. 7—Glide planes of K single crystals. Radius of primitive circle = 7·5 cm.

5—GLIDE PHENOMENA

Sodium crystals stretched by a few per cent show well-marked glide planes, as exemplified by fig. 8, Plate 1, which shows a sodium crystal extended by 4 %, turned so as to be viewed along a line in the glide plane normal to the axis of the wire. The longitudinal marks are left by the tube wall, and have no significance. Fig. 9, Plate 1 shows another crystal, extended by 5 %. The spacing of the glide planes in these crystals is large compared to that of α-iron crystals, a series of measurements on one sodium crystal giving an average separation of 0·069 mm. At greater extension a finer structure becomes visible between the original glide planes, which is easily masked by a thin film of oxide.

The heads of the glide bands are apt to be irregular, as shown in fig. 10, Plate 1, which would indicate that the glide planes are not strictly planes, but permit small variations. Taylor (Taylor and Elam 1926) has shown with α-iron that, while the glide direction is [111] there is no definite glide plane, and has put forward a model in which the glide elements are represented by hexagonal rods. The irregularity of the heads indicates that glide can take place for small distances on planes through the [111] direction which make an angle with the main glide plane, this being an average plane from which deviations over short lengths are permitted.

Double glide occasionally occurs, as shown in fig. 11, Plate 1, the crystal being crossed by a double system of slip bands. In two cases the angle between the two sets of planes was measured, and proved to be 87·3° and 85·7° respectively, which agrees within experimental error with $\cos^{-1} 1/14 = 85{\cdot}9°$, the angle between (123) and $(\bar{3}\bar{1}2)$. This confirms the X-ray identification of {123} as glide planes.

After a certain amount of extension, of the order of 10 %, has taken place the crystals often present an appearance of alternate bands, as shown in fig. 12, Plate 2. At first it was thought that this was a twinning phenomenon, but there are several reasons against this explanation. The bands do not appear suddenly, as do twinning bands, but gradually become more and more distinct as the extension proceeds. They are distributed all along the wire, in such a way that the crystal is divided equally between the alternate layers. Two further difficulties were revealed by X-ray photographs: first, that when an X-ray beam was sent through the crystal at right angles to the axis and in the plane of the picture in fig. 12, so as to include several layers, only one Laue pattern was produced, and not two, as would be expected if a definite reorientation of the lattice had taken place in alternate layers, and secondly that, while the boundary in two cases came out to be near a (103) plane, in other cases it was no simple crystallographic plane. Further, the boundaries were often not planes, but were branched, as shown in fig. 12, at the places indicated by the arrows.

On the other hand, the appearance can be explained as due to double

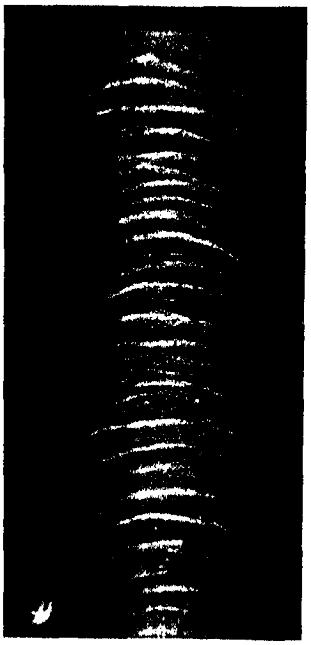

Fig. 10

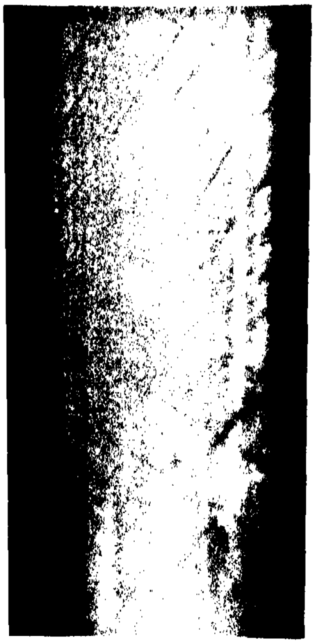

Fig. 11

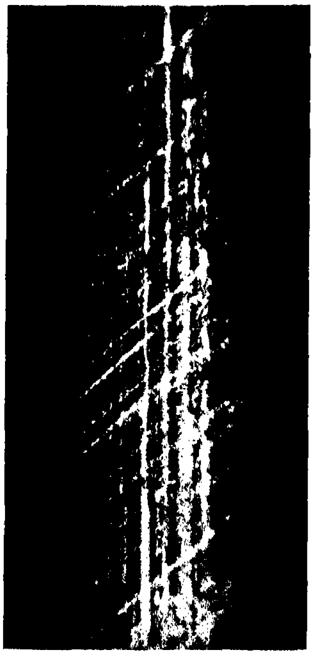

Fig. 8

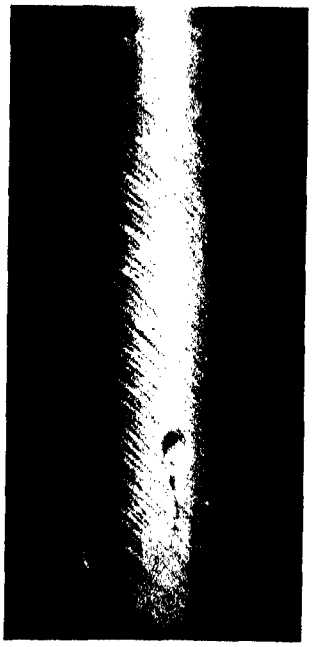

Fig. 9

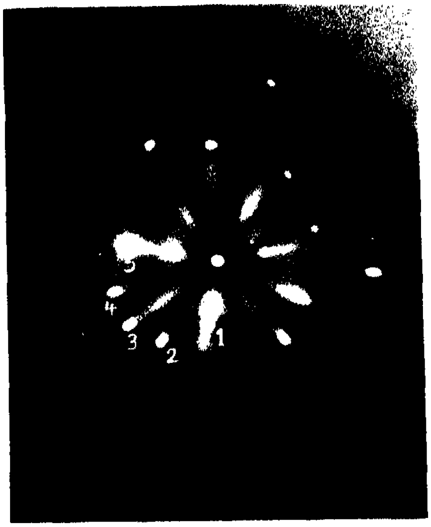

FIG. 3

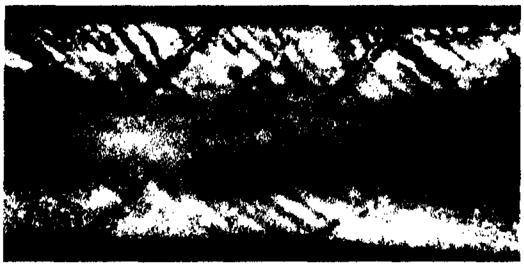

FIG. 12

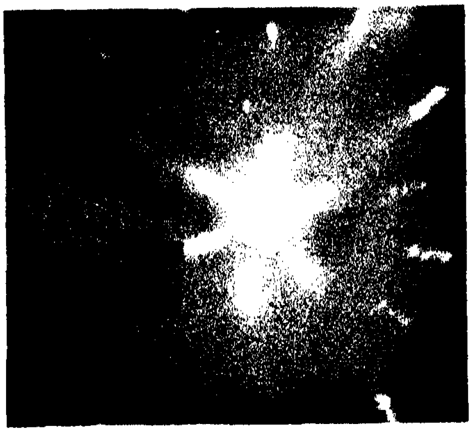

FIG. 14

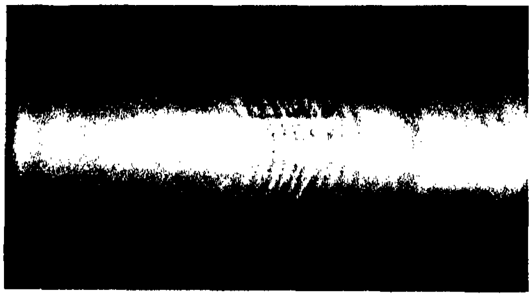

FIG. 13

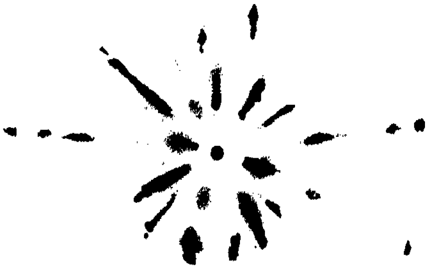

FIG. 15

glide taking place in alternate segments. Supposing the glide to be taking place on {123} planes in the [111] direction, the calculated angle between the planes in adjacent segments agrees within experimental error with that measured. A case of such double glide in alternate segments, for a hexagonal crystal with two glide directions equally inclined to the axis of stress, is given by Andrade and Roscoe (1937).

In one case there were indications of a second system of Laue spots, as points were found that could not be included in the main system. There were not sufficient of the superfluous spots, however, to enable a second system to be identified. In this case there was no alternating system of bands, such as is shown in fig. 12, but only one boundary. X-ray examination showed this boundary to be within 9° of a (111) plane. This plane fulfils the geometrical conditions necessary, if the twinning takes place along a [00$\bar{1}$] direction. It is possible, then, that sodium twins in this manner, but the evidence is weak.

6—GLIDE DIRECTION

The question of the glide direction can be investigated optically (Chalmers 1932; Roscoe and Hutchings 1933). Let α be the angle between the glide direction of the glide ellipse and the projection of the axis of the unstretched wire on the glide plane, β the angle between the major axis and the projection of the stretched wire on the glide plane. Then

$$\sin(\alpha-\beta) = \sin\alpha\,\frac{\tan\chi}{\tan\chi_0}$$

and

$$\tan\alpha = \frac{\sin\beta}{\cos\beta-\dfrac{\tan\chi}{\tan\chi_0}}.$$

The angle χ can be directly measured, and χ_0 found by the well-known formula

$$\frac{\sin\chi_0}{\sin\chi} = \frac{l}{l_0} = \epsilon.$$

The angle β can be derived from measurement of the shape of the elliptic trace, which is found by photographing the traces from a direction normal to the slip band, as shown in fig. 13, Plate 2, special care being taken to make the protecting layer of grease thin and uniform. Naturally all the bands but three or four are out of focus. The major axis is fixed by first finding the centre of the ellipse, by drawing parallel chords and joining the mid-points to fix a diameter, and then joining this centre to the point where the tangent is normal to the line from the centre, found by trial. From β, knowing χ and χ_0, we can find α. The projection of the axis of the stretched wire on the glide plane is known from the pole figure prepared from the X-ray work, and knowing $(\alpha-\beta)$ we can find the pole for the glide direction on the stereographic diagram. This being known, we can at once find its crystallographic direction.

In two cases the glide direction was confirmed by taking a photograph with the crystals so disposed that the beam of X-rays passed along this direction. Fig. 14, Plate 2 shows a picture obtained in this way, the threefold symmetry characteristic of a [111] axis being clearly shown. Closer analysis shows that the departure of the glide direction from the [111] direction is 4°, which is not in excess of the experimental error, as it is difficult to set the crystal with the experimentally found glide direction accurately along the path of the X-ray beam.

In the two cases directly confirmed in this way the glide direction was nearly along the projection on the glide plane of the wire axis, i.e. nearly coincided with the direction of greatest resolved shear. In the case of one crystal, where the [111] direction made an angle of 24° with the projection, the surface unfortunately oxidized too badly for the glide direction to be determined, but the glide plane was accurately found to be a {123} plane. A potassium crystal, No. V, for which the [111] direction made an angle of 13° with the projection, gave definitely asymmetrical glide ellipses, from which an angle of 12° 30′ was found. We can say, then, that in such cases as were accurately measured the glide direction was [111], but that no measurements have been made in a case where $\eta=\alpha-\beta$, the experimentally found value of the angle between the projection of the wire axis on the glide plane and the glide direction, exceeded 13°.

7.—CRYSTAL BREAK-UP

Crystals which have been considerably extended ($\epsilon > 1{\cdot}036$ say) show a deformation of the simple Laue spots. An elongation of the spots has often been observed, and is well known under the name asterism (Schmid and Boas 1935, p. 205). With sodium and potassium crystals, however, we obtain not a smearing of the spot into a continuous band, but a series of discrete spots which become more widely separated as the extension increases. Fig. 15, Plate 2 shows a sodium crystal for which $\epsilon = 1{\cdot}30$. The deformation of the spots corresponds well with a rotation of crystallites about a single crystallographic axis, in the glide plane and normal to the glide direction. Fig. 16 is a theoretical figure for the loci of Laue spots from a body-centred cubic crystal when the crystal rotates about an axis parallel to the photographic plate, of the type prepared by Yamaguchi (1929). The family of continuous lines represents the loci, the broken lines represent the angles of rotation written against them. The spots shown in fig. 15 have been transferred to this diagram, and it will be seen that they correspond well, on the whole, to a rotation about a single axis. The extreme range of rotation indicated by the spots is about the same in all cases, for a crystal that has suffered a given amount of shear, namely 13° in the case of the crystal represented in fig. 15.

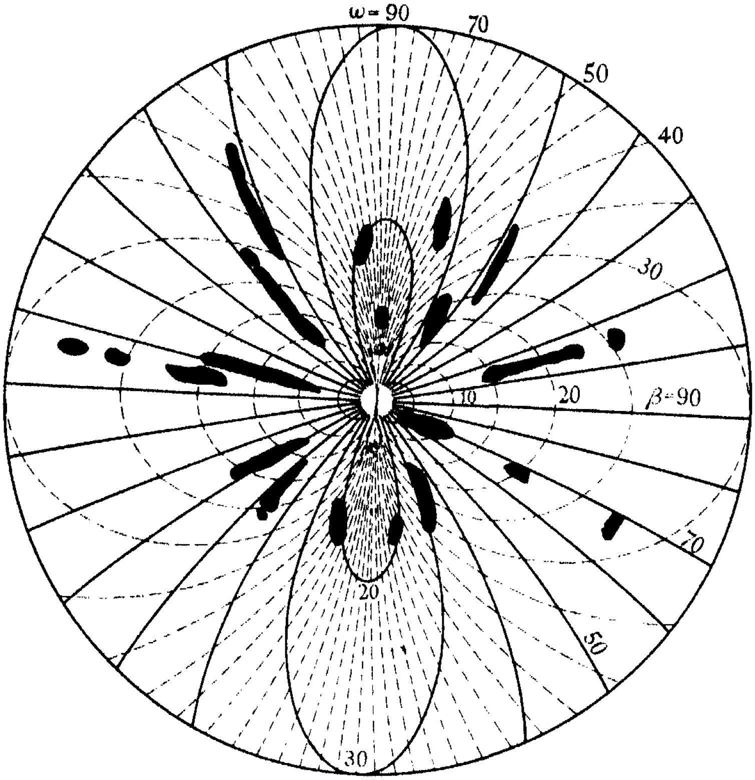

Fig. 16

The material to hand is somewhat scanty for a discussion of the formation of these spots, but rough measurements have been made of the angle of rotation corresponding to the separations. This has been done by counting the number of spots in a few of the well-defined cases, and dividing the angular distance between the extreme spots by the number of spacings.

In the case of three crystals, where the average shear was respectively 0·22, 0·30, 0·45, the average rotation corresponding to adjacent spots came out to be 0·83°, 1°, 1·6°, that is, as far as the rough nature of the experiments will allow a definite conclusion to be drawn, the steps of rotation are proportional to the shear. The X-ray beam will traverse a large number of glide planes (about ten), and the question arises whether on a given glide plane all the crystallites have rotated by the same amount, an amount which differs from glide plane to glide plane, or whether all the rotations are represented on one plane. A puzzling feature is that all the spots appear in about equal intensity and that the rotation shown by each spot seems to increase continuously as the shear increases. The simplest explanation would seem to be that the rotation takes place in layers of various thickness, each a simple multiple of a certain factor. The shear within the glide lamina is very large, as compared to the average shear, for the "packet" between two of the visible glide planes is undeformed.

It is to be noted that discontinuous asterisms have been obtained before with rock salt (Konobejewsky and Mirer 1932; Manteuffel 1931).

8—DISCUSSION

The mechanical behaviour of the body-centred cubic lattice offers, as has been pointed out, a wide range of phenomena which it is difficult to reconcile in a general scheme of behaviour. It is well known that, to explain any of the features of plastic behaviour of metals it is necessary to invoke some system of crystalline dislocations, or flaws, and the differences from metal to metal, and even from experimenter to experimenter (cf. Taylor, Elam, Fahrenhorst and Schmid) may be dismissed as due to differences of this feature in specimens prepared and handled in different ways. This mode of explanation is not, however, very satisfactory, and it seems better, in the first instance, to suppose that this type of lattice does not vary in general properties from case to case, and to see if there are variations of experimental circumstance which may account for the divergent results.

As regards the present experiment, it is in the first place to be remarked that crystals of the metals sodium and potassium are very much softer than those of the tungsten, α-iron and β-brass used by other experimenters, or, to put it differently, that we have worked very much nearer to the melting-point. Secondly, crystals grown by our method appear to be very free from strain, and uniform. Sodium and potassium contract on solidification,* and leave the tube very easily; the whole wire always forms on crystal. The iron crystals were made by a recrystallization method.

We found that the glide took place along the [111] direction within experimental error, say 4°. The only worker who has found exceptions to this rule is Elam, working with β-brass and with α-iron, who finds that, while this is the most common direction, it is not invariable. She proceeded to very large extensions, and there seems to have been no definite evidence that the crystals maintained their single crystal nature. Her method of fixing the crystallographic axes is that originally used by Taylor and Elam, which appears to be open to fairly large errors, but she does not give data which allow any estimate to be made. The fact that, for β-brass, Taylor always found [111] as the direction, she attributes to the small deformation which he used (5–15 %). This may be so, but, in the absence of a drastic X-ray examination to prove that the crystal has preserved its nature, small extensions seem to be preferable.

An examination of our results, however, shows that even where the angle between the glide direction and the projection of the wire axis on the glide plane (line of greatest slope, in Elam's phrase) is 13° the glide direction is still, within a degree or two, the [111] direction, and the glide plane a {123} plane. It may be added that the [111] direction is the most closely packed direction, and that with the exception of Elam, all workers hitherto have found the glide direction to be the most closely packed direction, although the glide plane is not the most closely packed plane.

As regards the glide plane, it so happened that the range of χ_0 shown by our different crystals was not very large, from 30 to 51°. A preferred direction of the crystallographic axes is often a feature of crystals prepared by cooling from the melt in the way used by us (Andrade and Roscoe 1937; Greenland 1937).

It cannot be deduced from our results, then, that a {123} plane is *always* the glide plane, whatever the angle χ which it makes with the wire axis, for in our experiments χ always lay within a certain limited range. It seems, however, safe to say that, if this angle is within 15° of the 45° inclination the glide plane is such a plane, and that in this case the [111] direction is the glide direction, even when it makes an angle of 10° or more with the line of greatest slope. We have no definite proof that it is still the glide direction in the case where α was 24°, because the full X-ray examination was not carried out, but the glide plane was definitely {123} in this case.

Our experimental method of fixing the crystallographic directions seems to offer certain advantages over those used by other experimenters on the body-centred crystal. It includes the use of all the spots, and is not dependent on the relative intensities, except in so far as they are used as rough guides to facilitate the identification of the planes. On the other hand the method of Müller, used by Taylor and Elam, makes use of only one or two spots, and assumes that they are due to {110} planes, which are supposed to give the most intense reflection. In our experience, however, the reflection from {112} planes is sometimes as strong, or stronger. Our slip planes are always well marked, and, except in the case of double glide, only one system appears. Our results are, then, particularly definite as compared for example with those of Fahrenhorst and Schmid, who made chief use of the movement of the wire axis with reference to the crystallographic frame, during extension. Their results on α-iron give as probable (they do not put it higher) the same glide elements as we have obtained with sodium and potassium: viz. the {123} plane and [111] direction.

---

* For sodium the density of the solid is 0·952, of the liquid 0·929: for potassium the figures are 0·851 and 0·830; in both cases at the melting-point of the metal.

Our results have all been obtained at comparatively small extensions, not exceeding 5 %. This was done purposely, since for large extensions the results are much complicated by crystal break-up (see § 7). It is for larger extensions that the anomalies in Elam's work chiefly occur. The X-ray method which she uses is not adopted to show how far the crystal has preserved its identity. If there is much break-up on the glide planes, of the type which we have found, irregular results are to be expected.

Taylor found for α-iron no definite glide plane, but only a glide direction. Evidence that the plane is not as definite as the direction, even for our crystals, is given by the shape of the heads of the glide traces, which shows irregularities such as might be obtained if, while on the whole the plane was a {123}, glide could take place on other planes making small angles with the main plane.

While we have found (123) as the slip plane, in this investigation, Elam found for β-brass that (110) and (112) were often operative. We do not suggest that (123) is always the slip plane in body-centred crystals, for Mr. Tsien and Miss Chow, working in this laboratory, have found with molybdenum that {112} planes are operative at low temperatures (15–300° C.), while {110} planes are operative at temperatures in the neighbourhood of 1000° C. The work is being extended to still higher temperatures.

Such different behaviour at different temperatures has been found with hexagonal metals: with magnesium, for instance (0001) is the glide plane at atmospheric temperature, but $(10\bar{1}1)$ or $(10\bar{1}2)$ also come into action at higher temperatures, e.g. 225° C. With α-iron Gough found that [111] was invariably the glide direction, and that the slip took place on pairs of planes, either {110} and {123}, or {112} and {123}, the two partners of a pair being situated on opposite sides of the maximum resolved shear stress. Apparently, then, with body-centred crystals as a class, {123}, {110} and {112} are possible glide planes, and conditions not yet elucidated determine which shall be operative.

SUMMARY

Sodium and potassium are of particular interest as belonging to the body-centred cubic system of crystals, data as to which are scanty and conflicting. Undeformed single crystal rods of the metals have been prepared, and extended under conditions which minimize surface oxidation. The glide elements have been determined by an X-ray method which employs all the Laue spots. It has been found that the glide plane is (123) and the glide direction [111]. The question of double glide, and of crystal break-up, is discussed.

REFERENCES

Andrade and Roscoe 1937 *Proc. Phys. Soc.* **49**, 152.
Chalmers, B. 1932 *Phil. Mag.* **14**, 612.
Clay, R. E. 1934 *J. Sci. Instrum.* **11**, 371.
Elam, C. F. 1936 *Proc. Roy. Soc.* A, **153**, 273.
Fahrenhorst and Schmid 1932 *Z. Phys.* **78**, 383.
Goucher 1924 *Phil. Mag.* **48**, 229, 800.
Gough 1928 *Proc. Roy. Soc.* A, **118**, 498.
Greenland, K. M. 1937 *Proc. Roy. Soc.* A, **163**, 28, 34.
Konobejewsky, S. and Mirer, I. 1932 *Z. Krystallogr.* **81**, 69.
Manteuffel, I. 1931 *Z. Phys.* **70**, 109.
Roscoe, R. and Hutchings, P. J. 1933 *Phil. Mag.* **16**, 703.
Schmid, E. 1931 *Z. Elektrochem.* **37**, 447.
Schmid, E. and Boas, W. 1935 "Kristallplastizitat". Berlin.
Taylor, G. I. 1928 *Proc. Roy. Soc.* A, **118**, 1.
Taylor, G. I. and Elam 1926 *Proc. Roy. Soc.* A, **112**, 337.
Yamaguchi 1929 *Sci. Rep. Inst. Phys. Chem. Res. Japan*, **11**, 151.

Preparation of Single Crystal Wires of Metals of High Melting Point

By E. N. da C. Andrade, F.R.S.
Quain Professor of Physics in the University of London

(*Received* 22 *June* 1937)

[Plate 3]

Introduction

Various methods of preparing single crystal wires of metals have been devised (see, e.g. Schmid and Boas 1935; Andrade and Roscoe 1937), but they all demand furnaces which reach the melting point, the transformation point, or the recrystallization temperature of the metal. In the case of metals where the temperature in question is very high the general methods call, then, for high temperature furnaces which are costly and often troublesome to control. The method to be described eliminates the need of such a furnace, and would seem to have a wide application. The wire is maintained at a high temperature by a current passing through it, and a subsidiary temperature gradient is applied.

General Method

The essence of many of the methods in use is a travelling temperature gradient, of magnitude $dT/dx = G$, covering a small length of the metal rod or wire; if the temperature on one side of this length is above, that on the other side below, the melting point of the metal, then, with suitable conditions, single crystals can always be grown. These conditions have been shown to be that G/V must have a high value, and G a value not exceeding a certain limit, where V is the velocity of travel (Andrade and Roscoe 1937). Similar conditions should apply when, in the case of transition from one crystal form to another, the temperature of transition is substituted for the melting point.

It seemed to me likely that, providing the wire were maintained at a temperature at which crystal growth is rapid, then a superimposed moving temperature gradient might lead to the formation of a single crystal from a polycrystalline wire, by promoting preferential growth from the high temperature side in the region of the gradient.

With these considerations in view, the following method was devised. A long wire is maintained at a high uniform temperature by the passage of an electric current. It is surrounded by an evacuated tube, so that, except near the ends, where conduction has an effect, the heat losses are mainly by radiation. A small furnace surrounds the tube for a short length. The temperature of the furnace need not be especially high: in particular it may be considerably lower than that of the wire, for its function is to raise the temperature by diminishing the heat lost by radiation from the wire. A temperature gradient will thus be established in the regions of the wire near the ends of the furnace. This furnace travels slowly along the tube, as can be easily arranged, for instance, by setting the tube vertically and lowering the furnace by a wire which is paid out by clockwork. As a variant of this procedure the wire may be enclosed under a bell jar, and the furnace may surround it closely, the whole being *in vacuo*. This method has not yet been tried, but may prove to have some advantages. Still another possible method would be to surround the wire by a short travelling tube, highly polished, which would diminish the radiation losses and so raise the temperature locally.

Alternatively, the temperature gradient may be confined to a restricted part of the wire, and the temperature of the whole wire gradually lowered. In the region of the gradient the spot at which the temperature is critical (e.g. transition temperature) will then travel along, and we may expect, in the region of the gradient, a single crystal to be formed, which, with slow cooling, will subsequently extend along the whole wire.

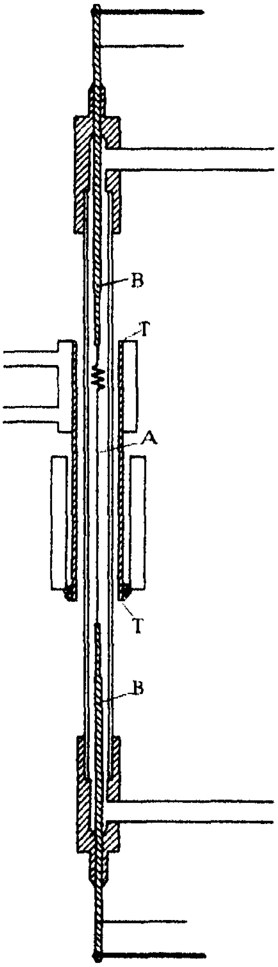

Fig. 1

Application of the Method

The method was first tried out, by Dr. Greenland and myself, to prepare wires of α-iron, the transition temperature of the α-form being about 900° C. The method of stationary temperature gradient and progressive cooling of the wire was adopted. Fig. 1 shows the arrangement. *A* is the iron wire, about 1 mm. in diameter, wound into a small spring at one end in order to keep it straight when it expands on heating. The wire is gripped at both ends by steel rods *BB*, drilled to receive it. These rods pass through brass caps, furnished with tubes for evacuation. The wire is surrounded by a quartz tube, to which the brass caps are cemented. The temperature gradient is maintained in a copper tube *TT*, one end of which is heated by a small furnace to a temperature of about 200° C., while the other end is kept cool by water circulation. The whole wire is first maintained at a temperature well above 900° C., the necessary current, about 15 amps., being drawn from accumulator cells. The temperature is estimated from the electrical resistance. The current is then steadily diminished by regulating carbon rheostats, until it is well below the transition point. The slow cooling takes about 15 min.

Very good single crystal wires of α-iron have been formed in this way. Fig. 2, Plate 3 shows such a wire extended, the slip bands being well marked, but with irregular outline, as is to be anticipated from the work of Taylor and Elam (1926).

The method of the travelling temperature gradient, produced by a moving furnace, has been successfully applied by Tsien and Chow in my laboratory to the manufacture of single crystals of molybdenum, which have not previously been made, and it is hoped to extend it to other metals of high melting point. The limitation of the method is that, owing to the high currents required, the wire must not be too thick, but it must be remembered that the potential needed is very low, and that currents of 200 to 300 amp. may be safely taken from modern cells, or even more if the cells are connected in parallel.

REFERENCES

Schmid and Boas 1935 "Kristallplastizitat." Berlin: Springer.
Andrade and Roscoe 1937 *Proc. Phys. Soc.* **49**, 152.
Taylor and Elam 1926 *Proc. Roy. Soc.* A, **112**, 337.

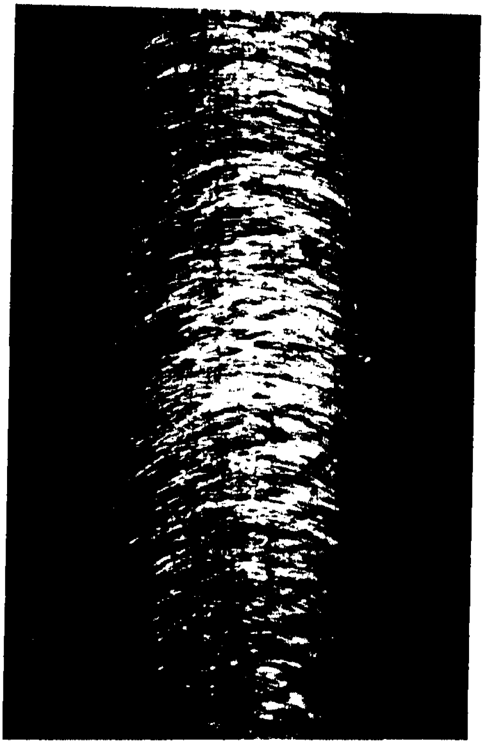

FIG. 2

(*Facing p.* 18)

The Glide of Single Crystals of Molybdenum

By L. C. Tsien and Y. S. Chow

Physics Laboratory, University College, London

(*Communicated by E. N. da C. Andrade, F.R.S.—*
Received 22 *June* 1937)

[Plates 4, 5]

1—Introduction

As pointed out in the paper by Andrade and Tsien, the situation as regards body-centred crystals is such that further information as to the glide element of crystals of this class is needed. In particular, there is considerable uncertainty as to the glide plane, different crystallographic planes being, apparently, operative with different metals. It is possible that with body-centred crystals the planes on which glide takes place depend upon the temperature with reference, say, to the melting point of the metal, since with certain hexagonal crystals such as magnesium, fresh planes have been found to come into operation at high temperatures. Molybdenum, which crystallizes in the body-centred system, has an extremely high melting point, about 2630° C., and so offers a wide range of temperature for experiment. In the following pages work on the glide elements in the temperature range 20–1000° is described, and it is shown that while the glide plane at the lower temperatures is (112), at high temperature it is (110). The glide direction is in all cases [111], thus confirming the rule that the glide direction is the most closely packed direction. It is hoped later to extend the determinations to higher temperatures.

2—Preparation of the Crystals

The crystals were prepared by the method devised by Professor Andrade for metals of high melting point, in which the wire is maintained at a high temperature by a current passing through it, and a local temperature gradient, which slowly travels down the wire, is obtained by a small subsidiary furnace surrounding the wire. For this method it is desirable not to use too thick a wire, and the metal used was 0·25 mm. in diameter, supplied by the Tungsten Manufacturing Company. If such a wire be maintained by the passage of a current at a temperature some 1000° C.

below its melting point, the individual crystallites grow, until the appearance shown in fig. 1, Plate 4 is obtained, where some of the crystals extend right across the wire. The crystal boundaries in this picture have been revealed by etching with dilute nitric acid.

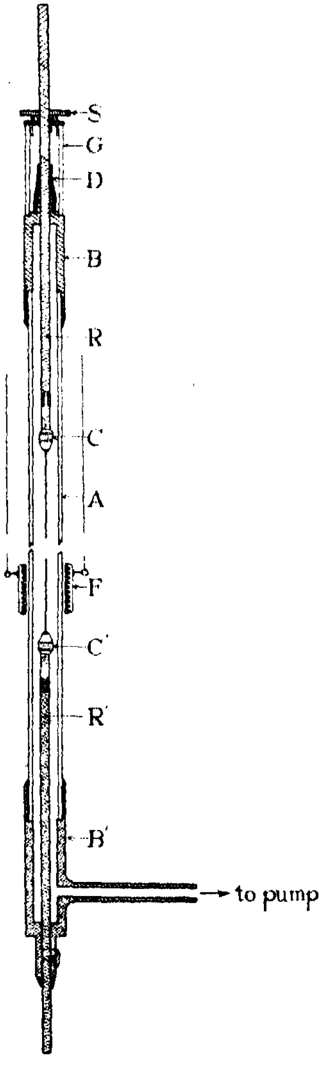

Fig. 2

However, with simple heating, we never obtained crystals longer than 2 mm. At Professor Andrade's suggestion a travelling temperature gradient was superposed on a wire heated to an approximately uniform temperature by the passage of a current. It was found that this enabled us to prepare single crystals of any length required. The apparatus used is shown in fig. 2. The transparent fused silica tube, *A*, 21 cm. long and 1·3 cm. in diameter, is fitted into the two brass caps, *B* and *B'*, the latter of which is furnished with a tube for evacuation. Through these caps pass brass rods, *R* and *R'*, each carrying pin chucks, *C* and *C'*, the wire, usually 11 cm. long, being firmly held by these chucks.

The lower rod does not move, and is sealed to its holder with hard wax. Owing to the expansion of the wire at high temperatures the upper rod is adjustable, so that the wire may be maintained taut. The nut *S*, supported by a short glass tube *G*, can be turned so as to withdraw the rod, rotation of which is prevented by a key fitting into a groove. The joints between the rod and the holder *B* is made vacuum-tight by the rubber sleeve *D*. The current through the wire is furnished by a 12 V accumulator battery, capable of safely supplying currents up to 200 amp. The quartz tube is surrounded by a small electric furnace, *F*, about 1·2 cm. long: this furnace is maintained at about 1000° C. by a current of some 3 amp. The furnace is suspended by wires, and can be steadily lowered by clockwork.

The wire is carefully polished with Hubert emery papers from No. 0 to No. 0000 successively. It is then inserted in the apparatus and maintained at a temperature of about 1800° C. by the passage of a current of 5 amp. or so. The temperature is estimated firstly by comparing the resistance of the wire with its resistance at room temperature, and secondly by calculating the temperature necessary if the heat generated, as given by the current and the potential drop over the wire, is to be dissipated by radiation. The necessary data on the electrical resistivity of, and the radiation by, molybdenum are given by Esper and Knoll (1936). While the wire is maintained at high temperature considerable evaporation takes place, and a film of metal forms on the walls of the quartz tube. However, this evaporation does not harm the metal surface, which remains smooth. The resistivity measurements gave a temperature of about 1800° C., but the radiation calculations gave a lower temperature, viz. 1500° C. It is probable that the resistivity measurements are more reliable, but no particular attention has been devoted to the point at this stage, since only the roughest estimate of the temperature is required. Taking the temperature of the wire as 1800° C., an approximate calculation shows that the temperature where the wire is surrounded by the furnace should be about 60° C. above that of the remoter parts of the wire.

In general, satisfactory single crystals several centimetres long can be easily obtained by this method. Occasionally two crystals grow side by side for a considerable distance, fig. 3, Plate 4 shows such a case, in which each crystal chances to be so orientated that double glide takes place in it. The extension, of some 40 %, was carried out at 300° C. Assuming, in accordance with the results described later, that the glide plane is (112) and the glide direction is [111], then both crystals must have a [110] direction parallel to the wire axis, but a rotation of approximately 90° about the wire axis is necessary to bring the lattice of one crystal into coincidence with that of the other.

3—DETERMINATION OF GLIDE PLANE AND GLIDE DIRECTION

The glide elements of the crystal were determined by means of Laue photographs. The spots were transferred to a stereographic projection, which was then rotated so as to give a simple figure which could be compared with certain standard figures. The general procedure is described in the paper on sodium and potassium (Andrade and Tsien 1937). Certain minor alterations have been introduced for application to molybdenum. In view of the high density (10·3 g./c.c.) penetrating X-rays must be used. White radiation from a tungsten target at a voltage of 70 kV was employed, corresponding to a shortest wave-length of 0·0176 A. A certain amount of trouble was experienced with the Shearer tube owing to sparking over the lamp chimney used as the body of the tube. A fused silica tube 20 cm. long and 4·8 cm. in diameter was substituted, which proved to be very satisfactory. The water cooling of the target was also improved.

Owing to the fineness of the single crystal wires the diameter of the cylindrical aperture which isolated the X-ray beam was reduced to 0·3 mm. The crystal was held in a pin chuck attached to a goniometer mounting, so arranged that the crystal plane could be adjusted in azimuth and declination. The wire was always arranged so that one vertical plane contained the wire axis, the X-ray beam and the normal to the glide plane. The distance from the crystal to the photographic plate was 3·3 cm. and the usual time of exposure 4 or 5 hr.

The crystals were stretched at three different temperatures, viz. 20, 300 and 1000° C. For 300° C. the wire held in the apparatus shown in fig. 2 was surrounded by a furnace, and the stretching carried out by rotating the nut *S*. For 1000° C. heating was effected by passing a current down the wire itself, the temperature being estimated by resistance measurement. This method of heating the wire is not altogether satisfactory, since local thinning immediately leads to local rise of temperature, which leads to further thinning, the cumulative effect resulting in early fracture. A small furnace consisting of a tungsten tube has since been made, and will be used for work at higher temperatures.

At temperatures in the neighbourhood of 1000° C. the glide packets are broad and marked, and considerable glide takes place on each glide plane, as shown in fig. 4, Plate 4, for which the extension is 28 %. At this temperature fracture takes place on a glide plane, as is also clear from fig. 4, Plate 4. At lower temperatures, e.g. 300° C., the glide planes are close and less plainly marked, so that naturally less slip takes place on the individual planes, as shown in fig. 5, Plate 4, for which the extension is 12 %. At still lower temperature, e.g. room temperature, the slip planes are still lighter and closer, as shown in fig. 6, Plate 4.

A curious effect was noticed in certain cases of extension at 1000° C. The exposed surfaces of the glide planes were marked at certain places by shallow furrows, parallel to the glide direction, as shown in fig. 7, Plate 5. These furrows all start at certain lines parallel to the wire axis, probably drawing marks, which were visible on the surface of the crystal before extension. These lines would therefore appear to consist of particularly hard material, either material abraded from the die, or deformed crystallites of the metal itself, produced by some irregularity of the die.

Determinations of the glide plane were made on seven different wires at

FIG. 1. × 16

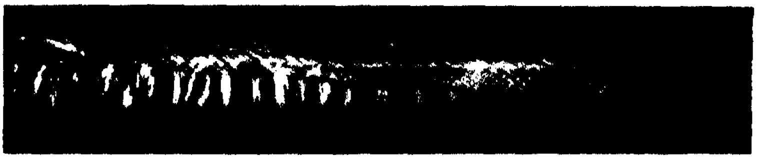

FIG. 3. × 60

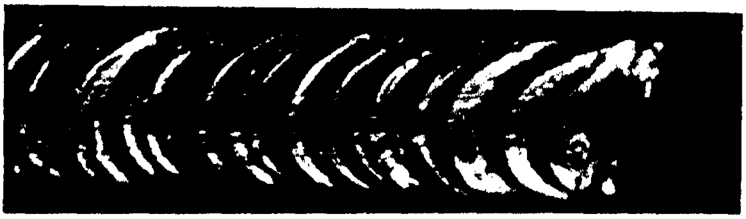

FIG. 4. × 80

FIG. 5. × 60

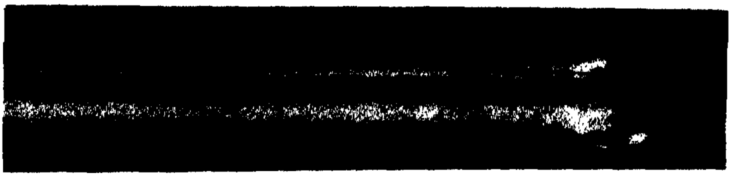

FIG. 6. × 60

(*Facing p.* 22)

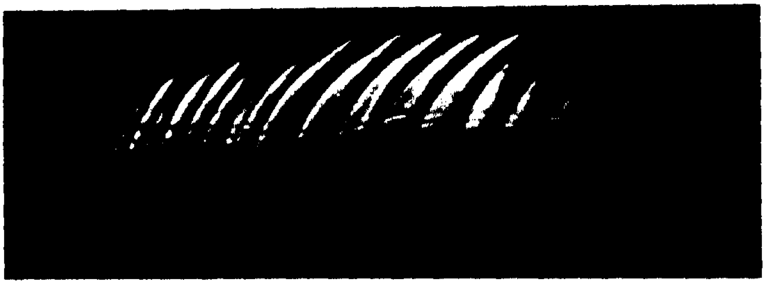

Fig. 7. × 150

Fig. 11

1000° C., on three wires at 300° C. and one wire at 20° C. In the case of two of the wires at 300° C. and of the one wire at 20° C., where extension was considerable, double glide took place, so that for each of the wires in question two determinations of the glide plane could be made. The seven determinations of the glide plane at high temperatures are shown in fig. 8, which represents a limited part of the stereographic projection for which the radius of the primitive circle is 10 cm. and the principle zone axis is [110]. The open circles represent the poles of the glide planes, as found experimentally. The centre of gravity of these determinations clearly lies very close to the (110) plane.

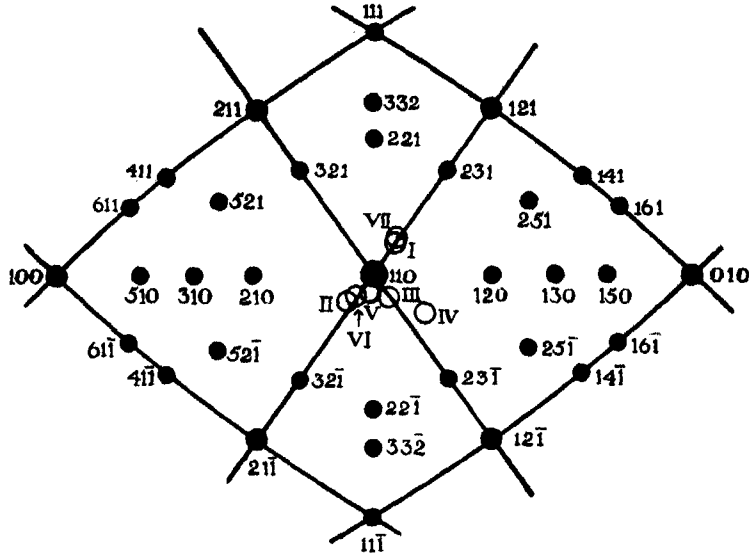

Fig. 8—Glide plane of molybdenum crystals at high temperature. (Radius of primitive circle = 10 cm.)

The glide plane results for 300° C. and for 20° C. are shown together in fig. 9 where the principal zone axis is [112]. Determinations at 20° C. are indicated by the open squares, while those at 300° C. are indicated by triangles. Four of the determinations at 300° C. are so close together that a system of concentric squares has to be used. We conclude from the observations here represented that the glide plane at these temperatures is (112).

The glide directions were experimentally found by determining the shape of the elliptic trace of the slip band, as explained in the paper of Andrade and Tsien (1937). The angle between the glide direction and the projection of the wire axis on the glide plane was calculated in the way described, and from this the glide direction could be fixed on the pole figure. The determinations at all temperatures are shown together on the pole figure, fig. 10, for which the principle zone axis is [111]. It will be seen that in all cases the [111] direction is indicated as the glide direction.

An interesting case, giving a clear indication of the glide direction, is represented by the Laue photograph shown in fig. 11, Plate 5. It was taken with a crystal extended by 40 % at 300° C. which showed double glide. The beam was normal to the intersection of the two sets of glide planes, and bisected the angle between them. The pattern shows the high degree of symmetry to be expected, and analysis reveals that glide has taken place on the planes (112) and ($\bar{1}\bar{1}2$), in directions [$\bar{1}\bar{1}1$] and [111] respectively, the axis of the wire being in a direction [110].

The results obtained with all crystals are given in Table I. The last three columns are given in order to show that the small deviation which the glide direction sometimes shows from the [111] direction is a more or less random one, and not such as to make the glide directions coincide

TABLE I

Crystal No.	Working temp. °C.	ϵ	χ_0	Angle between glide plane and			ψ	ϕ	η
				[110]	[112]	[123]			
I	1000	1·05	55·5°	6°	24·5°	13°	2°	2°	0°
II	1000	1·155	47°	6°	24°	12°	1°	8°	8·8°
III	1000	—	—	4°	26°	15°	4°	4°	0°
IV	1000	1·19	51°	10°	20°	11°	4°	8°	6·7°
V	1000	1·27	49°	3°	28°	17°	1·5°	1·5°	0°
VI	1000	1·21	54·5°	5°	25°	14°	1·5°	3°	4·5°
VII	1000	1·08	54·5°	6°	24°	15°	4°	2°	4·8°
VIII	300	1·05	41·5°	25°	6·5°	8°	5°	5°	0°
IX	300	1·40	36°	30°	0°	10°	0°	0°	0°
			36°	30°	0°	10°	0°	0°	0°
X	300	1·46	36°	30°	0°	10°	0°	0°	0°
			36°	30°	0°	10°	0°	0°	0°
XI	20	—	35·5°	31°	4°	13°	4°	4°	0°
			35·5°	31°	4°	13°	4°	4°	0°

with the projection of the wire axis on the glide plane, which in many cases differs by but little from the glide direction. The angle ψ is the measured angle between the glide direction and the [111] direction; ϕ is the angle between the projection of the wire axis on the glide plane and the [111] direction; and η is the angle between the glide direction and the projection of the wire axis. The results are also exhibited in fig. 12,

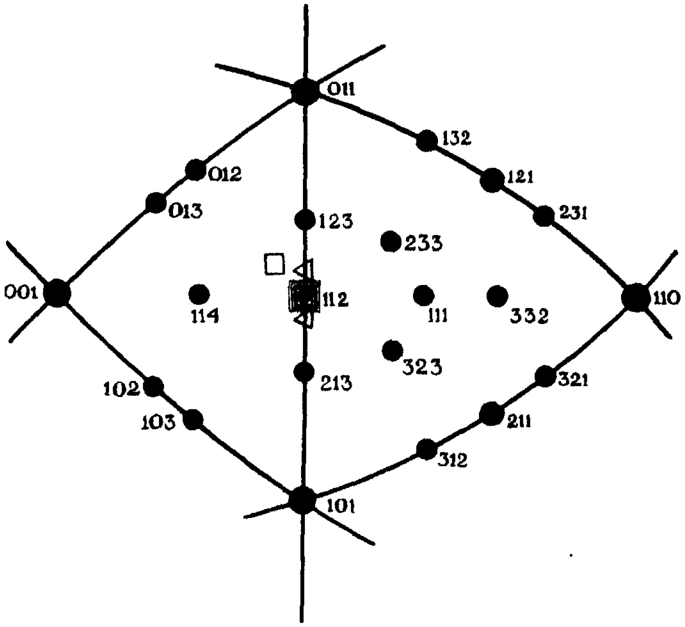

FIG. 9—Glide plane of molybdenum crystals at lower temperatures. (Radius of primitive circle = 10 cm.) □ = 300° C.; △ = 15° C.

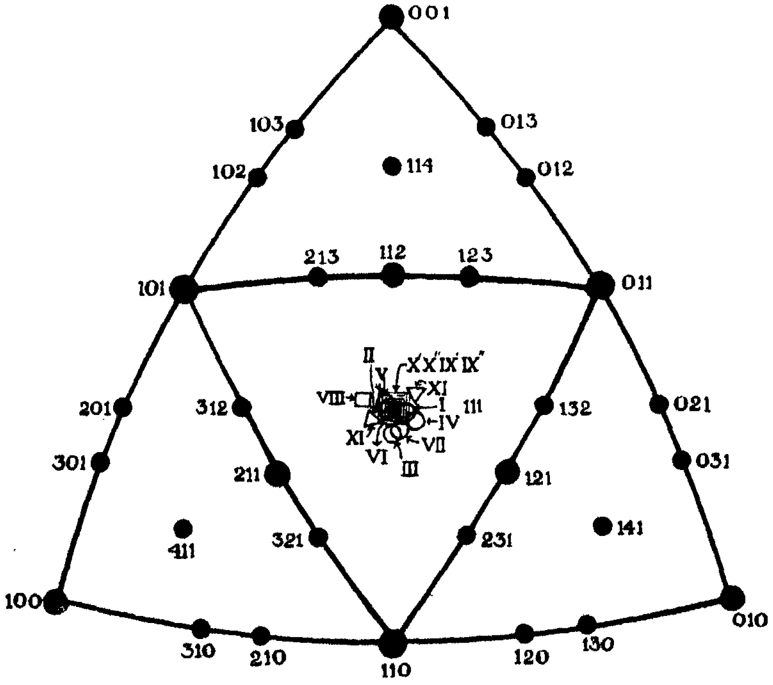

FIG. 10—Glide directions of molybdenum single crystals. (Radius of primitive circle = 10 cm.) ○ = 1000° C.; □ = 300° C.; △ = 15° C.

where A is the [111] axis; P is the projection of the wire axis on the glide plane; and G is the glide direction, exhibited in stereographic projection. The cases where all three coincide are not included. It will be seen that while P and G sometimes coincide, on other occasions they lie on opposite sides of the [111] direction A, with G much nearer to it than P. We are therefore probably justified in saying that the glide direction is, within experimental error, the [111] direction, rather than the line of greatest resolved shear.

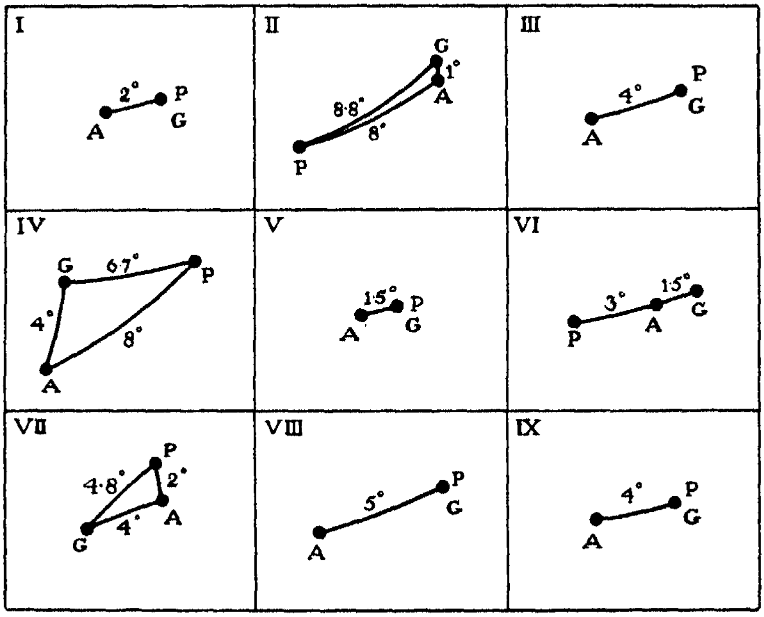

FIG. 12

4—DISCUSSION

It appears from the results described that the glide direction of molybdenum single crystals is always a [111] direction, which is a close packed line. There is no close packed plane in a body-centred structure: the closest packed is the (110) plane, followed by (100), with atomic surface densities of 0·892 and 0·630 respectively, compared with the surface density at close packing as 1. For (112), which is operative for molybdenum at low temperatures, it is 0·514: for (111) it is 0·364. It is clear, however, that closeness of packing on the plane is not, in general, a determining factor for the body-centred crystal, since for sodium and potassium the glide plane is (123) (Andrade and Tsien 1937), for which the packing is 0·337.

The temperature effect seems to be clearly established. If only the three crystals IX, X and XI are considered it might appear that the orientation relative to the direction of stress was the determining factor, and not the temperature, since in all these crystals two {112} planes were equally inclined to the wire axis. However, crystal VIII, where the orientation is different, glides on a plane, which, while it deviates 6° (probably within experimental error for a crystal, like this one, not very favourable for measurement) from a {112} plane, deviates considerably more from a {123} or a {110} plane. Moreover, for this crystal there is a pair of planes, equally inclined to the wire axis at 57°, which deviate only 7° from two {110} planes, and the projection of the wire axis on these two planes falls exactly on two [111] directions. The conditions were very similar to those in other crystals (Nos. I to VII) which were found to glide on {110} planes at higher temperatures, so that, if there were no temperature effect, glide in crystal VIII would have also been on {110} planes.

On the other hand, critical examination of the crystals extended at high temperature revealed no tendency to glide on a {112} plane. Such a change of glide plane with the temperature has already been established by Boas and Schmid (1931) with aluminium crystals (face-centred cube), where the glide direction was always [111], and the glide plane (111) at room temperature, but (100) above 400° C. Here the glide is on the less closely packed plane at higher temperature, while with molybdenum the glide is transferred to the more closely packed plane at higher temperature. This is another indication that closeness of packing has nothing to do with the plane selected as glide plane.

In conclusion the writers wish to take this opportunity of expressing their gratitude to Professor E. N. da C. Andrade, F.R.S., for his guidance and constant encouragement during the course of this work.

SUMMARY

Single crystals of molybdenum have been prepared from wire 0·25 mm. in diameter, by the method described by Andrade for metals of high melting point. Such crystals have been extended at three temperatures, viz. 20, 300 and 1000° C. The identification of the glide plane and glide direction in each case has been carried out by Laue photographs, the method employed making use of all the spots for identification. The

glide direction is always a [111] direction. The glide plane is different at different temperatures, being a (110) plane at 1000° C. and a (112) plane at 300 and 20° C.

REFERENCES

Andrade, E. N. da C. 1937 *Proc. Roy. Soc.* A, **163**, 16.
Andrade, E. N. da C. and Tsien, L. C. 1937 *Proc. Roy. Soc.* A, **163**, 1.
Boas, W. and Schmid, E. 1931 *Z. Phys.* **71**, 703.
Esper and Knoll 1936 "Werkstoffkunde der Hochvakuumtechnik." Berlin: Julius Springer.

Slip Bands on Mercury Single Crystals

By K. M. GREENLAND, PH.D.

(*Communicated by E. N. da C. Andrade, F.R.S.—*
Received 22 *June* 1937)

[Plates 6, 7]

1—INTRODUCTION

In the course of an experimental investigation of the factors determining the critical shear stress of mercury single crystals, it became clear that the distortion of the crystals by gliding took place in a way very different from that illustrated by the classical Polanyi model of gliding. This model represents the crystal in the form of a rod of circular cross-section, which, when stretched, separates into a number of inclined disks or glide lamellae which slide over each other. The planes defining the lamellae are crystallographic and are called glide planes. The relative displacement of the glide lamellae results in the appearance of markings on the crystal surface which are the traces of the intersection of the glide planes with the surface. These, according to the Polanyi model, are elliptical in shape, and so have been called "glide ellipses", but in this paper the more general term "slip band" will be used.

This representation of the process of distortion is in perfect accord with the observed phenomena in the majority of metal crystals. Their slip bands are perfect in shape and can be shown, by X-ray examination, to correspond closely to the traces of crystallographic planes.

There are, however, certain exceptions of which α-iron (Taylor and Elam 1926; see also Osmond and Cartaud 1906) and β-brass (Elam 1936) are notable examples, where the slip bands, while approximating in shape to the geometrical figure formed by intersection of the crystal surface by an inclined plane, are very wavy and branched. In the course of the present work on mercury, slip bands of both the regular and irregular types have been observed on the crystals, and the systematic examination to be described has shown that the shape of the bands formed by stretching depends upon the nature of any previous strain which the crystal has received. The nature of the surface disturbance by which the slip band is made visible has also been investigated and found not to be so simple as the Polanyi model suggests.

The crystals used in this work are in the form of wires 1 to 4 cm. long and 2 mm. in diameter, maintained at a temperature of −60° C. They are grown by the method developed by Andrade and Hutchings (1935). The apparatus in which they are examined is fully described in another paper by the present writer (Greenland 1937).

2—FORMATION OF THE SLIP BANDS

The mechanical resistance of the mercury lattice at −60° C. is very small, and shear may easily be caused by slight bending of the wire. Such bending produces slip bands which are faint but perfect ellipses. When the bent wire is extended by, say, 1 %, these bands, however faint initially, become much more pronounced, indicating that extension is occurring by slip on the surfaces which they represent. The bands now have the shape required by the conventional conception of glide as a relative displacement of parallel blocks of the crystal defined by crystallographic glide *planes*. Further extension results in the appearance of more slip bands, both between and beyond the original bands, and the wire then presents the appearance characteristic of a stretched single crystal (fig. 1, Plate 6).

When all possibility of accidental distortion is removed and the crystal wire extended by a pure tension, the slip bands bear little resemblance to those shown in fig. 1, Plate 6, for, as shown in fig. 2, Plate 6, they are remarkably wavy and branched. They still conform roughly to an elliptical shape, and the irregularity is greatest near the "heads" (i.e. ends of the major axes) of the approximate ellipses. Near the ends of the minor axes the bands are quite regular and parallel. As described elsewhere (Greenland 1937), the glide direction in these experiments always chanced to be within a few degrees of the direction of the major axis of the glide ellipse. From this, it follows that the bands are regular where they run in the direction of glide and irregular at right-angles to this direction. We may say, then, that under pure tension alone, glide takes place in a common direction at all points but that the glide surfaces are not single crystallographic planes. They may be regarded as being made up of a number of "glide strips" (each, perhaps, the result of the passage of a Taylor dislocation) which are all parallel to a common glide direction but distributed over a number of neighbouring lattice planes.

Great care in handling the crystals is necessary if the irregular slip bands are to appear. The monocrystalline wire is mounted for stretching by "welding" its ends to polycrystalline wires held in the chucks, as it is almost impossible to avoid bending or twisting the crystal if it is itself secured in the chucks. The joints are made by bringing the ends of the wires into contact and touching with a hot steel wire. The ends melt and run together to form a strong joint (Greenland 1937).

If the unstrained wire is twisted, very fine and regular slip bands appear (fig. 3, Plate 6). With the wire illuminated from one end, the four quarters of each ellipse are alternately light and dark, as would be expected if deformation occurs by the relative rotation of adjacent slices of crystal defined by crystallographic glide planes. Extension of the crystals after they have received torsional strain sometimes results in intensification of the bands produced by torsion, but more often the resulting bands are irregular and correspond roughly to a new set of planes nearly, but not quite, coincident with the torsion planes. Figs. 4 and 5, Plate 6, illustrate the two cases.

The average spacing of the first slip bands produced by pure tension is 5×10^{-2} mm.; by bending, 2×10^{-2} mm.; by torsion, 1×10^{-2} mm. It is a notable feature of the mercury single crystal that any substantial increase in extension is provided by an increase in the number of glide planes. The amount of glide of which each glide surface is capable soon reaches its limit, which is of the order of 5×10^{-3} mm. On the other hand, the rate of hardening of the crystal as a whole is very small (Greenland 1937).

Since a crystal under pure tension glides on irregularly shaped surfaces, it is to be expected that pure compression should produce similar glide surfaces. To test this, cylindrical single crystals 1·5 cm. in diameter and 1 cm. long were grown in a glass mould and compressed axially. Fig. 6, Plate 6, shows the appearance at the "heads" of the slip bands. At the ends of the minor axes of the approximate ellipses the slip bands are regular, as in the case of pure tension.

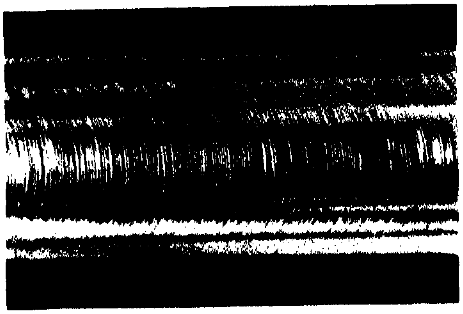

FIG. 1. × 16

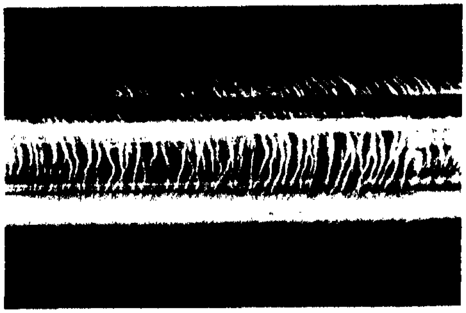

FIG. 2. × 16

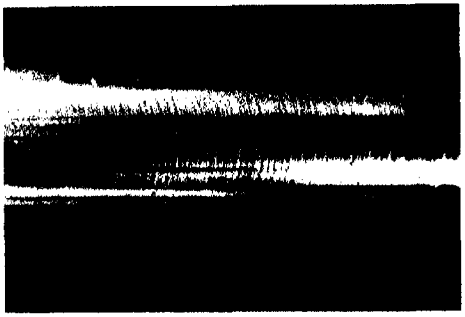

FIG. 3. × 16

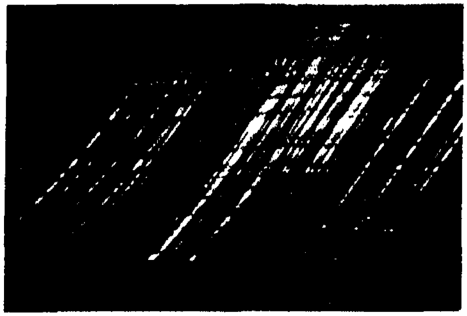

FIG. 4. × 80

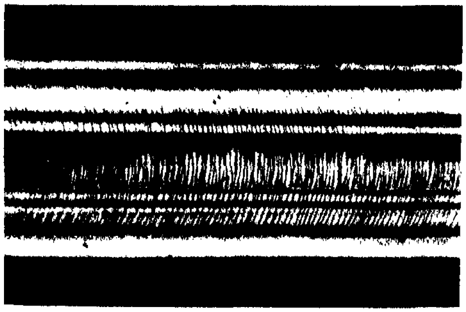

FIG. 5. × 16

FIG. 6. × 80

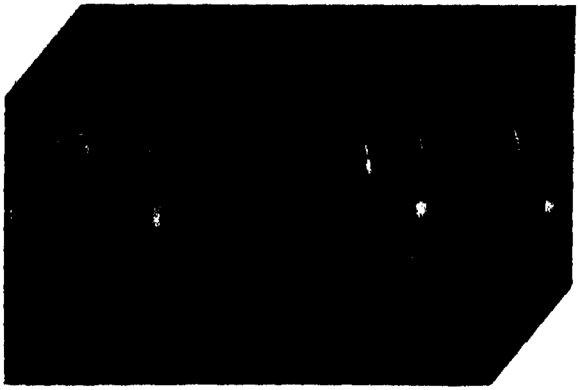

FIG. 7. × 80

FIG. 9. × 80

There is a close resemblance between the slip bands of fig. 6, Plate 6, and those obtained by Taylor and Elam (1926) with compressed crystals of α-iron. This is interesting in view of the fact that the irregularity of the α-iron and β-brass slip bands (Elam 1936) has been regarded as a particular property of the body-centred cubic lattice of those metals, whereas the mercury unit cell, while approximating to a cube, is face-centred.

In an investigation into the yielding of the crystals under known stresses (Greenland 1937), the writer has found indications that the formation of a macroscopic glide surface is effected by the linking together of minute faults in the lattice; the process is facilitated by bending the crystal. Further, it is found that the preliminary bending, with the consequent formation of regular slip bands, often lowers the critical shear stress by a considerable amount. From this, it is concluded that once a glide surface has been formed, the resistance of the lattice to a shear stress is lessened. This is consistent with the observation, described above, that when a slightly bent crystal is extended, glide takes place on the planes already sheared by bending. It is also noticeable that when a set of slip bands produced by stretching is superimposed on a set due to torsion, as illustrated in fig. 5, Plate 6, the bands of the extension set tend to run along those of the torsion set. This is often a very striking effect.

The possibility of propagation of any kind of dislocation in the lattice depends upon the mobility of the atoms in its neighbourhood and this is generally supposed to be provided by their thermal energy. The ability to control the type of slip band by suitable treatment of the crystal may well be due to the high degree of mobility of the dislocation consequent upon the nearness of the working temperature to the melting point in these experiments.

No extensive observations have yet been made with mercury crystals at lower temperatures, but a few crystals were stretched at −180° C. They usually extended by twinning, but occasionally by gliding. The slip bands were extremely close and regular.

3—NATURE OF SLIP BANDS

An examination of the nature of the surface disturbance which produces what we call a slip band has been made by illuminating the surface with a parallel pencil of light. The surface is very smooth, and a specular reflection can be received by the observing microscope.* Thus, by suitable adjusting of the angle of incidence so that the slip band appears bright, any change of inclination of the surface at the band can be detected and measured.

---

* It will be convenient to refer to the direction of the wire axis as "horizontal", and to that of the axis of the microscope receiving the reflected ray as "vertical".

According to the hitherto accepted mechanism, a slip band is the result of a break in the crystal surface, a small section of the actual glide surface being exposed owing to the displacement. Contrary to this, the observations on mercury have shown that each slip band owes its first appearance not to a break in the crystal surface, but to a very slight tilt of a narrow strip of the surface, at the periphery of the glide plane or glide surface. A newly formed slip band is only visible when the incident beam is as nearly as possible vertical.

As the amount of glide is increased, the angle between the crystal surface at the head of a slip band and the adjacent undistorted surface increases from zero to a value which in the case of a prominent band approaches that of the inclination of the glide surface itself. Owing to the disposition of the crystal wire in the apparatus, reflected light cannot be received from the wire surface at the head of a prominent band except at those places, to either side, where the surface is rounded. The double line of reflexion then visible is shown in fig. 7, Plate 7.

Fig. 8 shows (*a*) the profile of the surface at the head of a slip band as revealed by the method of observation just described, and (*b*) the appearance required by the hitherto accepted mechanism of formation; in both diagrams the plane of the diagram is parallel to the axis of the wire, and the broken line indicates the slope of the glide plane. A number of glide planes on which different amounts of glide have taken place should result in the surface at the heads of the bands having a profile as shown in fig. 8*c*. A photograph (fig. 9, Plate 7) has been obtained which confirms this conclusion. The inclination of the glide planes to the wire axis was 35°, but the greatest inclination of the surface at the prominent slip bands was only about 20°. Figs. 8*d* and 8*e* illustrate the observed and theoretical appearances of a slip band formed by compression.

If the glide plane were to break through the surface of the wire, as fig. 8*b* suggests, the slip band would at first appear as a very fine line, whereas it actually appears as a strip often 5–10μ in width. The surface of a mercury crystal in fact behaves as though it were an elastic skin. The effect may be due to a surface layer of polycrystalline or vitreous composition—the highly polished appearance of the surface suggests surface flow—or, as seems more likely, the surface tension may be high enough to produce the skin effects. Tammann (1926) has shown that when crystallites are formed under certain conditions, the surface tension of the

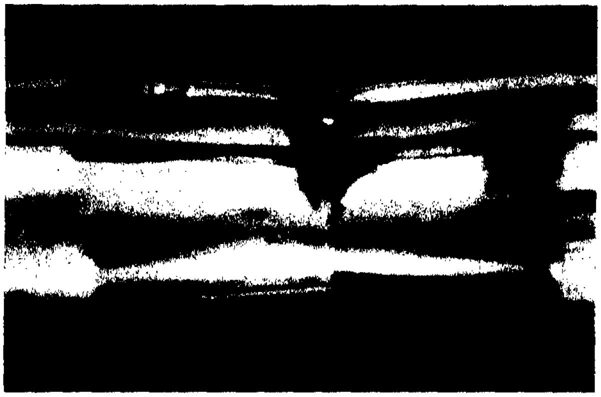

Fig. 3. × 16

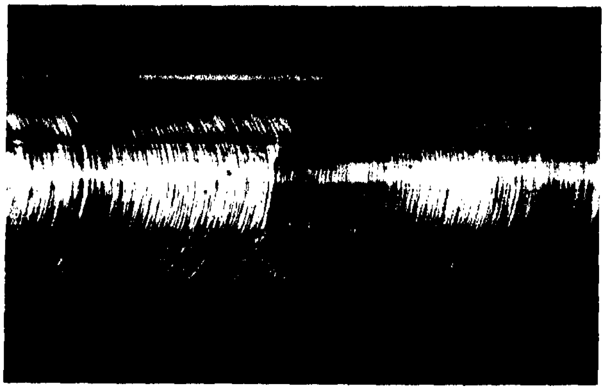

Fig. 4. × 16

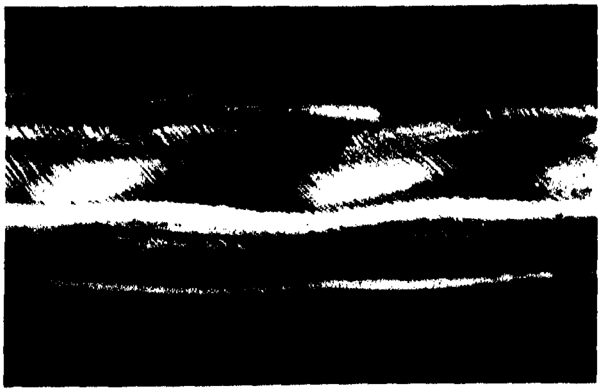

Fig. 5. × 16

(*Facing p.* 32)

solid material is high enough to round off their sharp edges. The edges of the band might be rounded in this way, but it hardly accounts for their initial breadth. Alternatively each slip band may represent a group of very close parallel glide planes. The general appearance of the slip band does not accord with the view that glide starts at cracks in the surface. If surface tension can round off the edges of crystallites or of glide surfaces, it could prevent the formation of surface cracks.

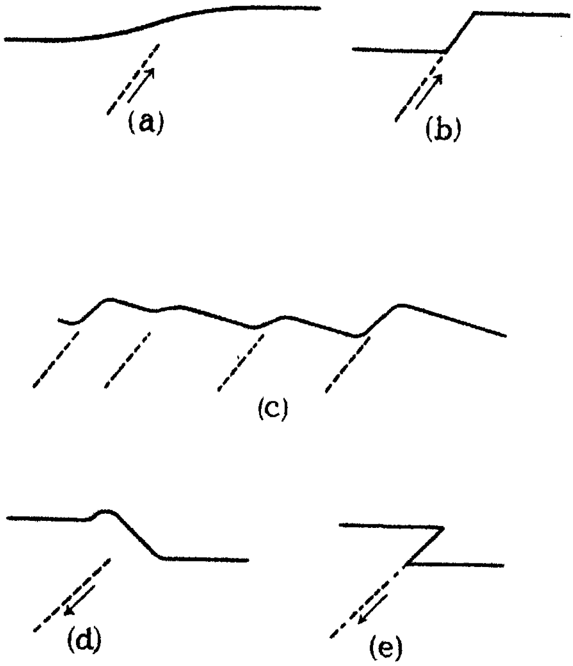

Fig. 8

The writer desires to acknowledge the very helpful interest shown throughout the course of this work by Professor E. N. da C. Andrade, F.R.S., at whose suggestion it was undertaken.

4—Summary

Whether the slip bands formed on single crystal wires of mercury at − 60° C. are plane or irregular depends upon the nature of the stress to which the wires are subjected. Stretching a wire which has not previously been strained produces slip bands which are approximately elliptical, but very wavy and branched near the ends of the major axes.

If the wire is slightly bent subsequent extension leads to perfectly plane bands, which multiply in number when the wire is stretched.

Torsional strain results in very close elliptical bands, but a new set of imperfectly elliptical bands sometimes appears on stretching the wire.

The bands formed by pure tension indicate gliding on surfaces which are not planes but are made up of glide elements having a common glide direction.

The surface of the crystal behaves as an elastic skin in that it shows no break at the slip bands.

REFERENCES

Andrade E. N. da C. and Hutchings, P. J. 1935 *Proc. Roy. Soc.* A, **148**, 120.
Elam, C. F. 1936 *Proc. Roy. Soc.* A, **153**, 273.
Greenland, K. M. 1937 *Proc. Roy. Soc.* A, **163**, 34.
Osmond and Cartaud 1906 *J. Iron Steel Inst.* No. **111**.
Tammann, G. 1926 "The States of Aggregation." London: Constable and Co.
Taylor, G. I. and Elam, C. F. 1926 *Proc. Roy. Soc.* A, **112**, 337.

The Critical Shear Stress of Mercury Single Crystals

BY K. M. GREENLAND, PH.D.

(Communicated by E. N. da C. Andrade, F.R.S.—
Received 22 *June* 1937)

[Plate 8]

1—INTRODUCTION

The influence of very small quantities of impurity on the critical shear stress of metal single crystals has an important bearing on the mechanism of their plastic deformation. For investigations in this field, mercury is a very suitable metal: its impurity content can easily be reduced to an extremely low level (Hulett 1911) and it contains no dissolved gases (Hulett 1911). Also, as first pointed out by Andrade (1914), single crystal wires of this metal can be prepared without difficulty.

The low melting point of mercury (−38·8° C.) is far from being a disadvantage. The crystals can be maintained at −60° C., and at a temperature so near the melting point the thermal agitation may be expected to accentuate phenomena not observable at lower temperatures, if such agitation plays the important part in the mechanism of glide ascribed to it (Taylor 1934; Polanyi 1934; Orowan 1934). As a possible instance of this, the experiments to be described have revealed the existence of a preliminary "set" preceding the true plastic yield. Widely differing forms of slip band have also been observed, and are described elsewhere (Greenland 1937). It is hoped that these results will throw further light on the mechanism of glide.

The main object of this study of mercury single crystals has been to measure the critical shear stress of crystals of the purest mercury obtainable and of mercury containing small measured quantities of another metal (silver). The general form of the stress-strain curves has also been examined in its bearing on the critical shear stress.

2—PURIFICATION OF THE MERCURY

The commercial mercury is shaken first with strong caustic soda solution, then with 1 : 6 nitric acid, to remove grease. It is then thoroughly washed with water and distilled in a quartz vacuum still at a rate of about 800 g./hr. After this treatment, the mercury is clean in the ordinary laboratory sense, but still contains traces of any metals of low boiling point which were originally present. To remove these traces, the method of distillation described by Hulett (1911) is used, in which the unwanted metals are oxidized in the vapour state by a stream of air. The pressure is maintained at about 25 mm. of mercury. At this pressure mercuric oxide dissociates while the oxides of the other metals remain in solid form and are deposited as scum. The deposition takes place mainly in the bulb containing the boiling mercury, but it is found that a little oxide is carried over with the mercury vapour into the distillate. The necessity of filtering the distillate, together with the desirability of keeping it free from atmospheric contamination has led to an elaboration of the design of the still described by Hulett.

In place of the collecting bottle, which in the original design was connected to the condenser tube by a ground-glass joint, the condenser tube discharges into a vertical conical bulb (*A*, fig. 1) containing a Jena glass filter disk. This bulb acts as a reservoir for the distillate, since the filter disk is too fine to allow the mercury to run through under its own weight. By means of a side tube and taps, the pressure in the space below the filter disk may be reduced, and the rest of the apparatus brought to atmospheric pressure, whereupon the mercury is forced through the disk and collects in a detachable bulb, *B*. With a little practice the exact quantity for one crystal can be drawn off by suitable manipulation of the taps. Not only is waste of the mercury thus avoided, but also it is kept in clean, dry air up to the moment of use.

A sample of mercury distilled in this way was examined for impurities by Messrs. Adam Hilger, using a method in which 1 part in 10^6 of added silver was certainly detectable. No trace of impurity was detected. Andrade and Hutchings (1935), who used the same method of distillation, estimate the impurity content as being not greater than 1 part in 10^8 and the measurements to be described later on the variation of critical shear stress with impurity content support this conclusion. When placed in a bottle cleaned with special thoroughness, this pure mercury was found to wet the glass, producing a concave meniscus.

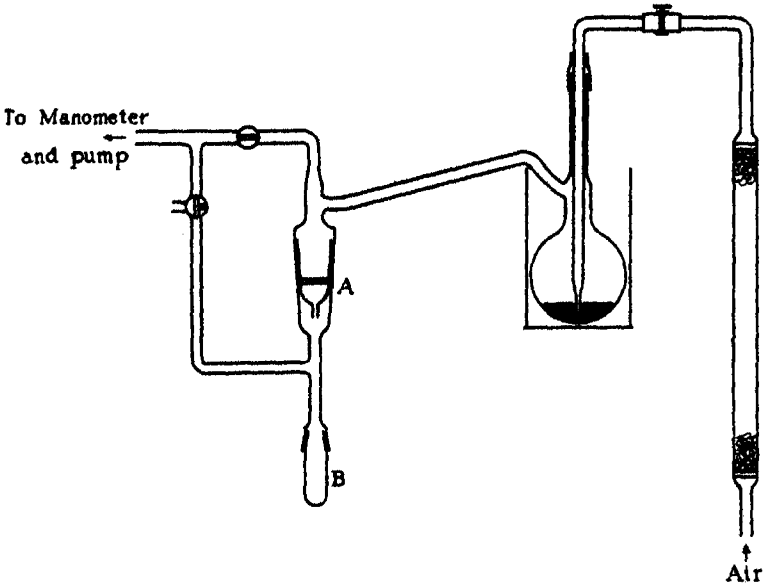

Fig. 1

3—Preparation of the Crystals

The crystals are in the form of wires 1 to 5 cm. in length and between 1 and 2 mm. diameter. They are grown by freezing a thread of the liquid metal in a thick-walled capillary tube, the tube being slowly lowered into the freezing mixture so that the solidification begins at one end of the thread and extends along its length. The method is described in detail by Andrade and Hutchings (1935).

4—APPARATUS

The design of the apparatus in which the crystals are examined is based on that originally used by Andrade and Hutchings (1935).

The crystal is gripped in two pin chucks, C_1 and C_2, fig. 2, immersed in ethyl alcohol contained in a copper bath B. The bath is V-shaped in section, and is itself immersed in a freezing mixture of solid carbon dioxide and methylated spirits. The alcohol is thus maintained at about −60° C. The Dewar flask D containing the freezing mixture is contained in a box, packed with cork dust, from the ebonite lid of which the copper bath is suspended, the lid being cut away above the bath. The box is placed beneath a brass platform (HH), which carries a travelling microscope and also the ebonite support for the chuck C_1.

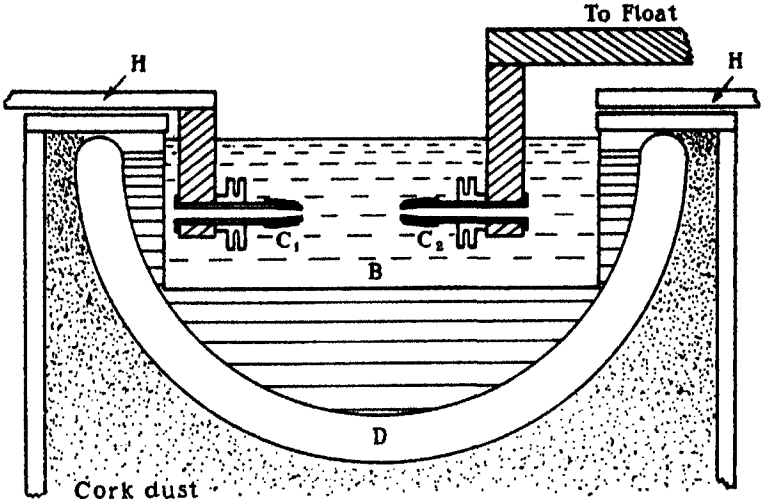

FIG. 2

The other chuck C_2 has two alternative mountings. In one the chuck support is screwed to a sliding plate, whose motion is constrained so that the chuck moves only along the line of its axis. The motion is controlled by a screw rotated by hand. This mounting is used when it is desired to examine the appearance of the crystal while it is being stretched.

The second mounting is used when a measured tension is to be applied to the crystal. The chuck bearing is screwed to one end of a wooden batten carried on an iron block. This floats in a mercury bath placed close to one side of the platform H. The float is guided by a steel rod mounted on the bath which passes between two pairs of pegs sheathed with glass and screwed into the batten. The gap between the two pegs of each pair is just large enough to permit frictionless motion along the rod without allowing any appreciable side-play. The batten can be clamped by a device so designed that no displacement of the chuck occurs at the moment of clamping.

If both ends of the crystal are gripped in the chucks, there is a danger of the crystal being bent or twisted when the second chuck is tightened. To avoid this, one end is secured in the fixed chuck and the other end "welded" to a polycrystalline (strong) mercury wire held in the moving chuck. The joint is made by bringing the ends of the wires into contact and touching with a hot steel wire. The ends melt and run together to make a strong joint. A picture of such a weld is shown in fig. 3, Plate 8.

In order that the crystal may be rotated about its axis without twisting, the chucks each carry a disk in which six radial holes are drilled (see fig. 2). The uppermost hole in each disk may then be engaged by the prongs of a double tommy-bar, and the two chucks rotated together.

The necessity of applying to the crystal a uniformly increasing tension and of allowing the crystal to extend freely made it desirable to eliminate such sources of friction as, for instance, pulleys. In the system finally adopted a soft iron plunger hangs inside a large solenoid carrying a variable current. The plunger (17·5 cm. long, 870 g. in weight) is suspended horizontally by four steel wires so that one end is at the centre of the solenoid, leaving about 9 cm. projecting. The length of the suspension is 70 cm., and the gravitational restoring force on the plunger when the crystal extends is negligible within the range of extensions dealt with. The plunger is coupled to the floating batten which carries the moving chuck by a nut, running on a threaded rod projecting from the plunger, which engages the forked end of a vertical rod carried by the batten. The threaded rod is long enough to allow the fork to be engaged by the nut without bringing the plunger out of its equilibrium position, whatever the length of the crystal in the chucks.

The solenoid current is taken from the 220 V. D.C. supply mains, and is controlled by a potentiometer. It is measured with an instrument shunted so that a full-scale deflexion corresponds to a tension on the crystal of 150 g. wt. When the crystal is being extended the actual readings giving the applied tension are taken on this instrument. It has been calibrated by applying known forces to the plunger and adjusting the solenoid current to bring the plunger into its equilibrium position.

5—METHOD OF MEASURING CRITICAL SHEAR STRESS

The critical shear stress S of a monocrystalline wire which glides under a critical tensional force W is given by

$$S = \frac{W}{A} \sin \chi_0 \cos \lambda_0, \qquad (1)$$

where A is the area of cross-section of the wire, χ_0 the inclination of the glide planes to the wire axis, and λ_0 the angle between the glide direction and the wire axis.

The angle χ_0 is easily measured by turning the wire until the slip bands are seen as straight lines and measuring their inclination to the wire with a rotating eyepiece fitted with a circular scale. There is, however, no direct indication of the glide direction.

The unit cell of the mercury lattice is a face-centred rhombohedron. Andrade and Hutchings (1935) found that glide normally takes place on the rhombohedral faces and twinning on a particular diagonal plane. If glide always occurred on the specified planes, the lattice orientation could be deduced from the orientation of two sets of glide planes, or from one set of glide planes and a twinning boundary. True double glide is, however, rare and did not occur in any of the particular crystals used for strength measurements. A second, and sometimes a third, set of slip bands can be artificially induced by bending or twisting the crystal slightly, but it appears that under these stresses glide does not take place on the rhombohedral faces. For instance, measurements of the angles between the sets of glide planes thus induced were made on seventeen crystals and, of the twenty-six angles obtained, only five were within 2° of the theoretical angle between the rhombohedral faces. Moreover, the other twenty-one did not correspond to any other fundamental angles in the mercury lattice. The slip bands induced by bending or twisting are therefore of no value for determining the lattice orientation, because they are not, apparently, related to any simple lattice planes. On the rare occasions when true double glide did occur, Andrade and Hutchings's conclusions as to the glide planes were confirmed.

It is not surprising that glide under bending or torsional stresses does not occur on the rhombohedral faces as in the normal case of pure tension. For instance, there is no reason why a "closest line of packing" in the lattice, which is a controlling factor in glide under pure tension, should have an influence on the selection of glide planes when the stress is applied by a couple.

Twinning nearly always occurs, but here again measurements are of little value, since a considerable extension is necessary before the boundaries become sufficiently well developed. Figs. 4 and 5, Plate 8, show the appearance, from different points of view, of a twinned crystal after an extension of 8 %. At such extensions the lattice orientation is quite different from its original position before glide began, since not only does the inclination of the glide planes to the wire axis decrease but also the sections of crystal between the glide planes rotate so as to bring the glide direction nearer to that of maximum shear on the glide planes. When, however, these two directions already coincide before strain, so that $\lambda_0 = \chi_0$, no rotation occurs and with the lattice in such a position the heads of twinning and glide ellipses lie on the same generator of the wire surface (Andrade and Hutchings 1935, p. 132). The glide direction cannot therefore be found by geometrical considerations unless twin boundaries appear in this particular position. X-ray photographs would, of course, settle the point, but taking such photographs of wires of solid mercury offers certain difficulties.

If it is assumed that $\lambda_0 = \chi_0$, the expression for the critical shear stress becomes

$$S' = \frac{W}{A} \sin \chi_0 \cos \chi_0 .$$

We shall call S' the "apparent" critical shear stress and S, as given by (1), the "true" shear stress. By measuring the apparent shear stress of a number of crystals we should obtain a series of results varying, not about a mean, but above a minimum which is the true shear stress. This is the method for finding the true shear stress which has been adopted in this work. As will be shown later, the variation in apparent critical shear stress is not nearly as great as would be expected if, in a series of experiments on different wires, the lattice wire were orientated at random with respect to the wire axis, and the glide took place in a particular crystallographic direction.

A graphical method is used to determine the tension which is just sufficient to cause gliding. The usual stress-strain, or hardening, curve cannot conveniently be obtained with mercury at $-60°$ C. on account of the very small hardening, which results in considerable flow with time under low stresses.

The extent of this flow is illustrated in fig. 6, showing the percentage extension of two monocrystalline wires plotted against time, the applied force being constant. The curves are obtained by increasing the force until the critical force is exceeded by a small amount and then keeping it steady while the shift of the moving end of the wire is measured with the travelling microscope at half-minute intervals. The following data are relevant:

Curve	Temperature of wire ° C.	Diameter of wire mm.	χ_0	Critical shear stress (apparent) g./mm.^{2}	Shear stress at zero of curve (apparent) g./mm.^{2}
I	$-65°$	2	41°	17·0	23·6
II	$-65°$	2	60°	18·1	19·4

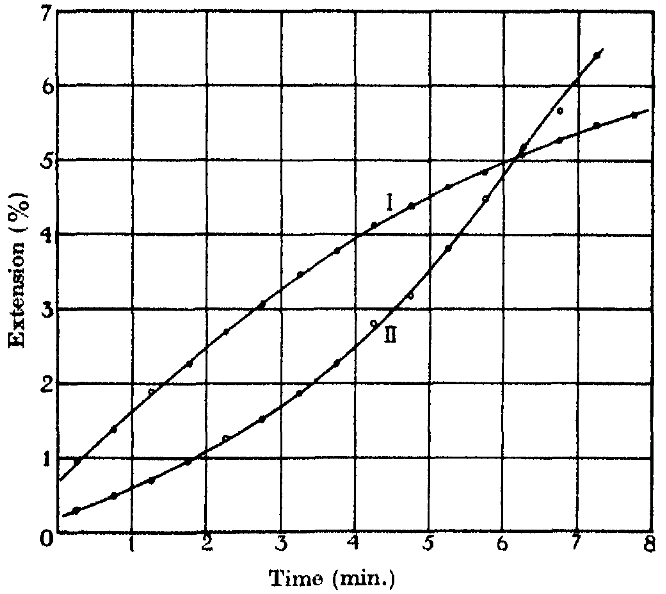

FIG. 6

In curve II the rate of extension shows a considerable *increase* as elongation continues. Here the geometrical softening effect is large on account of the high value of χ_0 (and consequently of λ_0), for not only does the value of $\sin \chi_0 \cos \lambda$ increase more rapidly for a given decrease in λ when λ is large but also the rate of decrease of λ during extension is greater. This geometrical softening, then, is apparently sufficient to outweigh the lattice hardening.

It will be seen from these curves that after 8 min. the rate of flow is still considerable. The flow of a number of crystals has been measured for greater lengths of time and it is found that under stresses slightly exceeding the critical shear stress the rate of extension per cm. settles down to about

20μ per min. and continues at that rate with very little diminution for at least 1 hr. It is therefore quite impossible to obtain true hardening curves for mercury at temperatures 20–30° below its melting point, and it is consequently necessary to include the time element in the measurements in order to obtain a smooth curve for the determination of the critical force.

This has been done by controlling the solenoid current with a potentiometer of which the slider is advanced by a screw mechanism, rotated by a slow-motion electric motor. The current is thus increased at a uniform slow rate such that the rate of increase of applied tension is about 7 g. wt. per min. Although the time element is introduced arbitrarily, its relation to the applied stress is always the same and the curves obtained are strictly comparable.

As the solenoid current increases, the displacement of a point at the "free" end of the crystal wire is measured at intervals of 30 sec. with a travelling microscope. The screw head is divided in $\frac{1}{100}$ths of a millimetre, and estimations of $\frac{1}{10}$th of a division are made. The readings of solenoid current are taken 15 sec. after each microscope reading. The two sets of readings are plotted against time on the same graph, so that with the aid of the calibration curve, the force at any extension may be read off. This is not, as explained above, the force necessarily required to produce that extension, because above a certain stress flow is taking place all the time.

The general form of the composite graph obtained in this way is shown in fig. 7, in which the full curve *OABC* is the percentage extension of the crystal and the broken line represents the solenoid current. The *O–A* extension is shown as a straight line but actually the method of measuring this extension is not sufficiently delicate to reveal its true form. The order of the magnitude of the extensions at *A* and *B* may be seen in fig. 8.

Seven crystals were examined, mainly to test the feasibility of the method, and the results are summarized in Table I.

The terms "regular" and "irregular" in column III refer to the shape of the slip bands. In another paper by the present writer (Greenland 1937), the dependence of the shape of the slip bands upon the type of applied stress is described, and it is there shown that stretched crystals exhibit perfectly elliptical slip bands only if they have been slightly bent or twisted before stretching. These bands are called "regular" bands. The "irregular" bands are formed when pure tension is applied to a previously unstrained crystal; although approximately elliptical they are wavy and branched.

The glide directions are unknown, except for No. 3, where the position of the twinning bands showed that the glide direction coincided with the projection of the axis of the wire in the glide plane. The shear stresses calculated for No. 3 are therefore "true" shear stresses.

TABLE I

I	II	III	IV	V	VI
				Apparent shear stress at	
Crystal No.	χ_0	Type of slip band	Temp. ° C.	*A* g./mm.^{2}	*B* g./mm.^{2}
1	35°	Irregular	− 65°	11·6	17·0
2	38°	Regular	− 52°	6·6	16·3
3	40°	Regular	− 65°	6·7	15·2
4	40°	Irregular	− 70°	6·6	18·0
5	49°	Regular	− 65°	4·2	18·0
6	52°	Irregular	− 70°	11·3	16·4
7	53°	Regular	− 70°	13·2	17·0

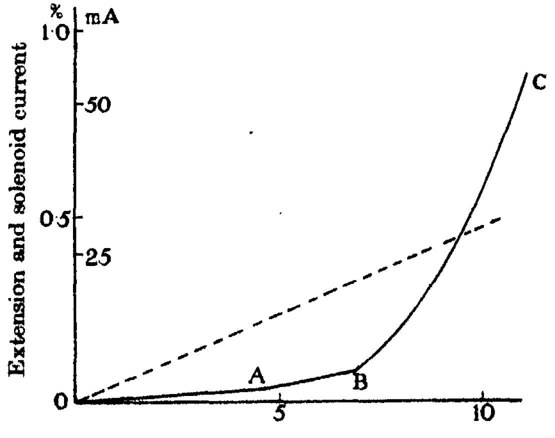

FIG. 7

6—INTERPRETATION OF THE STRESS-STRAIN CURVES

The extension as far as the point *A* is entirely elastic, since it all disappears if the tension is removed. Between *A* and *B* the increase of extension for a given increase of tension is greater than it is below *A*, and the wire takes on a permanent set. This is not, however, due to slip on macroscopic glide planes because no slip bands appear during this extension and there is no creep. After a sudden increase in the rate of extension at *B*, slip bands begin to appear and the extension becomes a function of time as well as of applied tension. Flow curves similar to those in fig. 6 can be obtained by holding the stretching force constant at any value above that at *B*. It is evident, then, that the point *B* represents commencement of the shearing of the crystal by glide. The true critical shear stress is therefore defined as the component of stress in the glide direction due to the tension corresponding to the point *B*. As predicted, the one "true" critical shear stress (crystal No. 3, Table I) is slightly lower than the other values in the column. The physical process represented by the region *A*–*B* will be discussed later.

The variation in the measured values of apparent critical shear stress above the true critical shear stress is much less than would be expected with a random orientation of crystal axis with respect to the wire axis in different specimens, so that it appears that, with the method adopted for preparing the crystals, the glide direction is always within a few degrees of the direction of maximum shear on the glide plane. For a set of glide planes inclined at an angle χ_1 to the wire axis, the angle λ_1 between the glide direction and the wire axis may have any value between χ_1 and an upper limit given by the condition (see p. 39)

$$\sin\chi_1\cos\lambda_1 = \sin\chi_2\cos\lambda_2, \tag{2}$$

where χ_2 and λ_2 refer to a second set of crystallographically equivalent glide planes. For orientations such that λ_1 is greater than this upper limit, the set distinguished by the suffix 2 would become the actual glide planes. Equation (2) can be solved algebraically by substituting the appropriate direction cosines, and it is found that when, for instance $\chi_1 = 45°$, the difference between the true and apparent critical shear stresses may be as much as 270 %, assuming that glide takes place on the rhombohedral faces. If this assumption is correct, we must conclude that the conditions of growth result in a limitation of the lattice orientation to within a few degrees of some preferential orientation. Andrade and Tsien (1937) have found that a preferential orientation does occur in the case of sodium. On the other hand, the greater tension required to reach the critical shear stress when all the rhombohedral faces are unfavourably orientated may be more than sufficient to induce glide in a less closely packed, but more favourably orientated, direction.

7—CRITICAL SHEAR STRESS OF PURE MERCURY

The preliminary measurements have shown that the method adopted is a practicable one. Further, comparison of the data in columns III and IV, Table I, with the results in column VI shows that the type of slip band and the permitted variation of temperature have no marked effect on the critical shear stress. Closer control of the type of slip band and of temperature is, therefore, unnecessary.

The rate of growth of the crystals for the trial measurements was generally 3 mm./min., but, to test whether small accidental variations in the rate would affect the critical shear stress, crystals 1, 2 and 3 were grown at 10 mm./min. The measured critical shear stresses of these three include the greatest and least values in the whole series, so it is safe to conclude that variations in the rate of growth have no effect.

The possible effect of a variation in the time between growing and stretching a crystal must not be overlooked. It is well known that the strength of a newly drawn quartz fibre decreases with time, and that this is attributed to the slow formation of sub-microscopic cracks in the surface. If, then, the abnormally low critical shear stress of single crystals is in any way due to the presence of cracks, internal or superficial, and if the cracks form slowly, the strength will decrease with the age of the crystal. Crystal No. 2 was extended a few minutes after growing, Nos. 3, 4 and 5 were kept at $-80°$ C. for 24 hr., and Nos. 1, 6 and 7 for 48 hr., before stretching, but column VI shows no evidence of any relation between the age and the strength of the crystal.

The crystals in the preliminary experiments were all made from the same sample of distilled mercury, but there was reason to believe that the stock from which the distillation was made had been contaminated with chromium which had been used in other experiments by a worker using the same still. A fresh supply of commercial mercury was therefore obtained and distilled several times in a new vacuum still. The special "bubbling" still was thoroughly cleaned by the method previously described, and the mercury from the vacuum still distilled in it twice. The quantity of mercury in the reservoir after the second distillation was sufficient for all the experiments, including those on silver amalgams, now to be described. It is, therefore, certain that, whatever the degree of purity of the distillate, it remained the same throughout the series.

Six crystals were made with the pure mercury, and curves of their extension plotted by the method developed in the preliminary experiments. Table II gives the principle data and the critical shear stresses.

For the first two crystals examined (Nos. 8 and 11) the solenoid current was increased at a rate higher than the standard rate. These were trial crystals used to determine the approximate critical tension, and the results for them cannot be given so much weight, since their curves are less precise. Moreover it is known that the critical shear stress of single crystals depends to some extent on the rate of loading.

TABLE II

Crystal No.	χ_0	Type of band	Critical shear stress (apparent) g./mm.^{2}
8	32°	Regular	(7·8)
9	36°	Regular	7·0
10	37°	Regular	7·4
11	42°	Irregular	(8·2)
12	48°	Regular	5·6
13	61°	Regular	7·1

Temperature: −55° C. to −65° C.

Crystal No. 12 was evidently an abnormal crystal. Several instances of these particularly weak crystals will be noticed in dealing with the results for contaminated mercury and in view of the closeness of the other results we have rejected No. 12. That the rejection is justified is well supported by the fact that of the remaining five, that having the lowest apparent critical shear stress (No. 9) showed twinning bands of which the heads were very nearly in line with the heads of the slip bands. As explained, a crystal with twin boundaries so placed should have the minimum apparent critical shear stress.

It is therefore concluded that the critical shear stress of the purest mercury obtainable is 7·0 g./mm.^{2} This is the lowest value recorded for any metal single crystal.

8—CRITICAL SHEAR STRESS OF MERCURY CONTAINING IMPURITY

Silver was chosen as the metal with which to contaminate the mercury. It can be obtained as very fine wire, in which form very small quantities can easily be measured off. It was first added in the proportion 1 : 10^4, about 6 cm. of wire being required for 0·6 c.c. of mercury. The wire appeared to dissolve immediately, but the solution was allowed to stand for 24 hr. and was thoroughly shaken before use.

Four crystals were made from this amalgam and were examined in exactly the same way as were those of pure mercury. Table III contains the relevant data and the results.

The amount of impurity in the purest mercury obtainable for these experiments was estimated at 1 part in 10^8. In view of the considerable

TABLE III

Crystal No.	χ_0	Type of band	Critical shear stress (apparent) g./mm.^{2}
14	35°	Irregular	22·9
15	42°	Regular	22·8
16	47°	Irregular	23·6
17	52°	Regular	18·3

Temperature: $-55°$ C. to $-62°$ C.

increase in strength with an additional impurity of 1 in 10^4 it seemed probable that an addition of 1 part of silver in 10^6 would give a measurable increase in strength. Accordingly 3·4 mm. of silver wire were dissolved in 3·4 c.c. of the pure mercury, and the critical shear stress of the crystals measured as before.

The data and results are shown in Table IV.

TABLE IV

Crystal No.	χ_0	Type of band	Critical shear stress (apparent) g./mm.^{2}
18	26°	Regular	3·3
19	39½°	Regular	10·6
20	42½°	Regular	8·2
21	46½°	Irregular	14·0
22	50°	Regular	14·0
23	53°	Regular	14·8
24	60°	Regular	8·0

Temperature: $-58°$ C. to $-62°$ C.

In crystal No. 21 the position of the twinning bands indicated that $\lambda_0 = \chi_0$, so that the result is a true critical shear stress.

A final set of measurements was taken at a silver concentration of 1 : 10^3 (160 cm. of wire in 1·6 c.c. of mercury). At this concentration the silver dissolved with difficulty and the solution must have been nearly saturated (Hulett (1911) suggests that 1 part of silver in 200 of mercury forms a saturated solution at 200°). As a consequence of the greater strength of the crystal wires, it was necessary to abandon the "welding" method for mounting them, and to secure both ends in the chucks.

Seven crystal wires were grown and examined in the usual way. The results are given in Table V and the curves reproduced in figs. 8 and 9.

The glide direction in crystal No. 27 is known to have been such that $\lambda_0 = \chi_0$.

TABLE V

Crystal No.	χ_0	Type of band	Critical shear stress (apparent) g./mm.^{2}
25	27°	Irregular	30·7
26	31°	Irregular	30·5
27	47°	Regular	28·0
28	48°	Irregular	24·7
29	49°	Irregular	18·5
30	53°	Regular	22·7
31	65°	Regular	31·2

Temperature: − 55° C. to − 62° C.

9—DISCUSSION OF RESULTS

At each silver concentration there is a group of crystals (three for purest mercury; three at $1:10^6$ of silver; three at $1:10^4$; four at $1:10^3$) for which the total variation in critical shear stress is about 10 %. The other results are in every case much lower than these consistent values and exhibit no regularity. Moreover, in the cases where the glide direction λ_0 was known to have had the minimum value $\lambda_0 = \chi_0$, the critical shear stress was the lowest result in the consistent group. It therefore seems certain that the lower irregular results are due to some extraneous effect.

To meet the objection that the method of preparing the silver amalgams might result in an inhomogeneous solution and so cause variations in the strength of the crystals, crystal No. 27 was allowed to melt after examination and the identical specimen of mercury used for Nos. 28 and 31. As these crystals embrace both high and low values in the $1:10^3$ group the variation in strength cannot be due to a badly mixed solution. Furthermore, the lowest value in the $1:10^6$ group is considerably lower than the lowest value for the purest mercury.

On examining the records of the crystals for an explanation of these lower random results, it was found that the very weak crystal No. 18 (Table IV) had been accidentally bent some 2° in ejecting it from the growing tube, and had to be straightened before being secured in the stretching apparatus. This produced several slip bands ("regular", as expected). Another crystal, also made of the $1:10^6$ amalgam, which had been bent 5–10°, flowed for 10 min. under a constant stress of 5·5 g./mm.^{2}, reaching an extension of 1 %.* The one extra-weak crystal of the purest mercury (No. 12, Table II), showed very regular slip bands close to the fixed chuck, an indication that bending had taken place there, probably

---

* Not included in the tabulated results, as no curve was obtained.

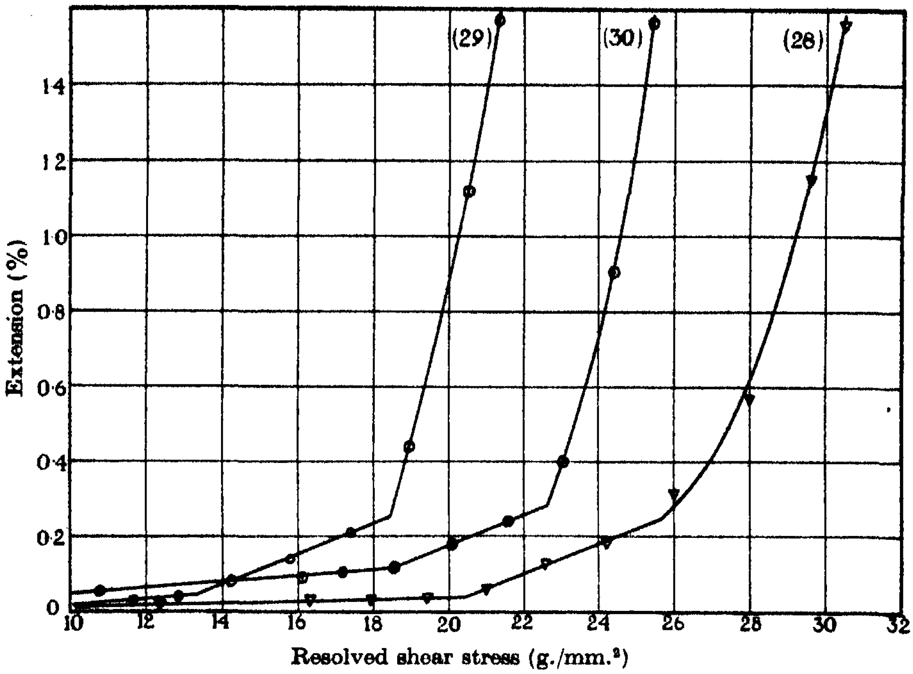
Extension (%)
0
0·2
0·4
0·6
0·8
1·0
1·2
1·4
(29)
(30)
(28)
10
12
14
16
18
20
22
24
26
28
30
32
Resolved shear stress (g./mm.²)

FIG. 8

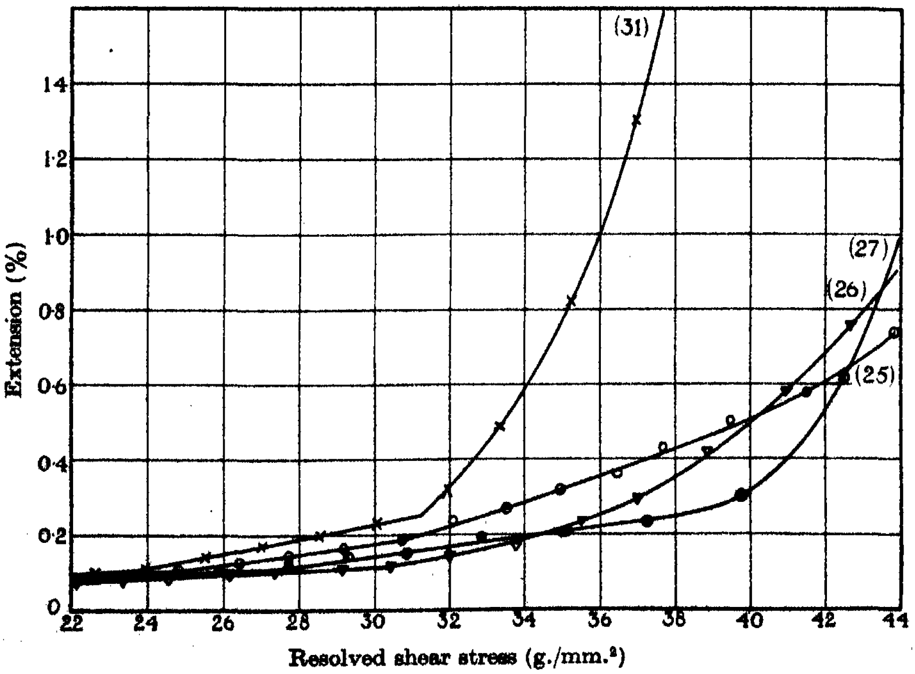
Extension (%)
0
0·2
0·4
0·6
0·8
1·0
1·2
1·4
(31)
(27)
(26)
(25)
22
24
26
28
30
32
34
36
38
40
42
44
Resolved shear stress (g./mm.²)

FIG. 9

in tightening the chuck. In the 1 : 10^4 group (Table III), the weak No. 17 had been bent 5° to ensure "regular" slip bands. The weak crystals 28 and 30 (Table V) showed faint slip bands before being stretched, caused by the securing of both ends in the chucks.

The fact that these anomalous results were given by crystals on which slip bands had already been formed by preliminary bending suggests that some preliminary process normally occurring in the lattice to form the complete glide planes has been hastened by the bending and that once the glide planes have been formed the resistance to shear is lessened. Some results on the formation of the slip bands (Greenland 1937) agree well with this hypothesis, for they show that, when a bent crystal is stretched, glide takes place by preference on the planes already sheared by bending. It appears, then, that isolated low values of critical shear stress are due to an artificial lowering of the actual shear stress. Its value at each silver concentration will therefore be taken as the lowest of the group of consistent values of apparent critical shear stress. The values to which extra weight may be given on account of a knowledge of the glide direction confirm the correctness of this method of selection.

The "preparation" of the glide planes may take the form of a setting up and growth of faults or "dislocations" which, when the critical shear stress is reached, run together to form complete glide planes. The permanent set which precedes plastic flow in these crystals (section *A–B*, fig. 7) may be connected with this preliminary activity on the glide planes. The observed absence of any preliminary permanent set in the curves of the badly bent crystals No. 17 (Table III) and 18 (Table IV) accords with this view. The behaviour of the crystals of the 1 : 10^3 amalgam is also interesting, for this solution must be saturated, or nearly so, and it is thought that the effect of the presence of so great a number of foreign atoms has been either partly to "seal" the faults in the lattice or to prevent their formation, and thereby to impede the motion at each glide plane (cf. Chalmers 1936, p. 442). The ground for this suggestion is that in the case of the four crystals (Nos. 25, 26, 27, 31, Table V) which show a consistently high strength, not only was the rate at which glide proceeded less than it was for purer mercury, but the preliminary set representing the development of the faults is in two cases indistinguishable, in the curves, from the normal elastic strain. On the other hand, the three weaker crystals, Nos. 28, 29, 30, all have a marked microscopic yield and the extension is much more rapid, as though the glide planes had succeeded in breaking away through the spreading of the dislocations, as in the more dilute amalgams.

Chalmers (1936) has detected a preliminary set preceding the normal gliding of tin single crystals. The order of this "micro-creep" in tin is 10^{-5} cm./cm., compared with 10^{-3} cm./cm. for mercury. This disparity is not of great consequence and is probably accounted for by the great difference in the relation of working temperature to melting point.

The micro-creep of tin continues at an appreciable rate for some minutes but approaches a final value which is independent of the stress, provided that the latter is less than the critical shear stress. In this property, mercury differs from tin, for with mercury the extension in the micro-yield region becomes sensibly constant after a few seconds if the tension is applied suddenly, but increases in proportion to the stress up to the macro-yield point. Chalmers explains, however, that tin recovers its micro-plasticity after resting for several hours. In mercury at a relatively higher temperature the recovery may take place so rapidly that the strain does not lag appreciably behind the stress. The flow properties of mercury at −60° C. have already shown that it either escapes the usual hardening effect of macroscopic gliding or recovers quickly from it.

The final results of critical shear stress are given in Table VI.

TABLE VI

Silver content	Critical shear stress g./mm.^{2}
Minimum ($1 : 10^8$?)	7·0
$1 : 10^6$	14·0
$1 : 10^4$	22·8
$1 : 10^3$	28·0

The selected results do not indicate any marked difference in strength between the regular and irregular types of glide.

In fig. 10 the critical shear stress has been plotted as a function of amount of impurity. The impurity content of the purest mercury appears by extrapolation (shown by the full line) to be not greater than the equivalent of $1 : 10^8$ of silver which agrees with the estimation quoted in § 2.

If the residual impurity in the purest mercury is equivalent to a silver content of $1 : 10^8$, the critical shear stress would appear, from the direction of the full curve, to fall to zero at some finite degree of purity. A more reasonable forecast is suggested by the broken curve, which is drawn for a residual impurity content equivalent to a $1 : 10^9$ silver concentration, which does not appreciably affect the curve for concentrations above 10^{-6} impurity. In this case, the critical shear stress approaches a limiting value of about 5 g./mm.^{2} for absolute purity.

The author wishes to express his sincere thanks to Professor E. N. da C. Andrade, F.R.S., for having initiated and provided every facility for the carrying out of this work, and for the valuable advice and encouragement which he has extended throughout its course.

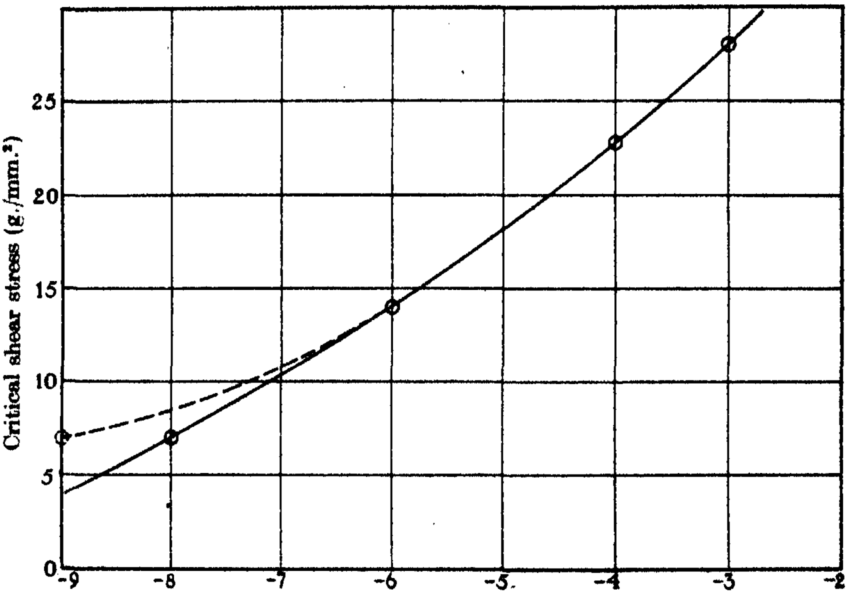

Impurity content (log ratio Ag:Hg)

FIG. 10

10—SUMMARY OF RESULTS

The critical shear stress of single crystal wires of very pure mercury and of mercury containing small quantities of silver has been measured at a temperature of − 60° C. The value for the purest mercury is 7·0 g./mm.² and the strength is progressively increased by addition of small quantities of silver up to 28·0 g./mm.² at a silver concentration of 1 : 10³. The critical shear stress at absolute purity appears by extrapolation to be not greater than 5 g./mm.².

There is no evidence of a difference in critical shear stress for the regular and irregular types of glide.

The crystallographic hardening at temperatures near the melting point is very small.

A permanent set immediately preceding the true plastic yield has been observed in the majority of extended crystals. It appears to represent the generation of glide planes from minute faults within the crystal.

REFERENCES

Andrade, E. N. da C. 1914 *Phil. Mag.* **27**, 869.
Andrade, E. N. da C. and Hutchings, P. J. 1935 *Proc. Roy. Soc.* A, **148**, 120.
Andrade, E. N. da C. and Tsien, L. C. 1937 *Proc. Roy. Soc.* A, **163**, 1.
Chalmers, B. 1936 *Proc. Roy. Soc.* A, **156**, 427.
Greenland, K. M. 1937 *Proc. Roy. Soc.* A, **163**, 28.
Hulett, G. A. 1911 *Phys. Rev.* **33**, 307.
Orowan, E. 1934 *Z. Phys.* **89**, 614.
Polanyi, M. 1934 *Z. Phys.* **89**, 660.
Taylor, G. I. 1934 *Proc. Roy. Soc.* A, **145**, 362.

Critical Phenomena in Gases—I

BY J. E. LENNARD-JONES, F.R.S. AND A. F. DEVONSHIRE
The University Chemical Laboratory, Cambridge

(*Received* 27 *July* 1937)

1—INTRODUCTION

The exact measurements of the isotherms of gases have proved extremely valuable in the determination of interatomic forces. For this purpose it has been found necessary to express the *pv* values of a gas as a finite power series in the density or in the pressure, and the coefficients so obtained have been compared with theoretical expressions in terms of interatomic fields. Many accounts of the method have been given and it is not necessary to give further details here (cf. Lennard-Jones 1931).

While these methods are valid for gases at low densities where binary encounters are predominant, they fail for gases at high densities such as obtain in the neighbourhood of the critical point. Michels and his collaborators (Michels and others 1937) have recently studied the isotherms of gases at pressures as high as 3000 atm., and they find that the usual method of representing isotherms as simple functions of density or pressure ceases to be useful. The equation of state of van der Waals was astonishingly successful in accounting for the critical phenomena of gases and the form of the isotherms for temperatures below the critical temperature. Other empirical equations of state, for example that of Dieterici, were even more successful in reproducing the observed relations between the critical pressure, volume and temperature, and their very success has often obscured the fact that they were not logical theories of critical phenomena in gases, based as they were on arguments which were valid only for gases of low concentration. Thus the van der Waals equation, valuable as it has been and useful as it still is, implies that the internal energy of a vapour and its liquid phase is proportional only to the first power of the density, and this cannot be true for gases or vapours at densities comparable with those of liquids. The problem still remains of explaining why gases exhibit critical properties and of correlating the observed values of the critical temperature with the forces which atoms or molecules exert on each other.

Fowler, following the work of Bragg and Williams on order and disorder in alloys (Bragg and Williams 1935), has recently made a definite advance in the theory of the critical adsorption of atoms on surfaces. The essential step in his treatment is that he takes the heat of adsorption to be a linear function of the concentration of adsorbed atoms, and by statistical methods finds a critical temperature below which adsorbed atoms would tend to condense into a two-dimensional liquid phase (Fowler 1936). Another interesting development in the theory of condensed phases has been made by Tonks (1936), who has shown that the equation of state of a one-dimensional gas can be obtained by considering the properties of a single atom in a cell of length determined by the density. Similar considerations, applied to two- and three-dimensional assemblies, lead to equations of state valid for high concentrations, and suitable interpolation formulae are given which yield the correct form at low and high concentrations. The treatment is limited to hard elastic spheres, which exert no external forces on each other and depends on the use of the virial theorem in a manner similar to that used for gases of low concentration.

The object of this paper is to attempt to find an equation of state and other properties of gases at high concentrations in terms of interatomic forces of the same general type as has been used extensively by one of the authors in other connexions. The main idea is that an atom in a dense gas is to be regarded as confined for most of its time to a cell, and that its average environment is something like that of an atom in a liquid or a crystal. This picture can only be looked upon as a rough first approximation, for it neglects the possibility of the migration or diffusion of atoms from one cell to another, but it is probably better than attempts to deal with a dense gas by methods which depend essentially only on binary encounters. We use the methods of statistical mechanics and attempt to evaluate the partition function for a dense gas for a field in which the repulsive and attractive fields can be represented by inverse power laws, though the method is applicable to any law of force. The resulting equation of state has the right kind of properties and in the particular cases of neon, argon, hydrogen and nitrogen, using the interatomic fields previously determined, a direct calculation of the critical temperature has been made.

2—GASES AT SMALL AND LARGE DENSITIES

When the density of a gas is small, its equation of state can be represented by the formula

$$pv = kNT\left(1+\frac{B}{v}\right), \tag{1}$$

where, as usual, N is the total number of molecules in a gas of volume v, and B is the virial coefficient; k is the usual gas constant. For moderate densities it is necessary to take many more terms in the expression on the right involving higher inverse powers of v. The equation (1) is valid under the same conditions as the van der Waals equation which may be regarded as a special form of it.

For molecules of spherical symmetry, which exert on each other a field of potential $\phi(r)$, the theoretical formula for B is

$$B = 2\pi N\int_0^\infty r^2\{1-e^{-\phi(r)/kT}\}\,dr, \tag{2}$$

or

$$= \frac{2\pi N}{3kT}\int_0^\infty r^3 f(r)\, e^{-\phi(r)/kT}\,dr, \tag{3}$$

where $f(r)$ is the force between two molecules.

For any given law of force B can thus be evaluated as a function of temperature, and compared with the values of B determined from the isotherms. In this way interatomic forces have been determined.

The internal potential energy of a gas can easily be derived from B, for, if $\bar{\phi}$ is the average potential energy of any one atom in the field of the rest, we have

$$\bar{\phi} = \nu\int_0^\infty 4\pi r^2\,\phi(r)\, e^{-\phi(r)/kT}\,dr, \tag{4}$$

where ν is the average concentration of the gas. From equation (2) or (3) we then get

$$\bar{\phi} = -2(\nu/N)\,kT^2(dB/dT), \tag{5}$$

and the average potential energy of the whole assembly is

$$\Phi = N\bar{\phi}/2 = -\nu kT^2(dB/dT), \tag{6}$$

or, in terms of the volume,

$$\Phi = -\frac{NkT^2}{v}\frac{dB}{dT}. \tag{7}$$

This relation can also be obtained by the use of the thermodynamic formula

$$\left(\frac{\partial U}{\partial v}\right)_T = T\left(\frac{\partial p}{\partial T}\right)_v - p \tag{8}$$

and equation (1). This gives

$$U = -\frac{NkT^2}{v}\left(\frac{dB}{dT}\right) + U_0(T), \tag{9}$$

where U_0 is a constant of integration, independent of the volume but dependent on temperature, and clearly refers to the value of U for an ideal gas.

It is instructive in passing to compare two alternative definitions of the internal pressure of gases. The *internal pressure* p_i of a gas is sometimes defined by either side of equation (8), and so is given by

$$p_i = (NkT^2/v^2)(dB/dT). \tag{10}$$

On the other hand, equation (1) can be written as

$$p = \nu kT + p_s, \tag{11a}$$

where

$$p_s = NkT\,B/v^2, \tag{11b}$$

and p_s has been shown (Lennard-Jones 1924) to be equal to the stress across unit area of a plane in the gas due to the interatomic forces and is positive when the stress is one of repulsion. This has been called the ***statical*** pressure. We see from (9) and (11) that p_i and p_s do not refer to the same thing; in fact

$$p_i = T^2\frac{d(p_s/T)}{dT}. \tag{11c}$$

Observations of the isotherms of gases show that B is negative at low temperatures and increases to positive values at high temperatures (through the Boyle point, where it vanishes); it has a maximum and then begins to fall again. Hence from (7) we infer that Φ behaves in a similar way. At very high temperatures it becomes positive, implying that owing to the high translational energies the atoms are penetrating deeply into each other's repulsive fields. We note also from (10) that at low temperatures p_i is positive, while from (11b) p_s is negative. This is a matter of definition; p_i is a measure of the tendency of the gas to compress itself, while p_s, as defined above, is a measure of its tendency to expand.

Returning now to the discussion of internal energy we see from (9) that U is a linear function of the density in the region in which this expression is valid, viz.

$$U = U_0 + \alpha\rho. \tag{12}$$

The curves given by Michels for the energy of CO_2 gas as a function of density show clearly that while the energy is proportional to the density for small enough densities, there are considerable deviations for larger pressures (Michels 1937, fig. 1). There is no adequate theory at present to explain the observations. We can see in a general way that (12) will cease to be valid. In a dense gas an atom will be surrounded by a number of others and will be moving in the field of several at the same time. Of course at high temperatures there will be continual change of the immediate neighbours of the complex, surrounding any one atom, but the average potential energy of each will be of the same order of magnitude as that of an atom in a crystal. The potential energy of any one in its position of equilibrium is given approximately by

$$\phi_0 = c\phi(r_0),$$

where c is the number of nearest neighbours, if we neglect the effect of more distant atoms. If we adopt for ϕ a form of potential which has proved to be a useful representation of the fields of inert gases, viz.

$$\phi = \frac{\lambda}{r^n} - \frac{\mu}{r^m}, \tag{13}$$

where n and m are integers, then we get for the potential energy of the assembly

$$\Phi = \frac{N}{2}\phi_0 = \frac{Nc}{2}\phi(r_0), \tag{14}$$

where r_0 is the equilibrium value of the distance between nearest neighbours when all are at rest. The relation between Φ and the density, neglecting heat motion, is then of the form

$$\Phi = \lambda'\rho^{n/3} - \mu'\rho^{m/3}. \tag{15}$$

The temperature-dependent part of Φ the energy is given by Einstein or Debye expressions as long as the amplitude of vibration about the mean position is small, but when the amplitude becomes large it is to be anticipated that Φ will be a more complicated function of density, temperature and the interatomic fields. Between these extremes of very low and very high densities, the theory will be more difficult. It is the object of this paper to develop a method which may be regarded as a step towards a theory of gases at moderate densities.

3—A MODEL OF A GAS AT MODERATE DENSITIES

If we adopt the hypothesis that for moderate densities each atom may be considered to be enclosed by its neighbours in a box of definite dimensions, then we have the following picture. At first the box is so large that the *potential within it is fairly uniform except near the boundary, where there is a region of low potential energy; the enclosure is, in fact, like a box with* an adsorbing surface, and the enclosed atom will tend to be near it. As the density of the gas increases and the size of the box diminishes, the fields of the adsorbing surface will begin to overlap as in figs. 1 (a_1) and 1 (a_2), giving an energy barrier in the centre which diminishes with the density.

Finally, a stage is reached at which the barrier disappears, the minimum of the potential energy is at the centre and remains there for all greater densities as in fig. 1 (b), but owing to the increasing overlap of the repulsive fields the absolute minimum of potential begins to rise with increasing concentration. We thus have two types of field, one of type (a) and one of type (b), depending on the density.

These features may be represented roughly by a simple model. We suppose every atom to be confined to a spherical box in which the potential energy is uniform for any given size but changes as the size changes. Thus we suppose the potential energy to vary with the radius R according to a law such that it is zero for large R, and then falls steadily as R decreases until it reaches its greatest negative value at $R = R_0$, when it begins to rise again, eventually becoming positive. We denote this function by $\chi(R)$ or by $\chi(v)$, where v is the average volume occupied by each atom.

We now suppose that the partition function of the whole assembly can be expressed as a product of the partition functions of the individual atoms. We shall examine this assumption later in the paper. We assume that each atom moves on the average in the same field and is confined to the same volume. The partition function of each atom is then given by

$$\begin{aligned} f &= \iiint e^{-(p_x^2+p_y^2+p_z^2)/2mkT} \int_0^R e^{-\chi(v)/kT}\, 4\pi r^2\, dr/h^3 \\ &= \frac{(2\pi mkT)^{\frac{3}{2}}}{h^3}\, e^{-\chi(v)/kT}\, \frac{4\pi R^3}{3} \\ &= \frac{(2\pi mkT)^{\frac{3}{2}}}{h^3}\, v e^{-\chi(v)kT}, \end{aligned} \tag{16}$$

the value of χ, as explained, being constant within the cell, and v being taken now for the volume available for one atom.

We could improve upon this model by taking into account the finite size of the atoms. Thus we could represent them by a diameter σ and then, supposing the centres of the surrounding atoms to be situated on the surface of the cell, the above expression must be replaced by

$$f = \frac{(2\pi mkT)^{\frac{3}{2}}}{h^3} e^{-\chi(v)/kT} \frac{4\pi(R-\sigma)^3}{3}$$

$$= \frac{(2\pi mkT)^{\frac{3}{2}}}{h^3} e^{-\chi(v)/kT} \alpha v\left(1-\frac{\sigma}{R}\right)^3, \tag{17}$$

where $\alpha v = 4\pi R^3/3$ and α is a numerical constant; for example, if the atoms were arranged regularly throughout space as a face-centred cubic crystal, we should have $\alpha = 4\pi\sqrt{\tfrac{2}{3}}$. For the above expression to be valid we must have $R > \sigma$ and also the "available" regions for neighbouring atoms must not overlap; this latter condition implies that $R < 2\sigma$. Within these limits, however, there lies the interesting range of densities near the critical point.

Equating the partition function of the whole assembly to f^N, we then get for the free energy $A(=U-TS)$

$$A = -NkT\log f, \tag{18}$$

and the pressure is given by

$$p = NkT\left(\frac{\partial}{\partial v}\log f\right)_T.$$

Using (16) we then get $$p = NkT\left\{\frac{1}{v} - \frac{\chi'(v)}{kT}\right\}, \tag{19}$$

and using (17) we get for the second model (atoms of finite size)

$$p = \frac{NkT}{v\left\{1-\left(\frac{v_0}{v}\right)^{\frac{1}{3}}\right\}} - N\chi'(v), \tag{20}$$

an equation very similar to that of van der Waals' when $\chi(v)$ has the special form of $-a/v$.

It is not necessary for our purpose to deal with this more complex form of the equation of state; the simple form (19) leads to critical phenomena if a suitable form for $\chi(v)$ be chosen. We have seen that $\chi(v)$ must vanish for large v, reach a minimum for a finite value of v and thereafter must increase as v decreases. A suitable function with these properties is

$$\chi(v) = \frac{\alpha}{v^{\nu}} - \frac{\beta}{v^{\mu}}, \tag{21}$$

where $\nu > \mu$. If the second term is to represent van der Waals attractive fields we must have $\mu \approx 2$.

Critical temperature, pressure and volume are given by

$$\left(\frac{\partial p}{\partial v}\right)_T = 0 = -\frac{1}{v^2} - \frac{1}{kT}\left\{\frac{\nu(\nu+1)\alpha}{v^{\nu+2}} - \frac{\mu(\mu+1)\beta}{v^{\mu+2}}\right\}, \tag{22}$$

$$\left(\frac{\partial^2 p}{\partial v^2}\right)_T = 0 = \frac{2}{v^3} - \frac{1}{kT}\left\{\frac{-\nu(\nu+1)(\nu+2)\alpha}{v^{\nu+3}} + \frac{\mu(\mu+1)(\mu+2)\beta}{v^{\mu+3}}\right\}. \tag{23}$$

These equations give the critical volume v_c at once as

$$v_c^{\nu-\mu} = \frac{\nu^2(\nu+1)\alpha}{\mu^2(\mu+1)\beta}, \tag{24}$$

while the critical temperature T_c is given by

$$kT_c = -v_c^2\chi''(v_c) = \frac{\mu(\mu+1)\beta}{v_c^{\mu}}\frac{\nu-\mu}{\nu} \tag{25}$$

on using (24). If we denote by v_m the value of v at which $\chi(v)$ assumes its minimum value, we have

$$v_m^{\nu-\mu} = \nu\alpha/\mu\beta, \tag{26}$$

and

$$\chi(v_m) = -\frac{\beta}{v_m^{\mu}}\frac{\nu-\mu}{\nu}. \tag{27}$$

Using these relations and (24) in (25), we find

$$\frac{kT_c}{|\chi(v_m)|} = \mu(\mu+1)\left[\frac{\mu(\mu+1)}{\nu(\nu+1)}\right]^{\mu/(\nu-\mu)}. \tag{28}$$

Further, the Kamerlingh Onnes constant K is given by

$$\frac{1}{K} = \frac{p_c v_c}{NkT_c} = 1 + \frac{\chi'(v_c)}{v_c\chi''(v_c)} = \frac{\mu\nu}{(\mu+1)(\nu+1)}. \tag{29}$$

Taking $\nu = 4$ and $\mu = 2$, corresponding to a repulsive potential varying as an inverse twelfth power of the distance and attractive potential varying as an inverse sixth power, we find

$$v_c/v_m = 1{\cdot}82, \quad kT_c = (1{\cdot}8)\,|\,\chi(v_m)\,|, \quad K = 1{\cdot}87. \tag{30}$$

The Kamerlingh Onnes constant is actually about 3·7 for many gases, and to obtain better agreement with experiment it would be necessary to consider the finite size of the atom in its cell as was done in equation (20). We note, however, that the model gives a simple linear relation between the critical temperature and the maximum absolute value of the potential in the cell. A somewhat similar relation is obtained by the more detailed calculations below.

4—THE EQUATION OF STATE OF A GAS AT MODERATE DENSITIES—CRITICAL PHENOMENA

Having seen that the simple considerations of the preceding section lead to an equation of state with the right kind of properties, at any rate as regards critical phenomena, we now proceed to consider the problem more closely and to try to find an equation of state in terms of interatomic forces. Instead of assuming the potential of an atom within its available volume to be constant, we must endeavour to find its potential due to all its immediate neighbours as a function of position and also as a function of the size of the available volume.

We shall use as before the approximation that the partition function of a dense gas can be expressed as a product of the partition functions of the individual members of the assembly, each member being confined to a cell from which all others are excluded. This approximation is probably the more reasonable, the greater the density. Whereas in a sparse gas binary encounters alone are important and an atom can migrate or diffuse rapidly from one part of a vessel to another, in a dense gas an atom will be imprisoned by its immediate neighbours and will make more multiple encounters than binary ones and will escape from one environment to another the more slowly the greater the density. We neglect this possibility of migration as being an infrequent event compared with the time spent in any given cell. None the less it is of interest to examine the error introduced for a case for which the approximation is least justified, that is, for a perfect gas.

Let N be the number of atoms in a gas and v the total volume. Then if we divide v into N cells, each of volume v/N, the partition function for a particle in such a cell will be given by

$$f(T) = [(2\pi m\,kT)^{\frac{3}{2}}/h^3]\,(v/N), \tag{31}$$

and the partition function for the whole system by

$$F(T) = [f(T)]^N, \tag{32}$$

whereas the correct partition function is given by

$$F^*(T) = [(2\pi m\,kT)^{\frac{3}{2}}\,v/h^3]^N/N!, \tag{33}$$

so that the ratio is $$\frac{F(T)}{F^*(T)} = \frac{N!}{N^N} = (2N\pi)^{\frac{1}{2}}\,e^{-N}.$$

When N is large the difference of the free energies is approximately

$$kT\{\log F^* - \log F\} = kT\left(\log \frac{F^*}{F}\right) = kT\,N,$$

and the difference of the free energies per atom is kT. This difference, depending only on N and the temperature, will thus not affect the equation of state when it is derived by the usual formula from the partition function.

We shall now suppose that the system consists of N particles moving in a volume v which is divided in some regular way into N equal cells each of volume v^*, and that each particle is confined to one of these cells. Each particle will be moving in the field of the others, which will vary with time, and to obtain the partition functions for the individual particles we must replace this field by some suitable average. The simplest assumption we can make is that the average field in which any one atom moves is that due to its immediate neighbours when each is in its equilibrium position, that is, at the centre of its own cell; and we shall consider this case as a suitable first approximation.

Since atomic fields fall off very rapidly with distance we shall consider only nearest neighbours. The problem we have to deal with, therefore, is that of a particle moving in the field of a number of other particles symmetrically arranged on the surface of a sphere. If the number of immediate neighbours is large (it will generally be about twelve), the field within the cell will have a high degree of symmetry, and it will be sufficient for our purpose to replace the actual field by one which is spherically symmetrical about the centre of the cell. This may be obtained by taking a suitable average. We may take the average field, as the atom within the cell describes a sphere about the centre. This is equivalent to the average potential produced within the cell when the nearest neighbours take up all positions with equal probability on the surface of a sphere.

Let a be the average distance between nearest neighbours and let $\phi(a)$ be their mutual potential energy at this distance apart. We suppose one particle kept fixed while the other is moved about a sphere of radius r, described by the vector $\mathbf{a}+\mathbf{r}$. The average potential of the particles is then given by

$$\bar{\phi}(r) = \tfrac{1}{2}\int_0^\pi \phi\{(r^2+a^2-2ar\cos.\theta)^{\frac{1}{2}}\}\sin\theta\,d\theta. \tag{34}$$

If c is the number of nearest neighbours, the average potential energy within a cell for $r<a$ may be written as

$$\psi(r) = c\bar{\phi}(r). \tag{35}$$

In order to make further progress it is necessary to take particular forms of $\phi(r)$. For a monatomic gas a convenient function is

$$\phi(r) = Ar^{-n}-Br^{-m}, \tag{36}$$

and then

$$\psi(r) = \frac{c}{2}\left[\frac{A}{(n-2)a^n}\left(\frac{a}{r}\right)\left\{\left(1-\frac{r}{a}\right)^{-n+2}-\left(1+\frac{r}{a}\right)^{-n+2}\right\}\right.$$
$$\left.-\frac{B}{(m-2)a^m}\left(\frac{a}{r}\right)\left\{\left(1-\frac{r}{a}\right)^{-m+2}-\left(1+\frac{r}{a}\right)^{-m+2}\right\}\right]. \tag{37}$$

For the special case of $n = 12$, $m = 6$, which has been found to represent the fields of some of the inert gases satisfactorily (Lennard-Jones 1931), we get

$$\psi(r) = \frac{c}{2}\left[\frac{A}{a^{12}}\left(\frac{a}{10r}\right)\left\{\left(1-\frac{r}{a}\right)^{-10}-\left(1+\frac{r}{a}\right)^{-10}\right\}-\frac{B}{a^6}\left(\frac{a}{4r}\right)\left\{\left(1-\frac{r}{a}\right)^{-4}-\left(1+\frac{r}{a}\right)^{-4}\right\}\right],$$

which may be written in the form

$$\psi(r)-\psi(0) = c[Aa^{-12}l(y)-Ba^{-6}m(y)], \tag{38}$$

where

$$y = r^2/a^2, \tag{39}$$

$$l(y) = [1+12y+(25{\cdot}2)y^2+12y^3+y^4](1-y)^{-10}-1, \tag{40}$$

and

$$m(y) = (1+y)(1-y)^{-4}-1. \tag{41}$$

Since a^3 is proportional to v^* the specific volume, we may write the equation for $\psi(r)$ in the form

$$\psi(r)-\psi(0) = \Lambda\{(v_0^*/v^*)^4 l(y)-2(v_0^*/v^*)^2 m(y)\}, \tag{42}$$

where Λ and v_0^* are constants, chosen so that

$$\Lambda(v_0^*/v^*)^4 = cAa^{-12}, \quad 2\Lambda(v_0^*/v^*)^2 = cBa^{-6}. \tag{43}$$

Putting $v_0 = Nv_0^*$, and $v = Nv^*$, we also have

$$\psi(r)-\psi(0) = \Lambda\{(v_0/v)^4\, l(y) - 2(v_0/v)^2\, m(y)\}. \tag{43a}$$

Some representative curves for $\psi(r)$ for certain values of (v_0/v) are shown in fig. 1. Curves (a_1) and (a_2) have a potential barrier at the centre while (b) has not. It is found that the field ceases to have this central hump when (v/v_0) is of the order of 1·6. At the critical volume $(v/v_0 = 2{\cdot}2)$, the height of the hump is approximately $kT_c/2$; at $v/v_0 = 3{\cdot}16$ it is $(0{\cdot}9)\, kT_c$.

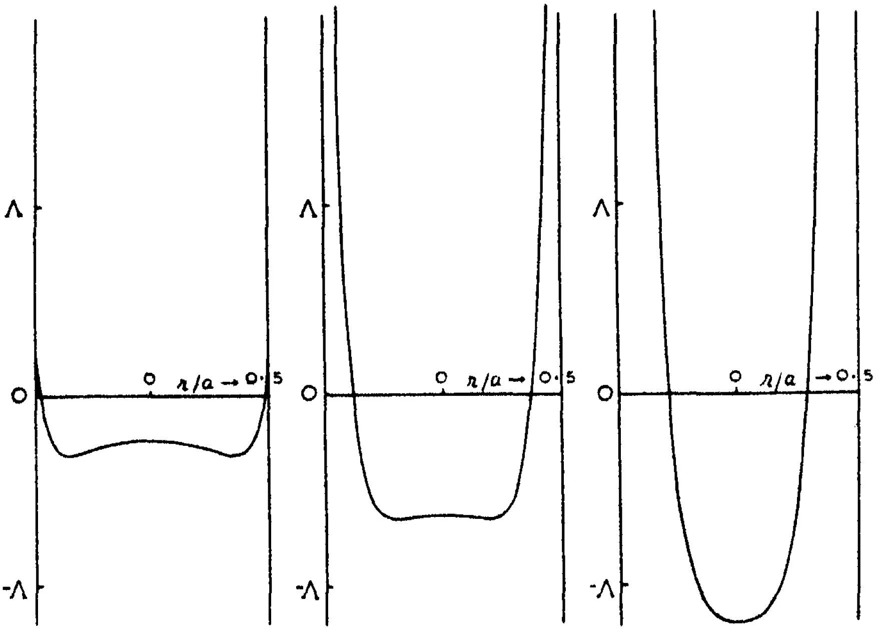

(a_1) (a_2) (b)

FIG. 1—The potential field within a cell; curves (a_1), (a_2) and (b) correspond to $(v_0/v)^2 = 0{\cdot}10$, $0{\cdot}30$, and $0{\cdot}70$ respectively.

The partition function for a particle moving in this field, when the energy zero is taken to be that of a particle at $r = 0$, is given by

$$f(T) = (2\pi mkT)^{\frac{3}{2}}\, h^{-3}\int_0^{a/2} 4\pi r^2 \exp\{[\psi(r)-\psi(0)/kT]\}\, dr$$

$$= (2\pi mkT)^{\frac{3}{2}}\, h^{-3}\, 2\pi a^3 \int_0^{\frac{1}{4}} y^{\frac{1}{2}} \exp\left[\frac{\Lambda}{kT}\left\{-\left(\frac{v_0}{v}\right)^4 l(y) + 2\left(\frac{v_0}{v}\right)^2 m(y)\right\}\right] dy, \tag{44}$$

where we have neglected the contribution to the partition function from portions of the cell outside the sphere of radius $a/2$, but this is certainly small owing to the repulsive field except at high temperatures. The partition function for the whole system, when the energy zero is that of an atom at rest at infinity, is then

$$F(T) = f(T)^N \exp\left[\frac{N}{kT}\,\tfrac{1}{2}\left\{2A\left(\frac{v_0}{v}\right)^2 - A\left(\frac{v_0}{v}\right)^4 + \alpha(v)\right\}\right], \tag{45}$$

where $\alpha(v)$ is an extra term inserted to take account of the interaction of particles which are not nearest neighbours. For a face-centred cubic structure the interaction between such particles increases the attractive term in the potential energy by about 20 % and has a negligible effect on the repulsive term (Lennard-Jones and Ingham 1925, Table I). We have therefore

$$F(T) = f(T)^N \exp\left[\frac{N}{kT}\left\{1{\cdot}2A\left(\frac{v_0}{v}\right)^2 - 0{\cdot}5A\left(\frac{v_0}{v}\right)^4\right\}\right]. \tag{46}$$

The expression

$$\psi^*(0) = \left\{-2{\cdot}4A\left(\frac{v_0}{v}\right)^2 + A\left(\frac{v_0}{v}\right)^4\right\} \tag{47}$$

is the potential energy of each atom when the atoms are at the centres of their cells. It has a maximum value equal to 1·44 when $\left(\frac{v_0}{v}\right)^2 = 1{\cdot}2$; $v_0^*(= v_0/N)$ is thus approximately 1·1 times the specific volume v^* of the crystal at the absolute zero, and A is 1·39 times the heat of sublimation at the absolute zero.

The equation for the partition function may be written

$$\frac{1}{N}\log F(T) = \frac{A}{kT}\left\{1{\cdot}2\left(\frac{v_0}{v}\right)^2 - 0{\cdot}5\left(\frac{v_0}{v}\right)^4\right\} + \log\left(2\pi\frac{\sqrt{2}v}{N}\right) + \log g + \frac{3}{2}\log\left(\frac{2\pi mkT}{h^2}\right), \tag{48}$$

where g is a function of (A/kT) and of (v_0/v) only, viz.

$$g = \int_0^{\frac{1}{4}} y^{\frac{1}{2}} \exp\left[\frac{A}{kT}\left\{-\left(\frac{v_0}{v}\right)^4 l(y) + 2\left(\frac{v_0}{v}\right)^2 m(y)\right\}\right] dy. \tag{49}$$

We have used the relation $a^3 = \sqrt{2}\,v^*$ for a face-centred cubic structure. All the equilibrium properties of the system may now be readily derived. For example, the pressure is given by

$$\begin{aligned} p &= kT\frac{\partial}{\partial v}\log F(T) \\ &= \frac{NkT}{v}\left[1 - \frac{A}{kT}\left\{2{\cdot}4\left(\frac{v_0}{v}\right)^2 - 2\left(\frac{v_0}{v}\right)^4\right\} - \frac{4A}{kT}\left\{\left(\frac{v_0}{v}\right)^2\frac{g_m}{g} - \left(\frac{v_0}{g}\right)^4\frac{g_l}{g}\right\}\right], \end{aligned} \tag{50}$$

where g_m and g_l are also functions of (Λ/kT) and (v_0/v) only, given by

$$g_m = \int_0^{\frac{1}{4}} y^{\frac{1}{2}}\, m(y) \exp\left[\frac{\Lambda}{kT}\left\{-\left(\frac{v_0}{v}\right)^4 l(y) + 2\left(\frac{v_0}{v}\right)^2 m(y)\right\}\right] dy \tag{51}$$

and
$$g_l = \int_0^{\frac{1}{4}} y^{\frac{1}{2}}\, l(y) \exp\left[\frac{\Lambda}{kT}\left\{-\left(\frac{v_0}{v}\right)^4 l(y) + 2\left(\frac{v_0}{v}\right)^2 m(y)\right\}\right] dy. \tag{52}$$

Similarly the mean energy per atom is given by

$$\begin{aligned}\bar{E} &= \frac{k}{N} T^2 \frac{\partial}{\partial T} \log F(T) \\ &= \Lambda\left\{0{\cdot}5\left(\frac{v_0}{v}\right)^4 - 1{\cdot}2\left(\frac{v_0}{v}\right)^2 + \Lambda\left(\frac{v_0}{v}\right)^4 (g_l/g) - 2\Lambda\left(\frac{v_0}{v}\right)^2 (g_m/g) + \frac{3}{2} kT\right\},\end{aligned} \tag{53}$$

and the specific heat by

$$\begin{aligned}c_v = \frac{\partial E}{\partial T} = k\Bigg[\frac{3}{2} + \left(\frac{\Lambda}{kT}\right)^2 \Bigg\{\left(\frac{v_0}{v}\right)^8 \left(\frac{g_{ll} g - g_l^2}{g^2}\right) - 4\left(\frac{v_0}{v}\right)^6 \left(\frac{g_{lm} g - g_l g_m}{g^2}\right) \\ + 4\left(\frac{v_0}{v}\right)^4 \left(\frac{g_{mm} g - g_m^2}{g^2}\right)\Bigg\}\Bigg],\end{aligned} \tag{54}$$

where
$$g_{ll} = \int_0^{\frac{1}{4}} y^{\frac{1}{2}}\, l^2(y) \exp\left[\frac{\Lambda}{kT}\left\{-\left(\frac{v_0}{v}\right)^4 l(y) + 2\left(\frac{v_0}{v}\right)^2 m(y)\right\}\right] dy, \tag{55}$$

and g_{lm}, g_{mm} are given by similar expressions.

We note that the *average* value of the potential energy of each atom in its cell is

$$\begin{aligned}\bar{\psi}(v, T) &= \int_0^{a/2} \psi(r)\, 4\pi r^2 \exp[-\psi(r)/kT]\, dr \Big/ \int_0^{a/2} 4\pi r^2 \exp[-\psi(r)/kT)]\, dr \\ &= -k \frac{\partial \log g}{\partial(1/T)} + \psi(0) \\ &= \Lambda\left[\left(\frac{v_0}{v}\right)^4 \frac{g_l}{g} - 2\left(\frac{v_0}{v}\right)^2 \frac{g_m}{g}\right] + \psi(0).\end{aligned} \tag{56}$$

Hence the average potential energy in a cell, referred to the potential at the centre as zero, is

$$\chi(v, T) = \bar{\psi}(v, T) - \psi(0) = \Lambda\left[\left(\frac{v_0}{v}\right)^4 \frac{g_l}{g} - 2\left(\frac{v_0}{v}\right)^2 \frac{g_m}{g}\right]. \tag{57}$$

We see from (53), using (47) and (57), that the mean energy per atom is

$$E = \tfrac{1}{2}\psi^*(0) + \chi(v, T) + \tfrac{3}{2}kT, \tag{58}$$

and the total energy is NE. The factor $\frac{1}{2}$ in the first term is due to the fact that this term arises from the mutual potential energy of atoms, and it might be expected that a similar factor should appear in the second term, since this also is due to the extra mutual potential when the atoms are disturbed from the centres of their cells. Some justification for the non-appearance of this factor may be made as follows.

Let P and Q be the mean positions of two atoms and P' and Q' be simultaneous positions of the atoms near P and Q respectively. Let $PQ = a$, $PP' = r_1$, and $QQ' = r_2$. Then we have for the mean potential of the two atoms as they describe spheres of radii r_1 and r_2 about P and Q respectively (to the second order)

$$\begin{aligned}\overline{\phi(P'Q')} &= \phi(a) + \overline{\Sigma(x_1 - x_2)\,\phi_x} + \overline{\Sigma\tfrac{1}{2}(x_1 - x_2)^2\,\phi_{xx}} \\ &= \phi(a) + \tfrac{1}{2}\{\overline{x_1^2}\,\phi_{xx} + \overline{y_1^2}\,\phi_{yy} + \overline{z_1^2}\,\phi_{zz}\} + \tfrac{1}{2}\{\overline{x_2^2}\,\phi_{xx} + \overline{y_2^2}\,\phi_{yy} + \overline{z_2^2}\,\phi_{zz}\} \\ &= \phi(a) + \frac{1}{6}(r_1^2 + r_2^2)\left(\frac{\partial^2\phi}{\partial a^2} + \frac{2}{a}\frac{\partial\phi}{\partial a}\right) \\ &= \phi(a) + \chi_1 + \chi_2, \end{aligned} \tag{59}$$

where χ_1 is the extra average energy of one atom due to its disturbance from the centre and χ_2 the corresponding energy of the other atom. Hence we get two χ terms for each ϕ term.

The values of g, g_l and g_m calculated by numerical integration for two values of A/kT and a range of values of v/v_0 are given in Table I. The isotherms, deduced from them, are shown in fig. 2.

TABLE I—THE FUNCTIONS OF g, g_l AND g_m

		$A/kT = 9$			$A/kT = 10$		
v/v_0	$(v_0/v)^2$	g	g_l	g_m	g	g_l	g_m
1·195	0·7	0·00180	0·000910	0·000173	0·00161	0·000747	0·000139
1·291	0·6	0·00295	0·002042	0·000372	0·00269	0·001723	0·000316
1·414	0·5	0·00515	0·00511	0·000875	0·00478	0·00441	0·000762
1·581	0·4	0·00964	0·01462	0·00228	0·00916	0·01315	0·00208
1·826	0·3	0·01957	0·0495	0·00670	0·01920	0·0468	0·00643
2·236	0·2	0·0437	0·2211	0·02366	0·0445	0·2156	0·02347
2·575	0·15	0·0676	0·543	0·0482	0·0700	0·546	0·0493
3·162	0·1	0·1069	1·635	0·1084	0·1125	1·667	0·1126

From these functions we deduce the equation of state from equation (50), the values of pv/NkT being given in Table II. The isotherm for $A/kT = 9$

appears to be close to the critical one, so far as can be judged from its graph. From the relations (43) we have

$$A = cB^2/4A, \tag{60}$$

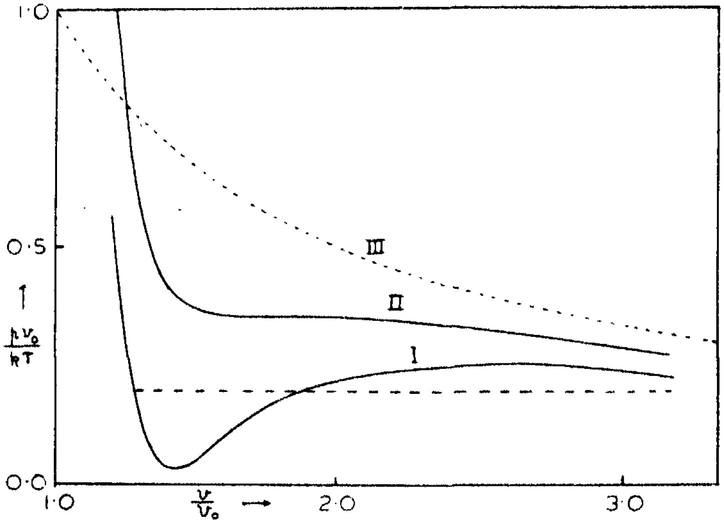

Fig. 2—Calculated isotherms. Curve I corresponds to $kT = A/9$, and curve II to $kT = A/10$ with the saturated vapour phase shown dotted. The upper curve is the isotherm of a perfect gas.

Table II—Calculated Isotherms of Gases in the Critical Region

		$A/kT = 10$		$A/kT = 9$	
v/v_0	$(v_0/v)^2$	pv/NkT	pv_0/NkT	pv/NkT	pv_0/NkT
1·195	0·7	0·675	0·565	1·202	1·006
1·291	0·6	0·218	0·169	0·765	0·593
1·414	0·5	0·046	0·033	0·573	0·406
1·581	0·4	0·149	0·094	0·568	0·359
1·826	0·3	0·348	0·191	0·644	0·353
2·236	0·2	0·531	0·237	0·788	0·352
2·575	0·15	0·642	0·249	0·825	0·320
3·162	0·1	0·721	0·224	0·877	0·277

and so, adopting the value $c = 12$ for a face-centred cubic arrangement, we can derive the critical temperature from the formula

$$kT_c = cB^2/36A = B^2/3A. \tag{61}$$

Now from the potential function given in (36) for two atoms for $n = 12$, $m = 6$ we have

$$|\phi(r)|_{\max} = B^2/4A, \tag{62}$$

and so

$$kT_c = (4/3)\,|\phi(r)|_{\max}, \tag{63}$$

which is similar to the result obtained in equation (30) by the simple model. The values of the critical temperature, calculated from this formula using the force fields given elsewhere by Lennard-Jones (1931, p. 475, Table I or p. 476, fig. 3), are given in Table III, and they are remarkably close to those observed.

TABLE III—CRITICAL TEMPERATURES

	$\|\phi\|_{\max}/k$	T_c(calc.)	T_c(obs.)
H_2	31	41	34
Ne	36	48	44
N_2	96	128	126
Ar	121	161	150

It is difficult to determine the critical volume accurately from the calculated curves without excessive labour, but it seems to be about $2v_0^*$, which is equal to 2·2 times the specific volume at the absolute zero. This value is rather too small. The calculated value of $p_c v_c/kT_c$ is about 0·7, whereas the experimental value for many gases is about 0·27.

We have not included helium in this table because throughout this paper we have used classical statistics, and quantum effects are likely to be appreciable in this case. The formula does, however, give the order of magnitude of the critical temperature even for helium. The method used in this paper could be extended to include quantized vibrations. We may conclude that the method reproduces the essential features of gases at high concentrations and encourages further investigations on similar lines. It is hoped in a later paper to calculate by similar methods the critical temperature of a film or two-dimensional gas with a view to finding whether it is higher or lower than that of the three-dimensional gas.

One of the authors is indebted to the Department of Scientific and Industrial Research for a grant.

SUMMARY

An attempt is made to find an equation of state of a gas at large densities in terms of interatomic forces. The main idea is that an atom in a dense gas is to be regarded as confined for most of its time to a cell, and that its average

environment is something like that of an atom in a liquid or crystal. This method abandons the attempt to calculate the properties of a dense gas from binary encounters only but considers an atom as subject to a multiple encounter all the time. The methods of statistical mechanics are used to derive an equation of state and the formulae are applied to the inert gases, for which the interatomic fields are known. The calculated values of the critical temperature are found to be close to those observed.

REFERENCES

Bragg, W. L. and Williams, E. J. 1934 *Proc. Roy. Soc.* A, **145**, 699.
— — 1935 *Proc. Roy. Soc.* A, **151**, 540.
Fowler, R. H. 1936 *Proc. Camb. Phil. Soc.* **32**, 144.
Lennard-Jones, J. E. 1924 *Proc. Camb. Phil. Soc.* **22**, 105.
— 1931 *Proc. Phys. Soc.* **43**, 461.
Lennard-Jones, J. E. and Ingham, A. E. 1925 *Proc. Roy. Soc.* A, **107**, 636.
Michels, A. and Michels, C. 1937 *Proc. Roy. Soc.* A, **160**, 348.
Michels, A., Bijl, A. and Michels, C. 1937 *Proc. Roy. Soc.* A, **160**, 376.
Michels, A., Blaisse, B. and Michels, C. 1937 *Proc. Roy. Soc.* A, **160**, 358.
Tonks, L. 1936 *Phys. Rev.* **50**, 955.

Reaction Kinetics in Films. The Hydrolysis of Long-Chain Esters

BY A. E. ALEXANDER AND E. K. RIDEAL, F.R.S.

(*Received* 29 *July* 1937)

INTRODUCTION

The hydrolysis of the simple esters of the short-chain fatty acids in the bulk phase has been investigated under a variety of conditions (Moelwyn-Hughes 1933, pp. 87, 245). This has now been extended to the insoluble esters of the long-chain acids and alcohols. These are also of interest biologically, since the natural breakdown and resynthesis of fats are probably interfacial reactions.

The work of Hughes and Rideal (1933) on the oxidation of the unsaturated fatty acids, and of Fosbinder and Rideal (1933) on the alkaline hydrolysis of γ-stearolactone, has shown that these interfacial or two-dimensional reactions may differ from those in homogeneous solution; chiefly in the possibility of controlling the true steric factor. In the present work also it has been found that the velocity of reaction between long-chain esters and alkali can be markedly altered by suitable changes in the molecular orientation. Such effects have been discussed in a previous communication (Alexander and Schulman 1937).

The saponification of the fats when emulsified has been studied by numerous workers (Lipp and Miller 1913; Lascaray 1928; McBain, Humphreys and Kawakami 1929; McBain and Kawakami 1930), and discussed theoretically by Treub (1917, 1923). They found that reaction occurs solely at the interface, thus depending upon the degree of dispersion. It is not possible to study accurately their reaction kinetics when emulsified, since the particle size of the emulsions (and therefore the interfacial area at which reaction occurs) depends upon the substrate and is affected by the hydrolysis products. As monolayers on aqueous substrates the hydrolysis can be followed quantitatively by use of a Langmuir-Adam trough in conjunction with the surface-potential modification of Schulman and Rideal (1931). The hydrolysis

$$R.\mathrm{COO}.R' + \mathrm{H_2O} \rightarrow R.\mathrm{COOH} + R'\mathrm{OH}$$

is accompanied by concurrent changes in both the molecular area and the phase-boundary potential. It is also possible to determine the effects produced by changes in the nature of the film (condensed, expanded or gaseous), in the molecular orientation and intermolecular spacing, and by the products of reaction when these remain in the film.

A few results have been obtained for acid-catalysed hydrolysis, the rate of which is, however, too slow for accurate study. With the alkaline saponification, using fairly concentrated solutions of base, the essentially bimolecular reaction

$$R.\mathrm{COO}.R_1 + \mathrm{OH}' \rightarrow R.\mathrm{COO}' + R_1\mathrm{OH}$$

behaves pseudo-unimolecularly, since the concentration of OH′ remains sensibly constant.

EXPERIMENTAL

The apparatus used was essentially the same as that described in previous communications from this laboratory (Gee and Rideal 1935). Film pressures could be measured with an accuracy of about 0·2 dynes/cm., and the thermostating arrangement gave a working range of about 3–40° C. All reactions were carried out at constant surface pressure, since the velocity was found to be dependent upon this factor. As strongly alkaline substrates (generally normal caustic soda) were employed, particular precautions had to be taken against contamination. With the exception of the platinum strips used to confine the film there was no metal in contact with the solution, the trough being made of pyrex and the float of mica. By these precautions and the use of very pure caustic soda (for which we have to thank Imperial Chemical Industries), the rate of contamination, as measured by the rate of change of the surface potential, could be made very small.

The preparation of the esters used has been given in a previous communication (Alexander and Schulman 1937).

EVALUATION OF VELOCITY CONSTANTS

The velocity constant (k) of the reaction can be determined from a knowledge of the observable quantities A (area per molecule) and ΔV (change in surface potential).

For the pseudo-unimolecular reaction we have at constant temperature

$$N = N_0 e^{-kt}, \tag{1}$$

where N_0 = initial number of ester molecules, N = number of ester molecules at time t, k = pseudo-unimolecular velocity constant.

If the rate is proportional to the number of collisions of the hydroxyl ions on the film, then

$$k = ZA_0 e^{-E/RT},$$

where Z = number of collisions of OH′ ions with surface per unit area per second, A_0 = area of the ester molecule, E = activation energy of the reaction. Therefore $\log_e k = \log_e ZA_0 - E/RT$.

Hence a plot of $\log_e k$ against $1/T$ gives E, assuming ZA_0 to remain sensibly constant.

If molecular areas are additive then the usual equation for a unimolecular reaction holds, namely

$$\frac{A - A_\infty}{A_0 - A_\infty} = e^{-kt}, \tag{2}$$

where A_0 = initial area per molecule (i.e. total area/N_0), A_∞ = final area per molecule, A = area per molecule at time t.

If surface potentials are additive, then

$$\begin{aligned} \Delta V &= \Delta V_{\text{ester}} + \Delta V_{\text{products}} \\ &= (4\pi n\mu)\,\text{ester} + (4\pi n\mu)\,\text{products}. \end{aligned}$$

At constant surface pressure this rearranges to

$$\frac{A\,.\,\Delta V - A_\infty\,.\,\Delta V_\infty}{A_0\,.\,\Delta V_0 - A_\infty\,.\,\Delta V_\infty} = e^{-kt}, \tag{3}$$

where the symbols have their usual significance.

At constant area this reduces to

$$\frac{\Delta V - \Delta V_\infty}{\Delta V_0 - \Delta V_\infty} = e^{-kt} \tag{4}$$

—the form used by Hughes and Rideal (1933), Fosbinder and Rideal (1933) and Schulman and Rideal (1933).

Experimentally only two important cases arise: (1) when both reaction products are soluble, (2) when one is soluble and the other insoluble.

1—*Reaction Products both Soluble*

The reaction can then be followed by area change alone provided that this is determined by the true rate of reaction and not by the rate of diffusion of the products away from the film.

Then since $A_\infty \Delta V_\infty = 0$ and $\Delta V = \Delta V_0$,

equation (3) reduces to $A = A_0 e^{-kt}$. (5)

2—*One Product Soluble, the other Completely Insoluble*

In this case both area and potential undergo change at constant surface pressure. The velocity constant can be evaluated by means of equations (2), (3) or (4).

By measurements of the surface area and surface potential of mixed films of ester and product (when the latter is insoluble) it is possible to examine the validity of equations (2) and (3). Deviations from equation (2) were found, but equation (3) was obeyed within the limits of the experimental error (see below). The work of Schulman and Hughes (1935) has also indicated that in the case of ester-acid and ester-alcohol mixtures the dipole interaction as measured by the change in the vertical component of the apparent dipole moment is small. Further evidence for the validity of equation (3) is given in the present work.

EXPERIMENTAL RESULTS

Alkaline Hydrolysis

Adam and Miller (1933) found that on strongly alkaline solutions the soaps of the long-chain fatty acids were insoluble, and formed expanded films, the stability of which was increased by greater chain length and higher alkalinity. Hence in order to evaluate velocity constants by the use of the above equations it was necessary to choose the two variables (chain length and alkalinity) such that the soap was either completely insoluble, or else dissolved into the substrate as rapidly as it was produced.

To study the effects of the variables previously discussed, the following esters have been examined over a range of temperatures:

Trilaurin, tripalmitin, α-α'-dipalmitin, α-monopalmitin, ethyl palmitate, n-butyl palmitate, methyl stearate and octadecyl acetate. In addition ethyl stearate, cetyl palmitate and cetyl propionate have been examined at 21° C., to determine the effect of the molecular orientation on the reaction velocity.

In order to compare the experimental velocities with those calculated from the kinetic theory the method of Fosbinder and Rideal (1933) was followed. The so-called "steric factor" $p = \dfrac{\text{observed velocity } (v)}{\text{calculated velocity } (N_0')}$.

Trilaurin.

Type of film: liquid expanded.

The F-A and ΔV-A characteristics of a film of trilaurin on a substrate of $N/500$ NaOH were first examined, the F-A measurements being found to agree with those of Gorter and Grendel (1926).

It was found impossible to use buffer solutions in any hydrolysis studied, as even with trilaurin (the most reactive of the esters) on a borate buffer of pH 12·3 the rate of hydrolysis was too slow. On these buffer solutions trilaurin gave an expanding film, showing that the soap produced was remaining in the film. This is to be ascribed to the salting-out effect of the buffer salts, since lauric acid on pure NaOH solution (N/100–N/2) was soluble with extreme ease and formed no stable films.

On using pure NaOH solution (generally N/5) as substrate trilaurin gave a contracting film, the area-time curve being unimolecular in form (equation (5)). Fig. 1 shows the variation of k_{uni} with NaOH concentration. As found for reactions involving an ion and a polar molecule, the rate was proportional to the concentration of the catalysing ion, i.e. $k_{\text{uni}} = k_{\text{bi}}\, C_{\text{OH}'}$. From the slope k_{bi} at 25° C. $= 4\cdot7 \times 10^{-3}$ l./g.mol./sec.

When the reaction was studied at different surface pressures, i.e. at different areas per molecule, it was found that increasing the pressure produced a marked increase in the apparent activation energy, whereas the alteration in absolute velocity was not so pronounced (Table I and fig. 2). It was not possible to work outside the range $F = 5$–17 dynes/cm., since at higher pressures the films were unstable, and at lower ones the area-time curve begins to deviate from its unimolecular form on account of the soap not being completely displaced from the film. On injecting a very dilute solution of the soap under the ester spread on N/500 NaOH at various surface pressures, no penetration could be detected at pressures of 5 dynes and greater, confirming the view of Schulman and Hughes (1935) that the ester-ionized acid complex is a very weak one.

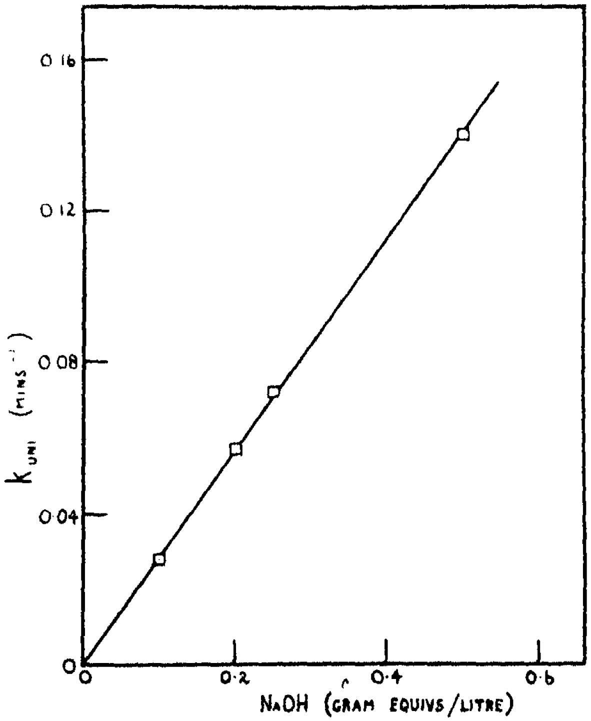

FIG. 1—Trilaurin at 25° C., $F = 5{\cdot}4$ dynes/cm. $k_{uni} \sim [\text{NaOH}]$.

A comparison of the experimental and calculated velocities (Table I) shows that E and "p" increase together, so that increase of pressure has the effect of diminishing the deviations from the "theoretical" rate.

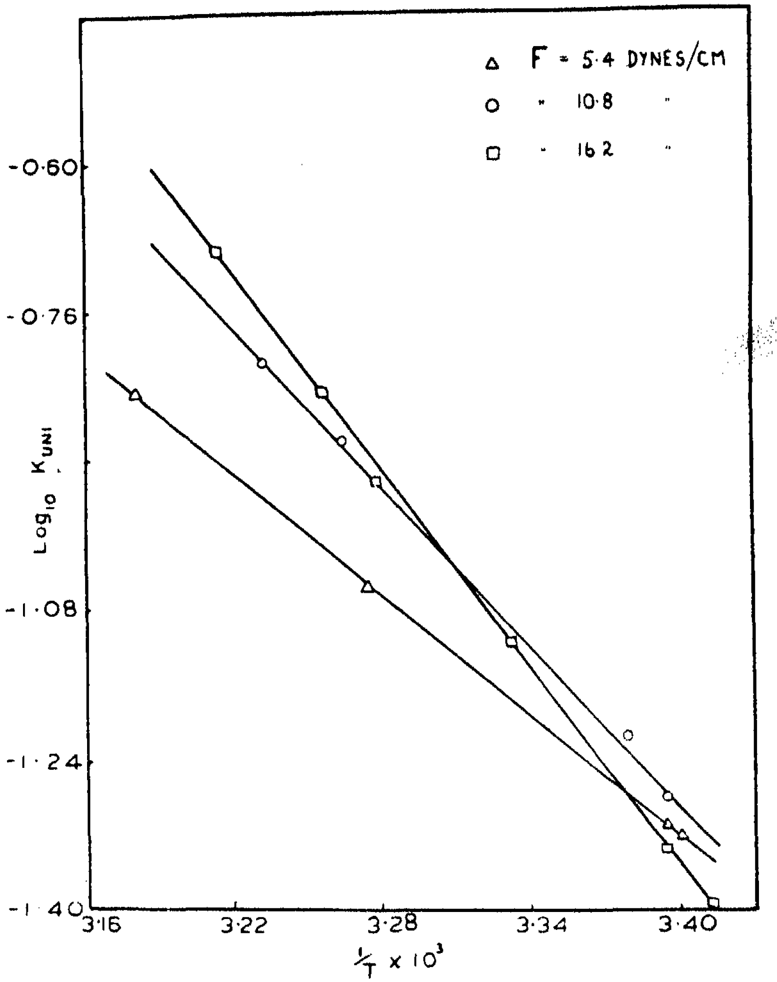

Fig. 2—Trilaurin on N/5 NaOH, $\log_{10} k_{\text{uni}} \sim 1/T$. Variation of E with F.

The experimental velocities on N/5 NaOH at different compressions are given below.

$F = 5{\cdot}4$ *dynes/cm.*

$T°$ C. ...	21	21	21·5	25	32·5	41·5
$k_{\text{uni}} \times 10^2$ min.$^{-1}$	4·85	4·76	4·88	5·68	8·73	14·15

$F = 10{\cdot}8$ *dynes/cm.*

$T°$ C. ...	21·5	22·9	33·3	36·3
$k_{\text{uni}} \times 10^2$ min.$^{-1}$	5·25	6·10	12·61	15·23

$F = 16{\cdot}2$ *dynes/cm.*

T° C. ...	20	21·5	23·0	27·0	32·0	34·0	38·0
$k_{\text{uni}} \times 10^2$ min.$^{-1}$	4·05	4·61	5·98	7·65	11·4	14·2	19·65

TABLE I—TRILAURIN ON N/5 NaOH. $T = 20°$ C.

F	E cal.	$k \times 10^3$	A A^2/mol.	$v \times 10^{11}$ sec.$^{-1}$	N_0^1	$p = v/N_0^1$
5·4	10,000	0·745	93·6	0·797	$7{\cdot}1 \times 10^{16}$	$1{\cdot}1 \times 10^{-6}$
10·8	13,200	0·787	83·2	0·946	$3{\cdot}0 \times 10^{14}$	$3{\cdot}1 \times 10^{-4}$
16·2	16,100	0·671	76·7	0·874	$2{\cdot}15 \times 10^{12}$	$4{\cdot}1 \times 10^{-2}$

F is given in dynes/cm.

k is the unimolecular velocity constant expressed in sec.$^{-1}$.

Glycerides of Palmitic Acid.

Tripalmitin, α-α'-dipalmitin and α-monopalmitin were studied on a substrate of N NaOH. In these cases, since the soap produced was insoluble, it was expected that equation (3) would hold, or at least that a similar behaviour to ethyl palmitate (see below) would be observed. In point of fact the curves obtained differed from those of ethyl palmitate in having an initial sharp fall over a period of a few minutes. The reason for this was not apparent until the α-mono compound was studied, when the remarkable result was obtained that this was appreciably soluble in the strong alkali used.

The values for the rates and activation energies are therefore only approximate ones.

Palmitic Acid.

Type of film (on N NaOH): highly expanded.

The area and surface potential of this acid on N NaOH were determined for the value of $A_\infty \Delta V_\infty$ for use in equation (3). The results are given in fig. 3. The change of surface potential is opposite in sign to that of the esters, being about -50 mV. The values for the area agree with those of Adam and Miller (1933).

Tripalmitin.

Type of film: solid condensed.

Tripalmitin on N NaOH gave a solid condensed film of the usual limiting area (about 63 A^2/mol.), so that hydrolysis was accompanied by a large increase in area. The solubility of the α-monopalmitin which must be produced at one stage caused the area-time curve to resemble one for an autocatalytic reaction.

In no case by plotting either the surface potential or the apparent dipole moment against the time was a discontinuity observed, indicating that each stage in the reaction

$$\text{Tripalmitin} \xrightarrow[k_1]{} \text{Dipalmitin} \xrightarrow[k_2]{} \text{Monopalmitin} \xrightarrow[k_3]{} \text{Soap}$$

occurred more rapidly than those preceding it. This was verified from measurements with the other two esters which gave $k_3 > k_2 > k_1$, the experimental values at 21° C. being 0·028, 0·030 and 0·054 min.$^{-1}$. That the hydrolysis of triglycerides proceeds in stages has been known for some time (see Lipp and Miller 1913). The velocity constant for tripalmitin is seen to be only about one-eighth that for the expanded film of trilaurin, probably due to the protecting action of the glyceride residue as previously discussed

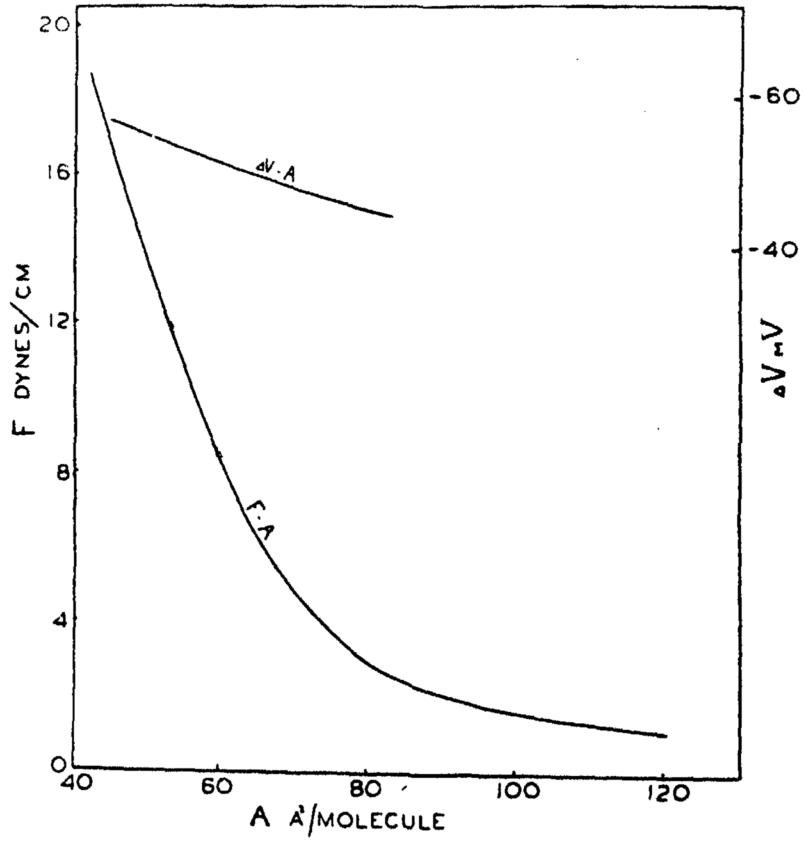

Fig. 3—Palmitic acid on N NaOH at 20° C. *F·A* and *ΔV·A*.

(Alexander and Schulman 1937). In this connexion the results obtained by Newitt, Linstead, Sapiro and Boorman (1937), on the effect of pressure on the hydrolysis of esters, are of interest. They found that whereas linseed oil reacted rapidly with dilute alkali, no hydrolysis of tristearin could be detected, even after 6 days at 5000 atm. pressure ($T = 17°$ C.). It is known that the unsaturated glycerides present in linseed oil form films of the expanded type as given by trilaurin, whereas tristearin resembles tripalmitin in giving a solid condensed film. The results discussed in this paper and in the previous one (Alexander and Schulman 1937) suggest that the change in the packing of the molecules in the interfacial film is responsible for these differences in the rates of hydrolysis.

α-α'-Dipalmitin.

Type of film: condensed.

Films of α-α' and α-monopalmitins were found by Schulman and Hughes (1935) to be impenetrable to all the usual penetrating agents, this being ascribed to the protecting action of the sheath of hydroxyl groups beneath the ester film. No effect was, however, observed on the rate of reaction, so that the effect of this sheath on the diffusion of hydroxyl ions to the ester group must be small.

The activation energy was of the same order of magnitude as for tripalmitin, i.e. about 20,000 cal.

α-Monopalmitin.

Type of film (on N NaOH): highly expanded.

When the kinetics of this ester on N NaOH were examined it was found that the film was highly expanded, the area being about 65 A^2 and the initial value of ΔV about 130 mV at $F = 5{\cdot}4$ dynes/cm. and $T = 21°$ C. The corresponding values on N/100 NaOH were about 30 A^2 and 210 mV. The marked effect of the strong alkali on the film is doubtless due to the ionization of the free hydroxyl groups in the ester molecule, as previously noted by Schulman and Hughes (1932) with the long-chain alcohols. We can thus account for the fall in potential, the expansion of the film, and also the solubility observed on the N NaOH substrate. (The ester appears to be quite insoluble on N/100 NaOH and lower *p*H's.)

The activation energy was much lower than for the two previous cases, being about 15,000 cal.

Ethyl Palmitate.

Type of film: partially expanded at room temperature.

Even in the expanded state the rate of hydrolysis was much slower than for trilaurin; so normal alkali was employed as substrate. Under these conditions the soap produced was insoluble, so the velocity constants were evaluated by equation (3). The validity of this equation was first tested by measuring the F-A and ΔV-A relationships of mixed films of ester and soap on N NaOH at 21° C. The results (fig. 4) showed that within the experimental error the assumption was justified.

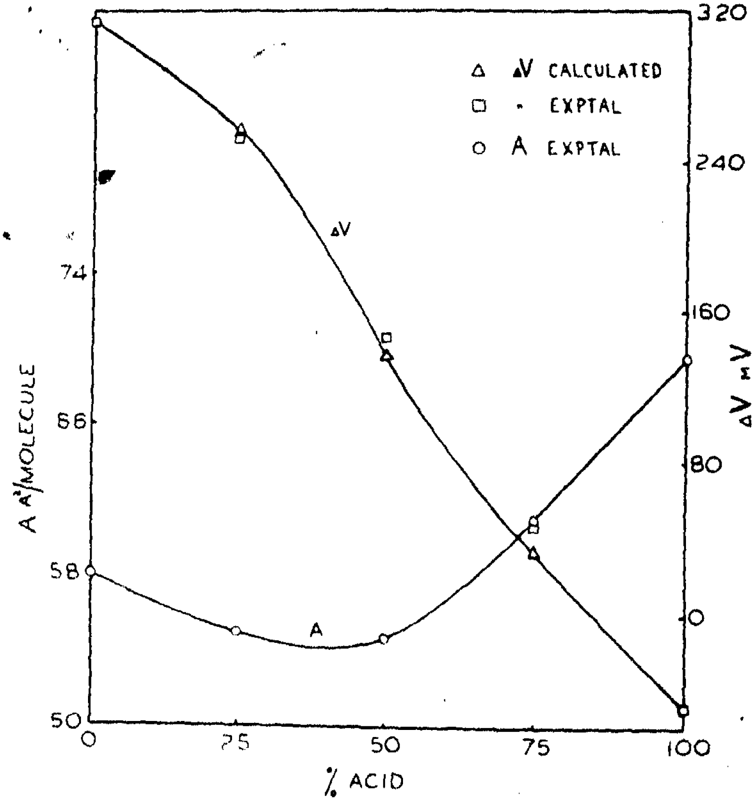

FIG. 4—Palmitic acid—Ethyl palmitate mixtures on N NaOH at 21° C. A and ΔV ~ Composition.

It was found that the velocity constant for the condensed state was only about one-eighth that for the expanded. This has been ascribed to the sheath of short ethyl chains in the condensed state protecting the ester group from attack by the OH′ ions, and with other similar effects has been discussed fully in the previous communication (Alexander and Schulman 1937). The velocity in the condensed state was too small to permit the evaluation of the activation energy.

In no case was a linear relatic p found between log $(A.\Delta V - A_\infty.\Delta V_\infty)$ and t; the velocity continually easing with time. That this was not due to contamination of the surf as shown by making up mixed films of

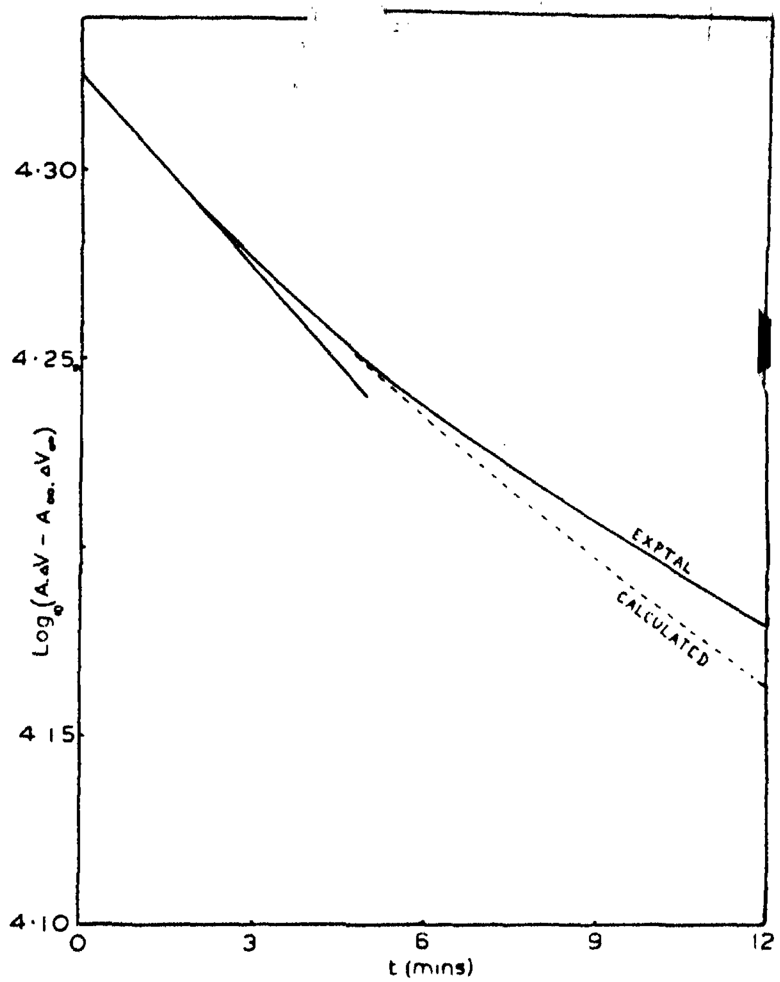

Fig. 5—Ethyl palmitate on N NaOH at 21·3° C., $F = 3$ dynes/cm.
$\text{Log}_{10}(A.\Delta V - A_\infty.\Delta V_\infty) \sim t$.

75 % ester, 25 % acid and showing that the initial slope so obtained agreed closely with that given by the pure ester after 25 % had decomposed. This was found to be the case at all temperatures (fig. 5). For example, in one experiment the initial velocity constant of 0·038 min.$^{-1}$ had fallen after 25 % decomposition to 0·022 min.$^{-1}$, that is, a decrease of about 40 %. The

initial slope of the mixture containing % ester, 25 % acid at the same temperature gave a velocity constant 23 min.$^{-1}$, in good agreement with the previous value. It appeared ble that the soap produced formed a complex with the undissoc ester (Schulman and Hughes 1935), this complex breaking down ver rate than the pure ester. Assuming that complex formation in ixture was nearly complete, then the rate of complex breakdown could be found by using such a mixture, and then by taking the initial slope of the ester curve as giving the decomposition rate for the [redacted] r, it should be possible to reproduce the experimental curve

If k_1 = velo [redacted] r the free ester, k_2 = velocity constant for the complex, [redacted] ing relationship should hold:

$$[redacted]\,(A_0.\Delta V_0 + A_\infty.\Delta V_\infty)}{A_0.\Delta V_0 - A_\infty.\Delta V_\infty} = \frac{2k_1}{2k_1 - k_2} e^{-(2k_1-k_2)t} - \frac{k_2}{2k_1 - k_2}.$$

When $k_2 = k_1$ (i.e. complex and ester decompose at the same rate), this equation reduces to the ordinary form. This equation was tested and found not to hold (fig. 5). It would also be expected on this view that with mixtures of more than 50 % soap the velocity constant should remain approximately the same, since only the complex would be present. In point of fact this is not so, increasing the amount of soap always decreasing the rate at all concentrations studied (up to 75 % soap). The explanation of the retarding effect of the soap must therefore be sought in some other direction. Since the reaction involves the change from a non-ionized molecule having a comparatively weak external field to an ionized one (the soap) with a powerful external field, it seems probable that the retardation is due to the alteration in the electrostatic field outside the monolayer (see later). The hydrophilic soap ions penetrate into the solution to a greater extent than the ester molecules, so that the rate of upward diffusion of the hydroxyl ions is reduced. Assuming that the retardation was due to the formation of a potential barrier (E_ϵ) which increased during the course of the reaction, then the velocity constant (k) is given by the equation

$$k = pZA_0 e^{-E_A/RT} e^{-E_\epsilon/RT}.$$

The initial velocity constant $k_0 = pZA_0 e^{-E_A/RT}$, since E_ϵ is then zero. Therefore $k/k_0 = e^{-E_\epsilon/RT}$.

Using synthetic mixtures the ratio k/k_0 was determined at 25 % and 50 % reaction (i.e. 3 ester : 1 soap and 1 ester : 1 soap), and hence the corresponding values of E_ϵ calculated. These were found to be approximately 325 and

630 cal./g.mol. respectively, indicating an approximately linear relationship between E_6 and the amount of reaction; and, within the experimental error, they appeared to be independent of the temperature.

If the acid produced remained unionized, as in the catalysis by H^+ ion (see below), then no such slowing-up effect was observed, the plot of $\log (A . \Delta V - A_\infty . \Delta V_\infty)$ against t being linear over the longest periods measured (about half-reaction).

From the initial slopes of the curves given by equation (3) at various temperatures it was possible to determine the activation energy for the pure ester in the expanded state. At an area of about 60 A^2 per molecule ($F = 3$ dynes/cm.) this was found to be 12,000 cal., very close to the value for the analogous reaction in homogeneous solution (about 11,300 cal.). This corresponds to a "p" factor of $0{\cdot}9 \times 10^{-5}$.

Experimental velocities on N NaOH *substrate*, *$F = 3$ dynes/cm.*

$T°$ C. ...	18·8	19·1	21·3	26·7	28·3	30·0
$k_{\text{uni}} \times 10^2$ min.$^{-1}$	3·34	3·32	3·73	5·68	6·33	7·09

n-*Butyl Palmitate.*

Type of film: expanded.

This ester resembled ethyl palmitate very closely with an activation energy (A about 60 A^2, $F = 3$ dynes/cm.) of 11,800 cal., i.e. identical within the experimental limit with that of the former ester.

Experimental velocities on N NaOH *substrate*, *$F = 3$ dynes/cm.*

$T°$ C. ...	18·0	21·2	25·0	31·2
$k_{\text{uni}} \times 10^2$ min.$^{-1}$	3·12	3·97	5·06	7·66

Methyl Stearate.

Type of film: condensed.

Although the condensed films of ethyl palmitate and ethyl stearate hydrolysed too slowly to enable the activation energy to be determined, it was hoped that shortening the alcohol radical chain length might decrease the protecting action and so increase the velocity sufficiently to enable this to be done. The effect was to increase the velocity some four times, but even so the pronounced slowing-down effect caused by the liberated soap in these condensed films made evaluation of the initial velocity constant very difficult. A value of *ca.* 17,400 cal. was obtained for the activation energy, giving a "p" factor of 0·12.

Experimental velocities on N NaOH *substrate*, *$F = 3$ dynes/cm.*

$T°$ C. ...	15·1	18·0	21·2	23·0	25·0	27·1	28·0
$k_{\text{uni}} . 10^2$ min.$^{-1}$	0·92	1·41	2·09	2·27	2·88	3·41	3·80

Octadecyl Acetate.

Type of film: condensed.

This ester is the reverse of the previous ones in having a short-chain acid and long alcohol radical. It hydrolysed extremely rapidly, some thirty times more quickly than the condensed films of ethyl stearate and ethyl palmitate under identical conditions. The octadecyl alcohol which was produced underwent slow ionization on the strong alkali as previously noted by Schulman and Hughes (1932). Fortunately this had little effect on the evaluation of the velocity constants, the reaction over the first few minutes obeying equation (3) accurately. The activation energy could be obtained with reasonable accuracy, being found to be 17,600 cal.; so that "p" = 1·2 or unity within the limits of experiment.

Experimental velocities on N NaOH *substrate,* $F = 3$ *dynes/cm.*

T° C. ...	18·9	20·9	20·9	23·7	26·1	29·0	31·6	32·0
k_{uni} min.$^{-1}$	0·127	0·143	0·146	0·203	0·275	0·32	0·396	0·433

Ethyl Stearate, Cetyl Propionate and Cetyl Palmitate.

These were examined at one temperature only (21° C.), and the results have already been discussed (Alexander and Schulman 1937). Cetyl palmitate was interesting since in this case both reaction products were insoluble and remained in the film.

Experimental results on N NaOH, $T = 21$° C.

Ethyl stearate	$F = 3$ dynes/cm.	$k = 0·006$ min.$^{-1}$
	10·8 ,,	0·005 ,,
Cetyl propionate	3 ,,	0·084 ,,
	9 ,,	0·021 ,,
Cetyl palmitate	0·2 ,,	≃ 0·18 ,,

Acid Hydrolysis

The H$^+$ ion is a much less powerful catalyst than the OH′ ion for the bulk hydrolysis, and a similar behaviour was observed with these long-chain esters in films. Even octadecyl acetate on a substrate of 5N HCl was only attacked very slowly, at 21° C. and $F = 3$ dynes/cm. $k_{bi} = 1·9 \times 10^{-3}$ l./g.mol./min., or some hundred times slower than on the alkaline substrates. For the bulk reaction the OH′ ion is about one thousand times as active as the H$^+$ ion. This difference between the catalytic ratio of the OH′ and H$^+$ ions for the film and bulk reactions is due to the OH′ ion, since the velocity for the acid-catalysed reaction is approximately the same in the film and in solution. This may be due to the presumably greater ease of passage through the ester barrier of the H^+ ion as compared with the OH' ion.

It was found that in this case, where the liberated acid did not ionize, equation (3) was obeyed strictly over periods as long as the half-reaction time.

Owing to the slow velocity in all cases it was impossible to measure the effect of molecular orientation as had been done for the alkaline hydrolysis. The velocity for the expanded film of ethyl palmitate could be measured, but not for the condensed, since in the latter case the changes of area and potential were too small.

Octadecyl Acetate.

Type of film: condensed.

This was the only ester for which an attempt was made to determine the activation energy, which was found to be very approximately 20,000 cal. This may be slightly greater than the bulk value (17,000 cal.), but the lower experimental accuracy in this case does not permit of a decision. The value of 20,000 cal. would correspond to a "p" factor of approximately unity, but no great reliance can be placed on this figure.

Experimental velocities on 5N HCl *substrate, $F = 3$ dynes/cm.*

$T°$ C. ...	19·9	22·9	24·4	26·0	28·7
$k_{bi} \times 10^3$ (l./g.mol./min.)	1·68	2·16	2·90	3·30	4·12

DISCUSSION OF RESULTS

The relevant experimental facts may be summarized as follows:

(*a*) In the expanded state the velocity and activation energy approximate to those for the bulk reaction.

(*b*) On compression the activation energy increases with but slight changes in velocity, so that the "p" factor in the kinetic equation $k = pZe^{-E/RT}$ also increases, until in the condensed state its magnitude appears to be of the order of unity.

(*c*) The nature of the film (*per se*) has little effect on the reaction velocity, but the latter is very dependent on the molecular orientation.

(*d*) The soap produced, if remaining in the film, exerts a marked depressing action on the reaction velocity.

The hydrolysis of esters in bulk has been shown to be very responsive to pressure (Newitt, Linstead, Sapiro and Boorman 1937), the velocity increasing with the pressure. This, however, cannot be compared with the effect of pressure on these two-dimensional reactions, since in this case pressure affects only one and not both of the reactants. The majority of the reactions involving an ion and a polar molecule have been shown to proceed with approximately the normal "gas kinetic" velocity (Moelwyn-Hughes 1936*b*), the "*p*" factor in the kinetic equation generally lying between 0·2 and 5. The ester hydrolysis is one of the exceptions, since "*p*" is of the order 10^{-4}. The closeness of this value and of the activation energy to those found for the esters in the expanded state suggests that the mechanism is the same in the two cases, as might be anticipated from the known two-dimensional freedom of the molecules in expanded films (Langmuir 1933). If it be assumed that the true value of "*p*" is unity and that by some mechanism the apparent activation energy has been depressed, then the value of the activation energy for the bulk reaction must be about 17,800 cal., i.e. $k \simeq Ze^{\frac{-17,800}{RT}}$. A value very close to this figure with "p" $\simeq 1$ has indeed been found for the condensed films of these long-chain esters. Thus, on this view, transition of the ester molecules from the expanded to the condensed state has removed the factor which is operative in reducing the Arrhenius activation energy to an anomalously low value.

Part of the change in activation energy may be associated with the electrostatic contribution (E_ϵ) to the activation energy, due to the interaction of the OH′ ion with the polar ester group. That such interaction is of importance in these surface reactions is shown by the effect of the ionized soap molecules in reducing the velocity by slowing up the diffusion of the OH′ ions to the film. This electrostatic contribution has recently been evaluated by Moelwyn-Hughes (1936*a*). In the case of these two-dimensional reactions the film is made up of a plane of similarly orientated dipoles, so that the OH′ ion has to surmount a repulsive barrier before it can penetrate the film, since it is known that the ester group is orientated with the negative end of the dipole towards the substrate. The height of the barrier, that is, the contribution E_ϵ to the activation energy, increases with closer packing of the dipoles. An approximate calculation for an ion (charge $Z_B\epsilon$) at a distance "r" from an array of vertically orientated dipoles each of length "b" and separated from each other by a distance "a", gives

$$E_\epsilon \simeq -\frac{4Z_B\epsilon^2N}{D}\left[\frac{1}{\sqrt{(r^2+a^2/2)}}-\frac{1}{\sqrt{\{(r+b)^2+a^2/2\}}}\right]e^{-\kappa(r+b/2)}.$$

Taking $a = 22\,\text{A}^2$, $b = 0{\cdot}8\,\text{A}$ (assuming a value of 3·6 Debyes for the ester moment in the *cis* position), $Z_B = -1$ for the OH′ ion, and $D = 7$ (from the surface potential measurements), then the maximum value of E_ϵ is 2800 cal.

when $r \simeq 1$A. This maximum value is only about one-half the experimental difference of 5600 cal. (i.e. 17,600–12,000 cal.), and in addition would not account for the large variations in "p". In this case therefore it would appear that the ion-dipole interaction alone is insufficient to explain the experimental facts.

A second factor which may have to be taken into account is the possibility that the internal degrees of freedom can contribute to the activation energy (Hinshelwood 1927; Fowler and Rideal 1927; Fowler 1936). Removal of a certain number of degrees of freedom from the ester molecule (as is known to occur on condensation), would explain the variation in the activation energy, but has the effect of decreasing and not increasing "p". Thus the contribution from the internal degrees of freedom must be small.

The nature of the activating collisions must be a contributory, if not the determining factor, in the estimation and interpretation of the "p" term. The kinetics of saponification reactions in the bulk phase would seem to require collisions of a ternary kind, involving a molecule of ester, one of water and the catalysing OH′ ion. An approximate expression for the frequency of such collisions is

$$Z_{\mathrm{S,W,OH'}} = \frac{3\pi N\sigma\eta n_{\mathrm{S}} n_{\mathrm{OH'}}}{2M_{\mathrm{S}} n_{\mathrm{W}}} \quad \text{(Moelwyn-Hughes 1933, p. 250).}$$

The activation energy, on this view, equals the Arrhenius value plus the correction for the variation of collision frequency with temperature. This increases the activation energy by about 4400 cal. and makes "p" of the order of magnitude unity for saponification both in the bulk phase and in the expanded film region (Fosbinder and Rideal 1933). Adopting the same method for the results obtained for the expanded state then the value of "p" is reduced from 10^{-5} to about 1/60. If, in addition, allowance be made for the fact that in the expanded state the area occupied by the ester head-group is considerably less than the total area occupied per molecule (the ratio being about $20\mathrm{A}^2/60\mathrm{A}^2$, i.e. *ca.* 1/3), then "p" is reduced to 1/20 in excellent agreement with the value of about 1/14 for the bulk reaction (Moelwyn-Hughes 1933, p. 252). At high compressions the film may be regarded as so compact a structure that collisions of the water molecules with it no longer determine the rate, which is then governed solely by the rate of approach of the OH′ ions to a virtually solid surface. In other words, transition from the expanded to the condensed state is accompanied by a change in the mechanism of the reaction. In the limiting case, therefore, when the motions of the ester molecule have been completely removed, the ordinary kinetic theory should be applicable. The results of compression and for the condensed state for these long-chain ester films are in accord with this view.

On the assumption that the activation energy in the condensed state is the same for all the esters (i.e. 17,600 cal.), then the values of "p" less than unity observed for the condensed films of methyl and ethyl stearates are probably due to a true steric hindrance. As would be expected, the deviations of "p" from unity increase from the methyl to the ethyl ester, the value of "p" in the latter case being about 3×10^{-2}.

We are indebted to Professor Hilditch for the specimen of trilaurin, to Professor Adam for those of ethyl and n-butyl palmitates, tripalmitin and α-monopalmitin; to the Chemical Society for a grant for the purchase of materials, and to the Department of Scientific and Industrial Research for a maintenance grant (A.E.A.). For many interesting and very helpful discussions on kinetics we have pleasure in thanking Dr. E. A. Moelwyn-Hughes.

MELTING POINTS OF ESTERS

Trilaurin 46·0° C., tripalmitin 64·2° C., α-α'-dipalmitin 71·0° C., α-monopalmitin 75·5° C., ethyl palmitate 25·0° C. Those for the other esters have already been given (Alexander and Schulman 1937).

SUMMARY

By means of the film technique of measuring surface pressures and surface potentials the hydrolysis of long-chain esters in monolayers has been quantitatively followed on both alkaline and acid substrates. Equations have been developed to evaluate the velocity constants and the conditions for their validity noted.

The reaction velocity has been found to be very sensitive to changes in the molecular orientation and to the products of reaction if these remain in the film. The activation energy and the velocity in the expanded state approximate to those in homogeneous solution, and on compression to the condensed state the activation energy rises although the absolute velocity only changes slightly. Where there is no true steric hindrance the value of "p" in the condensed state appears to be of the order of magnitude unity, i.e. the ordinary kinetic theory $k = Ze^{-E/RT}$ is obeyed. The reason for the small values of "p" in the expanded state and in solution are discussed. It is concluded that the high energy of activation as found for the condensed

state (*ca.* 18,000 cal.) is the correct one, and that the true value of the steric factor is never less than about 3×10^{-2} in these cases under discussion.

REFERENCES

Adam, N. K. and Miller, J. G. F. 1933 *Proc. Roy. Soc.* A, **142**, 401–15.
Alexander, A. E. and Schulman, J. H. 1937 *Proc. Roy. Soc.* A, **161**, 115–27.
Fosbinder, R. J. and Rideal, E. K. 1933 *Proc. Roy. Soc.* A, **143**, 61–75.
Fowler, R. H. 1936 "Statistical Mechanics", 2nd ed. p. 707. Camb. Univ. Press.
Fowler, R. H. and Rideal, E. K. 1927 *Proc. Roy. Soc.* A, **113**, 570–84.
Gee, G. and Rideal, E. K. 1935 *Proc. Roy. Soc.* A, **153**, 116–41.
Gorter, E. and Grendel, F. 1926 *K. Akad. Wet. Amst.* **29**, 1262–74.
Hinshelwood, C. N. 1927 *Proc. Roy. Soc.* A, **113**, 230–33.
Hughes, A. H. and Rideal, E. K. 1933 *Proc. Roy. Soc.* A, **140**, 253–69.
Langmuir, I. 1933 *J. Chem. Phys.* **1**, 756–76.
Lascaray, L. 1928 *Rev. gén. Colloïdes*, **6**, 32–44.
Lipp, A. and Miller, P. 1913[ii] *J. prakt. Chem.* **88**, 361–94.
McBain, J. W., Humphreys, C. W. and Kawakami, Y. 1929 *J. Chem. Soc.* pp. 2185–97.
McBain, J. W. and Kawakami, Y. 1930 *J. Phys. Chem.* **34**, 580–92.
Moelwyn-Hughes, E. A. 1933 "Kinetics of Reactions in Solution." Oxford Univ. Press.
— 1936*a* *Proc. Roy. Soc.* A, **157**, 667–79.
— 1936*b* *Acta Physicochim. U.R.S.S.* **4**, 173–224.
Newitt, D. M., Linstead, R. P., Sapiro, R. H. and Boorman, V. E. J. 1937 *J. Chem. Soc.* pp. 876–83.
Schulman, J. H. and Hughes, A. H. 1932 *Proc. Roy. Soc.* A, **138**, 430–50.
— — 1935 *Biochem. J.* **29**, 1243–52.
Schulman, J. H. and Rideal, E. K. 1931 *Proc. Roy. Soc.* A, **130**, 259–94.
— — 1933 *Biochem. J.* **27**, 1581–97.
Treub, J. P. 1917 *K. Akad. Wet. Amst.* **20**, 35–63.
— 1923 *Rec. trav. Chim. Pays-Bas*, **42**, 556–67.

Nitrogen Oxides in Internal Combustion Engine Gases

By T. K. Hanson, B.A. and A. C. Egerton, F.R.S.

(*Received* 31 *July* 1937)

INTRODUCTION

An account was given in a paper entitled "Proknocks and Hydrocarbon Combustion" (Ubbelohde, Drinkwater and Egerton 1935) of some experiments made to trace the source of the nitrogen peroxide which had been found by sampling the products from the cylinder of a petrol engine at various stages of the stroke. Those experiments indicated that it was not simply a matter of nitric oxide formed by the flame giving rise to the nitrogen peroxide, for different results were obtained using different exhaust-valve surfaces. Nevertheless it seemed probable that the flame should be mainly responsible for the formation of nitric oxide, and so further experiments have been made. In order to make progress it was essential to determine the amount of nitric oxide as well as the amount of nitrogen peroxide, and analytical methods had to be devised to do this. The first part of this note deals with the methods of determining small quantities (of the order of 10^{-4} mol. fraction) of total nitrogen oxides and of nitrogen peroxide, and the second part with the results of analyses of the gases sampled from the cylinder of internal combustion engines by the methods described by Egerton, Smith and Ubbelohde (1935) and by Drinkwater and Egerton for the C.I. engine in a paper shortly to be published.

1—ANALYTICAL METHODS

Nitrogen Peroxide

The concentration of nitrogen peroxide was determined by absorption in water followed by colorimetric estimation of the nitrite thus formed. The same reagent as used for the previous work, viz. a Griess-Islovsky solution: 0·1 g. α-naphthylamine in 100 c.c. N/100 acetic acid 5 c.c.; 0·5 g. sulphanilic acid in 100 c.c. N/100 acetic acid 5 c.c.; glacial acetic acid 10 c.c. The gases were bubbled through 5 c.c. of this reagent diluted to 50 c.c. with water in a sintered glass washer. The amount of acetic acid present is of importance. If there is too much present, absorption of the nitrogen peroxide is incomplete. On the other hand, if the acetic acid concentration is too low the formation of the pink compound is too slow and its decomposition too rapid for the maximum colour intensity to be attained. Absorption of the nitrogen peroxide was shown to be about 98 % complete in the first washer using a train of more than one washer.

The reaction is a slow one; it takes about half an hour for the maximum colour to develop. The pink compound formed decomposes slowly; this decomposition may be stopped by adding to the solution an equal volume of glacial acetic acid. Standard tints made up in this manner may be kept for several weeks. In this respect Hollins (1936) recommends the use of commercial alcohol as a stabilizing agent; acetic acid was found to be still more effective. Standard tints for the colorimeter were made from M/1000 nitrite solution. The results gave good agreement with the standard tints obtained from known amounts of nitrite ion.

The method is one of extreme delicacy for the estimation of small quantities of nitrogen peroxide (10^{-11} mol. fraction), but the accuracy of the estimation by the methods adopted would not be more than about ± 3 %.

The method of analysis was checked using air containing a known concentration of nitrogen peroxide. The required concentration of nitrogen peroxide was obtained:

(*a*) by passing air over solid nitrogen peroxide at a constant low temperature, and

(*b*) by introducing a measured slow stream of nitric oxide into a measured air stream.

Total oxides of nitrogen

There were only two chemical methods available which seemed likely to succeed in estimating the amount of nitric oxide:

1—Oxidation to nitrogen peroxide and determination with the Griess reagent.

2—Oxidation to nitric acid and determination with phenol disulphonic acid.

Much work has been done by Gas Companies on the estimation of small amounts of nitric oxide in coal gas, owing to the effect that nitric oxide has in causing gum to form in gas pipes, etc. None of the methods developed was satisfactory for the problem in hand, because those methods involve doubtful correction factors and can be applied only when the composition of the gas to be analysed is approximately constant. This condition certainly does not apply to the gas extracted from the cylinder of an internal combustion engine during different parts of the cycle. Any method which involved correction factors and which was not strictly quantitative had to be avoided.

Two methods devised for the estimation of nitric peroxide have found general application:

1—The oxidation of nitrogen peroxide with an aqueous oxidizing agent.

2—The oxidation of nitrogen peroxide by oxygen with or without a catalyst.

Referring to method 1, Guyer and Weber (1933) and Hollins (1936) used aqueous potassium permanganate as the oxidizing agent. Other oxidizing agents have been tried by the authors but found not so satisfactory as permanganate. The gas was passed through a spiral washer containing acid permanganate and then through a solution of the Griess reagent. The yield of nitrogen peroxide is low. Hollins found that a correction factor of three should be applied at the optimum gas flow of 1 cu. ft./hr.; Guyer and Weber found that the correction factor varied with the concentration of nitric oxide in the gas. A number of experiments were performed to investigate the possibility of modifying this method so that it might be employed for the estimation of nitric oxide in engine cylinder gases. Mixtures for analysis were prepared by introducing a small volume of nitric oxide at low pressure into a large volume of nitrogen. It was found that when the gas flow was low, over 90 % of the nitric oxide remained in the permanganate as nitric acid. With a small flow of gas, as must be the case when samples of gas are being taken from an engine cylinder, the yield of nitrogen peroxide depended on: (*a*) the concentration of nitric oxide, (*b*) the rate of gas flow, (*c*) the temperature, and (*d*) the type of washer used for the oxidation. Even at the optimum gas flow rate, a constant correction factor probably only applies to a very limited range of nitric oxide concentration. The method is no doubt suitable for the very small concentration of nitric oxide in town's gas, but could not be adapted for the present work.

The second method, the oxidation of nitric oxide to nitrogen peroxide by oxygen, was used by Fulweiler (1935). Using oxygen alone, the yield of nitrogen peroxide was low and a variable correction factor had to be applied. In a later modification of the method butadiene was used as a catalyst and an improved yield of nitrogen peroxide was obtained. As the gases obtained from an engine might, and probably do, contain substances which catalyse the oxidation of nitric oxide to nitrogen peroxide, this method is of little value.

In view of the difficulties involved in converting nitric oxide to nitrogen peroxide the first alternative for the estimation of nitric oxide was abandoned and both nitric oxide and nitrogen peroxide were converted into nitric acid, this compound being then estimated colorimetrically with phenol disulphonic acid. The difficulty then arose in absorbing the nitric oxide by the oxidizing agent. A bubbling method was first used, for it had been shown that nitric oxide is completely absorbed by acid permanganate if the rate of gas flow is sufficiently low. It was not found easy however to estimate nitric acid accurately in the presence of a large excess of permanganate, but the following method was found to be fairly satisfactory. The acid permanganate was made up with rather less than the theoretical amount of sulphuric acid. After the nitrogen oxides had been absorbed, hydrogen peroxide was added until the solution was colourless and a slight precipitate of manganese dioxide was brought down. After the manganese dioxide had been filtered off, the now neutral solution was evaporated and the nitric acid estimated in the usual manner. The method was not sufficiently accurate because the solid residue was too bulky and it was impossible to ensure that the phenol disulphonic acid reagent reacted completely with the residue.

Hydrogen peroxide, since it leaves no residue, was a more convenient oxidizing agent. However, it is impossible completely to absorb the oxides of nitrogen by washing unless a lengthy absorption train was used, and this was ruled out on account of the large dead space involved. The gases to be estimated therefore were collected in an evacuated vessel and allowed to stand for several hours in presence of hydrogen peroxide.

The samples from the engine could not be collected direct into the evacuated vessel, for leakage would occur along the sampling valve gland; by making connexion with the valve through a variable leak so regulated that the pressure inside the sampling valve was always slightly above atmospheric, this difficulty was overcome.

The oxidizing agent used was 25 vol. hydrogen peroxide containing 1 % normal sulphuric acid. The nitric acid thus formed was estimated colorimetrically by the phenol disulphonic acid method. This method of analysis proved to be satisfactory and as little as 5×10^{-6} g.-molecules of nitric oxide in a sample could be estimated with an error of not more than $\pm 2 \cdot 5$ %. Standard M/100 potassium nitrate solution was used along with the phenol disulphonic acid reagent as standard for comparison in the colorimeter.

2—ANALYSES OF GASES SAMPLED FROM ENGINES

Production of Nitrogen Oxides in a C.I. Engine

The engine used was a Crossley-Ricardo single cylinder compression ignition engine fitted with sampling valve (Drinkwater and Egerton—paper in course of publication). The engine speed was 600 r.p.m. The fuel used was

Anglo-American diesel oil. As a rule the engine was run so that the water inlet temperature was 10° C. and the outlet temperature 55° C., but the outlet temperature could be varied from 10 to 95° C., if required.

Fig. 1 shows the formation of the nitrogen oxides in the engine. The separate curves* refer to measurements of:

A—Nitrogen peroxide at no load.
B—Nitrogen peroxide; load 2·41 h.p.
C—Total nitrogen oxides at no load.
D—Total nitrogen oxides; load 2·41 h.p.

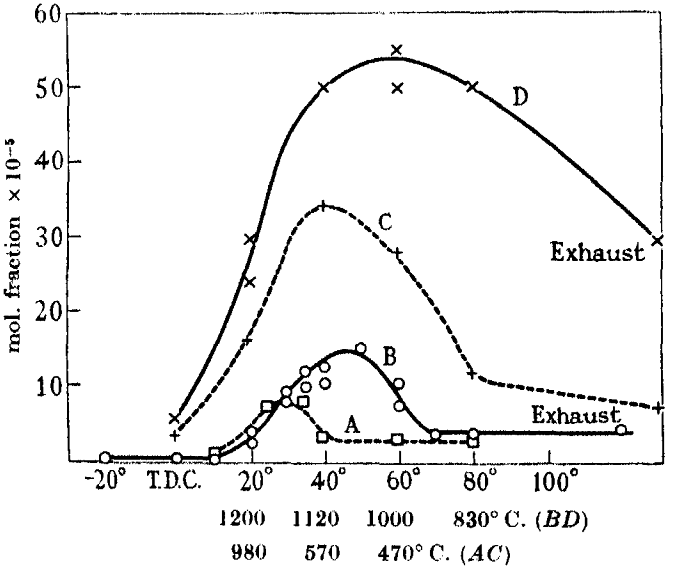

Fig. 1

The samples were taken from the comet chamber with the valve flush with the wall, the nitrogen oxides commenced to be formed about the same moment after injection as combustion was shown to commence (Drinkwater and Egerton), and increased to a maximum later in the stroke. The maximum for nitrogen peroxide was 30–40° after T.D.C. The nitrogen peroxide then decreased but the total oxides increased for another 20° and then began to diminish. At light loads very little nitric oxide is present in the exhaust, nearly the whole being present as nitrogen peroxide ($4 \cdot 10^{-5}$ mol. fraction).

---

* The mol. fraction or number of mols. per mol. of total gas is plotted against degrees of crank angle, for instance in fig. 1, curve *D*, the maximum concentration of total oxides of nitrogen is given by the fraction $50 . 10^{-5}/1$.

These experiments were carried out under conditions where there was considerable excess of oxygen present throughout the stroke. The decrease in the total oxide concentration is possibly due to absorption of the nitrogen oxides by oil or other products present in the cylinder the nitrogen peroxide being removed more rapidly; it does not seem to be due to re-establishment of equilibrium $2NO \rightleftharpoons O_2 + N_2$ at the lower temperatures in the cylinder during the later part of the stroke, for this explanation is not borne out by the results obtained with the petrol engine.

Fig. 2 shows the effect of water-jacket temperature on the concentration of nitrogen peroxide. The results were obtained when the water outlet temperature was 10, 55 and 95° C. Maxima of the nitrogen oxide concentrations varying between 30 and 60° after T.D.C. are again shown in these experiments. With the cold walls (10° C.) the amount of nitrogen peroxide formed was much less, as if it was being removed by absorption by moisture as well as by oil on the walls of the cylinder.

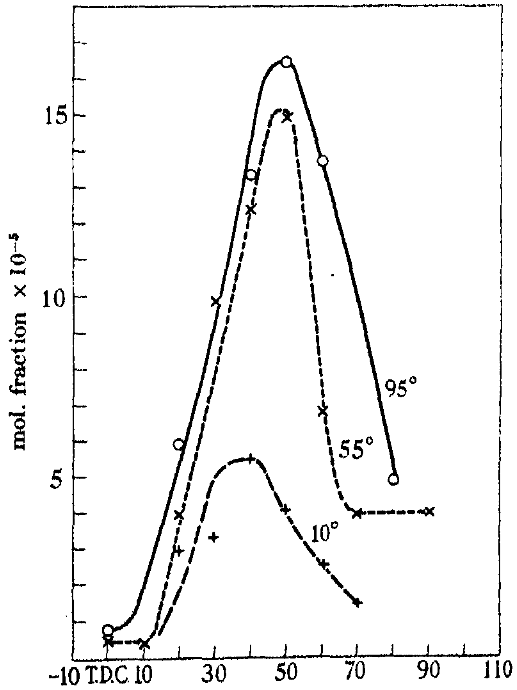

Fig. 2

The average temperatures of the gases in the cylinder are given in fig. 1. The average temperature at point of maximum pressure was 1200° for curves *B* and *D* and 1050° for curves *A* and *C*. These were low because the engine was running at slow speed under light load and required little fuel. Local flame temperature in the comet head would presumably be higher, and the maximum nitrogen oxides formed (0·06 %) were such as might be expected from the known figures for the nitrogen oxide equilibrium.

Production of Nitrogen Oxides in the Petrol Engine

The engine employed was the Delco knock-rating unit mentioned in previous papers. The following engine conditions were maintained throughout:

Fuel: Shell No. 1 petrol.
Speed: 600 r.p.m.
Water jacket temperature: 100° C.
Spark: 22°.

Figs. 3 and 4 show the production of nitrogen oxides at two different loads. The figures are drawn to very different scale. In the latter case continuous heavy detonation occurred, in the former case the engine was just not knocking. The difference in the yield of nitrogen oxides is very marked.

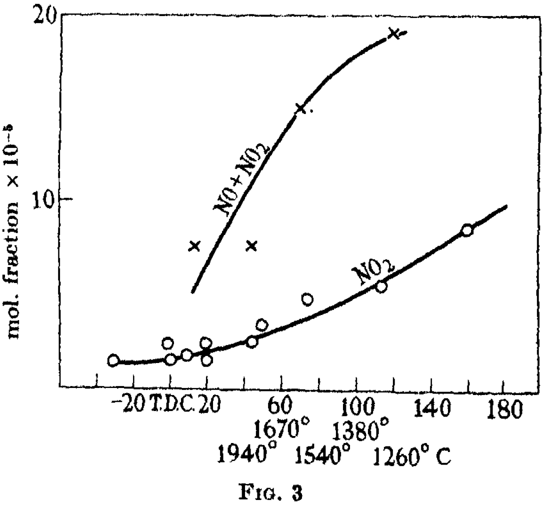

Fig. 3

In the case of the petrol engine, both nitrogen peroxide and total oxides increased throughout the expansion stroke in spite of falling temperature. The temperature at point of maximum pressure (+28°) was 1787° C. for the experiments shown in fig. 3 and was 2900° C. at +16° for those in fig. 4. The corresponding equilibrium amounts of nitric oxide (Lewis and v. Elbe 1935) would be about 0·6 and 1·6 % respectively, taking into account the oxygen concentration at the maximum temperature. The maximum concentrations found are therefore in both cases less than the amount which can be formed thermally in the flame, but in both cases the amounts are greater than would correspond to the temperature prevailing in the cylinder later in the stroke. For the experiments recorded in fig. 4 the flame would have reached the valve and all the combustion taken place by 20° after T.D.C. (Egerton and others 1935, p. 446, fig. 5). It is known that the actual flame breadth is small and the reaction is complete within quite a narrow region, so that the continued increase in the formation of nitric oxide (up to as much as $5 \cdot 10^{-3}$ mol. fraction) in spite of falling temperature is remarkable and may be connected with the presence of excited molecules which apparently exist (Withrow and Rassweiler 1932) in the charge and give rise to luminosity long after passage of the flame proper. The appreciable concentration of nitrogen peroxide is remarkable, because the oxygen concentration was low (< 2 %). If it was formed as the gases cool down, varying the length of time between sampling and analysing should have affected the result, but this was not the case. The amount of nitric oxide to nitrogen peroxide found was approximately 4 : 1.

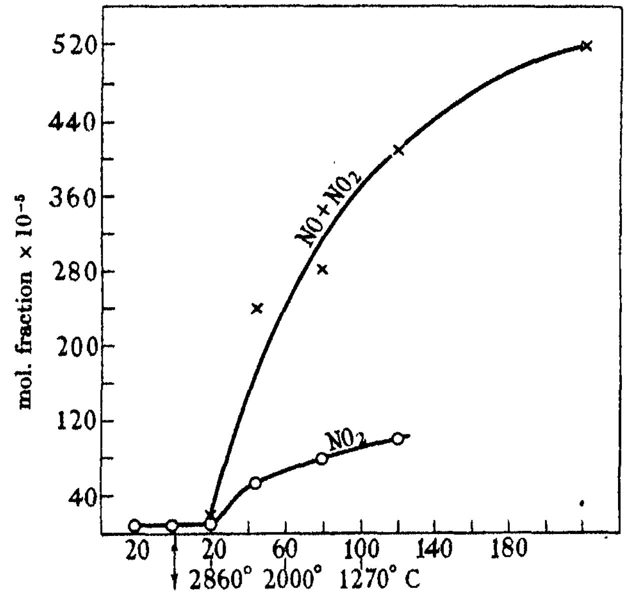

Fig. 4

Fig. 5 shows the effect of load on the production of nitrogen peroxide. The rise in concentration of nitrogen peroxide when knocking commenced was very marked. The values shown in this curve were all obtained at a constant sampling position, namely + 100°. The concentrations shown in fig. 5 are somewhat lower than the values given in fig. 4. This was probably due to the fact that the results shown in fig. 5 were obtained shortly after new oil had been added to the engine.

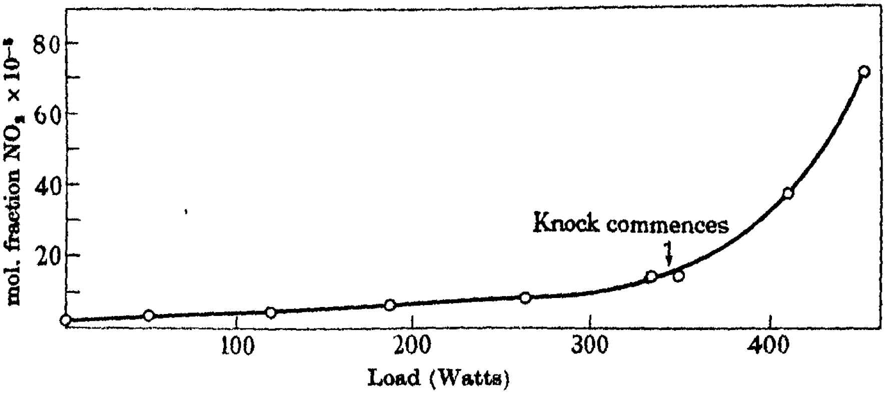

FIG. 5

It was found that the addition of new oil to the sump of the petrol engine caused a decrease in the concentration of the nitrogen peroxide in the later part of the expansion stroke. After about 20 hr. running, however, the concentration of nitrogen peroxide rose to the value previously obtained and then remained at that value; the oil apparently does not thereafter remove more than a constant small amount of nitrogen peroxide.

Determination of Temperature of Gases in the Engine Cylinder

The temperatures in the cylinder have been determined using the Farnborough Indicator with the Diesel engine and the Standard Sunbury Oscillograph Indicator with the petrol engine in conjunction with a cinematograph camera. Pressures less than 2 atm. were measured by connecting a manometer to the sampling valve. A calibrated orifice meter measured the air supply.

For the petrol engine, the conditions were:

(*a*) Load 0·209 kW.
Maximum pressure 224 lb./sq. in. at 28° after T.D.C.
Volume at maximum pressure 6·2 cu. in.
Air flow 2·04 ft./min.

(*b*) Load 0·456 kW.
Maximum pressure 496 lb./sq. in. at 16° after T.D.C.
Volume at maximum pressure 5·0 cu. in.
Air flow 2·35 ft.^{3}/min.

Correcting for the residuals, the number of gram-molecules of gas present in the cylinder after combustion for 100 g./molecules of air input was found and the temperature at maximum pressure calculated from the above pressure and volume measurements; this gave the figure 2907° C. in the case (*b*). This figure was checked by another method using the figures of Lewis and v. Elbe (1935) for specific heat of the gas and the heat of combustion of the fuel corrected for the carbon monoxide in the gas obtained from the analysis by the sampling method. As the oxygen was just all consumed by + 10° and the flame reaches the valve close to T.D.C. under these particular engine conditions, the sampled gases are probably fairly representative of the contents of the cylinder and the correction for the carbon monoxide sufficiently accurate. The result by this method was 2887° C., i.e. within 20° of the other estimate. Once the maximum temperature was obtained, it was easy to deduce the other temperatures from the indicator diagrams (see fig. 6).

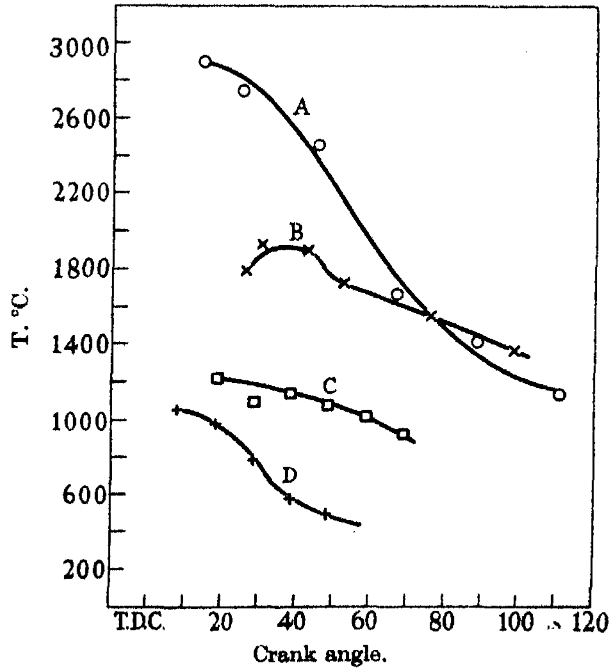

A—Petrol engine, load 0·456 kW. *B*—Petrol engine, load 0·209 kW.
C—Diesel engine, load 2·41 h.p. *D*—Diesel engine, no load.

FIG. 6

The authors are grateful to the Air Ministry for loan of the Indicators, and to the Salter's Institute and Trinidad Leaseholds, Ltd., for grants

(to T. K. H.), and to the Gas Light and Coke Co. for information relating to determination of nitric oxide in town's gas.

CONCLUSION

These experiments show that the nitrogen oxides have their origin amongst the hot gases in the engine cylinder, that they tend to be removed by the oil, that they are affected by the cylinder-wall temperature, that they increase rapidly under detonating conditions, and that the increase in nitrogen peroxide noted in previous experiments during the compression stroke must have been due to nitric oxide in residual gas combining with oxygen (the reaction being catalysed possibly by the valve surfaces).

Experiments have been carried out on the effect of nitrogen oxides in the dilution that they occur in the engine cylinder, on lubricating oils; and it has been found that they cause rapid gumming of the oil, acting as catalysts for the oxidation of the oil. It is therefore important to study the behaviour of various kinds of fuel as regards the amount of nitrogen oxides produced and the experiments are therefore being extended.

REFERENCES

Egerton, Smith and Ubbelohde 1935 *Phil. Trans.* A, **234**, 433–521.
Fulweiler 1935 *Amer. Gas (Engng) J.* **142**, 27.
Guyer and Weber 1933 *Brennst.-Chemie*, **14**, 405.
Hollins 1936 *Trans. Instn Gas. Engrs, Lond.*, **147**, .
Lewis and v. Elbe 1935 *J. Amer. Chem. Soc.* **4**, 612–14.
Ubbelohde, Drinkwater and Egerton 1935 *Proc. Roy. Soc.* A, **153**, 103–15.
Withrow and Rassweiler 1932 *J. Industr. Engng Chem.* **24**, 528–38.

The Interaction of Atoms and Molecules with Solid Surfaces

X—The Activation of Adsorbed Atoms by Metallic Electrons

By J. E. Lennard-Jones, F.R.S. and E. T. Goodwin
The University Chemical Laboratory, Cambridge

(*Received* 5 *August* 1937)

1—Introduction

One object of this series of papers (Lennard-Jones and others 1935–7) is to consider in detail the mechanism of condensation, migration and evaporation of atoms and molecules at solid surfaces and to try to find the processes which govern the transition from one state to another. It has been shown that under certain conditions the thermal vibrations of a solid may activate an adsorbed atom from one vibrational state to a higher one or even eject it from the surface altogether. But the theory there developed is limited in the sense that it deals only with the transfer of single quanta to or from the solid, and consequently the quantized vibrational levels of the adsorbed atom must be closer together than the largest single quantum of energy which the solid can emit. An attempt has been made (Strachan 1937) to find the probability of the simultaneous emission or absorption of several quanta by the solid, and the indication is that the probability of several such simultaneous events is small. Now when atoms are bound to solid surfaces by valency forces, the vibrational levels are widely spaced compared with those of the solid, and many thermal quanta must be transferred simultaneously to the adsorbed atom to change its state of vibration. While this process may occur in nature, it seemed desirable to look for other possible processes whereby adsorbed atoms could be activated to higher vibrational states. One such possible mechanism, in metals at any rate, is by the transfer of energy from the conduction electrons. A simple calculation by classical methods indicates that in a typical case a surface atom may suffer as many as 10^{15} collisions per second with the "free" electrons of a metal, and as, according to modern views, these electrons are moving with an energy of several volts, there is here an ample reservoir of energy from which adsorbed atoms may absorb energy or to which they can re-emit it, and thus change their vibrational state, or indeed, also their electronic state.

In this paper we make an attempt to estimate the frequency with which adsorbed atoms are activated by the conduction electrons of the underlying metal. The problem is not an easy one and certain approximations are necessary to render the analysis tractable, but they have been so designed as to represent as closely as possible the physical conditions of the actual process and to indicate the orders of magnitude of the principal quantities involved.

2—THE INTERACTION OF METALLIC ELECTRONS AND AN ADSORBED ATOM

We suppose that an atom X is adsorbed on the surface of a metal and that it may be regarded as attached to one of the metal atoms M, the two forming a complex MX. We are interested mainly in the vibration of X and M relative to each other, and so the first simplification we introduce is to suppose that the MX axis is perpendicular to the surface and remains so, the motion of X parallel to the surface being ignored. The free electrons of the metal are considered as independent in the sense usually adopted in the theory of metals, each electron being assumed to move in the averaged field of all the other electrons. We then calculate the interaction of one such electron with the MX group and subsequently sum over all the conducting electrons.

Let ρ denote the internuclear distance between M and X and let $\mathbf{r}$ (or r, θ, ϕ) specify the position of a conduction electron in the metal relative to a fixed point C on the nuclear axis (to be chosen later) and MX as polar axis. The wave equation of the interacting MX and electron systems is then

$$\left\{\frac{h^2}{8\pi^2 m}\nabla_{\mathbf{r}}^2+\frac{h^2}{8\pi^2 M}\frac{\partial^2}{\partial\rho^2}+\frac{h}{2\pi i}\frac{\partial}{\partial t}-V(\mathbf{r})-V(\rho)-V(\mathbf{r},\rho)\right\}\Phi(\mathbf{r},\rho,t)=0, \quad (1)$$

where m and M denote the mass of the electron and the reduced mass of the MX group respectively; $V(\mathbf{r})$, $V(\rho)$ and $V(\mathbf{r},\rho)$ are the potential energies of the electron, the mutual interaction of metal and adsorbed atom, and the interaction of electron and the MX group respectively. We solve this equation in the usual way in terms of the solutions of the equation obtained from that above by setting $V(\mathbf{r},\rho)$ equal to zero. These latter solutions are of the type

$$\psi_{\lambda\mu}(W,\mathbf{r})\,\phi_n(\rho)\,e^{2\pi it(W+E_n)/h}, \quad (2)$$

where

$$\psi_{\lambda\mu}(W,\mathbf{r})\,e^{2\pi itW/h}$$

is a solution of
$$\left\{\frac{h^2}{8\pi^2 m}\nabla_r^2+\frac{h}{2\pi i}\frac{\partial}{\partial t}-V(\mathbf{r})\right\}\psi=0, \tag{3}$$

and $\phi_n(\rho)\,e^{2\pi i t E_n/h}$ is a solution of
$$\left\{\frac{h^2}{8\pi^2 M}\frac{\partial^2}{\partial\rho^2}+\frac{h}{2\pi i}\frac{\partial}{\partial t}-V(\rho)\right\}\phi=0. \tag{4}$$

The state of the electron is described by three quantum numbers, W a continuous variable, which refers to the total energy of the electron, and λ, μ which refer to the angular coordinates. The adsorbed atom, being described by one coordinate, requires only one quantum number n to specify its state of vibration. The wave functions which are solutions of (3) and (4) are supposed normalized to give

$$\int\phi_{n'}^*(\rho)\,\phi_n(\rho)\,d\rho=\delta_{nn'}, \tag{5}$$

$$\int\psi_{\lambda'\mu'}^*(W',\mathbf{r})\,\psi_{\lambda\mu}(W,\mathbf{r})\,d\tau=\delta_{\lambda\lambda'}\delta_{\mu\mu'}\delta(W'-W). \tag{6}$$

We write for the solution of (1)
$$\Phi(\mathbf{r},\rho,t)=\sum_q a_{\lambda,\mu,n}(W,t)\,\psi_{\lambda\mu}(W,\mathbf{r})\,\phi_n(\rho)\,e^{2\pi i t(W+E_n)/h}, \tag{7}$$

where the summation $\sum_q$ is over *all* quantum numbers; it extends over all the discrete quantum numbers λ, μ and n, and implies an integration over all values of W. If we suppose that initially the combined system is in a state described by the discrete quantum numbers λ, μ and n while the continuous variable lies in the range W to $W+dW$, or symbolically
$$|a_{\lambda'\mu'n'}(W',0)|^2=\delta_{\lambda\lambda'}\delta_{\mu\mu'}\delta_{nn'}\delta(W'-W), \tag{8}$$

and if the perturbing interaction $V(\mathbf{r},\rho)$ is sufficiently small to allow of the supposition that the coefficients $a_{\lambda\mu n}$ remain sensibly constant during the time of interaction, then the usual method of solution leads to

$$\begin{aligned}&|a_{\lambda',\mu',n'}(W',t)|^2\,dW'\\&\quad=|(W'\lambda'\mu'n'\,|\,V\,|\,W\lambda\mu n)|^2\,\frac{4\sin^2\pi t\{(W+E_n-W'-E_{n'})/h\}}{(W+E_n-W'-E_{n'})^2}\,dW\,dW'\\&\quad=\Gamma_{W\lambda\mu n}^{W'\lambda'\mu'n'}\,dW\,dW',\end{aligned} \tag{9}$$

where
$$(W'\lambda'\mu'n'\,|\,V\,|\,W\lambda\mu n)=\int\psi_{\lambda'\mu'}^*(W',\mathbf{r})\,\phi_{n'}^*(\rho)\,V(\mathbf{r},\rho)\,\psi_{\lambda,\mu}(W,\mathbf{r})\,\phi_n(\rho)\,d\tau\,d\rho. \tag{10}$$

Then $\Gamma^{W'\lambda'\mu'n'}_{W\lambda\mu n}\,dW\,dW'$ is interpreted as the probability of transition from the initial state dW, λ, μ, n to another state dW', λ', μ', n'. This definition of Γ requires the electronic wave functions in the continuous variables W and W' to be normalized with respect to energy as in (6).

3—EVALUATION OF THE MATRIX ELEMENTS

In order to evaluate the matrix element given by (10) it is necessary to have a detailed knowledge of $V(\mathbf{r})$, $V(\rho)$ and $V(\mathbf{r}, \rho)$. A study of the surface and conduction properties of metals has provided some information about $V(\mathbf{r})$, and infra-red spectra something about the field between two atoms in a diatomic molecule, but there is at present no indication of the nature of the interaction between an electron and a group such as MX. It is known, however, that most diatomic molecules which contain unlike atoms have a dipole moment, and we may be fairly certain that most neutral atoms attached to a metallic surface lead to the existence of a dipole moment. There will thus be a long-range interaction with the electrons of the metal of the type

$$V(\mathbf{r}, \rho) = e\mu(\rho)\cos\theta/r^2, \tag{11}$$

but the potential at short distance will probably be much more complicated than this because of the complex electronic system of the group MX. Presumably "exchange" or other forces of a like nature will lead to repulsive forces at small values of r, and these will be discussed presently.

The origin from which the dipole field is measured must be chosen so that (11) is as accurate a representation of the distant field as possible, and the most suitable one is the equilibrium position of the centre of charge of the electronic system MX. The dipole moment $\mu(\rho)$ will be a function of the extension of the link between M and X. For small changes from the equilibrium value ρ_0 of ρ, we can write

$$\mu(\rho) = \mu(\rho_0) + (\rho - \rho_0)\left(\frac{d\mu}{d\rho}\right)_0 + \dots, \tag{12}$$

and this will be valid for states of small vibrational quantum number. The matrix element of $\mu(\rho)$ with respect to the vibrational states is then nearly the same as that of $\rho(\partial\mu/\partial\rho)_0$, for the matrix element of the constant term in (12) vanishes because of the orthogonal properties of the wave functions and those of the squares and higher powers of ρ prove to be of a smaller order of magnitude than those of ρ.

Under these conditions we have

$$(W'\lambda'\mu'n' \mid V \mid W\lambda\mu n) = e(\partial\mu/\partial\rho)_0\, g^{\lambda'\mu'W'}_{\lambda\mu W}\,\rho_{n'n}, \tag{13}$$

where
$$g^{\lambda'\mu'W'}_{\lambda\mu W} = \int \psi^*_{\lambda'\mu'}(W', \mathbf{r})\,(\cos\theta/r^2)\,\psi_{\lambda\mu}(W, \mathbf{r})\,d\tau \tag{14A}$$

and $\rho_{n'n}$ is the matrix element of ρ, viz.

$$\rho_{n'n} = \int \phi^*_{n'}(\rho)\,\rho\,\phi_n(\rho)\,d\rho. \tag{14B}$$

To proceed further we must now find suitable wave functions $\psi_{\lambda\mu}(W, \mathbf{r})$ and $\phi_n(\rho)$.

3·1—*The Electronic Wave Functions*

One method of representing the field in which the "free" electrons of a metal move is to take a constant potential inside the metal and to suppose that there is a potential discontinuity at the surface. To preserve the essential features of this field we shall suppose that there is a constant potential inside the metal except for a region within a distance r_0 of the origin from which r is measured. Within this hemisphere we shall suppose that the potential jumps by an amount χ. This change in potential is a rough attempt to represent the change in the environment of M due to the fact that its valency electron is no longer free but is shared with X to produce a homopolar bond. The group MX is thus more inert with respect to an electron than other metallic atoms, and there is accordingly a short-range repulsive field surrounding it. The amount of this discontinuity will probably be of the same order as the work function of the metal, though it is not necessarily identical with it for the same reason that the work function is raised or lowered by the presence of adsorbed films. In accordance with this picture it would be natural to assume a discontinuity of amount χ' at the rest of the surface to represent the work function of the clean metal. Then at the flat part of the hemisphere there would have to be a further potential discontinuity of amount $\chi' - \chi$.

If we were interested mainly in the escape of electrons from the system, this picture of the potential field would be necessary, but the main problem of this paper is to consider the effect of the electrons on the vibrating system MX. We are thus concerned with the interaction of those electrons which in classical language are said to "collide" with the system MX or in quantal language penetrate into the hemispherical region of potential χ. The electrons which collide with the surface outside the hemispherical region will have little or no effect on the MX group, and so it will not affect the phenomenon we wish to study if χ' is made infinite while χ remains finite. It simplifies the mathematics if this picture is adopted, as the electron wave functions can be expressed in terms of simple functions. It suffers from one defect in that the centre of charge of the MX electronic system is assumed to be at the centre of the hemisphere and this is identified with the surface. It also causes the wave functions to vanish at the centre of charge of MX which they would not actually do though they would probably be small owing to the effect of the χ-region.

The mathematical representation of the field is thus

$$V(r) = 0 \text{ when } r > r_0 \text{ and } \theta < \tfrac{1}{2}\pi,$$

$$V(r) = \chi \text{ when } r < r_0 \text{ and } \theta < \tfrac{1}{2}\pi,$$

$$V(r) = \infty \text{ for all } r \text{ when } \theta > \tfrac{1}{2}\pi,$$

and the wave equation for the electrons for $\theta < \frac{1}{2}\pi$ is

$$\left.\begin{aligned} &\nabla^2\psi + (8\pi^2 m/h^2)\, W\psi = 0 && \text{for } r > r_0,\\ &\nabla^2\psi + (8\pi^2 m/h^2)\,(W-\chi)\,\psi = 0 && \text{for } r < r_0.\end{aligned}\right\} \tag{15}$$

The boundary conditions are $\psi = 0$ at $\theta = \frac{1}{2}\pi$, while ψ and $\partial\psi/\partial r$ must be continuous at $r = r_0$. If we write

$$k^2 = 8\pi^2 m W/h^2, \quad \kappa^2 = 8\pi^2 m(\chi - W)/h^2, \tag{16}$$

the appropriate solutions† are for $r > r_0$,

$$\psi_{\lambda,\mu}(W, \mathbf{r}) = N_{\lambda\mu}(W)\, Y_\lambda^{|\mu|}(\theta, \phi)\, \{J_{\lambda+\frac{1}{2}}(kr) + \alpha_{\lambda\mu}(W)\, J_{-(\lambda+\frac{1}{2})}(kr)\}/(kr)^{\frac{1}{2}}, \tag{17}$$

and for $r < r_0$

$$\psi_{\lambda,\mu}(W, \mathbf{r}) = N_{\lambda\mu}(W)\, Y_\lambda^{|\mu|}(\theta, \phi)\, \beta_{\lambda\mu}(W)\, I_{\lambda+\frac{1}{2}}(\kappa r)/(\kappa r)^{\frac{1}{2}}, \tag{18}$$

where $\lambda - \mu$ is odd; $J(kr)$ and $I(\kappa r)$ denote the usual Bessel functions (cf. Watson 1922) and Y_λ^μ a Legendre function.

---

† The electronic wave functions could be improved by taking into account the effect of the constant part of the dipole, given in (12). This has been examined and has been found to be equivalent roughly to changing the *order* of the Bessel functions. It was considered to be a refinement which would hardly justify the extra labour involved, at any rate at this stage.

The constants N, α and β are determined by the continuity relations

$$\{J_{\lambda+\frac{1}{2}}(kr_0)+\alpha_{\lambda\mu}(W)\,J_{-(\lambda+\frac{1}{2})}(kr_0)\}/(kr_0)^{\frac{1}{2}} = \beta_{\lambda\mu}(W)\,I_{\lambda+\frac{1}{2}}(\kappa r_0)/(\kappa r_0)^{\frac{1}{2}}, \tag{19}$$

$$\left[\frac{d}{dr}\frac{J_{\lambda+\frac{1}{2}}(kr)}{(kr)^{\frac{1}{2}}}\right]_{r_0}+\alpha_{\lambda\mu}(W)\left[\frac{d}{dr}\frac{J_{-(\lambda+\frac{1}{2})}(kr)}{(kr)^{\frac{1}{2}}}\right]_{r_0} = \beta_{\lambda\mu}(W)\left[\frac{d}{dr}\frac{I_{\lambda+\frac{1}{2}}(\kappa r)}{(\kappa r)^{\frac{1}{2}}}\right]_{r_0}, \tag{20}$$

together with the normalizing condition (6).

$Y_\lambda^{|\mu|}(\theta, \phi)$ denotes the normalized angular part of $\psi_{\lambda\mu}(W, \mathbf{r})$, viz.

$$Y_\lambda^{|\mu|}(\theta, \phi) = \{(2\lambda+1)/2\pi\}\{(\lambda-|\mu|)!/(\lambda+|\mu|)!\}^{\frac{1}{2}}\,P_\lambda^{|\mu|}(\cos\theta)\,e^{i\mu\phi}, \tag{21}$$

the 2π in the denominator replacing the usual 4π because of the limited range of θ. Since $\lambda-\mu$ must be odd, λ can take all positive integral values and

$$\mu = \lambda-1, \quad \lambda-3, \quad \ldots, \quad -(\lambda-3), \quad -(\lambda-1).$$

Equation (20), with the application of the recurrence relations for the Bessel functions, leads to

$$\alpha_{\lambda\mu}(W) = \alpha_\lambda(k) = \frac{kr_0 J_{\lambda-\frac{1}{2}}(kr_0)\,I_{\lambda+\frac{1}{2}}(\kappa r_0)-\kappa r_0 J_{\lambda+\frac{1}{2}}(kr_0)\,I_{\lambda-\frac{1}{2}}(\kappa r_0)}{kr_0 J_{-(\lambda-\frac{1}{2})}(kr_0)\,I_{\lambda+\frac{1}{2}}(\kappa r_0)+\kappa r_0 J_{-(\lambda+\frac{1}{2})}(kr_0)\,I_{\lambda-\frac{1}{2}}(\kappa r_0)}, \tag{22 A}$$

$$\beta_{\lambda\mu}(W) = \beta_\lambda(k) = (k\kappa)^{\frac{1}{2}}\frac{J_{\lambda-\frac{1}{2}}(kr_0)\,J_{-(\lambda+\frac{1}{2})}(kr_0)+J_{-(\lambda-\frac{1}{2})}(kr_0)\,J_{\lambda+\frac{1}{2}}(kr_0)}{kJ_{-(\lambda-\frac{1}{2})}(kr_0)\,I_{\lambda+\frac{1}{2}}(\kappa r_0)+\kappa J_{-(\lambda+\frac{1}{2})}(kr_0)\,I_{\lambda-\frac{1}{2}}(\kappa r_0)}, \tag{22 B}$$

and using the formula

$$J_p(x)\,J_{-p+1}(x)+J_{p-1}(x)\,J_{-p}(x) = 2(\sin p\pi)/\pi x$$

we have

$$\beta_\lambda(k) = \frac{(-1)^\lambda(2/\pi)\,(\kappa/k)^{\frac{1}{2}}}{(kr_0)\,J_{-(\lambda-\frac{1}{2})}(kr_0)\,I_{\lambda+\frac{1}{2}}(\kappa r_0)+\kappa r_0\,J_{-(\lambda+\frac{1}{2})}(kr_0)\,I_{\lambda-\frac{1}{2}}(\kappa r_0)}. \tag{22 C}$$

Since $\alpha_{\lambda\mu}(W)$ and $\beta_{\lambda\mu}(W)$ are here written as functions of k (κ being known when k is given from (16)), and since they are independent of μ, we have abbreviated them to $\alpha_\lambda(k)$ and $\beta_\lambda(k)$.

The normalization factor $N_{\lambda\mu}(W)$ can be obtained by a method due to Fues (1926*a*), of which an example has been worked out in Paper II (Strachan, 1935) or by making the range of r large but finite and working out the normalization factor for each discrete state in the usual way and then allotting to each such state a weight unity. The density of states as the range increases can easily be found and the appropriate normalization factor for the continuum inferred. The asymptotic form of a normalized wave function in radial coordinates for very large r contains a diverging part

$$e^{-ikr}/h^{\frac{1}{2}}v^{\frac{1}{2}}r,$$

and, if it is a standing wave, a similar converging part, where $k = 2\pi mv/h$ and v is the velocity. This implies that the influx of electrons of energies between W and $W+dW$ across a large sphere in unit time is dW/h. In conformity with this we find

$$N^2_{\lambda\mu}(W) = N^2_{\lambda}(k) = \frac{4\pi^2 mk}{h^2(1+\alpha^2_{\lambda})}, \tag{23}$$

and this completes the determination of $\psi_{\lambda\mu}(W, \mathbf{r})$.

3·2—*The Evaluation of* $g^{\lambda'\mu'W'}_{\lambda\mu W}$

The integral $g^{\lambda'\mu'W'}_{\lambda\mu W}$, defined in equation (14A), can now be expressed as the product of two factors, one involving an integration with respect to r and the other an integration over the angular coordinates. The latter integral is

$$y^{\lambda'\mu'}_{\lambda\mu} = \left\{\frac{2\lambda+1}{2\pi}\frac{(\lambda-|\mu|)!}{(\lambda+|\mu|)!}\right\}^{\frac{1}{2}}\left\{\frac{2\lambda'+1}{2\pi}\frac{(\lambda'-|\mu'|)!}{(\lambda'+|\mu'|)!}\right\}^{\frac{1}{2}}$$

$$\times\int_0^{\frac{1}{2}\pi}\int_0^{2\pi} P^{|\mu|}_{\lambda}(\cos\theta)\,P^{|\mu'|}_{\lambda'}(\cos\theta)\,e^{i(\mu-\mu')\phi}\cos\theta\sin\theta\,d\theta\,d\phi, \tag{24}$$

where $P^{\mu}_{\lambda}(\cos\theta)$ is the usual Legendre function, normalized to have a value of unity at $\theta = 0$. The integral is zero unless $\mu = \mu'$ and then we require, writing x for $\cos\theta$,

$$\int_0^1 P^{|\mu|}_{\lambda}(x)\,P^{|\mu|}_{\lambda'}(x)\,x\,dx \tag{25}$$

for $\lambda-\mu$ and $\lambda'-\mu$ both odd.

Using the relation

$$(2\lambda+1)\,x\,P^{|\mu|}_{\lambda}(x) = (\lambda-|\mu|+1)\,P^{|\mu|}_{\lambda+1}(x)+(\lambda+|\mu|)P^{|\mu|}_{\lambda-1}(x), \tag{26}$$

we find that the evaluation of (25) depends on

$$\int_0^1 P^{|\mu|}_{\lambda}(x)\,P^{|\mu|}_{\lambda'\pm 1}(x)\,dx. \tag{27}$$

Now it can be shown that

$$(n-n')(n+n'+1)\int_0^1 P_n^{|m|}(x)\,P_{n'}^{|m|}(x)\,dx = (n'-|m|+1)\,P_n^{|m|}(0)\,P_{n'+1}^{|m|}(0)$$
$$-(n-|m|+1)\,P_{n+1}^{|m|}(0)\,P_{n'}^{|m|}(0). \quad (28)$$

For one of the integrals in (26) we have $n=\lambda$, $n'=\lambda'+1$, $m=\mu$, so that, $n-|m|$ and $n'+1-|m|$ being both odd, the first term on the right-hand side of (27) vanishes. A similar result follows also for the other integral in (26). We thus find

$$\int_0^1 P_\lambda^{|\mu|}(x)\,P_{\lambda'}^{|\mu|}(x)\,x\,dx = \frac{P_\lambda^{|\mu|+1}(0)}{(2\lambda'+1)}\left\{\frac{\lambda'-|\mu|+1}{(\lambda-\lambda'-1)(\lambda+\lambda'+2)}\,P_{\lambda'+1}^{|\mu|}(0)\right.$$
$$\left.+\frac{\lambda'+|\mu|}{(\lambda-\lambda'+1)(\lambda+\lambda')}\,P_{\lambda'-1}^{|\mu|}(0)\right\}, \quad (29)$$

and since

$$P_n^{|m|}(0) = (-1)^{\frac{n-|m|}{2}}\frac{1.3\ldots(n+|m|-1)}{2.4\ldots(n-|m|)}, \quad (30)$$

where $(n-|m|)$ is even, and

$$P_n^n(0) = 1.3\ldots(2n-1), \quad (31)$$

we have finally for $y_{\lambda\mu}^{\lambda'\mu'}$, when $\mu=\mu'$ and $(\lambda-\mu)$ and $(\lambda'-\mu)$ are both odd,

$$y_{\lambda\mu}^{\lambda'\mu'} = (-1)^{\frac{\lambda+\lambda'}{2}-|\mu|}\left\{\frac{(2\lambda+1)(\lambda-|\mu|)!}{(\lambda+|\mu|)!}\right\}^{\frac{1}{2}}\left\{\frac{(2\lambda'+1)(\lambda'-|\mu|)!}{(\lambda'+|\mu|)!}\right\}^{\frac{1}{2}}$$
$$\times\frac{1.3\ldots(\lambda+|\mu|)}{2.4\ldots(\lambda-|\mu|-1)}\,\frac{1.3\ldots(\lambda'+|\mu|)}{2.4\ldots(\lambda'-|\mu|-1)}$$
$$\times\frac{2}{(\lambda+\lambda')(\lambda+\lambda'+2)(\lambda-\lambda'-1)(\lambda-\lambda'+1)}. \quad (32)$$

This is symmetrical in λ and λ' as it ought to be. When $\lambda=|\mu|+1$ or $\lambda'=|\mu|\pm 1$, then the equation (31), instead of (30), must be substituted in (29).

When $\lambda=\lambda'$ we have

$$y_{\lambda\mu}^{\lambda\mu} = \frac{(-1)^{\lambda-|\mu|+1}(2\lambda+1)}{2\lambda(\lambda+1)}\,\frac{(\lambda-|\mu|)!}{(\lambda+|\mu|)!}\left\{\frac{1.3\ldots(\lambda+|\mu|)}{2.4\ldots(\lambda-|\mu|-1)}\right\}^2. \quad (33)$$

We shall write

$$\sum_\mu |y_{\lambda\mu}^{\lambda\mu}|^2 = y(\lambda). \quad (33\text{A})$$

The integral in $g_{\lambda\mu W}^{\lambda'\mu'W'}$ involving r is

$$z_{\lambda\lambda'}(k,k') = \frac{N_\lambda(k)\,N_{\lambda'}(k')}{(kk')^{\frac{1}{2}}}$$

$$\times\left[\int_{r_0}^{\infty}\{J_{\lambda'+\frac{1}{2}}(k'r)+\alpha_{\lambda'}(k')\,J_{-(\lambda'+\frac{1}{2})}(k'r)\}\,\{J_{\lambda+\frac{1}{2}}(kr)+\alpha_\lambda(k)\,J_{-(\lambda+\frac{1}{2})}(kr)\}\frac{dr}{r}\right.$$

$$\left.+\beta_\lambda(k)\beta_{\lambda'}(k')\,(kk'/\kappa\kappa')^{\frac{1}{2}}\int_0^{r_0}I_{\lambda'+\frac{1}{2}}(\kappa'r)\,I_{\lambda+\frac{1}{2}}(\kappa r)\frac{dr}{r}\right], \qquad (34)$$

so that we can write

$$g_{\lambda\mu W}^{\lambda'\mu'W'} = y_{\lambda\mu}^{\lambda'\mu'}\,z_{\lambda\lambda'}(k,k'), \qquad (35)$$

and the probability of a transition depends as is seen from (9) and (13) on

$$|(W',\lambda',\mu',n'\,|\,V\,|\,W,\lambda,\mu,n)|^2$$

$$= e^2(\partial\mu/\partial\rho)_0^2\,|\,\rho_{n'n}\,|^2\cdot|y_{\lambda\mu}^{\lambda'\mu'}\,|^2\,|\,z_{\lambda\lambda'}(k,k')\,|^2. \qquad (36)$$

This has non-zero values only when $\mu=\mu'$.

Now eventually we shall have to consider *all* processes which lead to a transition in the vibrating system MX of the type n to n', so that we shall have to examine the relative importance of all transitions which involve a change from λ to λ', as well as those which involve a change from k to k'. The effect of the former is represented by $|\,y_{\lambda\mu}^{\lambda'\mu'}|^2$, and it appears from equation (32) that for a given λ this quantity has its largest value when $\lambda=\lambda'$; for example, when $\lambda=\lambda'=1$ and $\mu=0$, the value of $|\,y_{\lambda\mu}^{\lambda'\mu}\,|^2$ is 9/16, and the next possible transition permitted by the selection rules is $\lambda=1$, $\lambda'=3$, $\mu=0$, for which $|\,y_{\lambda\mu}^{\lambda'\mu}\,|^2$ is 7/192. It appears also that $z_{\lambda\lambda'}(k,k')$ is larger when $\lambda=\lambda'$ than for other transitions, and since the main object of this investigation is to search for the order of magnitude of the probability of an interchange of energy between metallic electrons and the vibrating group MX, it will be sufficient to confine attention to those transitions for which $\lambda=\lambda'$. For them it is possible to evaluate the integral $z_{\lambda\lambda'}(k,k')$ in finite terms.

Let $Z_p(x)$ denote any linear combination of $J_p(x)$ and $N_p(x)$, where

$$N_p(x) = \{J_p(x)\cos p\pi - J_{-p}(x)\}/\sin p\pi,$$

then†

$$\int Z_p(kx)\,Z_p(k'x)\frac{dx}{x} = \frac{k'}{p}\int Z_p(kx)\,Z_{p-1}(k'x)\,dx - \frac{1}{p}\int Z_p(kx)\frac{dZ_p(k'x)}{dx}dx.$$

---

† The formulae used in the subsequent analysis are to be found in Jahnke and Emde (1933).

There is a similar relation in which k and k' are interchanged on the right-hand side and, adding the two together, we have

$$\int_{x_1}^{x_2} Z_p(kx)\, Z_p(k'x) \frac{dx}{x} = \frac{1}{2p}\Big[k' \int_{x_1}^{x_2} Z_p(kx)\, Z_{p-1}(k'x)\, dx$$
$$+ k\int_{x_1}^{x_2} Z_p(k'x)\, Z_{p-1}(kx)\, dx - Z_p(kx_2)\, Z_p(k'x_2) + Z_p(kx_1)\, Z_p(k'x_1)\Big]. \quad (37)$$

Further

$$\int_{x_1}^{x_2} Z_p(kx)\, Z_{p-1}(k'x)\, dx$$
$$= -\frac{1}{k}\int_{x_1}^{x_2} - kx^{-(p-1)}\, Z_p(kx)\, x^{p-1}\, Z_{p-1}(k'x)\, dx$$
$$= -\frac{1}{k}\int_{x_1}^{x_2} x^{p-1}\, Z_{p-1}(k'x) \frac{d}{dx}\Big[x^{-(p-1)}\, Z_{p-1}(kx)\Big] dx$$
$$= -\frac{1}{k}\Big[Z_{p-1}(kx)\, Z_{p-1}(k'x)\Big]_{x_1}^{x_2} + \frac{k'}{k}\int_{x_1}^{x_2} Z_{p-1}(kx)\, Z_{p-2}(k'x)\, dx,$$

from which we infer that

$$\int_{x_1}^{x_2} Z_{\lambda+\frac{1}{2}}(kx)\, Z_{\lambda-\frac{1}{2}}(k'x)\, dx = -\frac{1}{k}\Big[Z_{\lambda-\frac{1}{2}}(kx)\, Z_{\lambda-\frac{1}{2}}(k'x) + \frac{k'}{k} Z_{\lambda-\frac{3}{2}}(kx)\, Z_{\lambda-\frac{3}{2}}(k'x)$$
$$+ \ldots + \left(\frac{k'}{k}\right)^{\lambda-1} Z_{\frac{1}{2}}(kx)\, Z_{\frac{1}{2}}(k'x)\Big]_{x_1}^{x_2} + \left(\frac{k'}{k}\right)^{\lambda} \int_{x_1}^{x_2} Z_{\frac{1}{2}}(kx)\, Z_{-\frac{1}{2}}(k'x)\, dx. \quad (38)$$

Now since $Z_{\lambda+\frac{1}{2}}(kx)$ can be set equal to $J_{\lambda+\frac{1}{2}}(kx)$ or $J_{-(\lambda+\frac{1}{2})}(kx)$ and since

$$I_{\lambda+\frac{1}{2}}(\kappa x) = i^{-(\lambda+\frac{1}{2})} J_{\lambda+\frac{1}{2}}(i\kappa x),$$

we have, substituting from (38) into (37), the following formulae for the integrals occurring in (34):

$$\int_{x}^{\infty} J_{\pm(\lambda+\frac{1}{2})}(kx)\, J_{\pm(\lambda+\frac{1}{2})}(k'x) \frac{dx}{x}$$
$$= \frac{1}{2\lambda+1}\Big[J_{\pm(\lambda+\frac{1}{2})}(kx)\, J_{\pm(\lambda+\frac{1}{2})}(k'x) + \left(\frac{k'}{k} + \frac{k}{k'}\right) J_{\pm(\lambda-\frac{1}{2})}(kx)\, J_{\pm(\lambda-\frac{1}{2})}(k'x) + \ldots$$
$$+ \left\{\left(\frac{k'}{k}\right)^{\lambda} + \left(\frac{k}{k'}\right)^{\lambda}\right\} J_{\pm\frac{1}{2}}(kx)\, J_{\pm\frac{1}{2}}(k'x) \mp \frac{1}{\pi}\left\{\left(\frac{k'}{k}\right)^{\lambda+\frac{1}{2}} + \left(\frac{k}{k'}\right)^{\lambda+\frac{1}{2}}\right\} Si(k+k')\,x$$
$$+ \frac{1}{\pi}\left\{\left(\frac{k'}{k}\right)^{\lambda+\frac{1}{2}} - \left(\frac{k}{k'}\right)^{\lambda+\frac{1}{2}}\right\} Si(k'-k)\,x \pm \left(\frac{k}{k'}\right)^{\lambda+\frac{1}{2}}\Big], \quad (39)$$

for $k' > k$, upper and lower signs being taken together throughout.

$$
\begin{aligned}
&\int_x^\infty J_{\lambda+\frac{1}{2}}(kx)\,J_{-(\lambda+\frac{1}{2})}(k'x)\frac{dx}{x} \\
&= \frac{1}{2\lambda+1}\Bigg[J_{\lambda+\frac{1}{2}}(kx)\,J_{-(\lambda+\frac{1}{2})}(k'x) - \left(\frac{k'}{k}+\frac{k}{k'}\right)J_{\lambda-\frac{1}{2}}(kx)\,J_{-(\lambda-\frac{1}{2})}(k'x) + \ldots \\
&\quad + (-1)^\lambda\left\{\left(\frac{k'}{k}\right)^\lambda + \left(\frac{k}{k'}\right)^\lambda\right\} J_{\frac{1}{2}}(kx) J_{-\frac{1}{2}}(k'x) \\
&\quad - (-1)^\lambda \frac{1}{\pi}\left\{\left(\frac{k'}{k}\right)^{\lambda+\frac{1}{2}} + \left(\frac{k}{k'}\right)^{\lambda+\frac{1}{2}}\right\} Ci(k+k')\,x \\
&\quad + (-1)^\lambda \frac{1}{\pi}\left\{\left(\frac{k'}{k}\right)^{\lambda+\frac{1}{2}} - \left(\frac{k}{k'}\right)^{\lambda+\frac{1}{2}}\right\} Ci(k'-k)\,x\Bigg],
\end{aligned} \tag{40}
$$

$$
\begin{aligned}
&\int_0^x I_{\lambda+\frac{1}{2}}(\kappa x)\,I_{\lambda+\frac{1}{2}}(\kappa' x)\frac{dx}{x} \\
&= -\frac{1}{2\lambda+1}\Bigg[I_{\lambda+\frac{1}{2}}(\kappa x)\,I_{\lambda+\frac{1}{2}}(\kappa' x) - \left(\frac{\kappa'}{\kappa}+\frac{\kappa}{\kappa'}\right)I_{\lambda-\frac{1}{2}}(\kappa x)\,I_{\lambda-\frac{1}{2}}(\kappa' x) + \ldots \\
&\quad + (-1)^\lambda\left\{\left(\frac{\kappa'}{\kappa}\right)^\lambda + \left(\frac{\kappa}{\kappa'}\right)^\lambda\right\} I_{\frac{1}{2}}(\kappa x)\,I_{\frac{1}{2}}(\kappa' x) \\
&\quad + (-1)^{\lambda+1} \frac{1}{2\pi}\left\{\left(\frac{\kappa'}{\kappa}\right)^{\lambda+\frac{1}{2}} + \left(\frac{\kappa}{\kappa'}\right)^{\lambda+\frac{1}{2}}\right\} \{Ei(\kappa+\kappa')\,x - Ei(-\overline{\kappa+\kappa'}\,x)\} \\
&\quad + (-1)^{\lambda+1} \frac{1}{2\pi}\left\{\left(\frac{\kappa'}{\kappa}\right)^{\lambda+\frac{1}{2}} - \left(\frac{\kappa}{\kappa'}\right)^{\lambda+\frac{1}{2}}\right\} \{Ei(\kappa-\kappa')\,x - Ei(\kappa'-\kappa)\,x\}\Bigg].
\end{aligned} \tag{41}
$$

In these formulae $Si(x)$, $Ci(x)$ and $Ei(x)$ denote the usual logarithmic integrals

$$
Si(x) = \int_0^x \frac{\sin u}{u}\,du, \quad Ci(x) = -\int_x^\infty \frac{\cos u}{u}\,du, \quad Ei(x) = \int_\infty^{-x} \frac{e^{-u}}{u}\,du. \tag{42}
$$

With the above formulae the evaluation of $g_{\lambda\mu W}^{\lambda'\kappa' W'}$ for $\lambda = \lambda'$ and $\mu = \mu'$ can be regarded as completed.

3·3—*The Wave Functions of the Vibrator and the Evaluation of $\rho_{n'n}$*

The simplest method of representing a vibrator is by a simple harmonic oscillator. If in equation (4) we substitute

$$
V(\rho) = \tfrac{1}{2}M(2\pi\omega_0)^2\rho^2, \tag{43}
$$

where ω_0 is the frequency of vibration in a classical sense, then the matrix elements of ρ are (Sommerfeld 1929)

$$\rho_{n,n-1} = (hn/8\pi^2 M\omega_0)^{\frac{1}{2}}, \tag{44}$$

$$\rho_{n,n+1} = (h\overline{n+1}/8\pi^2 M\omega_0)^{\frac{1}{2}}, \tag{45}$$

and all the rest are zero. The vanishing of all the matrix elements except for one quantum transitions is a disadvantage of the linear oscillator representation and we must accordingly seek other better representations of the vibrator. There are two such available which lead to soluble wave equations, one introduced by Fues (1926*b*) and the other by Morse (1929).

Fues writes the potential energy in the form

$$V(\rho) = -(2\pi\omega_0)^2 I\left[\frac{\rho_0}{\rho} - \frac{1}{2}\left(\frac{\rho_0}{\rho}\right)^2\right], \tag{46}$$

which has a minimum at $\rho = \rho_0$ and leads to vibrations of classical frequency ω_0 when the amplitude is small. I is the moment of inertia of the MX molecule.

We then obtain for the wave function†

$$\phi_n(\rho) = N_n\left(\frac{\rho}{\rho_0}\right)^{\alpha+\frac{1}{2}} e^{-b_n\rho/\rho_0} L^{2\alpha}_{2\alpha+n}(2b_n\rho/\rho_0), \tag{47}$$

and the energy levels are given by

$$E_n = -\frac{h^2}{8\pi^2 I}\alpha^2\left\{1 + \frac{1}{\alpha}(n+\tfrac{1}{2})\right\}^{-2}, \tag{48}$$

where
$$b_n = \alpha\left\{1 + \frac{1}{\alpha}(n+\tfrac{1}{2})\right\}^{-1}, \tag{49}$$

and
$$\alpha = \frac{4\pi^2\omega_0 I}{h} = \frac{h\omega_0}{h^2/4\pi^2 I}. \tag{50}$$

Thus α is the ratio of the first vibrational transition to the first rotational transition of a free molecule such as MX. It is a dimensionless constant, of order of magnitude in typical cases about 100; for example, for copper hydride $\alpha = 122{\cdot}5$ about. $L^{\beta}_{\beta+\gamma}(x)$ denotes the generalized Laguerre polynomial, given by the series

---

† We have, of course, no angular factors and hence an extra factor ρ in our formula for $\phi_n(\rho)$ compared with Fues'. Also we are omitting terms in $1/\alpha^2$ which are very small.

$$L^{\beta}_{\beta+\gamma}(x) = e^{i\pi(\beta+\gamma)}\frac{\Gamma(\beta+\gamma+1)}{\gamma!}$$

$$\times\left\{x^{\gamma}-\frac{(\beta+\gamma)\gamma}{1!}x^{\gamma-1}+\frac{(\beta+\gamma)(\beta+\gamma-1)\gamma(\gamma-1)}{2!}x^{\gamma-2}\right\}$$

$$= e^{i\pi\beta}\{\Gamma(\beta+\gamma+1)\}^2\sum_{\nu=0}^{\gamma}(-)^{\nu}\frac{x^{\nu}}{\Gamma(\beta+1+\nu)\,\nu!(\gamma-\nu)!}, \tag{51}$$

with β in general not an integer, γ a positive integer or zero. The normalization factor is†

$$N_n = \frac{(2b_n)^{\alpha+1}}{(\rho_0)^{\frac{1}{2}}}\left\{\frac{n!}{(2\alpha+2n+1)\{\Gamma(2\alpha+n+1)\}^3}\right\}^{\frac{1}{2}}. \tag{52}$$

Substituting (47) in the formula for $\rho_{nn'}$ we obtain after integration

$$\rho_{n'n} = \rho_{nn'} = \frac{\rho_0^2 N^*_{n'} N_n\{\Gamma(2\alpha+n+1)\,\Gamma(2\alpha+n'+1)\}^2}{(b_n+b_{n'})^{2\alpha+3}}$$

$$\times\sum_{\mu=0}^{n'}\sum_{\nu=0}^{n}\frac{(-)^{\mu+\nu}(c_{n'})^{\mu}(c_n)^{\nu}\,\Gamma(\mu+\nu+2\alpha+3)}{\Gamma(2\alpha+\mu+1)\,\Gamma(2\alpha+\nu+1)\,\mu!\,\nu!(n'-\mu)!\,(n-\nu)!}, \tag{53}$$

where $$c_n = 2b_n/(b_n+b_{n'}), \quad c_{n'} = 2b_{n'}/(b_n+b_{n'}), \tag{54}$$

so that $$c_n + c_{n'} = 2, \quad c_n/c_{n'} = b_n/b_{n'}.$$

Substituting for N_n and $N^*_{n'}$ from (52), we then get

$$\rho_{nn'} = \frac{\rho_0(c_n c_{n'})^{\alpha+1}}{(b_n+b_{n'})}\left\{\frac{n!\,\Gamma(2\alpha+n+1)}{2\alpha+n+1}\,\frac{n'!\,\Gamma(2\alpha+n'+1)}{2\alpha+n'+1}\right\}^{\frac{1}{2}}$$

$$\times\sum_{\mu=0}^{n'}\sum_{\nu=0}^{n}\frac{(-)^{\mu+\nu}(c_n)^{\nu}(c_{n'})^{\mu}\,\Gamma(\mu+\nu+2\alpha+3)}{\Gamma(2\alpha+\mu+1)\,\Gamma(2\alpha+\nu+1)\,\mu!\,\nu!\,(n'-\mu)!\,(n-\nu)!}. \tag{55}$$

The Morse potential function is

$$V(\rho) = De^{-2au} - 2De^{-au}, \tag{56}$$

where $u = \rho - \rho_0$. This has a minimum of depth D at $\rho = \rho_0$; the constant a has the dimensions of a reciprocal of a length, $1/a$ being proportional to the width of the potential trough at half depth. The wave functions, which are solutions of the equation obtained by substituting (56) in (4), can be written

---

† These normalization coefficients differ from those given by Fues (*loc. cit.*) which seem to be incorrect; cf. Condon and Morse (1929, equation (21·5)).

$$\phi_n(u) = N_n \exp(-de^{-au})\,(2de^{-au})^{d-n-\frac{1}{2}}\, L^{2d-2n-1}_{2d-n-1}(2de^{-au}), \tag{57}$$

where

$$N_n = \left\{\frac{a(2d-2n-1)\,n!}{[\Gamma(2d-n)]^3}\right\}^{\frac{1}{2}}, \tag{58}$$

and $L^{2d-2n-1}_{2d-n-1}(2de^{-au})$ denotes the generalized Laguerre polynomial, defined in (51).

The corresponding energy levels are

$$E_n = -D\left(1-\frac{n+\frac{1}{2}}{d}\right)^2, \tag{59}$$

where

$$d = \frac{2\pi(2MD)^{\frac{1}{2}}}{ah}. \tag{60}$$

The formula for the frequency of the classical vibrations of zero amplitude is

$$\omega_0 = \frac{a}{2\pi}\sqrt{\frac{2D}{M}}, \tag{61}$$

so that

$$d = \frac{2D}{h\omega_0}, \tag{62}$$

and is a dimensionless constant whose value, for copper hydride, is 25·0. It is a measure of the number of discrete energy levels.

Now

$$\begin{aligned}
\rho_{n'n} &= \int_{-\infty}^{\infty} \phi^*_{n'}(u)\, u\phi_n(u)\, du \\
&= \int_{-\infty}^{\infty} \phi^*_{n'}(u) \operatorname*{Lt}_{y\to 0} \left\{\frac{(2d)^y-(2de^{-au})^y}{(2d)^y ay}\right\} \phi_n(u)\, du \\
&= -\frac{N_n N_{n'}}{a} \operatorname*{Lt}_{y\to 0} \frac{1}{y}\int_{-\infty}^{\infty} \exp(-2de^{-au})\,(2de^{-au})^{2d+y-n-n'-1} L^{*\,2d-2n'-1}_{2d-n'-1}(2de^{-au}) \\
&\qquad \times L^{2d-2n-1}_{2d-n-1}(2de^{-au})\, du,
\end{aligned} \tag{63}$$

the other term vanishing by the orthogonality conditions and the inversion of the limit and the integral being justified by the rapid convergence of the integral at ± ∞. Hence

$$\rho_{n'n} = -\frac{N_n N_{n'}^*\{\Gamma(2d-n)\,\Gamma(2d-n')\}^2}{a^2}$$

$$\times \operatorname*{Lt}_{y\to 0} \frac{1}{y}\int_0^\infty e^{-v} v^{2d+y-n-n'-2} L^{*\,2d-2n'-1}_{\;2d-n'-1}(v)\, L^{2d-2n-1}_{2d-n-1}(v)\, dv$$

$$= -\frac{N_n N_{n'}^*}{a^2}\{\Gamma(2d-n)\,\Gamma(2d-n')\}^2$$

$$\times \operatorname*{Lt}_{y\to 0} \frac{1}{y} \sum_{\mu=0}^{n'} \sum_{\nu=0}^{n} \frac{(-)^{\mu+\nu}\Gamma(2d+y-1-n-n'+\mu+\nu)}{\Gamma(2d-2n'+\mu)\,\Gamma(2d-2n+\nu)\,\mu!\,\nu!\,(n'-\mu)!\,(n-\nu)!}. \tag{64}$$

The double summation can be written

$$\sum_{\mu=0}^{n'} \frac{(-)^{\mu}}{\Gamma(2d-2n'+\mu)\,\mu!\,(n'-\mu)!} \sum_{\nu=0}^{n} (-)^{\nu} \frac{\Gamma(2d+y-1-n-n'+\mu+\nu)}{\Gamma(2d-2n+\nu)\,\nu!\,(n-\nu)!}. \tag{65}$$

Now suppose $n > n'$, then it follows that

$$2d-1-n-n'+\mu+\nu > 2d-2n+\nu$$

provided $\mu > 0$, and then we have

$$\Gamma(2d-2n+\nu) = \frac{\Gamma(2d-1-n-n'+\mu+\nu)}{(2d-n-n'+\mu+\nu-2)\ldots(2d-2n+\nu)}. \tag{65 A}$$

In using this formula later we must carefully note the conditions under which it is valid. If for particular values of n, n' and μ (such as $n = n'+1$ and $\mu = 0$) there is equality of $2d-1-n-n'+\mu+\nu$ and $2d-2n+\nu$, then the denominator of (65 A) must be taken to be unity.

In general then for $\mu > 0$ and $n > n'$ we can write for the summation on the right of (65)

$$\sum_{\nu=0}^{n} (-)^{\nu} \frac{\left\{ \begin{array}{l} (2d-2n+\nu)(2d-2n+\nu+1)\ldots \\ \qquad (2d-n-n'+\mu+\nu-2)\,\dfrac{\Gamma(2d+y-1-n-n'+\mu+\nu)}{\Gamma(2d-1-n-n'+\mu+\nu)} \end{array} \right\}}{\nu!\,(n-\nu)!}. \tag{66}$$

Now the double summation in (65) vanishes when $y = 0$ by the orthogonality property of the wave functions. Using this fact we infer that

$$\operatorname*{Lt}_{y\to 0}\frac{1}{y}\times \text{the expression (66)}$$

$$= \sum_{\nu=0}^{n}(-)^{\nu}\frac{(2d-2n+\nu)\dots(2d-n-n'+\mu+\nu-2)\,\Psi(2d-n-n'+\mu+\nu-1)}{\nu!\,(n-\nu)!}, \tag{67}$$

where $$\Psi(x) = \frac{\Gamma'(x)}{\Gamma(x)} = \frac{d}{dx}\{\log\Gamma(x)\}.$$

Now $$\Psi(1+x) = \Psi(x)+\frac{1}{x},$$

and so $$\Psi(\nu+x) = \Psi(x)+\frac{1}{x}+\frac{1}{x+1}+\dots+\frac{1}{x+\nu-1}.$$

Hence $$\Psi(2d-n-n'+\mu+\nu-1) = \Psi(2d-n-n'+\mu-1)+F_{\mu}(\nu), \tag{67A}$$

where $F_{\mu}(\nu)$ is a function of ν for a given μ and is given by

$$F_{\mu}(\nu) = \sum_{\nu=1}^{\nu} 1/(2d-n-n'+\mu+\nu-2). \tag{67B}$$

Making this substitution we find

$$\operatorname*{Lt}_{y\to 0}\frac{1}{y}\,[\text{expression (65)}]$$

$$= \sum_{\mu=0}^{n'}\sum_{\nu=0}^{n}(-)^{\mu+\nu}\frac{(2d-2n+\nu)\dots(2d-n-n'+\mu+\nu-2)\,\Psi(2d-n-n'+\mu-1)}{\Gamma(2d-2n'+\mu)\,\mu!\,(n'-\mu)!\,\nu!\,(n-\nu)!}$$
$$+\sum_{\mu=0}^{n'}\sum_{\nu=1}^{n}(-)^{\mu+\nu}\frac{(2d-2n+\nu)\dots(2d-n-n'+\mu+\nu-2)\,F_{\mu}(\nu)}{\Gamma(2d-2n'+\mu)\mu!\,(n'-\mu)!\,\nu!\,(n-\nu)!}. \tag{68}$$

Now the first of these double summations contains as a factor

$$\sum_{\nu=0}^{n}(-)^{\nu}\frac{(2d-2n+\nu)\dots(2d-n-n'+\mu+\nu-2)}{\nu!\,(n-\nu)!},$$

and this is equal to

$$\sum_{\nu=0}^{n}(-)^{\nu}\left[\left(\frac{d}{dt}\right)^{n-n'+\mu-1}\frac{t^{2d-n-n'+\mu+\nu-2}}{\nu!\,(n-\nu)!}\right]_{t=1}$$
$$= \left[\left(\frac{d}{dt}\right)^{n-n'+\mu-1} t^{2d-n-n'+\mu-2}\,(1-t)^{n}\right]_{t=1}.$$

This expression vanishes if $n > n - n' + \mu - 1$, that is $\mu \leqslant n'$. We deduce finally that

$$\rho_{n'n} = -\frac{1}{a}\{(2d-n-1)\,n!\,\Gamma(2d-n)\}^{\frac{1}{2}}\{(2d-n'-1)\,n'!\,\Gamma(2d-n')\}^{\frac{1}{2}}$$

$$\times \sum_{\mu=0}^{n'}\sum_{\nu=1}^{n}(-)^{\mu+\nu}\frac{(2d-2n+\nu)\dots(2d-n-n'+\mu+\nu-2)\,F_\mu(\nu)}{\Gamma(2d-2n'+\mu)\,\mu!\,(n'-\mu)!\,\nu!\,(n-\nu)!}. \tag{69}$$

The lack of symmetry is due to the fact that we have assumed n to be greater than n'. The formula when n' is greater than n is obtained from (69) by the simple interchange of n, n' throughout.

It is of interest to compare the formulae (69) and (55) for $\rho_{n'n}$ derived for the Fues and Morse potential fields respectively.

We consider firstly the $1 \to 0$ transition, that is $n = 1$, $n' = 0$. This is a case where $n = n' + 1$ and so for $\mu = 0$ the denominator of (65 A) and the corresponding numerator of (69) must be equated to unity, as already noted. Then

$$\rho_{01} = 1/a(2d-2)^{\frac{1}{2}}$$

and when α, d are large compared with unity, we find that (55) and (69) reduce to

$$\left.\begin{aligned} |\rho_{10}| &= \rho_0\sqrt{\frac{1}{2\alpha}},\\ |\rho_{10}| &= \frac{1}{a(2d)^{\frac{1}{2}}}. \end{aligned}\right\} \tag{70}$$

Now if we equate the expressions for V, $\frac{\partial V}{\partial \rho}$, $\frac{\partial^2 V}{\partial \rho^2}$, in the Morse and Fues theories so as to make the curves fit as closely as possible near the minimum, we get

$$a = \frac{1}{\rho_0}, \quad d = \alpha, \tag{71}$$

and the two expressions of (70) become identical. This is to be expected, since for small vibrations it is the form of the energy curve $V(\rho)$ near the minimum that is of importance. Both reduce to $\sqrt{\frac{h}{8\pi^2 M\omega_0}}$, the value of the matrix element for a simple harmonic oscillator of frequency ω_0.

For the 2 → 0 transition with $n = 2$, $n' = 0$, we have approximately

$$\left.\begin{aligned} |\rho_{20}| &= \frac{\rho_0}{2\alpha\sqrt{2}}, \\ |\rho_{20}| &= \frac{1}{2ad\sqrt{2}}, \end{aligned}\right\} \tag{72}$$

respectively. These expressions are again equal when the relations (71) hold good. Actually using the constants as determined for each potential field by the methods usually employed, we find for copper hydride

$$|\rho_{20}| = (2{\cdot}1)\,10^{-11}\text{ cm. and } (4{\cdot}7)\,10^{-11}\text{ cm.}$$

respectively. There is now a difference of a factor 2 between the two results and, from the form of the formulae (69), (55), we expect the discrepancy to increase with increasing n. This is due to the fact that the Fues wave functions are very poor for large vibrational quantum numbers, yielding, for example, for copper hydride a dissociation energy of 14·6 V compared with the observed value of 3·0 V. The Morse potential field is a better representation of actual fields between atoms and for higher quantum states the formulae given above for this field are to be preferred.

4—The Total Probability of Activation and Deactivation

In order to obtain the probability of a transition, whereby the vibrating MX changes its state from n to n' owing to electron impacts, we have to multiply the transition probability $\Gamma^{W'\lambda'\mu'n'}_{W\lambda\mu n}$ given in (9), by a factor $\varpi_W(1-\varpi_{W'})$, where ϖ_W is the probability of finding the initial electronic state occupied, and $(1-\varpi_{W'})$ the probability of finding the final state unoccupied. It is then necessary to sum over all the conduction electrons, and to include a factor 2 to account for electron spin. Thus

$$G_{n,n'} = \int dW \int dW' \sum_{\lambda}\sum_{\mu}\sum_{\lambda'}\sum_{\mu'} 2\varpi_W(1-\varpi_{W'})\,\Gamma^{W'\lambda'\mu'n'}_{W\lambda\mu n}. \tag{73}$$

Now the integrand contains a factor

$$\frac{4\sin^2\dfrac{\pi t}{h}(W+E_n-W'-E_{n'})}{(W+E_n-W'-E_{n'})^2},$$

and this has a sharp maximum for those energy values for which energy is conserved. We thus obtain the integral with respect to W' by giving to $\varpi_W(1-\varpi_{W'})\,|\,(W'\lambda'\mu'n'\,|\,V\,|\,W\lambda\mu n)\,|^2$ its value appropriate to conservation of energy, extending the limits of integration to $\pm\infty$ and using the formula

$$\int_{-\infty}^{\infty}\frac{\sin^2 x}{x^2}\,dx=\pi.$$

Thus $$G_{n,n'}=\frac{4\pi^2 t}{h}\,e^2\left(\frac{d\mu}{d\rho}\right)_0^2\int dW\sum_{\lambda}\sum_{\mu}\sum_{\lambda'}\sum_{\mu'}2\varpi_W(1-\varpi_{W'})\,|\,g_{\lambda\mu W}^{\lambda'\mu'W'}\,|^2\,|\,\rho_{nn'}\,|^2, \tag{74}$$

where $W'=W+E_n-E_{n'}$. Then from (33), (33 A) and (35) we have, taking only transitions in which $\lambda=\lambda'$ as explained in the previous section,

$$\begin{aligned}G_{n,n'}&=\frac{4\pi^2 t}{h}\,e^2\left(\frac{d\mu}{d\rho}\right)_0^2\int dW\sum_{\lambda}2\varpi_W(1-\varpi_{W'})\,y(\lambda)\,|\,z_{\lambda\lambda}(k,k')\,|^2\,|\,\rho_{n'n}\,|^2\\&=\frac{4\pi^2 t}{h}\,e^2\left(\frac{d\mu}{d\rho}\right)_0^2|\,\rho_{n'n}\,|^2\sum_{\lambda}y(\lambda)\int 2\varpi_W(1-\varpi_{W'})\,|\,z_{\lambda\lambda}(k,k')\,|^2\,dW.\end{aligned} \tag{75}$$

This is for a transition $n\rightarrow n'$, and we have supposed in calculating $\rho_{n'n}$ that $n>n'$.

Now for electrons obeying the Fermi-Dirac statistics we have†

$$\varpi_W=\frac{1}{1+\exp\{(W-\overline{W})/kT\}}, \tag{76}$$

and

$$\varpi_W(1-\varpi_{W'})=\exp(W'-\overline{W})/kT/[1+\exp(W-\overline{W})/kT][1+\exp(W'-\overline{W})/kT], \tag{76 A}$$

where $$\overline{W}=\frac{h^2}{8\pi^2 m}\,(3\pi^2 N)^{\frac{2}{3}}, \tag{77}$$

N being the number of conducting electrons per unit volume of the metal. For a transition $n\rightarrow n'$ in which $n>n'$, we have

$$h\nu_{nn'}=E_n-E_{n'}=W'-W, \tag{78}$$

approximately; if T is not very high so that $h\nu_{nn'}\gg kT$ and if $W<\overline{W}$, while $\overline{W}+h\nu_{nn'}>W'>\overline{W}$, then we have very nearly

$$\varpi_W=1,\quad \varpi_{W'}=\exp(-h\nu/kT), \tag{79}$$

where $h\nu=W'-\overline{W}$ approximately.

---

† The k appearing in the Boltzmann factor is not likely to be confused with that used elsewhere in this paper.

An examination of the definition of $y(\lambda)$ given in equation (33A) shows that it is a pure number; in fact,

$$y(\lambda) = (\overline{\cos\theta})^2_\lambda, \tag{80}$$

where $(\overline{\cos\theta})_\lambda$ is a suitably defined mean value of the $\cos\theta$ term occurring in the perturbing potential energy (or energy of coupling) given in (11).

Similarly $z_{\lambda\lambda}$, defined in (34), is a mean value of the $1/r^2$ term in the perturbing potential taken over wave functions which are normalized with respect to energy. It follows that $z_{\lambda\lambda}(k, k')$ has the dimensions of $[\text{energy}]^{-1} L^{-2}$ and so we can define a length $R_\lambda(k)$, such that

$$(h\nu_{nn'})\,|\,z_{\lambda\lambda}(k, k')\,| = 1/R^2_\lambda(k). \tag{81}$$

Then we can write equation (75) in the form

$$G_{n,n} = [1-\exp(-h\nu_{nn'}/kT)]\,[8\pi^2 t/h]\,[e^2\,|\,\rho_{n',n}\,|^2\,(d\mu/d\rho)^2_0]\sum_\lambda (\overline{\cos\theta})^2_\lambda \times (h\nu_{nn'})^{-2}\int_{\overline{W}-h\nu_{nn'}}^{\overline{W}} R_\lambda^{-4}(k)\,dW. \tag{82}$$

The first term in the squared brackets gives the dependence of $G_{n,n'}$ on temperature; the second term has the dimensions of an $[\text{energy}]^{-1}$ and is the result of integrating the term

$$\frac{4\sin^2 \pi t(W+E_n-W'-E_{n'})/h}{(W+E_n-W'-E_{n'})^2}$$

over the range of the energy W'; the third term has the dimensions of $[\text{energy}]^2 L^4$, while the summation over λ has the dimensions of $[\text{energy}]^{-1} L^{-4}$. We accordingly define a length R_0 by the equation

$$R_0^{-4} = (h\nu_{nn'})^{-1}\sum_\lambda (\overline{\cos\theta})^2_\lambda \int_{\overline{W}-h\nu_{nn'}}^{\overline{W'}} R_\lambda^{-4}(k)\,dW, \tag{83}$$

and then we can write

$$G_{n,n'} = \frac{[1-\exp(-h\nu_{nn'}/kT)]\,[8\pi^2 t/h]\,[e^2\,|\,\rho_{n',n}\,|^2\,(d\mu/d\rho)^2_0]}{[(h\nu_{nn'})\,R_0^4]}. \tag{84}$$

It is then obvious that $G_{n,n'}$ has the dimensions of a pure number, as it should, being a probability.

The transition probability per unit time for the n to n' vibrational jump, that is, for deactivation from a higher to a lower level is

$$\mathcal{G}_{n,n'} = G_{n,n'}/t \quad [\text{deactivation } n \to n'], \tag{85}$$

and the mean life time $\tau_{n,n'}$ before the MX group is deactivated from the state n to the state n' may be defined as the reciprocal of $\mathscr{G}_{n,n'}$. Then

$$\tau_{n,n'} = \frac{h\nu_{nn'} R_0^4}{[1-\exp(-h\nu_{nn'}/kT)]\,[8\pi^2/h]\,[e^2\,|\,\rho_{n',n}\,|^2\,(d\mu/d\rho)_0^2]}, \tag{86}$$

and when $h\nu_{nn'} \gg kT$ we find that $\tau_{n,n'}$ is nearly independent of temperature.

The probability of excitation from a lower state n' to a higher one n can be shown to be related to $\mathscr{G}_{n,n'}$ by the formula

$$\mathscr{F}_{n',n} = \mathscr{G}_{n,n'} \exp(-h\nu_{nn'}/kT) \quad [\text{excitation } n' \to n]. \tag{87}$$

It may be useful to recall at this stage the meaning of the various terms which occur in the above formula for $\tau_{n,n'}$. The term $(d\mu/d\rho)_0$ is the rate of change of the dipole moment of the group MX with extension of the link (ρ) near the equilibrium position, $\rho = \rho_0$, while $\rho_{n'n}$ is the matrix element of ρ with respect to the vibrational wave functions; it is given in explicit terms in (55) and (69) and depends not only on the quantum numbers n and n', characterising the initial and final vibrational states, but also on the constants of the field between X and M. The length R_0 has just been defined in (83).

5—NUMERICAL APPLICATIONS AND DISCUSSION OF THE RESULTS

In order to discover the orders of magnitude of the quantities involved in the preceding formulae we have considered in some detail the particular example of hydrogen adsorbed on copper. For this purpose we may regard the CuH as an electronic system similar to the diatomic copper hydride, for which the necessary data are available (Jevons 1932). We have $M = (1{\cdot}636)\,10^{-24}$ g., $\rho_0 = (1{\cdot}46)\,10^{-8}$ cm., $D = 3{\cdot}00$ e-volts, and the classical frequency $\omega_0 = 1939{\cdot}9$ cm.$^{-1}$. From this information we can derive the constants of the Morse field, viz. $a = (1{\cdot}517)\,10^{8}$ cm.$^{-1}$, and $d = 25{\cdot}0$. The energy quanta $h\nu_{nn'}$ for the first few levels are $h\nu_{01} = 0{\cdot}23$ e-volt, $h\nu_{12} = 0{\cdot}22$ e-volt, $h\nu_{23} = 0{\cdot}21$ e-volt, while $h\omega_0 = 0{\cdot}24$ e-volt.

There are no figures available for $(d\mu/d\rho)_0$, but Bartholomé (1933) has deduced values of this quantity from infra-red absorption measurements for HCl and HBr. He obtained $(0{\cdot}086)\,e$ for HCl, and $(0{\cdot}075)\,e$ for HBr. We have therefore taken $(0{\cdot}08)\,e$ as a reasonable estimate of this quantity for CuH.

For the underlying metal we have for copper a value 6·98 e-volt for W and a value 11·36 e-volts for χ (Hughes and du Bridge 1932, p. 75), the work function thus being 4·38 e-volts. The number of free electrons may be taken to be (8·5) 10^{22} per c.c. (Fowler 1929, p. 545).

In calculating R_0, which occurs in equation (83), it is convenient to introduce a length $R_{\lambda 0}$, defined by the equation

$$h\nu_{nn'} . R_{\lambda 0}^{-4} = \int_{\overline{W}-h\nu_{nn'}}^{\overline{W}} R_{\lambda}^{-4}(k)\,dW, \tag{88}$$

so that (83) becomes

$$R_0^{-4} = \sum_{\lambda} (\overline{\cos\theta})_{\lambda}^{2} R_{\lambda 0}^{-4}. \tag{89}$$

The range of integration over W is usually so small that $R_\lambda(k)$ varies very little within it, and so we may equate $R_\lambda(k)$ and $R_{\lambda 0}$. The latter quantity is a function of r_0, the radius of the hemispherical cavity surrounding the surface complex, but is found not to be very sensitive to it. Thus for $r_0 = 10^{-8}$ cm. we find for the 3 → 2 transition

$$R_{10} = (4{\cdot}54)\,10^{-8}\text{ cm.},\quad R_{20} = (5{\cdot}70)\,10^{-8}\text{ cm.},\quad R_{30} = (6{\cdot}67)\,10^{-8}\text{ cm.},$$

while for $r_0 = 0$, we find the corresponding values

$$R_{10} = (4{\cdot}29)\,10^{-8}\text{ cm.},\quad R_{20} = (5{\cdot}58)\,10^{-8}\text{ cm.},\quad R_{30} = (6{\cdot}65)\,10^{-8}\text{ cm.}$$

As is clear in this example $R_{\lambda 0}(r_0)$ approaches $R_{\lambda 0}(0)$ as λ increases. This may be proved mathematically by examining the asymptotic behaviour of the Bessel functions for large λ, and may be understood physically, since wave functions with a large λ correspond to states which in a classical sense have a large angular momentum about the origin of the MX group and do not penetrate near to it. Consequently for large λ we may use the formula (cf. Watson 1922, p. 405)

$$\begin{aligned} R_{\lambda 0}^{-4} &= (R^*)^{-4}\left|\int_0^\infty J_{\lambda+\frac{1}{2}}(kr)\,J_{\lambda+\frac{1}{2}}(k'r)\,(dr/r)\right|^2 \\ &= (R^*)^{-4}(2\lambda+1)^{-2}(k/k')^{2\lambda+1}, \end{aligned} \tag{90}$$

when $k < k'$; in this expression R^* is defined by the relation

$$(R^*)^{-2} = (h\nu_{nn'})\,(8\pi^2 m/h^2), \tag{91}$$

and is the length of a one-dimensional box of uniform potential in which an electron would have an energy of $h\nu_{nn'}$ in its lowest state. For the 3 → 2 transition ($h\nu_{nn'} = 0{\cdot}21$ e-volt) we find $R^* = (4{\cdot}24)\,10^{-8}$ cm.

To evaluate R_0 from (89) it is now necessary to investigate the dependence of $(\overline{\cos\theta_\lambda})^2$ on λ. By definition, equations (80), (33 A) and (33),

$$(\overline{\cos\theta})^2_\lambda = \left\{\frac{2\lambda+1}{2\lambda(\lambda+1)}\right\}^2 \sum_{\mu=-(\lambda-1)}^{\lambda-1} \frac{(\lambda-|\mu|)!^2}{(\lambda+|\mu|)!^2} \left\{\frac{1.3\ldots(\lambda+|\mu|)}{2.4\ldots(\lambda-|\mu|-1)}\right\}^4, \tag{92}$$

where the summation extends over the values $\lambda-1, \lambda-3, \ldots$ to $-(\lambda-1)$.

The summation in the expression on the right, which we may denote by $g(\lambda)$, is equal to the coefficient of $z^{\lambda-1}$ in the expansion of $[F(\frac{3}{2}, \frac{3}{2}; 1; z)]^2$, where F is a hypergeometric function. By solving in series the differential equation satisfied by F^2 (Whittaker and Watson 1927, p. 298, ex. 10) we obtain the following recurrence relation

$$2\lambda^3 g(\lambda+1) - (2\lambda+1)(2\lambda^2+2\lambda-1)\, g(\lambda) + 2(\lambda+1)^3 g(\lambda-1) = 0.$$

This is useful in obtaining the first few values of $g(\lambda)$ and also in deriving an asymptotic formula for large λ. Putting $g(\lambda)$ proportional to λ^m we find for large λ,

$$g(\lambda) \propto \lambda^3,$$

and so

$$(\overline{\cos\theta})^2_\lambda \propto \lambda.$$

For the first few values of λ it appears that

$$(\overline{\cos\theta})^2_\lambda = (2\lambda+1)^2/16\lambda, \tag{93}$$

very nearly and, as it has the correct asymptotic form for large λ, we may regard it as valid approximately over the whole range of λ.

From (89) and (90) we then have

$$[R_0^{-4}]_{r_0=0} = (R^*)^{-4} \sum_1^\infty (1/16\lambda)\,(k/k')^{2\lambda+1}$$

approximately, leading to

$$[R_0^{-4}]_{r_0=0} = (R^*)^{-4} \frac{1}{16}\left(1 - \frac{h\nu_{nn'}}{\overline{W}}\right)^{\frac{1}{2}} \log_e(\overline{W}/h\nu_{nn'}).$$

When, as in the example cited, $h\nu_{nn'}$ is of the order of $1/20$, or $1/30$ of $\overline{W}$, only the logarithmic term is relevant, and even this is not very large, so that R_0 is of the order of $2R^*$.

For other values of r_0 we can write

$$[R_0^{-4}]_{r_0} = \sum_1^\infty (\overline{\cos\theta})^2_\lambda \{R_{\lambda 0}^{-4}(r_0) - R_{\lambda 0}^{-4}(0)\} + [R_0^{-4}]_{r_0=0},$$

and the first series usually converges rapidly, e.g. in the case here considered it is sufficient to take three terms.

Typical values of R_0, obtained for $r_0 = 10^{-8}$ cm., are (9·3).10^{-8} cm. for the 1 → 0 transition of CuH, (8·98).10^{-8} cm. for the 2 → 1 transition and (8·63).10^{-8} cm. for the 3 → 2 transition.

The corresponding times for deactivation, obtained from the formula (86), are

$$\tau_{1,0} = (5{\cdot}5).10^{-12}\text{ sec.},$$
$$\tau_{2,1} = (3{\cdot}5).10^{-12}\text{ sec.},$$
$$\tau_{3,2} = (1{\cdot}7).10^{-12}\text{ sec.}$$

The variation of τ according to the transition is due almost entirely to the dependence of $\rho_{nn'}$ on the quantum numbers. For transitions of this type $(n+1) \rightarrow n$, the formula for the linear oscillator could be used, but for other types of transition this model would give zero probability. The Morse potential field, on the other hand, leads to

$$\tau_{3,0} = (3).10^{-9}\text{ sec.}$$

for a direct 3 → 0 transition. It may be observed that all these times are long compared with the period of a single vibration of the CuH, which is equal to (1·7) 10^{-14} sec. A typical time between successive activations is $t_{2,3} = (3{\cdot}5)\ 10^{-9}$ sec. at 1000° K. In applying these results to surface migration we may note that $n = 3$ corresponds to the lowest energy state for which migration is possible ($E = 0{\cdot}61$ e-volt; cf. Lennard-Jones 1932) and we may conclude that the duration of time of an excited state is of the order of 10^{-12} sec. and is nearly independent of the temperature. The time between successive activations is of the order of 10^{-12} sec. multiplied by a Boltzmann exponential factor, appropriate to the energy of activation.

We have not taken into account the effect of lattice periodicity of the metal on the electronic wave functions, or on the number of electrons available for the interaction. The effect on the wave functions is in general small, and can hardly modify our results appreciably. Also for many metals the available electrons will be given with fair accuracy by the usual Fermi formula. For an insulator, however, there would be no possible final state for the electron, $1-\varpi'$ would become zero, as would the transition probabilities. In such a case other mechanisms, such as activation by elastic waves, must be considered (cf. Lennard-Jones 1935–6).

Finally we may remark that our results are not sensitive to changes in r_0 or the work function of the metal, due, no doubt, to the long-range nature of the dipole field. If the interaction at short distances became for any reason more important, then the results would be more sensitive to r_0 and to the work function.

The final formulae do not involve N, the number of electrons, explicitly but only through $\overline{W}$, the maximum energy of the conduction electrons at the absolute zero. This is due to the fact that only a small group of electrons with energies in the neighbourhood of $\overline{W}$ can make effective collisions owing to the Pauli principle. It may be of interest to add that if these electrons be regarded as bombarding the MX group in a classical sense with their appropriate energy $\overline{W}$, and the target be considered to be a sphere of radius 1A half immersed in the metal, then the efficiency of the collisions in causing activation is of the order of 1 %. This is of the same order as the efficiency of slow electrons when bombarding molecules in a gas (Massey 1935). No doubt similar methods could be used to find the change in the free path of the conduction electrons due to hydrogen or other atoms dissolved in a metal.

SUMMARY

It is shown in this paper that atoms adsorbed on a metal may be excited to higher vibrational states by the conduction electrons of the underlying metal. Calculations are made of the frequency with which excitation occurs by this mechanism and also of the length of time before the atom loses vibrational energy to the solid by the same process. In a typical example the time of excitation is found to be of the order of 10^{-12} sec. and is nearly independent of the temperature. The time between successive activations is of the order of 10^{-12} sec., multiplied by a Boltzmann exponential factor, appropriate to the energy of activation. These values are not sensitive to the work function of the metal or to the number of conduction electrons and reasons are given for these results. The efficiency of the electrons which can cause activation and can be regarded as "colliding" with the adsorbed atom is of the order of 1 %.

REFERENCES

Bartholomé 1933 *Z. phys. Chem.* B, **23**, 131.
Condon and Morse 1929 "Quantum Mechanics." McGraw Hill Book Co.
Fowler 1929 "Statistical Mechanics," 1st ed. Camb. Univ. Press.
Fues 1926*a* *Ann. Phys., Lpz.*, **81**, 281.
— 1926*b* *Ann. Phys., Lpz.*, **80**, 367.
Hughes and du Bridge 1932 "Photoelectric Phenomena." McGraw Hill Book Co.
Jahnke and Emde 1933 "Funktionentafeln." Berlin.
Jevons 1932 "Report on Band Spectra of Diatomic Molecules." The Physical Society.
Lennard-Jones 1932 *Trans. Faraday Soc.* **28**, 333.

Lennard-Jones and Strachan 1935 *Proc. Roy. Soc.* A, **150**, 442.
Lennard-Jones and Devonshire 1936 *Proc. Roy. Soc.* A, **156**, 6, 29 and 37.
— — 1937 *Proc. Roy. Soc.* A, **158**, 242, 253 and 269.
Massey 1935 *Trans. Faraday Soc.* **31**, 556.
Morse 1929 *Phys. Rev.* **34**, 57.
Sommerfeld 1929 "Wellenmechanik." Braunschweig.
Strachan 1935 *Proc. Roy. Soc.* A, **150**, 456.
— 1937 *Proc. Roy. Soc.* A, **158**, 591.
Watson 1922 "Bessel Functions." Camb. Univ. Press.
Whittaker and Watson 1927 "Modern Analysis." Camb. Univ. Press.

The Interaction of Atoms and Molecules with Solid Surfaces

XI—The Dispersal of Energy from an Activated Link

By J. E. LENNARD-JONES, F.R.S.
The University Chemical Laboratory, Cambridge

(*Received* 5 *August* 1937)

One of the problems which has been considered in this series of papers (Lennard-Jones, Strachan, Devonshire, Goodwin 1935–7) is the activation of the vibrational states of an atom adsorbed on a surface and the converse problem of the deactivation from one vibrational state to another. Various mechanisms have been examined, such as the interaction of the adsorbed atom with the thermal vibrations of the solid and also with the conduction electrons of a metal, and in each case it has been found that deactivation occurs in a time which is of the order of a few vibrations of the adsorbed atom. In this connexion it is instructive to examine a simple problem which is of a similar type and can be solved by classical methods.

Let the positions of a number of similar atoms forming a one-dimensional chain when in equilibrium be denoted by

$$x = na, \quad n = 0, \pm 1, \pm 2, \ldots,$$

and let ξ_n denote the lateral displacement of the nth atom from its equilibrium position. When the relative displacements are small, the potential energy due to a relative shift of two neighbouring particles can be written as

$$\tfrac{1}{2}\kappa(\xi_n - \xi_{n-1})^2,$$

and the energy of the system when in a state of vibration is

$$\sum_n \tfrac{1}{2}m\dot{\xi}_n^2 + \sum_n \tfrac{1}{2}\kappa(\xi_n - \xi_{n-1})^2.$$

The motion of the nth particle is then determined by the equation

$$m\ddot{\xi}_n = \kappa(\xi_{n+1} - \xi_n) + \kappa(\xi_{n-1} - \xi_n). \tag{1}$$

Writing $$\omega^2 = \kappa/m, \quad u_{2n} = \dot{\xi}_n, \quad u_{2n+1} = \omega(\xi_n - \xi_{n+1}), \tag{2}$$

so that ω has the dimensions of a frequency, we have

$$\begin{aligned} \dot{u}_{2n} &= \omega(u_{2n-1} - u_{2n+1}), \\ \dot{u}_{2n+1} &= \omega(u_{2n} - u_{2n+2}), \end{aligned}$$

which can be combined into the single equation

$$\dot{u}_s = \omega(u_{s-1} - u_{s+1}); \tag{3}$$

where s is any integer.

This is an equation which has been considered by many authors, and a particular solution has been found in terms of Bessel functions (Havelock 1910; Schrödinger 1914; Bateman 1932), viz.

$$u_s = AJ_{s-\sigma}(2\omega t), \tag{4}$$

where A and σ are arbitrary constants.

We suppose that initially all the particles are at rest and one of them, say the one at the origin, is given an initial velocity v, so that the initial conditions are

$$u_{2n} = v,$$

and all other u's are zero. A solution which satisfies these conditions is

$$u_s = vJ_s(2\omega t), \tag{5}$$

for, when $t = 0$, all the J's vanish except J_0 which is equal to unity.

Once the motion has begun and all the other atoms are disturbed, it is difficult to partition the energy among the various links, but it is reasonable to adopt the convention that whenever the relative motion of two neighbouring atoms is zero the energy stored in that link is equal to the appropriate potential energy term $\frac{1}{2}\kappa(\xi_n - \xi_{n-1})^2$, whether that corresponds to a maximum extension or contraction of the link. The two-atomic system may at that moment be moving as a whole and thus contributing to the energy of the complete system, but the atoms having reached the end of an oscillation are not moving relatively to one another.

The relative positions of two neighbouring atoms are given by equations (2) and (5), viz.

$$\xi_{n-1}-\xi_n = u_{2n-1}/\omega = (v/\omega)\,J_{2n-1}(2\omega t),$$

and so

$$\xi_0-\xi_{-1} = (v/\omega)\,J_1(2\omega t) = -(\xi_1-\xi_0).$$

The potential energy in each of the two centre links is then

$$W_{0,1} = \tfrac{1}{2}\kappa(\xi_0-\xi_{-1})^2 = \tfrac{1}{2}\left(\frac{\kappa v^2}{\omega^2}\right)[J_1(2\omega t)]^2 = \tfrac{1}{2}mv^2\,[J_1(2\omega t)]^2 \qquad (6)$$

on using the definition of ω given in equation (2). This has its maximum values when the derivative of $J_1(2\omega t)$ is zero. This is also the condition that $\dot{\xi}_{-1}$, $\dot{\xi}_0$ and $\dot{\xi}_1$ shall be equal, as can be verified from equation (2), using (5).

The roots of $J_1'(2\omega t)$ are not at first equally spaced but rapidly become so, and are then separated by intervals of π. It is convenient to use the period of this ultimate motion as a standard of time. This period, it may be noted, is proportional to the period which a diatomic molecule would have if composed of two atoms of the same kind. Thus, writing

$$2\omega T = 2\pi$$

we have

$$2\omega t = 2\pi t/T.$$

In the first column of Table I the roots of $J_1'(2\omega t)$ are given, and in the second column the intervals of time between successive maxima and minima measured in units of T.

TABLE I—POTENTIAL ENERGY IN EACH OF THE CENTRE LINKS AT GREATEST AND LEAST EXTENSIONS

$2\omega t$	t/T	$J_1(2\omega t)$	$W_{0,1} \div \frac{1}{2}mv^2$
1·84	—	0·5819	0·3387
5·34	0·55	−0·3461	0·1198
8·54	0·51	0·2733	0·0747
11·70	0·51	−0·2333	0·0544
14·85	0·50	0·2070	0·0428

From this table it is evident that the energy of extension in one of the centre links and the equal energy of compression in the other link at the first maximum is equal to just over one-third of the energy initially given to the system. At this instant the three centre particles are still moving forward each with a velocity $(0{\cdot}3167)v$ and their combined kinetic energy is $(0{\cdot}3012)\frac{1}{2}mv^2$, so that all but 2 % of the energy is still stored in the three centre particles. The forward motion of the centre atom does not cease until $2\omega t$ is equal to 2·405 and that of the atoms on each side of it until $2\omega t = 5{\cdot}135$.

The rapid dispersal of energy from the centre links is evident from the last column of the table. After one complete period of $(\xi_1 - \xi_0)$ the potential energy of each centre link has fallen to less than one-quarter of its value at the first maximum. Since for large t the asymptotic behaviour of $J_1(2\omega t)$ is given by

$$(\pi\omega t)^{-\frac{1}{2}}\cos(2\omega t - \tfrac{3}{4}\pi),$$

we see that ultimately the potential energy of the centre link at the maxima is inversely proportional to the time and the rate of loss of energy to the inverse square of the time. The energy stored in the centre link depends on ωt, and so, according to this classical method of solution, the same fraction of energy is lost after each period of vibration whatever the masses or force constants (κ) of the atoms. The greater the "natural" period ω, the quicker is the dispersal of energy in time.

From the asymptotic behaviour of $J_{2s+1}(2\omega t)$, which gives the lengths of the sth link at any instant, viz.

$$J_{2s+1}(2\omega t) \sim (\pi\omega t)^{-\frac{1}{2}}\cos\left(2\omega t - \frac{4s+3}{4}\pi\right),$$

we infer that ultimately neighbouring links differ in phase by an amount π and so are opposite in phase. The centre portion of the chain settles down to the normal mode of highest frequency (neighbouring atoms in opposite phase) with an amplitude which diminishes as the disturbance spreads along the chain.

While all the atoms begin to be disturbed from the moment the centre atom is given its initial impulse, the disturbance of a distant link does not reach its maximum value for an appreciable time. The first maximum of $J_{2s+1}(2\omega t)$, when s is large, is given approximately by (Jahnke and Emde 1933, p. 211)

$$2\omega t = (2s+1) + (0{\cdot}809)(2s+1)^{\frac{1}{3}},$$

and so the time which elapses before the extension of the sth link reaches its first maximum is given approximately by

$$t = (2s+1)T/2\pi,$$

where T has been defined above as the "natural" period of vibration. From this point of view the disturbance may be regarded as spreading outwards with a velocity which is ultimately equal to $a\omega$.

It seems reasonable to infer that similar results would be obtained from the classical theory for the analogous problem of an atom of one kind attached to the end of a long chain of atoms of another kind, assuming the end atom set in motion with a given velocity. The result that the energy is dissipated in times of the order of one or two vibrations is in harmony with the results obtained in preceding papers by the method of quantum mechanics for the deactivation of adsorbed atoms from higher to lower vibrational states.

SUMMARY

A problem is discussed which is analogous to the deactivation of an atom adsorbed on a surface from a higher to a lower vibrational state. One atom of an infinite chain of atoms is assumed to be set in motion, the others being initially at rest, and the rate of loss of energy is discussed. It is shown that according to the classical theory the energy of the links which join the disturbed atom to its neighbours is reduced to less than one-quarter of its initial value in one complete vibration. The rate of loss of energy is ultimately proportional to the inverse square of the time.

REFERENCES

Bateman 1932 "Partial Differential Equations" p. 228. Camb. Univ. Press.
Havelock 1910 *Phil Mag.* (6) **19**, 191.
Jahnke and Emde 1933 "Funtionentafeln." Berlin.
Lennard-Jones and Devonshire 1936 *Proc. Roy. Soc.* A, **156** 6, 29 and 37.
— — 1937 *Proc. Roy. Soc.* A, **158**, 242, 253 and 269.
Lennard-Jones and Goodwin 1937 *Proc. Roy. Soc.* A, **163**, 101.
Lennard-Jones and Strachan 1935 *Proc. Roy. Soc.* A, **150**, 442.
Schrödinger 1914 *Ann. Phys., Lpz.* **44**, 916.

The Interaction of Atoms and Molecules with Solid Surfaces

XII—Critical Phenomena in a Two-Dimensional Gas

By A. F. Devonshire, Ph.D.

The University Chemical Laboratory, Cambridge

(*Communicated by J. E. Lennard-Jones, F.R.S.—*
Received 12 *August* 1937)

1—Introduction

In a paper recently published by Professor Lennard-Jones and the author (Lennard-Jones and Devonshire 1937) the equation of state of a gas at high concentrations has been calculated in terms of the interatomic fields. The equation found had the right kind of properties and, in particular, using the interatomic fields previously determined from the observed equation of state at low concentrations (Lennard-Jones 1931), the critical temperature was given correctly to within a few degrees for the inert gases.

In this paper we shall apply the same method to determine the equation of state of a two-dimensional gas. Although such a gas cannot strictly be obtained in practice, an inert gas adsorbed on a surface (or in fact any gas held by van der Waals' forces only) would probably behave very much like one, the fluctuations of the potential field over the surface not being of much importance. In confirmation of this it may be noted that the specific heat of argon adsorbed on charcoal was found by Simon (Simon 1935) to be equal to that of a perfect two-dimensional gas down to 60° K. A gas adsorbed on a liquid would be an even better representation of a two-dimensional one. Some measurements on the adsorption of krypton and xenon on liquid mercury have been made by Cassel and Neugebauer (Cassel and Neugebauer 1936), and they found no trace of any critical phenomena though they worked at temperatures considerably below the critical temperature of xenon. Our results are in agreement with this, for they show that the critical temperature of a two-dimensional gas should be about half that of the corresponding three-dimensional one.

2—Calculation of the Equation of state

As in the three-dimensional case we shall use the approximation of expressing the partition function of a dense gas as a product of the partition functions of the individual members of the assembly, each member being confined to a cell from which all others are excluded. We shall suppose that the system consists of N particles moving in an area s which is divided in some regular way into N equal cells each of area s^*, and that each particle is confined to one of these cells. As before we shall assume that the average field in which any one atom moves is that due to its immediate neighbours when each is in its equilibrium position, that is at the centre of its own cell. Such a field will have a high degree of symmetry, and it will be sufficient for our purpose to replace the actual field by one which is circularly symmetrical about the centre of the cell. This may be obtained by taking the average field as the atom within the cell describes a circle about the centre.

Let a be the average distance between nearest neighbours and $\phi(r)$ their mutual potential energy at a distance r apart. Then if one particle is kept fixed while the other is moved about a circle of radius r described by the vector $\mathbf{a}+\mathbf{r}$ the average potential of the particles is given by

$$\bar{\phi}(r) = \frac{1}{\pi}\int_0^\pi \phi\{(r^2+a^2-2ar\cos\theta)^{\frac{1}{2}}\}\,d\theta. \tag{1}$$

If c is the number of nearest neighbours the average potential energy within a cell for $r<a$ may be written as

$$\psi(r) = c\bar{\phi}(r). \tag{2}$$

For a monatomic gas a convenient form for $\phi(r)$ is given by

$$\phi(r) = Ar^{-n}-Br^{-m}, \tag{3}$$

and then

$$\psi(r) = \frac{c}{\pi}\int_0^\pi \{A(r^2+a^2-2ar\cos\theta)^{-n/2}-B(r^2+a^2-2ar\cos\theta)^{-m/2}\}\,d\theta. \tag{4}$$

Now
$$\int_0^\pi \frac{d\theta}{(d+b\cos\theta)} = \frac{\pi}{(d^2-b^2)^{\frac{1}{2}}},$$
when $d>b$, and hence

$$\int_0^\pi \frac{d\theta}{(d+b\cos\theta)^r} = \frac{\pi(-)^{r-1}}{(r-1)!}\frac{\partial^{r-1}}{\partial d^{r-1}}\left\{\frac{1}{(d^2-b^2)^{\frac{1}{2}}}\right\}, \tag{5}$$

so that

$$\psi(r) = c\left[A\frac{(-)^{n/2-1}}{(n/2-1!)}\frac{\partial^{n/2-1}}{\partial d^{n/2-1}}\left\{\frac{1}{(d^2-b^2)^{\frac{1}{2}}}\right\}-B\frac{(-)^{m/2-1}}{(m/2-1)!}\frac{\partial^{m/2-1}}{\partial d^{m/2-1}}\left\{\frac{1}{(d^2-b^2)^{\frac{1}{2}}}\right\}\right], \tag{6}$$

where
$$d = r^2+a^2, \quad b = 2ar,$$

provided m and n are both even.

For the special case of $n = 12$, $m = 6$, which has been found to represent the fields of some of the inert gases satisfactorily (Lennard-Jones 1931), we get

$$\psi(r) - \psi(0) = c[Aa^{-12} l_s(y) - Ba^{-6} m_s(y)], \tag{7}$$

where

$$y = r^2/a^2, \tag{8}$$

$$l_s(y) = (1+y)(1+24y+76y^2+24y^3+y^4)(1-y)^{-11} - 1, \tag{9}$$

and

$$m_s(y) = (1+4y+y^2)(1-y)^{-5} - 1.$$

Since a^2 is proportional to s^*, the specific area, we may write the equation for $\psi(r)$ in the form

$$\psi(r) - \psi(0) = A_s\{(s_0^*/s^*)^6 l_s(y) - 2(s_0^*/s^*)^3 m_s(y)\}, \tag{10}$$

where A_s and s_0^* are constants, chosen so that

$$A_s(s_0^*/s^*)^6 = cAa^{-12}, \quad 2A_s(s_0^*/s^*)^3 = cBa^{-6}. \tag{11}$$

Putting $s_0 = Ns_0^*$, and $s = Ns^*$, we also have

$$\psi(r) - \psi(0) = A_s\{(s_0/s)^6 l_s(y) - 2(s_0/s)^3 m_s(y)\}. \tag{12}$$

The partition function for a particle moving in this field, when the energy zero is taken to be that of a particle at $r = 0$, is given by

$$\begin{aligned} f(T) &= (2\pi mkT)\,h^{-2}\int_0^{a/2} 2\pi r \exp[\{\psi(r) - \psi(0)\}/kT]\,dr \\ &= (2\pi mkT)\,h^{-2}\,\pi a^2 \int_0^{\frac{1}{4}} \exp\left[\frac{A_s}{kT}\left\{-\left(\frac{s_0}{s}\right)^6 l_s(y) + 2\left(\frac{s_0}{s}\right)^3 m_s(y)\right\}\right] dy, \end{aligned} \tag{13}$$

where we have neglected the contribution to the partition function from portions of the cell outside the circle of radius $a/2$. The partition function for the whole system, when the energy zero is that of an isolated atom at rest on the surface, is then

$$F(T) = [f(T)]^N \exp\left[\frac{N}{kT}\frac{1}{2}\left\{2A_s\left(\frac{s_0}{s}\right)^3 - A_s\left(\frac{s_0}{s}\right)^6 + \alpha(s)\right\}\right], \tag{14}$$

where $\alpha(s)$ is an extra term inserted to take account of the interaction of particles which are not nearest neighbours. For a hexagonal structure the interaction between such particles increases the attractive term in the potential energy by about 6 % and has a negligible effect on the repulsive term. We have therefore

$$F(T) = [f(T)]^N \exp\left[\frac{N}{kT}\left\{1{\cdot}06A_s\left(\frac{s_0}{s}\right)^3 - 0{\cdot}5A_s\left(\frac{s_0}{s}\right)^6\right\}\right], \tag{15}$$

which may be written in the form

$$\frac{1}{N}\log F(T) = \frac{\Lambda_s}{kT}\left\{1{\cdot}06\left(\frac{s_0}{s}\right)^3 - 0{\cdot}5\left(\frac{s_0}{s}\right)^6\right\} + \log\left(\frac{2\pi s}{\sqrt{3N}}\right) + \log g + \log\left(\frac{2\pi mkT}{h^2}\right), \tag{16}$$

where g is a function of (Λ_s/kT) and of (s_0/s) only, viz.

$$g = \int_0^{\frac{1}{2}} \exp\left[\frac{\Lambda_s}{kT}\left\{-\left(\frac{s_0}{s}\right)^6 l_s(y) + 2\left(\frac{s_0}{s}\right)^3 m_s(y)\right\}\right] dy. \tag{17}$$

We have used the relation $a^2 = 2s^*/\sqrt{3}$ for a hexagonal structure. All the equilibrium properties of the system may now be readily derived and, in particular, the two-dimensional pressure is given by

$$\begin{aligned} p_s &= kT\frac{\partial}{\partial s}\log F(T) \\ &= \frac{NkT}{s}\left[1 - \frac{\Lambda_s}{kT}\left\{3{\cdot}18\left(\frac{s_0}{s}\right)^3 - 3\left(\frac{s_0}{s}\right)^6\right\} - \frac{6\Lambda_s}{kT}\left\{\left(\frac{s_0}{s}\right)^3\frac{g_m}{g} - \left(\frac{s_0}{s}\right)^6\frac{g_l}{g}\right\}\right], \end{aligned} \tag{18}$$

where g_l and g_m are functions of (Λ_s/kT) and (s_0/s) only,

$$g_m = \int_0^{\frac{1}{2}} m_s(y)\exp\left[\frac{\Lambda_s}{kT}\left\{-\left(\frac{s_0}{s}\right)^6 l_s(y) + 2\left(\frac{s_0}{s}\right)^3 m_s(y)\right\}\right] dy, \tag{19}$$

and g_l is given by a similar expression. Similarly the mean energy per atom is given by

$$\begin{aligned} \bar{E}_s &= \frac{k}{N}T^2\frac{\partial}{\partial T}\log F(T) \\ &= \Lambda_s\left\{0{\cdot}5\left(\frac{s_0}{s}\right)^6 - 1{\cdot}06\left(\frac{s_0}{s}\right)^3 + \left(\frac{s_0}{s}\right)^6\frac{g_l}{g} - 2\left(\frac{s_0}{s}\right)^3\frac{g_m}{g}\right\} + kT, \end{aligned} \tag{20}$$

and the specific heat at constant area by

$$\begin{aligned} c_s = \frac{\partial E_s}{\partial T} = k\Bigg[1 + \left(\frac{\Lambda_s}{kT}\right)^2\Bigg\{\left(\frac{s_0}{s}\right)^{12}\left(\frac{g_{ll}g - g_l^2}{g^2}\right) - 4\left(\frac{s_0}{s}\right)^9\left(\frac{g_{lm}g - g_lg_m}{g^2}\right) \\ + 4\left(\frac{s_0}{s}\right)^6\left(\frac{g_{mm}g - g_m^2}{g^2}\right)\Bigg\}\Bigg], \end{aligned} \tag{21}$$

where $$g_{ll} = \int_0^{\frac{1}{2}} l^2(y)\exp\left[\frac{\Lambda}{kT}\left\{-\left(\frac{s_0}{s}\right)^6 l(y) + 2\left(\frac{s_0}{s}\right)^3 m(y)\right\}\right] \tag{22}$$

and g_{lm}, g_{mm} are given by similar expressions.

The values of g, g_l, and g_m calculated by numerical integration for two values of A_s/kT and a range of values of s/s_0 are given in Table I. The isotherms deduced from them are shown in fig. 1.

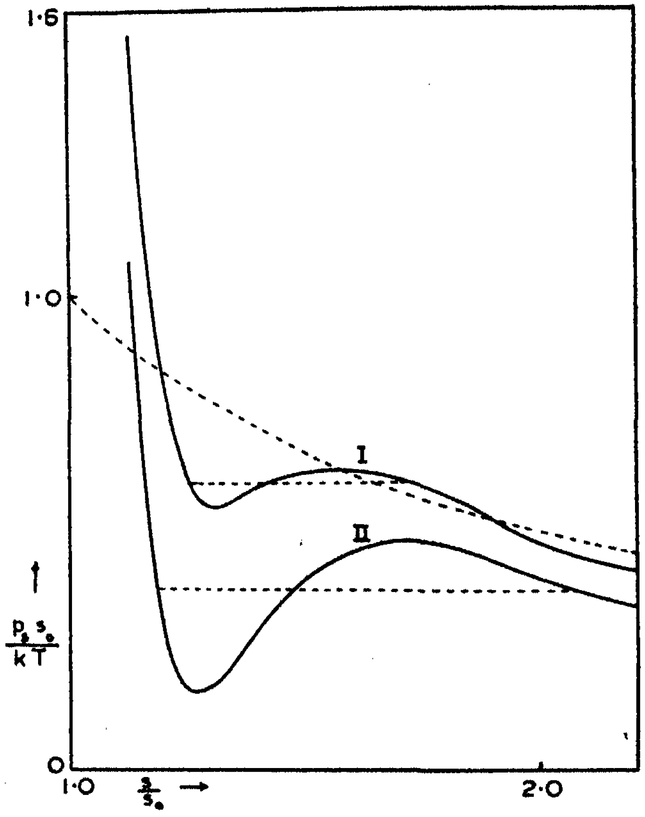

FIG. 1—Calculated isotherms. Curve I corresponds to $A_s/kT = 9$, curve II to $A_s/kT = 10$, and the dotted curve to a perfect gas. The saturated vapour phase is shown dotted.

TABLE I—THE FUNCTIONS g, g_l, AND g_m

		$A_s/kT = 9$			$A_s/kT = 10$		
s/s_0	$(s_0/s)^3$	g	g_l	g_m	g	g_l	g_m
1·126	0·70	0·01250	0·00518	0·001128	0·01162	0·00446	0·000982
1·186	0·60	0·01840	0·01090	0·002277	0·01730	0·00957	0·002018
1·260	0·50	0·02891	0·02580	0·00508	0·02763	0·02324	0·00462
1·357	0·40	0·04912	0·0714	0·01286	0·04806	0·0665	0·01212
1·494	0·30	0·0917	0·2403	0·03764	0·0928	0·2347	0·03723
1·710	0·20	0·1902	1·085	0·1344	0·2011	1·119	0·1405
1·882	0·15	0·2844	2·733	0·2799	0·3081	2·910	0·3018
2·154	0·10	0·4317	8·44	0·644	0·4791	9·26	0·716

From these functions we deduce the equation of state from equation (18), the values of $p_s s/NkT$ being given in Table II. The isotherm for $A_s/kT = 9$ is fairly close to the critical one and an extrapolation shows that the critical temperature is given approximately by $A_s/kT_s = 8{\cdot}6$. From the relations (11) we have

$$A_s = cB^2/4A,$$

and so, adopting the value $c = 6$ for a hexagonal arrangement, we can derive the critical temperature from the formula

$$kT_s = B^2/5{\cdot}7\,A.$$

Comparing this with the value T_c of the critical temperature found for the three-dimensional case (Lennard-Jones and Devonshire 1937) we have

$$T_s/T_c = 0{\cdot}53.$$

The critical area is given approximately by $s/s_0 = 1{\cdot}4$, that is when the mean distance of the atoms apart is 1·18 times that in a diatomic molecule.

TABLE II—CALCULATED ISOTHERMS FOR A DENSE, TWO-DIMENSIONAL GAS

		$A_s/kT = 9$		$A_s/kT = 10$	
s/s_0	$(s_0/s)^3$	$p_s s/NkT$	$p_s s_0/NkT$	$p_s s/NkT$	$p_s s_0/NkT$
1·126	0·70	1·741	1·546	1·185	1·052
1·186	0·60	1·052	0·887	0·467	0·394
1·260	0·50	0·749	0·594	0·205	0·163
1·357	0·40	0·780	0·575	0·321	0·237
1·494	0·30	0·932	0·624	0·597	0·400
1·710	0·20	1·048	0·613	0·818	0·478
1·882	0·15	1·019	0·541	0·840	0·446
2·154	0·10	0·911	0·423	0·754	0·350

In conclusion I should like to thank Professor J. E. Lennard-Jones, F.R.S., for suggesting the problem and for many helpful discussions with him while it was being carried out. I am also indebted to the Department of Scientific and Industrial Research for a grant.

SUMMARY

A method previously used to find the equation of state of a three-dimensional gas at large densities is applied to the two-dimensional case. Two isotherms are calculated, and it is estimated that the critical temperature of a gas in two dimensions should be about half the critical temperature of the same gas in three dimensions.

REFERENCES

Cassel and Neugebauer 1936 *J. Phys. Chem.* **40**, 523.
Lennard-Jones 1931 *Proc. Phys. Soc.* **43**, 461.
Lennard-Jones and Devonshire 1937 *Proc. Roy. Soc.* A, **163**, 53.
Simon 1935 *Z. phys. Chem.* B, **28**, 189.

A Comparison of the Absorption Spectra of some Typical Unsymmetrical Cyanine Dyes

BY BERNARD BEILENSON, NELLIE I. FISHER AND FRANCES M. HAMER

(*Communicated by Sir William Pope, F.R.S.—Received* 5 *June* 1937)

INTRODUCTION

A study has recently been made of the absorption spectra of eleven series of typical symmetrical cyanine dyes; each series comprised, in general, four members, in which two similar heterocyclic nuclei were linked by one, three, five, and seven methenyl groups (Fisher and Hamer 1936). The correlation of frequencies of maximum absorption with changes in chemical constitution proved so interesting that it seemed desirable to extend our work to other series of cyanine dyes, having two dissimilar, instead of two similar, nuclei. The object, with which we set out, was to combine each of the nuclei already studied with every other one, in order to ascertain how exactly the absorption maximum of each unsymmetrical cyanine thus obtained is the mean of those of the two related symmetrical dyes. That it is approximately the mean has been often accepted as axiomatic. For instance, Mills and Odams (1924) considered the structure of their new 2 : 4′-carbocyanine to be confirmed by the fact that its absorption maximum was intermediate in position between those of the 2 : 2′- and 4 : 4′-carbocyanines.

As before, ethiodides were selected for the study, and our aim was to examine purified specimens of the compounds, under standard conditions, in methyl alcoholic solution.

EXPERIMENTAL

The original scope of the work was restricted by the difficulty of preparing unsymmetrical tricarbocyanines, which class was finally omitted; in the dicarbocyanine series, members containing a benzoxazole or naphthoxazole nucleus were omitted, as also those containing more than one quinoline nucleus. The whole of the indo-series (IV in the original paper, Fisher and Hamer 1936) was also left out, on account of the inaccessibility of the quaternary salt used as starting-point, and three simple cyanines were also omitted. Altogether 105 unsymmetrical cyanines have been prepared and examined.

Of the simplest type, in which the nuclei are joined by one : CH · group, surprisingly few are described in the scientific literature: in these isolated instances, individual references are given. Since the patent literature, however, contains some account of other compounds of this type, or of general methods by which they may be prepared, a list of such references is given below.*

In the series in which the nuclei are joined by the three-carbon chain, : CH · CH : CH ·, still fewer individual references to scientific literature can be given, but here important general methods of preparation, applied to certain examples, are to be found in the patents.†

In the series in which the nuclei are joined by the five-carbon chain, : CH · CH : CH · CH : CH ·, the only references are those of the patents.‡

In preparing some of the unsymmetrical carbocyanines, it was occasionally found that, although a halogen determination on the purified compound might give a satisfactory result, nevertheless a test of the photographic sensitizing action revealed contamination by one or both of the related symmetrical substances. For this reason, each of the purified compounds was subjected, not only to a halogen determination, but also to the extremely delicate photographic test, and, if necessary, was then further purified, before its absorption spectrum was examined.

The names of the compounds prepared are given below, following the nomenclature described by one of us (Hamer 1934). The series are numbered as in the original paper on symmetrical cyanines (Fisher and Hamer 1936) and the graphic formulae show the skeletons (to be taken in conjunction with the static formulae VII and VIII), which are characteristic of the nuclei.

---

* Brooker and Kodak Ltd., B.P. 378,455, B.P. 380,140 and B.P. 385,267/1930. I. G. Farbenind. A.-G., B.P. 386,791 and B.P. 388,898/1931, B.P. 423,792/1932, B.P. 423,827/1933. Ilford Ltd. and Hamer, B.P. 387,167/1931. Kendall, B.P. 424,559/1933, B.P. 438,420/1934. Kodak Ltd., B.P. 408,571/1932.

† I.C.I. Ltd., Piggott and Rodd, B.P. 344,409/1929, B.P. 354,898/1930.

‡ I.C.I. Ltd., Piggott and Rodd, B.P. 355,693/1930. I. G. Farbenind. A.-G., B.P. 434,234 and B.P. 434,235/1933.

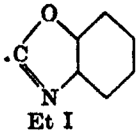

I

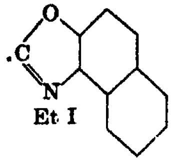

I A

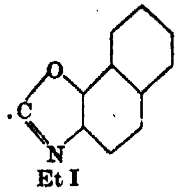

I B

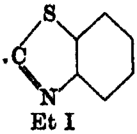

II

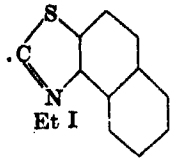

II A

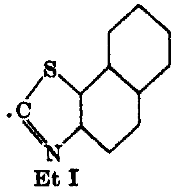

II B

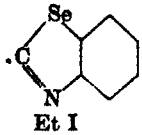

III

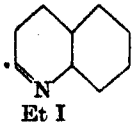

V

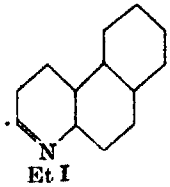

V B

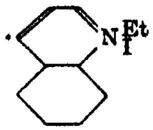

VI

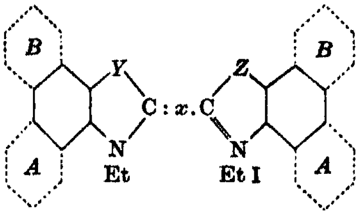

VII

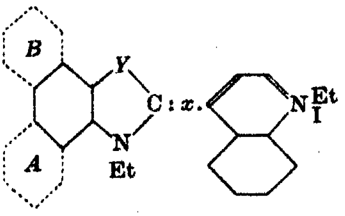

VIII

The original numbering of the series has been extended; thus, for example, I × I A indicates that unsymmetrical series which is related to the two symmetrical series, I and I A. The unsymmetrical compounds derived from any pair out of the series I, I A, I B, II, II A, II B, III, V, and V B may be represented by the general formula VII, where *Y* and *Z* are —O—, —S—, —Se—, or · CH : CH ·. The nuclei in such an unsymmetrical dye differ from one another, either by virtue of a difference in *Y* and *Z*, or because of the presence of a fused-on benzene ring in one of the positions indicated by dotted lines (*A* for series I A and II A, *B* for series I B, II B, and V B), or from both these causes. Where series VI is involved, the general formula is VIII. In the simple cyanine series, *x* (in formulae VII and VIII) is : CH ·, in the carbocyanine series it is : CH · CH : CH ·, and in the dicarbocyanine series : CH · CH : CH · CH : CH ·.

For arranging the rather unwieldy number of substances, it seemed logical to take first that nucleus which is characteristic of series I and combine it with the nuclei characteristic of each of the other series, in order (I A, I B, II, II A, II B, III, V, V B, and VI), then to take the nucleus characteristic of I A and combine it, in order, with each of the remaining nuclei (I B, II, II A, II B, III, V, V B, and VI), and so on.

I × I A:
  2:2′-Diethyl-3:4-benzoxacyanine iodide (**1**).
  2:2′-Diethyl-3:4-benzoxacarbocyanine iodide (**2**).

I × I B:
  2:2′-Diethyl-5:6-benzoxacyanine iodide (**3**).
  2:2′-Diethyl-5:6-benzoxacarbocyanine iodide (**4**).

I × II:
  2:2′-Diethyloxathiacyanine iodide (**5**).
  2:2′-Diethyloxathiacarbocyanine iodide (**6**).

I × II A:
  2:2′-Diethyl-3′:4′-benzoxathiacyanine iodide (**7**).
  2:2′-Diethyl-3′:4′-benzoxathiacarbocyanine iodide (**8**).

I × II B:
  2:2′-Diethyl-5′:6′-benzoxathiacyanine iodide (**9**).
  2:2′-Diethyl-5′:6′-benzoxathiacarbocyanine iodide (**10**).

I × III:
  2:2′-Diethyloxaselenacyanine iodide (**11**).
  2:2′-Diethyloxaselenacarbocyanine iodide (**12**).

I × V:
  2:1′-Diethyloxa-2′-cyanine iodide (**13**) (Brooker and Keyes 1935).
  2:1′-Diethyloxa-2′-carbocyanine iodide (**14**) (Ogata 1934*b*).

I × V B:
  2:1′-Diethyl-5′:6′-benzoxa-2′-cyanine iodide (**15**).
  2:1′-Diethyl-5′:6′-benzoxa-2′-carbocyanine iodide (**16**).

I × VI:
  2:1′-Diethyloxa-4′-cyanine iodide (**17**).
  2:1′-Diethyloxa-4′-carbocyanine iodide (**18**).

I A × I B:
  2:2′-Diethyl-3:4:5′:6′-dibenzoxacyanine iodide (**19**).
  2:2′-Diethyl-3:4:5′:6′-dibenzoxacarbocyanine iodide (**20**).

- I A × II:
  - 2:2′-Diethyl-3:4-benzoxathiacyanine iodide (**21**).
  - 2:2′-Diethyl-3:4-benzoxathiacarbocyanine iodide (**22**).
- I A × II A:
  - 2:2′-Diethyl-3:4:3′:4′-dibenzoxathiacyanine iodide (**23**).
  - 2:2′-Diethyl-3:4:3′:4′-dibenzoxathiacarbocyanine iodide (**24**).
- I A × II B:
  - 2:2′-Diethyl-3:4:5′:6′-dibenzoxathiacyanine iodide (**25**).
  - 2:2′-Diethyl-3:4:5′:6′-dibenzoxathiacarbocyanine iodide (**26**).
- I A × III:
  - 2:2′-Diethyl-3:4-benzoxaselenacyanine iodide (**27**).
  - 2:2′-Diethyl-3:4-benzoxaselenacarbocyanine iodide (**28**).
- I A × V:
  - 2:1′-Diethyl-3:4-benzoxa-2′-cyanine iodide (**29**).
  - 2:1′-Diethyl-3:4-benzoxa-2′-carbocyanine iodide (**30**).
- I A × V B:
  - 2:1′-Diethyl-3:4:5′:6′-dibenzoxa-2′-cyanine iodide (**31**).
  - 2:1′-Diethyl-3:4:5′:6′-dibenzoxa-2′-carbocyanine iodide (**32**).
- I A × VI:
  - 2:1′-Diethyl-3:4-benzoxa-4′-cyanine iodide (**33**).
  - 2:1′-Diethyl-3:4-benzoxa-4′-carbocyanine iodide (**34**).
- I B × II:
  - 2:2′-Diethyl-5:6-benzoxathiacyanine iodide (**35**).
  - 2:2′-Diethyl-5:6-benzoxathiacarbocyanine iodide (**36**).
- I B × II A:
  - 2:2′-Diethyl-5:6:3′:4′-dibenzoxathiacyanine iodide (**37**).
  - 2:2′-Diethyl-5:6:3′:4′-dibenzoxathiacarbocyanine iodide (**38**).
- I B × II B:
  - 2:2′-Diethyl-5:6:5′:6′-dibenzoxathiacyanine iodide (**39**).
  - 2:2′-Diethyl-5:6:5′:6′-dibenzoxathiacarbocyanine iodide (**40**).
- I B × III:
  - 2:2′-Diethyl-5:6-benzoxaselenacyanine iodide (**41**).
  - 2:2′-Diethyl-5:6-benzoxaselenacarbocyanine iodide (**42**).
- I B × V:
  - 2:1′-Diethyl-5:6-benzoxa-2′-cyanine iodide (**43**).
  - 2:1′-Diethyl-5:6-benzoxa-2′-carbocyanine iodide (**44**).
- I B × V B:
  - 2:1′-Diethyl-5:6:5′:6′-dibenzoxa-2′-cyanine iodide (**45**).
  - 2:1′-Diethyl-5:6:5′:6′-dibenzoxa-2′-carbocyanine iodide (**46**).
- I B × VI:
  - 2:1′-Diethyl-5:6-benzoxa-4′-cyanine iodide (**47**).
  - 2:1′-Diethyl-5:6-benzoxa-4′-carbocyanine iodide (**48**).
- II × II A:
  - 2:2′-Diethyl-3:4-benzthiacyanine iodide (**49**).
  - 2:2′-Diethyl-3:4-benzthiacarbocyanine iodide (**50**).
  - 2:2′-Diethyl-3:4-benzthiadicarbocyanine iodide (**51**).

II × II B:
2:2′-Diethyl-5:6-benzthiacyanine iodide (**52**).
2:2′-Diethyl-5:6-benzthiacarbocyanine iodide (**53**).
2:2′-Diethyl-5:6-benzthiadicarbocyanine iodide (**54**).

II × III:
2:2′-Diethylselenathiacyanine iodide (**55**).
2:2′-Diethylselenathiacarbocyanine iodide (**56**).
2:2′-Diethylselenathiadicarbocyanine iodide (**57**).

II × V:
2:1′-Diethylthia-2′-cyanine iodide (**58**) (Hamer 1928).
2:1′-Diethylthia-2′-carbocyanine iodide (**59**) (Ogata 1934*b*).
2:1′-Diethylthia-2′-dicarbocyanine iodide (**60**).

II × V B:
2:1′-Diethyl-5′:6′-benzthia-2′-cyanine iodide (**61**).
2:1′-Diethyl-5′:6′-benzthia-2′-carbocyanine iodide (**62**).
2:1′-Diethyl-5′:6′-benzthia-2′-dicarbocyanine iodide (**63**).

II × VI:
2:1′-Diethylthia-4′-cyanine iodide (**64**) (Braunholtz and Mills 1922).
2:1′-Diethylthia-4′-carbocyanine iodide (**65**).
2:1′-Diethylthia-4′-dicarbocyanine iodide (**66**).

II A × II B:
2:2′-Diethyl-3:4:5′:6′-dibenzthiacarbocyanine iodide (**67**).
2:2′-Diethyl-3:4:5′:6′-dibenzthiadicarbocyanine iodide (**68**).

II A × III:
2:2′-Diethyl-3′:4′-benzselenathiacarbocyanine iodide (**69**).
2:2′-Diethyl-3′:4′-benzselenathiadicarbocyanine iodide (**70**).

II A × V:
2:1′-Diethyl-3:4-benzthia-2′-cyanine iodide (**71**) (Hamer 1928).
2:1′-Diethyl-3:4-benzthia-2′-carbocyanine iodide (**72**).
2:1′-Diethyl-3:4-benzthia-2′-dicarbocyanine iodide (**73**).

II A × V B:
2:1′-Diethyl-3:4:5′:6′-dibenzthia-2′-cyanine iodide (**74**).
2:1′-Diethyl-3:4:5′:6′-dibenzthia-2′-carbocyanine iodide (**75**).
2:1′-Diethyl-3:4:5′:6′-dibenzthia-2′-dicarbocyanine iodide (**76**).

II A × VI:
2:1′-Diethyl-3:4-benzthia-4′-cyanine iodide (**77**) (Keyes and Brooker 1937).
2:1′-Diethyl-3:4-benzthia-4′-carbocyanine iodide (**78**).
2:1′-Diethyl-3:4-benzthia-4′-dicarbocyanine iodide (**79**).

II B × III:
2:2′-Diethyl-5′:6′-benzselenathiacarbocyanine iodide (**80**).
2:2′-Diethyl-5′:6′-benzselenathiadicarbocyanine iodide (**81**).

II B × V:
2:1′-Diethyl-5:6-benzthia-2′-cyanine iodide (**82**) (Hamer 1928).
2:1′-Diethyl-5:6-benzthia-2′-carbocyanine iodide (**83**).
2:1′-Diethyl-5:6-benzthia-2′-dicarbocyanine iodide (**84**).

II B × V B:
2:1′-Diethyl-5:6:5′:6′-dibenzthia-2′-cyanine iodide (**85**).
2:1′-Diethyl-5:6:5′:6′-dibenzthia-2′-carbocyanine iodide (**86**).
2:1′-Diethyl-5:6:5′:6′-dibenzthia-2′-dicarbocyanine iodide (**87**).

II B × VI:
2:1′-Diethyl-5:6-benzthia-4′-cyanine iodide (**88**) (Keyes and Brooker 1937).
2:1′-Diethyl-5:6-benzthia-4′-carbocyanine iodide (**89**).
2:1′-Diethyl-5:6-benzthia-4′-dicarbocyanine iodide (**90**).

III × V:
2:1′-Diethylselena-2′-cyanine iodide (**91**) (Brooker and Keyes 1935).
2:1′-Diethylselena-2′-carbocyanine iodide (**92**).
2:1′-Diethylselena-2′-dicarbocyanine iodide (**93**).

III × V B:
2:1′-Diethyl-5′:6′-benzselena-2′-cyanine iodide (**94**).
2:1′-Diethyl-5′:6′-benzselena-2′-carbocyanine iodide (**95**).
2:1′-Diethyl-5′:6′-benzselena-2′-dicarbocyanine iodide (**96**).

III × VI:
2:1′-Diethylselena-4′-cyanine iodide (**97**).
2:1′-Diethylselena-4′-carbocyanine iodide (**98**).
2:1′-Diethylselena-4′-dicarbocyanine iodide (**99**).

V × V B:
1:1′-Diethyl-5:6-benz-2:2′-cyanine iodide (**100**) (Hamer 1928).
1:1′-Diethyl-5:6-benz-2:2′-carbocyanine iodide (**101**) (*cf.* Mills and Raper 1925).

V × VI:
1:1′-Diethyl-2:4′-cyanine iodide (**102**) (Hamer 1928).
1:1′-Diethyl-2:4′-carbocyanine iodide (**103**) (Mills and Odams 1924, Ogata 1932, 1934*a*).

V B × VI:
1:1′-Diethyl-5:6-benz-2:4′-cyanine iodide (**104**).
1:1′-Diethyl-5:6-benz-2:4′-carbocyanine iodide (**105**).

The absorption curves of the methyl alcoholic solutions were obtained exactly as described in the earlier paper (Fisher and Hamer 1936), and for this work we are deeply indebted to Messrs. N. Groet and E. E. Richardson, and Dr. L. A. Jones, all of the Eastman Kodak Company, and to Mr. R. B. Morris and Dr. A. S. Roy, of Kodak Ltd.

In the absorption curves, density is, as before, plotted against wavelength (mμ). In every figure the dotted line refers to the simple cyanine, in which the nuclei are linked by one :CH· group, the curve with alternate dots and dashes refers to the corresponding carbocyanine, and the curve outlined by dashes is that of the dicarbocyanine.

As the number of curves is so large, only those involving the simplest series (I, II, III, V, and VI) have been selected for publication, whilst those involving series with a fused-on benzene ring (I A, I B, II A, II B, and

V B) have been omitted. Fig. 1 contains the curves for the cyanines and carbocyanines of series I × II, I × III, I × V, and I × VI: the dicarbocyanines of these four series were not obtained. Fig. 2 comprises the curves for the cyanines, carbocyanines and dicarbocyanines of series II × III, II × V, and II × VI. Fig. 3 contains the curves for the corresponding sets of the series III × V and III × VI, whilst fig. 4 contains those for the cyanine and carbocyanine of series V × VI.

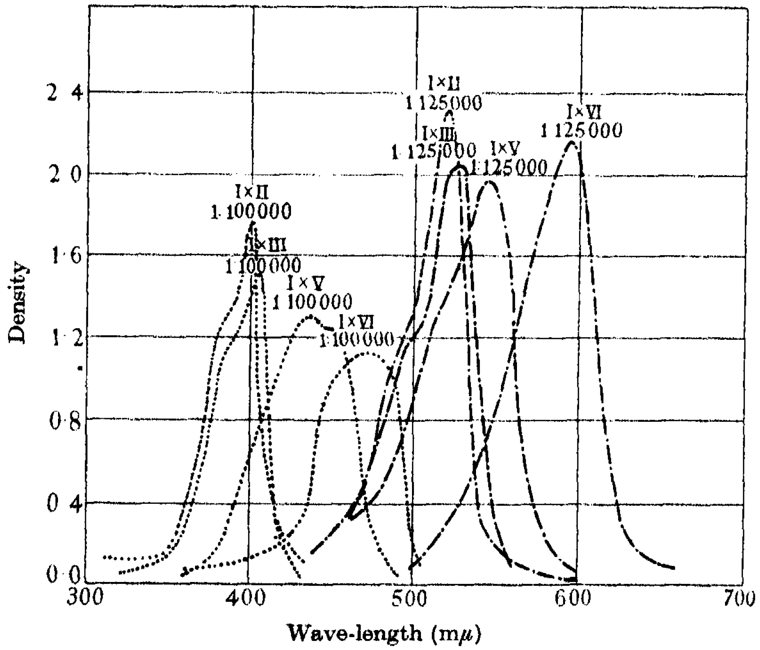

FIG. 1

In the simple cyanine series, compounds **25** and **100** have a secondary band on the short wave-length side of the principal band, whilst an inflexion, more or less marked, occurs on that same side of the curve of each of the following: nos. **5** (fig. 1), **7**, **9**, **11**, **33**, **37**, **39**, **47**, **58** (fig. 2), **61**, **71**, **74**, **82**, **91** (fig. 3), **102** (fig. 4), and **104**. (As in the earlier paper (Fisher and Hamer 1936), the parts of the curves lying at a wave-length less than 350 or 375 mμ have not been considered.) No. **13** (fig. 1) is strikingly abnormal, in that the secondary band lies on the long wave-length side of the principal band, and nos. **15**, **29**, and **43** tend towards the same abnormality, in having an inflexion on that side of the curve.

In the carbocyanine series, secondary bands in the normal position occur in the curves of nos. **28**, **34**, **101**, **103** (fig. 4), and **105**, and inflexions in

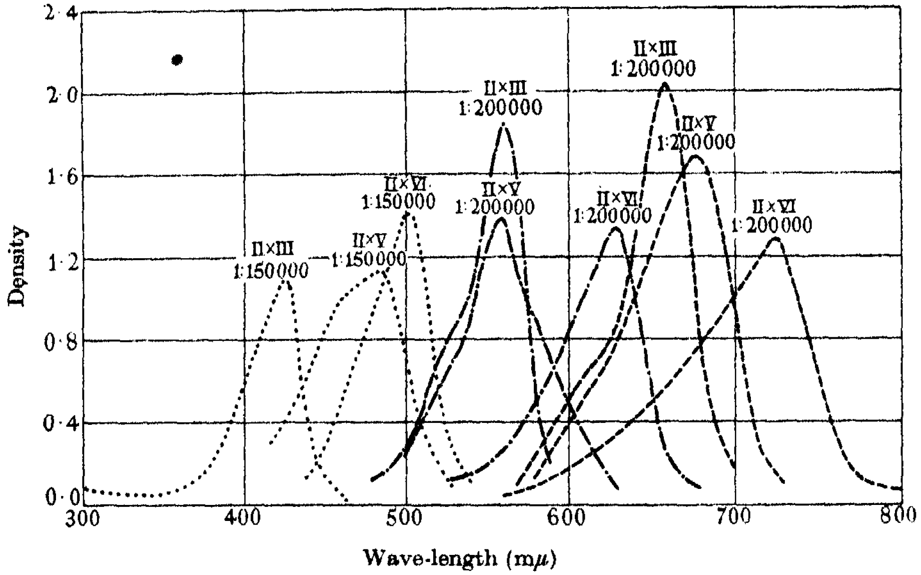
2·4
2·0
1·6
1·2
0·8
0·4
0·0
Density
300
400
500
600
700
800
Wave-length (mμ)
II×III
1:200000
II×III
1:200000
II×V
1:200000
II×VI
1:150000
II×V
1:200000
II×VI
1:200000
II×VI
1:200000
II×III
1:150000
II×V
1:150000

Fig. 2

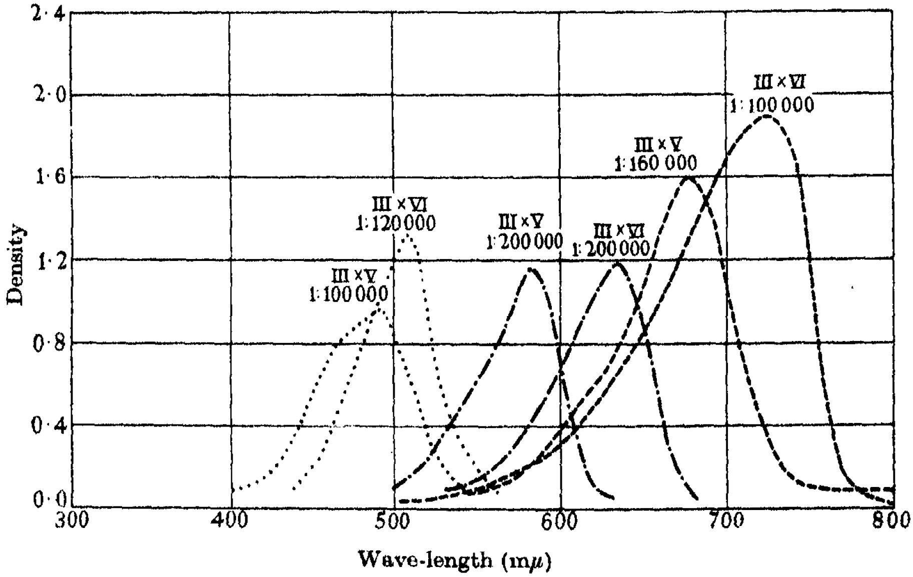
2·4
2·0
1·6
1·2
0·8
0·4
0·0
Density
300
400
500
600
700
800
Wave-length (mμ)
III×VI
1:100000
III×V
1:160000
III×VI
1:120000
III×V
1:200000
III×VI
1:200000
III×V
1:100000

Fig. 3

those of nos. **2**, **4**, **6** (fig. 1), **8**, **10**, **12** (fig. 1), **14** (fig. 1), **20**, **22**, **24**, **26**, **30**, **36**, **38**, **40**, **42**, **44**, **53**, **56** (fig. 2), **67**, **69**, **78**, **80**, **83**, and **89**.

In the dicarbocyanine series, the curves of nos. **51**, **54**, **57** (fig. 2), **68**, **70**, **81**, and **84** show inflexions on the normal side.

Of the eight compounds which show a definite secondary band, six contain a quinoline nucleus.

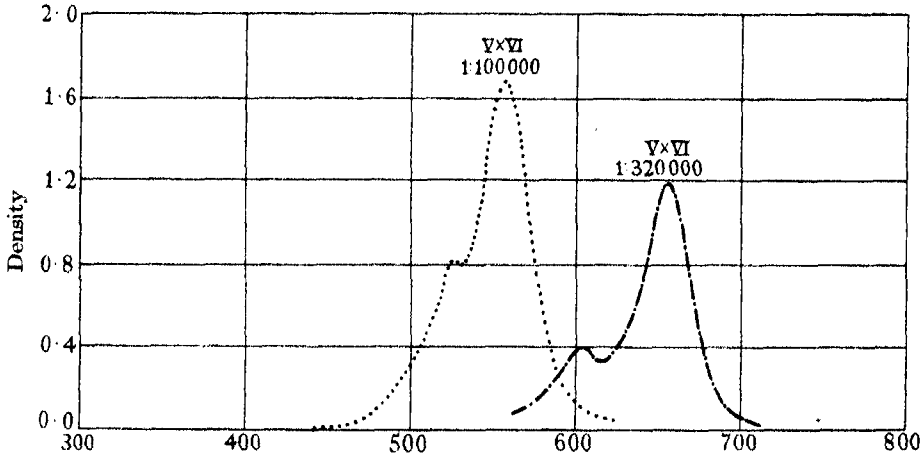

FIG. 4

In Table I are given the values of the absorption maxima of all the simple cyanines, as read from the curves. Table II contains the values of the absorption maxima of the carbocyanines, and Table III those for the dicarbocyanines. In Tables I–III, the numbers of the symmetrical series, to which the unsymmetrical dyes are related, are to be read both horizontally and vertically. It is clear that, along the diagonals (top left to bottom right corner), data relating to the symmetrical compounds of the first paper are to be found (Fisher and Hamer 1936). These compounds have the Roman numerals originally assigned to them; the two numbers accompanying each are the values found (Fisher and Hamer 1936) for the wave-length of maximum absorption (mμ), and for the frequency of maximum absorption, respectively, of their methyl alcoholic solutions, the former value being printed in italics. The numbers in heavy type are those given to the compounds in the present paper. Below the diagonal, the italicized number, which accompanies each dye number, is the value now found for the wave-length of maximum absorption, whilst the number below it is the corresponding frequency of maximum absorption. Above the diagonal, the

TABLE I—SIMPLE CYANINE SERIES. ABSORPTION MAXIMA AND FREQUENCIES OF MAXIMUM ABSORPTION

Frequencies to be multiplied by 10^{12} to give true values

CH	I Oxa-	I A Oxa- 3:4:3′:4′- dibenz.	I B Oxa- 5:6:5′:6′- dibenz.	II Thia-	II A Thia- 3:4:3′:4′- dibenz.	II B Thia- 5:6:5′:6′- dibenz.	III Selena-	V 2:2′-	V B 2:2′- 5:6:5′:6′- dibenz.	VI 4:4′-
I	I *372* 807	**1** *387* 775	**3** *383* 782	**5** *397* 756	**7** *414* 725	**9** *412* 727	**11** *400* 749	**13** *447* 671	**15** *462* 649	**17** *482* 622
I A	**1** *391* 767	IV *402* 746	**19** *398* 753	**21** *412* 728	**23** *429* 699	**25** *427* 702	**27** *415* 722	**29** *462* 649	**31** *477* 628	**33** *497* 603
I B	**3** *383* 783	**19** *394* 761	VII *395* 760	**35** *408* 734	**37** *425* 705	**39** *424* 707	**41** *412* 728	**43** *458* 655	**45** *474* 633	**47** *494* 607
II	**5** *402* 746	**21** *410* 732	**35** *410* 732	X *422* 711	**49** *439* 683	**52** *437* 686	**55** *425* 705	**58** *472* 636	**61** *487* 615	**64** *507* 591
II A	**7** *416* 721	**23** *430* 698	**37** *428* 701	**49** *437* 686	XIV *456* 658	— *454* 660	— *442* 678	**71** *489* 613	**74** *504* 595	**77** *524* 572
II B	**9** *420* 714	**25** *431* 696	**39** *428* 701	**52** *438* 685	— — —	XVIII *453* 662	— *441* 680	**82** *487* 615	**85** *503* 596	**88** *523* 573
III	**11** *406* 739	**27** *416* 721	**41** *414* 725	**55** *427* 703	— — —	— — —	XXII *429* 699	**91** *475* 631	**94** *491* 611	**97** *511* 587
V	**13** *437* 686	**29** *450* 667	**43** *450* 667	**58** *486* 617	**71** *503* 596	**82** *502* 598	**91** *490* 612	XXIX *522* 575	**100** *537* 558	**102** *557* 538
V B	**15** *445* 674	**31** *467* 642	**45** *467* 642	**61** *498* 602	**74** *511* 587	**85** *515* 582	**94** *503* 596	**100** *537* 559	XXXIII *553* 543	**104** *573* 523
VI	**17** *470* 638	**33** *490* 612	**47** *495* 606	**64** *503* 596	**77** *523* 573	**88** *521* 576	**97** *507* 592	**102** *557* 538	**104** *571* 525	XXXVI *593* 506

Observed Values

Calculated Values

TABLE II—CARBOCYANINE SERIES. ABSORPTION MAXIMA AND FREQUENCIES OF MAXIMUM ABSORPTION

Frequencies to be multiplied by 10^{12} to give true values

Calculated Values

3CH	I Oxa-	I A Oxa- 3:4:3′:4′- dibenz.	I B Oxa- 5:6:5′:6′- dibenz.	II Thia-	II A Thia- 3:4:3′:4′- dibenz.	II B Thia- 5:6:5′:6′- dibenz.	III Selena-	V 2:2′-	V B 2:2′- 5:6:5′:6′- dibenz.	VI 4:4′-
I	II *485* 619	**2** *499* 601	**4** *500* 600	**6** *521* 576	**8** *541* 554	**10** *539* 556	**12** *527* 569	**14** *545* 550	**16** *560* 536	**18** *594* 505
I A	**2** *497* 604	V *513* 585	**20** *514* 583	**22** *535* 561	**24** *555* 540	**26** *553* 542	**28** *541* 554	**30** *559* 537	**32** *574* 523	**34** *608* 493
I B	**4** *498* 602	**20** *515* 582	VIII *515* 583	**36** *536* 560	**38** *556* 539	**40** *554* 541	**42** *542* 553	**44** *560* 536	**46** *575* 522	**48** *609* 492
II	**6** *520* 577	**22** *535* 561	**36** *535* 561	XI *557* 539	**50** *577* 520	**53** *575* 522	**56** *563* 532	**59** *581* 516	**62** *596* 503	**65** *630* 476
II A	**8** *537* 559	**24** *556* 539	**38** *554* 541	**50** *577* 520	XV *597* 503	**67** *595* 504	**69** *583* 514	**72** *601* 499	**75** *616* 487	**78** *650* 461
II B	**10** *536* 560	**26** *552* 544	**40** *550* 545	**53** *578* 519	**67** *594* 505	XIX *593* 506	**80** *581* 516	**83** *599* 501	**86** *614* 489	**89** *648* 463
III	**12** *527* 569	**28** *540* 555	**42** *540* 555	**56** *562* 534	**69** *582* 515	**80** *581* 516	XXIII *570* 526	**92** *587* 511	**95** *602* 498	**98** *637* 471
V	**14** *545* 550	**30** *562* 534	**44** *565* 531	**59** *560* 536	**72** *600* 500	**83** *597* 502	**92** *582* 515	XXX *605* 496	**101** *620* 484	**103** *654* 458
V B	**16** *555* 540	**32** *569* 527	**46** *575* 522	**62** *590* 508	**75** *607* 494	**86** *601* 499	**95** *592* 507	**101** *615* 488	XXXIV *635* 472	**105** *669* 448
VI	**18** *596* 503	**34** *613* 489	**48** *617* 486	**65** *630* 476	**78** *647* 464	**89** *653* 459	**98** *632* 475	**103** *656* 457	**105** *668* 449	XXXVII *704* 426

Observed Values

TABLE III—DICARBOCYANINE SERIES. ABSORPTION MAXIMA AND FREQUENCIES OF MAXIMUM ABSORPTION

Frequencies to be multiplied by 10^{12} to give true values

Calculated Values

5CH	I Oxa-	I A Oxa- 3:4:3′:4′-dibenz.	I B Oxa- 5:6:5′:6′-dibenz.	II Thia-	II A Thia- 3:4:3′:4′-dibenz.	II B Thia- 5:6:5′:6′-dibenz.	III Selena-	V 2:2′-	V B 2:2′-5:6:5′:6′-dibenz.	VI 4:4′-
I	III *580* 517	— *593* 506	— *594* 505	— *615* 488	— *635* 472	— *633* 474	— *620* 484	— *644* 466	— *659* 455	— *695* 433
I A	— — —	VI *606* 495	— *607* 494	— *628* 478	— *648* 463	— *646* 464	— *633* 474	— *657* 456	— *672* 446	— *708* 424
I B	— — —	— — —	IX *608* 494	— *629* 477	— *649* 462	— *647* 463	— *634* 473	— *658* 456	— *673* 446	— *709* 423
II	— — —	— — —	— — —	XII *650* 462	**51** *670* 447	**54** *668* 449	**57** *655* 458	**60** *679* 442	**63** *694* 432	**66** *730* 411
II A	— — —	— — —	— — —	**51** *672* 446	XVI *691* 434	**68** *689* 435	**70** *675* 444	**73** *699* 429	**76** *714* 420	**79** *750* 400
II B	— — —	— — —	— — —	**54** *672* 446	**68** *693* 433	XX *687* 437	**81** *673* 445	**84** *697* 430	**87** *712* 421	**90** *748* 401
III	— — —	— — —	— — —	**57** *659* 455	**70** *680* 441	**81** *677* 443	XXIV *660* 455	**93** *684* 438	**96** *699* 429	**99** *735* 408
V	— — —	— — —	— — —	**60** *676* 444	**73** *693* 433	**84** *695* 432	**93** *675* 444	XXXI *708* 434	— *723* 415	— *759* 395
V B	— — —	— — —	— — —	**63** *683* 439	**76** *695* 432	**87** *693* 433	**96** *679* 442	— — —	XXXV *738* 406	— *774* 388
VI	— — —	— — —	— — —	**66** *725* 414	**79** *755* 397	**90** *750* 400	**99** *722* 416	— — —	— — —	XXXVIII *810* 370

Observed Values

italicized number,* which accompanies each number denoting a dye, is the value for the wave-length of maximum absorption, as calculated by taking the mean of the values found for the appropriate pair of symmetrical dyes, whilst the number below it is the frequency corresponding to this value of the wave-length of maximum absorption.

DISCUSSION OF RESULTS

The above method of calculating the wave-length of maximum absorption and, from it, the frequency, is purely empirical. Since the subject is too complex to have yet received adequate theoretical treatment from the physical or mathematical standpoint, this empiricism is common to the various possible methods of calculation: it seemed well to choose the simplest, in preference to others which are more involved.

It is seen from Tables I–III that the agreement of the observed frequency with that thus calculated is sometimes almost exact. The instances of close agreement are most numerous in the carbocyanine series and least so in the simple cyanine series. For example, taking those frequencies which differ by not more than 5 units from the calculated values: out of forty-two simple cyanines nineteen show this close agreement, out of forty-five carbocyanines forty show it, and out of eighteen dicarbocyanines twelve show it. Again, taking cases where the agreement is so poor that the frequencies differ by more than 10 units from the calculated values: this occurs with fourteen of the simple cyanines, only one carbocyanine, and three dicarbocyanines.

It appears from the tables that the observed frequency is apt to diverge from the calculated value when one quinoline nucleus is present. Thus, of the eighteen dyes where the frequencies differ by more than 10 units from the calculated values, no less than seventeen contain one quinoline nucleus, the other one having none. On the other hand, cyanines containing one or two quinoline nuclei sometimes show excellent agreement of the observed and calculated values of the frequencies.

In Table IV are given the frequency decreases which occur when the number of carbon atoms in the chain joining the nitrogen atoms varies from 3 to 5 and from 5 to 7, but since the quinoline nucleus has been found to cause anomalies (Fisher and Hamer 1936), series involving this nucleus have been omitted from Table IV. Table V gives the corresponding values for those compounds in which one nucleus is quinoline, linked in the 2-position, and Table VI the values for those in which one nucleus is quinoline, linked in the 4-position; in this last table, however, the changes are from 5 to 7 and from 7 to 9 carbon atoms (formula VIII for Table VI, as compared with formula VII for Tables IV and V).

TABLE IV

	Number of C atoms in chain joining N atoms			Frequency differences when number of C atoms varies from	
Series	3	5	7	3 to 5	5 to 7
I × I A	**1** 767	**2** 604	—	163	—
I × I B	**3** 783	**4** 602	—	181	—
I × II	**5** 746	**6** 577	—	169	—
I × II A	**7** 721	**8** 559	—	162	—
I × II B	**9** 714	**10** 560	—	154	—
I × III	**11** 739	**12** 569	—	170	—
I A × I B	**19** 761	**20** 582	—	179	—
I A × II	**21** 732	**22** 561	—	171	—
I A × II A	**23** 698	**24** 539	—	159	—
I A × II B	**25** 696	**26** 544	—	152	—
I A × III	**27** 721	**28** 555	—	166	—
I B × II	**35** 732	**36** 561	—	171	—
I B × II A	**37** 701	**38** 541	—	160	—
I B × II B	**39** 701	**40** 545	—	156	—
I B × III	**41** 725	**42** 555	—	170	—
II × II A	**49** 686	**50** 520	**51** 446	166	74
II × II B	**52** 685	**53** 519	**54** 446	166	73
II × III	**55** 703	**56** 534	**57** 455	169	79
II A × II B	—	**67** 505	**68** 433	—	72
II A × III	—	**69** 515	**70** 441	—	74
II B × III	—	**80** 516	**81** 443	—	73

It was recorded that, in the symmetrical series, when the number of carbon atoms in the chain joining the nitrogen atoms varied from 3 to 5, the frequency decrease lay within the limits 188–155, provided series V and V B, involving quinoline nuclei, were omitted (Fisher and Hamer 1936). As seen from Table IV, very similar values are obtained now, the eighteen values lying within the limits 181–152. It was also recorded that, omitting series V and V B, when the number of carbon atoms in the chain joining the nitrogen atoms increased from 5 to 7, the frequency decreases lay between 79 and 72 (Fisher and Hamer 1936). Table IV shows that the present six values lie within these same limits.

It was found before that, where series V and V B were involved, the values were anomalously low (Fisher and Hamer 1936). Similarly here, Table V shows that, on passing from a 3- to a 5-membered carbon chain, when only one quinoline nucleus is present, the fourteen values of the frequency decrease vary from 136 to 81; the value for V × V B, where two quinoline nuclei are present, is 71. On passing from a 5- to a 7-membered chain, in dyes involving one nucleus of series V or V B, the 8 instances of Table V lie within the limits 92–62.

TABLE V

	Number of C atoms in chain joining N atoms			Frequency differences when number of C atoms varies from	
Series	3	5	7	3 to 5	5 to 7
I × V	**13** 686	**14** 550	—	136	—
I × V B	**15** 674	**16** 540	—	134	—
I A × V	**29** 667	**30** 534	—	133	—
I A × V B	**31** 642	**32** 527	—	115	—
I B × V	**43** 667	**44** 531	—	136	—
I B × V B	**45** 642	**46** 522	—	120	—
II × V	**58** 617	**59** 536	**60** 444	81	92
II × V B	**61** 602	**62** 508	**63** 439	94	69
II A × V	**71** 596	**72** 500	**73** 433	96	67
II A × V B	**74** 587	**75** 494	**76** 432	93	62
II B × V	**82** 598	**83** 502	**84** 432	96	70
II B × V B	**85** 582	**86** 499	**87** 433	83	66
III × V	**91** 612	**92** 515	**93** 444	97	71
III × V B	**94** 596	**95** 507	**96** 442	89	65
V × V B	**100** 559	**101** 488	—	71	—

TABLE VI

	Number of C atoms in chain joining N atoms			Frequency differences when number of C atoms varies from	
Series	5	7	9	5 to 7	7 to 9
I × VI	**17** 638	**18** 503	—	135	—
I A × VI	**33** 612	**34** 489	—	123	—
I B × VI	**47** 606	**48** 486	—	120	—
II × VI	**64** 596	**65** 476	**66** 414	120	62
II A × VI	**77** 573	**78** 464	**79** 397	109	67
II B × VI	**88** 576	**89** 459	**90** 400	117	59
III × VI	**97** 592	**98** 475	**99** 416	117	59
V × VI	**102** 538	**103** 457	—	81	—
V B × VI	**104** 525	**105** 449	—	76	—

Table VI shows that, where series VI is implicated, lengthening the carbon chain from 5 to 7 members leads to frequency decreases of 135–109 for seven series where a second quinoline nucleus is absent; but where series V and V B are also involved, then the values are lower, being 81 and 76, respectively. The same table shows the four values for the frequency decreases caused by lengthening the chain from 7 to 9 members, where series VI is involved but a second quinoline nucleus is absent, to vary from 67 to 59.

The values for the frequency decreases on lengthening the carbon chain, which joins the nitrogen atoms, from 5 to 7 are considerably greater in Table VI than they are in Table V. This difference appears to be related to the fact that every compound in Table V has two cyclic carbon atoms in the chain, whilst every one in Table VI has four cyclic carbon atoms in the chain; it confirms the earlier observation (Fisher and Hamer 1936) that the cyclic and non-cyclic carbon atoms are definitely not equivalent as regards their effect on the frequency.

The frequency decreases caused by adding two benzene rings, i.e. two C_4H_4 groups, one to each nucleus, become progressively smaller as the carbon chain joining the nitrogen atoms is lengthened. Apart from the quinoline series (V and V B), when this chain is 3-membered the five values which may be deduced from Table I vary from 50 to 45; when it is 5-membered, the six values deduced from Table II vary from 38 to 32; when it is 7-membered, the one value from Table III is 29. These numbers agree with those which have been recorded for the symmetrical series (Fisher and Hamer 1936). If a quinoline nucleus is present, the four values for a 3-carbon chain, from Table I, are lower, being 44–30, whilst the 4 for a 5-carbon chain vary from 42 to 23, and the two values for a 7-carbon chain are 11 and 12.

From Tables I–III may be read off over 100 values for the frequency change caused by introduction of one benzene ring, i.e. one C_4H_4 group. This is always a frequency decrease except in one instance: namely, in Table III, passing from II B × V to II B × V B, there is an increase of 1 unit. Even in those series where quinoline nuclei are absent, the frequency decreases caused by introduction of C_4H_4 are irregular in the simple cyanine and in the dicarbocyanine series. In the carbocyanine series, however, the regularity is much greater. Thus, apart from the series involving quinoline nuclei, in twenty-eight instances from Table II, the frequency decrease caused by introducing C_4H_4 varies only within the limits 22–13. The presence of a quinoline nucleus introduces irregularities and, of eighteen instances from Table II involving this nucleus, the frequency decrease caused by introducing the extra benzene ring varies within the limits 36–3.

SUMMARY

One hundred and five ethiodides, belonging to the unsymmetrical cyanine type, in which two dissimilar heterocyclic nuclei are linked by one, three, or five methenyl groups, have been prepared, and the absorption curves of their methyl alcoholic solutions were plotted under standard conditions.

The observed values of the wave-lengths of maximum absorption have been compared with those empirically calculated, by taking the mean of the wave-lengths of maximum absorption of the two related symmetrical cyanines, and from these mean values the frequencies of maximum absorption have been calculated. This empiricism is considered to be common to various other possible methods of calculation.

The agreement of the observed frequency with that thus calculated is sometimes very close. The best agreement is obtained in the carbocyanine series. When one quinoline nucleus is present, the observed frequency is apt to diverge from the calculated value.

The frequency decreases caused by lengthening the carbon chain joining the nitrogen atoms from 3 to 5 members are greater than those caused by lengthening it from 5 to 7 members in those series where quinoline is absent, and a certain regularity is observed in the values obtained, but the presence of a quinoline nucleus introduces anomalies. As regards their effect on frequency, cyclic and non-cyclic carbon atoms of the chain are not equivalent.

The frequency decreases caused by adding two extra benzene rings become smaller as the carbon chain joining the nitrogen atoms is lengthened, the values being lowered by the presence of a quinoline nucleus.

Introduction of one benzene ring almost always causes a frequency decrease, the values being most regular in the carbocyanine series. The presence of a quinoline nucleus introduces irregularities.

REFERENCES

Braunholtz and Mills 1922 *J. Chem. Soc.* **121**, 2004.
Brooker and Keyes 1935 *J. Amer. Chem. Soc.* **57**, 2488.
Fisher and Hamer 1936 *Proc. Roy. Soc.* A, **154**, 703.
Keyes and Brooker 1937 *J. Amer. Chem. Soc.* **59**, 74.
Mills and Odams 1924 *J. Chem. Soc.* **125**, 1913.
Mills and Raper 1925 *J. Chem. Soc.* **127**, 2466.
Hamer 1928 *J. Chem. Soc.* p. 206.
— 1934 "Thorpe's Dictionary of Chemistry", supplt., see Cyanine Dyes.
Ogata 1932 *Proc. Imp. Acad. Sci., Tokyo*, **8**, 119.
— 1934*a* *Bull. Inst. Phys. Chem. Res., Tokyo*, **13**, 549.
— 1934*b* *Bull. Inst. Phys. Chem. Res., Tokyo*, **13**, 556.

The Emission of the Latent Energy due to previous Cold Working when a Metal is Heated

By H. Quinney and G. I. Taylor, F.R.S.

(*Received* 19 *April* 1937)

Four principal methods have been used for measuring the latent heats in metals due to change of phase or state, or to cold working:

(1) The total heat at any stage can be measured at a number of temperatures by means of a calorimeter.

(2) The rate of cooling of the specimen can be measured and the latent heat deduced on the assumption of Newton's Law of Cooling.

(3) The rate of heating can be measured when the specimen is placed in a furnace the temperature of which rises at a known uniform rate, Newton's Law being used to deduce rate of increase of thermal energy.

(4) The specimen can be heated electrically in such a way that all the electrical energy is used in heating the specimen.

Of these (1) and (4) involve direct measurements of heat energy, while in (2) and (3) the amount of absorption or emission of heat is deduced indirectly from the heating or cooling curves.

(1) and (4) have been used for measuring specific heats or latent heat of fusion where large quantities of heat are concerned, but when it is desired to measure small quantities of latent energy, such as that stored up in a metal during cold working, (2) and (3) have been used because they permit of greater sensitivity, especially when they are applied differentially.

The latent energy retained by a metal after it has been subjected to cold working can be found by measuring the heat evolved and the mechanical energy expended during the cold working. The difference between these lies latent in the metal, and if the metal is heated the latent energy must be released before the melting point is reached.

Several attempts have been made to measure this latent energy. C. J. Smith (1929) measured the difference between the heat evolved when a gramme of cold-worked and annealed copper wire were dissolved in a solution of bromine in potassium bromide. This method is insensitive because the heat evolution, due to dissolving the annealed copper, is large compared with that due to the latent energy of internal strains in the cold-worked material.

The most sensitive method so far attempted is the differential method of Sato (1931). In this method two specimens were cut from the same bar of metal. One is cold worked and the other annealed. The external dimensions were identical and they were inserted in two equal holes in a block of silver which were heated at a uniform rate. They were insulated from the silver block by a silica lining. The difference T in temperature between the two specimens was measured. In accordance with usual procedure in differential measurements of this kind Newton's Law of Cooling is assumed, and if the thermal resistance of the two silica linings and surfaces of the specimens are identical the difference between the initial heat content of the two specimens is proportional to $\int T\,dt$, where t is the time. Sato found that it was not possible to get identical thermal resistance at the surface of the two specimens so that there was still a difference between the temperatures of the two specimens placed in his apparatus when they had received identical treatment.

To overcome this difficulty he first measured T, the difference in temperature between a strained and unstrained specimen, while raising their temperatures sufficiently high to remove all internal strain. After allowing the apparatus to cool, he reheated without moving the two specimens. If the difference in temperatures on the second heating is T_0, Sato takes the latent heat as proportional to $\int (T-T_0)\,dt$. As a qualitative method for finding the temperatures at which the release of latent energy occurs this method is admirable, but in order to make it yield quantitative results, several assumptions must be made which need considerable justification. If $1/K_1$ and $1/K_2$ are the thermal resistances between the silver block and the annealed and cold-worked specimens respectively, and if H_1 and H_2 are the differences in the energy content after heating to a given temperature, then $H_1 - H_2 = \int K_1(T_s - T_1) + K_2(T_s - T_2)\,dt$, where T_s is the temperature of the silver block.

Similarly on the second heating, if K_1 and K_2 are unaltered, $H_1 - H_2'$ the change in heat content on heating through the same range as before, then

$$H_1 - H_2' = \int K_1(T_s - T_1) + K_2(T_s - T_2')\,dt,$$

and combining (1) and (2) we have

$$H_2 - H_2' = K_2\int (T_2 - T_2')\,dt.$$

In order to use the method for determining latent heat it is necessary to determine K_2. This was done by means of a separate experiment in which the latent energy of a specimen of brass, subjected to a definite amount of cold work, was determined by a calorimeter.

If the value of K_2, so obtained by dividing $H_2 - H'_2$ found by the calorimeter for brass by $\int (T_2 - T'_2)\, dt$, can be assumed constant for all specimens which have received the same mechanical treatment and for all temperatures, the method can be used quantitatively for determining latent heats of cold work in specimens of the same material subjected to different amounts of cold work or in specimens of different materials.

Unfortunately no evidence is given in Sato's paper that this very drastic assumption is justified. It is difficult therefore to accept his results except in the case of brass subjected to the same amount of cold work as that with which the calorimeter experiments were made.

It may be significant that in the experiments to be described below, in which direct measurements of energy input were made, excellent agreement was found with Sato's results in this particular case of brass, but in most other cases there was wide disagreement between his measurements of the amount of latent heat and ours. The temperatures at which we found that the latent heat is liberated agree with those measured by Sato, though our method was too insensitive to allow of any very complete comparison in that respect.

The difficulty inherent in Sato's method occurs in practically all metallurgical investigations which are concerned with quantities of heat. So long as qualitative results only are desired, the heating and cooling curves of specimens contained in furnaces subjected to known rates of heating and cooling are useful. When quantitative results are needed, it is necessary to make so many assumptions regarding the transfer of heat through the surface of the specimens that results are frequently of little value.

In order to avoid the necessity for assuming, as Sato did, that the thermal resistances at the surfaces of specimens of different materials but of the same shape is the same, it is possible to devise a differential method in which only the lesser assumption is made that the thermal resistance of a specimen remains unchanged during two successive heatings.

In an apparatus sketched in fig. 1 two similar specimens, one cold worked and the other annealed placed in two arms of a silica U tube, were heated by two furnaces, made to be as nearly as possible identical in all respects, and supplied by the same current. The temperature difference between the specimens was measured as the pair of furnaces was heated to a temperature higher than that necessary for annealing. After cooling, the temperatures of both furnaces were again raised, and the difference between the temperatures of the two specimens again measured. The results in the cases of copper and aluminium are shown in figs. 2 and 3, where the abscissae refer to difference in temperature between the two specimens. The fact that none of the curves actually coincides with the axis must be attributed to some accidental difference between the furnaces. If this accidental difference is assumed to remain unchanged when the specimen is heated a second or third time without removal from the furnace, the difference between the curves obtained on the first and those obtained on the second or third heating must be due to some change in the specimen which occurs during the first heating. This change will be assumed to consist in the evolution of the latent heat due to cold working.

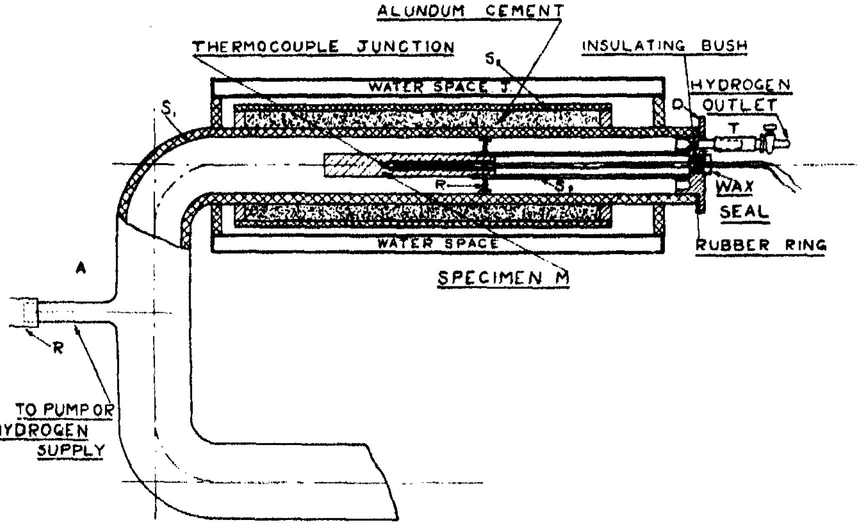

FIG. 1

On inspecting the curves of figs. 2 and 3 it will be seen that the curves for the second and third heating are identical, whereas the curve obtained during the first heating lies above them. In this respect the curves resemble those obtained by Sato, but they differ from them in an important particular. As the temperature rises the evolution of latent heat in Sato's experiments produces a transitory difference between the temperatures of the two specimens which disappears after the heat has ceased being evolved.

As explained above, the latent heat is proportional to the area of the time-temperature difference curve, but the actual magnitude of the latent heat can only be estimated when the thermal resistance between the specimen and the cell which contains it has been measured by some independent method.

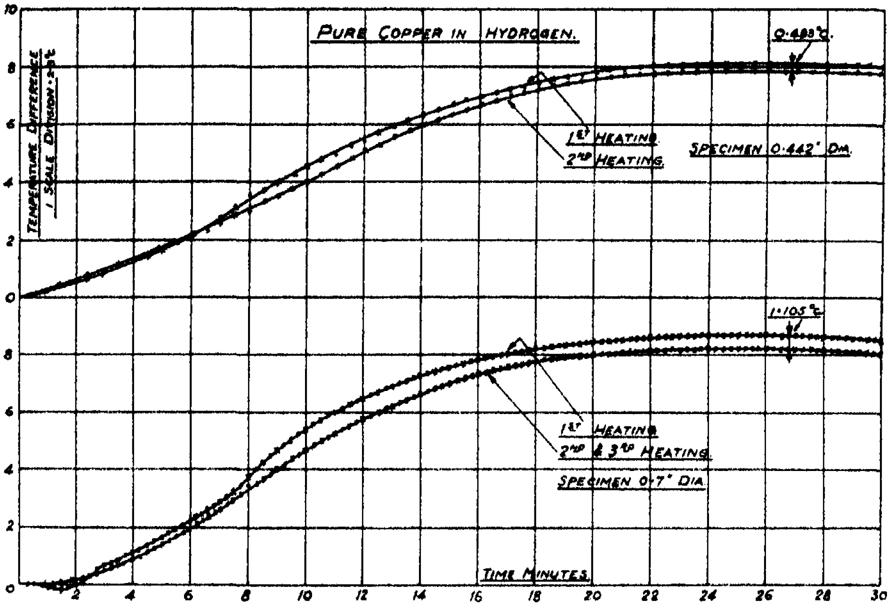

FIG. 2

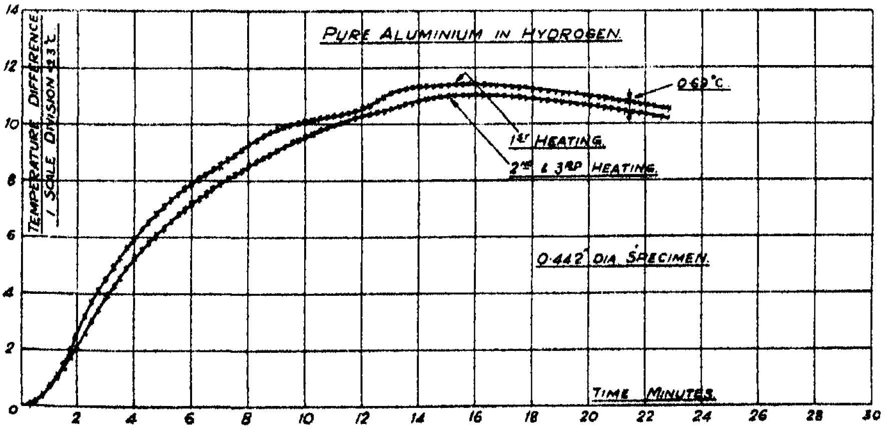

FIG. 3

In the present experiments the curves show that the evolution of latent heat causes the two curves to separate as soon as the heat begins to be evolved. As the temperature rises above that at which latent heat is given out the separation of the two curves begins to decrease, but soon attains a value which remains practically constant for the rest of the experiment.

In fig. 3, which refers to aluminium, this constant difference was 0·69° C. Fig. 2, which refers to copper, contains two pairs of curves, one for a specimen 0·442 in. in diameter and 4 in. long, and the other for a specimen 0·7 in. diameter and 4 in. long. Both had been subjected to the same amount of cold work per gramme. For these two copper specimens the constant temperature differences after losing their latent energy were 0·48 and 1·10° C.

This constant value which the temperature difference attains when all the latent energy has been evolved does not depend on the thermal resistance between the furnace and specimen, but is evidently connected with the fact that part of the furnace near the specimen can be regarded as being in thermal contact with the specimen.

CALCULATION OF LATENT HEAT FOR COPPER

If the specimens were very long in comparison with their diameter, the heat capacity of that part of the furnace, which might be regarded as being in thermal contact with the specimen, might be expected to be independent of the diameter of the specimen.

This assumption was verified by estimating directly the heat capacity per unit length of the furnace and comparing it with that deduced by the method which will now be described.

Assuming, therefore, that h the relevant part of the heat capacity of the furnace is identical for two specimens of different diameters, but the same length, it is possible to calculate h from the two measurements of the constant temperature differences, shown in fig. 2, which were made with copper specimens of the same length (4 in.) and diameter 0·442 in. and 0·70 in. respectively.*

The latent energy evolved by the smaller specimen was sufficient to raise the temperature of the specimen and furnace 0·483° C. If the evolution of latent energy due to cold work would have been sufficient to raise the temperature of the copper alone through θ° C.

$$\frac{\theta}{0{\cdot}483}=\frac{h+45{\cdot}7\sigma}{45{\cdot}7\sigma}, \tag{1}$$

where σ is the specific heat of copper and 45·7 g. is the weight of the smaller specimen. Similarly with the large specimen whose weight was 133 g. and temperature difference 1·105° C.

$$\frac{\theta}{1{\cdot}105}=\frac{h+133\sigma}{133\sigma}. \tag{2}$$

---

* This method has been used previously by Quinney (1929).

Since θ may be assumed the same with both specimens because the same amount of work per g. was done on each, θ and h/σ can be determined by solving (1) and (2).

The result is
$$\theta = 3\cdot37^\circ \text{ C.}, \tag{3}$$
and
$$h/\sigma = 273\cdot3. \tag{4}$$

In these specimens the work done in twisting was measured in the manner described in a previous paper (Taylor and Quinney 1934). In each case it was 4·6 cal./g. This would have been sufficient to raise the temperature 48·5° C. if the whole work had been turned into heat. The fraction of the work done which is absorbed and afterwards measured when it is released on reheating is therefore $3\cdot37/48\cdot5 = 0\cdot07$. 7 % of the cold work originally done on the specimen was therefore released in the form of heat during the first subsequent heating (to about 600° C.).

This is in close agreement with the results given in a previous paper (Taylor and Quinney 1934) where the latent energy was measured during the process of absorption. Fig. 6 of that paper shows the proportion of the cold work done in twisting copper rods which remains latent. It will be seen that over a great part of the range this was 7½ %. Referring to Table III (Taylor and Quinney 1934), it will be seen that for copper this fraction remained practically constant until cold work equivalent to 10·5 cal./g. had been done. The present specimens which had 4·6 cal./g. are therefore within this range.

Using the results obtained with copper specimens for determining the capacity for heat of the furnace, the latent energy contained in cold-worked aluminium and in 70/30 brass was measured.

ALUMINIUM

In the experiment represented in fig. 3 the observed final temperature difference between the annealed and the cold-worked specimen was 0·69° C. and the mass was 20 g., so that taking 0·22 as the specific heat the equation equivalent to (1) is:

$$\frac{\theta}{0\cdot69} = \frac{h + 20 \times 0\cdot22}{20 \times 0\cdot22}. \tag{5}$$

Taking the specific heat of copper 0·1, it will be seen from (4) that $h = 27\cdot3$. Thus from (5) $\theta = 4\cdot98^\circ$ C.

The work done on the specimen during twisting was equivalent to 11·1 cal./g. which is equivalent to a rise in temperature of $11\cdot1/0\cdot22 = 51^\circ$ C.

The fraction of the work done which is emitted as heat when the specimen is reheated is therefore 4·98/51 = 0·098, i.e. 9·8 %.

This may be compared with the proportion absorbed in Farren and Taylor's experiment (Farren and Taylor 1925) which was 8 %.

BRASS

Similar observations with 70/30 brass gave the proportion emitted as 15·8 %.

DESIGN OF CALORIMETER FURNACE

The method described above though free from the greatest defects of the differential method, as applied by Sato, still leaves room for much improvement. In the first place the heat capacity of the furnace is always so much greater than that of the specimen, that the difference in temperature between the annealed and the cold-worked specimen due to the release of the heat is only a small fraction of what it would be if the heat capacity of the furnace could be reduced till it was smaller than that of the specimen.

In the second place it is necessary to assume that the heat capacity of the part of the furnace in thermal contact with the specimen is the same for all specimens of the same length, provided this length is several times as great as the diameter of the furnace. This assumption appears to be true, because the results are in good agreement with those obtained by the use of other methods, but nevertheless it seemed desirable to attempt the design of apparatus which would not suffer from these disadvantages. In doing so it was noticed that the advantages which appear at first sight to favour differential methods are largely illusory. Two furnaces cannot be constructed so that they are really identical. It is only by the use of methods such as that of Sato in which both specimens are heated in the same furnace that the advantages of a differential method can be expected, and then, as we have seen, differences in the thermal resistance at the surface of different specimens may well produce far greater temperature differences than those due to cold work.

These considerations led us to abandon further attempts to use differential methods and to concentrate on devising a furnace in which fewer assumptions need be made about the nature of the thermal interchanges between the specimen and furnace.

In the apparatus now to be described the heat is supplied to the inner surface of a hollow specimen by means of a small electric furnace only

0·11 in. diameter and 1½ in. long. The whole of the electric energy input is therefore transferred to the specimen itself except for the small amount which is necessary to raise the temperature of the furnace and its support.

The thermal resistance between the interior-heating furnace and the specimen does not affect the amount of heat which flows into the specimen, though it does determine the amount by which the temperature of the furnace must exceed that of the specimen in order that all the heat produced by the furnace may pass into the specimen. At the surface of the specimen heat can be lost by convection or radiation. Convection losses are avoided by using a high vacuum. Radiation losses are avoided by a guard-ring furnace which almost completely surrounds the specimen, and is maintained at the same temperature as the specimen itself.

If the guard ring were completely closed, and accurately at the temperature of the specimen, there would be no loss or gain of heat through the outer surface of the specimen whatever its condition or radiative properties might be.

It is clear that with this design the thermal resistance and radiating properties of the surface have no influence on the heat measurements—or at any rate have only a small secondary influence, depending on the necessary departures from the ideal conditions of an infinitely small interior furnace, and a completely closed guard-ring furnace maintained at exactly the same temperature as the specimen.

Fig. 4 shows a sectional elevation of the furnace constructed in accordance with these principles. In this figure the hollow specimen is shown in position as *C* and the furnace as *D*.

Enlarged details of this part of the apparatus are shown inset.

The requirements which had to be satisfied were: (*a*) the specimen must be set on a support which is as good a non-conductor as possible, (*b*) the whole of the furnace must be inside the specimen, so that all heat which leaves it passes directly into the specimen, (*c*) the "guard-ring" furnace surrounding the specimen must be easily removable, so that the specimen and thermojunctions can be changed, (*d*) the apparatus must be vacuum tight and all heating and thermojunction leads must pass through vacuum-tight joints.

The first of these requirements (*a*) was attained by mounting the specimen on a silica post *B*, which was so designed that the cross-section near the specimen was as small as possible. This post, which was made by the Thermal Syndicate,* contained eight holes for wire leads. The two central

---

* The authors are indebted to Mr. Millar of the Thermal Syndicate for the preparation of this silica post.

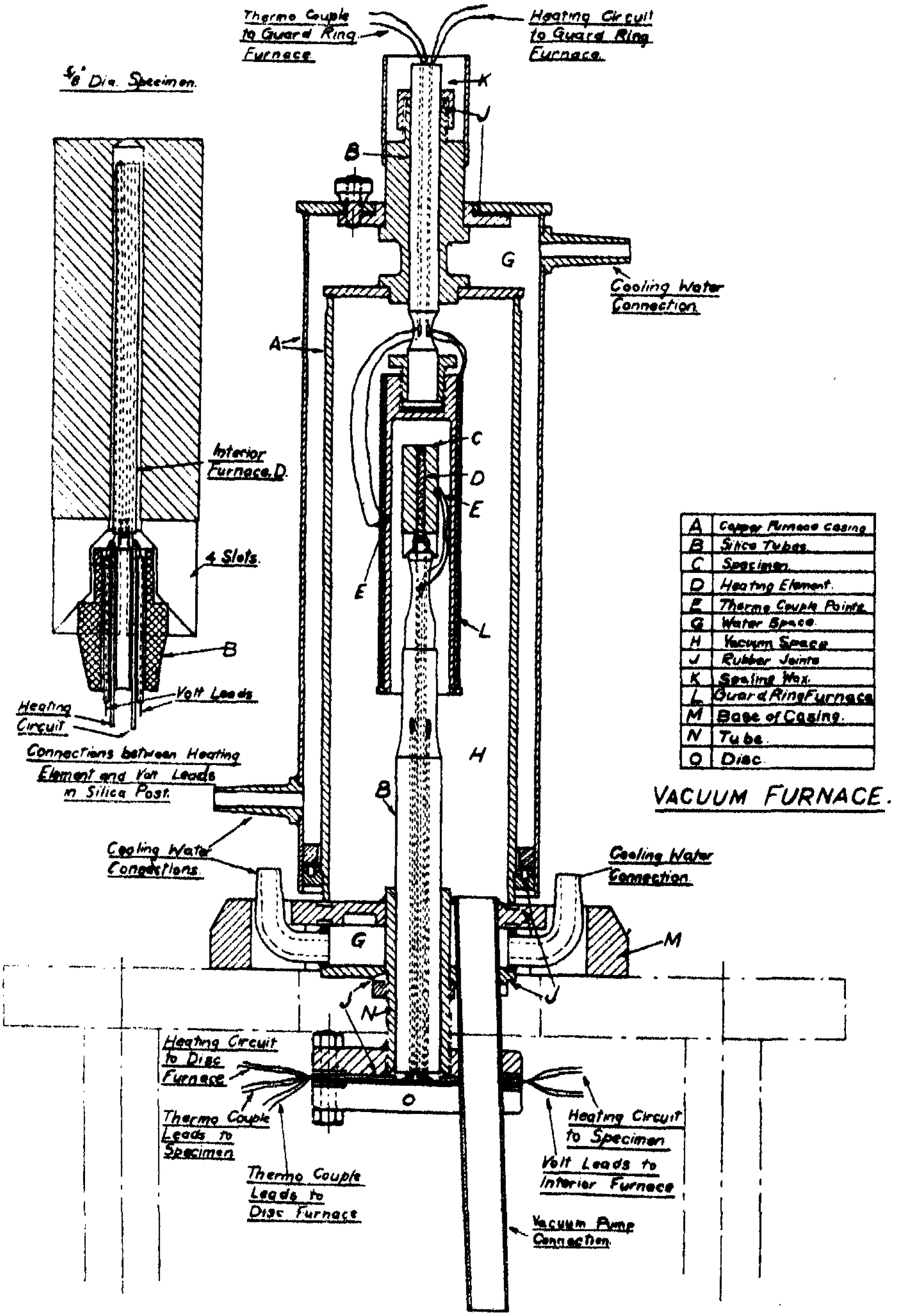
Thermo Couple to Guard Ring Furnace
Heating Circuit to Guard Ring Furnace
5/8" Dia. Specimen
K
J
B
G
Cooling Water Connection
A
C
D
E
E
L
Interior Furnace, D
4 Slots
B
Heating Circuit
Volt Leads
Connections between Heating Element and Volt Leads in Silica Post
H
B
Cooling Water Connections
Cooling Water Connection
M
G
J
J
N
O
Heating Circuit to Disc Furnace
Thermo Couple Leads to Specimen
Thermo Couple Leads to Disc Furnace
Heating Circuit to Specimen
Volt Leads to Interior Furnace
Vacuum Pump Connection
A Copper Furnace Casing
B Silica Tubes
C Specimen
D Heating Element
E Thermo Couple Points
G Water Space
H Vacuum Space
J Rubber Joints
K Sealing Wax
L Guard Ring Furnace
M Base of Casing
N Tube
O Disc
VACUUM FURNACE.

FIG. 4

ones conveyed the heating leads and also the two platinum potential leads for measuring the energy input to the furnace. These potential leads, which were themselves insulated by very small silica tubes, were fused to the two large gauge (0·018 in. diameter) platinum leads to the furnace. The small gauge (0·01 in. diameter) platinum wire of the furnace itself was fused to the upper end of these leads, and the lower ends were welded to the copper-heating leads which passed out of the furnace. By bringing the potential leads from a point which was actually inside the specimen (see inset fig. 4), it was possible to ensure that the measured energy input was wholly used inside the specimen.

The thermojunction *E* on the specimen consisted of a platinum-rhodium disk to which the wires were welded. This disk was screwed by a platinum-rhodium screw to the specimen. The thermojunction leads passed through two of the holes in the silica post.

(*b*) The furnace which is shown inset as *D*, in fig. 4, consisted of a silica tube 0·11 in. diameter and 1½ in. long containing six holes through which the platinum heating wire (0·01 in. diameter) was threaded. The cylindrical specimen was so formed that it rested on the top of the silica post, being thus electrically insulated from the furnace wire.

(*c*) The delicate nature of the electrical connexions of the heating element *D* made it necessary to construct a special slide so that the specimen could be moved into position and the thermocouple screwed on without risk of injury.

(*d*) After the specimen and thermojunctions had been placed in position it was necessary to bring the guard-ring furnace *L*, with all its electrical connexions, and the casing *A* into position and to make the joints vacuum tight. This operation was facilitated by attaching the guard-ring furnace to a silica post *B* which passed through the top of the casing, and was made vacuum tight by wax which was poured into the cup *K*, fig. 4.

The whole of the casing was made of copper and had a highly polished interior which was water jacketed in order to assist in maintaining repeatable temperature conditions inside the apparatus. It could be moved in a vertical slide and bedded down on to a vacuum-tight rubber ring *J* recessed into the base *M*.

To ensure the maintenance of the vacuum at the point where the wires from the heating element passed out of the furnace, a flange was brazed to the tube *N* which was brazed to the base in the casing *M*. This cylindrical flanged head which is drilled to take six ¼ in. diameter securing bolts carries a corresponding disk *O* by means of which it is possible to collect and compress all the leads which are conveyed through the silica post, between two layers of rubber, coated with vacuum grease as shown in the figure.

The guard ring was also heated with platinum wires 0·01 in. diameter carried in fifty fused alumina tubes kindly supplied for the purpose by Dr. Desch of the N.P.L. These tubes were attached vertically to the guard ring by three bindings of tungsten wire. The guard-ring tube itself was of nickel and was painted outside with a solution of silica gel and graphite to facilitate the transfer of heat by radiation from the furnace wire to the metallic nickel. Round the outside of the heating wires of the guard ring was bound a sheet of pure nickel insulated with a thin sheet of mica to prevent radiation to the casing.

Most of the specimens were ⅝ in. diameter and 2 in. long and contained a hole which originally fitted closely round the heating element, but in later experiments this hole was enlarged to facilitate the escape of any gas which might be given off by the specimen during heating.

The specimens after cold working in torsion were cut off to correct length, with a minimum of delay and the outside cylindrical surfaces were not machined after twisting. No grease or lubricant of any kind was used in drilling and machining the specimen, and the machining operations were done at a slow speed so as to avoid as far as possible any heating of the specimen. After washing in carbon tetrachloride and drying in ether the specimens were handled only by means of rubber finger stalls, to avoid any risk of introducing impurities. As soon as the thermocouple had been attached to the specimen the casing *A* was lowered into position and the apparatus was exhausted.

To carry out a test three observers were required. A heating current of about 2 amp. was found suitable for the interior furnace or heating element and the p.d. recorded by the potential leads attached to a high resistance (12000 Ω) voltmeter was generally about 6 V. The current in this interior furnace was controlled by hand during the whole of the test and maintained constant by one observer, who likewise recorded the voltmeter readings every ½ min.

To maintain the guard ring at the same temperature as the specimen, about 2 amp. were required. This current was adjusted where necessary by a second observer who recorded the difference between the readings of the thermocouple attached to the specimen and those of a similar one screwed to the nickel of the guard ring. Any difference which the controlling observer had been unable to eliminate were recorded by him every ½ min. A third observer recorded the temperature of the specimen by means of the potentiometer. The procedure was as follows: Having recorded every

½ min. the temperature of the specimen, it was possible, by means of a double pole change-over switch, to transfer the potentiometer to the guard-ring thermocouple; and the extent to which this was out of balance, if any, was recorded by the second observer who made the necessary adjustment of the guard-ring current to maintain balance. In this way five sets of readings were taken simultaneously, i.e. the current supplied to the interior furnace, potential drop between its potential leads, the temperature of specimen, that of the guard ring, and the guard-ring current.

In the early tests the vacuum was maintained throughout the test by having the whole apparatus attached directly to a Hyvac pump which was started some time before the beginning of the test. It was found, however, that in every case a considerable drop in potential at the potential leads of the interior furnace occurred soon after heating, and also occasionally during the first heating of a specimen. At the same time a small discharge tube attached to the apparatus indicated that this drop in potential was associated with a rise of pressure in the apparatus. This rise was attributed to a sudden evolution of gas which decreased the thermal resistance between the specimen and the heating element so that the heating wire became cooler and therefore suffered a corresponding drop in electrical resistance. Most metals at some stage appeared to give off gases which produced this effect, and it was only after a great many trials that methods were finally devised for overcoming this difficulty.

Some of our results were obtained before we had finally perfected these methods. In the case of copper for instance, in our early experiments we found a difference between the temperature-time curves of an annealed specimen obtained during the first and during subsequent heatings in the apparatus. We also found a difference between the first and subsequent heatings of a specimen which had been subjected to cold work after annealing. The temperature-time curves of the second and subsequent heatings of the annealed and of the cold-worked specimens were, however, found to be identical. It seemed therefore reasonable to suppose that the difference between these two differences was due entirely to the cold work. These differences are shown in fig. 5, and it will be seen that at temperatures above 350° C. they amounted to 13° C. for annealed and 18° C. for the cold-worked specimen. The difference, namely 5° C., was assumed to be due entirely to the latent energy due to cold work. This assumption, however, did not remain an unconfirmed assumption, because when methods for eliminating spurious effects had been perfected, the temperature-time curves of annealed and of cold-worked specimens were again compared, and it was then found that for the annealed specimen the curve obtained on the first heating was identical with that for subsequent heatings (see fig. 6), while for the cold-worked specimen there was at temperatures above (500° C.) a difference of 5° C. See fig. 7.

The cold-worked specimen in this case had received the same amount of cold work as in the early experiments, so that the agreement between the latent heats found in the two cases (namely that required to raise the temperature 5° C.) is proof of the truth of the assumption that the difference between the differences of the temperature-time curves on first and on subsequent heatings is due to the latent heat of cold work.

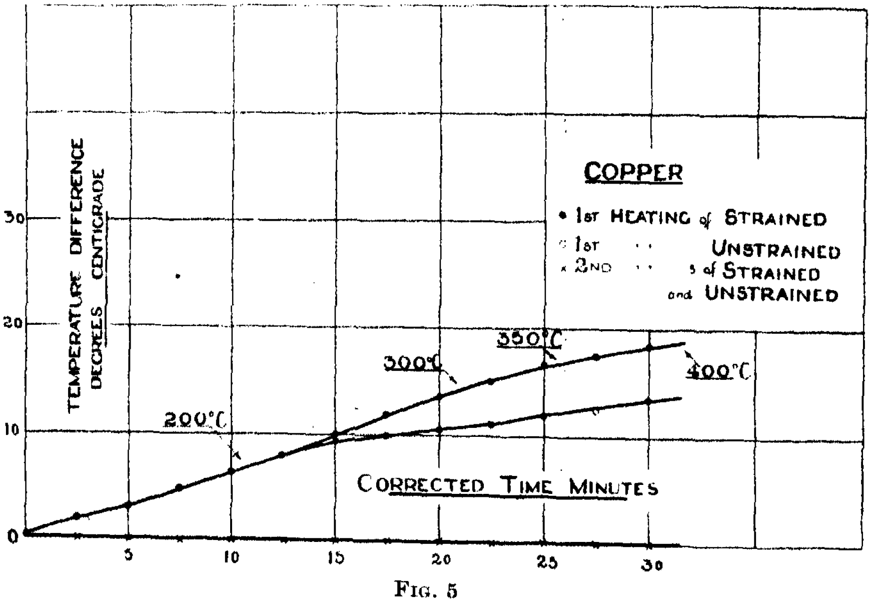

Fig. 5

The results shown in fig. 6 and onwards are those obtained after perfecting the apparatus in a number of respects enumerated below.

Instead of merely maintaining the vacuum for some time before commencing the test, the jackets were heated to a definite temperature well above the dew point, so that possible traces of moisture in the calorimeter were removed before commencing the test. During the whole of this time the calorimeter was exhausted by using a mercury vapour pump with the Hyvac pump as a backing pump.

The hole in the specimen into which the heating element fitted was enlarged and modified to allow any gases which might be evolved on heating to escape easily.

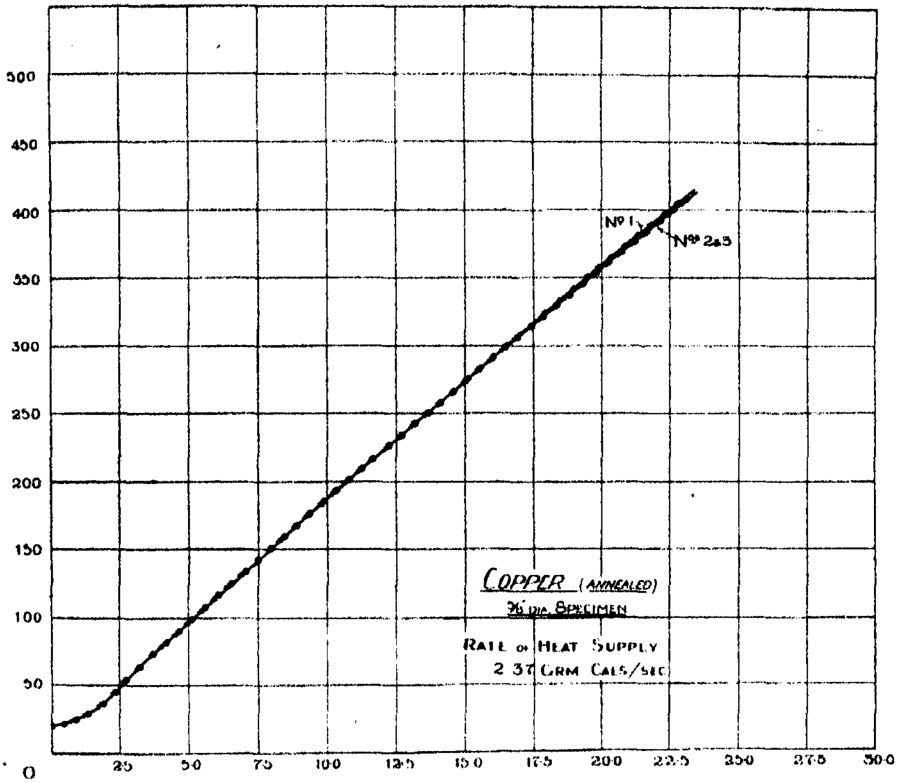
500
450
400
350
300
250
200
150
100
50
0
2·5
5·0
7·5
10·0
12·5
15·0
17·5
20·0
22·5
25·0
27·5
30·0
No 1
Nos 2 & 3
COPPER (ANNEALED)
⅜" dia. Specimen
Rate of Heat Supply
2·37 Grm Cals/sec

Fig. 6

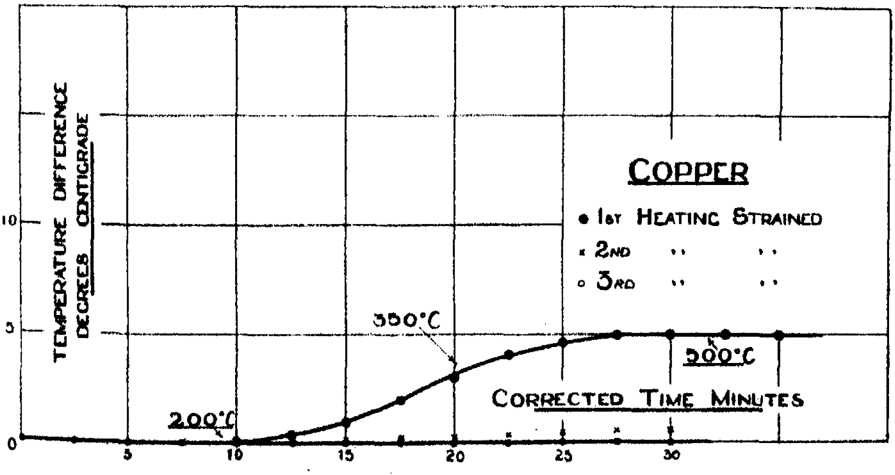
Temperature Difference
Degrees Centigrade
10
5
0
5
10
15
20
25
30
COPPER
● 1st Heating Strained
× 2nd " "
○ 3rd " "
350°C
500°C
200°C
Corrected Time Minutes

Fig. 7

The exhaust passage in the calorimeter was considerably enlarged to facilitate the removal of the gases and the pump was set working and allowed to run in all cases for at least 1 hr. before testing. In some cases the pump was allowed to continue for 24 hr. before the test was made.

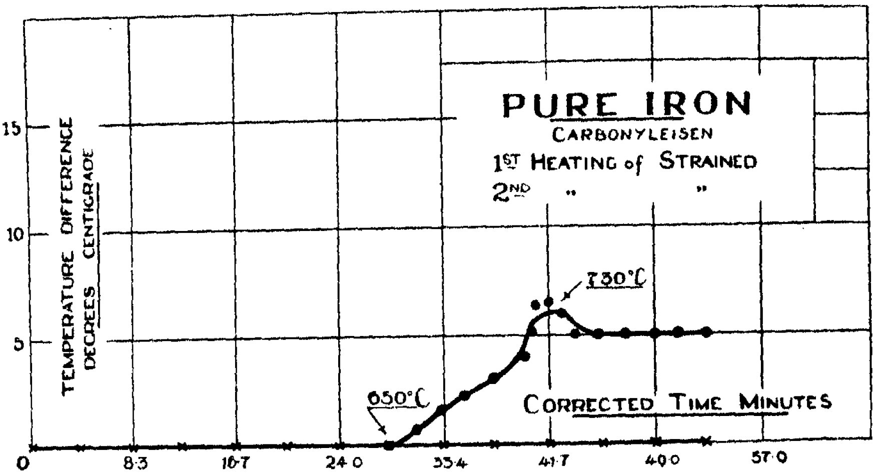

FIG. 8

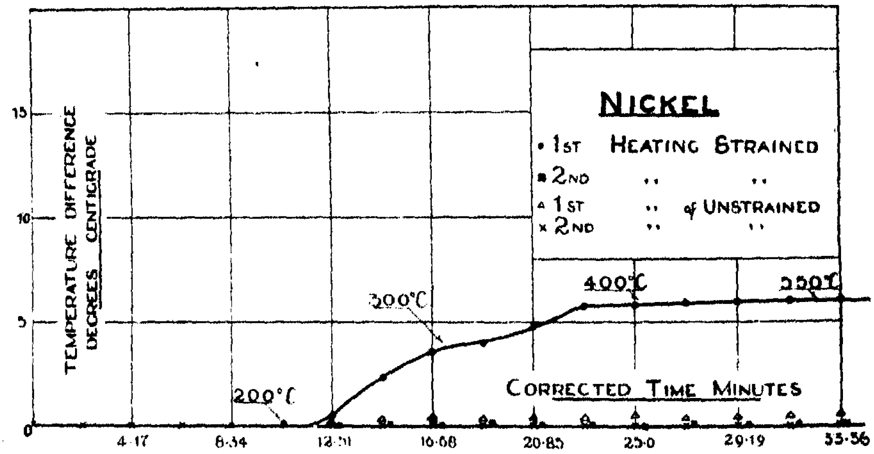

FIG. 9

These and other modifications resulted in an almost complete elimination of the lowering in the potential drop through the heating coils which had previously been obtained during the first heating. The temperature-time curves for first, second and third heatings of an annealed specimen were now in very close though not always perfect agreement.

As may be seen in fig. 7, a maximum difference of about 0·5° C. was found for copper between the second and third heatings, while for iron (fig. 8) no measurable difference was observed.

With nickel, fig. 9, the maximum difference between the second heating of the strained and the second heating of the unstrained specimens was only a small fraction of a degree. The points in fig. 9 represent the differences between the various heating curves and those of the second heating of the *unstrained* specimen. It will be seen that the points representing the second heating of the *strained* specimen lie very nearly exactly on the base line.

CORRECTION OF OBSERVED TEMPERATURE-TIME CURVES FOR VARIATION IN ENERGY SUPPLY

As already stated the current in the interior furnace was maintained constant, and in view of the fact that the potential drop was subject to variation during the test, the rate of heat supply to the specimen was not quite constant.

With the very perfect heat insulation which this apparatus ensures it seems certain that the rate of rise in temperature would be proportional to the heat input, accordingly it is possible to correct the observed temperature-time curves to an assumed standard constant heat input. The slope of these corrected temperature-time curves is then directly proportional to the specific heat of the metal.

The details of the method can be followed by referring to fig. 10, where the observed temperature-time and volt curves are shown. It will be seen that during the experiment the p.d. across the heating coil leads increased from 6·0 to 6·35 V. In this case the standard p.d. was taken as 6 V.

In taking the observations the potential difference between the ends of the heating coil was read every ½ min. Since the current is kept constant the corrected time for constant heat input is therefore proportional to the sum of all the readings of the voltmeter which had been taken since starting the test. In practice the sum of these readings was used as a convenient abscissa for the temperature-time curves, and the corrected time for a standard heat input nearly equal to the mean actual input was afterwards calculated. In this way the corrected temperature-time curve shown in fig. 10 was obtained.

Fig. 11 shows the temperature curve for tool steel also plotted to a corrected time base. This curve is the mean of three independent tests, the separate points being indistinguishable. The heat absorption at the recalescence point is seen to be 68° C.

It would be difficult to reproduce the temperature-time curves similar to that of fig. 10 on a scale which would permit the difference due to cold work to be appreciated. Accordingly the principal results of the measurements are here exhibited by means of curves showing the difference at any given time between the corrected temperature-time curves for the first and for subsequent heatings. Figs. 5, 7, 8 and 9, copper, iron and nickel for instance, which have already been described, are of this type.

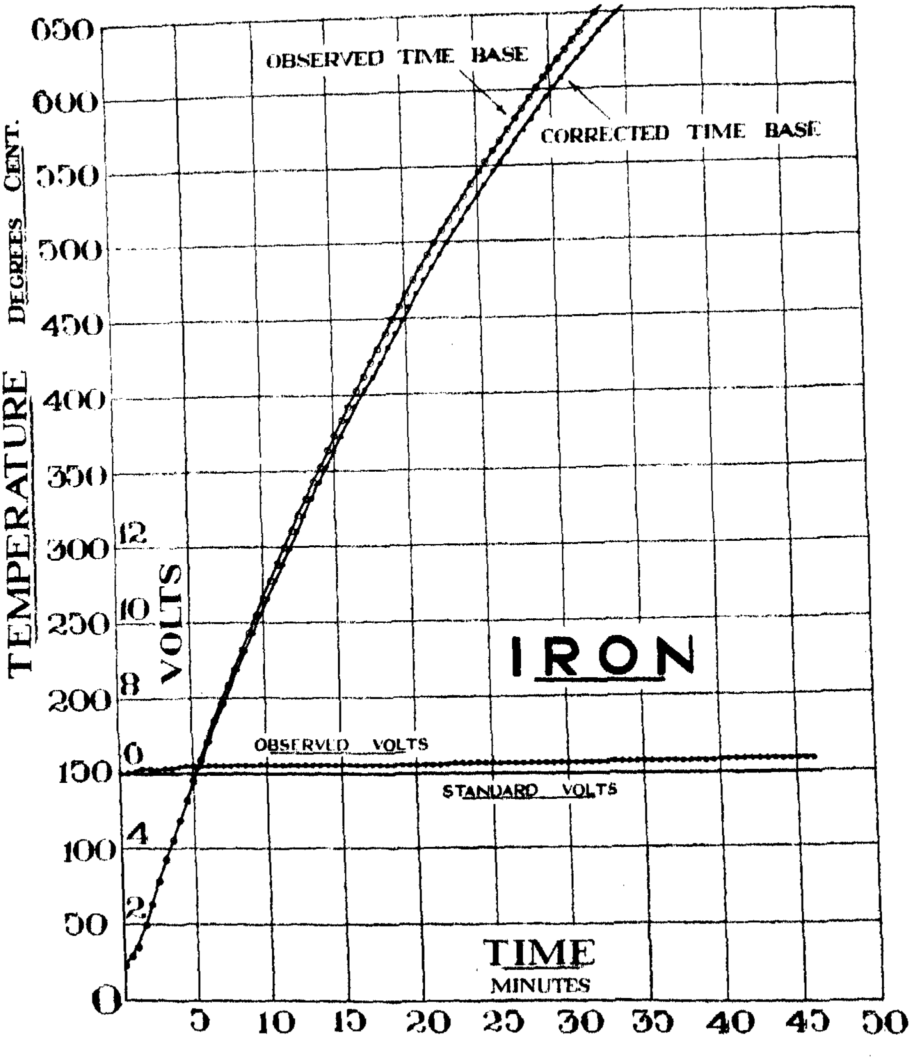

Fig. 10

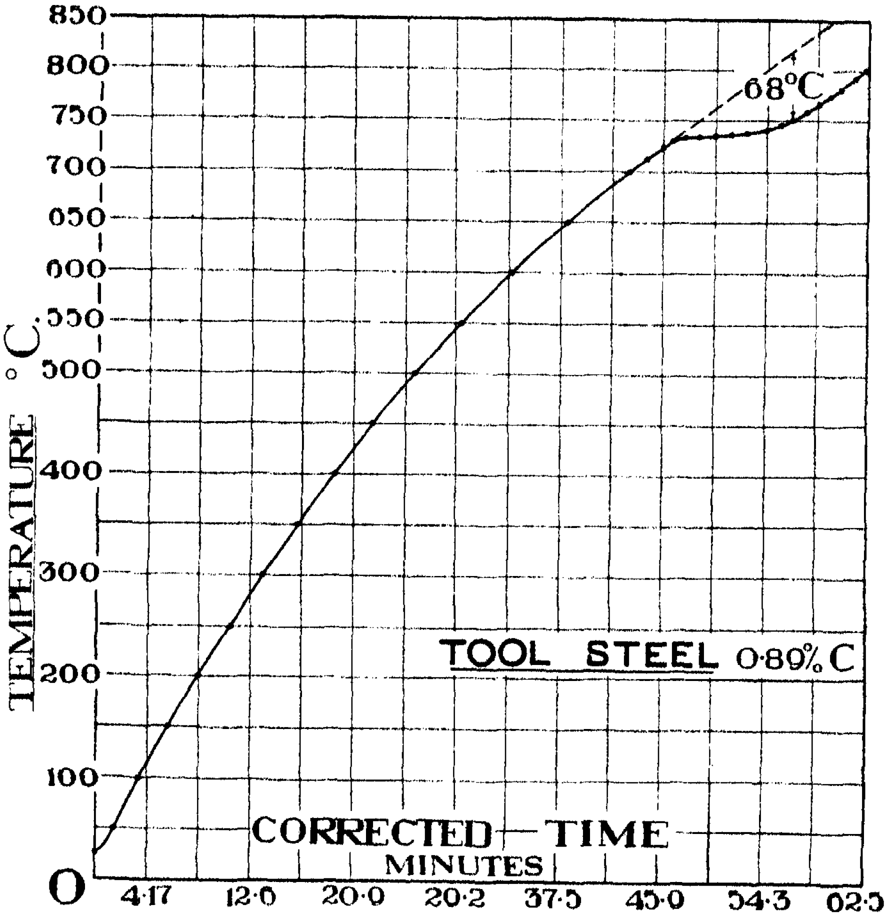

FIG. 11

RESULTS

Copper

It has already been mentioned that at a temperature of 500° C. the difference in temperature attributed to the release of internal energy due to cold work was 5° C. Assuming the specific heat of copper at 500° C. to be 0·10 this is equivalent to 0·5 cal./g. The mechanical work done on the specimen during twisting was measured by apparatus previously described and was in each case 5·6 cal./g. A fraction 0·5/5·6 (i.e. 9 %) of the mechanical work done was then released on reheating. This is in good agreement with the value 9·8 % found by the differential apparatus and is in fair agreement with the difference (7·5 %) between the work done and heat emitted during the process of twisting.

Nickel

The work done in twisting the nickel specimen referred to in fig. 9 was 13·9 g.cal./g. while the latent heat of cold work produced a difference in temperature (see fig. 9) between the strained and unstrained specimens of 6° C. at 400° C. Taking the specific heat of nickel at 400° C. to be 0·13, the latent heat of cold work was 6 × 0·13 = 0·78 cal./g.

The proportion of the cold work originally done on the specimen which is released on reheating is therefore 0·78/13·9 or 5·6 %.

Iron

For iron the corresponding figures are:

Work done in twisting = 7·83 g.cal./g.

Temperature difference due to release of cold work (see fig. 8) } 5° C. at 730° C.

The specific heat of iron between 700° C. and 800° C. is very variable. Measurements as low as 0·19 and as high as 0·29 seem to have been made. Using the mean value 0·24 the heat energy evolved is 5 × 0·24 = 1·2 cal./g. The work done was 7·83 cal./g. so that a proportion 1·2/7·83, i.e. 15 % of the total work done on the specimen, was given out during the heating.

Aluminium

Measurements were made with aluminium specimens, but it was found that volatilization of the metal in the vacuum furnace made the results unreliable.

Brass 70/30

Work done in twisting = 2·93 g.cal./g. Temperature difference due to release of cold work = 5·5° C. and taking 0·088 as the specific heat of the specimen, the heat energy evolved was 5·5 × 0·088 = 0·485 g.cal./g. That is, 14·7 % of the total work done on the specimen during twisting is given out on heating.

The results of Stott and Rosenhain (1933) and also those of Smith (1929) are not included in Table I as the cold work done in drawing the wires through the dies is not known.

Specific Heats

If the heat capacity of the interior furnace is negligible the slope of the corrected temperature-time curve is a measure of the specific heat of the metal at that temperature.

TABLE I

Metal	Heat equivalent of work done g.cal./g.	Energy absorbed during cold working / Work done on specimen	Energy emitted on heating / Work done on specimen	Authority
Cu	5·5	—	0·09	Present results
Cu	0·82	0·09	—	Farren and Taylor (1925)
Cu	0·96	0·075	—	Taylor and Quinney (1934)
,,	6·2	0·086		
,,	14·1	0·081		
Cu	18	—	0·018	Sato (1931)
,,	9·7	—	0·031	,,
,,	4·2	—	0·042	,,
Fe (pure)	7·8	—	0·15	Present results (vacuum calorimeter)
Fe (mild steel)	1·1	0·13	—	Farren and Taylor (1925)
Fe (decarburized mild steel)	3·2	0·09	—	Taylor and Quinney (1934)
	9·6	0·07	—	,,
Fe	16·1	—	0·008	Sato (1931)
,,	10·4	—	0·009	,,
Al	1·2	0·07	—	Farren and Taylor (1925)
Al (single crystal)	1·8	0·05	—	Farren and Taylor (1925)
Al	11·8	—	0·098	Present results (differential method)
Al	5·3	—	0·34	Sato (1931)
70/30 brass	4·67	—	0·16	Present results (differential method)
70/30 brass	2·93	—	0·15	Present results (vacuum calorimeter)
70/30 brass	1·12	—	0·24	Sato (1931)
,,	3·42	—	0·16	,,
,,	8·24	—	0·13	,,
Nickel	13·9	—	0·056	Present results (vacuum calorimeter)

In order to find the true specific heat from the curves it was therefore necessary to estimate the heat capacity of the furnace. This was done by estimating the capacity for heat of the parts of the internal furnace and further checking same by comparing the rate of rise of temperature of two specimens of pure copper of the same length but different diameters. Calling h the capacity for heat of the furnace the average value was 0·49 cal./° C. which is approximately 5 % of the capacity for heat of a nickel specimen. This value of h was determined as follows:

Copper specimens of the same length but different diameters weighing 82·07 g. and 24·80 g. respectively were used. From the corrected temperature-time curves the rates of rise of temperature in ° C./sec. were found at a number of temperatures ranging from 490° C. down to 100° C.

If θ_1 is the slope of the temperature-time curve for the large specimen, and θ_2 that for the smaller one, and if σ is the specific heat of the metal at any given temperature then, since the energy supplied was 10 W in both cases,

$$\begin{aligned}(82{\cdot}07\sigma + h) &= \frac{10}{4{\cdot}17} \times \theta_1 \\ &= H_1. \qquad (6)\end{aligned}$$

Similarly for the smaller specimen

$$\begin{aligned}(24{\cdot}80\sigma + h) &= \frac{10}{4{\cdot}17} \times \theta_2 \\ &= H_2, \qquad (7)\end{aligned}$$

where h = capacity for heat of furnace and adjoining material. The present results together with comparable result of previous experiments are given in Table I. In this table column 3 contains measurements made during the *absorption* of energy and column 4 contains measurements made during the *release* of energy on reheating.

In Table II the values of H_1 and H_2 are given for temperatures ranging from 490° C. downwards. Subtracting H_2 from H_1 the fourth line of the table gives 57·276, and dividing this by 57·27 the values of σ are given in the fifth line. Using these values of σ the value of h can be found by substituting in (7).

The values of h found in this way are given in line 6. It will be seen that except for the values at 100° C. and to a less extent at 490° C. the values are remarkably constant.

The mean of the series of values such as are shown in Table II was h = 0·49 g.cal./° C.

The heat capacity of the furnace was therefore always a small fraction of the heat capacity of the specimen; for instance, the specimen with least heat capacity was aluminium 5·5 cal./° C. The capacity for heat of furnace was therefore 9 % of specimen. The specimen with greatest capacity was 10·0 cal./° C. and the capacity for heat of the furnace was therefore 5 %. Errors in determining the heat capacity of the furnace give rise to only very small errors in the specific heats obtained.

Table II—Values of H_1 and H_2

Temperature (° C.)	490	400	350	250	200	150	100
$82{\cdot}07\sigma + h = H_1 =$	8·98	8·97	8·65	8·6	8·22	7·82	7·82
$24{\cdot}80\sigma + h = H_2 =$	3·145	3·052	3·01	2·95	2·86	2·72	2·61
$57{\cdot}27\sigma =$	5·84	5·93	5·64	5·65	5·36	5·10	5·21
$\sigma =$	0·102	0·1037	0·0985	0·0985	0·0936	0·0891	0·091
Values of h =	$+3{\cdot}145$ $-2{\cdot}540$	$+3{\cdot}052$ $-2{\cdot}57$	$+3{\cdot}01$ $-2{\cdot}49$	$+2{\cdot}95$ $-2{\cdot}44$	$+2{\cdot}86$ $-2{\cdot}36$	$+2{\cdot}72$ $-2{\cdot}21$	$+2{\cdot}61$ $-2{\cdot}29$
	=0·61	=0·48	=0·52	=0·51	=0·50	=0·51	=0·32

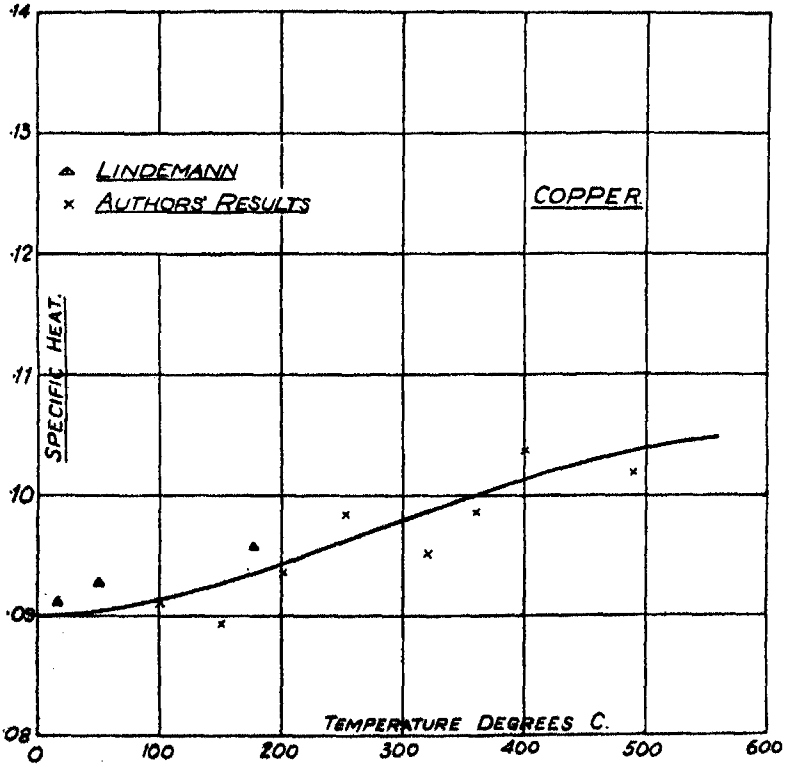

Fig. 12

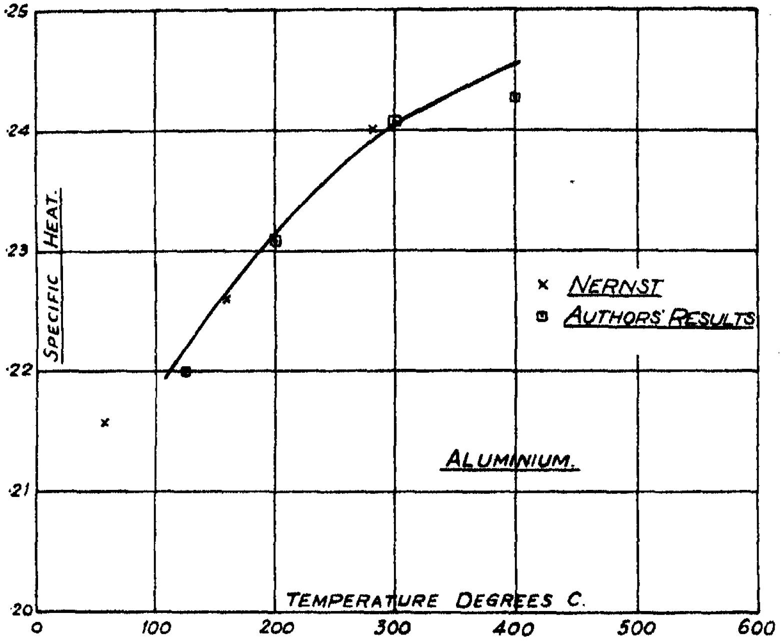
·25
·24
·23
·22
·21
·20
0
100
200
300
400
500
600
SPECIFIC HEAT.
× NERNST
AUTHORS' RESULTS
ALUMINIUM.
TEMPERATURE DEGREES C.

Fig. 13

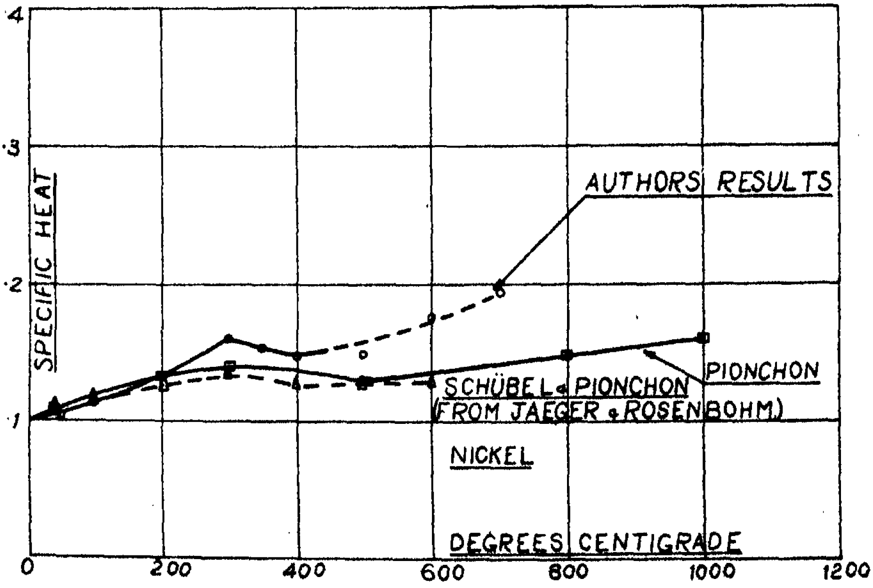
·4
·3
·2
·1
0
200
400
600
800
1000
1200
SPECIFIC HEAT
AUTHORS RESULTS
PIONCHON
SCHÜBEL & PIONCHON
(FROM JAEGER & ROSENBOHM)
NICKEL
DEGREES CENTIGRADE

Fig. 14

From the corrected temperature-time curves, using this value (0·49 g.cal./° C.) for the heat capacity of the furnace, the specific heats for copper, aluminium, nickel and iron are shown in figs. 12, 13, 14 and 15. The results obtained by other investigations are also shown. It will be seen that for aluminium and copper the results are in good agreement with those of Nernst and Lindemann (1911, 1912). For iron, steel and nickel, our values appear higher at higher temperatures.

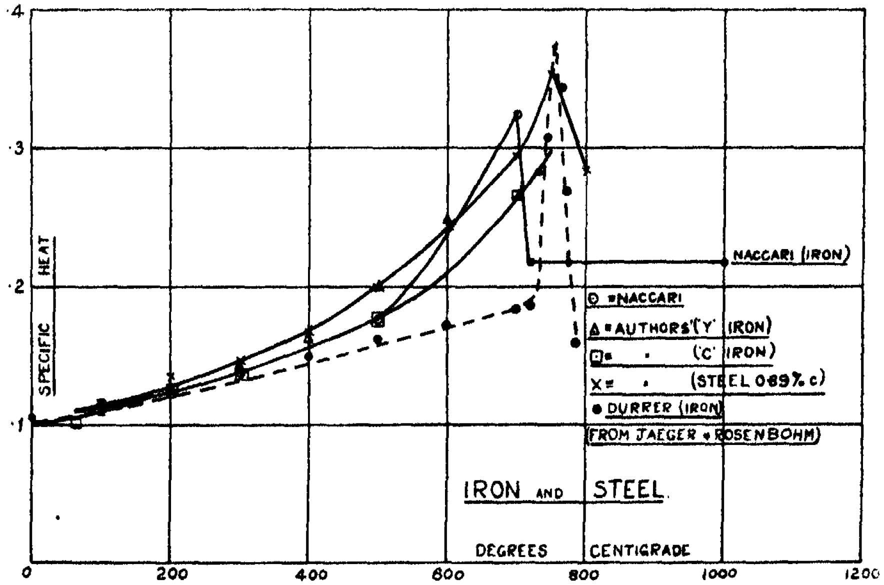

FIG. 15

In conclusion we wish to express our thanks to Professor C. E. Inglis, F.R.S. for permission to carry out the work in his laboratory.

REFERENCES

Farren, W. S. and Taylor, G. I. 1925 *Proc. Roy. Soc.* A, **107**, 422.
Nernst, W. and Lindemann, F. A. 1911 *S.B. preuss. Akad. Wiss.* p. 494.
— — 1912 *S.B. preuss. Akad. Wiss.* p. 1160.
Quinney, H. 1929 *Proc. Roy. Soc.* A, **124**, 591.
Sato, S. 1931 *Sci. Rep. Tohaku Imp. Univ.* **20**, 140–77.
Smith, C. J. 1929 *Proc. Roy. Soc.* A, **125**, 619.
Stott, V. H. and Rosenhain, W. 1933 *Proc. Roy. Soc.* A, **140**, 9.
Taylor, G. I. and Quinney, H. 1934 *Proc. Roy. Soc.* A, **143**, 307.

Spontaneous Emulsification, and Reactions Overshooting Equilibrium

By James W. McBain, F.R.S. and Ts-Ming Woo

Department of Chemistry, Stanford University, California

[Plates 9–12]

Spontaneous emulsification was discovered in 1878 by Johannes Gad (1878). He observed that when an oil containing fatty acid is placed quietly upon an alkaline solution with avoidance of stirring, streamers shoot out which at their ends disintegrate into minute droplets forming a milky emulsion. In the following year, Brücke (1879) confirmed Gad's numerous observations, showing that a higher concentration of alkali suppresses this motion, and instead gives rise to slowly swelling growths or "myelin forms", familiar since 1852 in medical literature (see Adami and Aschoff 1906).

The phenomenon of spontaneous emulsification appears to have been lost sight of during the past generation, apart from some observations recorded by Gurwitsch* in connexion with petroleum technology.

In a series of papers from 1879 to 1894, Quincke ascribed the spontaneous emulsification to spotty or local formation of soap at points in the interface which through lowering of surface tension immediately spread with sufficient violence to produce lateral currents of sufficient turbulence to tear off droplets. This provides a gross mechanical explanation of the formation of emulsion droplets based upon uneven lowering of surface tension in the interface.

Undoubtedly there is some truth in this picture of an "emulsifiant", which in this case is mechanical stirring although due to lowering of surface tension. Mechanical stirring appears to be an important or essential factor in the production of soap type emulsions of olive oil (Brücke 1879) and of asphaltic bitumens.

Similar spotty violent spreading, or "pockeling", is observed on a surface when materials that lower surface tension come into it from an inhomogeneous solution or from one containing suspended particles or drops of spreading materials (Wilson and Ford 1936; Ford 1936). For example, a drop of phenol or a minute crystal which may take an hour or more to dissolve when immersed in water, spreads instantaneously and dissolves in a few seconds when it happens to touch the surface. Similar sudden spreading was noticed by H. D. Bruce, also in this laboratory, when a drop of highly concentrated asphalt emulsion is brought up to the surface of a dish of water.

---

* Gurwitsch (1913), see Moore (1932); Müller (1907); Máday (1913); Harkins and Zollman (1926); Weichherz and Pletenjewa (1936) describe spontaneous emulsification in systems containing water, phenol, xylol and soap; Young (1936); Young (1937) confirms the ameboid motions described by Gad.

We have observed with toluene and water, and with medicinal paraffin oil (Nujol) and water, that the emulsification is sometimes at first mutual, into the oil and into the water. This occurs with 1 % "Gardinol" in Nujol placed side by side with water. In some systems spontaneously formed emulsions are permanent, in others they afterwards separate again.

There are two chief modes of experiment, one like Gad's where a drop or lens of oil is placed upon a large surface of aqueous solution, and the other in which deep layers of the two liquids rest upon each other in a test tube or beaker. In the former case the violent movement is noticed at the edges; whereas in the latter, prominences and droplets are extruded from the whole interface, even where the whole process occurs against the influence of gravity as when paraffin oil, containing palmitic acid, rests upon warm aqueous alkali and forms an emulsion in a soap solution that is lighter than water.

Gurwitsch emphasized what we regard as a more important alternative factor in spontaneous emulsification; namely, the molecular diffusion of substances across the interface. We have shown elsewhere (McBain and Dawson 1934, noted also in the ultra-centrifuge by Pedersen 1936) that diffusing columns drive along with them other substances, presumably by molecular collisions, concentrating these other substances in the direction of the diffusing column, so that a strong diffusing column can overcome a weak one in the opposite direction, or accelerate it if in the same direction. Gurwitsch's example was alcohol crossing from oil to water. It would be desirable to find another substance that does not lower surface tension and yet causes this effect.

In a series of theoretical papers, Raschevsky (1928*a*, *b*) discusses how diffusion alone without surface tension effects may suffice to subdivide a drop into smaller droplets.

In the following experiment, molecules of lauric acid carry along with them molecules of Nujol into water. The Nujol molecules then collect to form globules, some of which are stabilized by the soap thus formed. But many of the latter can be collected in a centrifuge to form a layer of pure Nujol. All analyses were made by Dr. M. E. Laing McBain.

1 g. of lauric acid dissolved in 19 g. of Nujol was placed quietly in a separating funnel upon 80 c.c. of N/20 NaOH in water, containing 0·0920 g. sodium. After 3 days the milky aqueous layer was carefully separated from the clear Nujol layer and placed in a Swedish angle centrifuge. This yielded a fairly clear Nujol layer over a white pasty layer over a clear aqueous layer. Analysis showed that the aqueous liquid originally placed in the centrifuge now contained 1·9 g. Nujol and 1·0 g. laurate radical and 0·0915 g. sodium. Thus 1 g. of lauric acid carried with it into the aqueous alkali 1·9 g. of Nujol, the 0·004 equivalents of alkali combining with the 0·005 equivalents of lauric acid to form a mixture of soap, acid soap and Nujol in the aqueous emulsion. In this experiment lateral streaming was not observed and there was merely a steady downward movement of emulsified Nujol through the whole quiet aqueous layer.

When 55 g. of Nujol containing 5 % of oleic acid were placed upon 45 c.c. of aqueous 0·0856N NaOH, the aqueous layer became 0·0861N with regard to oleate radical, half the weight of oleic acid still being left in the Nujol. Likewise when the oleic acid was increased to 15 % and the sodium hydroxide to 0·166N, again all the alkali in the aqueous layer was converted to oleate, the remainder of the oleic acid remaining in the Nujol. When 5 % cerotic acid (Eastman Kodak Company) was substituted for 5 % oleic acid, the opalescent aqueous layer became 0·00129N cerotate with 0·0843N NaOH.

We have observed spontaneous emulsification with "diglycol laurate" placed upon water, and with Nujol solutions of lauric acid (5 and 10 %), palmitic acid (1 %), sodium palmitate (1 %), acid sodium laurate (5 %), stearic acid (5 %), ammonium linoleate (½ %), montan wax (5 %), "Gardinol" (1 %), "Amoa" (1 %), trimethyl dodecyl ammonium bromide (1 %), and other neutral modern detergents placed upon water or various concentrations of alkali.

Spontaneous emulsification did not occur with Nujol placed upon sodium palmitate solution. This shows again that preformed soap is not an emulsifiant but is merely a stabilizing or protective agent for droplets that have been formed by some other means. To be active it must be forming or diffusing. We consider that there may be a further class of substances which are anti-emulsifiants through forming brittle or inelastic films.

Nujol containing lauric acid does not emulsify on water or 0·005N NaOH, or 0·55, 1·1, or 2·2N NaOH because the soap formed solidifies the interface in the latter cases and no interaction is possible in the first case. It does emulsify on 0·01, 0·02 and 0·04N NaOH. This is quite similar to the failure of water or dilute alkali to emulsify melted asphaltic bitumen with vigorous stirring, the process (Montgomerie 1923, 1927) being effective only over a limited range, above which the sodium salts are so insoluble in water that the emulsion reverses. Likewise Nujol containing pure stearic acid does not emulsify on 0·02N NaOH at room temperature where sodium stearate is insoluble in water, but does at once at 90° where it is very soluble. Similarly the sodium salt of cerotic acid is so insoluble in water that even at 80° no emulsification of Nujol, containing cerotic acid, was observed at any concentration of alkali (0·05–2·2N NaOH).

Beautiful demonstrations of the phenomena here discussed are obtained by first dyeing the oil layer with an oil soluble dye or with eosin. For example, with the latter, the diglycol laurate layer is yellow and sends out pink and white streamers from its lower surface. Similarly a water soluble dye such as methyl violet is useful in seeking droplets of water in the oil layer.

To convey some idea of one of the many forms which the phenomena here described may take and which are individual to each of the systems studied, photographs are given in fig. 1, Plates 9–11, showing the streamers which very slowly extend downwards into water from "diglycol laurate" placed upon its surface. They were taken by transmitted light in a plane parallel cell. The originally sharp interface is seen after 10 min. to be disintegrated (fig. 1*a*), streamers are well developed at 30 min. (fig. 1*b*), and much further extended at 1 hr. (fig. 1*c*). If a portion breaks off, it floats up again to the interface, and in any case, when after a day or so growth has neared the bottom of the vessel, the streamers bend round and slowly grow upwards. The surface appears to be solid and brittle, consisting of products of hydrolysis. Fig. 2, Plate 12 is included for the purpose of showing myelin forms very clearly as produced with the same reagent, "diglycol laurate," placed upon a lens of water in a watch glass.

Nujol containing a slight amount of glycerine, placed upon water, spontaneously becomes turbid through formation of a water-in-oil emulsion which settles, without breaking, in 3 or 4 days. The water layer remains clear throughout. It is tempting to suggest that this is due to the diffusion of water being much faster than that of glycerine, resulting in a new type of osmosis and a suggested mechanism of myelin swelling.

When a liquid consisting of 10% methyl alcohol and 90% toluene is placed quietly upon water in a test tube, the water remains clear but water droplets appear in the upper liquid forming a turbid emulsion. With 40% methyl alcohol and 60% toluene, the liquid remains clear but the water fills with emulsion to a depth of 2·5 cm. in 5 min., which diminishes to about 0·8 cm. after 2 hr. When ethyl alcohol is substituted for methyl alcohol in these experiments, similar results are obtained.

When the upper liquid consists of 10 % acetic acid and 90 % toluene, both it and the water layer remain clear and free from emulsion. When the acetic acid is increased to 40 %, a comparatively stable milky emulsion of visible droplets forms throughout the aqueous layer. Possibly it is the limited solubility of hydrochloric and sulphuric acids in toluene that does not suffice for spontaneous emulsification with water, although the diffusion of the acid is visible and the slightest stirring causes emulsification. Trisodium phosphate, casein, and sodium silicate are too insoluble in Nujol to produce spontaneous emulsification with water; but on shaking, sodium silicate emulsifies Nujol in water as well as water in Nujol, the latter being favoured by a lower concentration of silicate.

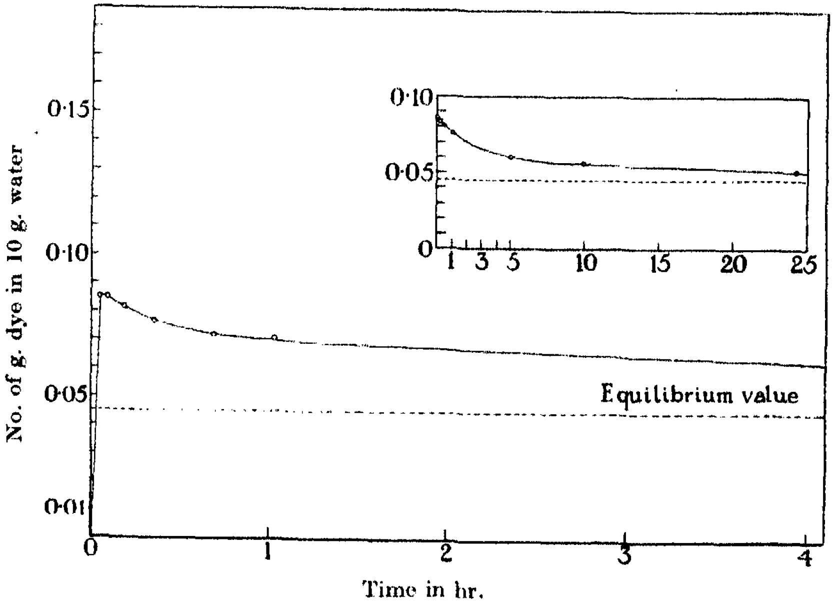

FIG. 3—Dye carried from toluene into water by diffusing soap, only the excess subsequently returning to the toluene

It has been shown elsewhere (McBain, J. W. and M. E. L. 1936) that a dilute aqueous solution of stable colloid will dissolve a small amount of water-insoluble dye, giving a true reversible equilibrium, any excess being neglected or expelled, the final concentration being dependent solely upon the total composition of the system and independent of its history. Now we have found, fig. 3, that when dye and soap are dissolved in toluene and this placed upon pure water, not only does all the soap pass into the water, but during the first few minutes it carries with it twice as much dye as it can retain. This excess of dye passes back again into the toluene during the next few days. It is easily shown that this is not due to local concentration of soap (an effect quantitatively in the opposite direction), and not due to toluene droplets carried along (for these are eliminated by filtration through dry filter paper, as shown by microscopic examination, before analysis). Hence this is again a case of a diffusion column of soap driving along dye molecules that get in its way until the soap has ceased to move, just as in our other diffusion experiments sugar diffusing through water carries before it a salt which was originally uniformly distributed, leaving the salt to find its way back when the movement of the sugar has slowed down.

In the actual experiments, 0·4 g. of potassium oleate and 0·1 g. of Yellow AB (benzene azo-β-naphthylamine) were dissolved in 2 c.c. of toluene, and this was placed upon 40 c.c. of 0·0406N KOH solution in a thermostat on a table mounted on a central pivot so that the normal to the table slowly described a cone, so slowly that the surface of the liquids was never broken. The amount of dye in the aqueous layer rose from 0 at first to a maximum of 0·0857 g. at 2 and 5 min., being double the equilibrium concentration of 0·0445 g. to which it gradually returned during the next few days. At 48 hr. it was 0·0490 g. Likewise the droplets of toluene which spontaneously appeared in the water disappeared during the next few days.

SUMMARY

The phenomenon of spontaneous emulsification in the absence of all external mechanical stirring, known to classical physics, was observed and studied. It is partly due to local movements resulting from lowered surface tension, but an important factor is the collision of molecules in diffusing columns driving other molecules with them.

REFERENCES

Adami, J. and Aschoff, L. 1906 *Proc. Roy. Soc.* B, **78**, 359.
Brücke, E. 1879 *S.B. Akad. Wiss. Wien*, **79**, 267.
Ford, T. F. 1936 *J. Phys. Chem.* **40**, 835.
Gad, J. 1878 *Arch. Anat. Physiol., Lpz.*, p. 181.
Gurwitsch, L. 1913 "Wissenschaftliche Grundlagen der Erdölebearbeitung", p. 200. Translation by Moore, H. (1932), p. 430. London: Chapman and Hall, Ltd.
Harkins, W. D. and Zollman, H. 1926 *J. Amer. Chem. Soc.* **48**, 80.
Máday, S. v. 1913 *Zbl. Physiol.* **27**, 381.
McBain, J. W. and Dawson, C. R. 1934 *J. Amer. Chem. Soc.* **56**, 52.

McBain, J. W. and McBain, M. E. L. 1936 *J. Amer. Chem. Soc.* **56**, 2610.
Montgomerie, J. A. 1923 British Patent No. 226,032.
— 1927 U.S. Patent No. 1,643,675.
Müller, A. 1907 "Allgemeine Chemie der Kolloide", p. 88. Leipzig: J. A. Barth.
Pedersen, K. O. 1936 *Nature, Lond.*, **138**, 363.
Rasohevsky, N. 1928*a* *Z. Phys.* **46**, 568.
— 1928*b* *Z. Phys.* **48**, 513.
Weichherz, J. and Pletenjewa, N. 1936 *Kolloidzschr.* **74**, 330.
Wilson, D. A. and Ford, T. F. 1936 *Nature, Lond.*, **137**, 235.
Young, P. A. 1936 *Trans. Amer. Micr. Soc.* **55**, 260.
— 1937 *Sci. Amer.* January, p. 28.

A Comment on the Paper by Sten von Friesen "On the Values of Fundamental Atomic Constants"

By J. S. E. Townsend, F.R.S.

(*Received* 17 *July* 1937)

My attention has been drawn to certain statements in this paper (von Friesen 1937) about the early measurements of the mass of negatively charged particles in gas. As it is generally understood that papers published by the Society have been recommended by one or more persons who are knowing and well skilled in the particular branch of natural knowledge to which the paper relates, and as these statements are contrary to the account which I have given of these constants in my book "Electricity in Gases", I may be permitted to point out that I am unable to find any support for the statements in question, and that there is an important omission.

I stated that Schuster (1890), in measuring e/m for negatively charged particles in a gas at low pressures, found numbers not much greater than the values for charged atoms. If e is in electromagnetic units, the value for hydrogen is about 10^4. Von Friesen, on the other hand, says that the first determinations of e/m were made by Schuster and J. J. Thomson, and that they found values of about 10^7; but as von Friesen makes no reference to any of Schuster's publications I do not know where his information comes from.

I made in my book a statement, which will also be found in most foreign books, that Wiechert (1897), in January 1897, first showed that the ratio e/m for a cathode-ray particle is between 2000 and 4000 times as great as that corresponding to an atom of hydrogen. I gave the reference to his paper, in which he described the method now known as Wiechert's method. Von

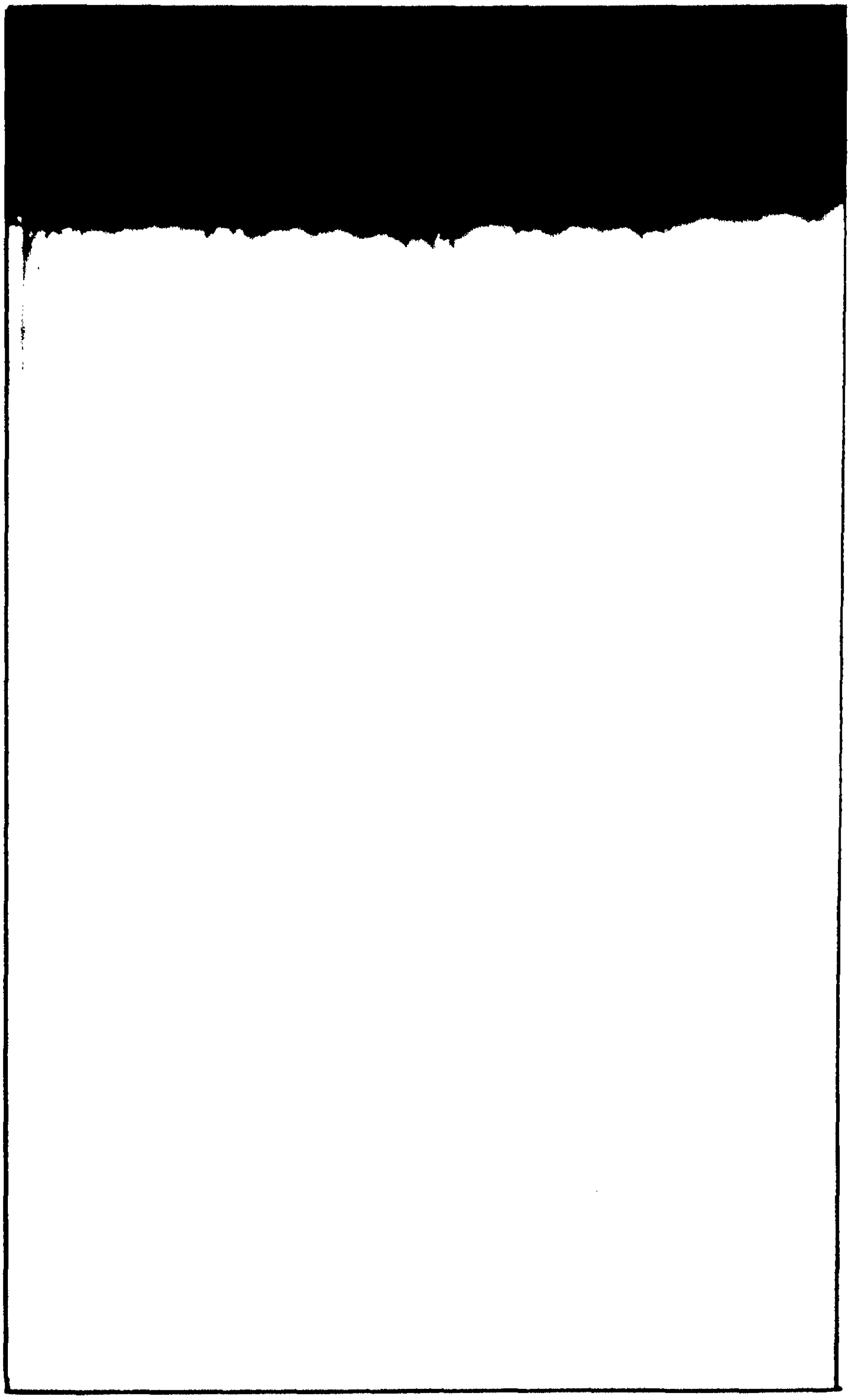

Fig. 1*a*—Spontaneous slow streaming of "diglycol laurate" downwards into water, photographed after 10 minutes.

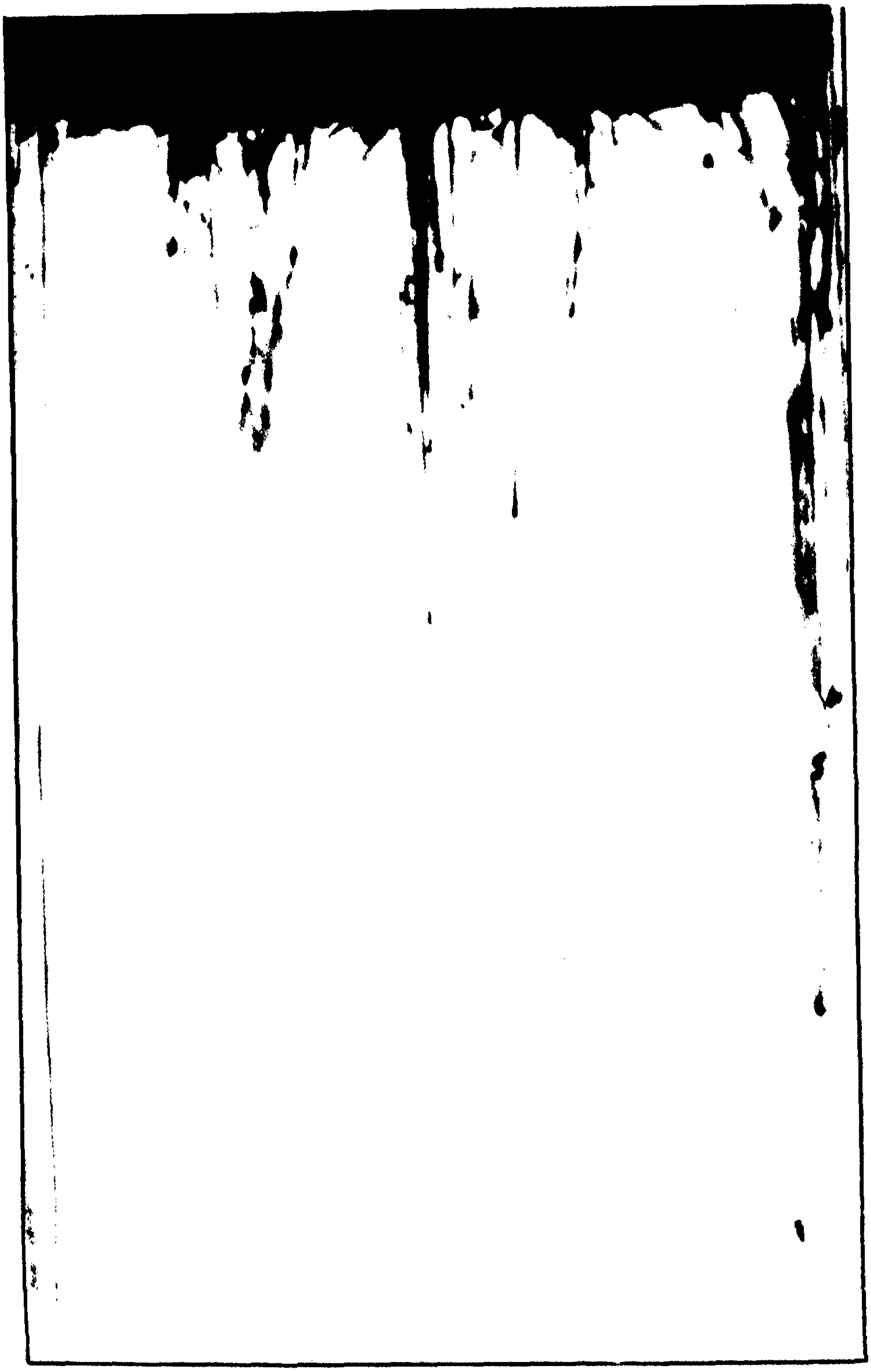

FIG. 1*b*—Spontaneous slow streaming of "diglycol laurate" downwards into water, photographed after 30 minutes.

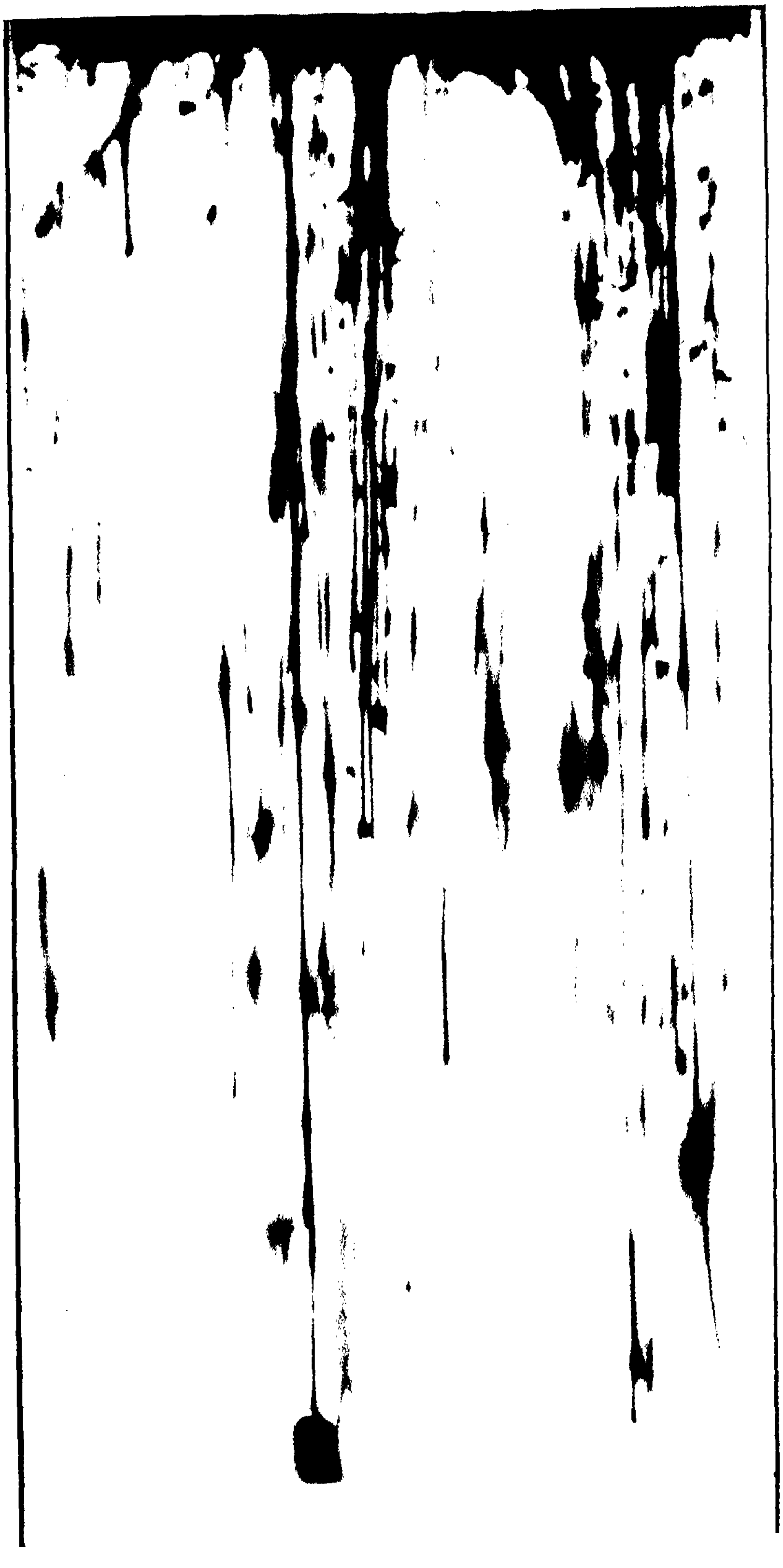

Fig. 1c—Spontaneous slow streaming of "diglycol laurate" downwards into water, photographed after one hour.

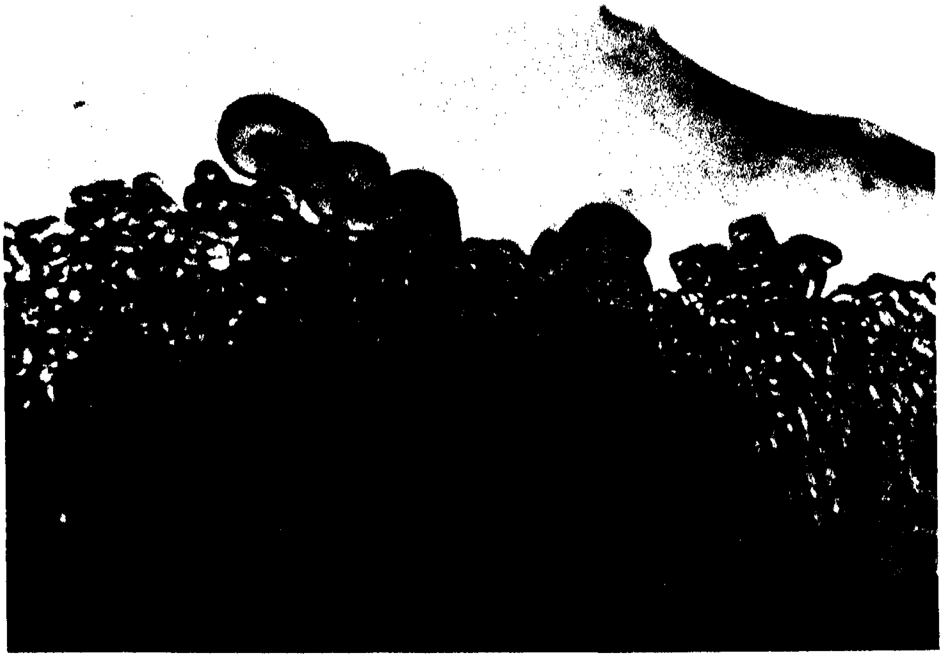

Fig. 3—A drop of "diglycol laurate" placed on a lens of water and spreading horizontally to give myelin forms.

Friesen gives a table containing the results of three recent experiments by Wiechert's method; but as he gives no reference to any of Wiechert's publications, it is impossible to find out from his paper the date of Wiechert's first experiments.

It therefore appears to me that the statement made by von Friesen concerning Schuster is incorrect; and since J. J. Thomson's first paper (1897) on the ratio e/m was published many months after Wiechert's paper, the statement concerning J. J. Thomson is also incorrect.

REFERENCES

Friesen, S. von 1937 *Proc. Roy. Soc.* A, **160**, 428–9.
Schuster, A. 1890 *Proc. Roy. Soc.* **47**, 526.
Thomson, J. J. October 1897 *Phil. Mag.* [5], **44**, 293.
Wiechert, E. 7 January 1897 *Beitr. Naturk. Preuss.* **38**, 1. There is an abstract in *Beibl. Ann. Phys.* **21**, 443, May 1897.

The Variation with Temperature of the Thermal Conductivity and the X-Ray Structure of some Micas

I—The Thermal Conductivity up to 600° C.

By R. W. Powell, B.Sc. and Ezer Griffiths, D.Sc., F.R.S.
Physics Department, National Physical Laboratory, Teddington, Middlesex

(*Received* 21 *August* 1937)

INTRODUCTION

The authors recently had occasion to measure the thermal conductivities of several varieties of mica up to a temperature of 600° C. In the course of this work it has been observed that whereas the thermal conductivities of the muscovite varieties of mica alter but little over this temperature range, the thermal conductivities of certain phlogopite micas decrease to about one-third of their initial values when the micas are heated to about 200° C. In such cases there is incomplete reversibility in the thermal conductivity temperature curve on cooling.

Subsequent examination of these micas by means of X-ray crystal analysis has revealed the fact that in those samples which suffered appreciable change in conductivity, the arrangement of the elementary crystals composing the mica laminae becomes displaced from their ordered setting at approximately the same temperature as the thermal conductivity change. The present paper describes the thermal conductivity experiments, which are believed to be the first determinations carried out on mica to high temperatures. In the paper which follows, Mr. W. A. Wood describes the X-ray experiments on some of these samples of mica.

The material studied consisted of samples of phlogopite micas from Madagascar and Canada and muscovite micas from India. These were supplied by Messrs. Wiggins* who also kindly advised on the technique for cutting the specimens. For the present experiments disks 1 in. in diameter were cut from larger irregular plates. Those selected for test were free from air films and uniform in thickness, and the surface laminae were removed after cutting so that the specimens were free from surface blemishes.

EFFECT OF LOADING ON THE THICKNESS OF THE SPECIMENS OF MICA

Before commencing the thermal conductivity measurements the weight and dimensions of each specimen were determined. To measure the thickness the specimen was placed between two optically flat plates of glass and the distance between the external glass faces measured by a micrometer screw gauge. This measurement was also carried out under a uniformly applied pressure equivalent to 176 lb./sq. in., corresponding to the condition under which most of the thermal conductivity measurements were made.

The results obtained from the particular samples studied are set out in Table I. In general the compressibility of the phlogopite varieties are greater than those of the muscovite varieties, whilst it will be seen that specimen No. 1 of Madagascan light amber phlogopite mica was far softer than any of the other micas.

DESCRIPTION OF APPARATUS AND METHOD USED FOR THE DETERMINATION OF THE THERMAL CONDUCTIVITIES

A divided bar method was used to determine the thermal conductivities of the micas up to temperatures of about 600° C. The details of the apparatus are shown in fig. 1. The disk of mica to be tested is sandwiched between two metal rods. The rods were composed of "glowray", a nickel-chromium alloy. Since it was important to maintain a clean metal surface in contact with the mica, these end-faces were faced with platinum. Thin sheets of platinum were hard soldered to the rods and were afterwards polished until the surfaces were optically flat. The metal rods were supported vertically, the end of the lower rod being a taper fit into a block of glowray.

---

* Messrs. F. Wiggins and Sons, 102 Minories, London, E.C. 2.

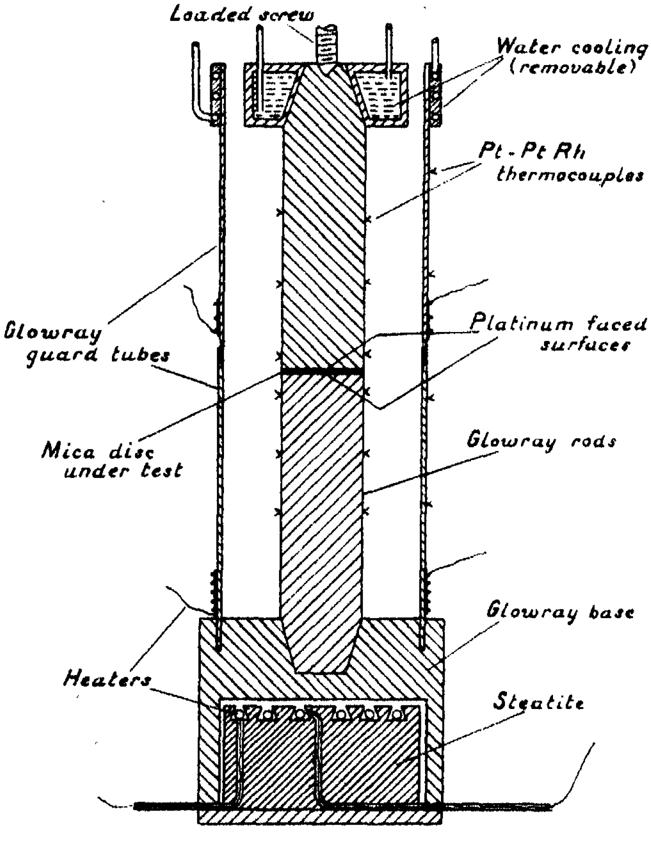

Divided bar and test specimen.

FIG. 1

The latter contained a spiral heater of coiled nichrome wire recessed in a steatite former. The rods were surrounded by a glowray "guard tube" 6·3 cm. in diameter which was also securely fixed in metallic contact with the metal base. The guard tube was in two sections so as to introduce a discontinuity similar to that caused in the gradient along the rods by the presence of the mica specimen. Water cooling units could be attached to the upper end of the rod and guard tube when necessary so as to control

TABLE I—EFFECT OF LOADING ON THE THICKNESS OF THE SPECIMENS OF MICA

Locality	Description	Sample No.	Weight (g.)	Diameter (cm.)	Unloaded Thickness (cm.)	Unloaded Density (g./cm.^{3})	Loaded 176 lb./sq. in. Thickness (cm.)	Loaded 176 lb./sq. in. Density (g./cm.^{3})	$\frac{\text{Unloaded thickness}}{\text{Loaded thickness}}$
				Phlogopites					
Madagascar	Amber light	1	1·400	2·48	0·135	2·15	0·109	2·66	1·24
,,	,, ,,	(after heating)	1·400	2·48	0·117	2·48	0·104	2·79	1·12
,,	,, dark	2	1·472	2·48	0·109	2·80	0·105	2·90	1·04
,,	,, ,,	3	1·692	2·48	0·128	2·74	0·122	2·87	1·05
,,	,, ,,	3 (second specimen)	1·986	2·48	0·145	2·83	$0{\cdot}143_7$	2·86	1·01
Canada	Dark	4	0·520	2·49	$0{\cdot}037_6$	2·84	$0{\cdot}035_8$	2·98	1·05
,,	Medium	5	1·285	2·47	$0{\cdot}094_8$	2·83	$0{\cdot}094_2$	2·85	1·01
,,	,,	6	1·328	2·50	$0{\cdot}096_3$	2·81	$0{\cdot}096_0$	2·82	1·00
,,	Light	7	1·115	2·48	$0{\cdot}086_4$	2·67	$0{\cdot}081_2$	2·84	1·06
,,	,,	8	0·690	2·48	$0{\cdot}051_3$	2·79	$0{\cdot}048_4$	2·95	1·06
				Muscovites					
India	Clear brown	9	0·770	2·46	$0{\cdot}056_8$	2·85	$0{\cdot}056_5$	2·87	1·01
,,	Clear green	10	0·940	2·47	$0{\cdot}068_4$	2·87	$0{\cdot}068_7$	2·86	1·00
,,	Clear pale green	11	0·818	2·46	0·061	2·82	$0{\cdot}060_8$	2·83	1·00
,,	Clear ruby	12	1·358	2·48	$0{\cdot}099_8$	2·82	$0{\cdot}099_4$	2·83	1·00
,,	Clear stained ruby	13	$0{\cdot}924_5$	2·48	$0{\cdot}068_1$	2·81	$0{\cdot}067_1$	2·85	1·01

the temperature gradient. To measure the temperature of the rods six platinum platinum-rhodium thermocouples were pegged into each rod. These were arranged in pairs at opposite ends of a diameter and at distances of approximately 0·35, 2·5 and 4·9 cm. from the face in contact with the mica disk. Thermocouples were also attached to the guard tube.

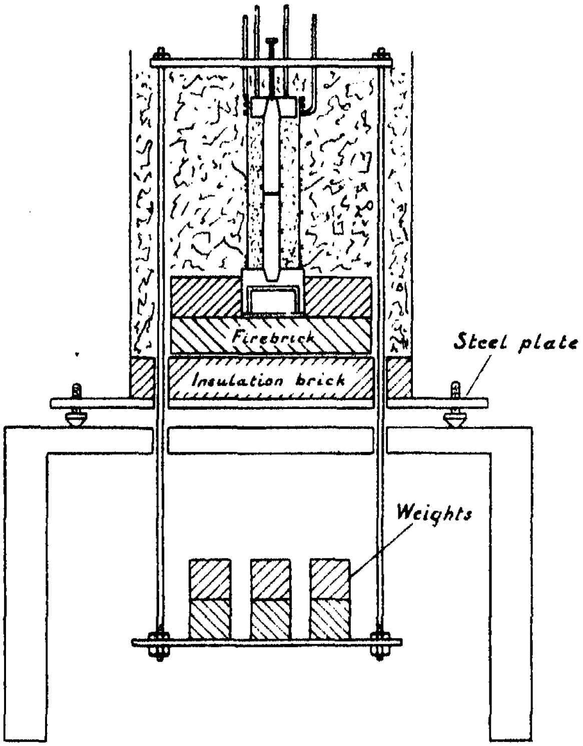

General arrangement of apparatus.

FIG. 2

Fig. 2 shows the general arrangement of the apparatus together with the loading device. The latter was a steel frame carrying a plate, the whole being suspended from a hardened steel point resting in a depression in the centre of the upper rod. The rods stood on several inches of insulating brick supported on a base plate of ½ in. steel fitted with levelling screws. In order to minimize transfer of heat by convection and radiation the interspace between the rods and the guard tube was filled with sil-o-cel, an insulating powder which has a thermal conductivity of the order of 0·0002 g. cal./cm./sec. The exterior of the guard tube was well lagged with magnesia-asbestos.

To determine the thermal conductivity of a specimen of mica a gradient in temperature was established in the rods, and the temperature of the guard tube adjusted so that when steady conditions were attained corresponding points on the rod and guard tube were at approximately the same temperatures. The measurement of the temperature gradients in the rods for this matched condition enabled the heat flow through the mica to be calculated. The temperature distribution in each rod was approximately linear and by extrapolating smooth curves drawn through these points to the metal mica interfaces the temperature discontinuity introduced by the mica specimen was determined. A similar test was carried out on a very thin specimen of mica, and the temperature drop produced by unit heat flow evaluated for each specimen. Assuming the contact resistance between the mica and metal to be the same in each case, the difference between these two temperature drops is equal to the temperature drop which would be established by unit heat flow in a specimen of mica of thickness equal to the difference between the two specimens tested. The value of the temperature drop through the thin specimen, of about 0·003 cm. in thickness, increased during the course of the work from about 1·6 to 3·0° C. per calorie. This was no doubt due to deterioration in the perfection of the metal surfaces. For the thicker phlogopite specimens the temperature drop across the thin specimen amounted to less than 10 % of that across the thick specimen.

In the course of the work on the micas some measurements were made in which the loading screw was thermally insulated from the rod by a disk of ebonite so that the cooling coil functioned as a flow calorimeter. This enabled a determination to be made of the thermal conductivity of the rod. The mean of several measurements at a temperature of about 220° C. together with the electrical resistivity gave a value for the Lorenz function which was in close agreement with that for a 80 : 20 nickel-chromium alloy which had been studied over the range from 20 to 800° C. (Powell 1936). Since the electrical resistivities of the two alloys at 23° C. were the same and differed by only 5 % at 570° C. it was assumed that the thermal conductivity of the glowray up to 800° C. could be derived from that of the 80 : 20 alloy to the order of accuracy required in the present investigation. No correction has been applied to allow for heat flow from the lower to the upper rod which is not conducted through the mica. That such a correction was relatively unimportant was shown by the fact that the substitution of alumina, a powder of much higher conductivity, for the sil-o-cel had no appreciable effect on the observed conductivity of the mica.

In fig. 3 are shown the values obtained for the thermal conductivities of two specimens cut from the same sheet of Canadian medium phlogopite. The thickness of one specimen was about half that of the other and the values are seen to be in good agreement. A marked decrease is observed in the thermal conductivity in the neighbourhood of 200° C. This decrease may occur over a narrower range of temperature than that shown in fig. 3 where the thermal conductivity is plotted at the corresponding mean temperatures, since in tests on the thicker specimens, for example, the temperature drop through the mica was of the order of 20° C. at temperatures below this change point and 5 to 7 times as much above.

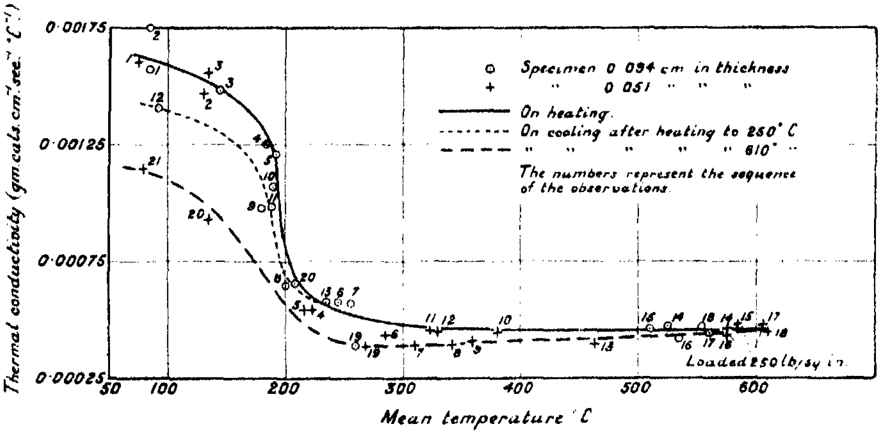

Variation of the thermal conductivity of Canadian medium phlogopite (Sample N°5) with temperature. (Normal loading 176 lb/sq.in.)

FIG. 3

EFFECT OF PRESSURE ON THE THERMAL CONDUCTIVITY

During the normal test on a specimen of mica a load equivalent to 176 lb./sq. in. was applied, but from time to time the effect of variations in this load was determined. Approximately doubling or halving the applied load on the specimens of Indian muscovite mica produced but little alteration in the thermal conductivities.

Changing the load from 176 lb./sq. in. to 250 lb./sq. in. on a specimen of Canadian phlogopite when at temperature of 575° C. had but a small effect on the thermal conductivity, although this specimen showed a considerable change in thermal conductivity on first heating, see fig. 3. The very compressible specimen of Sample No. 1, the light amber Madagascan phlogopite, also showed no measurable change on reducing the pressure from 176 to 74 lb./sq. in. (see fig. 5).

The effect of pressure on the thermal conductivity of a specimen of Madagascan dark amber phlogopite however was found to be appreciable and has been studied in some detail. The results obtained are summarized in Table II.

Table II—Effect of Pressure on the Thermal Conductivity of Madagascan Dark Amber Phlogopite

(This is Sample No. 3 (second specimen) of Table I)

Pressure	Thermal conductivity		
lb./sq. in.	At 100° C.	At 300° C.	At 500° C.
23	0·0011	$0{\cdot}0005_5$	$0{\cdot}0005_5$
48	0·0014	0·0006	$0{\cdot}0006_5$
176	0·0016	$0{\cdot}0008_5$	0·0009
330	0·0018	0·0011	0·0012

Effect of Temperature on the Thermal Conductivity

The five specimens of Indian muscovite mica studied showed but slight variation of the thermal conductivity with temperature over the range 100–600° C. The values obtained for the different samples did not depart by more than 18 % from the mean value of 0·0016 g. cal./cm./sec./° C.

The results for the phlogopite micas are of some significance inasmuch as they indicate a change in thermal conductivity at a temperature between 150 and 250° C. amounting in some cases to a decrease to one-third of its initial value. It will be seen from an inspection of the data given in figs. 3 and 4 that the thermal conductivity of these micas is nearly independent of temperature above about 250° C.

A structural change appears to take place in the neighbourhood of 200° C. which is only partially reversed on cooling and reference to fig. 3 shows that the extent of this recovery decreases as the maximum temperature to which the specimen is heated is increased.

The marked change in the neighbourhood of 200° C. is not confined to the Canadian phlogopite micas but is also shown by a sample of Madagascan mica, see data for Sample No. 3, fig. 5. This specimen was cut from a different sheet to that for which results are given in Table II, and it is seen to have a lower thermal conductivity for the same degree of loading. It was also more compressible at normal temperatures (see Table I) and it is interesting to observe from the data in fig. 5 that Sample No. 1, amber light Madagascan mica, which was extremely compressible, possessed the lowest initial thermal conductivity.

The X-ray examination of the Canadian phlogopite micas, which is described in the following paper, indicates that the change on heating to about 200° C. is due to the tilting of the planes of individual mica crystals between the limits ± 5 degrees and also to irregular changes in the spacing of the atomic planes.

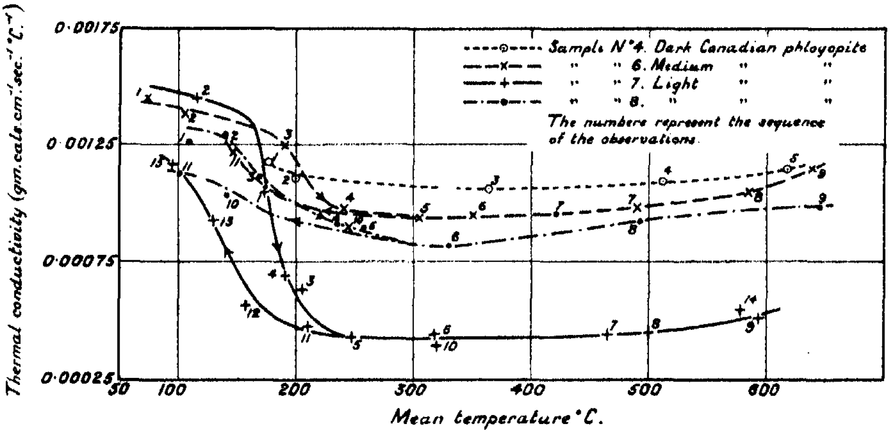

Variation of the thermal conductivities of Canadian phlogopites (Samples N^{os} 4, 6, 7 & 8) with temperature. (Normal loading 178 lb/sq in.)

FIG. 4

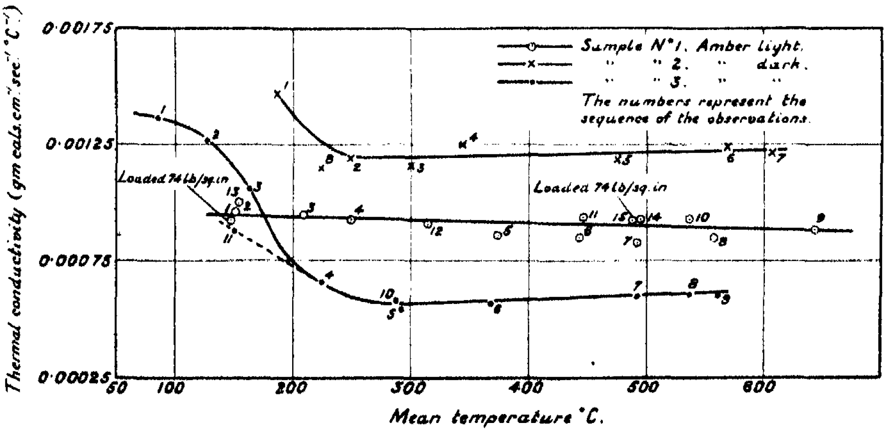

Variation of the thermal conductivities of Madagascan phlogopites (Samples N^{os} 1, 2 & 3) with temperature. (Normal loading 178 lb/sq.in.)

FIG. 5

It is considered that the surface crystals become stepped as a result of the heat treatment though still giving an approximately plane surface. In consequence of this the thickness of the air films within the mica may become increased. It can be shown, however, that an increase in air film of as much as 15 % of the original mica thickness would be necessary to account for the observed decrease in thermal conductivity.

Our thanks are due to the British Electrical and Allied Industries Research Association for permission to publish some of the data obtained in an investigation carried out at the Laboratory on their behalf. Also to Mr. M. J. Hickman for his work in connexion with the construction of the apparatus and with observations.

SUMMARY

The divided bar method has been adapted for the determination of the thermal conductivities of mica up to a temperature of 600° C. A disk of mica about 1 mm. in thickness is clamped between cylindrical rods of nickel chromium alloy of known thermal conductivity. To eliminate effects due to oxidation the plane surfaces of the rods are faced with platinum. A correction for temperature discontinuities at the mica metal interfaces is obtained by experiments using extremely thin mica laminae.

Phlogopite micas show, in varying degree, a pronounced decrease in thermal conductivity in the region of 200° C. which is only partially reversible on cooling. The effect is ascribed to the tilting of the elementary crystals of mica on heating.

The muscovite micas tested do not show this effect and their thermal conductivity changes but little with temperature.

REFERENCE

Powell 1936 *Proc. Phys. Soc.* **48**, **388**.

The Variation with Temperature of the Thermal Conductivity and the X-ray Structure of some Micas

II—The X-ray Examination of the Structure

By W. A. Wood, M.Sc.

Physics Department, National Physical Laboratory,
Teddington, Middlesex

[Plates 13–15]

It has been shown by Mr. R. W. Powell and Dr. E. Griffiths in Part I of this paper that the thermal conductivity of certain types of mica changes with temperature in an anomalous way. The present section deals with the alterations in crystalline structure exhibited by similar specimens during a cycle of temperature varying from 16 to 400° C. The results show that, in contrast with the usual effect of annealing, the heat treatment of mica may bring about a pronounced mosaic formation without apparent change in external appearance; that this structure is not necessarily stable but may revert appreciably on cooling to the initial state; and that these particular thermal and structural characteristics are interdependent. Measurements of the thermal expansion of the lattice constant perpendicular to the cleavage plane indicate that the transition to the mosaic structure does not, however, affect the perfection of atomic arrangement in the individual crystallites.

SPECIMENS

Of a number of mica specimens examined, the following typical four are described in detail:

(i) Specimen No. 4, Canadian dark phlogopite.
(ii) Specimen No. 5, Canadian medium phlogopite.
(iii) Specimen No. 6, Canadian medium phlogopite.
(iv) Specimen No. 7, Canadian light phlogopite.

Specimens 4 and 6 represent micas showing only minor changes, and specimens 5 and 7 micas showing abnormal changes in thermal conductivity on heating.

METHOD

To measure the state of crystalline structure a modified form of X-ray spectrometer was designed in which the essential feature was that the film recording the X-ray reflexions moved in synchronism with the specimen, as the latter was rotated through the reflecting positions. This was ensured in a simple way by using a circular camera which could be mounted on the circumference of the spectrometer table that carried the specimen. As the table was rotated or oscillated, both specimen and camera moved similarly through the same angle. On passing through the reflecting position, a perfect specimen gave a sharp image of the slit system, since each element of the crystal reflected simultaneously; the different elements of an imperfect crystal, however, though reflecting at the same Bragg angle θ, did so at different times, according to the extent to which they deviated in tilt from the mean surface of the crystal, and thereby gave a reflexion which was drawn out into an irregular band.

The reflexions from each specimen were photographed, normally, at room temperature, 100, 200, 300, 400° C. in the rising half of a temperature cycle, and again at 300, 200, 100° C. and room temperature as the specimen cooled. The time of exposure at each temperature was 10–15 min., and the time taken to pass from one temperature to the next was 3–5 min. The incident beam consisted of CrK-radiation and the first two orders of reflexion from the cleavage plane were recorded; this gave the two lines due to the α component and the second order of the β component; the first order of the β wavelength was occasionally missed since it happened to occur at the boundary of the 15° angle of oscillation employed. These are the photographs reproduced in figs. 1–4.

It was essential also to find whether the fragmentation was accompanied by distortion of the atomic lattice. The point was investigated by measuring the spacing of the cleavage planes at temperatures up to 400° C., and by noting the resolution of high order spectra. This was done on the same spectrometer which would take a quarter-plate flat film in a stationary holder perpendicular to the incident X-ray beam and actually carrying the slit system. The film, pierced with a central hole to permit passage of the beam, thus recorded spectra deviated backwards through large angles. For this work, the 11th order spectrum given by CoK-radiation was used. Photographs were taken on the same film at room temperature, at 100, 200, 300 and 400° C. as the temperature of the specimen rose, and then, on an interchanged film, at 350, 250 and 150° C. and room temperature on cooling. Each temperature was held for ½ hr. and the time of transition from one to the next was 3 min. The $\alpha_1 \alpha_2$ doublet was well resolved and the displacement of the doublet between 16 and 400° C. was of the order of 5 mm. A precise check on the measured expansion was afforded by observation of the rise in temperature required to shift the doublet through the distance by which the components were separated, so that the α_2 component at the higher temperature coincided with the α_1 component obtained on the same film at room temperature. Then, by the Bragg reflexion condition, the ratio of the lattice spacings at the two temperatures is equal to the ratio of the α_2 and α_1 wave-lengths, which are known with high accuracy.

In the arrangement for heating, the mica specimen was clamped in contact with the face of a rectangular block of brass ($2 \times 1\frac{1}{4} \times \frac{1}{2}$ in.), which carried at the back a nichrome heating element screwed in position under a plate of steatite. The mica specimen, approximately $1 \times \frac{3}{8} \times \frac{1}{250}$ in., was held under rectangular brass bars, leaving a length of $\frac{1}{4}$ in. of specimen which was exposed at the base of a recess $\frac{1}{4}$ in. deep formed by the bars. The temperature was measured by thermocouples inserted underneath the clamping bars in contact with the mica and as near as possible to the exposed surface. The brass was itself mounted in a steatite block carried in an adjustable holder on the table of the spectrometer. The thermal inertia of the brass was sufficient to prevent undue fluctuations of temperature.

RESULTS

The results on the variation in crystalline state are conveniently set out in figs. 1–4 which portray the behaviour of specimens 4–7 respectively.

Those specimens, Nos. 4 and 6, which showed no appreciable change in thermal conductivity on heating, gave spectra which remained remarkably sharp throughout (figs. 1 and 3). Thus, for specimen 4, the sharpness indicates that the reflexion is confined to a few minutes of arc throughout the whole temperature cycle, and the final state is indistinguishable from the first. In specimen 6, a suspicion of change appears at the higher temperatures but not of the same order as the specimens considered next.

Those micas, Nos. 5 and 7, which showed* a marked drop in thermal conductivity at about 200° C., gave spectra which exhibited an extraordinary modification over the same range of temperature. Thus fig. 2 (specimen 5) shows at room temperature the sharp spectrum of a reasonably perfect structure; the lines possess more than one component, indicating a multiple crystal, but these components are sharp. This state is maintained at 100, 150 and 180° C. At 200° C., however, the reflexions alter abruptly;

---

* *Vide* Part I.

the lines deteriorate into irregular bands, thereby pointing to a marked degradation of the mica structure into a mass of crystallites tilted from the original positions by as much as five degrees. This condition persists at 300 and 400° C. on heating, and again at 300 and 200° C. on cooling. It is of particular interest to note the partial but distinct recovery in the final state at 18° C.; the improvement is not enough however to bring about a condition comparable with the original. The behaviour of specimen 7 (fig. 4) is similar. The degradation of this specimen, though more marked, does not occur so abruptly as in the preceding case. The specimen shows also the partial improvement, setting in about 200° C., in the cooling half of the cycle.

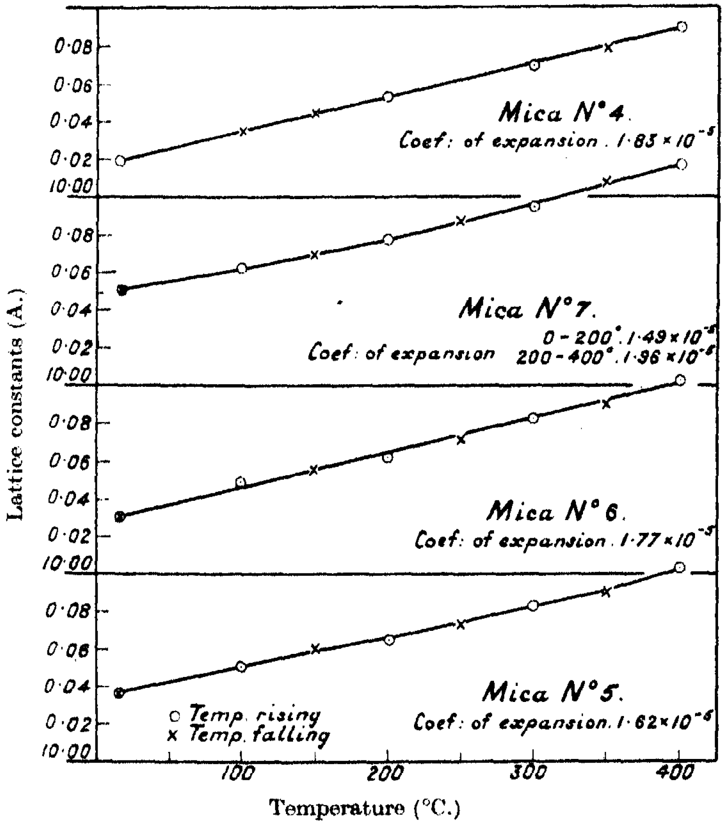

FIG. 5—Lattice constants and temperature, showing regular nature of expansion.

Now, if the above observations are compared with the thermal measurements set out in Part I, it will be seen that a remarkable parallelism exists between the degradation of crystalline structure and the decrease in thermal conductivity which characterizes the same micas at elevated temperatures.

The following further observations indicated that these structural changes alone appear to be responsible for the anomalies in thermal conductivity. In the first instance it was found that the lattice constant varied in a regular way through the critical temperatures. The results, deduced from the displacement of the $\alpha_1 \alpha_2$ doublet, are given in fig. 5 where the lattice constant is plotted against temperature. The expansion curve is smooth, and the points obtained in the rising and falling halves of the cycle lie on the same line. Secondly, the doublet, photographed under high resolution by the stationary back-reflexion method, gave no indication of radial diffusion. The case of the abnormal type of specimen is illustrated by fig. 6 where the photograph shows the doublets equally sharp at the different temperatures. (It is interesting to note in this figure the peripheral elongation of the doublets at the higher temperatures, confirming the fragmentation observed more directly by the method utilizing a moving camera.) There is therefore no distortion of the atomic lattice when the break-up of the large-scale crystal takes place, and the regular expansion suggests that no chemical changes are involved.

DISCUSSION

The fall in thermal conductivity of these micas at elevated temperatures is to be explained by the physical disturbances in the macrostructure in which an initially perfect crystal disintegrates into innumerable elements, themselves intrinsically perfect but differing very widely in orientation from the initial uniform formation. It is reasonable to suppose, as discussed in more detail in Part I of this paper, that the extra boundaries thus produced increase the resistance to the heat flow. It is a new and interesting point that such a mosaic formation may be brought about by a rise in temperature and may actually exhibit a partial recovery on cooling, and, as found subsequently, on ageing. The tendency to recovery and the critical temperature required suggest that the fragmentation is not due to escape of gas, known to be evolved by heated mica, but rather associated more intimately with the atomic structure. A possible explanation might be based on recent theories of imperfections in the crystalline state. According to these, there is a limit to which the element of a crystal may grow in size and remain a perfect "block". Sir W. H. Bragg has suggested that a limitation might be imposed by the cumulative effect of a slight irregularity in the packing of non-spherical atoms. The structure of mica, with its large diffuse oxygen atoms on the one hand and small compact metal ions on the other, would lend itself easily to such an effect. The increased thermal vibrations of the atoms at raised temperatures would then reasonably be expected to enhance the instability of a large block and explain the observed fragmentation of the crystal.

The author desires to express his thanks to the Electrical Research Association for kindly permitting publication of these results; to Mr. W. G. H. Turl who carefully constructed the X-ray spectrometer and was responsible for details of design; and to Mr. M. G. Harwood for assistance in carrying out the experimental work.

SUMMARY

An X-ray investigation has been made of the variation in structure exhibited by certain micas during a cycle of temperature ranging from 16 to 400° C. It has been found that the heat treatment may result in a very marked mosaic formation without apparent change in external appearance; that such a structure may not be final, but partially reversible on cooling; and that a close parallelism exists between these structural characteristics and measurements which show an anomalous fall in thermal conductivity at the same elevated temperatures. The thermal expansion of the lattice constant perpendicular to the cleavage plane has been measured; from these and from the radial sharpness of high order spectra inferences have been drawn in regard to the intrinsic perfection of atomic arrangement in the individual crystallites produced by breakdown of the large-scale crystal.

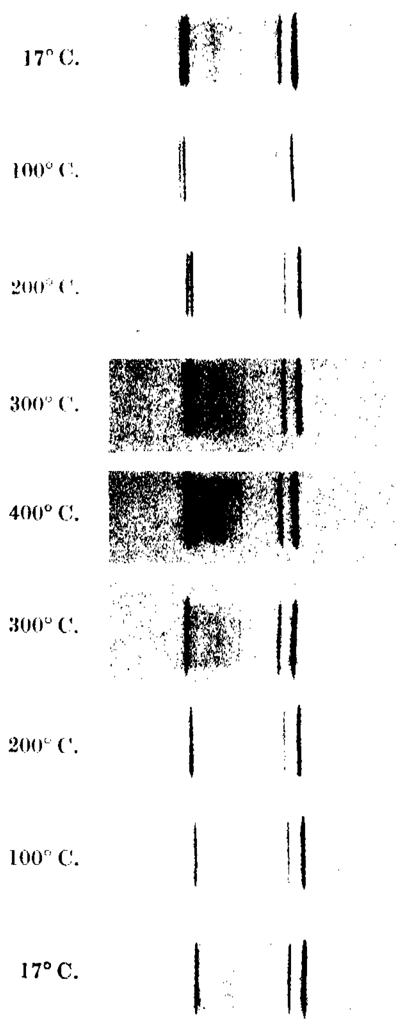

FIG. 1—(Specimen No. 4)

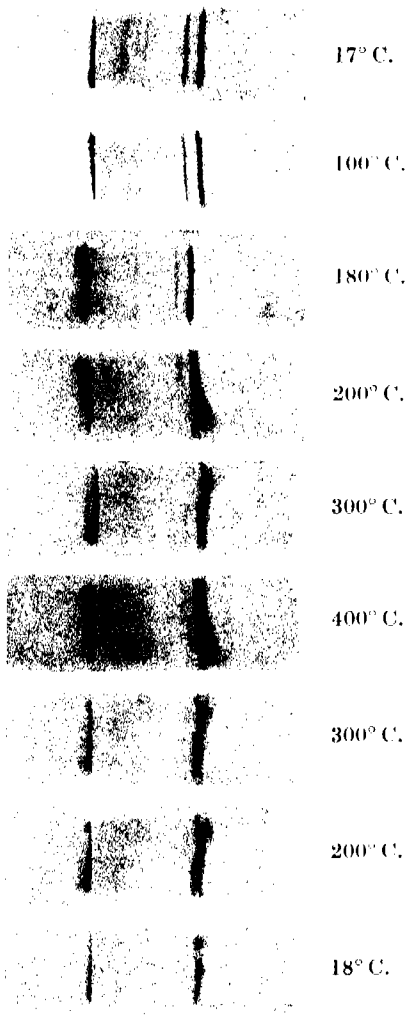

FIG. 2—(Specimen No. 5)

X-ray spectra of mica during temperature cycle.

FIG. 1—No change in perfection (steady thermal conductivity).
FIG. 2—Marked change at 200° C. (abnormal fall in thermal conductivity).

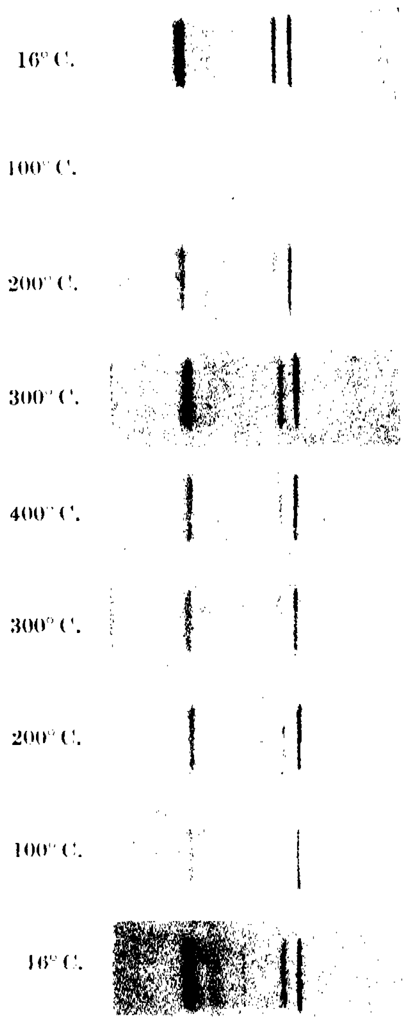

Fig. 3—(Specimen No. 6).

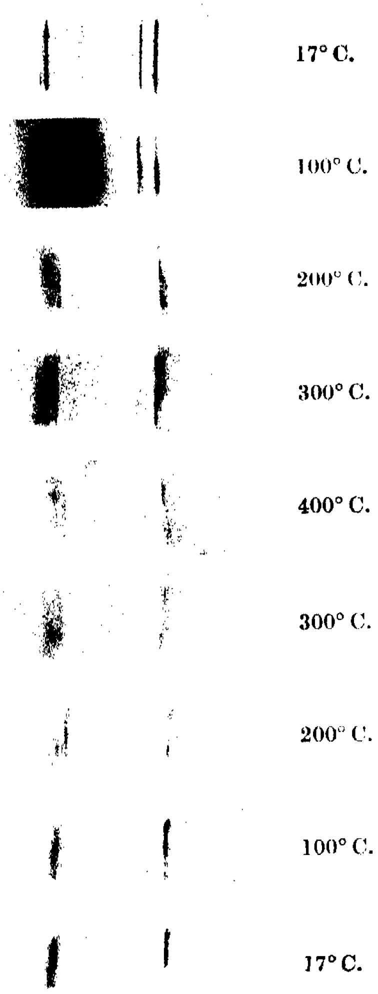

Fig. 4—(Specimen No. 7).

X-ray spectra of micas during temperature cycle.

Fig. 3—No change in perfection (steady thermal conductivity).
Fig. 4—Marked change at 200° C. (abnormal fall in thermal conductivity).

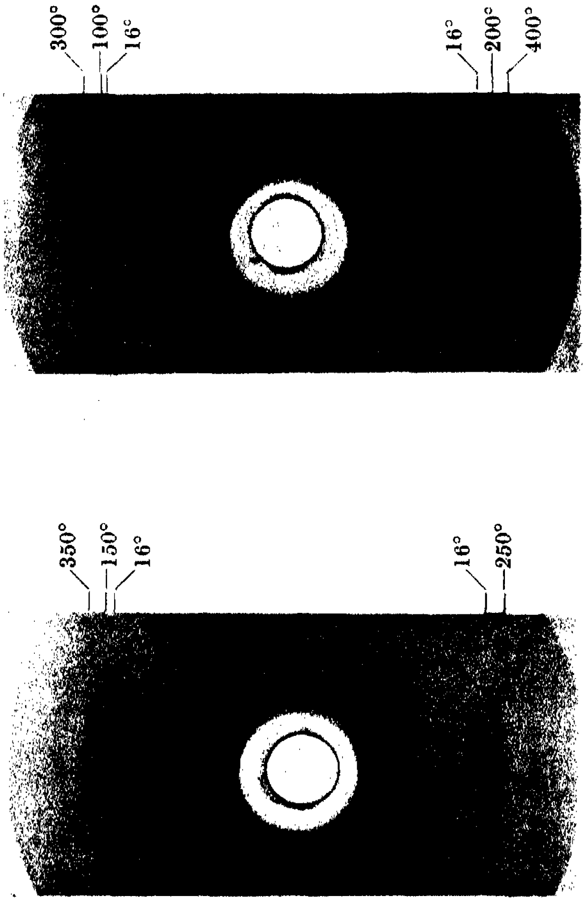

Fig. 6—(Specimen No. 5) showing shift of $\alpha_1\alpha_2$ doublet with temperature.

Note absence of radial diffusion despite breakdown of structure shown by same mica in fig. 2.

The Formation and Structure of Polymers of the Insoluble Cross-Linked Type

By R. G. W. Norrish, F.R.S. and E. F. Brookman

(*Received* 23 *August* 1937)

Staudinger, in a series of papers (1934, 1935, 1936) describes the formation of an insoluble polymer of styrene by the addition to the styrene, before polymerization, of small quantities of *p*-divinyl-benzene. This insolubility he explains by suggesting the formation of cross-linkages of divinyl-benzene between the long thread-like molecules of polystyrene to give three-dimensional macromolecules of exceedingly high molecular weight. By using increasing proportions of divinyl-benzene Staudinger obtained a series of polymers which varied from polystyrenes soluble in benzene through polymers of high swelling capacity to completely insoluble products. He considers that the cross-linkages of divinyl-benzene prevent the dispersion of the substance throughout the solvent, while it does not prevent the solvation of the long polystyrene chains. Thus, when few such cross-linkages are present, i.e. when the concentration of divinyl-benzene is low, the polymer will have a great tendency to go into solution through the solvation of the polystyrene chains, but will be prevented from becoming completely dispersed by the presence of the cross-linkages. The product will therefore have a high swelling capacity in those solvents in which the straight chain polystyrenes are soluble. This swelling capacity will decrease as the concentration of divinyl-benzene increases until completely insoluble polymers are obtained. Staudinger's presentation of the structure of his "cross-linked" polystyrene is as follows:

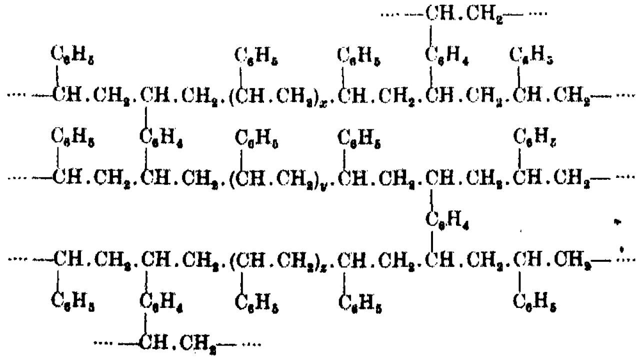

Blaikie and Crozier (1936) have recently found a similar example of an insoluble vinyl polymer. They polymerized vinyl acetate with divinyl-ether and obtained a polymer which was insoluble but had a high swelling capacity in the normal solvents for pure polyvinyl-acetate. This, in accordance with Staudinger's views, they consider to be due to the formation of cross-linkages of divinyl-ether between the long thread-like molecules of polyvinyl-acetate.* Reference may also be made to a paper by Morgan, Megson and Holmes (1936) in which the possibility of the cross-linking of vinyl polymers by divinyl substances is considered.

There exist various other illustrations of the connexion between the chemical structure of a macromolecule and its solubility in various solvents, but none more capable of such a simple and convincing explanation. For example, Koebner (1933) proposes a theory for the formation and constitution of the pheno-plastics, explaining the action of solvents on these polymers, while Kienle (1929, 1930) considers the properties of the glycol and glycerol phthalates with regard to their structure. In the latter case, the glycol phthalate grows into long thread-like molecules since each component has a functionality of two and is soluble, in contrast to the insoluble or highly swelling glycerol phthalate which can grow in three-dimensions, through the glycerol which has a functionality of three.

On Staudinger's view of the cross-linked structure of these polymers there should exist a series of compounds, similar to *p*-divinyl-benzene, which would possess this capacity for producing cross-linkages between the thread-like molecules of polystyrene or similar vinyl derivatives, and to confirm this view we considered it of interest to attempt an extension of his observations to other similar substances. As may be seen from the following experimental results such confirmation has been obtained and a series of cross-linking agents found, the efficiency of which, in the production of the insoluble type of polymer, depends both on the temperature used and on some intrinsic property of the cross-linking molecule.

The present investigation was limited to the study of the influence of various divinyl derivatives of the general formula $(CH_2:CH)_2X$ on the polymerizations of the typical monovinyl compounds, styrene and methyl methacrylate, with special reference to the dependence of the properties of the co-polymers upon the nature of the cross-linking agent used. The following compounds were used:

---

* They also obtained an insoluble polymer of pure vinyl acetate which, however, could, under certain conditions, be changed back into the soluble type. They account for the formation of such a polymer by assuming the formation of cross-linkages between the long threads of the soluble polymer by residual valencies and not by actual chemical cross-linkages as is the case with the co-polymer.

Divinyl-acetylene	$X = -C{\equiv}C-$
1 : 3 : 5-Hexatriene	$X = -CH{=}CH-$
1 : 5-Hexadiene, or diallyl	$X = -CH_2-CH_2-$
Divinyl ether	$X = -O-$
Divinyl sulphide	$X = -S-$
Divinyl sulphoxide	$X = -SO-$
Divinyl sulphone	$X = -SO_2-$

In addition to these compounds isoprene was used in an attempt to obtain a cross-linked polymer with styrene, since isoprene must possess this cross-linking property to a small extent, for both soluble and insoluble forms of polyisoprene are known (Staudinger 1936).

The production of these cross-linkages as determined by the formation of insoluble polymers appears to depend upon the electron attracting or repelling properties of the group X, although the group R in the polymerizing substance $CH_2 : CH . R$, e.g. styrene may, in like manner, influence the production of such insoluble polymers. We return to this influence of the groups R and X later.

EXPERIMENTAL

Preparation and Purification of Styrene, and Methyl-methacrylate

The styrene was prepared by the dehydration of β-phenyl-ethyl alcohol by distillation with anhydrous potassium hydroxide according to the method of Palfrey, Sabetay and Sontag (1932). The yield was almost theoretical and, after two distillations under reduced pressure, a little hydroquinone was introduced as a stabilizer. Immediately prior to use, the sample of styrene to be used was left in contact with solid caustic potash to remove hydroquinone and then distilled *in vacuo* into liquid air, the first and last small fractions being discarded.

The methyl-methacrylate used was a commercial sample which was freed from any impurities present and from polymerized material immediately before use by fractional distillation *in vacuo* into liquid air, the middle fraction alone being used.

Preparation and Purification of the Divinyl Compounds

1—*Divinyl Acetylene*, $CH_2 : CH : C : C.CH : CH_2$.

The divinyl acetylene was prepared by the controlled polymerization of acetylene by passing acetylene gas into a concentrated solution of cuprous ammonium chloride and allowing the mixture to stand at room temperature for about 7 days (Nieuwland and others 1931). By distillation of the mixture on an oil-bath a mixture of divinyl-acetylene and a tetramer of acetylene was obtained, from which the divinyl-acetylene was separated by distillation under reduced pressure. This was subjected to a further distillation under reduced pressure followed by distillation *in vacuo* into liquid air. The resulting liquid had a boiling-point of 45° C. under a pressure of 200 mm. of mercury.

When required for use sufficient of the divinyl-acetylene was distilled from the bulk of the substance into a liquid air-trap in order to free the sample from any polymerized material present. It was found that if the divinyl-acetylene is kept in an evacuated and sealed tube, the rate of polymerization is quite slow and the liquid may be kept at room temperature for some weeks without any appreciable amount of polymerization.

2—1 : 3 : 5-*Hexatriene*, $CH_2 : CH.CH : CH.CH : CH_2$.

This divinyl compound was prepared by the thermal decomposition of the mixture of diformates obtained by the action of 99 % formic acid on divinyl-ethylene glycol (van Romburgh and others, 1905, 1906, 1913, 1914). Equal weights of the glycol and of 99 % formic acid were heated together for ½ hr. at 105° C. and the excess acid removed under reduced pressure at 60° C. The mixture of diformates so obtained was heated on an oil-bath at atmospheric pressure to 160–220° C., the distillate being collected in a flask immersed in a freezing mixture. The upper layer containing the hexatriene was then washed twice with water and dried over caustic potash. After a fractional distillation over sodium and two distillations *in vacuo*, also over sodium, a sample of hexatriene was obtained having a boiling-point of 77·5–78·5° C.

The divinyl-ethylene-glycol was prepared by the reduction of acrolein with zinc-copper couple (Van Romburgh and others 1905, 1906, 1913, 1914; Farmer and others 1927).

This preparation is tedious and the yields obtained, particularly in the last stage, are poor.

3—1 : 5-*Hexadiene, or Diallyl*, $CH_2 : CH.CH_2.CH_2.CH : CH_2$.

This hydrocarbon was prepared by the coupling together of two allyl groups by a Grignard reaction with allyl bromide by the method of Cortese (1929). The allyl bromide was prepared from the corresponding alcohol (Adams 1921).

4—*Isoprene*, $CH_2 : C(CH_3).CH : CH_2$.

Isoprene was prepared by the cracking of limonene (Harries and Gottlob 1911; Staudinger and Klever 1911), using a modification of the method of Harries. The crude isoprene so obtained was then fractionally distilled, using an apparatus similar to that designed by Cooper and Fasce (1928). The use of a column of this type made it possible to obtain the isoprene almost pure at one distillation. A further fractional distillation was carried out *in vacuo* into liquid air and the middle fraction alone used for the experiments.

5—*Divinyl-sulphide*, $CH_2 : CH.S.CH : CH_2$.

The method of Bales and Nickelson (1922) was used. This consists of the elimination of two molecular proportions of hydrogen chloride from $\beta\beta'$-dichlorodiethylsulphide (mustard gas) with 20 % alcoholic potash. The impure sulphide, after drying with fused sodium sulphate, was distilled at atmospheric pressure, the fraction boiling at 85·5–86° C. being taken as the sample to be used. Before using this divinyl-sulphide as a cross-linking agent it was fractionally distilled *in vacuo* into liquid air, the first and last small fractions being discarded.

6—*Divinyl-sulphoxide*, $(CH_2 : CH.)_2SO$.

The sulphoxide was prepared by the removal of two molecular proportions of hydrogen iodide from $\beta\beta'$-diiododiethylsulphoxide by triethylamine, after the method of Alexander and McCombie (1931). The crude product consisted of a brownish liquid, which on distillation under reduced pressure yielded a fraction boiling at 84–85° C./15 mm. which was collected for use.

7—*Divinyl-sulphone*, $(CH_2 : CH.)_2SO_2$.

This was also prepared by the method of Alexander and McCombie (1931) by the removal of two molecular proportions of hydrogen chloride from $\beta\beta'$-dichlorodiethylsulphone by triethylamine. The crude product, which consisted of a yellowish liquid, was distilled at a pressure of 14 mm. of mercury, and the fraction boiling at 105–120° C. under this pressure collected. This distillate was then fractionally distilled under a pressure of 14–15 mm,, most of the liquid coming over at 108–109° C. This fraction was collected and used in the formation of the cross-linked type of polymer.

8—*Divinyl-ether*, $(CH_2 : CH.)_2O$.

We are indebted to Dr. McCombie for supplying us with a sample of divinyl-ether. This sample was purified and freed from any polymer present by distillation *in vacuo* into a trap cooled in liquid air.

The Polymerizations

The polymerizing mixtures used consisted of styrene or methyl-methacrylate containing varying percentages of one of the above divinyl compounds. The mixtures were prepared by the successive dilution with styrene or methyl-methacrylate of the mixture containing the highest percentage of cross-linking agent to be used. The concentrations used are expressed in the tables as percentages by volume. Before use both the polymerizing substance and the cross-linking agent were distilled *in vacuo* into liquid air to free them from any polymer present. Mixtures containing up to 20 % of divinyl compound were used.

The polymerizations were carried out in tubes of about 3 c.c. capacity which had previously been cleaned with chromic acid mixture and then washed with water. These tubes were allowed to soak for some days in distilled water and finally dried for use. About 2 c.c. of the polymerizing mixture was placed in each of these tubes which were then evacuated and sealed off while immersed in liquid air. The whole series of tubes containing mixtures with varying concentrations of cross-linking agent were then placed at the same time into an oil-bath electrically heated to the required temperature. It was found that the most convenient temperature for the styrene polymerizations was 120° C., while that for the polymerizations with methyl-methacrylate mixtures was 80° C. The temperatures of the oil-baths could be kept constant to within 2° C., which may be regarded as sufficiently accurate in view of the essentially qualitative nature of the experiments.

It was observed that with increasing concentration of the divinyl compound the rate of polymerization of the mixture decreased. This decrease was very marked with those divinyl compounds which produced the insoluble polymers most easily. In a series containing increasing proportions of the cross-linking agent all the tubes of the series were kept at the same temperature until the contents of every tube appeared to be solid or nearly solid. This effect on the rate of polymerization with the addition of cross-linking agent varies both with the amount and the nature of the agent used.

Co-polymerization of Styrene with Divinyl Compounds

Of the cross-linking agents used it was found that divinyl-acetylene and divinyl-sulphide were the best for the production of the insoluble type of polymer when styrene is used as the polymerizing medium. Isoprene and 1 : 5-hexadiene, while showing the property of reducing the rate of polymerization, do not give insoluble polymers with styrene even when up to 20 % of the divinyl compound is used. Divinyl-sulphone and 1 : 3 : 5-hexatriene show considerable cross-linking capacity, while divinyl-ether in concentrations up to 20 % does not produce an insoluble polymer with styrene although cross-linking has probably taken place to a small degree, since the polymers containing divinyl-ether form more viscous solutions than the corresponding pure polystyrene. The effect of the sulphoxide on the polymerization is not to produce polymers of the insoluble type. In this case the products after polymerizing for 14 days at 120° C. varied from a clear rubbery solid when 1 % of the sulphoxide was used to a dark red viscous liquid when 20 % was used. All these polymers were soluble in benzene and probably consisted of low polymers of styrene or a product of low molecular weight of some reaction between the styrene and the sulphoxide.

In Tables 1, II and III is given a summary of the properties of the various polymers obtained from styrene by using different cross-linking agents, special reference being made to the solubility or swelling properties in benzene.

Hexatriene was the first cross-linking agent used in this series, and since very little of this hydrocarbon was available at the time, the polymerizations over the whole range of concentrations from 0 to 20 % were not carried out. Mixtures containing 5 % of hexatriene were polymerized at 95, 120, 150 and 200° C. At the two lower temperatures a highly elastic jelly was formed which was insoluble in benzene, although it had a high swelling capacity in this solvent. At the higher temperatures this insoluble polymer was not formed. However, these polymers in solution in benzene had a higher viscosity, and therefore a higher molecular weight than the corresponding pure polystyrene.

It is unnecessary to describe in detail the properties of the polymers obtained with each cross-linking agent, and it is of greater interest to compare the capacity of these divinyl compounds for producing the three-dimensional type of polymer. This comparison for the co-polymers with styrene is shown in the preceding tables. It will be seen that the efficiency of the divinyl compounds used, as determined from the minimum concentration necessary for the production of the insoluble type of polymer, is as follows:

1—Divinyl-acetylene.
2—Divinyl-sulphide.
3—Divinyl-sulphone.
4—Hexatriene.
5—Divinyl ether, divinyl sulphoxide, diallyl and isoprene.

These last divinyl compounds do not act as effective cross-linking agents for styrene polymerization.

TABLE I—HYDROCARBONS USED AS CROSS-LINKING AGENTS FOR STYRENE

Percentage divinyl compound	Divinyl acetylene	Hexatriene	Diallyl	Isoprene
20	Brittle resin, easily powdered. Insol., no swelling capacity	—	—	Soluble glass
10	Light yellow rubber, easily powdered. Insol., no swelling capacity	—	Tough glass, soluble	—
5	Yellowish rubber, rather sticky, easily powdered. Insol., slight swelling capacity	Very elastic jelly. Insol., high swelling capacity	Tough glass, soluble	Tough glass, soluble
4	Yellowish rubber. Insol., limited swelling capacity	—	—	—
3	Yellowish rubber. Insol., limited swelling capacity	—	—	—
2	Slightly yellow rubber. Insol., medium swelling capacity	Tough solid. Partly insol., very high swelling capacity	Tough glass, soluble	—
1	Clear rubber. Insol., medium swelling capacity, no loss of form	—	—	Tough glass, soluble
0·1	Clear glass, can be bent although difficult to break. Insol., high swelling capacity, no loss of form	—	—	—
0·05	Clear tough glass. Insol., high swelling capacity, loss of form	—	—	—
0·00	Clear tough glass. Soluble. Typical polystyrene	Clear tough glass. Soluble. Typical polystyrene	Typical soluble polystyrene	Typical soluble polystyrene

TABLE II—DIVINYL-SULPHUR COMPOUNDS USED AS CROSS-LINKING AGENTS FOR STYRENE

Percentage divinyl compound	Sulphide	Sulphoxide	Sulphone
20	Very viscous liquid. Soluble	Dark red viscous liquid. Soluble	Clear jelly. Insol., very high swelling capacity
10	Yellowish rubber soft. Insol., slight swelling capacity	Orange viscous liquid. Soluble	—
5	Clear solid. Insol., medium swelling capacity	Light orange viscous liquid. Heterogeneous. Soluble	Clear soft yellow rubber. Insol., medium swelling capacity
4	Clear solid. Insol., swelling capacity greater than 5	Yellow very viscous liquid. Heterogeneous. Soluble	Hard tough yellowish glass. Insol., swelling capacity greater than 5
3	Clear glassy solid. Insol., swelling capacity greater than 4	Yellowish, very viscous liquid. Heterogeneous. Soluble	Hard tough yellowish glass. Insol., swelling capacity greater than 4
2	Similar to 3 but with higher swelling capacity	Clear viscous liquid. Almost colourless. Soluble	Hard tough glass. Medium swelling capacity greater than 3
1	Similar to 2 but with higher swelling capacity	Clear rubbery solid. Soluble	Similar to 2 but with higher swelling capacity
0·2	Clear glassy solid. High swelling capacity, slight loss of form. Partly soluble	—	—
0·1	Tough glass. Very high swelling capacity. Loss of form	Clear tough glass. Soluble	Clear tough glass. Soluble, giving very viscous solution
0·0	Clear tough glass. Soluble. Typical polystyrene	Clear tough glass. Typical soluble polystyrene	Clear tough glass. Typical soluble polystyrene

TABLE III—EXPERIMENTS WITH DIVINYL-ETHER IN STYRENE

Percentage divinyl ether	88 hr. at 75° C.	15 hr. at 120° C.
20	Very viscous liquid. Completely soluble	—
10	Very viscous liquid. Completely soluble	Clear elastic jelly. Completely soluble
5	Very viscous liquid. Can be drawn into long threads. Completely soluble	Clear elastic jelly. Completely soluble
4	Very viscous liquid. Can be drawn into long silky threads. Soluble	Clear tough jelly. Completely soluble
3	Similar to 4	Clear tough jelly. Harder than 4. Completely soluble
2	Elastic jelly. Completely soluble	Clear elastic glass. Completely soluble
1	Similar to 2	Clear glass. Soluble
0·0	Tough elastic jelly. Completely soluble	Hard tough glass. Typical soluble polystyrene

Co-polymerization of Methyl-Methacrylate with Divinyl Compounds

The general results with the production of insoluble polymers of methyl-methacrylate were the same as when styrene was used as the polymerizing medium, with the exception of the formation of an insoluble product with divinyl-ether as the cross-linking agent. As will be seen above, styrene does not form an insoluble co-polymer with divinyl ether either at 75 or 120° C. even when 20 % of the ether is used. Methyl-methacrylate, however, gives an insoluble product when polymerized with more than 3 % of the ether at 80° C.

All of the polymerizations with methyl-methacrylate were carried out in the manner described for the polymerizations with styrene. In the case of methyl-methacrylate it was found that the optimum temperature of polymerization was 80° C. with the exception of polymerizations with divinyl-acetylene in concentrations greater than 1 % and with hexatriene.

The mixtures containing 1 % or more of the divinyl-acetylene would not polymerize at 80° C., and after being heated at this temperature for 188 hr. were transferred to a bath at 120° C. for 70 hr. to complete the polymerization. The mixtures containing 0·4 and 0·5 % divinyl-acetylene were polymerized at 80° C. for 135 hr., while those containing less than 0·2 % were polymerized at 80° C. for 66 hr.

Below and in Tables IV and V is a summary of the properties of the polymers obtained using varying concentrations of the different divinyl compounds. It is found from an inspection of this data that the order of efficiency of divinyl compounds as cross-linking agents is the same as for the co-polymerization of styrene.

TABLE IV—DIVINYL-ACETYLENE USED AS CROSS-LINKING AGENT FOR METHYL-METHACRYLATE

Percentage divinyl-acetylene	Physical properties	Solubility in EtAc
20	Dark yellow resin, hard. Easily powdered—brittle	Completely insol., no swelling capacity
10	Light yellow rubbery solid. Easily powdered	Completely insol., no swelling capacity
5	Yellowish sticky jelly	Insol., limited swelling capacity
4	Yellowish jelly, containing considerable amount of monomer. Heterogeneous	Partly insol., high swelling capacity
3	Clear jelly or very viscous liquid	Partly insol., high swelling capacity
2	Very viscous liquid	Partly insol., high swelling capacity
1	Very viscous liquid	Partly insol., high swelling capacity
0·5	Very viscous liquid	Insol., high swelling capacity
0·4	Very viscous liquid	Insol., high swelling capacity
0·2	Elastic jelly	Insol., medium swelling capacity
0·1	Clear tough glass	Insol., limited swelling capacity
0·05	Tough glassy solid	Insoluble. Medium swelling capacity. No loss of form
0·01	Tough glassy solid	Partly soluble. High swelling capacity, with loss of form
0·001	Tough glassy solid	Soluble, to give very viscous solution
0·000	Tough glassy solid. Typical poly-methyl-methacrylate	Soluble, to give viscous solution

Methyl-methacrylate was polymerized at both 95 and 120° C. with 5 % of hexatriene. These polymers showed the insoluble properties of the cross-linked type of polymer, although they had a high swelling capacity in ethyl-acetate and acetone as solvents. A part of the polymer was also dissolved out by these solvents. The cross-linking ability of hexatriene is by no means as great as that of divinyl-acetylene.

Isoprene and diallyl (1 : 5-hexadiene) do not give insoluble co-polymers with methyl-methacrylate, even with mixtures containing as much as 10 % of the divinyl compound.

TABLE V—DIVINYL-ETHER AND DIVINYL-SULPHIDE USED AS CROSS-LINKING AGENTS FOR METHYL-METHACRYLATE

Percentage divinyl compound	Ether	Sulphide
20	White opaque solid. Easily crushed. Insol., no swelling capacity	Hard tough solid. Yellowish but clear. Insol., slight swelling capacity
10	White opaque solid. Less brittle than 20. Insol., limited swelling capacity	Hard tough clear glass. Insol., slight swelling capacity
5	Hard tough clear glass. Many bubbles. Medium swelling capacity, no loss of form	Hard tough glass. Insol., slight swelling capacity
4	Hard tough glass. Many bubbles. Very high swelling capacity, with loss of form	—
3	Hard tough glass. Few bubbles. Just soluble, giving very viscous solution	—
2	Hard tough glass. Only one bubble. Soluble, giving viscous solution	Hard tough glass. Insol., limited swelling capacity
1	Hard tough glass. No bubbles. Completely soluble	Hard tough glass. Insol., limited swelling capacity
0·5	—	Similar to 1 but with higher swelling capacity
0·0	Hard tough glass. Typical soluble poly-methyl-methacrylate	Hard tough glass. Typical soluble poly-methyl-methacrylate

DISCUSSION

It has been shown in the above series of experiments that the addition of small percentages of a divinyl compound $(CH_2:CH.)_2X$ to a polymerizing monovinyl compound $CH_2CH.R$ has a profound effect on the properties and the nature of the polymer obtained. This consists of a decrease in the rate of polymerization and the formation of insoluble polymers. These polymers vary from insoluble and infusible discoloured resins, formed when high concentrations of the divinyl compound are used, through insoluble rubbery substances and glasses of limited swelling capacity to glasses of high swelling capacity and finally to completely soluble polymers. The percentage of the divinyl compound required to produce a polymer of a given swelling capacity depends upon the group *X* in addition to the temperature. This dependence on the temperature has been shown by Staudinger (1936) with his co-polymers of styrene and *p*-divinyl-benzene. That the percentage also depends upon the nature of the group *R* in the monovinyl compound used, is shown below by comparing the co-polymers of styrene, vinyl-acetate and methyl-methacrylate with divinyl-ether.

In general the properties of the co-polymers of styrene and methyl-methacrylate with various divinyl compounds are similar to those of styrene and *p*-divinyl-benzene obtained by Staudinger, and collectively they furnish considerable support for his view of the structure of this type of macromolecule. Following Staudinger's presentation of the structure of his insoluble polystyrene we can now state his formula in the more general form:

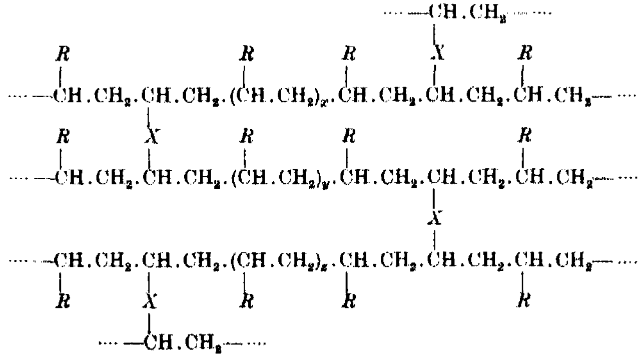

The polymerizing substance $CH_2:CH.R$ may be styrene, methyl-methacrylate or any similar substance such as vinyl-acetate (Blaikie and Crozier 1936), which polymerizes to give long thread-like molecules.

In the divinyl compounds used it is interesting to consider the effect of changing the group *X*. The cross-linking capacity of the compound clearly depends upon some property conferred on the vinyl groups by the group *X*, the function of which, we suggest, is the same as the function of the group *R* (e.g. Cl, C_6H_5, etc.) in the monovinyl compounds, i.e. the induction of a permanent dipole moment in each of the vinyl groups. It is upon their intensity of polarization that the reactivity of the vinyl groups must ultimately depend, the molecules of monomer tending to orientate themselves, and to polymerize by a chain reaction when once active centres have been produced. This idea is supported by the fact that there is generally a complete absence of lower polymers in the reaction products, the factor controlling the rate of reaction being the production of active centres, while the subsequent polymerization to a long thread-like molecule is extremely rapid.

The prerequisite of a good cross-linking agent is thus that the group *X* should induce a strong dipole in the two vinyl groups, so that these may enter actively into the alignment of molecules and produce the three-dimensional polymer, the structure of which is given above. The group *X* must therefore be possessed of either electron attracting, or electron repelling, properties, and it may be expected that the efficiency of the divinyl compound as a cross-linking agent may be correlated with the electron affinity of this activating group. It will be seen from the preceding experiments that this is in effect the case. For example, of the three divinyl hydrocarbons used, divinyl-acetylene containing the comparatively strong negative group $—C{\equiv}C—$ is by far the most efficient as a cross-linking agent. On reducing the electron affinity of this electro-negative group by the addition of hydrogen, we first get hexatriene which still possesses marked cross-linking properties although by no means as strong as those of divinyl acetylene, while on further addition of hydrogen we obtain diallyl, with the electrically neutral group $—CH_2.CH_2—$, which has no cross-linking capacity at all. Similarly with the sulphur compounds, when we change the electrical properties of the group *X* by the addition of oxygen to the sulphur atom. Thus the electro-negative group $—S—$ in divinyl-sulphide confers on that compound marked cross-linking properties, but when the lone pair of electrons on this sulphur atom are used up by the addition of oxygen to give the sulphoxide, these properties disappear. On the further addition of an oxygen atom to give the sulphone, the group becomes effectively electropositive (cp. SO_2Cl_2, etc.), and the cross-linking properties again become apparent. Thus the order of cross-linking capacity appears to be the same as that of the order of electron attraction or repulsion.

The group *R* of the monovinyl compound does not affect this order of cross-linking capacity, although on changing *R* the actual minimum percentage of the divinyl compound necessary to produce an insoluble polymer does of necessity change, since the resulting change in the strength of the dipole in the vinyl group of this monovinyl compound must have an effect similar to that taking place by the changing of the group *X* in the divinyl compound. This is shown most markedly in the preceding experiments by the co-polymerization of styrene and methyl-methacrylate respectively with divinyl-ether; styrene will not form an insoluble co-polymer with the ether, although a small amount of cross-linking must occur, since the solutions of this polymer have higher viscosities than similar solutions of a pure polystyrene; methyl-methacrylate, on the other hand, forms an insoluble co-polymer with divinyl-ether when the latter is present in concentrations greater than 3 %, while vinyl-acetate requires about 10 % of ether to give an insoluble co-polymer.

A specific effect of these cross-linking agents also appears in the reduction of the rate of polymerization, the extent to which this occurs being dependent both upon the concentration and the nature of the divinyl compound used. As a first approximation it may be said that the order of efficiency in decreasing the rate of polymerization is the same as that of the cross-linking ability. The diminution in the rate of polymerization rises rapidly with increasing concentration of the divinyl compound. A series of kinetic measurements are being carried out in an attempt to find the relationship between these two effects and also to put these co-polymerizations on a sound theoretical basis.

We wish to express our thanks to the Department of Scientific and Industrial Research for an Assistantship granted to one of us (E.F.B.), which enabled this work to be carried out, and also to the Chemical Society for grant towards the purchase of materials. We are also indebted to Mr. J. Bottomley for help in preparing the divinyl-sulphur compounds, to Dr. H. McCombie for helpful advice during their preparation, and to Messrs. The Imperial Chemical Industries for a supply of methyl-methacrylate.

SUMMARY

A series of cross-linking agents have been described together with the properties of their co-polymers with monovinyl compounds. Support is given to Staudinger's view of the structure of this class of polymer and a general formula given for such a structure. The view is expressed that the electronic properties of the group X in the divinyl compound $(CH_2:CH.)_2X$ determines the cross-linking properties in the same way as the electronic properties of R in the monovinyl compound $CH_2:CH.R$ determines the ease of polymerization of those compounds. The effect of the presence of the divinyl compound on the rate of polymerization is also noted.

REFERENCES

Adams, R. 1921 "Organic Syntheses", **1**, 3. New York: J. Wiley and Sons.

Alexander, J. R. and McCombie, H. 1931 *J. Chem. Soc.* **134**, 1913–18.

Bales, S. H. and Nickelson, S. A. 1922 *J. Chem. Soc.* **121**, 2137–9.

Blaikie, K. G. and Crozier, R. N. 1936 *Industr. Engng. Chem.* **28**, 1155–9.

Cooper, C. M. and Fasce, E. V. 1928 *Industr. Engng. Chem.* **20**, 420–1.

Cortese, F. 1929 *J. Amer. Chem. Soc.* **51**, 2266–9.

Farmer, E. H., Laroia, B. D., Switz, T. M. and Thorpe, J. F. 1927 *J. Chem. Soc.* **130**, 2937–58.

Harries, C. D. and Gottlob, K. O. 1911 *Ann. Phys., Lpz.*, **383**, 228–9.

Kienle, R. H. and Hovey, A. G. 1929 *J. Amer. Chem. Soc.* **51**, 509–19.

Kienle, R. H. 1930 *Industr. Engng. Chem.* **22**, 590.

Koebner, M. 1933 *Angew. Chem.* **46**, 251–6.

Morgan, G. T., Megson, N. J. L. and Leighton Holmes, E. 1936 *J. Soc. Glass Techn.* **20**, 19–34.

Nieuwland, J. A., Calcott, W. S., Downing, F. B. and Carter, A. S. 1931 *J. Amer. Chem. Soc.* **53**, 4197–202.

Palfrey, L., Sabetay, S. and Sontag, D. 1932 *C.R. Acad. Sci., Paris*, **195**, 1392–4.

Romburgh, P. van and Dorssen, W. van 1905 *Proc. K. Akad. Wet. Amst.* **8**, 541–4, 565–8.

—— —— 1906 *Proc. K. Akad. Wet. Amst.* **9**, 111–15.

Romburgh, P. van 1913 *Proc. K. Akad. Wet. Amst.* **15**, 1184.

Romburgh, P. van and Muller, P. 1914 *Proc. K. Akad. Wet. Amst.* **16**, 1090–3.

Staudinger, H. and Klever, H. W. 1911 *S.B. Akad. Wiss. Wien*, **44**, 2212–15.

Staudinger, H. and Heuer, W. 1934 *S.B. Akad. Wiss. Wien*, **67**, 1164–72.

Staudinger, H. and Husemann, E. 1935 *S.B. Akad. Wiss. Wien*, **68**, 1618–34.

Staudinger, H. 1936 *Trans. Faraday Soc.* **32**, 323–32.

Photochemical Reactions in the Fluorite Region
II—Photochemical Decomposition of Formaldehyde Vapour

By R. G. W. Norrish, F.R.S. and W. Albert Noyes, Jr.

(*Received* 27 *August* 1937)

The photochemical decomposition of formaldehyde in the near ultra-violet has been the subject of several investigations. It is known (Norrish and Kirkbride 1932) that the products are chiefly carbon monoxide and hydrogen, and that neither the composition of the products nor the quantum yield depends appreciably on wave-length.

Recently Price (1935) has investigated the far ultra-violet absorption spectrum of formaldehyde. The first band observed in this region occurs at about 1745 A and is very diffuse, whereas the first bands in acetaldehyde (Price 1935) and acetone (Noyes, Duncan and Manning 1934) occur at longer wave-lengths and are relatively much sharper. Price ascribes this diffuseness to a predissociation resulting from the interaction of the upper state in formaldehyde with the ground state and assumes that the primary dissociation at about 1745 A should be

$$CH_2O \xrightarrow[1745\,A]{h\nu} CH_2 + O. \qquad (1)$$

Sidgwick and Bowen (1931), in summarizing heats of dissociation of various bonds, give 160 kcal. for the heat of dissociation of the carbon-oxygen bond in formaldehyde. This corresponds, in fact, to about 1780 A, which lends support to the assumption made by Price (1935). Since heats of combustion and other thermochemical data enter into the calculation of this figure, the oxygen atom in equation (1) would be formed, presumably, in the ground state (^3P). The state of the CH_2 group is more uncertain and would probably be that formed in the (hypothetical) dissociation of ethylene when the energy customarily assigned for the dissociation of the carbon-carbon double bond in that compound is absorbed. Whether or not this corresponds to any definite spectroscopic state of the CH_2 group is at present unknown, and moreover, the products resulting from the "adiabatic" dissociation of formaldehyde in its ground state cannot be predicted with absolute certainty.

It should be emphasized, moreover, that large uncertainties (Kistiakowsky 1937; Herzberg 1937) exist at present in the heats of dissociation of various bonds in organic compounds, so that a precise prediction of the wave-length which would cause reaction (1) is impossible. Suffice to say that various means of arriving at this figure lead to widely varying results.

Consequently it is of interest to ascertain whether the products of photochemical decomposition of formaldehyde are the same in the far as in the near ultra-violet. Following a primary dissociation as in equation (1), the following products might result: C_2H_4, O_2, HCOOH, CO_2, H_2O, CO, H_2, C_2H_6, CH_4. Higher hydrocarbons could only be formed by a complicated series of secondary reactions. Indeed, the formation of methane and ethane may be considered as relatively improbable. Following reaction (1) it would seem impossible for any sequence of reactions to lead to a 1 : 1 ratio of carbon monoxide to hydrogen. In the following experiments an attempt has been made to ascertain the nature and quantities of the products formed in the fluorite region of the absorption spectrum. It seems that the products in the far ultra-violet differ little if at all from those in the near ultra-violet, and that there is no experimental evidence for assuming a rupture of the C=O bond.

EXPERIMENTAL METHOD

The hydrogen lamp has been described (McDonald and Norrish 1936). An additional cell which could be filled with a gas to serve as colour filter was inserted between the reaction vessel and the lamp (*loc. cit.* fig. 1).

Acetone was used in many of the experiments as a colour filter. It absorbs in the same general region as formaldehyde in the near ultra-violet and would serve to reduce the reaction due to that region of absorption. The sample used transmitted strongly from 1720 to 1780 A (Noyes, Duncan and Manning 1934; Duncan 1937), but otherwise absorbed all wave-lengths below about 1965 A completely at the pressures used.

Mercury vapour was present in the colour filter cell to prevent sensitized reaction due to the 2536 and 1849 A lines of mercury.

Formaldehyde was prepared by heating paraformaldehyde. While precautions were taken to remove oxygen and water by discarding a large amount of formaldehyde before each run, the apparatus could not be baked out due to the presence of the ground joints and the fluorite windows. Consequently some polymerization of the formaldehyde always took place.

Since small amounts of decomposition product were obtained, an apparatus free from stopcocks was used to reduce possibilities of error.

During the first series of experiments, liquid hydrogen was used to condense all of the gases but hydrogen, the latter being removed by a Toepler pump and measured. The gases uncondensed by liquid nitrogen were then collected and measured. These would include CO, O_2, C_2H_4, C_2H_6, CH_4. However, some formaldehyde always came over at the same time, thus preventing this method from being exceedingly precise for small amounts of gas. In some experiments the additional gas liberated at − 155° C. (pentane mush) was collected. This proved to be small. An attempt to pump off the formaldehyde at − 77° C. and determine the products condensible at that temperature gave negative results. Such a method would be wholly unreliable for small amounts of water, formic acid, etc.

A second method of analysis was also used. A McLeod gauge bulb was fitted at the top of the capillary with two projections, one containing copper oxide and the other magnesium perchlorate, to act as drying agent. The gas was compressed into this part of the apparatus and the copper oxide heated. The pressures were read at constant volume by bringing the mercury to a fixed position in the capillary. Water would be removed by the magnesium perchlorate. Three runs were made in the near ultra-violet. The percentages H_2 found (i.e. the decrease in pressure divided by the initial pressure times 100) were: 48, 47, 49, av. 48. The average percentage hydrogen reported by Norrish and Kirkbride (1932) is 47·2. This method of analysis seems to work satisfactorily, therefore, in the case when the products are chiefly carbon monoxide and hydrogen. The apparatus is referred to below as "the analysis gauge".

RESULTS

a—Approximate Determination of Amounts of Reaction in Various Wave-Length Regions

By determining the amounts of decomposition under various experimental conditions, using a quartz window and the acetone filter, one finds the approximate distribution of quantity of reaction with wave-length given in Table I, due allowance (15 %) having been made for reflexion and absorption at the quartz window.

TABLE I—APPROXIMATE FRACTION OF REACTION PRODUCTS IN VARIOUS WAVE-LENGTH REGIONS

(*a*) 1300–3500 A (fluorite alone)	1·00
(*b*) 2300–3500 A (fluorite plus quartz)	0·64
(c) 1300–1800 A (difference)	0·36

These figures are subject to some uncertainty due to the presence of the formaldehyde polymer. Of the reaction due to radiation transmitted by fluorite plus the acetone filter (12–14 mm. pressure, 4·2 cm. thick), it was similarly found that approximately 10 % is due to the region embracing the 1745 A band of formaldehyde. This agrees with the following facts: (1) the hydrogen continuum is weak on the long-wave side of the Lyman bands; (2) although the absorption coefficient of formaldehyde is high at 1745 A, the band is only 30–40 A wide, while the near ultra-violet absorption region extends well over 1000 A in length.

Of the 36 % of the reaction due to the far ultra-violet, the vast majority must be caused by the Lyman bands of hydrogen absorbed in the formaldehyde bands lying below about 1560 A (Price 1935).

b—Fractionation of Reaction Products using Various Condensing Temperatures

Table II presents results obtained in various attempts to fractionate the reaction products.

TABLE II—FRACTIONATION OF REACTION PRODUCTS. (VOLUME OF COLLECTING SYSTEM APPROXIMATELY 60 C.C.)

Run no.	Total pressure products uncondensed by liquid N_2 mm. × 10^2	Fraction uncondensed by liquid H_2	Fraction uncondensed by liquid N_2 but condensed by liquid H_2	Fraction uncondensed at − 155° C. but condensed by liquid H_2	Pressure acetone in filter mm.
3	9·3	0·45	0·55	—	0
4	3·14	0·49	0·51	—	~ 40
5	2·18	—	—	0·05	~ 40
6	4·81	—	—	0·04	~ 40
7	3·34	0·43	0·57	—	~ 40
11	6·94	—	—	0·02	0
13	6·11	0·40	0·60	—	0

In case successive runs were made on the same day without a long period of evacuation, runs after the first seemed to give anomalous results. This was evidenced by the fact that practically no hydrogen was formed and the total of gaseous products was greatly diminished. It seems probable that this phenomenon can be explained by the formation of a film of polymerized formaldehyde on the fluorite window which absorbed most of the radiation, for by continued pumping the polymer can be evaporated and the anomaly suppressed. The small amounts of gas pumped away under these circumstances may well have been monomeric formaldehyde vapour.

While the results in Table II are not very satisfactory, they seem to indicate that hydrogen is formed in the Schumann region to an extent not far different from that in the near ultra-violet. No definite conclusion, however, is possible from the small amount of gas obtained at − 155° C., except, perhaps, that carbon dioxide is not formed in large quantities.

c—Partial Analysis of Reaction Products

Table III presents results obtained using copper oxide to analyse the reaction products, as described on p. 223 above.

TABLE III—ANALYSIS OF PRODUCTS UNCONDENSED AT − 155° C.

Run no.	Pressure of products mm. on analysis gauge mm. P_1	Initial pressure CH_2O mm.	Pressure of products after heating CuO mm. on analysis gauge mm. P_2	$\frac{P_1 - P_2}{P_1}$	Pressure acetone in filter mm.	Time min.	Conditions
24	4·9	16	2·6	0·47	11·5	358	Quartz window
25	8·0	14	4·1	0·49	0	358	,,
20	3·3	14·5	1·7	0·48	11	341	Air in discharge tube
19	1·5	8·5	0·9	0·40	0	341	Fluorite window
22	7·2	16·5	4·35	0·40	12	374	,,
23	3·9	16	2·7	0·31	12	358	,,
26	6·8	16	4·05	0·40	0	358	,,

Finally, two runs were made in which liquid hydrogen was used to condense the gases other than hydrogen, the hydrogen was pumped off and the gases uncondensed at − 155° C. then subjected to analysis by copper oxide. Table IV gives the results obtained.

TABLE IV—ANALYSIS OF PRODUCTS OTHER THAN HYDROGEN

Run no.	Pressure of products including H_2 mm. × 10^3	Pressure of products in analysis gauge (without H_2) mm. P_1	Initial pressure CH_2O mm.	Pressure of products after heating CuO in analysis gauge mm. P_2	$\frac{P_2 - P_1}{P_1}$	Pressure acetone in filter mm.	Time min.
27	0·85	1·2	2·7	1·3	0·08	7	370
28	16·4	(*a*) 33·0	5	33·0	0	0	330
		(*b*) 17·5	—	17·9	0·02	—	—

The runs in Table IV were carried out at such low pressures of formaldehyde that practically no polymerization took place, and the absorption in the near ultra-violet would be very small. Further since the acetone removes only about 5 % of the radiation of wave-length larger than 2300 A, it is obvious from a comparison of the yield in runs 27 and 28 that in the latter over 90 % of the reaction occurred through the agency of radiation in the Schumann region.

In Table III, $P_1 - P_2/P_1$ represents the fraction hydrogen in the reaction products providing the hydrogen is mixed only with the following gases (which might be present): CO, CH_2O, CO_2, CH_4. These gases would cause no pressure change if present, since each would give one molecule of carbon dioxide per molecule initially present and water would be removed by the magnesium perchlorate. Of the other possible products remaining in the gas phase at − 155° C., oxygen would be removed either in oxidizing some of the other gases or some of the copper. Ethylene and ethane would both give two molecules of carbon dioxide for each molecule initially present.

Although it is difficult to correct properly for the effect of temperature due to cooling the trap with liquid hydrogen, runs 27 and 28 gave very closely the same percentage hydrogen as found previously.

$\frac{P_2 - P_1}{P_1}$ in Table IV would give the percentage of ethylene and ethane in the gases uncondensed at − 155° C. For run 27 this does not exceed experimental error due to the small amount of gas present, while for run 28 the results indicate beyond question that these gases are almost entirely absent. Moreover, they indicate that the gas uncondensed at − 155° C. (other than H_2) is either CO, CH_4, CH_2O or CO_2, or a mixture of these gases.

The amount of CO_2 and CH_2O in the gas phase at this temperature would be negligible. Methane could only be formed by a complicated set of secondary reactions. The evidence is thus very strong that this gas is carbon monoxide.

The vast majority of the decomposition of formaldehyde in the Schumann region must give carbon monoxide and hydrogen, the fraction of the latter being slightly lower than in the near ultra-violet. However, in the near ultra-violet the results of Norrish and Kirkbride (1932) indicate a slight trend toward lower fractions of hydrogen with increasing frequency. This may indicate that at short wave-lengths hydrogen atoms are formed as distinguished from hydrogen molecules, and that these may give secondary reactions with formaldehyde thus leading to the lower percentage of H_2 in the products.

The results as regards the individual band at 1745 A are not too conclusive, due to the small intensity of the source at this point. There is no reason to believe, however, that formaldehyde at this wave-length behaves differently than in the rest of the Schumann region.

We acknowledge with thanks a grant from the Royal Society which has been applied in part to the purchase of apparatus for this work.

SUMMARY

Formaldehyde decomposes in the Schumann region to give, as products uncondensed at -155° C., mainly hydrogen and carbon monoxide, the fraction of the former being slightly lower than in the near ultra-violet. No evidence is found in this work for a primary dissociation into methylene radicals and oxygen atoms. Most of the decomposition in these experiments must be caused by the wave-lengths lying below 1600 A where formaldehyde would absorb some of the Lyman bands of hydrogen.

REFERENCES

Duncan 1937 *J. Chem. Phys.* **3**, 131.
Herzberg 1937 *Chem. Rev.* **20**, 145.
Kistiakowsky 1937 *J. Phys. Chem.* **41**, 175.
McDonald and Norrish 1936 *Proc. Roy. Soc.* A, **157**, 480.
Norrish and Kirkbride 1932 *J. Chem. Soc.* p. 1518.
Noyes, Duncan and Manning 1934 *J. Chem. Phys.* **2**, 717.
Price 1935 *J. Chem. Phys.* **3**, 256.
Sidgwick and Bowen 1931 *Ann. Rep. Chem. Soc.* **28**, 401.

Thermal Radiation and Absorption in the Upper Atmosphere

By G. H. Godfrey, M.A., B.Sc., and W. L. Price, B.Sc., B.E.

(*Communicated by Lord Rutherford, O.M., F.R.S.—Received* 15 *June* 1937)

1—Introduction

In a recent paper, Martyn and Pulley (1936), from a study of radio and other observations, reached certain conclusions regarding the temperatures and constituents of the upper atmosphere. It is one of the objects of the present paper to examine whether the temperatures found by these authors are compatible with their assumption that solar radiation is the causal agency.

Much the greatest part of the solar radiation absorbed in the earth's atmosphere is in the ultra-violet region of the spectrum, and there is little doubt that this radiation is responsible for most of the ionization, excitation and dissociation known to exist in the gases of the high atmosphere. There is also little doubt that most of the energy so absorbed must be speedily degraded into thermal energy of molecular agitation.

In this paper we employ the known coefficients of absorption of the atmospheric gases and calculate from the mean solar constant and the distribution of energy in the solar spectrum the rate of absorption of energy. On the assumption that this energy is almost all degraded into heat in a matter of seconds, we calculate the rate of rise of temperature. When the temperature reaches a value such that the radiation emitted by the gas equals that absorbed, radiative equilibrium is attained, and the temperature at which this occurs depends only on the relative concentrations of the absorbing substances present and the external conditions.

The general problem of radiative equilibrium in a thick layer of gas can be solved analytically only for the case of a grey body, i.e. for an absorbing material which has the same coefficient of absorption for all wave-lengths.

The earth's atmosphere does not even approximate to a grey body, for although relatively few absorbing substances are present (viz. ozone, water vapour and molecular oxygen), they absorb selectively over a wide range of wave-lengths, and, moreover, their relative concentrations vary considerably at different heights.

As stated above we are mainly concerned in this paper with the regions of the ionosphere above 100 km. At these heights considerable simplification occurs, since the atmosphere above is of small absorptive thickness for ozone and water vapour.

The absorption by a layer of gas for a given wave-length is given by $1-\epsilon^{\alpha x}$, where α is the coefficient of absorption for that wave-length, and x is the thickness of the layer reduced to N.T.P.* When the absorption is small it simplifies to αx. If αx is small for all wave-lengths, the total absorption is a linear function of the thickness, and the layer may be described as thin. Under these conditions we may neglect the re-radiation from one part of a layer to another, and the incident radiation may be taken as uniform at all depths in the layer. It is a reasonable assumption that such conditions apply for the absorption of normally incident solar radiation by ozone and water vapour above 100 km.

For ozone, the maximum value of α is 276, so that $\alpha x < 0{\cdot}1$ provided $x < 1/3000$ cm. Martyn (1935) finds that the total pressure at 100 km. is equivalent to 1 cm. of air at N.T.P. It follows that $\alpha x < 0{\cdot}1$ provided the ozone concentration is less than 1/3000, which is a much higher concentration than is known to exist at any level of the atmosphere accessible to observation. We may therefore assume with reasonable safety that the ozone above 100 km. forms a thin layer.

Even if the whole atmosphere above 100 km. were water vapour, it would still be thin, owing to the low values of α for this substance.

For molecular oxygen, however, no such assumptions can be made, and care has had to be taken in allowing for absorption in the upper layers of this gas, even above the 100 km. level.

2—THE EQUATION OF RADIATIVE EQUILIBRIUM FOR A THIN HORIZONTAL LAYER OF THE ATMOSPHERE

The conditions of radiative equilibrium in a thin horizontal layer of the atmosphere are expressed by the following equation:

$$\begin{aligned} R\,dx &= R_1\,dx_1 + R_2\,dx_2 + \dots \\ &= \int_0^\infty (S_\lambda + 2s_\lambda + 2E_\lambda)(\alpha_\lambda\,dx_1 + \beta_\lambda\,dx_2 + \dots)\,d\lambda. \qquad (1) \end{aligned}$$

---

* In the case of water vapour, however, x is usually measured in cm. of precipitable water.

dx is the thickness of the layer of mixed gases when reduced to conditions of N.T.P. and dx_1, dx_2, etc., the corresponding quantities for the different constituents whose coefficients of absorption for a wave length λ are α_λ, β_λ, etc. R is the rate of radiation per c.c. of the mixture reduced to conditions of N.T.P. R_1 and R_2 have corresponding meanings with regard to the several constituents, and are given by

$$R_1 = 4\int_0^\infty \beta_{\lambda T}\alpha_\lambda \, d\lambda,$$

$$R_2 = 4\int_0^\infty \beta_{\lambda T}\beta_\lambda \, d\lambda, \text{ etc.,}$$

where $\beta_{\lambda T}$ is the total outward flux of wave-length λ from unit surface of a black body at temperature T.

S_λ is the solar radiation of wave-length λ received per second at the surface of the layer by unit area taken normally to the rays. The angle of incidence of these rays is not explicitly involved in the equation of equilibrium, because reduction in the surface density of the radiation due to obliquity is balanced by the increased absorption due to the longer path of the rays through the layer. The obliquity will, however, affect the value of S_λ itself, since this depends upon the amount of absorbing gas traversed by the rays before reaching the layer. s_λ is the rate at which the diffusive radiation from the atmosphere above is received by unit area of the layer, whilst E_λ is the corresponding quantity for the energy received from the lower layers and the earth.

The factor 2 before the symbols S_λ and E_λ is introduced to take account of the diffusive nature of the radiation, and the factor 4 in the expression for R_1 and R_2 allows for diffusion and for the fact that the radiation is emitted from both sides of the layer.

Since the volume concentrations of the different constituents in the layer may be defined by $C'_v = \frac{dx_1}{dx}$, $C''_v = \frac{dx_2}{dx}$, etc., the equation may be written

$$R = R_1 C'_v + R_2 C''_v + \ldots = \int_0^\infty (S_\lambda + 2s_\lambda + 2E_\lambda)(C'_v\alpha_\lambda + C''_v\beta_\lambda + \ldots)\, d\lambda.$$

We have, also, that $dx : dx_1 : dx_2$, etc., $= \frac{d}{\rho} : \frac{d_1}{\rho_1} : \frac{d_2}{\rho_2}$, etc., where d and ρ are respectively the densities of the mixture under its actual condition in the layer and at N.T.P., d_1, ρ_1, etc., being the corresponding quantities for constituents. Thus the equation may be written

$$\begin{aligned}\bar{R} &= \bar{R}_1 C'_m + \bar{R}_2 C''_m + \ldots \\ &= \int_0^\infty (S_\lambda + 2s_\lambda + 2E_\lambda)(C'_m \alpha_\lambda/\rho_1 + C''_m \beta_\lambda/\rho_2 + \ldots)\, d\lambda,\end{aligned}$$

where $\bar{R} = \dfrac{R}{\rho}$, $\bar{R}_1 = \dfrac{R_1}{\rho_1}$, etc., are the radiations per gram of mixture and constituent respectively and $C'_m = d_1/d$, $C''_m = d_2/d$, etc., are the mass concentrations.

In the text the distinguishing superscripts $'$, $''$, $'''$, refer to water vapour, ozone and molecular oxygen.

It is convenient to have a single term to represent the right-hand side of the equation. We shall denote it by Adx so that A is the absorption per c.c of gas at N.T.P. The absorption per gram of gas, viz. A/ρ, will be represented by $\bar{A}$.

The temperature at which this equation is satisfied can be found if the relative concentrations of the absorbing constituents are known.

3—DATA AND ASSUMPTIONS USED

We now consider the application of the equilibrium equation to regions of the atmosphere above 100 km. in height. The absorbing substances to be considered are water vapour, ozone and molecular oxygen and we denote their respective coefficients by α_λ, β_λ and γ_λ.

The values of α_λ, etc., have been taken from the investigations of Hettner (1918) on water vapour, of Fabry and Buisson (1913), Colange (1927) and Ladenburg and Lehmann (1906) on ozone and of Ladenburg and Van Voorhis (1933) on oxygen.

We have already pointed out that the whole region above the 100 km. level may be considered "thin" for absorption of solar radiation by water vapour and ozone at normal incidence. In the case of molecular oxygen it has been shown (Ladenburg and Van Voorhis 1933) that a strong absorption band exists in the ultra-violet, the maximum absorption coefficient being 490 at 1450 A. If we take the value given by Martyn and Pulley (1936, pp. 463–4) for the total atmospheric pressure at the level of the F region; viz. 5×10^{-8} cm. of mercury, and suppose that molecular oxygen has no greater concentration here than that at the earth's surface, it will be seen that γdx_3 does not exceed 0·05, so that here again thin layer conditions exist. We may thus, to a sufficient approximation, consider that the values to be given to S_λ in this region are those which it would have at the outer boundary of the atmosphere. These have been obtained from the work of Fabry and Buisson (1921), and Abbot (1913).

The values of E_λ corresponding to midsummer and midwinter, day and night at Sydney, have been calculated on the following assumptions:

(1) That the earth's surface radiates as a black body at the average temperature obtaining for each condition.

(2) That the absorption of this radiation by the atmosphere up to the 11 km. level is due to water vapour distributed according to Hergesell's formula for the relative humidity (Simpson 1928), taken in conjunction with a mean lapse rate of 6° C. per km., and that the absorption above this level is due to water vapour and ozone. The atmosphere is taken as saturated at the tropopause and above it the amount of water vapour is regarded as given by the hypothesis of complete mixing. The ozone is assumed to have the distribution given by Chapman (1934) with the exception that the amount of ozone below 11 km. has been placed, as regards its effect, at this level.

(3) That the ozone and water vapour so distributed reradiate day and night at the temperature given in column 4, Table II.

(4) That the earth's albedo can be neglected, since it is negligible in the infra red and reduced to a negligible amount in the ultra-violet by its outward passage through atmospheric ozone. In the visible region the coefficients of absorption are so small that the albedo does not require consideration.

4—CALCULATION OF EQUILIBRIUM TEMPERATURES

The values of $\bar{R}$ in ergs per second per gram are given in fig. 1 for mixtures of ozone and water vapour at temperatures up to 3000° K. and for different relative volume concentrations. The values of $\bar{R}$ for oxygen are given in the same figure for temperatures between 2500 and 3600° K. The value of $\bar{R}$ for oxygen at 2500° K. is about $1/10^7$ of that for water vapour or ozone, so that we may neglect the radiation by oxygen for lower temperatures when its concentration is less than 10^5 times that of these substances.

In the case of pure ozone the graph between 900 and 2000° K. is very nearly a straight line, and the radiation very accurately is proportional to the cube of the temperature. In the same figure are shown the radiations per gram molecule of ozone and water vapour respectively. It is worthy of note that for temperatures between 300 and 1500 °K., the radiation from a gram molecule of water vapour is within 20 % of that from a gram molecule of ozone. This fact is important in connexion with the rate of heating and will be discussed later. For present purposes it precluded the possibility of plotting volume concentrations in the graph as the curves for different mixtures of ozone and water vapour would have practically coincided.

TABLE I

Nature of incident radiation	Relative volume concentration of oxygen	Rate of absorption per gram of mixture of $O_3 + H_2O$ in c.g.s. units Ratio of $H_2O : O_3 + H_2O$ by mass 0·0	0·25	0·5	0·75	0·9	1·0
Sun, summer day	— —	$2\cdot63 \times 10^9$	—	—	$6\cdot59 \times 10^8$	—	$1\cdot89 \times 10^6$
Earth, summer day	— —	$7\cdot44 \times 10^6$	—	—	—	—	$1\cdot29 \times 10^7$
Earth, winter day	— —	$5\cdot98 \times 10^6$	$6\cdot93 \times 10^6$	$7\cdot88 \times 10^6$	$8\cdot83 \times 10^6$	$9\cdot4 \times 10^6$	$9\cdot78 \times 10^6$
Earth, summer night	— —	$5\cdot98 \times 10^6$	$6\cdot93 \times 10^6$	$7\cdot88 \times 10^6$	$8\cdot83 \times 10^6$	$9\cdot4 \times 10^6$	$9\cdot78 \times 10^6$
Earth, winter night	— —	$4\cdot47 \times 10^6$	$5\cdot16 \times 10^6$	$5\cdot85 \times 10^6$	$6\cdot53 \times 10^6$	$6\cdot95 \times 10^6$	$7\cdot22 \times 10^6$
Sun and earth, summer day	— —	$2\cdot64 \times 10^9$	$1\cdot98 \times 10^9$	$1\cdot33 \times 10^9$	$6\cdot69 \times 10^8$	$2\cdot78 \times 10^8$	$1\cdot48 \times 10^6$
Sun and earth, winter day Ratio $O_2 : O_3 + H_2O$ by volume which is constant throughout a range of $H_2O : H_2O + O_3$	0·0	$2\cdot64 \times 10^9$	$1\cdot98 \times 10^9$	$1\cdot33 \times 10^9$	$6\cdot69 \times 10^8$	$2\cdot75 \times 10^8$	$1\cdot17 \times 10^7$
	0·1	$2\cdot65 \times 10^9$	$1\cdot99 \times 10^9$	$1\cdot34 \times 10^9$	$6\cdot81 \times 10^8$	$2\cdot88 \times 10^8$	$2\cdot56 \times 10^7$
	0·3	$2\cdot66 \times 10^9$	$2\cdot00 \times 10^9$	$1\cdot36 \times 10^9$	$7\cdot05 \times 10^8$	$3\cdot15 \times 10^8$	$4\cdot90 \times 10^7$
	1·0	$2\cdot69 \times 10^9$	$2\cdot06 \times 10^9$	$1\cdot43 \times 10^9$	$7\cdot88 \times 10^8$	$4\cdot07 \times 10^8$	$1\cdot52 \times 10^8$
	9·0	$3\cdot12 \times 10^9$	$2\cdot65 \times 10^9$	$2\cdot20 \times 10^9$	$1\cdot74 \times 10^9$	$1\cdot47 \times 10^9$	$1\cdot28 \times 10^9$
	18	$3\cdot59 \times 10^9$	$3\cdot33 \times 10^9$	$3\cdot07 \times 10^9$	$2\cdot81 \times 10^9$	$2\cdot66 \times 10^9$	$2\cdot55 \times 10^9$
	30	$4\cdot23 \times 10^9$	$4\cdot23 \times 10^9$	$4\cdot23 \times 10^9$	$4\cdot23 \times 10^9$	$4\cdot23 \times 10^9$	$4\cdot22 \times 10^9$
	45	$5\cdot02 \times 10^9$	$5\cdot35 \times 10^9$	$5\cdot69 \times 10^9$	$6\cdot01 \times 10^9$	$6\cdot22 \times 10^9$	$6\cdot35 \times 10^9$
	60	$5\cdot82 \times 10^9$	$6\cdot48 \times 10^9$	$7\cdot15 \times 10^9$	$7\cdot79 \times 10^9$	$8\cdot20 \times 10^9$	$8\cdot48 \times 10^9$
	90	$7\cdot40 \times 10^9$	$8\cdot70 \times 10^9$	$1\cdot01 \times 10^{10}$	$1\cdot14 \times 10^{10}$	$1\cdot22 \times 10^{10}$	$1\cdot27 \times 10^{10}$
	180	$1\cdot22 \times 10^{10}$	$1\cdot55 \times 10^{10}$	$1\cdot87 \times 10^{10}$	$2\cdot21 \times 10^{10}$	$2\cdot41 \times 10^{10}$	$2\cdot54 \times 10^{10}$
	300	$1\cdot85 \times 10^{10}$	$2\cdot45 \times 10^{10}$	$3\cdot04 \times 10^{10}$	$3\cdot63 \times 10^{10}$	$3\cdot99 \times 10^{10}$	$4\cdot21 \times 10^{10}$
	450	$2\cdot64 \times 10^{10}$	$3\cdot57 \times 10^{10}$	$4\cdot49 \times 10^{10}$	$5\cdot41 \times 10^{10}$	$5\cdot97 \times 10^{10}$	$6\cdot35 \times 10^{10}$
	600	$3\cdot44 \times 10^{10}$	$4\cdot70 \times 10^{10}$	$5\cdot95 \times 10^{10}$	$7\cdot19 \times 10^{10}$	$7\cdot95 \times 10^{10}$	$8\cdot40 \times 10^{10}$
	900	$5\cdot02 \times 10^{10}$	$6\cdot93 \times 10^{10}$	$8\cdot85 \times 10^{10}$	$1\cdot08 \times 10^{11}$	$1\cdot19 \times 10^{11}$	$1\cdot27 \times 10^{11}$
	1800	$9\cdot8 \times 10^{10}$	$1\cdot37 \times 10^{11}$	$1\cdot76 \times 10^{11}$	$2\cdot14 \times 10^{11}$	$2\cdot38 \times 10^{11}$	$2\cdot54 \times 10^{11}$
Ratio $O_2 : H_2O$ by volume which is constant throughout a range of $H_2O : H_2O + O_3$	45	$2\cdot64 \times 10^9$	$3\cdot57 \times 10^9$	$4\cdot50 \times 10^9$	$5\cdot43 \times 10^9$	$5\cdot98 \times 10^9$	$6\cdot35 \times 10^9$
	90	$2\cdot64 \times 10^9$	$5\cdot15 \times 10^9$	$7\cdot68 \times 10^9$	$1\cdot02 \times 10^{10}$	$1\cdot17 \times 10^{10}$	$1\cdot27 \times 10^{10}$
	300	$2\cdot64 \times 10^9$	$1\cdot26 \times 10^{10}$	$2\cdot25 \times 10^{10}$	$3\cdot24 \times 10^{10}$	$3\cdot81 \times 10^{10}$	$4\cdot21 \times 10^{10}$
	450	$2\cdot64 \times 10^9$	$1\cdot79 \times 10^{10}$	$3\cdot31 \times 10^{10}$	$4\cdot84 \times 10^{10}$	$5\cdot74 \times 10^{10}$	$6\cdot35 \times 10^{10}$
	900	$2\cdot64 \times 10^9$	$3\cdot37 \times 10^{10}$	$6\cdot48 \times 10^{10}$	$9\cdot51 \times 10^{10}$	$1\cdot15 \times 10^{11}$	$1\cdot27 \times 10^{11}$
	1800	$2\cdot64 \times 10^9$	$6\cdot54 \times 10^{10}$	$1\cdot28 \times 10^{11}$	$1\cdot89 \times 10^{11}$	$2\cdot29 \times 10^{11}$	$2\cdot54 \times 10^{11}$
Mean molecular mass "*M*" of $O_3 + H_2O$		48·00	33·88	26·18	21·32	19·20	18·00
No. of g.-mol. of O_2 whose absorption is equivalent to 1 g.-mol. of the mixtures of O_3 and H_2O. Absorption of O_2 equals $7\cdot93 \times 10^7$ c.g.s. per g. = $2\cdot53 \times 10^9$ per g.-mol.		49·7	26·4	13·6	5·54	2·00	0·19

Table I gives the value, in the outer regions of the atmosphere, of the absorption per gram of ozone and water vapour of different relative concentrations with varying amounts of oxygen present. In these regions the incident radiation from the sun, S_λ, has the unattenuated value obtained directly from the solar constant. The value of E_λ used in the table has been calculated for midwinter conditions at Sydney as described in § 3. The table also gives $\bar{A}$ for ozone and water vapour alone at midsummer. From this table may also be obtained the number of gram molecules of oxygen whose rate of absorption of the solar radiation is equal to that of 1 g.-mol. of the above mixtures of ozone and water vapour.

The equilibrium temperatures corresponding to the mixtures of gases shown in Table I can be obtained by comparing their absorption with the radiation given by the curves of fig. 1. This has been done for midwinter conditions and the result is presented in figs. 2 and 3.

The full and dotted lines in fig. 2 give the equilibrium temperatures for different volume ratios of oxygen to water vapour in the one case, and of oxygen to a mixture of water vapour and ozone in the other. The curve giving the equilibrium temperatures for night time, when the absorption by water vapour only need be considered, is indicated in the figure. The remaining curves are for day-time conditions.

The information regarding the day-time absorption and equilibrium temperatures contained in these tables and graphs, although estimated for the outer boundary of the atmosphere, will apply to a depth such that the absorption of the sun's radiation is negligible compared with its incident value.

The vertical extent of this region will depend upon the zenith distance of the sun—that is upon the time of day, season and latitude. It also depends upon the constitution of the atmosphere, but it appears from fig. 6, which is discussed later, that above 250 km. and for zenith distances less than about 80°, S_λ remains sensibly constant. The absorption and the equilibrium temperatures at any point within the "F" region of the ionosphere are consequently given by these tables and figures provided the restriction as to the zenith distance is satisfied.

It follows that at these levels the seasonal variation in the absorption and day-time equilibrium temperatures will be due almost entirely to the change in E_λ, provided that the composition of the atmosphere does not alter from summer to winter. It will be seen from the table that this change in absorption is small, so that the variation from winter to summer conditions produces an alteration of the equilibrium temperature of about 12° only. This amount may seem surprisingly small in view of the large seasonal changes of temperature at lower levels, but it must be borne in mind that the obliquity of the sun's rays does not affect the proportion of S_λ absorbed and that the value of S_λ itself is constant at these levels.

Our conclusions on this point are at variance with those of Appleton and Naismith (1935), who find that the midsummer noon temperature is at

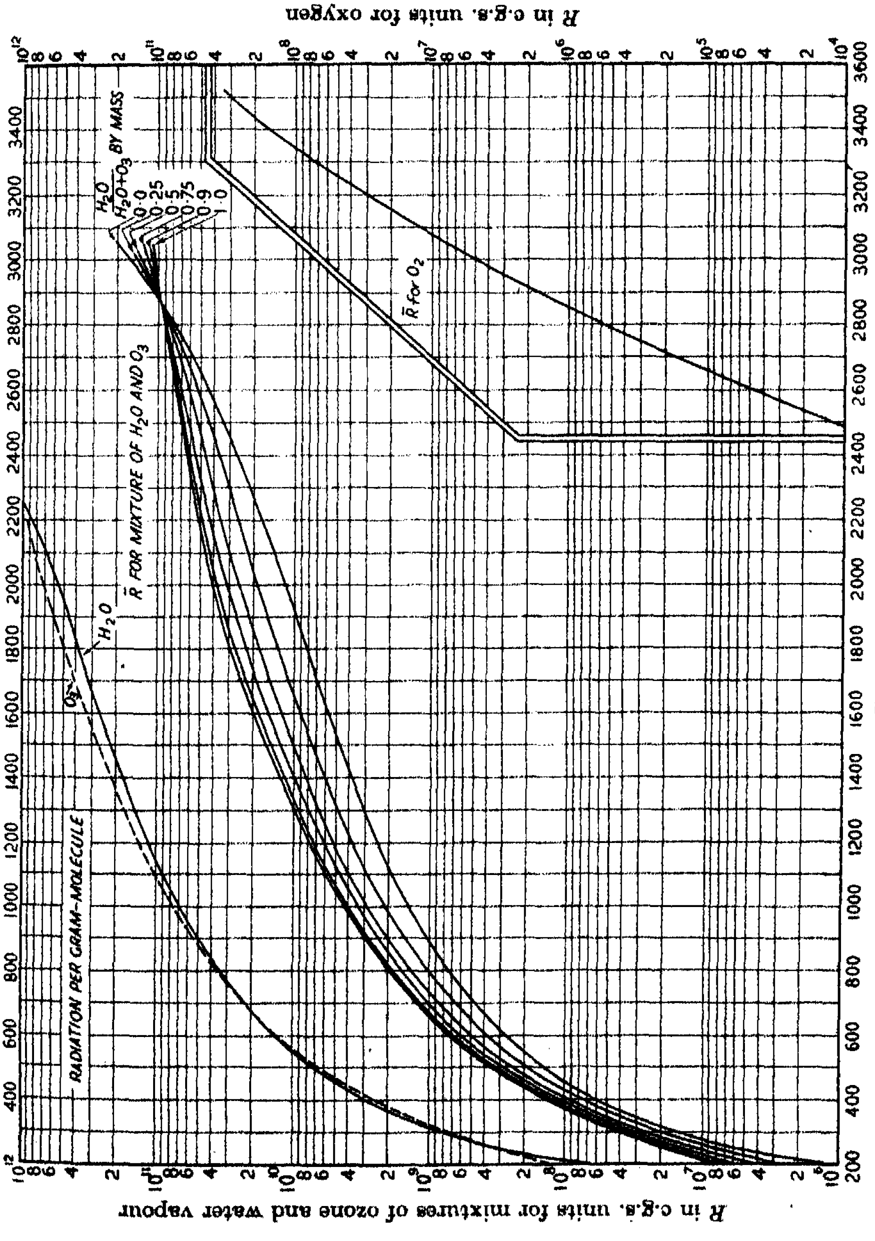

Fig. 1—Relation between $\bar{R}$ and temperature for several gases.

least four times that of midwinter noon; for, although, so far, we have discussed only equilibrium temperatures, yet it will be shown later that the noon temperatures at these heights, for the latitude considered by Appleton and Naismith, are within a few degrees of the actual temperatures.

TABLE II

Height above sea-level height in km.	Dissociation factor K	Mean molecular mass M	Winter temperature assigned to layer $T°$ K.	Total pressure P in cm. of Hg	Linear density of molecular oxygen g. km.	Calculated temperatures in degrees Kelvin			
						a	b	c	a_1
0	0	28·9	286	76·0	—	—	—	—	—
11	0	28·9	220	17·1	—	—	—	—	—
40	0	28·9	220	$1{\cdot}81 \times 10^{-1}$	—	—	—	—	—
60	0	28·9	450	$2{\cdot}36 \times 10^{-2}$	—	—	—	—	—
82	0	28·9	200	$1{\cdot}71 \times 10^{-3}$	$9{\cdot}25 \times 10^{-4}$	200 to 215	405	655	400
100	0	28·9	270	$1{\cdot}10 \times 10^{-4}$	$4{\cdot}40 \times 10^{-5}$				
105	0	28·9	310	$6{\cdot}05 \times 10^{-5}$	$2{\cdot}10 \times 10^{-5}$				
110	0	28·9	350	$3{\cdot}59 \times 10^{-5}$	$1{\cdot}11 \times 10^{-5}$	215	410	670	405
150	0·20	27·9	770	$2{\cdot}64 \times 10^{-6}$	$2{\cdot}85 \times 10^{-7}$	550	590	715	680
200	0·37	27·2	1150	$4{\cdot}85 \times 10^{-7}$	$1{\cdot}57 \times 10^{-8}$	1020	1030	985	1040
250	0·67	25·7	1300	$1{\cdot}39 \times 10^{-7}$	$3{\cdot}42 \times 10^{-9}$	1230	1230	1200	1240
285	0·67	25·7	1350	$6{\cdot}25 \times 10^{-8}$	$1{\cdot}47 \times 10^{-9}$	1350	1350	1350	1350
Time from which complete mixing occurs ...						4·0 p.m.	4·0 p.m.	4·35 p.m.	4·0 p.m.

$$\frac{\text{Total oxygen}}{\text{Air}} = 0{\cdot}232 \text{ by mass at all heights.}$$

We have attempted to present information regarding absorption and equilibrium temperatures for all concentrations of the absorbing constituents which might occur. Relative to water vapour the amounts by volume of oxygen range from 1800 to zero. It is considered that this gives the possible outside limits for the following reasons: Assuming saturation at the tropopause the ratio oxygen/water vapour there is about 2000, which gives approximately the upper limit assumed. The only factors tending to alter this ratio at higher levels for a given set of conditions at the tropopause are gravitational action and dissociation of the molecules. The action of the former, if mixing is incomplete, can only reduce this ratio. But as there is strong evidence in favour of mixing this reduction must be small. As regards the effect of dissociation there is spectroscopic evidence (Cabannes 1935) that the oxygen is partly in the atomic state at these heights. This would again reduce the proportion of molecular oxygen. It seems therefore that the upper limit has been taken sufficiently high.

On the other hand there is evidence of considerable supersaturation near the tropopause (Lepape and Colange 1935), so that taking this into account as well as the question of dissociation of the oxygen it has seemed necessary to discuss the case of relatively low concentrations of molecular oxygen.

The results are given for ozone mixed with water vapour in all proportions. This enables the required information to be obtained for any ratio of oxygen/ozone up to 1800, which we consider to be greater than is likely to occur.

The following facts are readily seen from the graphs: (1) The highest possible equilibrium day-time temperature is about 3300° K. and the actual equilibrium temperature may have any value between this and 230° K., the equilibrium temperature for water vapour alone; (2) for a concentration oxygen/water vapour having a value of about 1/60 the equilibrium temperature is about the same as that for ozone alone; (3) for concentrations oxygen/water vapour lying between 30 and 90, the presence of ozone does not affect the equilibrium temperature by more than 200° K.

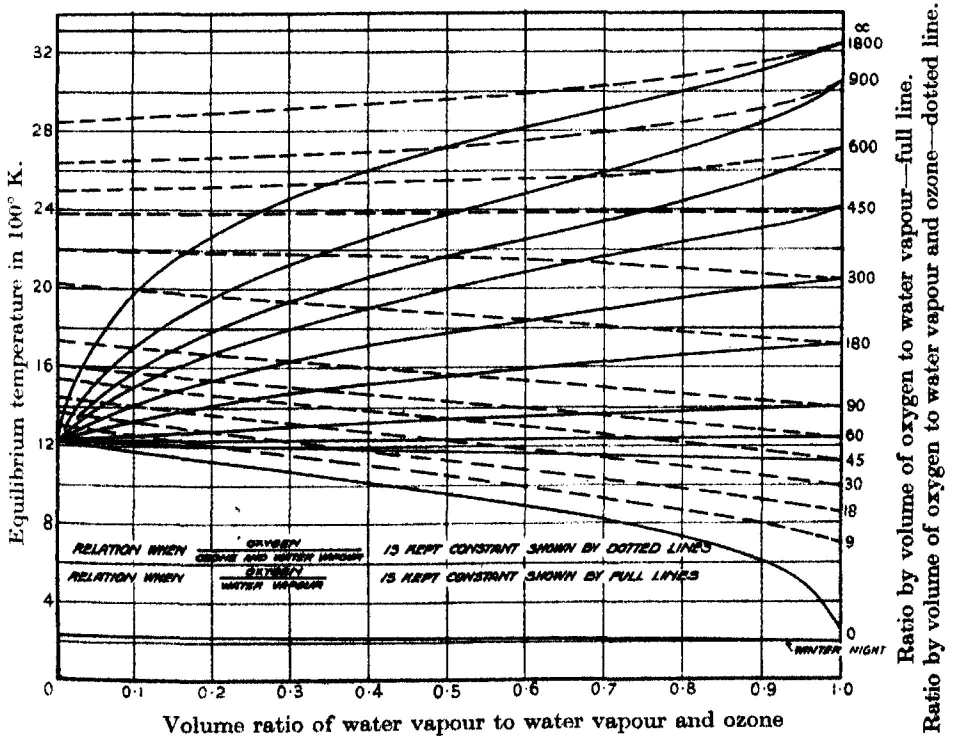

FIG. 2—Relation between winter day and night equilibrium temperatures and variations in the relative concentrations of oxygen, water vapour and ozone.

We proceed to discuss the significance of the equilibrium temperature. It is the temperature which would be ultimately reached by the layer under steady conditions of incident radiation and composition. Theoretically this temperature could not actually be attained except under ideal conditions of a convectionless atmosphere and in an infinite time.

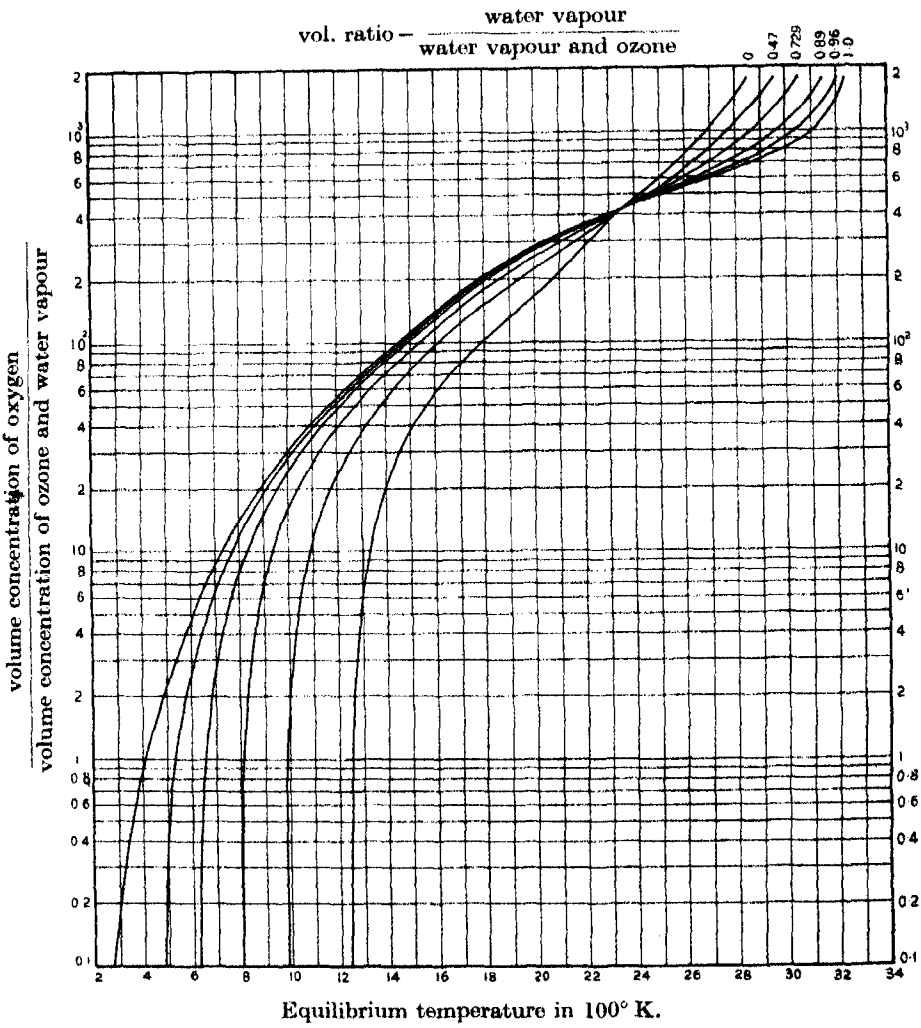

Fig. 3—Relation between winter day equilibrium temperatures and variations in the relative concentrations of oxygen, ozone and water vapour.

The temperatures given in figs. 2 and 3 are the highest which can exist under winter day-time conditions at the level considered and at the latitude of Sydney. For night-time conditions, on the other hand, they represent minimum values. In general, the effect of convection would be to lower the maximum and raise the minimum values in these regions. The results, although given for Sydney, apply almost exactly for other localities provided the sun's zenith distance does not exceed about 90°. Such small variations as occur are due to small changes in E_λ with latitude and to the slight effect of the obliquity of the sun's rays on S_λ.

The results given in figs. 2 and 3 in terms of the proportion of oxygen to mixture apply directly only to levels such as the F region where the energy received from the sun is undiminished. Interest attaches however to temperatures at lower levels, where the value of S_λ has been reduced through absorption by the oxygen above. The graphs and tables can be applied to these cases, for temperatures less than 2500° K., by replacing the actual concentration of oxygen at the point considered by an equivalent value. This is possible because at these temperatures the re-radiation by oxygen may be neglected as compared with its absorption. Thus if the ratio actual absorption of solar radiation/A is p and the actual concentration of molecular oxygen is C_m''', then the equivalent concentration of oxygen for the purpose of applying the graph is pC_m'''.

The value of the factor p depends on the mass of gas m in the oblique column of sectional area 1 sq. cm. through which the radiation has passed before reaching the layer and this dependence has been presented in fig. 4, where the quantity m is obtained from the abscissae of the graph on multiplying by the appropriate density. The value of m itself depends in turn on the obliquity of the incident radiation from the sun and the distribution of the absorbent material. Its value is given by

$$m = \int_0^\infty \frac{PM}{RT}\frac{dz}{dh}(1-k)\,C_m'''\,dh, \tag{2}$$

where k is the ratio of dissociated to total oxygen present at any point, R the universal gas constant, T the temperature, P the pressure of the mixture of all the gases, z and h the oblique and vertical distances traversed, M the mean molecular mass of the mixture, and C_m''' the mass concentration of oxygen, that is, the ratio of the total mass of oxygen (atomic and molecular) to the total mass of all the gases. The quantities h and z are related by the equation

$$\frac{dz}{dh} = \frac{r+h}{z+r\cos\chi} = \frac{r+h}{\sqrt{\{r^2\cos^2\chi + h(2r+h)\}}},$$

where r is the distance of the centre of the earth from the point considered and χ the sun's zenith distance.

An application of equation (2) to a particular case is discussed in § 6.

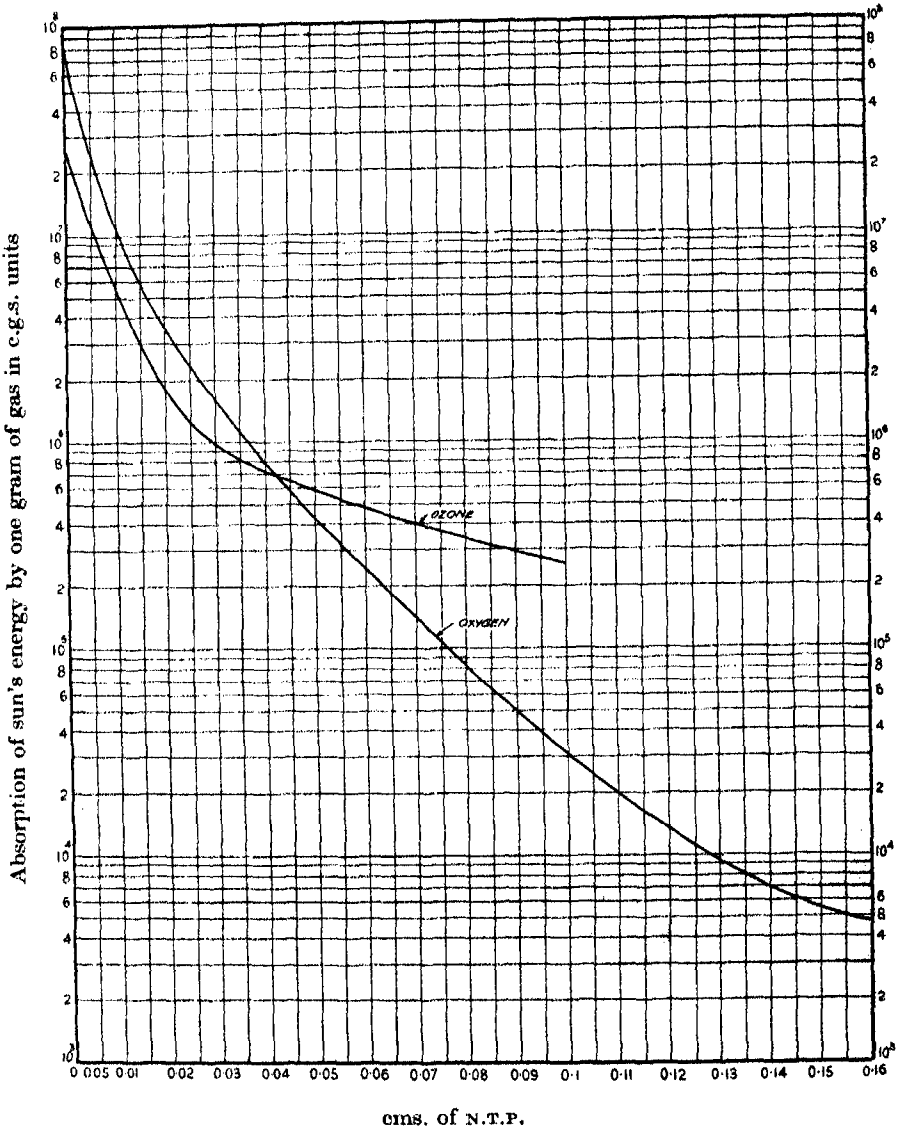

Fig. 4—Absorption of solar energy at various depths in the atmosphere.

5—Rates of Heating and Cooling

As mentioned above, the equilibrium temperatures can, theoretically, be reached only after an infinite time. We now consider how closely these temperatures are approached in the time available.

The rate of change of temperature depends upon the nett rate at which energy is gained or lost by the material present at the point. The relevant equation may be expressed in the form

$$\frac{dT}{\bar{A}-\bar{R}+\bar{B}}=\frac{dt}{K_\rho/M},$$

where M is the mean molecular mass of the whole mixture, T and t are the temperature and time respectively and $\bar{A}$ and $\bar{R}$ have the meanings given before. $\bar{B}$ is the rate of gain of heat per gram of material at the point, due to causes other than the radiation processes (e.g. convection or conduction). K_ρ is the specific heat at constant pressure in ergs per gram molecule of the mixture of gases which constitute the atmosphere at the point considered.

It is convenient to write the above equation in the form

$$\int_{T_1}^{T_2}\frac{dT}{\frac{M_R}{d_R}(\bar{A}-\bar{R}+\bar{B})d}=\int_{t_1}^{t_2}\frac{C_v\,dt}{K_\rho}=\frac{C_v(t_2-t_1)}{K_\rho}, \tag{3}$$

where M_R and d_R are the mean molecular mass and density respectively of the material that contributes to the radiation, C_v is the volume concentration of the same substances, and K_ρ and C_v are assumed to be independent of t. We shall consider the solution of this equation for the case where $\bar{B}$ is neglected. Using the data presented in the previous graphs, the integral on the left side of this equation has been graphically integrated and the results for different ranges of temperature are shown in figs. 5*a*, 5*b*, 5*c*. These sets of curves refer to mixtures of oxygen in varying proportions by volume with (*a*) water vapour, (*b*) water vapour and ozone in the ratio of 8/1 by volume, and (*c*) ozone alone. In each set the curves which have the same proportion of oxygen differ little from each other at temperatures below about 2800° K., and for this reason it is unnecessary to consider other proportions of water vapour to ozone.

As pointed out in § 4, these ratios can be extended to apply as equivalent values when appreciable absorption occurs above the layer considered. The quantity C_v on the right side of equation (3) refers in all cases to the actual concentrations existing at the point considered.

All the curves are asymptotic to the ordinates which represent the equilibrium temperatures for the mixtures considered. It will be noticed

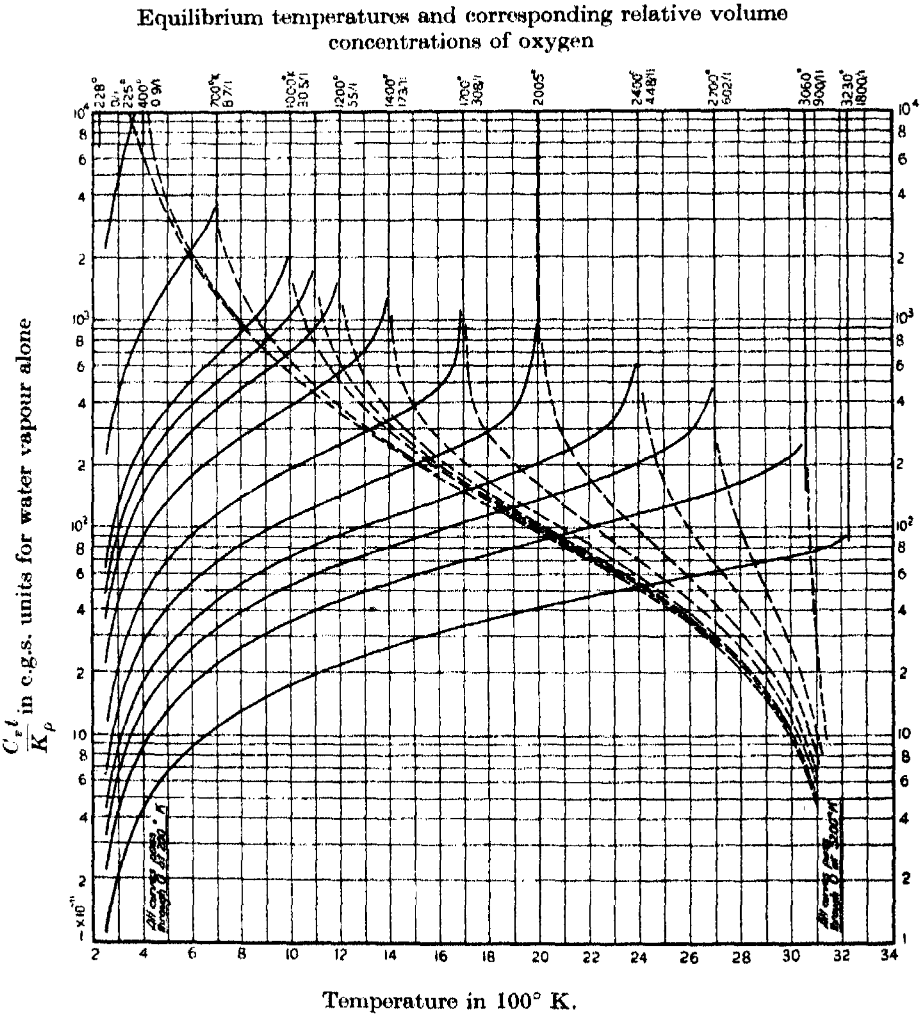

Fig. 5a—Relation between $\frac{C_v t}{K_p}$ and temperature for mixtures of oxygen and water vapour when rate of absorption varies so as to give different equilibrium temperatures.

that the actual temperatures approach to within a few degrees of the limiting values in a time short compared with that during which the region is exposed to solar radiation.

In using the cooling and heating diagrams, the equilibrium temperature for the given conditions of incident radiation and concentration of gases is

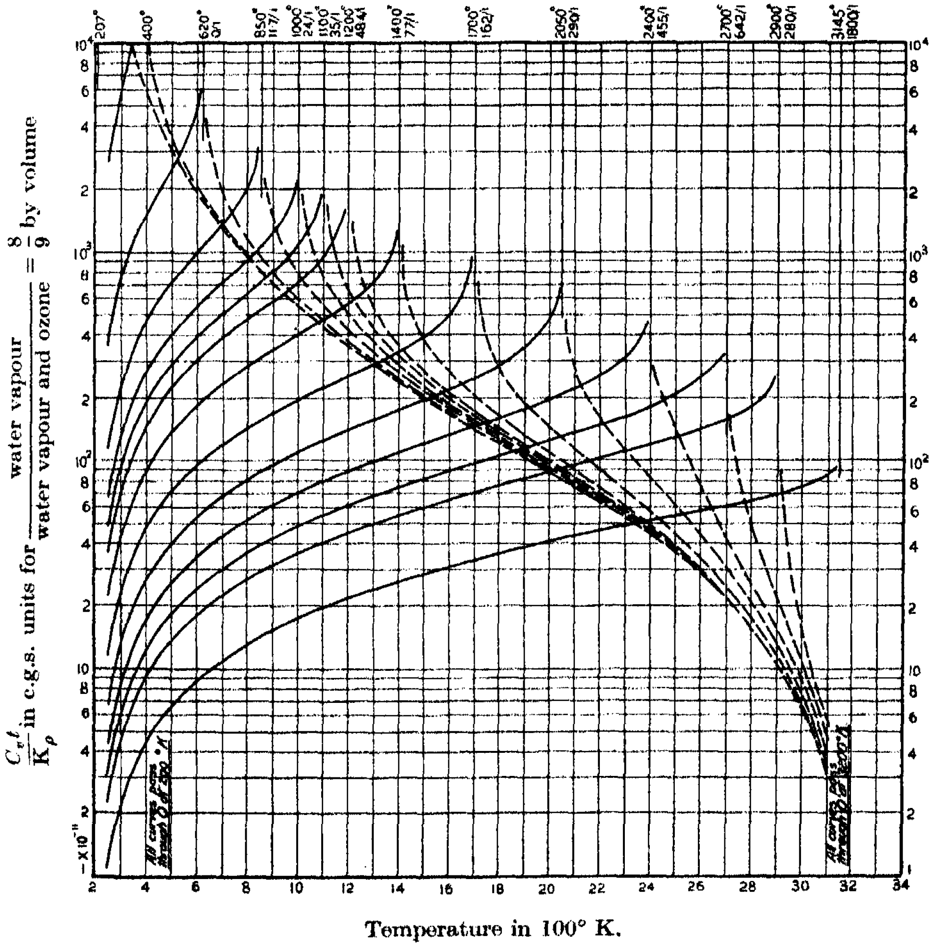
Equilibrium temperatures and corresponding relative volume concentrations of oxygen

FIG. 5*b*—Relation between $\frac{C_v t}{K_p}$ and temperature for mixtures of oxygen, water vapour and ozone when rate of absorption varies so as to give different equilibrium temperatures.

first ascertained from figs. 2 or 3. The changes in temperature for a given value of $C_v t$ are then found by inspecting the curve which is asymptotic to this temperature ordinate and which refers to the appropriate ratio ozone/water vapour. If the conditions which determine the equilibrium temperature are not steady but are changing in a known manner with time, approximate values of the temperature changes can be found by successive inspection of the changing curves.

Equilibrium temperatures and corresponding relative volume concentrations of oxygen

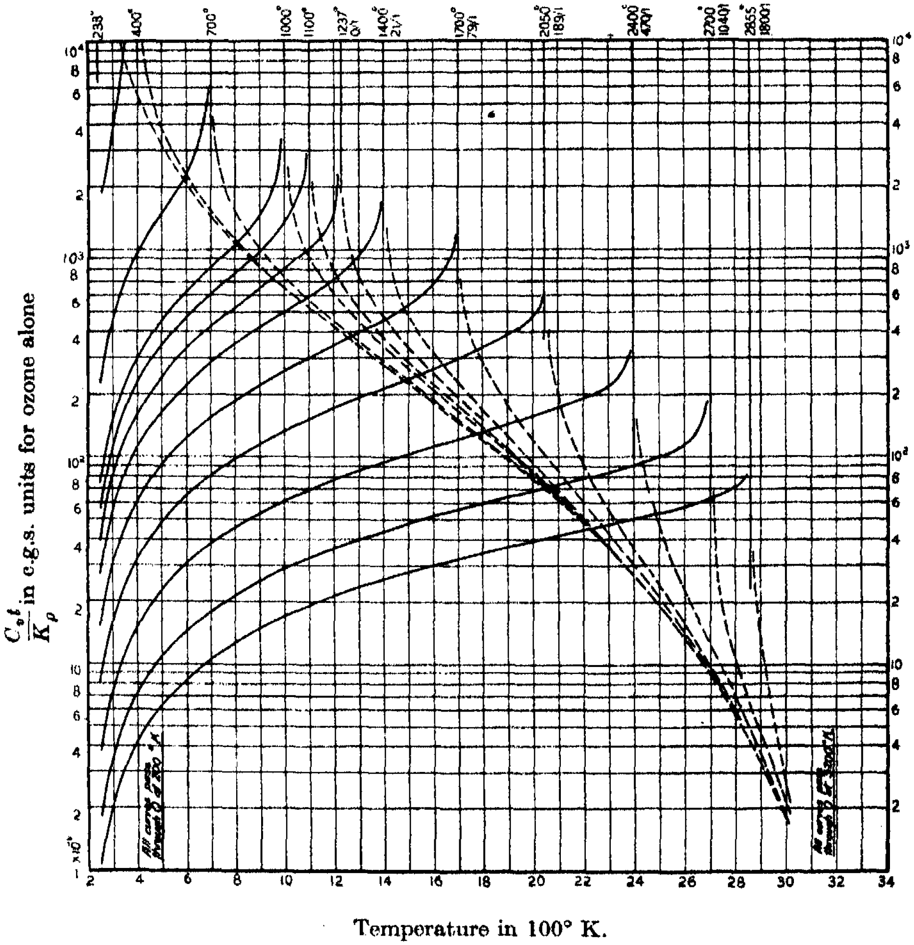

FIG. 5c—Relation between $\frac{C_v t}{K_p}$ and temperature for mixtures of oxygen and ozone when rate of absorption varies so as to give different equilibrium temperatures.

Recently Penndorf (1936) has calculated the rate of change of temperature in the main ozone layer below 50 km. to be 0·03 °C. per day. This estimate is much smaller than that indicated by Gowan's work (*vide* above reference to Penndorf for discussion by Dobson and Gowan). It may safely be assumed that at 50 km. S_λ is undiminished in the spectral region absorbed by ozone so long as the solar zenith angle does not exceed 90°. From Table I it follows that the noon rate of absorption is $2{\cdot}64 \times 10^9$ c.g.s. units/g. For an ozone concentration of $2/10^6$ by volume, the rate at which the temperature must rise is 3° C./hr. It appears therefore that our work offers considerable support for Dobson and Gowan's criticism of Penndorf's calculated figure.

6—STUDY OF A PARTICULAR CASE

In illustration of the above principles a particular case has been analysed, assuming the following conditions, which are suggested by the work of Martyn and Pulley (1936, pp. 461, 463, 464).

(*a*) Between the earth and the 105 km. level the pressure falls off by a factor of 10^6, while between the 100 km. and 285 km. levels, the corresponding factor during the night up to 1 a.m. is 2000.

(*b*) Between 1 a.m. and 3.30 a.m. the temperatures above the 100 km. level change by 30 %.

(*c*) The atmospheric gases are everywhere thoroughly mixed and the mass ratio oxygen (molecular and atomic together)/nitrogen does not alter with time. This restriction is not placed upon water vapour or ozone.

With these conditions assumed we now assign a temperature distribution at 1 a.m. and a degree of dissociation of oxygen (cf. Cabannes 1935) as shown in columns 4 and 2 of Table II. In this table the values of the temperatures up to the 110 km. level are in the main in accord with the findings of Martyn and Pulley (1936, p. 482). The principal difference is that at the 82 km. level, where these authors find a temperature minimum at 160° K., we have assumed a temperature minimum of 200° K. This is the equilibrium temperature corresponding to night-time conditions for water vapour alone and the actual temperature cannot be lower than this value.

From the assigned temperatures the pressures at the different heights have been calculated and the results compared with Martyn and Pulley's results.

The values shown in column 5 are seen to be in fair agreement with the results of these authors. Examining the case from the point of view of the cooling curves, it will be seen that the assumed drop in temperature from

1350 to 945° K. in 2½ hr. at the 285 km. level could be obtained with the following mixtures:

(1) Water vapour to air, 1/8900 by volume; or its equivalent, water vapour to oxygen, 1/543.

(2) Water vapour to ozone to air, 0·89/0·11/8500; or water vapour to ozone to oxygen, 0·89/0·11/450.

(3) Ozone to air, 1/7350; or ozone to oxygen, 1/450.

The day-time equilibrium temperatures corresponding to (1) and (2) are 2600 and 2525° K. If heating and cooling takes place uncomplicated by convection, then these temperatures would be reached in from 2½ to 3 hr. after sunrise and would be maintained almost until sunset, after which they would fall—at first rapidly. By 1 a.m. the air would have cooled to about 200° K. But Martyn and Pulley find that from sunset to 1 a.m. there is very little change in temperature, and at the latter hour the temperature is found to be 1350° K. There must therefore be some process which temporarily keeps the temperature nearly steady at this value, which is so much lower than is to be expected at sunset on the simple theory, and so much higher than the value which would exist at 1 a.m. Martyn and Pulley suggest that this process might be a large-scale convection bringing in warm air from the region heated in the day-time.

The temperature cannot, of course, be accurately constant during the early part of the night, but some idea of the effect of convection may be obtained by assuming it to maintain a constant temperature for some period prior to 1 a.m. This period must begin earlier than sunset, and the time of its commencement is shown in Table II for the different cases. In order to calculate this time of commencement, the total heat absorbed during the period has been equated to the total heat radiated at 1350° K. The total of absorption referred to is calculated for oxygen by the aid of fig. 6, which gives the value of the absorption by oxygen (relative to its maximum value) at different times after 12 noon. In the case of ozone it is assumed that the absorption is steady until sunset when it cuts off completely. Fig. 6 only applies to the distribution of temperatures and material referred to in this particular case.

If the assumption is made that the time so calculated is the same for the lower regions down to 80 km. (and this parallelism though arbitrary will probably be a fair approximation to the facts), then the temperature at 1 a.m. can be calculated for this level with the aid of fig. 6 by a process similar to that already described. These temperatures are shown in columns 7–10 of Table II, for the different concentrations mentioned before. A fourth case is given in column 10, for conditions in which water vapour and ozone are present in the day time in the proportions of 8/1 by volume, the ozone disappearing at night.

It will be seen that the agreement with the original temperatures assumed is reasonable down to the 150 km. level. This agreement holds irrespective of the ratio of ozone to water vapour. Between 80 and 110 km., when ozone is present in the amounts selected, the temperatures are always higher than those assumed and it is impossible to reach so low a temperature as 200° K. Between 150 and 110 km., when water vapour alone is present, the temperatures fall much more steeply than those assumed, but a smaller temperature gradient would not be inconsistent with the presence of water vapour as in case (1) if vertical convection be allowed.

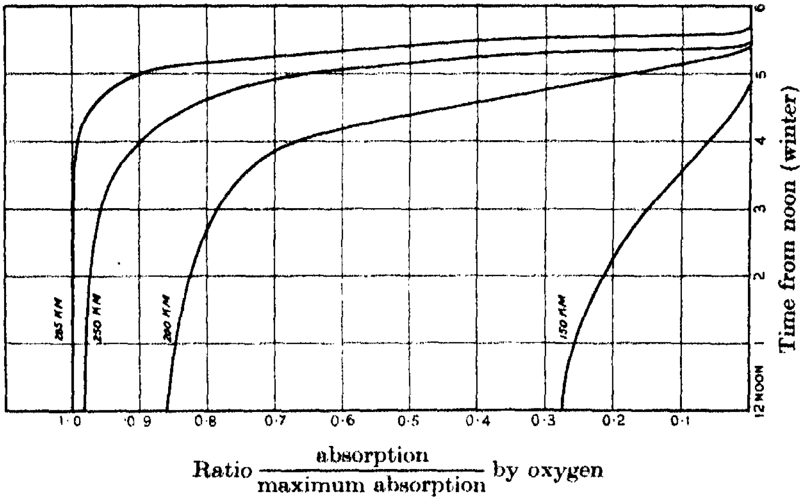

Fig. 6

7—Conclusions

In the light of present knowledge regarding the coefficients of absorption of the constituents of the atmosphere, it is found that a temperature higher than 3300° K. can not be attained in the atmosphere for any distribution or concentration of the constituents. A temperature as low as 200° K., however, can be reached at night-time in most latitudes.

All values of the temperature between these two limits are possible and the graphs and tables provided give a means of estimating the actual temperature at any point, and the time at which it occurs, when the conditions are known.

If a temperature of the order of 1200° K. exists in the *F* region as is suggested by Martyn and Pulley, and if the absorption is entirely due to ozone and water vapour, then the concentration of the latter must be small compared to the former (see fig. 2). The fact that this temperature appears to be maintained until 1 a.m. and falls rapidly thereafter is most satisfactorily explained as being due to convection coupled with the existence of considerably higher temperatures in the day-time. Such higher temperatures would not be possible if ozone and water vapour were the only absorbing agents.

On the other hand, these temperatures can be attained with any relative proportion of ozone and water vapour, and in fact without the presence of ozone, provided oxygen is present in the necessary proportion. The variations in temperature from night to night that seem to be indicated by the changes in ionization density in the *F* layer, and in the height of the layer itself, could be accounted for by changes in the quantity of water vapour present.

The authors desire to thank Dr. D. F. Martyn of the Radio Research Board of the Commonwealth Council for Scientific and Industrial Research for suggesting the investigation and for much helpful criticism during its progress.

They also wish to acknowledge the stimulating interest and advice of Dr. J. P. V. Madsen, Professor of Electrical Engineering, and Professor O. U. Vonwiller of the Physics Department, University of Sydney.

The work is published by permission of the Superintendent of Technical Education, Sydney.

SUMMARY

The conditions for radiative equilibrium in the atmosphere above the 100 km. level are examined, taking into consideration the absorbing properties of ozone, water vapour and molecular oxygen. Graphs are provided giving the equilibrium temperatures for different concentrations of these substances extending over a wide range. The investigations are primarily for the latitude of Sydney but changes of latitude within certain limits do not materially affect the results. Midwinter conditions are assumed, but here again seasonal changes are found to have negligible effects (except as they may affect the relative concentrations of the absorbing substances).

It is found that the existence of high temperatures, of the order 1000° C. or more, in the *F* region of the ionosphere, is a necessary consequence of the

presence of appreciable oxygen at these levels. Seasonal variations of these temperatures must be small, however.

The approach to equilibrium conditions in the time available is considered, and curves are given from which may be obtained the rates of cooling at night and of heating by day. An investigation is made of the discrepancy between the results of Penndorf and of Gowan on the rate of heating due to ozone at 50 km. The result obtained supports Gowan's estimates.

A case is analysed assuming the distributions of temperature and pressure suggested by Martyn and Pulley and an estimate is made of the effect of the convection which seems to be indicated by these authors' results.

REFERENCES

Abbot, C. G. 1913 *Ann. Astrophys. Obs. Smithson Inst.* **3**, 194–202.
Appleton, E. V. and Naismith, R. 1935 *Proc. Roy. Soc.* A, **150**, 685–708.
Cabannes, J. 1935 *C.R. Acad. Sci., Paris*, **200**, 1905–8.
Chapman, S. 1934 *Quart. J. R. Met. Soc.* **60**, 127–42.
Colange, G. 1927 *J. Phys. Radium*, **8**, 254–6.
Fabry, C. and Buisson, H. 1913 *J. Phys. Radium*, **5**, 196–206.
— — 1921 *J. Phys. Radium*, **21**, 197–226.
Hettner, G. 1918 *Ann. Phys., Lpz.*, **55**, 476–96.
Ladenburg, E. and Lehmann, E. 1906 *Ann. Phys., Lpz.*, **21**, 305–18.
Ladenburg, R. and Van Voorhis, C. C. 1933 *Phys. Rev.* **43**, 315–21.
Lepape, A. and Colange, G. 1935 *C.R. Acad. Sci., Paris*, **200**, 1340–2.
Martyn, D. F. 1935 *Proc. Phys. Soc.* **47**, 323–39.
Martyn, D. F. and Pulley, O. O. 1936 *Proc. Roy. Soc.* A, **154**, 455–86.
Penndorf, R. 1936 *Quart. J. R. Met. Soc.* Suppt. to vol. **62**, Atmospheric Ozone, Oxford Conference Papers, pp. 37–40.
Simpson, G. C. 1928 *Mem. R. Met. Soc.* **2**, 69–95.

The Size-Grading of Sand by Wind

By R. A. Bagnold

(*Communicated by G. I. Taylor, F.R.S.—Received* 17 *June* 1937)

In the course of experiments on the changes which take place in the size-grading of the grains when sands are picked up, transported and redeposited by a wind, it was found that by plotting the proportional weights of the constituent sieve-separated grades on a log scale, important changes can be observed in the character of the grading which are imperceptible when the usual grading diagram is used. Let the abscissa of the usual diagram be $R = \log$ diameter, so that δR is the log ratio between successive sieve apertures. If δp is the weight of a grade (total weight of sample unity), then the ordinate $\phi = \frac{\delta p}{\delta R}$. With an infinite number of sieves $\phi = \frac{dp}{dR}$. The whole area included under the diagram is $\int \phi \, dR = 1$.

1—The Grading Diagram

Fig. 1*a* shows the grading curve of a sample of dune sand, together with a suitably chosen "normal probability curve" $\phi' = \frac{a}{\sqrt{\pi}} e^{-a^2(R-R_0)^2}$, where R_0 is log (most frequent diameter). Though comparison is difficult owing to the low values of the ordinates representing the extreme grades, it is sometimes assumed that the grain-size distribution may be a random effect.

In fig. 1*b* the same two curves are plotted with $y = \log_{10}\phi$ as ordinate. The probability curve becomes a parabola

$$y' = \log_e \phi' = -a^2(R-R_0)^2 + \log B,$$

while in the case of the actual sand sample the curve is seen to depart very considerably from the parabolic probability form. The curves given by the analyses of a number of sand samples, when plotted in the manner of fig. 1*b*, suggested to me that the extreme grades tended to die away in proportional weight exponentially on each side of the mean diameter. Though I can find no theoretical reason why this should be so, as an approximate assumption it provides a useful method of specifying the grading of a sand by three quantities, the mean diameter, and two coefficients defining the slopes of the straight lines of fig. 1*b*. Sands in which the grading can be specified in this way I will call "regular sands".

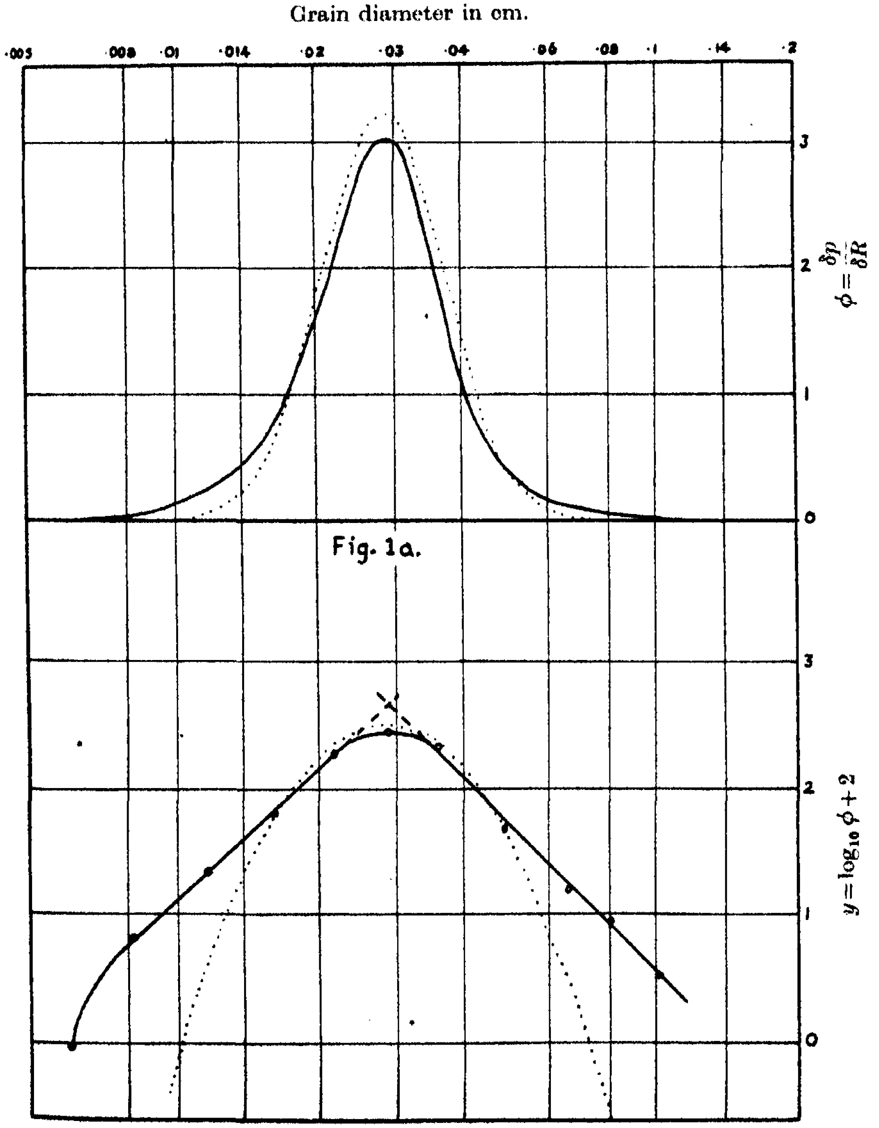

Fig. 1b.

Fig. 1—Comparison of sand-grading curve (heavy line) with probability curve (dotted). *a*, ordinates on usual linear scale; *b*, ordinates on log scale.

2—METHOD OF GRAIN-SIZE ANALYSIS

It was important that as many points as possible should be obtained on each side of every experimental grading curve. This meant very accurate estimation of the relative size limits used in the analyses. It is well known that the same analysis results are not obtained with sieves which, though they have the same apparent aperture, are made with a slightly different combination of mesh and wire gauge. A correction is necessary.

This correction was made as follows: A number of sand samples were obtained which gave, when analysed by the set of sieves in use, grading curves of more or less "regular" shape, but for which the position of the peak varied considerably along the scale of size. Now since the ordinate ϕ of the ϕ-R diagram is the quotient of the original weight divided by the log ratio of the limiting apertures, an error in estimating one of these apertures would cause a corresponding error in ϕ. It would also cause an error in the opposite sense in the ϕ of the next grade. The result would be a kink in the final grading curve.

Such a kink might, however, arise from a real irregularity in the sand grading. But if the kink occurs in a series of samples at the same grain size but in relatively different positions on the curves—e.g. on the left-hand slope of one and the right-hand slope of another—it is clearly due to an error in the size of the sieve. Further, if a slight adjustment can be made which causes the kink to disappear simultaneously in all positions on the curves, that adjustment is legitimate. Of the thirteen sieves used to cover the range of sand grain sizes such adjustment was found necessary in three cases.

3—THE CYCLE OF SAND MOVEMENT

At a certain wind strength sand grains begin to move at some point on the exposed surface. The motion continues down wind, and the mass of sand passing an observer in unit time increases as the observer moves down wind, till, for a homogeneous sand surface under a steady wind, it reaches a steady equilibrium value. This equilibrium sand flow proceeds on until some change in the conditions causes deposition to occur. There is in general therefore a limited length of surface up wind where sand removal takes place, followed by a length in which sand is neither removed nor deposited, followed again by a length where deposition occurs.

Sand Removal—The threshold wind required to start the removal depends on the diameter of the grains which cover and protect the surface. If the wind is feeble a removal takes place of the finer grades exposed on the surface, but the movement ceases when the surface becomes stabilized by the protection afforded by exposure of sufficient large grains on the surface. This limited removal clearly continues locally for a longer time if the large grains are relatively few.

If the wind is strong enough to move the largest grains, then removal proceeds indefinitely. In this case sand is ultimately removed in the same grading proportions as those of the underlying bed. Since large grains can be rolled along the surface by the bombardment of far smaller ones even by a gentle wind, removal also takes place indefinitely if the oncoming wind is carrying a little fine sand removed from elsewhere up wind. There is a distinction, affecting the grading of the removed sand, between sand removal by direct pick-up and removal stimulated by the bombardment of oncoming grains.

Transportation—The mass flow of removed sand consists (*a*) of a small proportion of very fine grains in true suspension; (*b*) of grains in saltation over the surface; (*c*) of the surface creep of grains rolled or impelled along the surface by the forward impact of grains descending from the saltation. Owing to a continuous interchange of grains between the saltation and the surface creep a rigorous distinction is impossible. In my experiments I define the surface creep as consisting of grains of such low velocity that they tumble over into a narrow transverse slot (fig. 2 inset) if such is cut in the

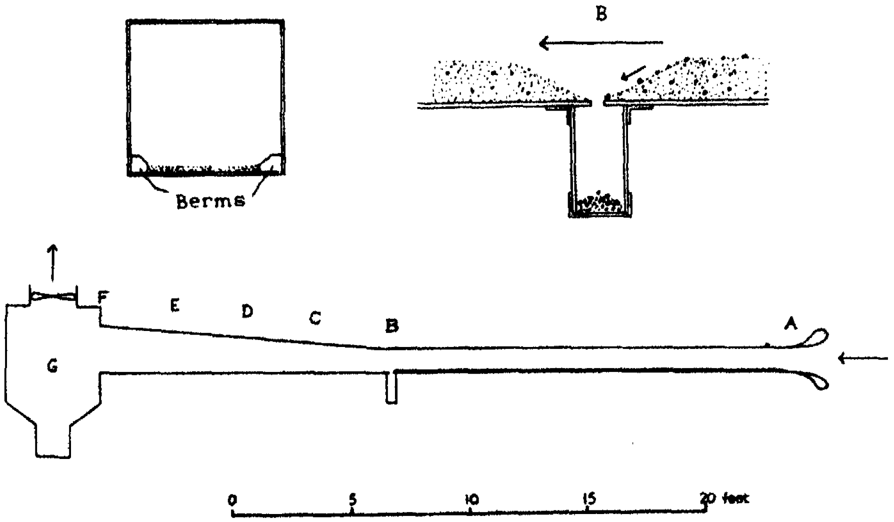

FIG. 2—General arrangement of apparatus.

floor beneath the sand bed. The rate of flow of the surface creep is of the order of 25 % of the total flow.

The surface creep consists of a large mass of sand (per unit area of surface) moving very slowly, whereas the saltation, carrying the bulk of the flow, consists of a relatively small mass moving at a speed of the order of half that of the wind. Hence in their journey down wind the grains in surface creep lag far behind those in saltation. It is doubtful, therefore, whether even over a continuous homogeneous sand bed a true homogeneous condition of sand flow can ever ensue over a considerable length of path. Wherever saltation occurs there is a complementary surface creep of relatively larger grains, and so the surface sand, except where deposition is taking place, tends to become coarser than that immediately beneath.

Deposition—There appear to be three ways by which grains reach their final resting places in a sand deposit. (*a*) True sedimentation, in which grains falling through slowly moving air strike the surface with insufficient forward velocity either to be carried on again or to jerk other surface grains forward. In the case of the very fine grains carried in true suspension this is probably the only method of deposition possible. (*b*) Accretion. The grains in saltation in a diminished wind may strike the surface with sufficient velocity to jerk other grains forward and so to contribute to a diminished surface creep, but some of the impacting grains may themselves come to rest in the process. Here the deposit is built up from the surface creep and from the saltation simultaneously. (*c*) Encroachment. If the surface is not continuous but contains an obstruction of any sort, e.g. an abrupt step up or down, the surface creep is held up while the saltation passes on. The resulting deposit, which need not require any diminution in the wind for its occurrence, consists only of the surface creep. In the case of a steep slope down, such as the slip-face of a dune, the surface grains roll over the crest of it and come to rest because they become sheltered from the impelling bombardment of the saltation. The slope encroaches down wind forming a relatively coarse deposit.

4—Experiments and Notation used to Express Results

Experiments were designed to find out by imitating the foregoing natural cycle of sand movement under controlled conditions (*a*) the changes which take place in the slopes of the asymptotes of "regular" sands and in the position of the peaks; and (*b*) how a sand of haphazard grading is transformed into a regular sand.

The wind tunnel used has already been described (Bagnold 1936). Deposition was brought about by inserting an expansion section at the down wind end to check the velocity of the air stream. The arrangement is shown in fig. 2. The sand bed was laid in the parallel tunnel *AB*. A transverse slot 2 cm. long and 0·5 cm. wide was cut in the centre of the floor at *B*, through which a sample of the surface creep could fall into a container. The sand removed by the wind from *AB* was deposited between *B* and *F*. Removal close to *A* could be stimulated by introducing a trickle of sand at *A*.

Difficulty was encountered owing to a tendency for the finer grains to separate out sideways and to collect in the zones of slow-moving air along the tunnel walls. This was reduced partially by adding smooth wood berms at each side as shown inset in fig. 2. The surface of the berm being free from the drag of the sand movement, the wind at the edge of the sand layer could, by a suitable adjustment of the width of the berms, be made as stong as that over the central sand portion of the floor.

Observations were made on (*a*) composition of the original bed sand; (*b*) composition of surface creep trapped at *B*; (*c*) relative weights and compositions of the deposits collected from *BC*, *CD*, *DE*, *EF* and of any carry-over found in the box *G*.

Results will be shown in diagrams of the form of fig. 1*b*, and the following terms will be used.

The "Carrier Grade" is the sand of grain diameters lying between the size limits bounding the rounded portion of the curve. It forms the bulk of the saltation and is the driving agent which impels the larger grains along the surface.

The "Peak Size" R_0 is defined by the intersection of the two asymptotes. The "Peak Height" $y_0 = \log_{10}\phi_0$ is the height of the intersection.

The "Small Grade Coefficient" s is the slope of the left-hand asymptote representing the grading of grains finer than the carrier grade. The "Coarse Grade Coefficient" c similarly refers to the right-hand side:

$$\frac{dy}{dR} = s,$$

$$y = \log_{10}\phi = \int s\,.\,dR + y_0 = s(R-R_0)+y_0$$

$$\phi = \phi_0 e^{2\cdot 3s(R-R_0)}, \quad \text{left-hand side,}$$

similarly

$$\phi = \phi_0 e^{2\cdot 3c(R-R_0)}, \quad \text{right-hand side.}$$

Some sand samples are composed of a number of constituent sands each having a different grading. If the area $\int \phi\, dR$ of the whole curve plotted as in fig. 1*a* is unity for a sample of unit weight, the grading of any constituent is shown comparatively by reducing all its ordinates ϕ by a constant f representing the ratio of the weight of the constituent to that of the whole. On the log scale of fig. 1*b* the constituent is represented by a curve lowered bodily through a distance $\log f$.

The "width of a sand" is defined by the expression $1/s + 1/c$ which is the length of the base of the triangle cut off by any abscissa divided by the height.

5—Results

(*a*) *Regular Sands*

In fig. 3*a* the heavy curve shows the grading of a wide sand compiled artificially from a stock range of separate grades. The grading coefficients s and c are 1·9 and 3·0 respectively. The peak size is 0·034 cm. The irregularity in the two finest grades was made accidentally during the mixing. It was purposely left uncorrected.

The thin continuous curves represent the grading of the constituent deposits collected in the sections *CD*, *DE*, *EF* of the expansion tunnel and that carried over into the box *G*. Each has been reduced in scale according to the relative weight of the deposit to the total weight collected. The deposit in *BC* was inseparable from the surface creep which accumulated there. It is omitted from fig. 3*a* for clearness.

It will be seen that the slopes of the deposit curves become steeper and that the peak size falls as the wind slackens, but that in spite of this the grading coefficients, though larger than those of the original sand, are both nearly constant throughout the deposition ($s_{\text{dep}} = 2\cdot 5$, $c_{\text{dep}} = 9$). Since, outside the limits of the carrier grade, any ordinate $\phi_R = \phi_0 e^{2\cdot 3s(R-R_0)}$, the sum of all ordinates ϕ_R of a set of deposits 1, 2, 3, etc. themselves lie on an exponential curve

$$(\phi_1 + \phi_2 + \phi_3 + \text{ etc.}) = e^{2\cdot 3sR}(\phi_{0_1} e^{-sR_{0_1}} + \phi_{0_2} e^{-sR_{0_2}} + \phi_{0_3} e^{-sR_{0_3}} + \text{ etc.}).$$

If, therefore, ${}_s\Phi_c$ represents the composition of unit mass of a regular sand with grading coefficients s and c, any group of regular sands of varying peak size but with constant grading coefficients can be mixed together in proportions A, B, C, etc., to form another regular sand

$$\Sigma\, {}_s\Phi_c = {}_s\Phi_c(A + B + C + \text{ etc.}).$$

The line *MN* joining the peaks of the four fractional deposits is approximately straight. Its slope $T = \dfrac{dY_0}{dR_0}$ is a measure of the rate of change of relative mass deposited at any place with the peak grain size at that place. $1/T$ may be called the "separation" caused by the process. Its value is here 0·11. It is remarkably small; only 1·55 % of the deposit had so far separated out that its peak size had shifted from 0·034 cm. for the original mixture to 0·029 cm.

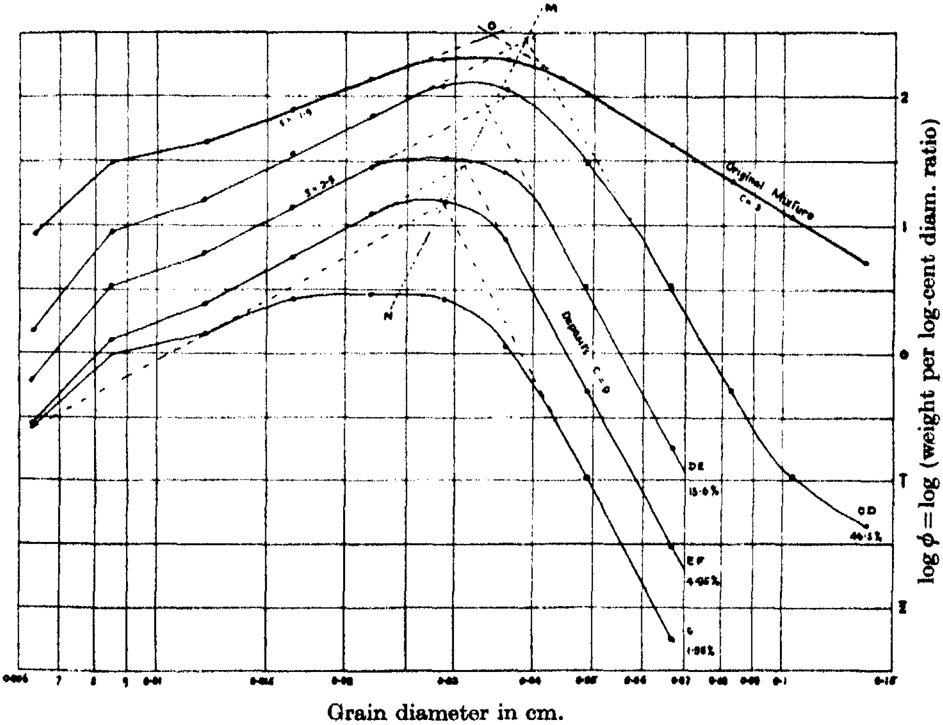

FIG. 3*a*—Last stage of removal by a moderate wind. Bed becoming coarser with consequent shift of the line *MN* to the right. Original bed mixture shown by heavy line $\left(\int \phi\, dR = 1\right)$. Fractional deposits in various places in the tunnel *CD*, *DE*, etc. shown by thin curves for which the ordinates have been reduced according to the proportion of sand by weight found at each place; e.g. for deposit in *CD* $\int \phi\, dR = 0{\cdot}465$. Total deposit for which $\int \phi\, dR = 0{\cdot}334 + 0{\cdot}465 + 0{\cdot}136 +$ etc. $= 1$ is shown by dotted line in fig. 3*b*.

Fig. 3*b* shows the composition of the surface creep (cross dotted), the first deposit *BC* omitted from fig. 3*a*, and the total sand movement (broken line) which is the sum of all the fractional deposits. On the left-hand side it will be noticed that the irregularity in the extreme grades is faithfully

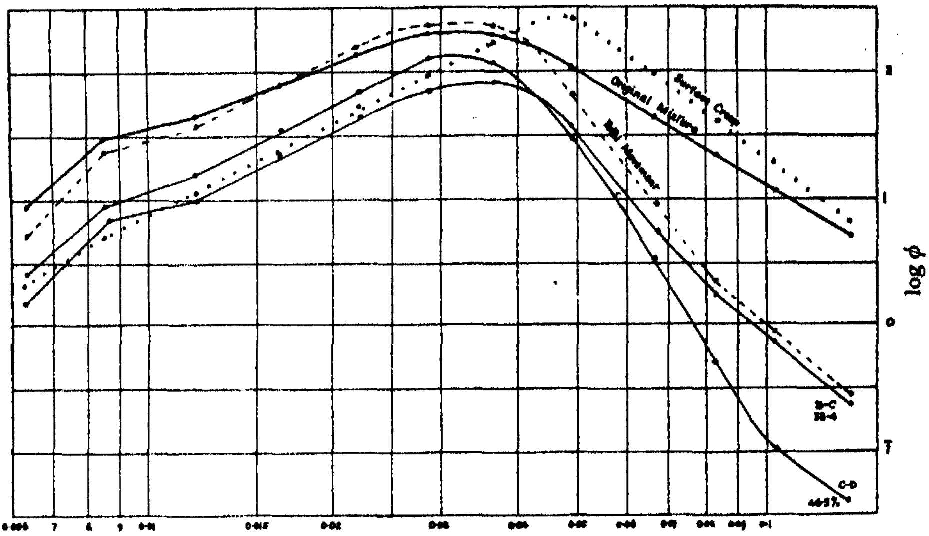

Grain diameter in cm.

FIG 3*b*—Other details omitted from fig. 3*a*. Extreme up-wind deposit between *B* and *C* shown by continuous curve. Total sand removed and deposited shown dotted. Surface creep collected by trap in tunnel floor shown cross dotted.

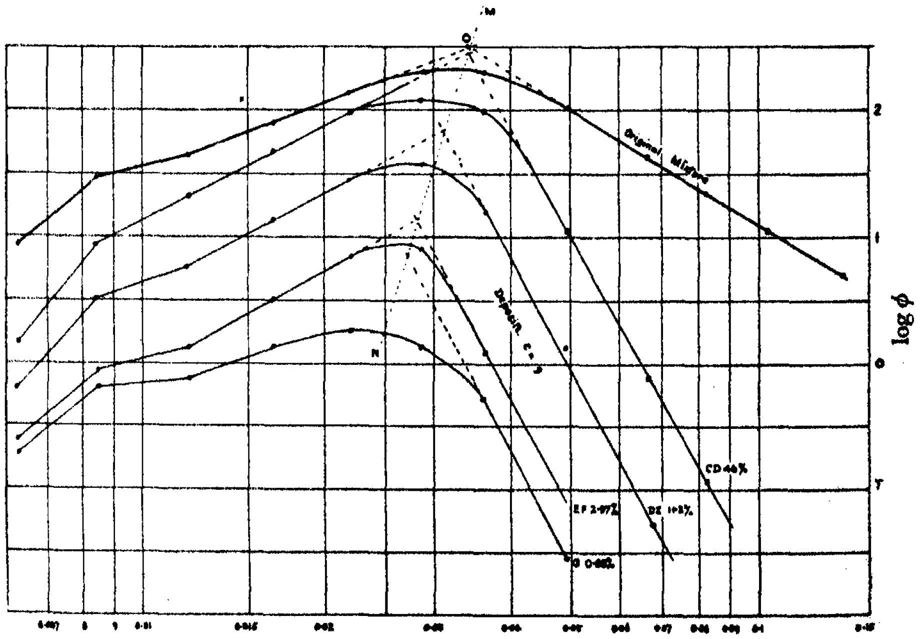

Grain diameter in cm.

FIG. 4—Early stage of removal by moderate wind.

reproduced in all the deposits, but that it has been almost flattened out in the case of the surface creep. On the right-hand side, the surface creep has taken up a new slope, steeper than the original but considerably flatter than that of the deposits. The peak size of the surface creep has shifted to the right. The advance of the surface creep and its mingling with the up-wind deposits is well marked by the extreme deposit grades bending up to become parallel with it. This is an example of the sum of two mixtures differing in grading coefficient.

The above was the result of a run under a moderate wind maintained till the surface became stable and motion ceased. During the later part of the run the failing supply of fine grains caused the carrier grade to become coarser. Consequently the line MN joining the peaks of the deposits passes to the right of the peak O of the original bed mixture. Fig. 4 resulted from a run of the same period—3 min.—when a fresh surface of the same sand was kept disturbed by a small incoming fall of sand at the mouth. The grading coefficients of the deposits are unchanged, but the line MN has shifted to the left so that it now passes through O. Since, however, the coarse grading coefficient c for the total sand removal is greater than that of the bed mixture, the consequent concentration of the coarsest grades on the removal bed must in time shift the whole deposit pattern to the right again.

In fig. 5 the same sand was exposed to a considerably stronger wind, above the threshold required to move the largest grains. On the left, the increased wind has made the slope of the deposits approach very closely to that of the bed mixture; but the slope of the surface creep has remained unchanged. The peak size of the surface creep has shifted still farther to the right, and the long line of eight analysis points illustrates well the persistence of the exponential relationship. Again the irregularity has straightened out. On the right the slope of the deposits remains unchanged at $c = 9$. The duration of the run was only 2 min. but the rapid removal, with its consequent coarsening of the removal bed, has already shifted the line MN to the right, and has steepened the right-hand slope of the surface creep. In the final state of steady movement the peak of the surface creep shifts so far to the right that its right-hand coefficient rises to the common value of 9 as shown by the dotted line in the figure.

Fig. 6 shows the behaviour of a natural "fine silver sand" as obtained from a builder's merchant. The peak size is finer than that of the artificial mixture; and the composition curve is typical of the sand of desert dunes. The wind in this case was lower than that in fig. 5 but was of corresponding strength having regard to the threshold wind required to move the coarsest grains. On the left the deposit slope is again nearly parallel to that of the original mixture. On the right it has taken up the same value as before, $c = 9$. The coarse grades of the surface creep have again taken up a slope intermediate between those of the deposits and of the original mixture.

Owing to the relative lack of coarse grains in this sand, the coarsening of the removal bed, as indicated by the shift of the line *MN* to the right, is considerably less than in the case of the "wide" sand.

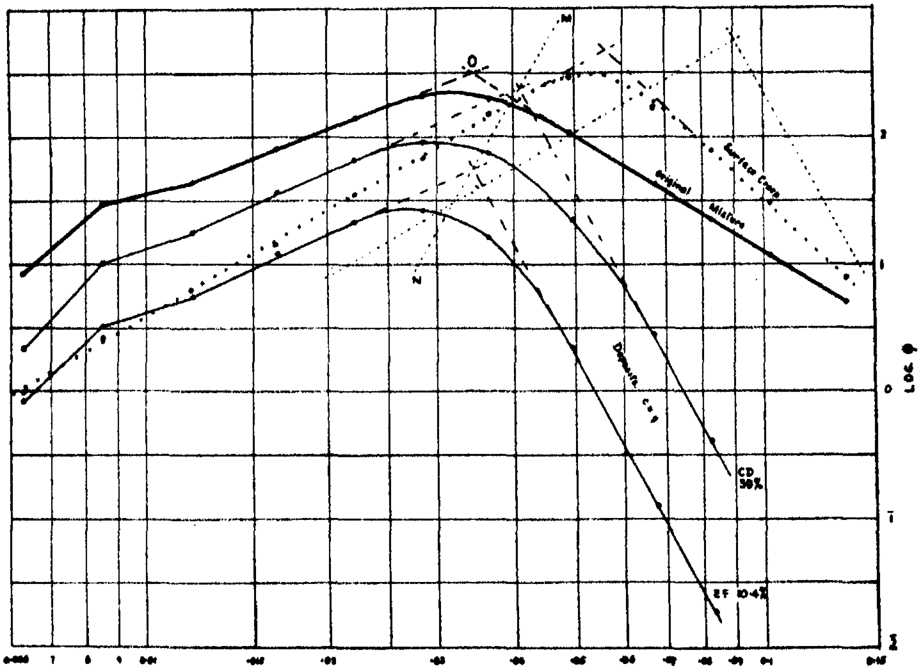

Grain diameter in cm.

Fig. 5—Grading effects of strong wind.

(*b*) *Irregular Sands*

The foregoing experiments show that regular sands tend to retain their exponential grading no matter how their coefficients may change. Further experiments were made to ascertain whether, and if so in what part of the cycle, a non-regular sand is transformed into a regular sand. The natural sand of fig. 6 was used; and by the addition of more sand (*a*) the extreme fine grade, and (*b*) the extreme coarse grade were separately increased about tenfold. Since changes in the grading on one side of a curve appear to have no appreciable effect on the other side, the irrelevant halves of the curves are omitted from fig. 7.

If the distortion n is defined as the ratio of the content of a grade actually present in a mixture to that of the same grade if it conformed to the general pattern of the regular grading curve, then the difference in the height y of the ordinate in the figure between the straight line and the actual curve is $\log n$.

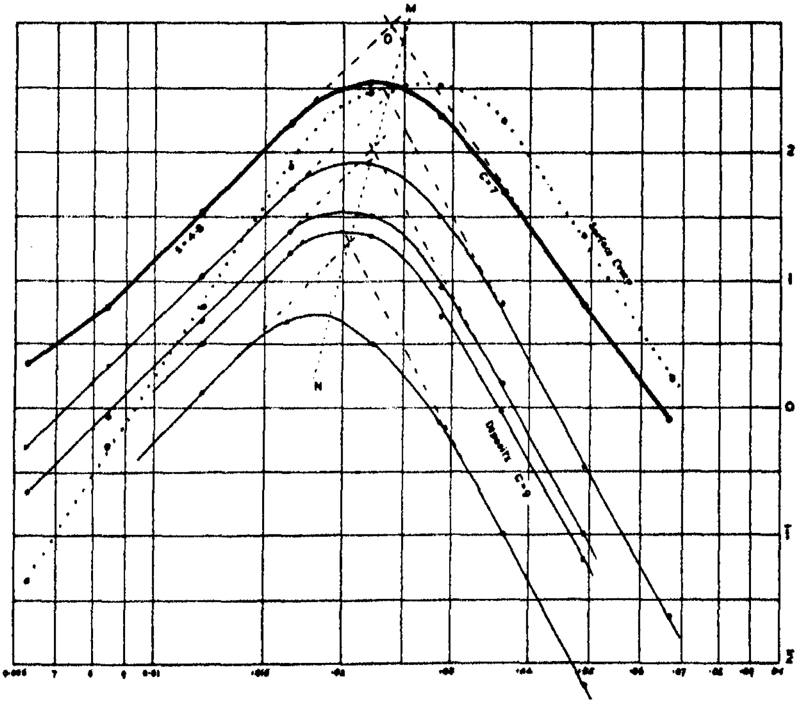

Grain diameter in cm.

FIG. 6—A "narrow" natural sand. Original bed mixture shown by heavy curve. *Fractional deposits shown by thin curves. Surface creep shown cross dotted.*

In fig. 7*a* the distortion artificially caused was about sevenfold for the extreme fine grade. In the deposits it will be seen that n has dropped, most pronouncedly in the early up-wind deposits, and to a lesser extent as the deposit dies off down wind. Most of the excess of the finest grade was left behind on the removal bed, where it formed smooth sheets over which the wind passed without causing any movement on them. Confirmation of this rather surprising rejection of fine sand in the pick-up process is given by fig. 3*b* where the slope of the total sand removed is steeper than that of the removal bed. In the case of the surface creep as trapped at B the distortion is much reduced.

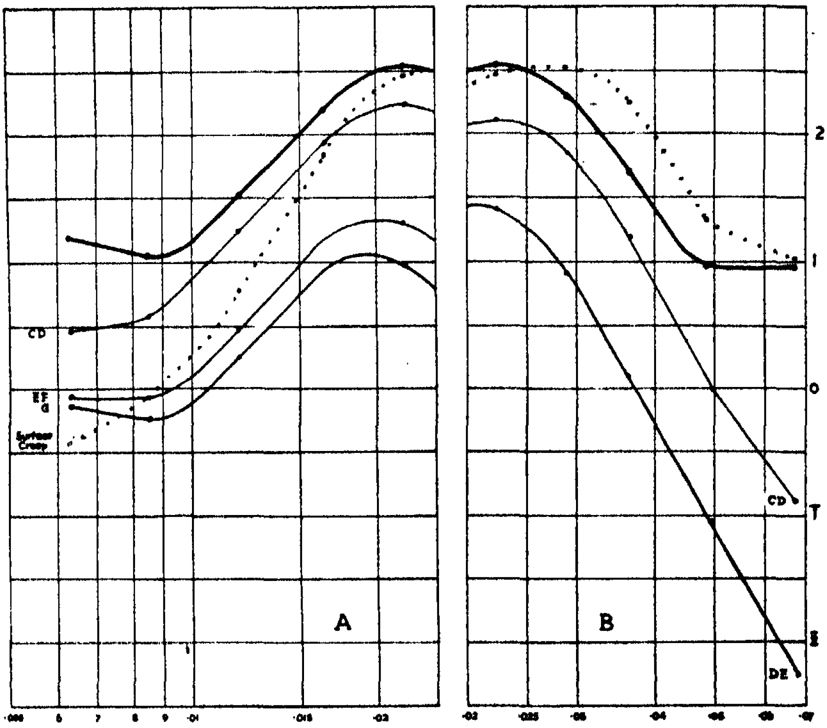

Grain diameter in cm.

Fig. 7—Effects of distortion of pattern of original bed mixture. Bed mixture shown by heavy curves—extreme grades on right and left increased, in turn, in weight by the addition of extra sand. On the right (coarse grains) the regular exponential grading tends to be restored in the successive down-wind deposits. On the left (fine grains) the restoration is most pronounced in the surface creep.

Fig. 7b shows the changes which took place in a distortion on the right of the curve, n was 10 for the original mixture. It was reduced least, to 6·3, in the case of the surface creep, and was progressively more reduced in the deposits till it had disappeared altogether as the deposit died away towards the down-wind end of the expansion tunnel. Again most of the excess of the distorted grade was left behind on the removal bed, where in this case it formed typical "residue ridges" (Bagnold 1937).

The tendency for sand grains to grade themselves according to the exponential relation $\log_{10}\phi = -c(R-R_0)$ is not confined to natural sands composed of a complete continuity of grain size. Fig. 8 shows the result of two experiments with a mixture consisting of a narrow carrier grade of almost uniform size and two coarser grades separated by gaps. As before, the grading tends to become linear, and c increases towards the apparent limiting value of 9 under the action of the wind.

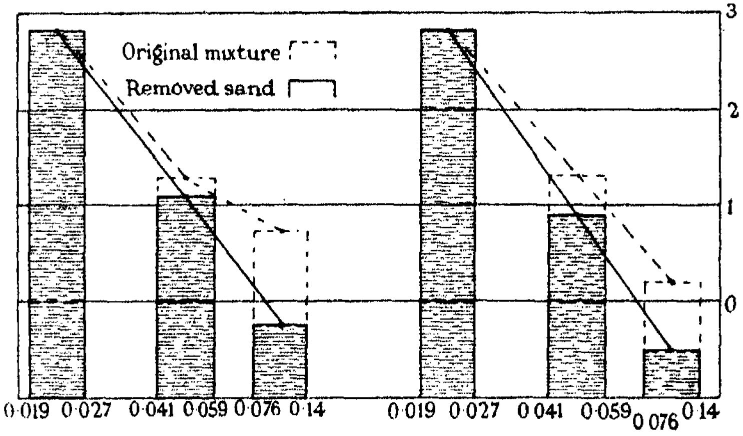

FIG. 8—Discontinuous grading. Tendency of thin sands each of nearly uniform grain size to assume and maintain the general exponential grading relation.

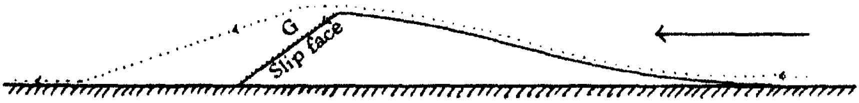

FIG. 9—Separation of saltation from surface creep at dune crest.

(c) *Grading of an Encroachment Deposit*

Observation of the movement of sand over a typical dune such as that shown in fig. 9 indicates that the dune advances down wind by the trapping of the surface creep, which is driven by the saltation over the crest into the shelter of the leeward slip-face. It seems, therefore, that most of the mass of the dune, above the level of the foot of the slip-face, is composed of sand which has been graded by a process similar to that of the slot method used to collect the surface creep; and it is this process which appears to be most effective in producing the exponential form of the left-hand side of the grading curve. Thus, while the steepness and the exponential grading of the right-hand side may be regarded as arising from the removal process, those of the left-hand side appear to be due to the separation of the surface creep at the dune crest. This is born out by the fact that the grading curves of samples I have analysed of sands taken from the great undulating desert sand accumulations, where no crest or slip-face exist, all have a very flat left-hand side with but little approach to regularity of form.

Since the analysis of samples of true dune sands also showed that in many cases the left-hand side of the curve was steeper than that of the surface creep in any of the preceding experiments, some further grading process was looked for. Such was found in the elutriating or winnowing action of the upward air current due to the wind eddy in the lee of the crest. For in imitation of this upward air current an in-draught of air was made to rise through the collecting slot at B (fig. 2); and as a result, though there was no change in the right-hand side of the curve or in the position of the peak, the left-hand side became considerably steeper. It is noteworthy that in this process, too, the altered left-hand side still retained its linear form.

It would seem from the above results that there is experimental evidence that the assumed grading law of the form $\phi \propto d^n$ is something more than a practical approximation, and that deposits of grains which have been removed and transported by the wind from a bed composed of sand graded in any irregular way tend to become graded according to the above law, most of the superfluous grains being left behind on the bed.

SUMMARY

The size-grading of samples of eolian sand deposits when plotted as weight per log-cent change in grain diameter against log diameter give curves which show that the extreme grades on each side of the mean diameter die away in percentage weight according to an exponential law. The exponential coefficients on each side differ in value. These and other coefficients defined in the paper numerically describe the grading of sand in a manner independent of the usual diagrammatic representation and of the sieve sizes used in its analysis.

By imitating experimentally a simple cycle of sand movement consisting of removal from a sand bed of known composition, transportation over the bed, and deposition under various conditions, the factors controlling the value of each coefficient separately have been investigated.

The tendency of sand to grade itself according to the above bi-exponential pattern was confirmed by experiments with sands whose grading pattern had been artificially distorted by the addition of extra sand of certain grades. The process by which the extra sand is rejected by the mixture is described.

The results are applied to the size-grading of a typical sand dune.

REFERENCES

Bagnold, R. A. 1936 *Proc. Roy. Soc.* A, **157**.
— 1937 *Geog. J.* **89**, 428.

The Angular Distribution of Protons Projected by Fast Neutrons

By P. I. Dee, M.A., *Fellow of Sidney Sussex College, Cambridge*
and C. W. Gilbert, Ph.D., *Fellow of Jesus College, Cambridge*

(*Communicated by Lord Rutherford, O.M., F.R.S.—Received* 24 *June* 1937)

[Plate 16]

1—Introduction

The nature of the interaction between neutron and proton has assumed great importance in modern nuclear theory, since it is now generally assumed that these two particles form the fundamental constituents of all nuclei. Little direct evidence exists, however, as to the nature of this interaction.

The stable existence of the deuteron shows that the force between neutron and proton is attractive, and for purposes of calculation a "square hole" potential well has generally been assumed. With this model some success has been obtained* in correlating the magnitudes of a number of experimentally measurable quantities such as (*a*) the binding energy of the deuteron, (*b*) the total cross-section for neutron-proton scattering (Tuve and Hafstad 1936; Amaldi and Fermi 1936*a*), (*c*) the cross-section for photoelectric disintegration of the deuteron (Chadwick and Goldhaber 1935), and (*d*) the cross-section for capture of neutrons by protons (Amaldi and Fermi 1936*b*). The interaction is not completely derivable from the above data, since the values of these quantities depend mainly upon r^2V, where r is the mean radius and V is the depth of the potential hole.

The magnitudes of the binding energies of some of the light nuclei (^{3}H, ^{3}He, ^{4}He) can be explained by assuming that the force between neutron and proton falls off very rapidly when the distance between the two particles increases beyond about 2×10^{-13} cm. (Wigner 1933; Thomas 1935; Feenberg 1935), but the law of variation of force with distance cannot be obtained from the experimental data. The calculations of these binding energies, however, involve assumptions as to the magnitudes of neutron-neutron and proton-proton forces.

---

* For a full account of the theoretical interpretation of these results see Bethe and Bacher (1936).

A more direct method of obtaining information about this interaction is by the investigation of the angular distribution of protons projected by fast neutrons, since the form of this distribution depends more markedly upon the width of the potential hole. According to Morse, Fisk and Schiff (1937), this angular distribution depends also upon the shape of the potential hole. Thus while Bethe and Bacher (1936) find that for a "square hole" interaction with $V = 0$ for $r > r_0$ the distribution would be isotropic for incident neutrons of energy less than 10^7 e-volts, Morse, Fisk and Schiff state that small but finite values of V for $r > r_0$ should give rise to marked differences from isotropy for much smaller neutron energies.

2—MODES OF REPRESENTING THE DISTRIBUTION OF SCATTERED PROTONS

Before considering the results which have been obtained upon the angular distribution of protons recoiling under the impacts of fast neutrons we shall briefly summarize the methods by which this distribution may be represented, since many workers, both theoretical and experimental, have chosen different schemes of representation of their results, rendering intercomparison difficult. Consider first the motion referred to the centre of gravity of the two particles which then approach one another along the line joining them each with velocity v. Let $(180° - \phi)$ be the angle through which each particle is deflected, the particles then receding after the collision, each with velocity v, in opposite directions. Then the required distribution function $f(\phi)$ is equal to the number of protons (or neutrons) scattered per unit solid angle in the direction ϕ, and an isotropic distribution corresponds to $f(\phi) =$ constant. The number of protons scattered between ϕ and $(\phi + d\phi)$ is then proportional to $f(\phi)\sin\phi\, d\phi$.

Consider now a collision specified as above in terms of ϕ, viewed from the co-ordinate frame of the laboratory. In this system, relative to which the proton is initially at rest, the incident neutron has velocity $2v$. It may readily be shown that if in these co-ordinates $\theta =$ the angle of projection of the proton relative to the direction of the incident neutron then $\phi = 2\theta$.

The number of protons scattered between θ and $(\theta + d\theta)$ is therefore proportional to $f(2\theta)\sin 2\theta\, d\theta$, which may also be written $f(2\theta)\, d(\cos 2\theta)$. The obvious method of investigation is therefore to count the number of recoil proton tracks occurring within equal intervals of $(\cos 2\theta)$, and the form of the function $f(2\theta)$ is then directly obtained.

For purposes of graphical representation a number of methods may be used:

(*a*) The numbers of observed angles of projection lying within equal intervals of cos 2θ are plotted as ordinates and the corresponding values of cos 2θ as abscissae. On such a histogram the important case $f(\phi) =$ constant appears as a line $y =$ constant.

(*b*) The same numbers as in (*a*) are taken as ordinates, while the corresponding values of 2θ are taken as abscissae. An isotropic distribution again appears as a line $y =$ constant.

(*c*) The numbers of recoil tracks with angles of projection lying between θ and $(\theta + d\theta)$ are taken as ordinates while the corresponding values of θ are taken as abscissae. (This is the method adopted by Harkins.) The ordinates of such a graph being proportional to $f(2\theta) \sin 2\theta$, an isotropic distribution appears as a sin 2θ curve with maximum at 45°.

(*d*) The numbers of particles scattered at angle θ per unit solid angle referred to the laboratory co-ordinates are taken as ordinates and the corresponding θ values as abscissae. The ordinates are obviously proportional to $f(2\theta) \sin 2\theta d\theta \div \sin \theta d\theta$, i.e. to $f(2\theta) \cos \theta$. Thus an isotropic distribution appears as a cosine curve with maximum at 0° and zero at 90°. (This method is adopted by Kurie 1933).

In view of the importance of easy intercomparison of past results and of the many results which doubtless will appear in the future, it seems desirable that a common practice should be adopted in future work.

Since the fundamental question at issue is the extent to which the distribution departs from isotropy, it would seem that either method (*a*) or (*b*) is to be preferred, since on these methods an isotropic distribution receives the simplest possible representation $y =$ constant.

For purposes of representation of experimental results method (*a*) has the great advantage that the area under the curve between any two values of cos 2θ is proportional to the number of particles observed in this angular range, so that so long as the main errors are statistical ones this representation is the most direct and most easily gives a correctly weighted distribution. We have used method (*a*) in the manipulation and representation of our results (figs. 5, 6).

For theoretical purposes the method (*b*) is the logical one and is much to be preferred to (*c*) or (*d*).

This representation is simply obtained from (*a*) and we have used it for comparison of our results with theory (fig. 8).

3—Experimental Results of other Workers

The experimental results of different workers on the form of the scattering distribution are widely contradictory. Thus Kurie (1933), from measurements on expansion chamber photographs of protons projected from a layer of paraffin by neutrons from a source of polonium and beryllium, obtains a distribution which shows wide departures from isotropy. Meitner and Philipp (1934), on the other hand, using a similar neutron source and measuring the angles of projection of 100 recoil protons originating in the gas of the expansion chamber, find a distribution which is isotropic within the large limits of statistical error. Similar results were obtained by Auger and Monod Herzen (1933) by measurements upon eighty-four recoil proton tracks. A more detailed study has been made by Harkins, Kamen, Newson and Gans (1935, 1936), who used neutron sources of beryllium mixed with mesothorium and thorium X and in some cases of beryllium mixed with radiothorium. They photographed 730 tracks of recoil protons originating in various hydrogenous gases in an expansion chamber. Their distribution, plotted according to method (*c*) § 2, shows a maximum at 25° instead of at 45° as would be the case for an isotropic distribution.

In criticism of the above results it must be noted that in all of these experiments the incident neutrons must have been widely inhomogeneous in velocity. Thus for the polonium-beryllium sources the neutrons might be expected to have energies from zero up to 10×10^6 e-volts, whilst the sources used by Harkins probably gave neutrons with energies from zero up to 12×10^6 e-volts with a maximum in the number × energy distribution at about 5×10^6 e-volts. Harkins states that 25 % of the neutrons had energies less than 10^6 e-volts.

The disadvantages of this inhomogeneity are twofold. In the first place it is probable that the required function $f(\phi)$ is different for different values of the energy of the incident neutrons, so that any satisfactory comparison of the results with theory is extremely difficult. But from an experimental standpoint there also exists a serious disadvantage. Consider, for example, the collision of neutrons of energy 10^6 e-volts with protons. The range in air at N.T.P. of a proton projected at angle $\theta = 0°$ with the direction of the incident neutron is 2·5 cm. For $\theta = 45°$, however, the range of the projected proton is 1·0 cm., while for $\theta = 60°$ the range is 4 mm. It is obvious that if for any reason there is a minimum detectable range of the projected protons the distribution obtained will show a deficit of scattered protons for large values of θ as compared with the true distribution. Whilst such effects upon the distribution may be negligible for neutrons of high energy, for which the ranges of the protons projected at large values of θ are still large, the presence of appreciable numbers of neutrons of lower energies may introduce considerable error. For all work with inhomogeneous neutrons it is therefore possible that, owing to this cause, a distribution which represented according

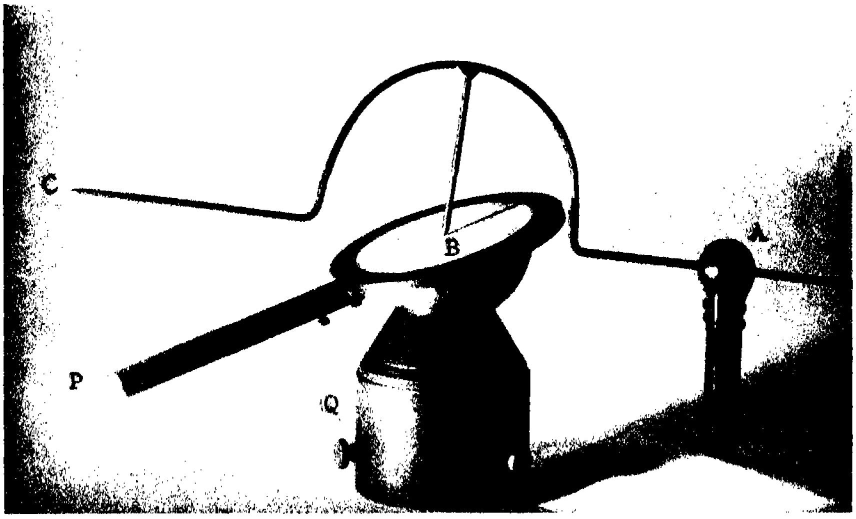

Fig. 1

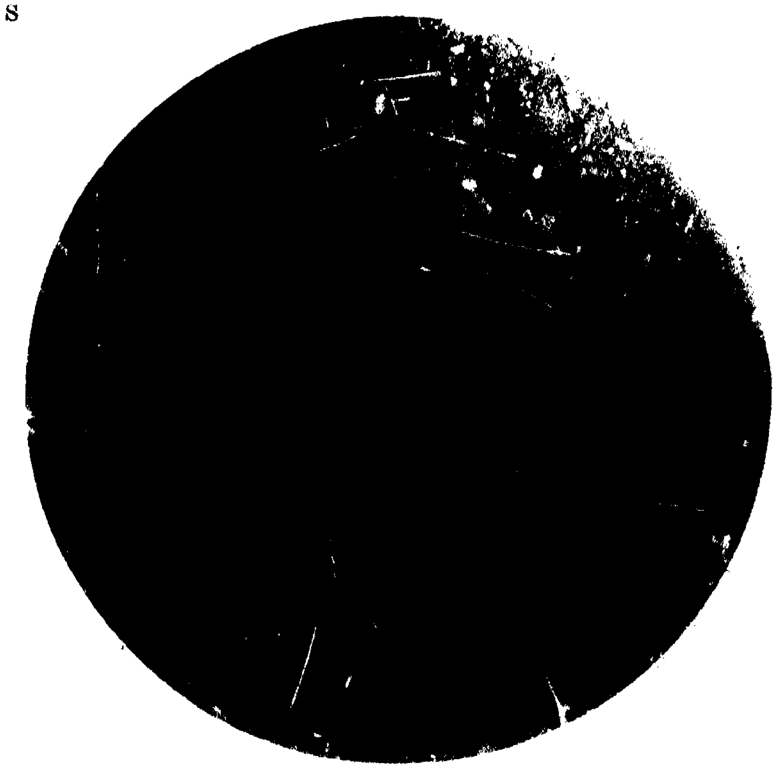

Fig. 2—Tracks of protons recoiling from the impacts of neutrons of $2\cdot4 \times 10^6$ e-volts energy. The neutron source was at the point *S*.

to (c) § 2 should show a maximum at 45° will in fact show a maximum at smaller angles.

The results of Harkins and of Kurie plotted according to this scheme show a maximum at 25°, and the possibility of this explanation of the departure from isotropy must be borne in mind. On the other hand, the advance notice of a paper by Kruger, Shoupp and Stallmann (1937) using the homogeneous neutrons from deuterium under deuteron bombardment would seem to be free from this error, and the results of these workers are in substantial agreement with the results of Harkins and of Kurie. Similar results have been found by Lampson, Mueller and Barton (1937) using a similar neutron source but detecting the recoil protons in a photographic emulsion. It is doubtful whether this method can have the same reliability as that of the expansion chamber.

Another feature of such experiments which may give rise to error lies in the fact that the path of the incident neutron does not appear on the photograph. The direction of the neutron has by all workers been assumed to be given by the direction of the line joining the neutron source to the point of origin of the track of the recoil proton. In other words the resulting distribution must include a certain percentage of recoil tracks which were due to neutrons which had not proceeded directly from the source. These effects of scattering of the neutrons by the matter surrounding the gas in the chamber might reasonably be expected to tend to conceal any departures from isotropy which may actually exist in the true distribution and can therefore only be regarded as a possible criticism of the methods which have yielded an isotropic distribution. As will be shown in the next section, we have adopted a method which should minimize both of these two main sources of experimental error. A further difficulty of such measurements lies in the large statistical error which must be present unless a great number of tracks are measured. The only distribution which contains more than 250 particles is that of Harkins, who measured 730 tracks. Our results refer to measurements upon about 2000 recoil proton tracks.

4—EXPERIMENTAL METHOD

We have seen from the preceding discussion that the important points to be considered in these experiments are (1) the use of homogeneous neutrons and (2) the elimination from the statistics of recoil tracks produced by neutrons which have not proceeded directly from the source.

We have accordingly used as a source in these experiments the homogeneous neutrons of $2{\cdot}4 \times 10^6$ e-volts energy, which are produced by bombarding with deuterons a target containing deuterium. In order to satisfy the second condition the recoil proton tracks were photographed in an expansion chamber containing a mixture of 60 % methane and 40 % argon at a total pressure of about 3·5 atm. Under these conditions the range of a proton projected at $\theta = 0^\circ$ with the direction of the incident neutron was about 3·5 cm. For all other values of θ the ranges were correspondingly less. We have thus been able to measure, for each recoil track, both the angle of projection relative to the line joining its point of origin to the source and also the length of the track. Each recoil track was then represented by a point upon a diagram having range and angle as ordinate and abscissa respectively. With strictly homogeneous neutrons, all proceeding directly from the source, and with negligible errors of measurement, all such points should then lie smoothly upon a theoretical curve relating the ranges and corresponding relative angles of projection of the protons. Conservation of momentum and energy are sufficient conditions for the calculation of this curve.

Allowing for the slight inhomogeneity of the neutrons, due to the effects of the finite bombarding energy of the deuterons, and for some errors of measurement, we might expect that the experimental points would show a concentration about the theoretical line, while recoil tracks due to scattered neutrons would be distributed at random over the diagram. A typical experimental diagram obtained in this way is shown in fig. 3. It is obvious that by the use of this method the tracks due to scattered neutrons can be eliminated from the required statistical distribution.

The above method of elimination of tracks due to scattered neutrons can only be used when the maximum length of the recoil tracks is small compared with the dimensions of the expansion chamber. Previous work upon this distribution has been carried out with expansion chambers operated at about atmospheric pressure. Under such conditions the tracks usually passed right across the chamber, so that this method of elimination of the effects of scattering could not be used.

Our choice of this method of elimination of tracks due to scattered neutrons, instead of the possible alternative method of constructing a chamber with such thin walls that the scattering of neutrons might be reduced to the lowest possible minimum, was partly conditioned by the necessary screening of the chamber from X-rays produced by the high-voltage apparatus. This screening was effected by a lead-lined hut, at the base of the accelerating tube, inside which the chamber was operated. It seemed possible that the number of neutrons scattered from the walls of this hut might not be negligible. The elimination of such scattered neutrons by the method which we have used would not be possible unless the chamber were constructed to work at fairly high pressures, and this condition would seem to preclude the use of such a thin-walled chamber.

The target used in this work was a disk of heavy aluminium hydroxide, 12 mm. in diameter, contained in a wide evacuated tube down which passed the beam of accelerated deuterons. The target lay in the median plane of the chamber, 17 cm. from its centre. The expansion chamber was 25 cm. in diameter and 6 cm. deep, these large dimensions being chosen in order to be able to select for measurement only those tracks which occurred within a certain chosen central region of the chamber. This region was chosen in such a manner that any recoil proton track which originated within it would appear completely whatever its direction of projection. No systematic errors could therefore be introduced into the statistics by the effects of the walls, etc., of the chamber. An expansion chamber of a water-piston type was developed in order to facilitate the use of a large chamber at high pressures. The general experimental method was the same as that described in earlier papers (Dee 1935). Two main series of photographs were taken, in which the voltages applied to the accelerating tube were 300 and 100 kV respectively. A typical photograph is shown in fig. 2, Plate 16.

5—REPROJECTION AND MEASUREMENT OF THE RECOIL TRACKS

In order to measure the ranges (l) and angles of projection (θ) of the protons relative to the direction of the incident neutrons it was necessary to develop a method which would be rapid in use, in order to deal with the great number of tracks required for a satisfactory statistics.

The two cameras used to photograph the recoil tracks were rigidly fastened together, and after a set of photographs had been taken they were removed as a unit from the expansion chamber support and placed upon two upright pillars fixed to a "reprojection" table. By illuminating the plates from behind, two images of the expansion chamber were produced about 15 cm. above the reprojection table top. This horizontal table top was hinged so that its height could easily be varied.

The apparatus shown in fig. 1, Plate 16 stood upon this table top. A steel hemisphere could slide smoothly in a concentric spherical cup which forms the upper surface of the support Q. The projected tracks were viewed upon the flat (white) surface of the hemisphere. By suitable adjustment of the position of Q upon the table top, and of the height of the latter, it was simple to arrange that the points of origin of the two projected images of any selected track lay both at the centre B of the hemisphere. By rocking the hemisphere in its cup this adjustment remained unaltered, while the whole lengths of the two images were brought into coincidence. The single track then observed coincides with the position (relative to the cameras) of the track which was photographed. The length (l) of the track was then read off. A thin diametral wire carried by a brass ring which could be rotated relatively to the steel hemisphere was then brought into coincidence with the track image. This ring also carried a pointer P in line with the diametral wire. Thus BP defined the direction of the recoil track in space. The angle θ between this direction and the direction of the incident neutron was measured by using the shaped rod which could slide smoothly through the centre A of the ball of a cup and ball joint. The centre of this ball occupied the same position relative to the cameras as had been occupied by the neutron source when the photograph was taken. The tip of the central prong was placed upon the origin of the track at B. The rod was constructed so that A, B and C were collinear, and hence this line defined the direction of the incident neutron. Further, BC was constructed equal in length to BP (16 cm.). Hence the angle θ was readily obtained by measurement of the distance CP ($= 32 \sin \theta/2$ cm.).

For the purpose of eliminating the recoil tracks due to scattered neutrons the value of θ for each recoil track was not calculated, the directly measured value of CP (d) being used on all such diagrams.

This method has proved very rapid in use and is sufficiently accurate for most expansion chamber measurements. (The support Q was actually a "pot" electromagnet, so that the hemisphere could easily be locked in position by passing current through its coil when desired. This feature has proved very useful when detailed measurements need to be made upon, for example, a disintegration fork produced in the gas.)

By this method the tracks of about 2000 recoil protons were measured and plotted upon l, d diagrams. Measurement was confined to tracks occurring within a selected region of the chamber as described in § 4. Every track originating within this region was measured. The measurement was not continued for ranges less than 5 mm. owing to the difficulties of measurement and elimination of the effects of scattering. A typical diagram is shown in fig. 3.

6—EXPERIMENTAL RESULTS

Twelve diagrams, similar to the one reproduced in fig. 3, were obtained by plotting the experimental points obtained in a number of runs under similar conditions. Preliminary experiments had given diagrams which showed much smaller concentration about the theoretical range-angle curve, this being mainly due to bombardment of the target tube down which the beam of accelerated deuterons passed. Conditions were much improved by making this tube wide, so that the beam of deuterons did not fall on any parts of the apparatus other than the actual target.

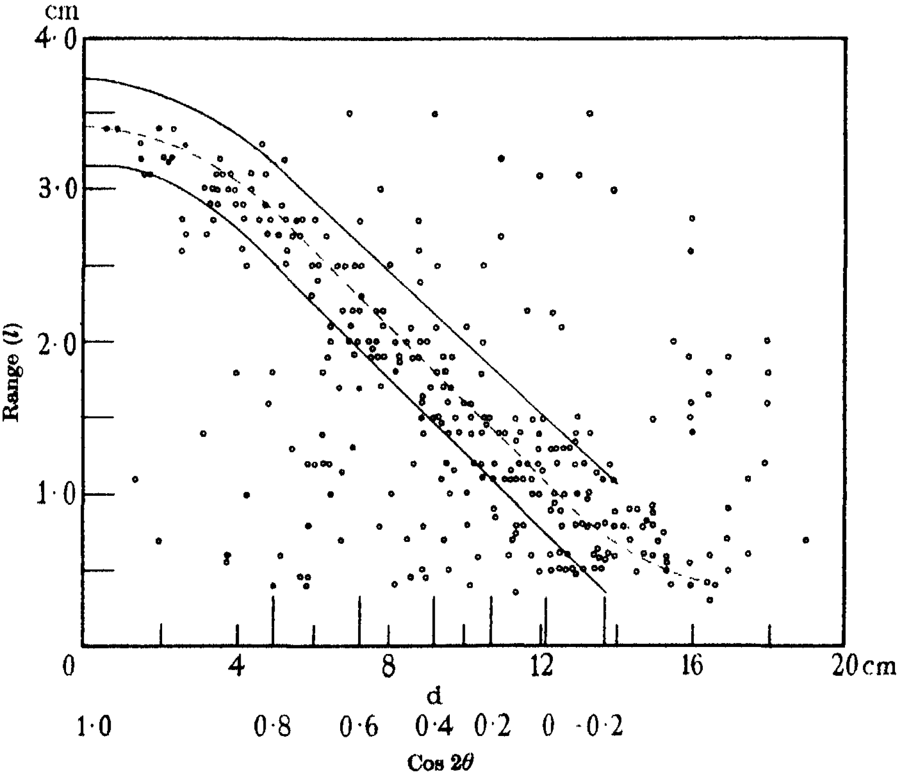

Fig. 3—Each point upon this diagram refers to a recoil proton track, plotted so that the ordinate represents the length of the track (*l*), and the abscissa the quantity *d*, which is a measure of the angle of projection of the proton relative to the direction of the incident neutron. The dotted line represents the theoretical relation between *l* and *d* for neutrons of energy 2·4 × 10^6 e-volts.

It is clear that the points are mainly concentrated in a band of width 3 cm. on the abscissa scale of *d*, which is a measure of the angle of projection of the recoil protons.

Four factors might be expected to contribute to the width of this band, namely, (1) effects of bombarding energy of the deuterons, giving rise to slight inhomogeneity of the incident neutrons, (2) the finite target area, (3) errors of measurement of the ranges and angles of the tracks and (4) small angle scattering of the neutrons in passing through the walls of the expansion chamber.

The energy of the neutrons would be $2\cdot4 \times 10^6$ e-volts for zero bombarding energy of the deuterons. For deuterons of energy E striking a thin target, the energy of the neutrons emitted at right angles to the direction of the bombarding beam would be greater than the above value by an amount $E/4$. Since disintegrations in the thick target used might have been effected by deuterons of all energies up to the maximum value of 300 kV, we conclude that the incident neutrons might have had energies varying between about 2·4 and $2\cdot5 \times 10^6$ e-volts. Calculation shows that the spread of d due to this cause should be about 2 mm. The effect of target area might be expected to give rise to a spread of d of about 14 mm. By reprojecting and measuring a few plates several times in succession the third effect was shown to account for a spread of d of about 7 mm. Calculation from the known cross-section for scattering showed that the fourth effect should be unimportant. We can therefore readily account for a total spread of 23 mm. and the agreement with the observed spread is considered sufficiently close.

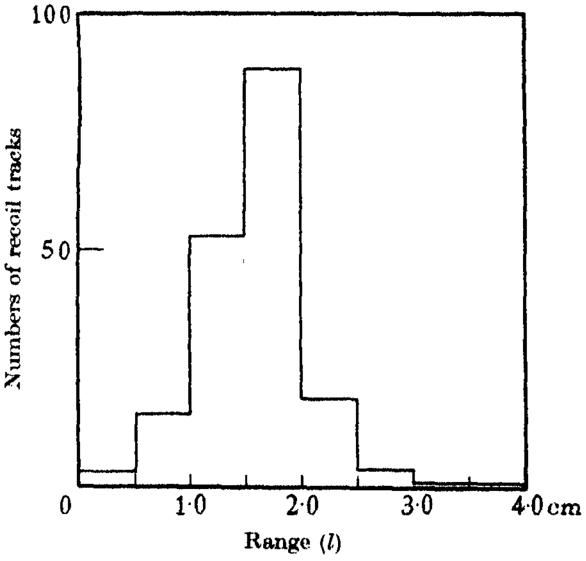

Cross-section of band $\cos 2\theta = 0\cdot4$ to $\cos 2\theta = 0\cdot2$

FIG. 4

In order to obtain the required distribution function and to eliminate the effects of scattered neutrons, graphs were plotted of the type shown in fig. 4, in each of which the numbers of points occurring within intervals of l

were plotted against l for a fixed interval of d. Upon such graphs the width of the main peak was approximately constant independently of the particular value of d for which this cross-section was made. The two full lines shown in fig. 3 were therefore drawn in such a manner as to include these main peaks. Using the diagrams such as fig. 3, counts were then made of the number of points included between these two lines for different intervals of d, chosen in such a manner that they corresponded to equal intervals of $\cos 2\theta$. Fig. 5 shows the results of this statistics, in which the ordinate scale represents this number of points (in all = 1534), and the abscissa scale the corresponding value of $\cos 2\theta$. The shaded area corresponds to the runs made with smaller bombarding energy, in which the experimental conditions were rather more satisfactory.

It should be noted that owing to the predominant character of the peaks, as illustrated by fig. 4, no very radical difference in this distribution can be introduced by small variations in the choice of the "allowed" breadth of the band of fig. 3, providing that the main peaks of the diagrams such as fig. 4 are included. To check this, and to make a correction for the background due to scattered neutrons, similar counts were made using a width of band twice that previously employed, with very similar results. As a correction for background the differences between the ordinates of these two distributions for each interval of $\cos 2\theta$ were then subtracted from the distribution shown in fig. 5. This in effect means that the background of fig. 5 is being taken as given by the density of points on fig. 3 in the neighbourhood of the main band. The result of this correction is shown in fig. 6, which includes data for 1111 recoil proton tracks.

A straight dotted line has been drawn to represent the probable shape of the distribution indicated by these experiments. The equation of this line is $N = N_0\{1 - \lambda(1 - \cos 2\theta)\}$, where $\lambda = 0{\cdot}14 \pm 0{\cdot}1$. The distribution obtained in this way shows therefore a small deficit of recoil tracks projected at large angles as compared with an isotropic distribution. It must be noted, however, that the method employed in making the correction for background might tend to introduce such a deficit into the distribution. Thus the effects of small deflexions of the tracks, errors of measurement, etc., would be more important for the protons projected with large values of θ, since the tracks are then relatively short. Hence it is possible that some of the tracks which have been taken as background should actually be included in the counts of the numbers lying within the allowed error limits, and that this error would be relatively more important for the higher values of θ.

Alternative methods of analysing the results have been used. The final result of such calculations shows that if the distribution be represented by a straight line, as described, the most probable value of λ is 0·1 ± 0·1.

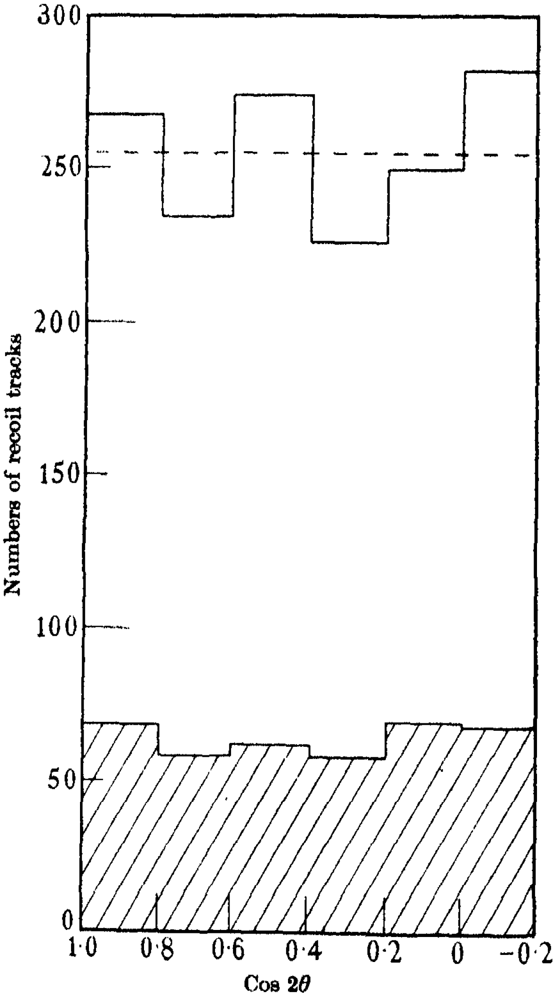

Fig. 5

Figs. 5 and 6—Numbers of recoil tracks {lying within the allowed band (see fig. 3)} with angles of projection corresponding to fixed intervals of cos 2θ. Fig. 5 without correction for scattered neutrons; fig. 6 (opposite) with correction for scattered neutrons. Shaded area = results of experiments with low bombarding energy of the deuterons.

7—DISCUSSION OF RESULTS

The experimental result given by fig. 6, which as shown in § 2 (*a*) represents the number of protons projected per unit solid angle (in the coordinate system relative to which the centre of gravity of the two particles is at rest) plotted against the corresponding values of the cosine of the common angle of deflexion, is reproduced in fig. 7, together with the results of Harkins. For the purpose of this comparison we have transformed his experimental representation from the mode of § 2 (*c*) to the mode (*a*). The areas under the two histograms are proportional to the numbers of tracks included in each statistical distribution. The two results are therefore widely contradictory. It will be seen that our result conforms much more closely to an isotropic distribution.

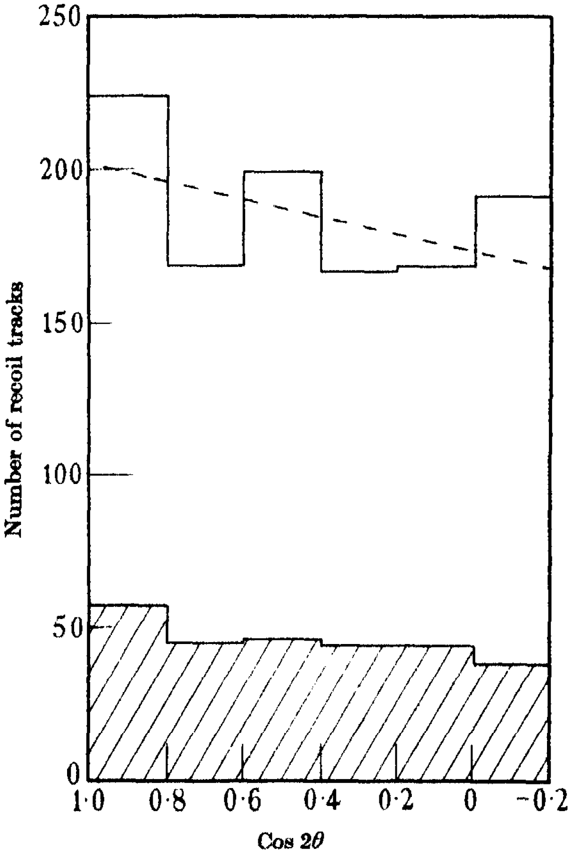

FIG. 6

The marked disagreement between the two results seems much too great to be accounted for by the difference in the energies of the neutrons used in the two experiments. The disagreement with the results of Kruger, Shoupp and Stallmann, who agree with Harkins in finding a peak in the distribution (§ 2 (c)) at 25°, could certainly not be explained in such a manner since the neutron source used by these workers was the same as that used in our experiments.

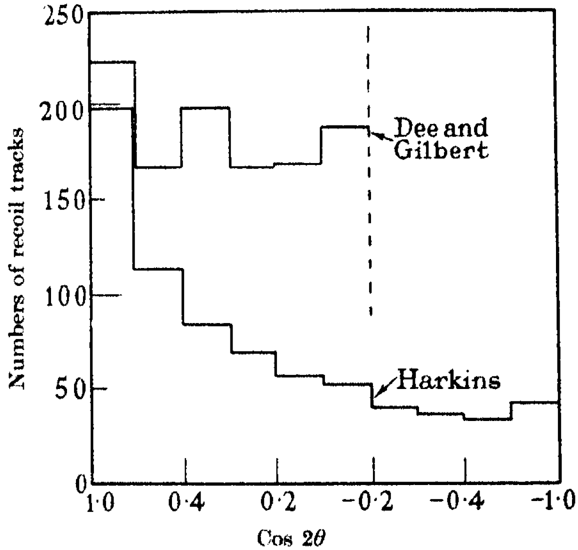

Fig. 7—*Angular distribution of recoil protons.* Numbers of recoil tracks within angular intervals which correspond to equal intervals of cos 2θ. Upper curve—result of these experiments, lower curve—result of Harkins.

It has been stated by Harkins that the large departure from isotropy indicated by his results could not be reconciled with the requirement of modern theory that no such anisotropy should be evident for the neutron energies used in his experiments (Bethe and Peierls 1935; Bethe and Bacher 1936). Our own experiments do not support this suggested inadequacy of the theory since the observed departure from isotropy is not much greater than the statistical errors involved.

On the other hand, Morse, Fisk and Schiff (1937) regard the results of Harkins as support for their assumption of an exchange interaction with a particular shape of potential hole, and claim that his results are in much better agreement with the results of their calculations than with the square hole potential previously assumed by Bethe and Bacher.

For this comparison with theory we have transformed the dotted line representing our averaged distribution (fig. 6) to the mode of representation of § 2 (*b*); see fig. 8, curve *A*. We show also upon this diagram Harkins's result (*B*) directly transformed from his smoothed curve and also the theoretical curves (*C*, *D*, *E*) of Morse, Fisk and Schiff, for different values of the energy (in the laboratory co-ordinates) of the bombarding neutrons.

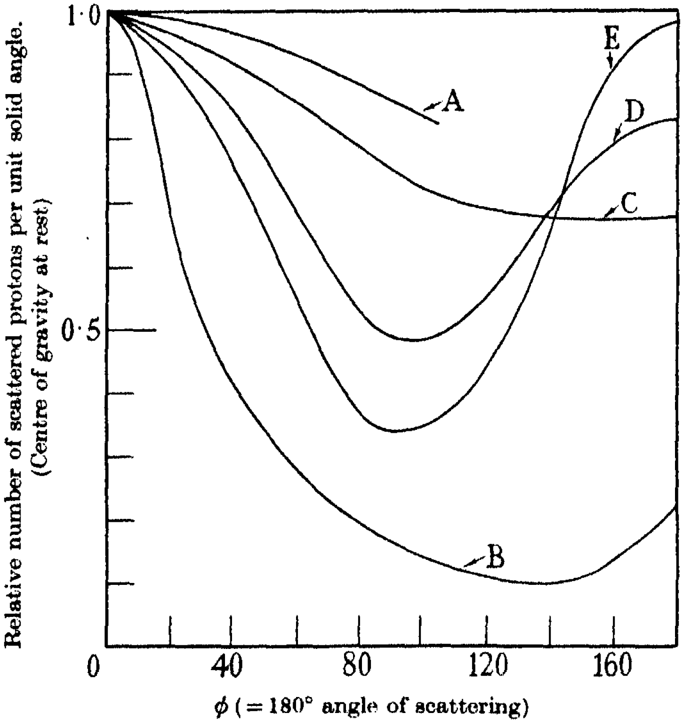

FIG. 8—*Angular distribution of scattered protons.* Curve *A*, experiments of Dee and Gilbert. Curve *B*, experiments of Harkins. Curve *C*, *D* and *E*, theoretical curves of Morse, Fisk and Schiff for neutrons of energies (in the laboratory co-ordinates) 5, 15, and 25 × 10^6 e-volts respectively.

Since the neutron energies used by Harkins had an upper limit of 12 × 10^6 e-volts and probably had a mean value of about 5 × 10^6 e-volts it is difficult to see how support for their view can be derived from these curves.

It might be thought that our own results are in better agreement with the predictions of Morse, Fisk and Schiff, but it should be emphasized that the departure from isotropy which we observe is not sufficiently great to enable any precise conclusions to be drawn as to the shape of the potential hole. According to recent calculations* by Massey and Buckingham (1937) our results could be fitted with a "square" hole of radius about $3 \cdot 0 \times 10^{-13}$ cm. and ordinary forces, whereas with an exponential, or inverse fifth power field, and ordinary forces, agreement could be obtained with a range of interaction of about $2 \cdot 5 \times 10^{-13}$ cm. The assumption of exchange forces is also shown by Massey and Buckingham to lead to departures from isotropy which would correspond to a preferential projection of the protons at large angles as compared with an isotropic distribution. These departures from isotropy, however, are small so that assumptions of "ordinary" or "exchange" forces are both compatible with our experimental results providing that the range of the interaction is less than $3 \cdot 0 \times 10^{-13}$ cm.

We wish finally to express our appreciation of Lord Rutherford's constant interest and encouragement. We are indebted to Drs. H. S. W. Massey and R. Peierls for many helpful discussions, and to Mr. J. C. Bower for some technical assistance.

SUMMARY

Expansion chamber photographs have been obtained of about 2000 tracks of protons recoiling from the impacts of neutrons of $2 \cdot 4 \times 10^6$ e-volts energy.

By measurement of the ranges and angles of projection of the protons relative to the direction of the incident neutrons the angular distribution function for the collision has been determined.

The function obtained is $N = N_0\{1 - \lambda(1 - \cos 2\theta)\}$ where N = the number of protons projected per unit solid angle in a direction making an angle θ with the direction of the incident neutrons. The value of λ obtained is $0 \cdot 1 \pm 0 \cdot 1$ and the distribution of scattered protons is therefore almost isotropic about the centre of gravity of the colliding particles. This result is at variance with that obtained by a number of experimenters who have observed angular distributions showing wide departures from isotropy. The result obtained lends support to the view that the force of interaction between neutron and proton is very small when the relative separation of the particles exceeds 3×10^{-13} cm.

REFERENCES

Amaldi and Fermi 1936*a* *Phys. Rev.* **50**, 899.
— — 1936*b* *Ric. Sci.* **1**, 56.
Auger and Monod Herzen 1933 *C.R. Acad. Sci., Paris*, **196**, 1102.

---

[*] We are indebted to H. S. W. Massey and R. A. Buckingham for giving us the results of these calculations.

Bethe and Peierls 1935 *Proc. Roy. Soc.* A, **149**, 176.
Bethe and Bacher 1936 *Rev. Mod. Phys.* **8**, 121.
Chadwick and Goldhaber 1935 *Proc. Roy. Soc.* A, **151**, 479.
Dee 1935 *Proc. Roy. Soc.* A, **148**, 623.
Feenberg 1935 *Phys. Rev.* **48**, 906.
Harkins, Kamen, Newson and Gans 1935 *Phys. Rev.* **47**, 511.
— — — — 1936 *Phys. Rev.* **50**, 980.
Kruger, Shoupp and Stallmann 1937 *Bull. Amer. Phys. Soc.* **12**, No. 2, 30.
Kurie 1933 *Phys. Rev.* **44**, 463.
Lampson, Mueller and Barton 1937 *Bull. Amer. Phys. Soc.* **12**, No. 2, 30.
Massey and Buckingham 1937 *Proc. Roy. Soc.* A, **163**, 281.
Meitner and Philipp 1934 *Z. Phys.* **87**, 484.
Morse, Fisk and Schiff 1937 *Phys. Rev.* **51**, 706.
Thomas 1935 *Phys. Rev.* **47**, 903.
Tuve and Hafstad 1936 *Phys. Rev.* **50**, 490.
Wigner 1933 *Phys. Rev.* **43**, 252.

The Nature of the Interaction between Neutron and Proton from Scattering Experiments

By H. S. W. Massey, Ph.D. and R. A. Buckingham, Ph.D.
Queen's University, Belfast

(*Communicated by R. H. Fowler, F.R.S.—Received* 25 *June* 1937)

Although our knowledge of atomic nuclei has expanded greatly in the last few years we are still in the lamentable position of having no certain information concerning the nature of the interaction between neutron and proton. Heisenberg's suggestion (1932), in the form as modified by Majorana (1933), that this interaction is of an exchange nature has been much used for the discussion of the binding energies of the heavy nuclei. It has the great advantage of providing a simple explanation of the proportionality of nuclear binding energies to the number of nuclear particles, but there is no direct experimental evidence that it is correct. The simplest way in which one can hope to test any assumed form of interaction is from observation of the collisions between neutrons and protons. Unfortunately the relative velocities of the colliding particles which would give the most decisive test are not easily realized in practice, but the recent advances in the technique of nuclear disintegration have provided a source of neutrons of homogeneous velocity which may be used to give results of a higher precision and definiteness than hitherto. It is our purpose in this paper to describe the results to be expected in such experiments on the assumption of either exchange or ordinary forces, for a variety of forms of interaction. The known binding energies of the nuclei H^2, H^3, He^3, He^4 enable us to restrict considerably the magnitude and range of the forces assumed, and we take account of this in all cases. It is found that there is a fair expectation of positive results from accurate experiments on the angular distribution of protons projected by neutrons of $2\frac{1}{2}$ mV energy provided that the form of the interaction does not approach too closely that of the spherical potential "well", i.e. provided there is an appreciable "tail" to the potential energy curve at large distances of separation.

The calculations have not been restricted to neutrons of this particular energy but have been carried out for energies up to 20 mV. This is important in order to examine what conclusions, if any, can be derived from the experiments already carried out with neutrons, having a wide range of velocities.

1—ORDINARY AND EXCHANGE INTERACTIONS BETWEEN NEUTRON AND PROTON—RESTRICTIONS FROM BINDING ENERGIES OF LIGHT NUCLEI

We suppose the interaction energy between neutron and proton to be capable of representation in the form

$$V_\xi(\mathbf{r})\,P,$$

where $\mathbf{r}$ is the position vector of the proton relative to the neutron and ξ depends on the spin of the two particles. P is an operator which is just unity for ordinary forces but which exchanges the space co-ordinates of the two particles if the force is an exchange one of the Majorana type. We have thus the interactions:

Spins	Exchange forces	Ordinary forces
Parallel ($\xi = t$)	$V_t(r)\quad P(1, 2)$	$V_t(r)$
Antiparallel ($\xi = s$)	$V_s(r)\quad P(1, 2)$	$V_s(r)$

The point at issue is whether the presence or otherwise of the operator $P(1, 2)$ can be verified by experiments on the collisions between slow neutrons and protons. To examine the possibilities in this direction we must consider what restrictions can be placed on the functions V_t, V_s; for the more definite we can make them, the more certain are any conclusions arrived at. We therefore consider a variety of functional forms for V_t, V_s as follows:

(i) Spherical "well" ... ... $V_\xi(r) = -C_\xi, \quad r<a$
$\quad\quad = 0, \quad r>a.$

(ii) "Gauss" potential ... ... $V_\xi(r) = -C_\xi e^{-r^2/a^2}.$

(iii) Inverse fifth power field ... $V_\xi(r) = -C_\xi, \quad r<a$
$\quad\quad = -C_\xi\left(\frac{a}{r}\right)^5, \quad r>a.$

(iv) Exponential field ... ... $V_\xi(r) = -C_\xi e^{-2r/a}.$

In all cases these functions involve only two unknown parameters, and it is assumed that the range of the interaction does not depend on the spins. It is, of course, possible that this is not correct, but we must make some such assumption to proceed at all. There is no *a priori* theoretical justification for any of the forms chosen, except perhaps for (iii), as the neutrino-field theory in its simplest form leads to a potential falling off inversely as the fifth power of the distance (Heisenberg 1934).

The following conditions enable us to restrict the values of the two constants which appear in each assumed function:

(*a*) The interaction energy for parallel spins must be such as to give the correct binding energy (2·2 mV) of the deuteron. This leads in each case to a functional relation between the constants C_t, a, which for fields (i) and (iv) can be written in analytical form. Thus, for (i)

$$\tan\left(\sqrt{(\alpha^2-\kappa^2)}\,a\right) = -\frac{\sqrt{(\alpha^2-\kappa^2)}}{\kappa}, \tag{1}$$

and for (iv)*

$$J_{\kappa a}(\alpha a) = 0, \tag{2}$$

where, in terms of the mass M of neutron or proton, and binding energy E_0 of the deuteron

$$\alpha^2 = \frac{4\pi^2 M}{h^2}C_t, \quad \kappa^2 = \frac{4\pi^2 M}{h^2}E_0.$$

The relation must be worked out numerically for the other two interactions. This has already been done by Bethe and Bacher (1936, p. 111) for the Gauss field, but values for the inverse fifth power field have been worked out specially for this paper and these are given in Table I. The method of deriving them is described in the appendix.

---

* For a proof of this result see Massey and Mohr (1935, p. 225).

(*b*) The interaction energy for antiparallel spins must be such as to give the large elastic cross-section, 4×10^{-23} cm.^{2}, for collision of slow neutrons with protons (Dunning, Pegram, Fink and Mitchell 1935). This requires that the singlet state of the deuteron be a virtual one of 30,000 e-volts energy.

TABLE I—CONSTANTS FOR INVERSE FIFTH POWER FIELD GIVING BINDING ENERGY EQUAL TO THAT OF THE DEUTERON

$a \times 10^{-13}$ cm.	1·5	2·0	2·5	3·0	3·5	4·0	5·0	6·0	7·0	8·0
$C_t a^2$	2·28	2·55	2·86	3·16	3·51	3·86	4·61	5·42	6·30	7·40

From this condition a functional relation between C_0 and a is obtained. For our purposes this may be taken as

$$C_s a^2 = 2{\cdot}31,\ 2{\cdot}69,\ 1{\cdot}56_5,\ 5{\cdot}78_5,$$

for the four cases respectively. These relations are strictly accurate for a virtual level of zero energy and hold quite closely in our case because of the low value of the energy of the virtual level.

(*c*) The force must be such as to give consistent results for the binding energy of the nuclei H^3, He^3 and He^4, assuming the same force between like particles in each case.

This does not provide nearly so definite a restriction as it might for, on the one hand, the non-existence of appreciable three-body forces is assumed, and on the other, there is no absolutely reliable means available for carrying out the calculations with precision. Further, to reduce the number of possibilities we must make some assumption concerning the range of the like particle forces and, as usual, we assume this to be the same as that for the neutron-proton force. Bearing these considerations in mind we can only hope to use the binding energies of the light nuclei to give a probable, but by no means certain, value to the range and hence from (*a*) and (*b*) to the magnitude of the interaction in each case (i)–(iv).

The method which we use for this purpose is that of the equivalent two-body problem in its simplest form, refinements lacking significance in view of the uncertain formulation of the method. As the procedure has been given by Bethe and Bacher (1936, p. 143) we will include only the briefest outline here.

The effective interaction between a neutron and proton in nuclei containing two of either or both, with opposite spin, is

$$\bar{V} = \tfrac{1}{4}V_s + \tfrac{3}{4}V_t,$$

and the influence of the exchange operator is unimportant. Denoting the like particle interaction (of range a and magnitude D) by U, it may be shown that to a close first approximation the equivalent two-body problem gives:

For H^3: Binding energy = that in a two-body problem with same mass as in H^2 but with a potential function of magnitude $2\bar{V} + U$ and range $a/\sqrt{2}$.

For He^4: In this case the two-body problem is for a potential function of magnitude $4\bar{V} + 2U$ and range $a/\sqrt{3}$.

By solving these two-body problems in the same way as for H^2 the values of U necessary to give the corrected values of the binding energies of H^3 and He^4 for functions V_t, V_s of various ranges satisfying (a) and (b) may be calculated. For some range of interaction the values of U derived from both nuclei will agree and this we take as the best value of the range a. The values found are given in Table II.

TABLE II—VALUES OF FIELD PARAMETERS GIVING AGREEMENT WITH OBSERVED BINDING ENERGY OF H^2, H^3 AND He^4

Form of field	$a \times 10^{13}$ cm.	$C_t a^2$	$C_s a^2$	Da^2	D/C_t
(i)	2·90	4·13	2·31	2·48	0·60
(ii)	2·32*	4·48	2·69	2·73	0·61
(iii)	2·2	2·66	$1{\cdot}56_5$	1·64	0·62
(iv)	2·4	10·36	$5{\cdot}78_5$	6·16	0·59

It is to be noted that for all fields the ratio D/C_t is nearly the same and D is not very different from C_s. This is in general agreement with the indications from the scattering of protons by protons† (Tuve, Heydenburg and Hafstad 1936; Breit, Condon and Present 1936).

We use the results of Table II as the basis of our calculations with the different fields, being careful to remember that they are only indications which may or may not be very reliable.

2—CALCULATION OF THE SCATTERING

Consider a beam of neutrons of velocity v passing through a gas of protons. The number of protons projected per unit solid angle in directions making angles between θ and $\theta + d\theta$ with that of the incident beam is then proportional to

---

* This value has been taken directly from Bethe and Bacher's article (1936) where it was obtained by an extended use of the equivalent two-body method. The elementary method employed for the other three fields gives $a = 2{\cdot}5 \times 10^{-13}$ cm. for this case.

† Rarita and Present (1937) have recently shown that the assumption of exact equality between C_s and D is inconsistent with the observed binding energies of ${}_1H^3$ and ${}_2He^4$ even when the calculations are carried out with the maximum possible precision.

$$\cos\theta\{\tfrac{1}{4}J_s(\pi-\theta)+\tfrac{3}{4}J_t(\pi-\theta)\}\,d\theta, \tag{3}$$

where

$$J_\xi(\theta) = |\Sigma(e^{2i\delta_{n\xi}}-1)(2n+1)P_n(\cos\theta)|^2. \tag{4}$$

$\delta_{n\xi}$ is such that the solution of the differential equation

$$\frac{d^2F_n}{dr^2}+\left\{\frac{4\pi^2M}{h^2}(\tfrac{1}{2}Mv^2-\epsilon^nV_\xi(r))+\frac{n(n+1)}{r^2}\right\}F_n = 0, \tag{5}$$

which vanishes at the origin, has the asymptotic form

$$F_n \sim \sin\left(\frac{\pi Mv}{h}r-\tfrac{1}{2}n\pi+\delta_{n\xi}\right). \tag{6}$$

For ordinary forces $\epsilon = 1$, for exchange forces of Majorana type $\epsilon = -1$. The total elastic collision cross-section is

$$\frac{h^2}{32\pi M^2v^2}\int_0^\pi\{J_s(\theta)+3J_t(\theta)\}\sin\theta\,d\theta$$
$$= \frac{h^2}{4\pi M^2v^2}\Sigma_n(\sin^2\delta_{ns}+3\sin^2\delta_{nt})(2n+1). \tag{7}$$

The convergence of the series depends on the fact that $\delta_{n\xi}$ is small for such n that

$$\frac{n(n+1)}{r^2} \gg V_\xi(r) \text{ for } kr \sim n.^* \tag{8}$$

As we restrict ourselves to neutrons with energies not greater than 20 mV it may be easily seen that for the values of the field parameters given in Table II the condition (8) is satisfied for all values of $n > 1$, and we must expect even the phases $\delta_{1\xi}$ to be small.

The calculation of $\delta_{0\xi}$, $\delta_{1\xi}$ for the various fields was carried out as follows:

In all cases $k = \dfrac{\pi Mv}{h}$, $k'^2 = k^2+\alpha^2$.

(i) Here we have the analytical expressions (Massey and Mohr 1935)

$$\delta_0 = \arctan\left(\frac{k}{k'}\tan k'a\right)-ka \quad \text{(for both ordinary and exchange forces)},$$

$$\delta_1 = \arctan(-)^n\frac{kJ_{n-\frac{1}{2}}(ka)J_{n+\frac{1}{2}}(k'a)-k'J_{n-\frac{1}{2}}(k'a)J_{n+\frac{1}{2}}(ka)}{kJ_{-n+\frac{1}{2}}(ka)J_{n+\frac{1}{2}}(k'a)+k'J_{n-\frac{1}{2}}(k'a)J_{-n-\frac{1}{2}}(ka)}$$

(for ordinary forces).

---

* See for example Mott and Massey (1933, p. 25).

δ_1 is obtained for exchange forces by replacing $J_{n\pm\frac{1}{2}}(k'a)$ by $I_{n\pm\frac{1}{2}}(k''a)$ where $k''^2 = \alpha^2 - k^2$.

(ii) and (iii) Both δ_0 and δ_1 were obtained for these fields by numerical integration of the equation (5).

(iv) δ_0 is given by the expression

$$\delta_0 = -ka(\log \tfrac{1}{2}\alpha a + C) + \sum_{n=1}^{\infty}\left(\frac{ka}{n} - \arctan\frac{ka}{n}\right) + \arctan\left\{\tan\left(\alpha a - \tfrac{1}{4}\pi - \arctan\frac{B}{A}\right)\tanh\left(\tfrac{1}{2}ka\pi\right)\right\}, \quad (9)$$

where
$$A = 1 - \sum_{r=1}^{\infty}\frac{(1+4k^2a^2)(3^2+4k^2a^2)\ldots\{(4r-1)^2+4k^2a^2\}}{(2r)!\,2^{6r}(\alpha a)^{2r}},$$

$$B = \sum_{r=1}^{\infty}\frac{(1+4k^2a^2)(3^2+4k^2a^2)\ldots\{(4r-3)^2+4k^2a^2\}}{(2r-1)!\,2^{6r-3}(\alpha a)^{2r-1}},$$

TABLE III—PHASE CONSTANTS FOR DIFFERENT FORMS OF THE NEUTRON-PROTON INTERACTION

			All forces		Exchange forces		Ordinary forces	
k in 10^{13} cm.$^{-1}$	Field	Range 10^{13} cm.	δ_{0t}	δ_{0s}	$-\delta_{1t}$	$-\delta_{1s}$	δ_{1t}	δ_{1s}
0·16	I	3·0*	2·286	1·168	0·0074	$0{\cdot}004_4$	0·0175	$0{\cdot}007_7$
(2·2 mV)	II	2·32*	2·260	1·435	$0{\cdot}012_0$	$0{\cdot}006_4$	—	—
	III	2·2*	2·290	1·300	$0{\cdot}017_0$	$0{\cdot}010_5$	0·030	$(0{\cdot}014_5)$
		3·0	2·225	—	$0{\cdot}042_5$	(0·024)	—	—
	IV	1·75	2·327	1·315	0·012	(0·007)	(0·019)	(0·010)
		2·4*	2·277	1·233	0·032	$0{\cdot}019_5$	0·056	0·026
0·25	I	3·0	1·928	1·096	0·025	0·016	0·068	0·028
(5·4 mV)	III	2·2	1·940	—	0·050	$0{\cdot}032_5$	0·097	$0{\cdot}046_5$
		3·0	1·840	—	0·110	(0·062)	—	—
	IV	2·4	1·930	1·077	(0·091)	0·055	0·176	0·080
0·40	I	3·0	1·482	0·925	0·086	0·056	0·271	0·102
(13·7 mV)	IV	1·75	1·622	1·010	0·113	(0·075)	0·201	(0·110)
		2·4	1·532	0·858	0·213	0·133	0·423	0·192
0·50	I	3·0	1·250	0·805	0·146	0·100	0·466	0·178
(21·5 mV)	II	2·32	—	—	0·206	0·141	—	—
	III	2·2	1·246	—	0·193	0·125	—	—
		3·0	1·136	0·656	0·372	0·201	—	—
	IV	2·4	1·330	0·731	0·297	0·180	—	—

I, Spherical "well" interaction. II, Gaussian interaction.
III, Spherical well and inverse fifth power interaction. IV, Exponential interaction.

* Ranges for which the binding energies of H^3, He^4 are correctly given by the equivalent two-body method. The value for the spherical well is actually $2{\cdot}9 \times 10^{-13}$ cm. but the difference from $3{\cdot}0 \times 10^{-13}$ cm. is unimportant and, in any case, phases may be obtained by interpolation from Table IV. Values in brackets are interpolated.

and $C = 0{\cdot}5772$, Euler's constant. The proof of this result is given in the appendix.

δ_1 must again be calculated by numerical integration.

The values of the phases calculated in this way for various cases are given in Table III. Because of the comparative ease of calculation a much greater range of values are given for the spherical well potential (i) in Table IV. From these it is possible to obtain a very good idea of values for other fields with parameters not included in the table.

TABLE IV—PHASE CONSTANTS GIVEN BY THE SPHERICAL "WELL" INTERACTION

k in 10^{13} cm.$^{-1}$	a in 10^{-13} cm.	All forces		Exchange forces		Ordinary forces	
		δ_{0t}	δ_{0s}	$-\delta_{1t}$	$-\delta_{1s}$	δ_{1t}	δ_{1s}
0·16 (2·2 mV)	1·5	2·41$_3$	1·12$_7$	0·0007$_4$	0·0005$_7$	0·0015	0·0009$_2$
	2·0	2·37$_1$	1·16$_5$	0·0019$_5$	0·0014$_0$	0·0039	0·0022
	2·5	2·32$_8$	1·17$_2$	0·0038$_5$	0·0025$_8$	0·0088	0·0042
	3·0	2·28$_6$	1·16$_8$	0·0071	0·0045	0·0175	0·0071$_5$
	3·5	2·24$_4$	1·15$_1$	0·0115	0·0069$_5$	0·0327	0·0114
	4·0	2·19$_9$	1·13$_0$	0·0180	0·0102	0·0577	0·0169
0·20 (3·4 mV)	1·5	2·27$_5$	1·15$_9$	0·0015	0·0011$_5$	0·0028	0·0017$_5$
	2·0	2·22$_2$	1·17$_2$	0·0036	0·0025$_8$	0·0075	0·0042
	2·5	2·16$_9$	1·16$_4$	0·0074	0·0050$_5$	0·0172	0·0081$_5$
	3·0	2·11$_6$	1·14$_2$	0·0133	0·0085	0·0345	0·0140
	3·5	2·06$_4$	1·11$_2$	0·0217	0·0132	0·064$_9$	0·0222
	4·0	2·01$_0$	1·08$_8$	0·0330	0·0192	0·116	0·032$_5$
0·25 (5·4 mV)	1·5	2·12$_5$	1·17$_4$	0·0029	0·0022	0·0055	0·0034
	2·0	2·06$_0$	1·16$_4$	0·0069	0·0050$_5$	0·0150	0·0081$_5$
	2·5	1·99$_3$	1·13$_5$	0·0139	0·0095$_5$	0·034	0·0159
	3·0	1·92$_8$	1·09$_6$	0·0248	0·0158	0·068	0·0272
	3·5	1·86$_3$	1·04$_9$	0·0399	0·0246	0·128	0·0422
	4·0	1·79$_7$	1·00$_3$	0·0600	0·0354	0·228	0·0615
0·40 (13·7 mV)	1·5	1·78$_7$	1·14$_2$	0·0111	0·0085	0·022$_5$	0·0140
	2·0	1·68$_6$	1·08$_8$	0·0264	0·0192	0·061	0·0325
	2·5	1·58$_1$	1·00$_3$	0·0511	0·0354	0·137	0·0615
	3·0	1·48$_2$	0·925	0·0860	0·0562	0·271	0·102
	3·5	1·38$_5$	0·845	0·131	0·081	0·475	0·151
	4·0	1·28$_8$	0·765	0·193	0·112	0·716	0·206
0·50 (21·5 mV)	1·5	1·62$_1$	1·09$_6$	0·021	0·015$_8$	0·044	0·0272
	2·0	1·49$_5$	1·00$_3$	0·048	0·035$_5$	0·118	0·0615
	2·5	1·37$_1$	0·905	0·090	0·061$_5$	0·255	0·114
	3·0	1·25$_0$	0·805	0·146	0·100	0·466	0·178
	3·5	1·13$_7$	0·708	0·218	0·136	0·703	0·246
	4·0	1·03$_2$	0·616	0·301	0·178	0·887	0·309

3—DISCUSSION OF RESULTS

As there are four parameters, δ_{0t}, δ_{0s}, δ_{1t}, δ_{1s}, required to specify a particular angular distribution, it would appear difficult to illustrate the great variety of possibilities. However, inspection of Table III reveals a number of simplifying features. First, for all fields which satisfy the binding energy requirements in the manner described in § 1, the phases δ_{0t}, δ_{0s} are nearly

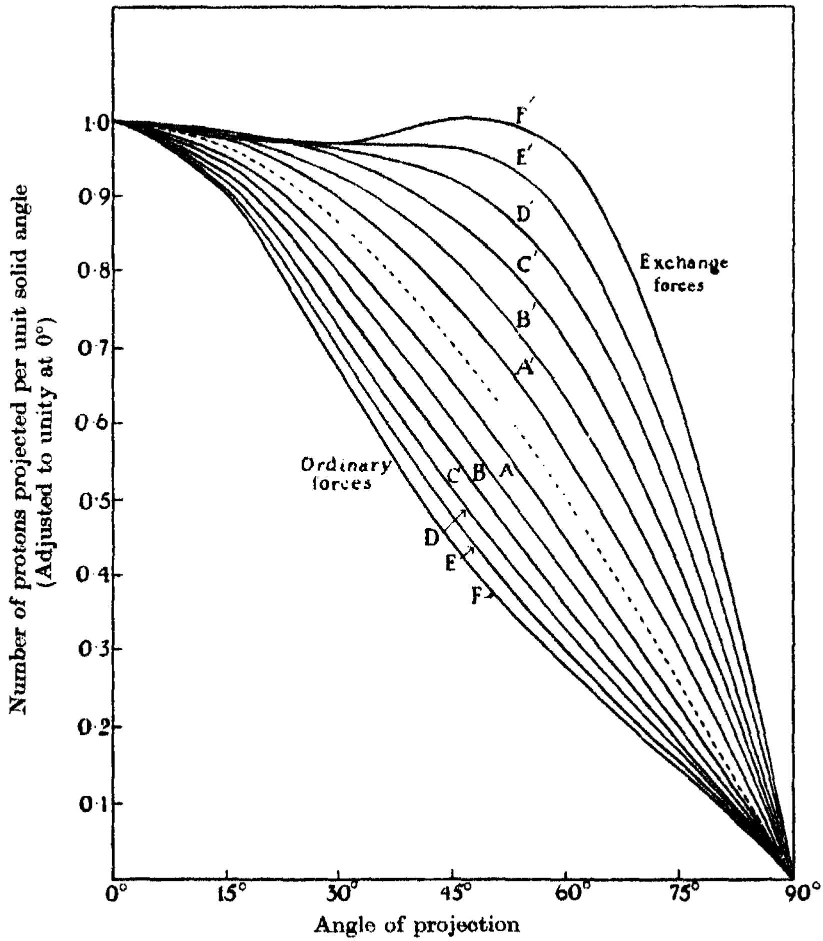

FIG. 1—Angular distributions per unit solid angle of protons projected by neutrons calculated with $\delta_{0t} = 2{\cdot}30$, $\delta_{0s} = 1{\cdot}25$. Curves *A*, *B*, *C*, *D*, *E*, *F* correspond to $\delta_{1t} = 0{\cdot}025$, $0{\cdot}050$, $0{\cdot}075$, $0{\cdot}100$, $0{\cdot}125$, $0{\cdot}150$ respectively, i.e. to ordinary forces. Curves *A′*, *B′*, *C′*, *D′*, *E′*, *F′* correspond to $\delta_{1t} = -0{\cdot}025$, $-0{\cdot}050$, $-0{\cdot}75$, $-0{\cdot}100$, $-0{\cdot}125$, $-0{\cdot}150$ respectively, i.e. to exchange forces. The broken curve corresponds to $\delta_{1t} = 0$.

independent of the form of the field for each particular neutron energy. Secondly, the phases δ_{1s} for such fields are roughly 0·6 time as great as the corresponding δ_{1t}. Since neither δ_{0s} nor δ_{1s} plays as important a role in determining the form of the angular distribution as the phases for the paralle spin interaction we suppose, for purposes of discussion, that $\delta_{1s} = 0{\cdot}6\delta_{1t}$ and that δ_{0s} bears a definite relation to δ_{0t} irrespective of the form of the field. With these assumptions we have calculated the angular distribution function (3) for four values of δ_{0t} and a variety of values of δ_{1t}, taking in each case a value of δ_{0s} agreeing with that to be expected from Table III and $\delta_{1s} = 0{\cdot}6\delta_{1t}$ throughout. Thus figs. 1, 2, 3, 4 represent the results for the four pairs of values $\delta_{0t} = 2{\cdot}30$, $\delta_{0s} = 1{\cdot}25$; $\delta_{0t} = 2{\cdot}10$, $\delta_{0s} = 1{\cdot}12$; $\delta_{0t} = 1{\cdot}90$, $\delta_{0s} = 1{\cdot}00$; $\delta_{0t} = 1{\cdot}70$, $\delta_{0s} = 0{\cdot}90$. In all the figures the magnitudes of the various ordinates have been adjusted to agree at 0°.

With this choice of zero order phases, fig. 1 represents the possibilities for various forms of interaction for neutrons of 2·2 mV energy, since for such neutrons it appears that $\delta_{0t} \simeq 2{\cdot}30$ independently of the form of field. Similarly the other figures refer to 3·6, 5·6, and 6·9 mV neutrons. Even if the field parameters chosen by the equivalent two-body method of § 1 are not exactly correct it is possible to estimate the proper value of δ_{0t} to be taken for each energy and again make use of the diagrams given. The only change, in fact, would be that they would refer to different values of the neutron energy.

The curves for negative δ_{1t} phases correspond to exchange forces, those for positive phases to ordinary forces. It will be seen then that the clearest distinction between these two possibilities arises for a long range interaction at the low energies of impact. Thus for 2·2 mV neutrons (fig. 1), exchange forces give rise to curves lying above that given by $\delta_{1t} = 0$, whereas the curves for ordinary forces all lie below. At this energy also the effect of a given finite value of δ_{1t}, in causing a departure from the curve for vanishing δ_{1t} at the smaller angles of scattering, is more marked than at higher energies. The reason for this is that for a clear distinction between angular distributions for positive and for negative δ_{1t} to occur, δ_{0t} should be approximately $3\pi/4$ (giving $\sin 2\delta_{0t} \simeq 1$) and at the same time δ_{1t} not too small. We have seen that the condition for δ_{0t} is satisfied by 2·2 mV neutrons. Although δ_{1t} increases at first with the neutron energy, δ_{0t} decreases and the corresponding decrease in $\sin 2\delta_{0t}$ may offset the increase in δ_{1t}. In fig. 4 the distinction between ordinary and exchange forces is not at all marked, since here $\delta_{0t} \simeq \pi/2$ and $\sin 2\delta_{0t}$ is small.

It would seem by reference to Table III that it should be possible to distinguish experimentally between ordinary and exchange forces using 2·2 mV neutrons if the form of the interaction is well represented by the exponential type of field (iv). The simplest way of interpreting experimental results is to determine which, if any, of the curves given for the particular neutron energy (figs. 1–4) most nearly agrees with the observed one. This decides the appropriate value of δ_{1t}, which can then be compared with those given in Table III. Unfortunately the experimental information available at present is not sufficiently definite for this purpose. Kurie (1933) and Harkins, Kamen, Newson and Gans (1936) have measured the number of protons projected at various angles by neutrons from a beryllium source and find a distribution departing markedly from that given by $\delta_{1t} = 0$. Their results are not in detailed agreement, but both find relatively more protons projected at small angles than would be expected if δ_{1t} is negligible.

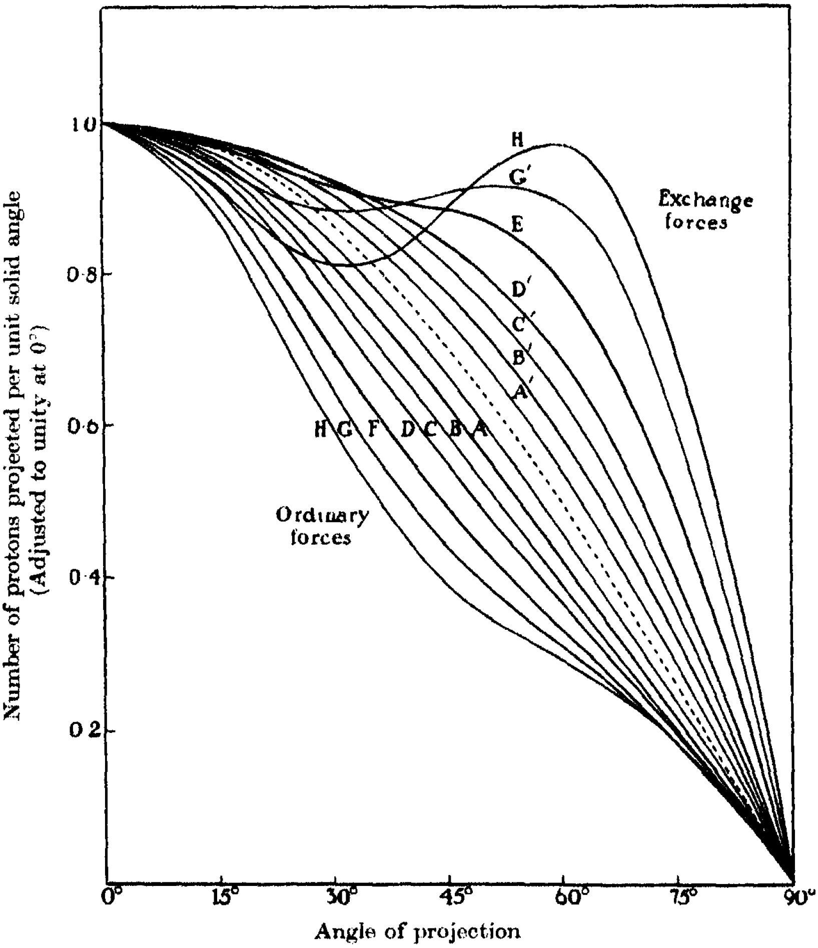

FIG. 2—As for fig. 1 with $\delta_{0t} = 2\cdot10$, $\delta_{0s} = 1\cdot12$. Curves *A*–*F*, *A′*–*F′* as before. Curves *G*, *H* refer to $\delta_{1t} = 0\cdot200$ and $0\cdot250$ respectively and *G′*, *H′* to the corresponding negative values.

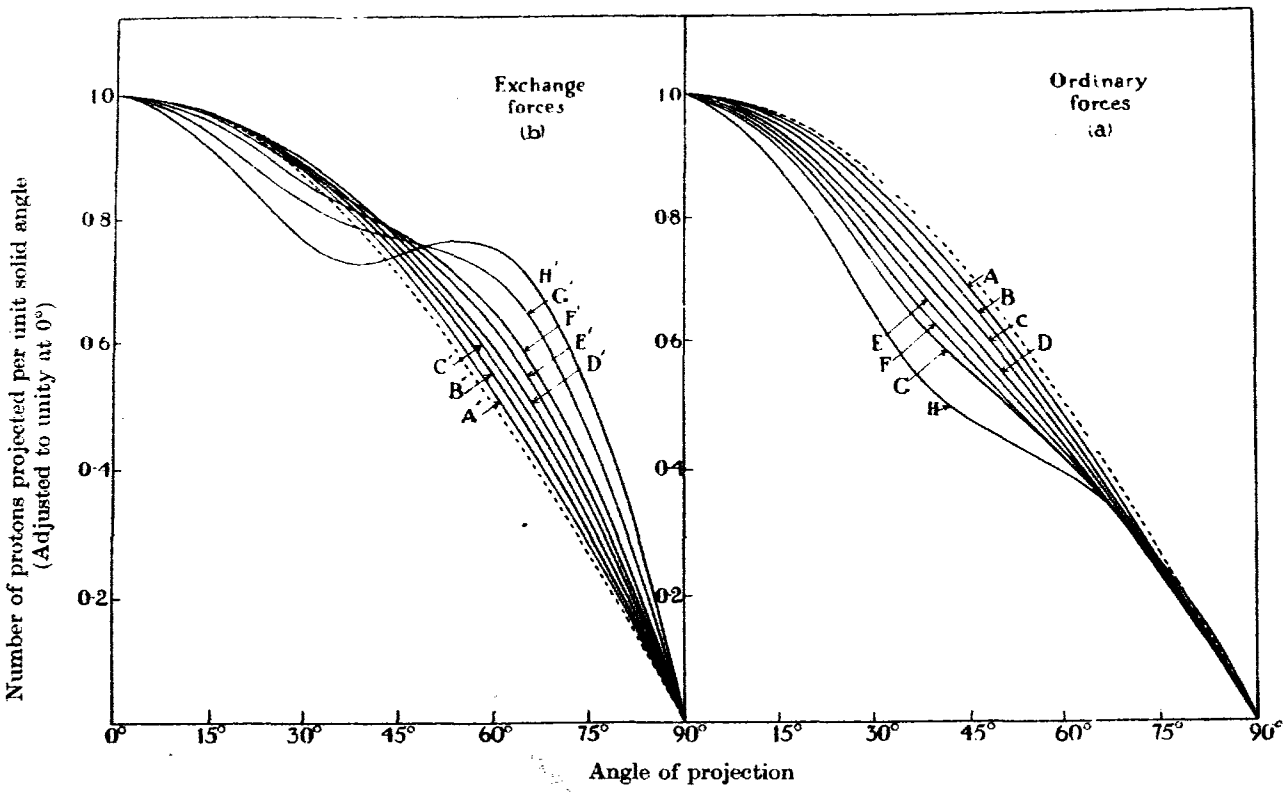

FIG. 3—As for figs. 1 and 2, with $\delta_{0t} = 1 \cdot 90$, $\delta_{0s} = 1 \cdot 00$.

(*a*) Curves *A*–*H* as before. (Ordinary forces.)

(*b*) Curves *A′*–*H′* as before. (Exchange forces.)

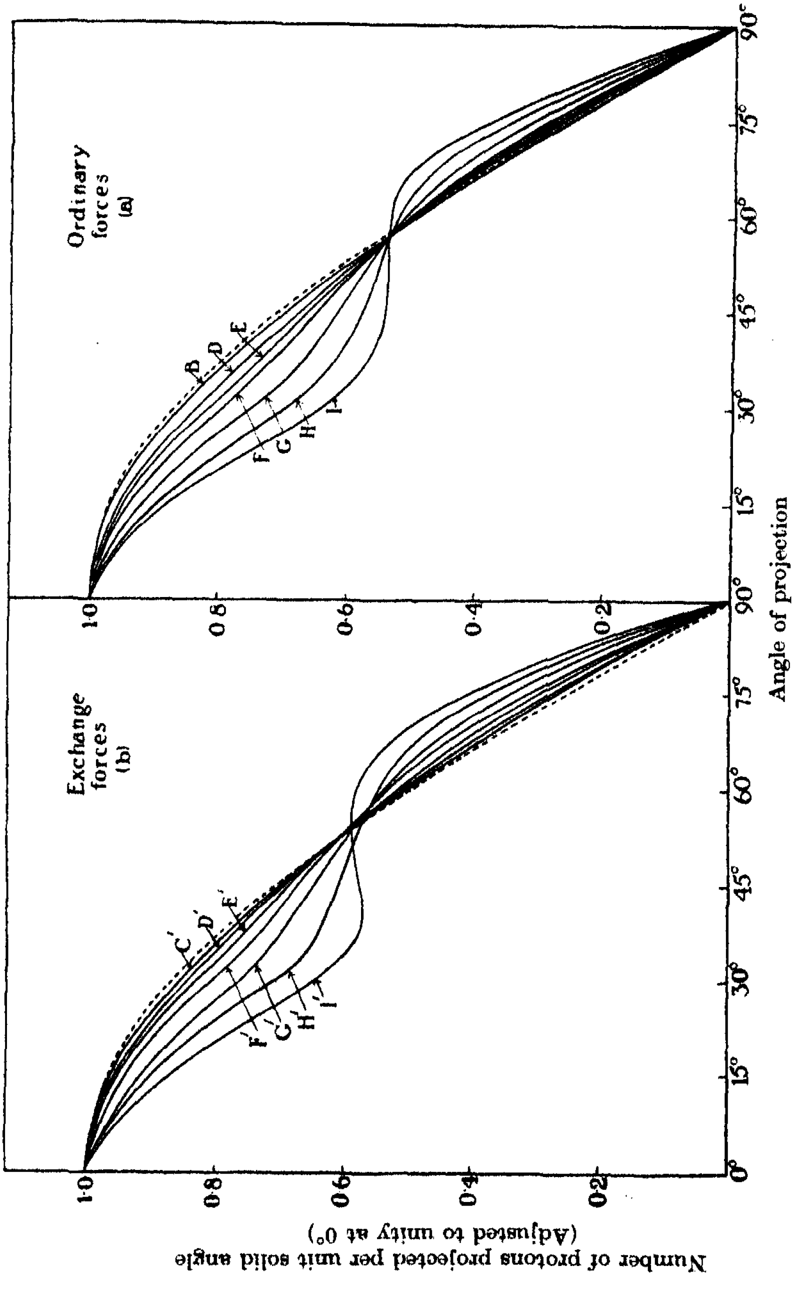

FIG. 4—As for preceding figures, with $\delta_{0t} \doteq 1\cdot70$, $\delta_{0s} = 0\cdot90$.

(*a*) Curves *B*–*H* as before. Curve *I* refers to $\delta_{1t} = 0\cdot300$. (Ordinary forces.)

(*b*) Curves *C*′–*H*′ as before. Curve *I*′ refers to $\delta_{1t} = -0\cdot300$. (Exchange forces.)

The difficulty in interpreting such results arises from the wide distribution in energy of the incident neutrons. It is probable that a large proportion of the neutrons used had energies in the neighbourhood of 5 mV, but there were certainly considerable numbers of much slower neutrons besides others of higher energy. This leads to difficulties not only in the direct comparison with theory but also in other directions discussed by Dee and Gilbert (1937). On these grounds it does not seem desirable to attempt any comparison with our theoretical results. It will suffice to say that, if we were to take the observed distribution as characteristic of 5·6 mV neutrons, comparison with the curves of fig. 3 shows that a positive δ_1 phase $> 0{\cdot}25$ (i.e. ordinary forces) would be necessary to explain the results. Reference to Table III shows that such a large value is most unlikely. It is true that Morse, Fisk and Schiff (1937), assuming exchange forces (i.e. $\delta_{1\xi} < 0$), have obtained theoretical distribution curves resembling the experimental ones, but in order to do this they found it necessary to suppose that the neutrons employed in the experiments had the almost inconceivably high energy of 20 mV.

In an accompanying paper Dee and Gilbert describe the results of a detailed examination of the distribution of protons projected by the neutrons arising from the reaction

$$ {}_1\mathrm{H}^2 + {}_1\mathrm{H}^2 \rightarrow {}_2\mathrm{He}^3 + {}_0n^1. $$

These neutrons form a homogeneous group with energy 2·2 mV, so no difficulties due to energy spread occur, and at the same time it is possible to allow for the scattering of the neutrons within the cloud chamber. However, a very great number of observations must be made to reduce the statistical error. The results when compared with the curves of fig. 1 correspond to $\delta_1 = 0{\cdot}075$, i.e. to ordinary forces, but the statistical error is such that it is really only possible to say that the true curve lies between those for $\delta_{1t} = 0{\cdot}075$ and $\delta_{1t} = 0{\cdot}0$. It is even possible, though unlikely, that δ_{1t} may have a small negative value, so we are not yet in a position to decide between ordinary and exchange forces. Until the statistical error of the observations is reduced further discussion would be pointless. The great desirability of further experimental results is evident.

We should like to express our thanks to Drs. Dee and Gilbert for their assistance in the discussion of experimental matters and for providing us with details of their own experimental results in advance of publication.

APPENDIX

I—*Calculations of the Binding Energy for the Fifth-Power Law Interaction*

The radial wave equations for the *s*-states in the field (iii) are

$$\frac{d^2\psi}{dr^2}+(\alpha^2-\kappa^2)\psi=0, \quad r<a,$$

$$\frac{d^2\psi}{dr^2}+\left\{\alpha^2\left(\frac{a}{r}\right)^5-\kappa^2\right\}\psi=0, \quad r>a;$$

where $$\alpha^2=4\pi^2MC/h^2, \quad \kappa^2=4\pi^2ME_0/h^2.$$

ψ must vanish for $r=0$ and remain finite in the range $0\leqslant r\leqslant\infty$. Since E_0 is a fixed binding energy the problem is one of determining the proper values of α^2 for given κ and various values of a. For the interaction of particles with antiparallel spins, E_0 can be taken as zero without important error, and it was found convenient to use Thomas's iterative method (1937) of determining proper values; three successive approximations in this method fix the value of α^2a^2 between 1·56 and 1·57. The problem for parallel spins, for which E_0 is not negligible, is best considered as a perturbation of the spherical "well" problem, in which the interaction vanishes for $r>a$. This gives quite a good approximation, and then the proper value of α^2 can easily be obtained as follows:

The radial wave equation in the form

$$\frac{d\eta}{dr}=\eta^2-\kappa^2+\alpha^2\left(\frac{a}{r}\right)^5,$$

where $$\eta=-\frac{1}{\psi}\frac{d\psi}{dr},$$

is integrated by a numerical method, inwards from large values of r to a, using the approximate value of a^2. When the value of η at a is obtained, the solution of the equation for $r<a$ is considered and the value of α^2 determined which gives the same value of η at a. This should agree with that used in the inward integration if it is the proper value; otherwise it is usually sufficiently accurate to adopt the mean of the two values of α^2. It is clear that the calculation is facilitated by choosing an interaction such as (iii), in which the potential is constant within $r=a$.

II—*Calculation of Zero Order Phases for the Exponential Field*

For this field, the radial wave equation for *s*-states can be written

$$\frac{d^2\psi}{dr^2}+(k^2+\alpha^2e^{-2r/a})\psi=0,$$

and we require a solution vanishing at the origin and with asymptotic form $\sin(kr+\delta_0)$. The substitution $x = e^{-r/a}$ enables one to obtain the general solution in the form

$$\psi = AJ_{ika}(\alpha a e^{-r/a}) + BJ_{-ika}(\alpha a e^{-r/a}).$$

This must vanish at the origin, so

$$A/B = -J_{-ika}(\alpha a)/J_{ika}(\alpha a).$$

For large r we now have, using the series expansion of the Bessel functions (Whittaker and Watson 1927),

$$\begin{aligned}\psi &\sim C\left\{\frac{e^{-ikr}}{\Gamma(1+ika)} J_{-ika}(\alpha a)\left(\frac{\alpha a}{2}\right)^{ika} - \frac{e^{ikr}}{\Gamma(1-ika)} J_{ika}(\alpha a)\left(\frac{\alpha a}{2}\right)^{-ika}\right\}\\ &= C' \sin(kr+\delta_0),\end{aligned}$$

where

$$\begin{aligned}\delta_0 &= \arg\left\{\frac{J_{ika}(\alpha a)}{\Gamma(1-ika)}\left(\frac{\alpha a}{2}\right)^{-ika}\right\}\\ &= -ka(0{\cdot}5772 + \log \tfrac{1}{2}\alpha a) + \sum_{n=1}^{\infty}\left(\frac{ka}{n} - \arctan\frac{ka}{n}\right) + \arg J_{ika}(\alpha a).\end{aligned}$$

The last term may conveniently be calculated by using the asymptotic expression for the Bessel functions:

$$\begin{aligned}J_n(z) \sim \left(\frac{2}{\pi z}\right)^{\frac{1}{2}}\Bigg[&\cos(z - \tfrac{1}{2}n\pi - \tfrac{1}{4}\pi)\\ &\times\left\{1 + \sum_{r=1}^{\infty}\frac{(-1)^r\{4n^2-1^2\}\{4n^2-3^2\}\ldots\{4n^2-(4\pi-1)^2\}}{(2r)!\,2^{6r}z^{2r}}\right\}\\ &+ \sin(z - \tfrac{1}{2}n\pi - \tfrac{1}{4}\pi)\sum_{r=1}^{\infty}(-1)^r\frac{\{4n^2-1^2\}\{4n^2-3^2\}\ldots\{4n^2-(4r-3)^2\}}{(2r-1)!\,2^{6r-3}\,z^{2r-1}}\Bigg],\end{aligned}$$

giving the formula (9) of § 2.

SUMMARY

The possibility of deciding the nature of the force between a neutron and proton from experiments on the angular distribution of protons projected by neutron collision is considered in detail. Calculations have been carried out for both ordinary and exchange types of interaction using four different functional forms—the "spherical well", the "Gauss" function, the spherical well plus inverse fifth power "tail", and the exponential function. Account is taken of the binding energies of $_1H^2$, $_1H^3$, $_2He^3$ and $_2He^4$ to limit the

possibilities, and it is found that it should be possible to distinguish between ordinary and exchange forces from experiments using neutrons with energies as low as 2·2 mV, provided the form of the interaction does not resemble the spherical well too closely. Tables and figures are provided which can be used to interpret experimental results. The available experimental information is not definite enough for any reliable conclusion to be drawn.

REFERENCES

Bethe and Bacher 1936 *Rev. Mod. Phys.* **8**, 82.
Breit, Condon and Present 1936 *Phys. Rev.* **50**, 825.
Dee and Gilbert 1937 *Proc. Roy. Soc.* A, **163**, 265.
Dunning, Pegram, Fink and Mitchell 1935 *Phys. Rev.* **48**, 265.
Harkins, Kamen, Newson and Gans 1936 *Phys. Rev.* **50**, 980.
Heisenberg 1932 *Z. Phys.* **77**, 1.
— 1934 Lectures at Cavendish Lab., Cambridge (unpublished).
Kurie 1933 *Phys. Rev.* **44**, 463.
Majorana 1933 *Z. Phys.* **82**, 137.
Massey and Mohr 1935 *Proc. Roy. Soc.* A, **148**, 206.
Morse, Fisk and Schiff 1937 *Phys. Rev.* **51**, 706.
Mott and Massey 1933 "Theory of Atomic Collisions." Oxford Univ. Press.
Rarita and Present 1937 *Phys. Rev.* **51**, 788.
Thomas 1937 *Phys. Rev.* **51**, 202.
Tuve, Heydenburg and Hafstad 1936 *Phys. Rev.* **50**, 806.
Whittaker and Watson 1927 "Modern Analysis." 4th ed. Camb. Univ. Press.

Electrosmosis between Plane Parallel Walls produced by High-Frequency Alternating Currents

By L. Rosenhead, Ph.D., D.Sc. and J. C. P. Miller, M.A., Ph.D.

(With Note by J. J. Bikerman)

(*Communicated by W. C. M. Lewis, F.R.S.—Received* 29 *June* 1937)

1—Introduction

The problem of the motion, under the influence of high-frequency alternating currents, of fluid between plane parallel walls whose distance apart is very small, appears to be of interest in certain branches of Physical Chemistry. The following paper contains a mathematical treatment of this type of motion under certain specified conditions. We are greatly indebted to Mr. J. J. Bikerman of the Chemistry Department of the University of Manchester for having brought the problem to our notice, and for having given us a great deal of information concerning the physics of the phenomena involved.

In general, when two different substances, or phases, have a common surface, there is an electrokinetic potential difference between them. This is produced by an electric double layer of ions in contact with the common surface. Consider the boundary between a solid and an electrolyte, and let us assume the solid to take a negative charge, as is almost invariably the case when the electrolyte is water or a very dilute aqueous solution. The negative layer consists, probably, of ions adsorbed *rigidly* to the surface. Near the surface, in the fluid, there will be a preponderance of positively charged ions held more or less firmly in position by electrostatic forces. Very close to the "rigid" layer of negative ions the electrostatic forces will be sufficiently great to keep the positive ions rigidly in place. As we leave the solid surface the forces diminish and ultimately a position is reached where diffusion and thermal forces overcome the electrostatic forces. Beyond this surface in the fluid there will still be a preponderance of positive ions, since the electrostatic forces will still be operative, but these ions will be mobile. At points remote from the solid surface there are approximately equal concentrations of positive and negative ions, and the liquid as a whole is electrically neutral. The equilibrium attained when electrostatic and diffusion forces are operating was first calculated by Gouy; the expression given by Gouy for the charge density is used in this paper. On applying an electric field the mobile ions in the layer near the surface begin to move towards one or other of the two electrodes as illustrated diagramatically in fig. 1, and this motion is transmitted to the liquid as a whole through the operation of viscous forces. As the fluid close to the walls contains more positive ions than negative ions greater forces will be called into play near the walls than in the body of the fluid, and, in a constant field, the liquid will move to the cathode. This phenomenon of the movement of a liquid over a fixed surface under the influence of an applied electric field is called "electrosmosis" or "endosmosis".

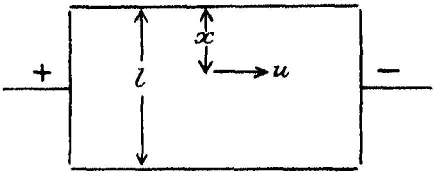

FIG. 1

Section 2 contains a list of the principal symbols used in the investigation and § 10 contains a summary of the principal results. The mathematical investigation is contained in the intervening sections.

2—LIST OF SYMBOLS

u is the velocity of the fluid in a direction parallel to the walls;
x the distance from one wall;
m the density of the liquid;
η its viscosity;
t the time;
l the distance between the walls;
$E\cos\omega t$ the field strength;
ν the valency of the ions of the electrolyte (which is assumed to be binary);
F the "faraday", equal to 96494 coulombs $= 2{\cdot}89 \times 10^{14}$ electrostatic units;
C the concentration of the electrolyte between the walls;
ζ the electrokinetic potential difference;
R Boltzmann's constant, equal to $8{\cdot}32 \times 10^7$ erg/degree;
T the absolute temperature;
D the dielectric constant of the solution;

$$A = \frac{\exp(-\nu F\zeta/2RT)+1}{\exp(-\nu F\zeta/2RT)-1}; \quad a = \log_e A;$$

$\alpha = 2\nu F(2\pi C/DRT)^{\frac{1}{2}}$; $\quad n^2 = m\omega/\alpha^2\eta$;

$8\nu FC\dfrac{Ae^{\alpha x}(A^2e^{2\alpha x}+1)}{(A^2e^{2\alpha x}-1)^2}$ is, according to Gouy (1910) and Bikerman (1933), the volume density of the electric charge in the liquid at a distance x from a plane wall;

$G = E.4\nu FC$; $H = G/\alpha^2\eta = E.4\nu FC/\alpha^2\eta$;

$\xi = \alpha(x-\frac{1}{2}l)$; $\lambda = a+\frac{1}{2}\alpha l$;

y, P and Q are functions, the last two real functions, of ξ (or of x), which are defined in such a way that u is the real part of

$$He^{i\omega t}y(\xi) \quad \text{and} \quad y = P+iQ,$$

so that
$$u = H(P\cos\omega t - Q\sin\omega t);$$

y_r and f_r are functions connected with the expansion of y as a series in powers of n^2, they are defined in § 5 for $r = 0, 1, 2, \ldots$, etc., and their expansions are given in equations (6·2), (6·3), (6·5). They are connected by the relation

$$y_r = f_r(\lambda+\xi)+f_r(\lambda-\xi);$$

Y_r is the value of y_r when $\xi = \pm\frac{1}{2}\alpha l$;

$F(x)$ and ϵ are defined by means of the relation

$$u = HF(x)\cos(\omega t-\epsilon);$$

$F(x) = (P^2+Q^2)^{\frac{1}{2}}$ is the greatest value of u/H attained at a given value of x;

$\epsilon = \tan^{-1}(-Q/P)$ is the phase-lag.

The orders of magnitude of some of the above constants, in the range of experiments considered, are given by the following set of approximate values:

$\eta = 10^{-2}$ g./cm.sec.; $m = 1$ g./cm.^{3}; $E = 10^{-2}$ g.$^{\frac{1}{2}}$/cm.$^{\frac{1}{2}}$sec.; $A = 1{\cdot}01$ to 2 (dimensionless); $8\nu FC$ about 10^9 g.$^{\frac{1}{2}}$/cm.$^{\frac{3}{2}}$sec.; $\alpha = 10^6$ cm.$^{-1}$; $l = 10^{-4}$ cm.; ω lies between 10^2 and 10^5 sec.$^{-1}$; αl is greater than 20; n^2 lies between 10^{-5} and 10^{-8}; $n\alpha l$ is less than 1 (the last three quantities are dimensionless).

In an electric field of constant strength the highest velocity (u) usually observed is less than 5×10^{-3} cm./sec. When $l = 10^{-4}$, electrical measurements of "surface conductivity" can be made with an error of ± 3 %, but when $l = 10^{-3}$ the error is roughly ± 20 %.

3—The Equation and the Complementary Solution

We consider the motion of fluid, between two plane parallel walls whose distance apart is l, under the influence of an applied electric field whose strength is $E\cos\omega t$. Accepting the formula suggested by Gouy (1910) for the volume density of the electric charge in liquid at a distance x from a plane wall, the equation to be satisfied by u, the velocity of the fluid in a direction perpendicular to x, is

$$m\frac{\partial u}{\partial t}-\eta\frac{\partial^2 u}{\partial x^2}=Ge^{i\omega t}\left[\frac{2Ae^{\alpha x}\{A^2e^{2\alpha x}+1\}}{\{A^2e^{2\alpha x}-1\}^2}+\frac{2Ae^{\alpha(l-x)}\{A^2e^{2\alpha(l-x)}+1\}}{\{A^2e^{2\alpha(l-x)}-1\}^2}\right], \quad (3\cdot1)$$

where
$$G=E.4\nu FC. \quad (3\cdot2)$$

The equation (3·1) is derived from the ordinary equations of motion of a viscous fluid on the assumption (i) that the velocities are so small that squares and higher powers can be neglected, and (ii) that the direction of the motion is parallel to the direction of the applied electric force. (In the experiments under investigation u is never greater than 5×10^{-3} cm./sec.) In the equation the electric force has been written as $Ee^{i\omega t}$, and this must be interpreted as meaning that the velocity u is the real part of the solution obtained from (3·1). Further, the boundary conditions to be satisfied by u are

$$u=0 \text{ at } x=0 \text{ and } x=l. \quad (3\cdot3)$$

Since the equation is linear in u, the solution may be split up into (i) a complementary solution and (ii) a particular integral. The complementary solution satisfies the equation

$$m\frac{\partial u}{\partial t}-\eta\frac{\partial^2 u}{\partial x^2}=0, \quad (3\cdot4)$$

and it can be shown very easily that the only solution of (3·4) which satisfies (3·3) is

$$u=\Sigma K_r\exp(-\eta r^2\pi^2t/l^2m)\sin(r\pi x/l), \quad (3\cdot5)$$

where the summation is over all integral values of r from 1 to ∞, and where each K_r is a constant.

The solution (3·5) represents the free oscillations. If we substitute $\eta=10^{-2}$, $l=10^{-4}$, $m=1$ c.g.s. units as typical values of the constants, we see that these oscillations die away very rapidly. The coefficients of t in the exponentials are always negative, and that coefficient which corresponds to $r=1$ is the one that is numerically least. The coefficient in this case is approximately (-10^7), so that the first term in (3·5) diminishes in the ratio $1/e$ in 10^{-7} sec.; other terms diminish even more rapidly. We shall therefore neglect the free oscillations in the following paragraphs.

4—CHANGE OF INDEPENDENT VARIABLE AND THE PARTICULAR INTEGRAL IN THE GENERAL CASE

The equation (3·1) can be simplified by a change of variable. We write

$$\xi = \alpha(x - \tfrac{1}{2}l), \quad \lambda = a + \tfrac{1}{2}\alpha l, \quad \text{where } a = \log_e A. \tag{4·1}$$

The equation now becomes

$$m\frac{\partial u}{\partial t} - \alpha^2\eta\frac{\partial^2 u}{\partial \xi^2} = Ge^{i\omega t}\left[\frac{\cosh(\lambda+\xi)}{\sinh^2(\lambda+\xi)} + \frac{\cosh(\lambda-\xi)}{\sinh^2(\lambda-\xi)}\right], \tag{4·2}$$

and the boundary conditions (3·3) become

$$u = 0, \quad \text{when } \xi = \pm\tfrac{1}{2}\alpha l. \tag{4·3}$$

We seek a solution of the form

$$u = (G/\alpha^2\eta)\,e^{i\omega t}y(\xi) = He^{i\omega t}y(\xi), \tag{4·4}$$

by which we mean that u is the real part of the expression on the right-hand side of (4·4). If

$$y(\xi) = P + iQ, \tag{4·5}$$

where P and Q are real functions, then

$$\begin{aligned} u &= H(P\cos\omega t - Q\sin\omega t) \\ &= HF(\tfrac{1}{2}l + \xi/\alpha)\cos(\omega t - \epsilon), \end{aligned} \tag{4·6}$$

where ϵ, the phase difference, and $F(x)$ are given by

$$\epsilon = \tan^{-1}(-Q/P), \quad F(x) = F(\tfrac{1}{2}l + \xi/\alpha) = (P^2+Q^2)^{\frac{1}{2}}. \tag{4·7}$$

Substituting (4·4) in (4·2), we find

$$\frac{d^2y}{d\xi^2} - i\frac{m\omega}{\alpha^2\eta}y = -[\coth(\lambda+\xi)\operatorname{cosech}(\lambda+\xi) + \coth(\lambda-\xi)\operatorname{cosech}(\lambda-\xi)], \tag{4·8}$$

$$\text{or} \quad y'' - in^2y = -[\coth(\lambda+\xi)\operatorname{cosech}(\lambda+\xi) + \coth(\lambda-\xi)\operatorname{cosech}(\lambda-\xi)], \tag{4·9}$$

where

$$n^2 = m\omega/\alpha^2\eta. \tag{4·10}$$

The equation (4·9) is a particular case of the more general equation

$$y'' - in^2y = S, \tag{4·11}$$

where S is an even function of ξ. The solution to this, which satisfies end conditions $y = 0$ when $\xi = \pm h$, is

$$y = \frac{1}{2n} e^{i3\pi/4}\Big[Y\cosh(n\xi e^{i\pi/4}) + \exp(n\xi e^{i\pi/4})\int_0^\xi \exp(-n\xi e^{i\pi/4})\,S\,d\xi$$

$$-\exp(-n\xi e^{i\pi/4})\int_0^\xi \exp(n\xi e^{i\pi/4})\,S\,d\xi\Big], \qquad (4{\cdot}12)$$

where $$Y = -\operatorname{sech}(nhe^{i\pi/4})\Big[\exp(nhe^{i\pi/4})\int_0^h \exp(-n\xi e^{i\pi/4})\,S\,d\xi$$

$$-\exp(-nhe^{i\pi/4})\int_0^h \exp(n\xi e^{i\pi/4})\,S\,d\xi\Big]. \qquad (4{\cdot}13)$$

This form of y is symmetrical about $\xi = 0$. A solution which is not symmetrical about $\xi = 0$, but which satisfies the same end conditions, can be obtained in a similar form when S is not even.

5—SUCCESSIVE APPROXIMATIONS TO THE PARTICULAR INTEGRAL

In the present case n^2 is a small non-dimensional quantity not exceeding 10^{-5}, so that we can approximate to the solution of (4·9) or (4·11) by means of an expansion in powers of n^2. We can write (4·11) in the form

$$(D^2 - in^2)\,y = S, \qquad (5{\cdot}1)$$

whence

$$\begin{aligned} y - L\cosh(n\xi e^{i\pi/4}) - M\sinh(n\xi e^{i\pi/4}) &= (D^2 - in^2)^{-1} S \\ &= \frac{1}{D^2}\left(1 + i\frac{n^2}{D^2} - \frac{n^4}{D^4} - i\frac{n^6}{D^6} + \ldots\right) S \\ &= y_0 + in^2 y_2 - n^4 y_4 - in^6 y_6 + \ldots, \end{aligned} \qquad (5{\cdot}2)$$

where L and M are constants and where

$$y_0 = \int^x dx \int^x S\,dx, \quad y_r = \int^x y_{r-1}\,dx. \qquad (5{\cdot}3)$$

We shall see later, from the inequality (6·7), that (5·2) is always valid if $n^2 \leqslant 1$. Putting

$$y_r = f_r(\lambda + \xi) + f_r(\lambda - \xi) = f_r\{\alpha x + a\} + f_r\{\alpha(l - x) + a\}, \qquad (5{\cdot}4)$$

and using the value of S given in (4·9), we have

$$f_0(z) = \log_e(\tanh \tfrac{1}{2}z), \tag{5·5}$$

and

$$f_r(z) = -\int_z^{\infty} f_{r-1}(z)\,dz. \tag{5·6}$$

(The limits of integration are chosen in this way because, as will be seen later in § 6, they make $f_r(\infty) = 0$ for all values of r.) Applying the boundary conditions, $y = 0$ when $\xi = \pm\tfrac{1}{2}\alpha l$, we find $M = 0$ and

$$y = L\cosh(n\xi e^{i\pi/4}) + y_0 + in^2y_2 - n^4y_4 - in^6y_6 + \dots, \tag{5·7}$$

where

$$L = -\operatorname{sech}(\tfrac{1}{2}n\alpha l e^{i\pi/4})\,(Y_0 + in^2Y_2 - n^4Y_4 - in^6Y_6 + \dots), \tag{5·8}$$

in which Y_r is the value of y_r when $\xi = \pm\tfrac{1}{2}\alpha l$. Since y_0 is an even function of ξ, y_2, y_4, etc. are also even functions of ξ; and as $\cosh(n\xi e^{i\pi/4})$ is another even function of the argument, we see that y is symmetrical about $\xi = 0$. Applying this to (4·4) we see that the velocity profile of the forced oscillations is symmetrical with respect to the walls. Though the free oscillations are not in general symmetrical in this way they are damped out very rapidly, and in practice the observed velocity profile is always a symmetrical one.

Now, if $|\theta| < \tfrac{1}{2}\pi$,

$$\operatorname{sech}\theta = 1 - \frac{E_1}{2!}\theta^2 + \frac{E_2}{4!}\theta^4 - \frac{E_3}{6!}\theta^6 + \dots, \tag{5·9}$$

where E_r is the rth Euler number (in particular $E_1 = 1$, $E_2 = 5$, $E_3 = 61$, $E_4 = 1385$, etc.), so that

$$\operatorname{sech}(\tfrac{1}{2}n\alpha l e^{i\pi/4}) = 1 - i\frac{E_1}{2!}(\tfrac{1}{2}n\alpha l)^2 - \frac{E_2}{4!}(\tfrac{1}{2}n\alpha l)^4 + i\frac{E_3}{6!}(\tfrac{1}{2}n\alpha l)^6 + \dots. \tag{5·10}$$

If we write $L = L_1 + iL_2$, where L_1 and L_2 are real, we have, from (5·8) and (5·10),

$$\begin{aligned} L_1 = -Y_0 &+ n^4\left\{Y_4 - \frac{E_1}{2!}(\tfrac{1}{2}\alpha l)^2Y_2 + \frac{E_2}{4!}(\tfrac{1}{2}\alpha l)^4Y_0\right\} \\ &- n^8\left\{Y_8 - \frac{E_1}{2!}(\tfrac{1}{2}\alpha l)^2Y_6 + \frac{E_2}{4!}(\tfrac{1}{2}\alpha l)^4Y_4 - \frac{E_3}{6!}(\tfrac{1}{2}\alpha l)^6Y_2 + \frac{E_4}{8!}(\tfrac{1}{2}\alpha l)^8Y_0\right\} + \dots, \end{aligned} \tag{5·11}$$

$$\begin{aligned} L_2 = &-n^2\left\{Y_2 - \frac{E_1}{2!}(\tfrac{1}{2}\alpha l)^2Y_0\right\} \\ &+ n^6\left\{Y_6 - \frac{E_1}{2!}(\tfrac{1}{2}\alpha l)^2Y_4 + \frac{E_2}{4!}(\tfrac{1}{2}\alpha l)^4Y_2 - \frac{E_3}{6!}(\tfrac{1}{2}\alpha l)^6Y_0\right\} - \dots. \end{aligned} \tag{5·12}$$

Finally, if $y = P+iQ$, where P and Q are real functions, we have

$$P = (y_0 - n^4y_4 + n^8y_8 - \ldots) + L_1\cosh(n\xi/\sqrt{2})\cos(n\xi/\sqrt{2}) \\ - L_2\sinh(n\xi/\sqrt{2})\sin(n\xi/\sqrt{2}), \quad (5\cdot13)$$

$$Q = (n^2y_2 - n^6y_6 + n^{10}y_{10} - \ldots) + L_1\sinh(n\xi/\sqrt{2})\sin(n\xi/\sqrt{2}) \\ + L_2\cosh(n\xi/\sqrt{2})\cos(n\xi/\sqrt{2}). \quad (5\cdot14)$$

6—THE FUNCTIONS $f_r(z)$

From (5·5) we have

$$f_0'(z) = \operatorname{cosech} z = 2/(e^z - e^{-z}) \\ = 2(e^{-z} + e^{-3z} + e^{-5z} + \ldots), \quad z > 0, \quad (6\cdot1)$$

whence

$$f_0(z) = \log_e \tanh \tfrac{1}{2}z = -2\left(\frac{e^{-z}}{1} + \frac{e^{-3z}}{3} + \frac{e^{-5z}}{5} + \ldots\right), \quad z > 0, \quad (6\cdot2)$$

and

$$f_{r-1}(z) = 2(-1)^r\left(\frac{e^{-z}}{1^r} + \frac{e^{-3z}}{3^r} + \frac{e^{-5z}}{5^r} + \ldots\right), \quad z \geqslant 0, \quad (6\cdot3)$$

for integral values of r greater than 1. All these functions vanish as $z \to \infty$, in accordance with their definitions in (5·5) and (5·6). These series are most useful when z is large.

For smaller values of z, we can write, if $0 \leqslant z < \pi$,

$$f_0'(z) = \operatorname{cosech} z = \frac{1}{z} - \tfrac{1}{6}z + \tfrac{7}{360}z^3 - \ldots + (-1)^s\frac{B_s \, . \, 2(2^{2s-1}-1)}{(2s)!}z^{2s-1} + \ldots, \quad (6\cdot4)$$

where B_s is the sth Bernoulli number. Hence

$$\left.\begin{aligned} f_0(z) &= \log_e \tanh \tfrac{1}{2}z = \log_e \tfrac{1}{2}z - \tfrac{1}{12}z^2 + \tfrac{7}{1440}z^4 - \tfrac{31}{90720}z^6 + \ldots, \\ f_1(z) &= z\log_e \tfrac{1}{2}z + 2T_2 - z - \tfrac{1}{36}z^3 + \tfrac{7}{7200}z^5 - \tfrac{31}{635040}z^7 + \ldots, \\ f_2(z) &= \frac{1}{2!}z^2\log_e \tfrac{1}{2}z - 2T_3 + 2T_2z - \tfrac{3}{4}z^2 - \tfrac{1}{144}z^4 + \tfrac{7}{43200}z^6 - \ldots, \\ f_3(z) &= \frac{1}{3!}z^3\log_e \tfrac{1}{2}z + 2T_4 - 2T_3z + T_2z^2 - \tfrac{11}{36}z^3 - \tfrac{1}{720}z^5 + \ldots, \\ f_4(z) &= \frac{1}{4!}z^4\log_e \tfrac{1}{2}z - 2T_5 + 2T_4z - T_3z^2 + \tfrac{1}{3}T_2z^3 - \tfrac{25}{288}z^4 - \ldots, \end{aligned}\right\} \quad (6\cdot5)$$

and so on.

In the above series the constants T_2, T_3, ... are given by

$$T_r = \sum_{p=0}^{\infty} \frac{1}{(2p+1)^r}, \tag{6·6}$$

these constants of integration being found from a comparison of (6·3) and (6·5) at $z = 0$. (The numbers T_r are tabulated on p. 92 of Dale's "Five-figure Tables of Mathematical Functions".) The values of $f_0(z)$, $f_2(z)$, $f_4(z)$ are given in Table I.

TABLE I

z	$-f_0(z)$	$-f_2(z)$	$-f_4(z)$	z	$-f_0(z)$	$-f_2(z)$	$-f_4(z)$
0	∞	2·1036	2·0090	0·5	1·4068	1·2311	1·2150
0·01	5·2983	2·0793	1·9889	0·6	1·2334	1·1108	1·0990
0·02	4·6052	2·0555	1·9689	0·7	1·0895	1·0028	0·9942
0·03	4·1998	2·0321	1·9491	0·8	0·9677	0·9057	0·8994
0·04	3·9122	2·0092	1·9295	0·9	0·8630	0·8183	0·8137
0·05	3·6891	1·9867	1·9102	1·0	0·7719	0·7396	0·7362
0·06	3·5069	1·9646	1·8910	1·2	0·6217	0·6045	0·6026
0·07	3·3528	1·9428	1·8720	1·4	0·5036	0·4943	0·4933
0·08	3·2194	1·9213	1·8532	1·6	0·4094	0·4044	0·4039
0·09	3·1018	1·9002	1·8346	1·8	0·3337	0·3309	0·3306
0·10	2·9966	1·8793	1·8162	2·0	0·2723	0·2709	0·2707
0·12	2·8146	1·8386	1·7800	2·2	0·2225	0·2217	0·2216
0·14	2·6609	1·7989	1·7445	2·4	0·1819	0·1815	0·1814
0·16	2·5279	1·7603	1·7097	2·6	0·1488	0·1486	0·1486
0·18	2·4106	1·7228	1·6756	2·8	0·1218	0·1216	0·1216
0·20	2·3059	1·6862	1·6423	3·0	0·0997	0·0996	0·0996
0·22	2·2113	1·6505	1·6095	3·5	0·0604	0·0604	0·0604
0·24	2·1250	1·6157	1·5775	4·0	0·0366	0·0366	0·0366
0·26	2·0458	1·5818	1·5461	4·5	0·0222	0·0222	0·0222
0·28	1·9726	1·5486	1·5153	5·0	0·0135	0·0135	0·0135
0·30	1·9046	1·5163	1·4851				
				6·0	0·0050	0·0050	0·0050
0·35	1·7531	1·4387	1·4124	7·0	0·0018	0·0018	0·0018
0·40	1·6226	1·3656	1·3432	8·0	0·0007	0·0007	0·0007
0·45	1·5083	1·2965	1·2775	9·0	0·0002	0·0002	0·0002
0·50	1·4068	1·2311	1·2150	10·0	0·0001	0·0001	0·0001

From Table I, or using the equations (6·3), we see readily that, for any fixed value of z not less than zero,

$$|f_0| > |f_1| > |f_2| > |f_3| > \ldots, \tag{6·7}$$

so that the series (5·2) is certainly valid if $n^2 \leqslant 1$. We note that $f_r(z)$ is approximately zero when z is big. Since αl is big, in our case greater than

20, we see that near $x = 0$, that is $\xi = -\frac{1}{2}\alpha l$, $f_r(\lambda - \xi) \doteqdot f_r(\alpha l + a)$ which is approximately zero. Hence here

$$y_r \doteqdot f_r(\lambda + \xi) \doteqdot f_r(\alpha x + a). \tag{6·8}$$

Similarly, near $x = l$,

$$y_r \doteqdot f_r\{\alpha(l - x) + a\}. \tag{6·9}$$

7—Formulae for Approximation

Before going on to consider a particular case, with particular numerical values of the constants, we expand P and Q in terms of powers of the small quantities n^2 and $(n\alpha l)^2$. We substitute in (5·13) and (5·14) the series

$$\left.\begin{aligned} \cosh\frac{n\xi}{\sqrt{2}}\cos\frac{n\xi}{\sqrt{2}} &= 1 - \frac{(n\xi)^4}{4!} + \frac{(n\xi)^8}{8!} - \dots, \\ \sinh\frac{n\xi}{\sqrt{2}}\sin\frac{n\xi}{\sqrt{2}} &= \frac{(n\xi)^2}{2!} - \frac{(n\xi)^6}{6!} + \dots, \end{aligned}\right\} \tag{7·1}$$

and also the values of L_1 and L_2 given in (5·11) and (5·12). We find, to an accuracy involving terms in n^4, that

$$P = P_0 - n^4 P_2 + \dots, \quad Q = n^2 Q_1 - \dots, \tag{7·2}$$

where

$$\left.\begin{aligned} P_0 &= y_0 - Y_0, \\ Q_1 &= y_2 - Y_2 + (\tfrac{1}{4}\alpha^2 l^2 - \xi^2)\,Y_0/2!, \\ P_2 &= y_4 - Y_4 + (\tfrac{1}{4}\alpha^2 l^2 - \xi^2)\left\{\frac{Y_2}{2!} - (\tfrac{5}{4}\alpha^2 l^2 - \xi^2)\frac{Y_0}{4!}\right\}. \end{aligned}\right\} \tag{7·3}$$

We note that $Q_1'' = P_0$, $P_2'' = Q_1$, where dashes indicate differentiation with respect to ξ.

Other quantities of interest are the greatest velocity $F(x)$ and the phase-lag ϵ, at different values of x. We find, as far as the term in n^4,

$$F(x) = F(\tfrac{1}{2}l + \xi/\alpha) = (P^2 + Q^2)^{\frac{1}{2}} = P_0 - n^4(P_0 P_2 - \tfrac{1}{2}Q_1^2)/P_0 + \dots, \tag{7·4}$$

$$\epsilon = \tan^{-1}(-Q/P) = n^2 Q_1/P_0 + \dots. \tag{7·5}$$

If we compare (7·3) with (5·4) we see that

$$P_0 = f_0(\alpha x + a) + f_0\{\alpha(l - x) + a\} - f_0(a) - f_0(\alpha l + a).$$

Thus, if n^2 is small and αl large, we have, when $x \leq \frac{1}{2}l$, the approximate relation

$$P \doteqdot P_0 \doteqdot f_0(\alpha x + a) - f_0(a), \tag{7·6}$$

which is independent of αl.

We may also find an approximation to Q_1 for the range $0 \leqslant x \leqslant l$. For, on consulting Table I and equations (7·3), we see that $(y_2 - Y_2)$ can be neglected, with an error of not more than 1 %, in comparison with the term $(\frac{1}{4}\alpha^2 l^2 - \xi^2) Y_0/2$, so that, approximately,

$$\begin{aligned} Q \doteqdot n^2 Q_1 &\doteqdot n^2(\tfrac{1}{2}\alpha l - \xi)(\tfrac{1}{2}\alpha l + \xi) Y_0/2 \\ &= n^2\alpha^2 x(l-x) Y_0/2. \end{aligned} \tag{7·7}$$

The relations (7·6) and (7·7) lead to the results

$$F(x) \doteqdot P_0, \quad \epsilon \doteqdot \tfrac{1}{2} n^2 \alpha^2 x(l-x) Y_0/P_0, \tag{7·8}$$

and, when $x = 0$, we find

$$\epsilon \doteqdot -\tfrac{1}{2} n^2 \alpha l Y_0 \sinh a = -\tfrac{1}{4} n^2 \alpha l Y_0 (A^2 - 1)/A. \tag{7·9}$$

The above considerations apply most strongly to the regions near the walls. In the central region of the fluid motion between the parallel walls, i.e. where $5 < \alpha x < \alpha l - 5$, say, we may approximate to the various functions by noting that $|f_0(\alpha x + a)|$ does not exceed $\frac{3}{4}$ % of $|f_0(a)|$. In this region $|y_0|$ is less than $2|f_0(\alpha x + a)|$, and $Y_0 = f_0(a)$ almost exactly, so that $|y_0|$ cannot exceed $1\frac{1}{2}$ % of $|Y_0|$. When $a = 0{\cdot}7$ (an extreme value) and $\alpha x = 5$, we find

$$y_0 = 0{\cdot}007 Y_0, \tag{7·10}$$

which is the biggest ratio of y_0/Y_0 in our range. We still have $(y_2 - Y_2)$ negligible in comparison with $(\frac{1}{4}\alpha^2 l^2 - \xi^2) Y_0/2$, so that in this region

$$P \doteqdot -Y_0, \quad Q \doteqdot n^2(\tfrac{1}{4}\alpha^2 l^2 - \xi^2) Y_0/2, \tag{7·11}$$

whence

$$F(x) \doteqdot -Y_0, \quad \epsilon \doteqdot n^2(\tfrac{1}{4}\alpha^2 l^2 - \xi^2)/2. \tag{7·12}$$

The maximum value of ϵ is thus seen to occur when $\xi = 0$ and is equal to

$$n^2\alpha^2 l^2/8. \tag{7·13}$$

Combining (7·4) and (7·11) we see that $|y|$, and therefore $|u/H|$, has approximately the constant value $(-Y_0)$ in the central range $5 < \alpha x < \alpha l - 5$, and this constant depends only on A if αl is large. The value of the constant is approximately

$$\begin{aligned} -Y_0 &\doteqdot -f_0(a) \\ &\doteqdot \log_e \coth \tfrac{1}{2} a = \log_e\{(A+1)/(A-1)\} = -\nu F\zeta/2RT. \end{aligned} \tag{7·14}$$

Hence, using the various definitions given in § 2, we see that in this central range the velocity is approximately $\frac{D\zeta}{4\pi\eta}E\cos(\omega t-\epsilon)$, which compares with Helmholtz's formula $\frac{D\zeta}{4\pi\eta}E$ for the electrosmotic velocity in a field of constant strength E (Helmholtz 1879; Perrin 1904).

Further, the maximum phase difference, which is $(n\alpha l)^2/8$, depends only on the non-dimensional number $n\alpha l$, and occurs at the centre of the range.

8—A Representative Case

As a numerical example we shall consider a case which, within the limits given for the various constants, gives the greatest maximum phase-lag ϵ.

We put $a = 0{\cdot}01$, $\alpha l = 100$, $n^2 = 10^{-5}$ and use the more accurate expansions (7·2) and (7·3). The detailed figures are given in Table II.

The main features of the solution are brought out by the table, though many of them are not pronounced because the chosen value of n, though the greatest allowed by our range, is not very large. It will be noted that, while P_0 has only one maximum, at the centre of the range ($\alpha x = 50$), $(P^2+Q^2)^{\frac{1}{2}}$ has two maxima, somewhere near $\alpha x = 15$, $\alpha x = 85$ and a minimum at $\alpha x = 50$. This depends upon the chosen values of n and αl. With smaller values of these constants $(P^2+Q^2)^{\frac{1}{2}}$ may possess only one maximum, which occurs, of course, at the centre of the range.

9—The Velocity Profile

Fig. 2 contains diagrams showing the variation of $F(x)$, the amplitude of u/H, which is equal to $(P^2+Q^2)^{\frac{1}{2}}$. This is the greatest value attained by u/H at various positions in the channel. Fig. 3 contains diagrams showing the variation of the phase-lag ϵ. Both figures refer to the numerical case con-

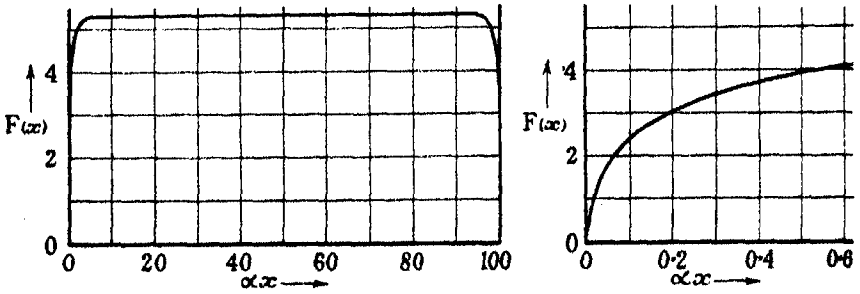

FIG. 2—Maximum values of $|u/H|$, i.e. $F(x)$, at various values of x.

TABLE II—$a = 0{\cdot}01$, $\alpha l = 100$, $n^2 = 10^{-5}$

αx	P_0	$P_2 \times 10^{-4}$	$Q_1 \doteqdot Q \times 10^5$	P	$(P^2+Q^2)^{\frac{1}{2}}$	$(-Q/P) \times 10^5$	ϵ
0	0	0	0	*	*	2·6	0′·09
0·02	1·0985	0·4	− 5·3			4·8	0′·17
0·04	1·6092	0·9	− 10·5			6·5	0′·22
0·06	1·9455	1·3	− 15·8			8·1	0′·28
0·08	2·1965	1·8	− 21·0			9·6	0′·33
0·10	2·3971	2·2	− 26·2			10·9	0′·37
0·15	2·7704	3·3	− 39·4			14·2	0′·49
0·20	3·0409	4·4	− 52·5			17·3	0′·59
0·25	3·2525	5·5	− 65·6			20·2	0′·69
0·30	3·4260	6·6	− 78·7			23·0	0′·79
0·4	3·6998	8·8	− 104·8			28·3	1′·0
0·5	3·9105	11·0	− 130·9			33·5	1′·2
0·6	4·0805	13·2	− 157·0			38·5	1′·3
0·7	4·2219	15·4	− 183·1			43·4	1′·5
0·8	4·3418	17·7	− 209·1			48·2	1′·7
0·9	4·4450	19·9	− 235·0			52·9	1′·8
1·0	4·5349	22·1	− 260·9			57·5	2′·0
1·2	4·6832	26·5	− 312·6			66·7	2′·3
1·4	4·7999	30·9	− 364·1			75·9	2′·6
1·6	4·8931	35·3	− 415·6			84·9	2′·9
1·8	4·9680	39·7	− 466·5			93·9	3′·2
2·0	5·0287	44·1	− 517·4			102·9	3′·5
2·5	5·1354	55	− 644	5·1353	5·1353	125	4′·3
3·0	5·1996	66	− 769	5·1995	5·1995	148	5′·1
3·5	5·2385	77	− 893	5·2384	5·2384	171	5′·9
4·0	5·2621	88	− 1015	5·2620	5·2620	193	6′·6
4·5	5·2763	99	− 1136	5·2762	5·2762	215	7′·4
5·0	5·2849	110	− 1256	5·2848	5·2848	238	8′·2
6·0	5·2933	131	− 1492	5·2932	5·2932	282	9′·7
7·0	5·2965	153	− 1723	5·2963	5·2963	325	11′·2
8·0	5·2976	174	− 1948	5·2974	5·2974	368	12′·6
9·0	5·2981	196	− 2168	5·2979	5·2979	409	14′·1
10·0	5·2982	216	− 2382	5·2980	5·2981	450	15′·5
12·0	5·2983	258	− 2796	5·2980	5·2981	528	18′·1
14·0	5·2983	298	− 3188	5·2980	5·2981	602	20′·7
16·0	5·2983	336	− 3558	5·2980	5·2981	672	23′·1
18·0	5·2983	374	− 3908	5·2979	5·2981	738	25′·4
20·0	5·2983	410	− 4237	5·2979	5·2981	800	27′·5
25·0	5·2983	491	− 4965	5·2978	5·2980	937	32′·2
30·0	5·2983	561	− 5561	5·2977	5·2980	1050	36′·1
35·0	5·2983	616	− 6025	5·2977	5·2980	1137	39′·1
40·0	5·2983	657	− 6356	5·2976	5·2980	1200	41′·2
45·0	5·2983	681	− 6555	5·2976	5·2980	1237	42′·5
50·0	5·2983	690	− 6621	5·2976	5·2980	1250	43′·0

* Blank spaces in these columns indicate that the values are indistinguishable from the values of P_0 for the same αx. In each of these columns the first value printed is the first to differ by as much as a unit in the fourth decimal place from the corresponding value in the column labelled P_0.

sidered in § 8. In each figure there are two diagrams, one giving the curves for the whole range of x, and the other, with different scales, showing the way in which the functions vary in the region near the wall where x is small.

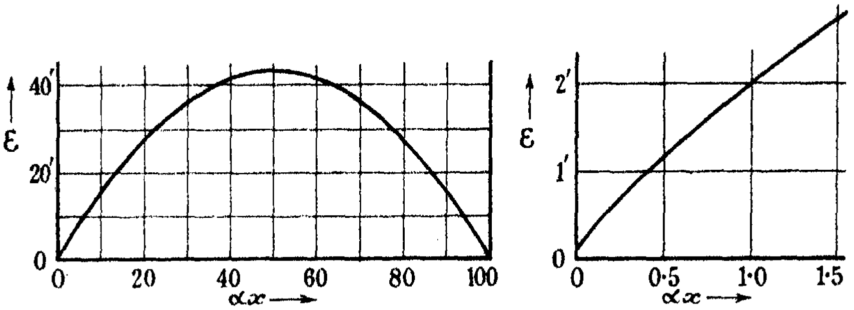

FIG. 3—Values of the phase-lag ϵ at various values of x.

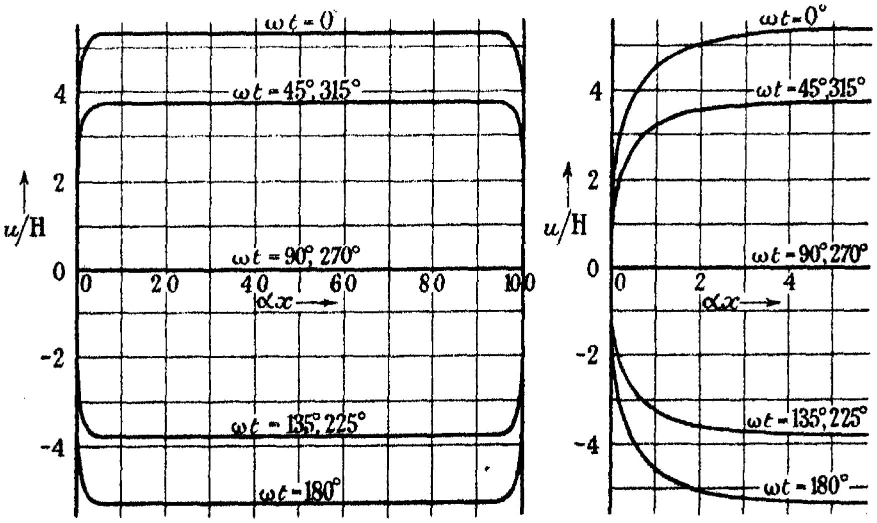

FIG. 4—Values of u/H. (The velocity profiles corresponding to $\omega t = 45°$ and $\omega t = 315°$ are not identical, but the difference is too small to be visible with the chosen scale. Similar remarks apply to the curves labelled $\omega t = 90°$, $270°$ and $\omega t = 135°$, $225°$.)

Reverting to equation (4·6) we see that the velocity is

$$u = H(P\cos\omega t - Q\sin\omega t). \tag{9·1}$$

This is a function of both αx and ωt, and curves are given in figs. 4 and 5 showing how u varies with αx for several different values of ωt. Again, two diagrams, with different scales for αx, are given in each figure. In fig. 4

the values of ωt cover the whole range 0°–360°, but fig. 5 is confined to the neighbourhood of $\omega t = 90°$, in which interesting results occur. The values of u/H from which these curves were derived are given in Table III. Between 180° and 360° the same figures apply, but with a change of sign corresponding to an increase of 180° in ωt. From the table it will be seen that the velocity profiles in fig. 4 corresponding to $\omega t = 45°$ and $\omega t = 315°$ are not identical, but the difference is too small to be visible with the chosen scale. Similar remarks apply to the curves labelled $\omega t = 90°$, 270° and $\omega t = 135°$, 225°.

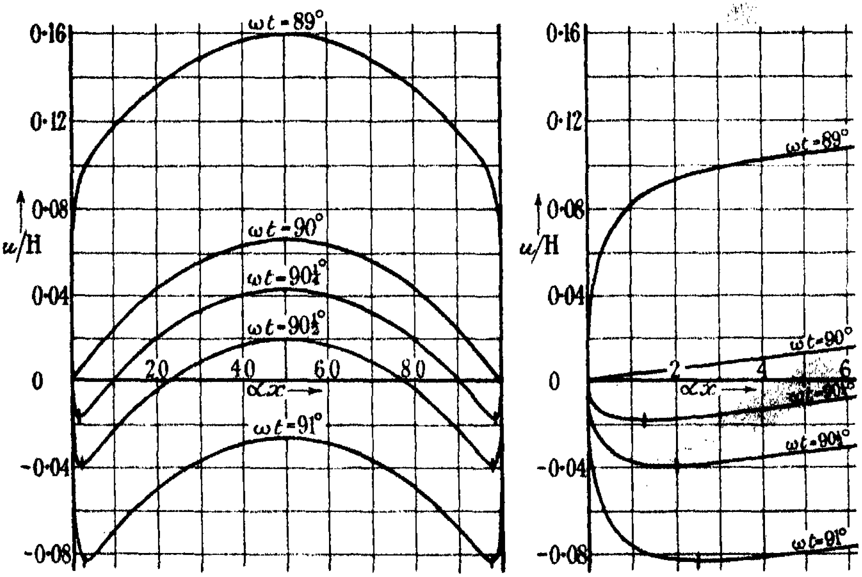

FIG. 5—Values of u/H in the neighbourhood of $\omega t = 90°$.

We note that the velocity can be expressed in the form

$$u = HF(x)\cos(\omega t - \epsilon),$$

so that, at any value of x, $u = 0$ when $\omega t = \epsilon + 90°$ or $\epsilon + 270°$. We note also from fig. 3 that ϵ increases from $x = 0$ to $x = \frac{1}{2}l$, so that those positions of x at which $u = 0$, apart from the permanent zeros at the walls themselves, will move continuously from the walls to the centre of the channel as t increases. In all cases, therefore, the velocity profile changes, from that in which u is positive everywhere and concave towards the x-axis to that in which it is negative everywhere and again concave towards the x-axis, according to the sequences of diagrams shown in figs. 4 and 5. The actual changes during the beginning of that period of transition during which ωt passes through the value 90° are shown in fig. 5. There is a similar set of figures corresponding to $\omega t = 270°$, but these are not shown.

TABLE III—VALUES OF u/H AT VARIOUS TIMES DURING A HALF-CYCLE
$a = 0{\cdot}01$, $\alpha l = 100$, $n^2 = 10^{-5}$

αx	$\omega t = 0°$	45°	89°	90°	90¼°	90½°	91°	135°
0	0	0	0	0	0	0	0	0
0·1	2·40	1·70	0·042	0·000	−0·010	−0·021	−0·041	−1·70
0·2	3·04	2·15	0·054	0·001	−0·013	−0·026	−0·053	−2·15
0·3	3·43	2·42	0·061	0·001	−0·014	−0·029	−0·059	−2·42
0·4	3·70	2·62	0·066	0·001	−0·015	−0·031	−0·064	−2·62
0·6	4·08	2·89	0·073	0·002	−0·016	−0·034	−0·070	−2·88
0·8	4·34	3·07	0·078	0·002	−0·017	−0·036	−0·074	−3·07
1·0	4·53	3·21	0·082	0·003	−0·017	−0·037	−0·077	−3·20
1·5	4·85	3·43	0·089	0·004	−0·017	−0·038	−0·081	−3·43
2·0	5·03	3·56	0·093	0·005	−0·017	−0·039	−0·083	−3·55
3·0	5·200	3·682	0·099	0·008	−0·015	−0·038	−0·083	−3·671
4·0	5·262	3·728	0·102	0·010	−0·013	−0·036	−0·082	−3·714
5·0	5·285	3·746	0·105	0·013	−0·010	−0·034	−0·080	−3·728
6·0	5·293	3·753	0·107	0·015	−0·008	−0·031	−0·078	−3·732
7·0	5·296	3·757	0·110	0·017	−0·006	−0·029	−0·075	−3·733
8·0	5·2974	3·760	0·112	0·019	−0·004	−0·027	−0·073	−3·732
9·0	5·2979	3·761	0·114	0·022	−0·001	−0·024	−0·071	−3·731
10·0	5·2980	3·763	0·116	0·024	+0·001	−0·022	−0·069	−3·729
15·0	5·2980	3·770	0·126	0·034	+0·011	−0·012	−0·059	−3·722
20·0	5·2979	3·776	0·135	0·042	+0·019	−0·004	−0·050	−3·716
30·0	5·2977	3·785	0·148	0·056	+0·032	+0·009	−0·037	−3·707
40·0	5·2976	3·791	0·156	0·064	+0·040	+0·017	−0·029	−3·701
50·0	5·2976	3·793	0·159	0·066	+0·043	+0·020	−0·026	−3·699

With our choice of the constants, the velocity profile with three stationary values, of the type shown in fig. 5, $\omega t = 91°$, persists for about a quarter of the complete cycle, but with smaller values of n and αl this period can be considerably reduced, even to a fraction of a degree. The magnitude of the dip in the velocity profile in the centre of the channel is never greater than 1 % of the maximum velocity attained there, and may be much less. This is below the limits of experimental error at present available and therefore may not have been observed.

10—SUMMARY OF THE PRINCIPAL RESULTS

1—The equation satisfied by the fluid flow is

$$m\frac{\partial u}{\partial t} - \eta\frac{\partial^2 u}{\partial x^2} = Ge^{i\omega t}\left[\frac{2Ae^{\alpha x}\{A^2e^{2\alpha x}+1\}}{\{A^2e^{2\alpha x}-1\}^2} + \frac{2Ae^{\alpha(l-x)}\{A^2e^{2\alpha(l-x)}+1\}}{\{A^2e^{2\alpha(l-x)}-1\}^2}\right].$$

The velocity, which is restricted to be zero at the walls, is the real part of u obtained from this equation.

2—When the field strength is $E\cos\omega t$, the velocity of the fluid is

$$HF(x)\cos(\omega t-\epsilon),$$

where
$$F(x) = P_0 - n^4(P_0P_2 - \tfrac{1}{2}Q_1^2)/P_0 + \ldots,$$

and
$$\epsilon = n^2Q_1/P_0 + \ldots,$$

which is also a function of x. In these expressions

$$P_0 = y_0 - Y_0,$$
$$Q_1 = y_2 - Y_2 + (\tfrac{1}{4}\alpha^2l^2 - \xi^2)\,Y_0/2\,!,$$
$$P_2 = y_4 - Y_4 + (\tfrac{1}{4}\alpha^2l^2 - \xi^2)\left\{\frac{Y_2}{2\,!} - (\tfrac{5}{4}\alpha^2l^2 - \xi^2)\frac{Y_0}{4\,!}\right\}.$$

The values of y_0, y_2, y_4 and Y_0, Y_2, Y_4 are obtained from Table I. The curve showing the variation of velocity along a line perpendicular to the walls is always symmetrical with respect to the walls.

3—The highest value of u obtaining at any point is given by the equation $u = HF(x)$, (cf. fig. 2 and Table II). If n^2 is small, $u \doteqdot H(y_0 - Y_0)$, and in the central region $5 < \alpha x < \alpha l - 5$,

$$u \doteqdot -HY_0 \doteqdot H\log_e\{(A+1)/(A-1)\} = -D\zeta E/4\pi\eta.$$

In the central region the velocity is approximately $\dfrac{D\zeta}{4\pi\eta}E\cos(\omega t-\epsilon)$ which should be compared with Helmholtz's formula $\dfrac{D\zeta}{4\pi\eta}E$ for the velocity in a field of constant strength E.

4—The phase difference ϵ increases continuously from the value

$$-\tfrac{1}{2}n^2\alpha lY_0\sinh a = \tfrac{1}{4}n^2\alpha l\,\frac{A^2-1}{A}\log_e\frac{A+1}{A-1}$$

at the walls to the value $n^2\alpha^2l^2/8$ at points half-way between the walls. Except near the walls, we have $\epsilon \doteqdot \tfrac{1}{2}n^2\alpha^2x(l-x)$, (cf. fig. 3 and Table II).

5—The curves showing the form of the velocity profile at various times during one cycle of the alternating current are shown in figs. 4 and 5. Although these curves refer to one set of values of the physical constants, they are characteristic of the whole range considered. It therefore appears that if the distance between the walls is of the order of magnitude which allows of a measurement of the surface conductivity (or of the electrosmotic velocity in the alternating field), that is if the Gouy theory can be applied, then the normal phenomena of electrosmosis exist, even with frequencies of the alternating current as high as 10^5/sec. For two periods during a complete cycle, the velocity profile shows a dip in the middle portion. This dip may persist for a quarter-cycle at a time or for a very much shorter period, depending on the chosen values of the constants. The magnitude of the dip is never greater than 1 % of the greatest velocity attained in the centre of the channel, and may be much less. This is below the limits of error associated with the present experimental technique, and this phenomenon therefore may not have been observed.

NOTE BY J. J. BIKERMAN

Electrokinetic phenomena represent the best, indeed almost the only, source of information concerning the potential difference between the surface and the body of a liquid.

Unfortunately, in the first approximation used by Helmholtz, the electrokinetic potential ζ can only be calculated with an uncertain multiplier. Thus Helmholtz believed ζ to be of the order of 5 V, whilst modern workers (Perrin 1904) accept values of ζ less than 0·1 V. It is even possible (in the first approximation) to account for the simplest electrokinetic phenomena without using a definite value of ζ at all. On the other hand, the formulae of Helmholtz are independent of the structure of the surface charge.

The situation changes when the second approximation of the theory is considered or effects of the second order are examined: (*a*) the value of ζ becomes unambiguous, and (*b*) the equations depend on the assumed structure of the surface charge. Dealing with the second order phenomena it is possible and convenient to use the surface conductivity as the fundamental property. This is the reason for its importance (Bikerman 1935). Electrosmosis is an effect of the first order, and only the second approximation of its theory depends on the assumed structure of the double layer; on the other hand, the surface conductivity is an effect of the second order and cannot be accounted for without an assumption concerning the structure of the double layer.

The surface conductivity has a twofold origin: (*a*) the surface layer of the liquid contains a different number of ions per cubic centimetre from the liquid in bulk, and (*b*) the surface layer of the liquid contains different numbers of positive and negative ions; it is charged so that its electrosmotic movement produces an electric current. In agreement with this the mathematical expression for the surface conductivity contains two terms. It was suggested (Bikerman 1933) that both terms depend upon the frequency of the alternating current used for measuring the surface conductivity, but in different ways. The first one is a simple concentration term and should show a "dispersion" at the same frequencies as the ordinary conductivity, that is, at about 10^7 cycles/sec. (By the "dispersion" of a quantity we mean the variation of the quantity considered with the frequency of the alternating current.) The second term presupposes the existence of a regular movement of the whole liquid and would, therefore, disappear at some lower frequencies. A consequence of this theory is that the magnitudes of both these terms are of the same order under the usual conditions, and, as a result, the values of the surface conductivity should fall, with rising frequency, to about one-half of their values for direct current. The exact knowledge of the dispersion of surface conductivity, that is, the extent of the fall and the frequency interval where it occurs, would be, for the science of electrokinetics, as useful as the discovery and investigation of the dispersion of ordinary conductivity was for the science of electrolytes (Debye and Falkenhagen 1928).

As far as experimental evidence is concerned (Urban, Feldman and White 1935) no difference has been noticed between the surface conductivity for direct current and 1000 cycles alternating current, and more extensive measurements have been planned both in England and in the U.S.A. In order to compare experimental evidence with theory it is necessary to calculate the critical interval of frequencies. Professor Rosenhead and Dr. Miller were kind enough to carry out investigations along these lines. They came to the unexpected conclusion that the dispersion of electrosmosis is not in evidence even at frequencies as high as 10^5 cycles/sec. This suggests that the dispersion of electrosmosis, if it occurs at all, occurs at frequencies at least as high as those which produce the Debye-Falkenhagen effect (10^7 cycles/sec.). Hence many important consequences follow, of which three may be mentioned here:

(1) The suggested checking of the theory of surface conductivity by measuring its dispersion is impracticable.

(2) The comparison (Abramson 1934) of the experimental results observed at various frequencies, with the formula for surface conductivity, taking both terms in the formula into consideration, is justified.

(3) The discrepancy between the surface conductivity values found by different observers cannot be attributed to the difference of the frequencies used.

REFERENCES

Abramson 1934 "Electrokinetic Phenomena." New York, U.S.A.
Bikerman 1933 *Z. phys. Chem.* A, **163**, 378.
— 1935 *Kolloidzschr.* **72**, 100.
Debye and Falkenhagen 1928 *Phys. Z.* **29**, 401.
Gouy 1910 *J. Phys. Radium*, (4), **9**, 457.
Helmholtz 1879 *Ann. Phys., Lpz.*, **7**, 337.
Perrin 1904 *J. Chim. phys.* **2**, 601.
Urban, Feldman and White 1935 *J. Phys. Chem.* **39**, 605.

A Discussion
on
Viscosity of Liquids

22 *April* 1937

G. I. TAYLOR, F.R.S.—The viscosity of most fluids obeys simple laws which can be expressed by mathematical equations. Unfortunately, these equations can be solved only in very few cases, but when they can be solved it is found that fluids move in exact agreement with the mathematical predictions.

This is now known to be true even in the case of turbulent motion, for a prediction based only on the law of viscosity has recently been made concerning the rate of decay of the energy of turbulent movement. This prediction has been verified experimentally. The difficulties which beset the mathematician who attempts to analyse turbulent flow are so great that some workers in the past have stated their belief that the law of viscosity does not apply in this case. They have even thought that there is an essential impossibility in analysing turbulent flow by means of the usual differential equations of motion for viscous fluids.

Though the common law of viscosity applies to most fluids, some exist which exhibit anomalous viscous properties. Some even possess a little rigidity. Anomalous properties may be conferred on a fluid by small particles immersed in it. Small spheres merely increase the macroscopic viscosity of the combination of fluid and spheres. Elongated solid bodies, however, tend to set themselves in certain special directions in relation to the stresses and thus confer anisotropic properties on the fluid.

It is noteworthy that the degree of anisotropy and also the proportional increase in viscosity of the mixture of fluid and particles over the viscosity of the fluid alone depends on the shape and total volume of the particles, but not on the number of particles.

When the fluid is made anisotropic by the addition of non-spherical solid particles the stresses due to any given motion do not have the same distribution as those in a similarly moving isotropic fluid. On the other hand, the stresses in the anisotropic fluids are proportional to the gradients just as they are in a viscous fluid.

When a fluid contains a large number of small drops of another fluid, it behaves like an isotropic fluid whose viscosity is increased proportionally to the volume of the drops provided that the stresses round the drops are not so great as to deform them from the spherical form which they assume under the action of surface tension.

When a fluid containing drops of another fluid is deformed so rapidly that the drops are appreciably deformed from their spherical shape, it not only becomes anisotropic, but also loses the property that the stresses are proportional to the velocity gradients.

J. D. Bernal, F.R.S.—I shall confine my contribution to the first aspect mentioned by Professor Taylor, that of the theory of viscosity of pure liquids.

The problem is that of relating the phenomena of viscosity of liquids to what we already know of their internal molecular structure. Most of the theories that have appeared so far have either been of a thermodynamic nature, approaching the problem of the viscosity of liquids from that of gases, or have made use of special models of the behaviour of liquid molecules which are difficult to reconcile with what we know of actual liquids. From the point of view of the molecular theory of liquids I have developed elsewhere (1937) viscosity is intimately linked with the rate of change of the mutual configuration of the molecules of a liquid. This rate of change is far slower than the normal vibrations of the molecules and would seem in certain cases, from the evidence of the anomalous absorption of ultrasonic waves (Biquard and Lucas 1937; Errera and others 1937), to have a characteristic time of the order of *ca.* 10^{-6} sec. Normally, changes of configuration occur equally in all directions and are in energy equilibrium with the thermal vibrations. As such they are responsible for the phenomena of diffusion and Brownian motion. If, however, the liquid is subject to shearing stresses those changes of configuration which tend to relieve the stress will be favoured at the expense of those that do not in a way formally equivalent to the motion of electrons in metals under an electric field. The elementary process of these configuration changes must be considered to be the interchange of neighbours between a pair of molecules as shown in fig. 1. Every such process implies an intermediate state in which the molecules are further apart and this involves a certain activation energy.

In this sense, as Eyring (1936) has pointed out, viscosity is essentially chemical kinetics. Two different forms of the process can be distinguished: one at low rates of shear and low viscosity in which a steady state can be maintained, and one at high rates of shear and high viscosity, in which the energy liberated can effectively change local temperature and lead to a homogeneous breakdown of the structure, which is apparent in plastic deformation. The magnitude of the activation energy is shown in the expression first developed by Guzman (1913) for the thermal coefficient of viscosity. The constant B varies considerably from substance to substance as Ward has shown, but if we consider it in relation to the melting-point certain regularities become apparent. The quantity B/T_f, where T_f is the melting-point, which may be called the viscosity entropy change of the substance, is for each chemical type of liquid relatively constant (see Table I).

For both ionic liquids and simple molecular liquids the values range about 6·2–8·4, but for metals they are almost half as great (2·6–4·2). This suggests at once that the phenomena of viscosity are closely linked with

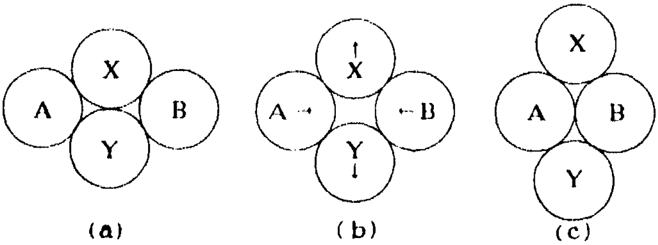

Fig. 1—Elementary process of place exchange of molecules in liquids. Configuration (*a*) changes to (*c*) passing through the higher energy state (*b*).

TABLE I

	T_f	V_{liq}/V_{sol}	B	$B/T_f \times 10^3$
NaCl	1077	1·40	9·10	8·44
NaBr	1028	1·39	8·00	7·79
KCl	1045	1·30	7·40	7·09
KBr	1003	1·30	7·96	7·93
AgCl	728	1·06	5·30	7·29
AgBr	703	1·08	4·85	6·90
$NaNO_3$	581	1·16	3·68	6·34
KNO_3	606	1·09	4·38	7·22
				Mean 7·38
A	84·0	1·18	0·524	6·24
N_2	63·4	1·27	0·468	7·39
CO	66·2	1·10?	0·463	7·00
CH_4	89·2	1·10?	0·740	8·31
O_2	54·8	1·26	0·406	7·41
				Mean 7·27
Na	371	1·04	0·96	2·59
K	335	1·04	1·15	3·43
Ag	1233	1·12	4·87	3·95
Zn	692	1·06	2·92	4·22
Cd	594	1·08	1·59	2·68
Hg	234	1·04	0·598	2·56
Pb	601	1·10	2·32	3·86
				Mean 3·33

those of volume change; as the chief difference between metals and the other types are the very much smaller volume changes occurring on melting (see Table I second column). The idea of the relation of viscosity to volume is not new; the theories of Batchinsky (1913) and McLeod (1923) make viscosity a function of free volume that is on the difference between the actual volume of the liquid V and another volume $\frac{V_0}{\lambda}$ either found empirically or derived from van der Waals' equation.

McLeod's law is $\frac{1}{\eta} = \frac{c}{(V - V_0)^A}$, Batchinsky's is the particular case where $A = 1$.

The present approach only differs in that it begins with the consideration of the crystalline solid and not of the gas, the volume V_0 being taken as that occupied by the crystal at absolute zero. To this extent it follows Eyring, by making viscosity depend on the existence of holes in the liquid. There is certainly a rough agreement with Batchinsky's law for substances as different as argon, mercury and sodium chloride.

The reason such theories have fallen into disfavour is largely due to a misunderstanding of the problem. It is not to be expected that any simple theory of viscosity can give good results for the great majority of the liquids known to organic chemists owing to the complexity of their molecules and the presence of active binding groups; this applies particularly to alcohols and acids. A more fundamental difficulty, however, is that V_0, the occupied volume, cannot be considered to be independent of temperature and pressure, and until we can calculate the really effective free volume any theories of viscosity based on it will be bound to give less accurate representations than purely empirical expressions. The results of Bridgeman (1931) for mercury, the simplest liquid he studied, have been supposed to have finally demolished any theories of viscosity based on volume alone, but if we allow V_0 to vary with the pressure and to have the same compressibility as solid mercury (actually of solid lead, as that of solid mercury has never been measured) we get a very good agreement with experiment even up to the highest pressures used by Bridgeman as can be seen from Table II.

It is clear that one of the effects of pressure is to increase the viscosity activation energy. If we take Bridgeman's results for mercury—those for more complex liquids are obviously of little use owing to internal molecular changes—we can see that B increases with the pressure. Extrapolating to negative pressure very roughly owing to the irregularity of the data we find that at a pressure of the order of $-50{,}000$ kg./sq. cm. B would vanish. A similar figure can be found by extrapolating the viscosity-pressure curves themselves. Such a process has obviously no physical significance, but it points to the relation of viscosity to the normal internal pressure of the liquid and it is interesting to note that the values obtained correspond to the value 45,000—found for a in Simon's melting-point formula (1929)

$$\log (a+p) = b+c\log T,$$

where p is the melting-point pressure at a temperature T. The fact that the viscosity of a liquid obeys simultaneously the laws

$$\eta(V-V_0) = \text{const. and } \eta = Ae^{B/RT}$$

points the dependence of both of these on configuration change in the liquid, such as would lead to an expression for the thermal dependence of the volume

$$V = V_0+Ae^{-B/RT}.$$

The actual expression must necessarily be more complex, as Eyring has shown (1937). It is clear, however, that we are approaching a state in which one common expression for the internal configuration of a liquid will give us directly not only the ordinary thermodynamic properties of specific heat and latent heat but the thermal expansion, the compressibility, the viscosity and the surface tension. What is needed at the moment would seem to be a more intimate collaboration between exponents of thermodynamic theory and the experimental physicists studying the molecular properties of liquids.

Table II—Variation of Viscosity with Pressure. If Batchinsky's Law was followed $(V-V_0)\,\eta$ should be independent of Temperature and Pressure

p Kg/ sq. cm.	V_0	V_{30}	$V_{30}-V_0$	η_{30}	$(V_{30}-V_0)\eta_{30}$ 0·000	V_{75}	$V_{75}-V_0$	η_{75}	$(V_{75}-V_0)\eta_{75}$ 0·000
1	1·0000	1·0555	0·0555	0·0152	843	1·0637	0·0637	0·0134	856
2000	0·9950	1·0478	0·0528	0·0159	840	1·0560	0·0610	0·0140	854
4000	0·9906	1·0407	0·0501	0·0166	833	1·0489	0·0583	0·0146	851
6000	0·9864	1·0341	0·0477	0·0174	829	1·0423	0·0559	0·0152	849
8000	0·9826	1·0280	0·0454	0·0182	826	1·0362	0·0536	0·0160	858
10000	0·9791	1·0225	0·0434	0·0191	828	1·0307	0·0516	0·0167	861
12000	0·9761	1·0175	0·0414	0·0200	828	1·0258	0·0497	0·0176	874

A. S. C. **Lawrence**—High viscosity has always been recognized as a characteristic of solutions of lyophilic colloids. This property is frequently, but not invariably, accompanied by gelation. Attempts were made to explain gelation as a solvation phenomenon but failed because the low concentration of solute required for gelation implied impossibly thick layers of bound solvent. Further, the bulk of liquid in gels is not bound. Free diffusion takes place through it: it can be replaced by other liquids without destroying the gel structure: Brownian motion goes on in it in the gel. It was then found that the sol-gel change did not involve change in several physical properties such as light scattering, electrical conductivity and osmotic pressure.

Many years, however, passed before it was recognized that this transition was not from true liquid to rigid gel: that the sols, from which the gel forms, possess anomalous mechanical properties and that gelation is no more than arrangement of the micelles into the gel structure. This may take several days in a sol, otherwise equilibriated, whose concentration is only just sufficient to form a gel with rigidity enough to support its own weight. Mechanical anomaly is detected in sols by measuring their apparent viscosity at different rates of shear. For normal liquids, the viscosity coefficient is independent of the rate of shear, but these sols have an apparent viscosity which increases at small rates of shear; often to enormous values when the rate is very small. Anomaly has also been observed in concentrated systems such as clay pastes, mud-pies, paints, etc. There is, however, a gap between these systems which require a concentration of disperse phase of 60 % or more and the lyophilic sols which show their anomaly with less than 1 %.

It is now accepted that gel structure is a meshwork of fibrils. This theory was put forward first on the quite unreliable evidence of microscopic or ultramicroscopic detection of fibrillar particles in coagels. True gels are, of course, optically empty. In the last few years, our knowledge of mechanically anomalous colloidal solutions has been increased largely by chemical work on linear polymerization. Formation of fibrils of great length/breadth ratio is rare as a crystal habit. Linear polymerization readily supplies fibrillar polymer molecules of very high length/breadth ratio. Staudinger, to whom we owe most of this knowledge, has suggested that, in solution, these particles will rotate and occupy an effective volume much larger than themselves and equal to $\pi(l/2)^2 b$, where l is their length and b their breadth. When the concentration of a solution is such that the total effective volume of all the particles is equal to the volume of the solution, any further addition of solute will cause interference and the viscosity/concentration curve will rise more steeply.

Mark has pointed out, however, that the chemically linear polymer molecules will not normally be geometrically linear; they will be coiled irregularly, and their increase of kinetic energy when the temperature is raised will mean that more work is required to draw the particles out into linear form. Hence the increase of elasticity of rubber with temperature. In solution the results are complicated. The effective volume is lowered considerably since the square of the geometrical length is involved. On the other hand, random kinetic oscillations of different parts of a long particle will increase the effective volume as the squares of the lengths of the oscillating parts. Further, increase of temperature should *increase* the viscosity effect due to the solute by increasing this kinetic motion. This effect will be offset to some extent by the decrease of viscosity of the solvent. Data, however, seem to be lacking on temperature coefficients of viscosity of these sols. The viscosity measured will be affected by the rates of shear employed. Coiled particles will be extended by high rates of shear, so increasing their effective volume for Staudinger's treatment. Kuhn has discussed the degradation of rigid particles by shear.

The general position is now reasonably clear. Anomalous viscosity occurs when some of the applied stress is used for any purpose other than the normal shearing of the fluid. Leaving out liquid/liquid suspensions, there are two possibilities: (1) plastic systems with a yield point above which flow may be Newtonian or anomalous according to conditions; and (2) systems in which the apparent viscosity increases with decrease of rate of shear, but without rigidity. These fall into two classes: (*a*) those containing *rigid* anisodimensional particles, in which increase of rate of shear increases orientation thereby decreasing the number at any moment lying across the velocity gradient and, therefore, the apparent viscosity. Any non-spherical particle-molecule or micelle- will show this effect provided that a velocity gradient sufficient to overcome the random kinetic motion of the particles can be applied. And (*b*) those containing *non-rigid* anisodimensional particles which can be stretched by flow. Cases of very large elastic recoil cannot be explained by this mechanism and seem to be due to the presence in the fluid of large lumps of weak gel which can be stretched to a very much greater extent than the single particles. Class 1 requires high concentration of solute. In class 2 anomaly can occur at any concentration. The mean space traced out by an anisodimensional particle is a double cone (fig. 2). Orientation increases the solid angle α until it approaches 180°. At this stage the conditions are fulfilled for Staudinger's treatment, except that in a sol flowing through a viscometer, orientation occurs only in an annular region whose thickness increases with rate of flow but never reaches the

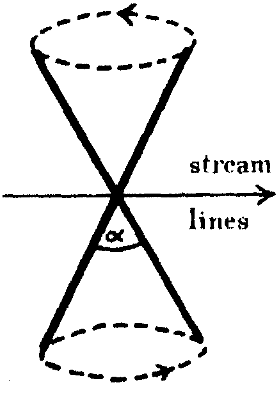

FIG. 2

radius of the tube. The method therefore seems to contain a serious systematic error.

The polymer molecule is usually only a few carbon atoms thick. It has not rigidity enough for gelation, and the more concentrated sols have high and anomalous viscosity. They are elastic liquids rather than rigid gels. This is reflected in the physical properties of the solid polymers. They are gluey or resin-like bodies. With the soaps dispersed in paraffin, I have been able to show directly the correlation between physical state of solute and mechanical properties of its dispersions. If soaps of the alkali metals are heated in paraffin, only swelling occurs at first, as the solvent has no direct dispersing effect upon the polar groups. When the temperature is raised higher, these are separated by thermal disruption and a clear solution is formed. On cooling to this temperature, the solution sets to a clear gel. The temperature is below the melting points of the soaps but strictly parallel to them in any series of kations with a common fatty acid or of fatty acid homologues with a common kation. On further cooling the gel changes abruptly to an opaque suspension of micro-crystals. This transition also is parallel to the change in the "solid" soaps from plastic to fully crystalline. In the cases of silver and aluminium soaps, stable homogeneous mechanically anomalous systems are formed also only over a temperature range corresponding with that over which the "solid" soaps are plastic.

In solutions of polymer molecules and of the soaps, the exteriors of the particles are lyophilic so that there is no cause for adhesion when they touch. With systems which owe their stability to adsorbed layers of ions, it is otherwise. Adhesion is a serious factor increasing rigidity. It varies with alteration of the surface electrical forces, either by addition of ions or by an external electric field.

Any attempt to treat colloidal systems by hydrodynamical theory must take into account the factors described, the relative importance of which varies largely in different systems. Especially, it must be recognized that the domain of colloid science is the range of particle size over which Brownian motion is a vital factor. The gelation phenomenon of "thixotropy" is due to this. If a gel is shaken and becomes a mobile liquid which resets on standing for some time, it is because Brownian motion is resolving the groups of anisodimensional particles with common orientation, due to the shaking, into the completely random structure required for gelation. Thixotropy is not therefore to be expected in systems of isodimensional particles. The increase of movement of particles with rise of temperature has been shown well in one case. Thixotropic gels of Fe_2O_3 reset after shaking more rapidly with increasing temperature—the temperature coefficient being much larger than that due to the simple increase of kinetic bombardment and corresponding to an energy of activation of some 30,000 kg. cal.

E. N. DA C. ANDRADE, F.R.S.—In attempting to construct a theory of liquid viscosity it is clear that we cannot proceed by adapting the theory of the viscosity of gases. The experimental fact that the viscosity of liquids decreases with rise of temperature, while that of gases increases with rise of temperature, is one indication; further, it is obvious from the most elementary considerations that there can be no question of a mean free path, or rather, of a free path at all, in liquids. The densities of the liquid and the solid form of any one substance differ by only a few per cent, so that it would appear more promising to regard a liquid as a kind of solid with a relaxed order, a loosened discipline, than as a dense gas: that is, by the time a gas has been compressed to a density of the liquid order of magnitude it has lost all these properties which we commonly regard as characteristic.

At the same time the type of mechanism that we require is one that will transfer momentum from one layer to another across planes parallel to the xy plane, supposing that the liquid is moving with velocity u in the x direction with a velocity gradient du/dz. Although there is no possibility of a molecule moving without collision through a distance of the order of a molecular diameter, it might be supposed that the viscous drag could be produced by the molecules diffusing from one layer of molecules to the next layer, taking their momentum with them unchanged. This, however, gives the wrong order for liquid viscosity in the one case where the self-diffusion of a liquid has been measured, namely, that of liquid lead, where the measurement has been made possible by the use of the radioactive isotope thorium B (Groh and Hevesey 1920). I have shown that the time for a molecule to move through its own diameter is $1 \cdot 9 \times 10^{-11}$ sec. (Andrade 1934), which leads to a coefficient of viscosity for liquid lead of the order of 2×10^{-4} as compared to the experimental value of the order 2×10^{-2}. This view of the mechanism is therefore untenable.

I suppose, on the other hand, that the local molecular field is not very different in the liquid and the solid state, since the distance between the molecules is much the same, and the arrangement is not grossly different (Prins 1936; Bernal 1937), especially for substances that crystallize in the closely packed state. The molecules in a liquid can then be regarded as vibrating about a mean position, which moves with a velocity very slow compared to the mean velocity of vibration, and can be neglected for a first approximation. It is assumed that the frequency of vibration, ν, of a molecule of a substance in the liquid state at the melting-point differs little from that of a molecule of the solid state at the same temperature. Further, the molecules come into close contact at each extreme libration: such contact has been assumed by Lindemann (1911) to characterize the transition from solid to liquid. It is also assumed that this contact, which may be considered as a momentary association, leads to a sharing of momentum between the two molecules in question. On these lines an expression for the coefficient of viscosity of a liquid at the melting-point can be easily derived: it is

$$\eta = \frac{4}{3}\frac{\nu m}{\sigma}, \tag{1}$$

where m is the mass of the molecule, and σ the average distance between the centres of molecules, so that $n\sigma^3 = 1$, where n is the number of molecules per unit volume. No doubt the constant $\frac{4}{3}$, derived on very rough assumptions, is only an approximation: even in the viscosity of gases at normal pressure, where the considerations are much simpler, the constant can only be evaluated with accuracy for monatomic gases.

There are various methods of measuring ν, but the more direct ones are not applicable to the class of substances which are best adapted for viscosity measurements. Lindemann, however, has, in his theory of melting, given an expression for ν in terms of the temperature of melting T, the volume of the gram-molecule V, and the atomic weight A, which is

$$\nu = C\sqrt{\frac{T}{AV^{\frac{2}{3}}}},$$

where C is $2\cdot8 \times 10^{12}$. Substituting, we have for the viscosity at melting-point

$$\eta = 5\cdot1 \times 10^{-4}\frac{(AT)^{\frac{1}{2}}}{V^{\frac{2}{3}}}. \tag{2}$$

The points to which I wish to direct attention are, firstly, that this formula, which contains no arbitrary constant, gives viscosities of the right order for monatomic liquids—and, indeed, for all liquids—and secondly, that for metals of close-packed crystal structure, which are clearly the simplest substances from the theoretical point of view, the agreement from substance to substance is striking. The recent measurements of Chiong (1936) have provided us with data on molten metals of very low viscosity, sodium and potassium, so that the viscosities of the molten metals, at melting-point, for which satisfactory measurements have been made, range from 0·0054 to 0·038. Fig. 3 shows the values given by the formula (2) plotted against the experimental values. All metals belonging to Hume-Rothery's Class I (close-packed, or approximately so) lie near a straight line bisecting the axes: gallium, bismuth and antimony belong to his Class III, where we cannot expect such good agreement.

Conversely, formula (1) may be used to find ν from the viscosity at melting-point, and Chiong has given a table comparing the values of ν so found with those derived from other methods.

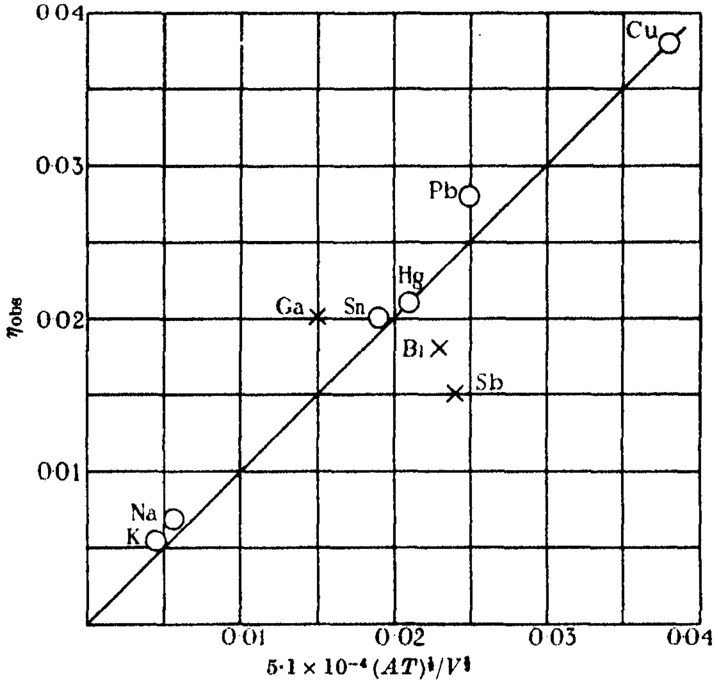

Fig. 3

The theory of the variation of viscosity with temperature is based upon ideas that have been admitted in the theory of gaseous association, namely, that whether combination takes place or not depends upon whether the molecules, at the instant of closest approach, are favourably disposed, say, in respect of either relative position or internal state. The simplest picture is, perhaps, that of some localization of charge which gives the molecules a potential energy, governed by the orientation of some molecular axis with respect to a local field, but the exact mechanism which makes the potential energy a minimum when the molecules are favourably disposed is immaterial. Whatever it may be, the temperature agitation will tend to prevent molecules being favourably disposed at the instant of closest approach. An application of Boltzmann's formula gives, allowing for the effect of expansion,

$$\eta v^{\frac{1}{3}} = Ae^{c/T.f(v)}, \tag{3}$$

where $f(v)$ expresses the variation of the local field with volume, due to changes of temperature. Taking as the simplest approximation $f(v) = 1/v$ we have

$$\eta v^{\frac{1}{3}} = Ae^{c/Tv}. \tag{4}$$

This formula is very successful in expressing the variation with temperature not only of molten metals, but also of a variety of organic compounds. It holds over a very wide range of viscosity; for instance, the viscosity of ethyl alcohol has been measured from −98° C., where the viscosity is 0·44, to 74° C., where it is 0·00476, a range of nearly a hundredfold, and the maximum departure at any temperature is less than 5 % of the viscosity at that temperature. For many substances, where the range of viscosities measured is as 1 to 3, or thereabouts, the discrepancies are within experimental error.

On the views put forward the viscosity should be independent of the temperature at very high temperatures. Spells (1936) has shown that for molten gallium, which has a very high boiling-point, the viscosity varies by only about 2 % from 1000 to 1100° C.

It is clear that any advance will be much facilitated by further data, especially systematic measurements made over a wide range of temperature with simple liquids whose other properties are known. Liquid metals would seem to be particularly appropriate, as only one kind of molecule is present, and that is monatomic in most cases, and of metals the close packed ones present the simplest case. At the present time experimental investigations on the viscosities of the molten alkali metals are proceeding at University College, and it is hoped to undertake in the near future a more extensive programme.

EMIL HATSCHEK—*Anomalous Viscosity in Suspensions of Spherical Particles*

The fact that suspensions of rigid and approximately spherical particles exhibited the same anomaly as lyophilic sols (gelatin, starch, etc.), viz. a decrease in viscosity with increasing rate of shear, was first demonstrated by Humphrey and Hatschek (1916). They investigated suspensions of rice starch (average diameter 3μ) in a mixture of toluene and carbon tetrachloride of the same density, in the concentric cylinder apparatus. The investigation was repeated and extended by Hatschek and Jane (1926), a mixture of viscous paraffin and carbon tetrachloride being used as medium with the object of obtaining higher absolute values. Fig. 4, which is taken from their paper, shows the deflexions of the inner cylinder plotted as ordinates against the angular velocity of the rotating outer cylinder as abscissae; for normal liquids in the laminar region these curves are of course straight lines parallel to the axis of abscissae. The viscosities tend to constant values which, however, are not always reached before turbulence sets in.

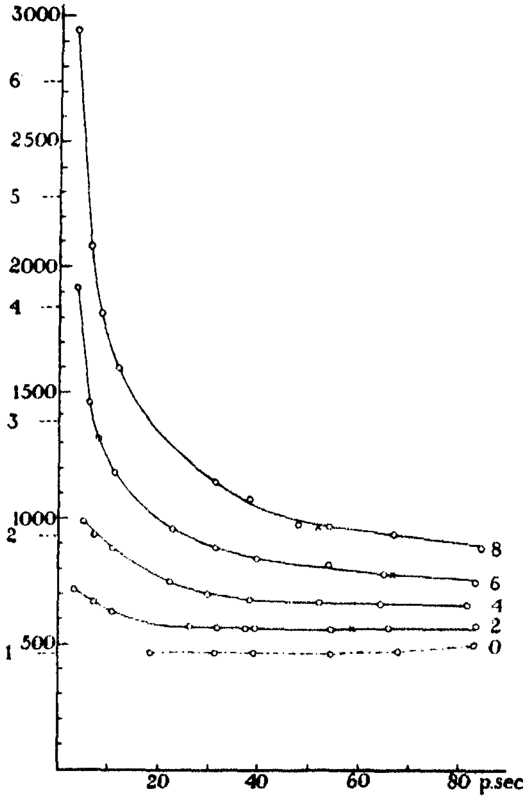

Fig. 4

To explain the behaviour described above it has been assumed that the virtual or effective volume of the particles is increased by a layer of adsorbed liquid and that, with increasing rate of shear, this layer is gradually stripped off. There is abundant evidence (e.g. from the sedimentation volume of powders) of the existence of such adsorbed layers.

An entirely different explanation of the anomaly is proposed by McDowell and Usher (1931) and supported by striking experimental evidence. These authors find that electrically neutral particles, like those of starch or carbon black in organic liquids, do not distribute themselves uniformly in the latter, but form clusters or ramifying aggregates. These occlude liquid which is no longer free, or may form a network with demonstrable rigidity, thus causing high viscosity at low rates of shear; with the progressive destruction of these structures at increasing rates the viscosity decreases.

The authors find that this process of aggregation can be prevented by the addition of "protective colloids" such as rubber or cellulose nitrate, and that suspensions thus protected do not exhibit any anomaly and behave like normal liquids.

These results give occasion for two remarks. The first is that it would now seem to be necessary to find an explanation for the aggregation of uncharged and unprotected particles, the cause of which is by no means self-evident.

The second is that the latest workers in this field (Eirich, Bunzl and Margaretha (1936)), have not found any anomaly with a suspension of uncharged and unprotected particles, viz. spores of *Lycoperdon bovista* in a mixture of paraffin and tetrachlorethane. Within the limits of concentration and velocity gradient investigated these behaved as normal liquids.

In systems in which both phases are liquid, i.e. emulsions, the particles are necessarily spherical unless their concentration is such that deformation by mutual contact takes place. With particles of uniform size—extremely difficult to obtain—and closest packing, contact would begin when the aggregate volume of particles amounts to 74·04 % of the total volume. With even two sizes of globules no general prediction is possible, but microscopic observation shows a considerable amount of deformation much below the limiting concentration.

Assuming particles of uniform size and in such concentration that they are deformed approximately into rhombododecahedra, which in laminar flow are alternately deformed into prisms and recover their original shape owing to the interfacial tension, the author has deduced the following conclusions (Hatschek 1911). Work has to be done in deforming the minimum polyhedra, which appears as increased viscosity. The amount of work done depends on the amount of recovery of the original shape, which in turn depends on the interfacial tension—necessarily low in stable emulsions—and on the rate of shear. As the latter increases, recovery becomes less and less complete, and when a certain rate is exceeded it ceases altogether. In terms of viscosity this means that the viscosity will decrease with increasing rate of shear and become constant beyond a certain value. This constant viscosity is given by the formula

$$\eta_r = \frac{1}{\sqrt[3]{(1-\phi)}},$$

in which η_r is the relative viscosity of the emulsion, that of the continuous phase being taken as 1, and ϕ is the fraction of the total volume occupied by the disperse phase; neither the viscosity of the latter nor the particle size appear in the equation.

These conclusions have been tested in an exhaustive investigation carried out with the concentric cylinder apparatus by Sibree (1930). Fig. 5 illustrates the decrease in viscosity with increasing rate of shear and the constant value eventually reached for four emulsions with the following percentages of disperse phase: [from top to bottom 75, 68.2, 60 and 50]; the dispersion medium was sodium oleate (1 %) in all cases, while the disperse phase was paraffin with an addition of bromoform sufficient to produce the same density as that of the soap solution.

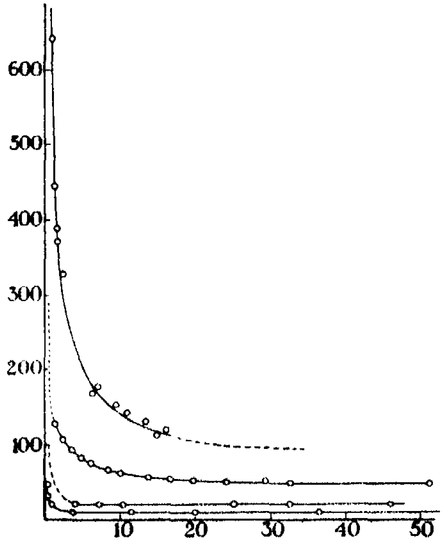

FIG. 5—Viscosity angular velocity curves.

According to the formula the viscosity of the emulsion should be independent of the viscosity of the disperse phase. Fig. 6, in which the coordinates have the same meaning as in figs. 4 and 5, shows that this holds for low rates of shear, but not exactly in the constant region. The emulsions were: A 50 % of viscous paraffin and B 50 % of limpid paraffin, the viscosities being respectively 64·2 and 1·7 (water = 1). The viscosities of the emulsions in the constant region were: A = 10·0 and B = 7·0, so that the effect of increasing the viscosity of the disperse phase over 37 times is, if not nil, at least very slight.

Finally, as regards the concentration function, the formula gives lower values of the viscosity than those found experimentally. If, however, the volume of disperse phase is multiplied with a factor varying within the narrow limits of 1·3 to 1·2, the agreement between calculated and experimental values is very good, and this holds for such extremes as limpid paraffin on the one hand and bitument on the other (Gabriel 1935).

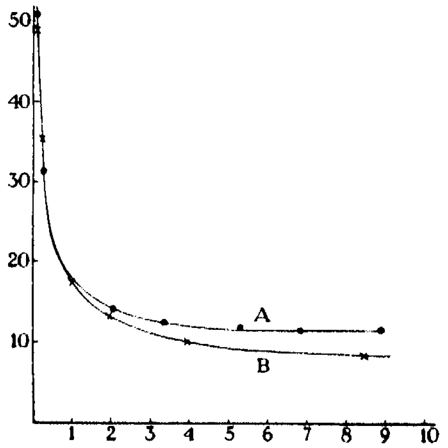

FIG. 6—Viscosity angular velocity curves at low rates of shear.

The meaning of this factor is for the present obscure. One obvious explanation is again an increase in the effective volume by adsorption layers, but this involves certain difficulties into which it is not necessary to go. Another possibility is, of course, that the stereometric assumptions made in deducing the formula are only a first approximation and might be improved by considering an assemblage of 14-faced polyhedra instead of the (unstable) dodecahedra.

It may be worth adding that Sibree (1934) has also investigated emulsions in which the disperse phase was air, i.e. froths, and that these show the same behaviour as emulsions with liquid disperse phase: the viscosity decreases with increasing rate of shear and eventually reaches a constant and fairly reproducible value.

R. K. SCHOFIELD—*The Viscosity of Flour Dough*

Henky (1929) and Eisenschitz (1933) have pointed out that it is necessary, when applying Maxwell's equation to the case of steady flow through a capillary or between concentric cylinders, to bear in mind that the direction of maximum shear does not coincide with the direction of maximum rate of shear, thereby resolving the apparent paradox that, in these systems, both remain constant. If, therefore, we wish to use Maxwell's equation to elucidate the behaviour of bodies that show solid (rigid) as well as fluid (viscous) properties, it is desirable to deform them in such a way that the direction of maximum shear and of maximum rate of shear are coincident. It is also desirable that the whole of the test piece should be strained uniformly.

These desiderata are practically fulfilled when a cylinder or prism of the material is extended axially. For this to be possible the material must be coherent. It is also desirable that the material should be soft, i.e. that its shear modulus should be very small in comparison with its bulk modulus, for, under these conditions the deformation can be regarded as the resultant of two simple shears each given numerically by the fractional elongation e, or better, $\log_e l/l_0$, while the corresponding shearing stresses, S, are numerically one-third of the tensile stress. Maxwell's equation then takes the form

$$\frac{de}{dt} = \frac{1}{n}\frac{dS}{dt} + \frac{1}{\eta}S,$$

and serves to define a rigidity modulus, n, and a viscosity, η, and enables us to evaluate these from measurements of e and S.

A dough made by kneading wheat flour with water is a very convenient material to investigate from this standpoint. One point that emerges in such a study (Schofield and Scott Blair 1933) is that a further term is needed to take account of elastic after-effect, since a cylinder of dough continues to contract for several minutes when released after being stretched. Thus de/dt has a finite negative value when both S and dS/dt are zero. Another term is evidently required. No grounds have so far been found for deciding the form of the additional term, but we have provisionally written it as $-d\alpha/dt$.

Maxwell's equation, thus amended, becomes

$$\frac{de}{dt} = \frac{1}{n}\frac{dS}{dt} - \frac{d\alpha}{dt} + \frac{1}{\eta}S.$$

The most direct way to determine η is to apply to a dough cylinder a known constant stress S for a series of short periods of time, Δt, separated by longer periods during which it is permitted free recovery. The length is noted each time just before the stress is applied when α may be taken as zero. In this way values are obtained of the rate of increase of permanent deformation, $\Delta e/\Delta t$, which must be divided into the shearing stress to obtain the viscosity.

The magnitude of the viscosity varies greatly for a given dough. It increases as the dough cylinder is stretched under constant shearing stress and for a given total extension is less the greater the shearing stress. A particular viscosity can, therefore, only be assigned to a dough when the shearing stress and total permanent deformation are specified.

Although we have been able to evaluate a viscosity of flour dough by using an equation developed by Maxwell for true fluids, it is clear that the mechanism that gives rise to viscosity in a flour dough is quite different from that which causes the viscosity of a true fluid. The dough is permeated by an extremely elastic protein network with insecure links between the positively and negatively charged groups (Schofield and Scott Blair 1937). Even a small deformation, when made for the first time, causes some links to break and the cylinder does not show complete elastic recovery. If the same stress is applied again a few more links may go, but on repeating the process a number of times a condition is reached when little further permanent deformation can be produced without increasing the stress. Quite a small rise in stress will considerably increase the rate of permanent deformation, since, as more links break, a bigger proportion of a higher stress falls on those that remain. Thus the viscosity increases with the amount of deformation under constant stress, and it is less the higher the stress.

REFERENCES

Andrade, E. N. da C. 1934 *Phil. Mag.* **17**, 497, 698.
Andrade, E. N. da C. and Chiong, Y. S. 1936 *Proc. Phys. Soc.* **48**, 247.
Batchinsky, A. 1913 *Z. phys. Chem.* **84**, 643.
Bernal, J. D. 1937 *Trans. Faraday Soc.* **33**, 27.
Biquard, P. and Lucas, R. 1937 *Trans. Faraday Soc.* **33**, 130.
Bridgeman, P. W. 1931 "Physics of High Pressure."
Chiong, Y. S. 1936 *Proc. Roy. Soc.* A, **157**, 264.
Eirich, F., Bunzl, M. and Margaretha, H. 1936 *Kolloidzeitschr.* **74**, 276.
Eisenschitz, R. 1933 *Kolloidzeitschr.* **64**, 184.
Errera, J., Claes, J. and Sack, H. 1937 *Trans. Faraday Soc.* **33**, 136.
Eyring, H. 1936 *J. Chem. Phys.* **4**, 283.
— 1937 *J. Phys. Chem.* **41**, 249.
Gabriel, L. 1935 "Technical Aspects of emulsions", p. 140 and following. London: A. Harvey.
Groh and Hevesey 1920 *Ann. Phys., Lpz.*, **63**, 85.
Guzman, J. de 1913 *An. Soc. esp. Fis Quim.* **11**, 353.
Hatschek, E. 1911 *Kolloidzeitschr.* **8**, 34.
Hatschek, E. and Jane, R. S. 1926 *Proc. Phys. Soc.* **38**, 274.
Henky, H. 1929 *Ann. Phys., Lpz.*, **2**, 617.
Humphrey, Edith and Hatschek, E. 1916 *Proc. Phys. Soc.* **38**, 274.
Lindemann 1911 *Phys. Z.* **11**, 609.
McDowell, C. M. and Usher, F. L. 1931 *Proc. Roy. Soc.* A, **409**, 564.
McLeod, D. B. 1923 *Trans. Faraday Soc.* **19**, 6.
Schofield, R. K. and Scott Blair, G. W. 1933 *Proc. Roy. Soc.* A, **141**, 72.
— — 1937 *Proc. Roy. Soc.* A, **160**, 87.

Sibree, J. O. 1930 *Trans. Faraday Soc.* **26**, 26.
— 1931 *Trans. Faraday Soc.* **27**, 161.
— 1934 *Trans. Faraday Soc.* **30**, 325.
Simon, F. 1929 *Z. anorg. Chem.* **178**, 309.
— 1931 *Z. anorg. Chem.* **203**, 219.
Spells, K. E. 1936 *Proc. Phys. Soc.* **48**, 299.
Prins, J. A. 1936 *Physica, 's Grav.*, **3**, 147.
Ward, A. G. 1937 *Trans. Faraday Soc.* **33**, 88.

On the Torsion of Conical Shells

BY R. V. SOUTHWELL, F.R.S.

(*Received* 30 *June* 1937)

INTRODUCTION AND SUMMARY

1—In my "Introduction to the Theory of Elasticity" (Chap. V) I have approached the torsion problem for circular shafts by way of the simpler case of a thin cylindrical shell. A rectangular plate of uniform thickness (fig. 1 *a*) will distort into a nearly rectangular parallelogram (fig. 1 *b*) under the action of uniform shearing stresses q applied to its four edges, and if the distorted plate *with stresses operative* is bent into a cylindrical form (fig. 1 *c*) the pair of opposite faces which are thereby brought into contact may be cemented together. Then their externally applied shear will cancel, leaving us with a cylindrical tube subjected to torsion; and the twist in the tube can be related with the shear strain in the originally flat plate.

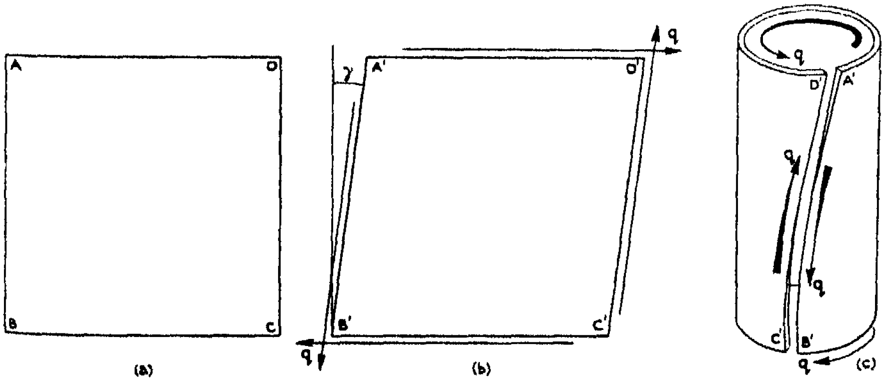

FIG. 1

An advantage of this treatment is that we can equally imagine the plate to be bent into a *non-circular* cylinder. Then by the same argument we arrive at the Bredt-Batho formula* for non-circular tubes, viz.

$$T = 2qtA, \tag{1}$$

where q stands for the intensity of shear stress in the tube wall,
t stands for the thickness of the tube wall, and
A stands for the area contained by its perimeter,
T stands for the applied torque.

The torque and twist can be related by considering the total strain-energy, and the warping of cross-sections, which is a well-known consequence of Saint-Venant's theory, can be deduced by a simple geometrical argument given in § 7 of this paper. It is not necessary (as in my book) to restrict the treatment to tubes of uniform thickness; for provided that t is small, so that q can be taken as constant across the thickness of the tube wall, qt will still be given by (1) although t varies round the perimeter of the cross-section, and the expressions for twist and warping are not seriously complicated. All of the results are supported (for tubes of small thickness) by exact calculations on orthodox lines.

2—In fact, whenever a stress distribution is known for a flat plate (of *small* but not necessarily of uniform thickness) which is stretched without being bent, we can deduce a new solution by imagining the strained plate to be wrapped round a rigid "former" and thereby to be bent into some developable surface.† (By taking the strained instead of the unstrained plate to have the specified form, we alter the stress system, but to a negligible extent. This is the basis of the principle of superposition.) Usually normal pressures between the plate and the former will be required for the maintenance of equilibrium; but the foregoing example shows that exceptions are possible, and in general it is clear that *transverse pressures will not be needed, if at every point a generator of the strained form bisects the (right) angle between principal stresses which are equal and opposite.*

3—A case of some importance is provided by thin conical shells, and detailed treatment of this problem may be useful in relation to the design of tapered wings and fuselages for aircraft. Without restriction on the degree of the taper it will be shown that an argument on the lines of § 1 leads to a generalization of the Bredt-Batho formula (1) which is easy to understand and to apply, and that the twist of the shell can be calculated without difficulty. As before the solution postulates that the torque is imposed in a particular way, and that strains are permitted to occur in accordance with theory.

---

* Cf. §§ 161, 162 (footnote), and supplementary note in p. 499 of my book.

† Caution is necessary when an effect of wrapping is to convert an equilibrating system of applied tractions into a system having a resultant; but the device would seem likely to be useful, e.g., for investigating the effect on torsional stiffness of constraints which prevent distortion of one or more terminal cross-sections.

Since warping was not considered in my book (attention is there confined to the stresses and the twist per unit length), this matter is discussed in relation to cylindrical tubes (§ 7) as a preliminary to the treatment of conical shells. It is shown that the calculated twist accounts in part, but not entirely, for the strain which must accompany the calculated shear stress: the remainder (of which the average value round the cross-section is zero) must be supplied by additional local distortion, and in a cylindrical tube the required distortion can arise from purely axial displacements, which involve no extension of the generators since they are the same for all cross-sections.

In a conical shell, on the other hand, displacements directed along the generators would entail extension of the plating, and therefore will not occur: instead, the shear strain which remains after allowance has been made for twist must be supplied by displacements directed along the surface and perpendicularly to the generators.* In order that they may not entail extension, these again must be accompanied by displacements normal to the surface, whereby the shapes of cross-sections will be changed. Unless the cone is circular they will also entail local changes of curvature, and in a shell of sensible thickness these changes will be resisted by flexural stresses; therefore a compromise must be effected in accordance with the principle of minimum strain-energy, and slight extension of the plating will result.† Nevertheless the solution gives a limit to which the actual occurrences will approximate as the thickness is reduced, and it is interesting to find that they differ thus fundamentally from what we might have expected on the basis of the results for a cylindrical shell. A deduction having practical importance is that diaphragms which resist changes in the shapes of cross-sections may be expected to have an appreciable stiffening effect when fitted to thin conical shells, whereas fitted to cylindrical shells they have no such effect.

---

* We can visualize a "former" (§ 2) composed of rigid disks which are free to turn about the axis of the cone, and we may assume that the plating is free to slip over its surface: then the twist will be common to the "former" and to the plating, whilst a relative slipping will provide the additional displacements.

† (*Added* 12 *July* 1937.) The required shear strain will be contributed in part by extension and in part by flexural strain, and the ratio of the two contributions will decrease as the square of the thickness. But the extensions resulting from given displacements along the generators will be proportional to the taper, which if small will have a relatively slight influence on the strains resulting from flexural displacements: therefore in the compromise *displacements* of the first type will have, relatively to those of the second, magnitudes decreasing with the thickness but varying (roughly) as the reciprocal of the taper. When the thickness is small and the taper considerable (as assumed in this paper) they will be negligible; but they will predominate when the thickness is considerable and the taper small, and they will constitute the whole of the required distortion when the taper is zero (i.e. in parallel tubes).

Part II is concerned with the question whether Saint-Venant's celebrated theory of torsion can be extended so as to include *thick* tubes and rods having the forms of non-circular cones. It is found (as we should expect from the foregoing results) that except in relation to sections of a special (circular or oval) type we can make no progress by assuming that the shapes of the cross-sections are not altered by torsional strain.

PART I—THE TORSION OF THIN CONICAL SHELLS

The Relation of Shear Stress to Torque

4—Just as a parallel tube can be constructed from a rectangular plate (cf. § 1), so a conical shell* can be constructed from a plate having the form of a curvilinear rectangle (fig. 2*a*). The centre of the curved edges will become the vertex of the conical shell (fig. 2*b*), and points on those edges, or on circles originally concentric with them, will lie at equal distances from the vertex of the cone, on closed curves which in this paper we shall term "cross-

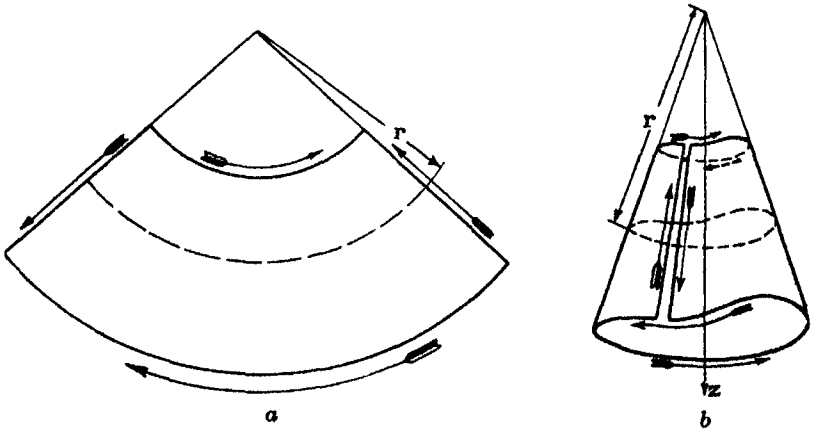

FIG. 2

---

* The word "shell" is here employed instead of "tube", in order to emphasize that no restriction is imposed upon the degree of the taper.

sections" of the shell. It is on these that we must concentrate attention, because they define the direction of the purely shearing stress; thus warping will be measured not (as for a cylindrical tube) in relation to plane sections, but in relation to curves of this kind. In tubes of small taper, or in cones which are nearly circular, they will be sensibly plane.

Thinking of the flat plate as part of a circular annulus subjected to uniform shear on its two concentric edges, and assuming its thickness to vary only with the distance from the centre,* it is easy to see that at other points the line-intensity of shear stress (qt) must be inversely proportional to r^2. Now imagining the plate to be bent into a conical shell, an argument on the same lines as before can be used to relate the shear with the resultant torque. We treat the thickness as negligible in comparison with the cross-sectional dimensions.

Let P, Q be two points on the same "cross-section" (r = const.) having co-ordinates x, y, z and $x+\delta x$, $y+\delta y$, $z+\delta z$ when z is taken along the axis of the cone and the origin of co-ordinates at its vertex (fig. 2*b*). Then PQ will be an elementary arc δs of the cross-section, and along this arc is operative a pure shear stress of uniform line-intensity $q_r t_r$ (say). The length of the arc is given by

$$\delta s = \sqrt{(\delta x^2 + \delta y^2 + \delta z^2)}, \tag{2}$$

and the total force of the shear stress is $q_r t_r \delta s$; so the component forces in the directions of x, y and z are respectively

$$q_r t_r . \delta x, \quad q_r t_r . \delta y, \quad q_r t_r . \delta z, \tag{i}$$

and the resultant action has components

$$q_r t_r \int_c dx, \quad q_r t_r \int_c dy, \quad q_r t_r \int_c dz, \tag{ii}$$

in which the integrals relate to the whole of the closed "cross-section", and accordingly vanish severally.

We deduce that the resultant action is a pure couple: its components about axes parallel to Ox, Oy, Oz will be given, according to (i), by

$$\left.\begin{aligned} M_x &= q_r t_r \int_c (y\,dz - z\,dy) = 2q_r t_r A_x, \\ M_y &= q_r t_r \int_c (z\,dx - x\,dz) = 2q_r t_r A_y, \\ T &= q_r t_r \int_c (x\,dy - y\,dx) = 2q_r t_r A_z, \end{aligned}\right\} \tag{3}$$

---

* qt will vary with r as r^{-2} under somewhat wider conditions. See Appendix.

in which the integrals again relate to the whole cross-section. Taken with due regard to signs they measure twice the areas (A_x, A_y, A_z) enclosed by its projections on the (y, z), (z, x) and (x, y) planes respectively. Thus we see from the third of (3) that the Bredt-Batho formula (1), properly interpreted, will still relate the shear stress with the applied torque.

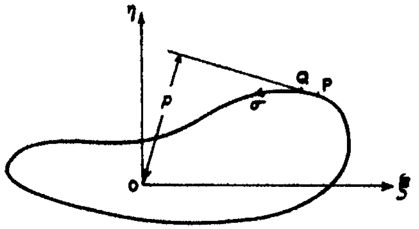

FIG. 3

5—Expressions for A_x, A_y, A_z can be obtained without difficulty. The shape of the cone can be specified by an equation relating ξ and η, the co-ordinates of the "datum section" made by the plane $(z = 1)$. Then the equation of the generator through $(\xi, \eta, 1)$ will be

$$\frac{x}{\xi} = \frac{y}{\eta} = z, \tag{iii}$$

and the co-ordinates of the point P (§ 4) which lies on this generator at a distance r from the vertex will be

$$x = \frac{\xi r}{\sqrt{(1+\xi^2+\eta^2)}}, \quad y = \frac{\eta r}{\sqrt{(1+\xi^2+\eta^2)}}, \quad z = \frac{r}{\sqrt{(1+\xi^2+\eta^2)}}. \tag{4}$$

Let Q correspond similarly with a second point $\xi + \delta\xi$, $\eta + \delta\eta$ in the "datum section", and write $\delta\sigma$ for the length of the elementary arc joining the first and second point. Then

$$\delta\xi = -\delta\sigma \cos(\eta, \nu), \quad \delta\eta = \delta\sigma \cos(\xi, \nu), \tag{iv}$$

ν denoting the normal to the datum section drawn outwards; and (since Q also lies at a distance r from the vertex) the co-ordinates of Q will be $x + \delta x$, $y + \delta y$, $z + \delta z$, where

$$\delta x = \frac{\partial x}{\partial \xi} . \delta\xi + \frac{\partial x}{\partial \eta} . \delta\eta$$

$$\left.\begin{aligned} &= \frac{-r . \delta\sigma}{(1+\xi^2+\eta^2)^{\frac{3}{2}}} [\xi\eta \cos(\xi, \nu) + (1+\eta^2)\cos(\eta, \nu)], \\ &\text{and similarly} \\ \delta y &= \frac{r . \delta\sigma}{(1+\xi^2+\eta^2)^{\frac{3}{2}}} [(1+\xi^2)\cos(\xi, \nu) + \xi\eta \cos(\eta, \nu)], \\ \delta z &= \frac{r . \delta\sigma}{(1+\xi^2+\eta^2)^{\frac{3}{2}}} [-\eta \cos(\xi, \nu) + \xi \cos(\eta, \nu)]. \end{aligned}\right\} \tag{5}$$

Substituting for x, y, z, dx, dy, dz from (4) and (5), we have from (3) the expressions

$$\left.\begin{aligned} 2A_x &= -r^2\int_c \frac{\cos(\xi,\nu)\,d\sigma}{(1+\xi^2+\eta^2)} = -r^2\int_c \frac{d\eta}{1+\xi^2+\eta^2},\\ 2A_y &= -r^2\int_c \frac{\cos(\eta,\nu)\,d\sigma}{(1+\xi^2+\eta^2)} = r^2\int_c \frac{d\xi}{1+\xi^2+\eta^2},\\ 2A_z &= r^2\int_c \frac{\xi\cos(\xi,\nu)+\eta\cos(\eta,\nu)}{1+\xi^2+\eta^2}\,d\sigma = r^2\int_c \frac{p\,d\sigma}{1+\xi^2+\eta^2},\end{aligned}\right\} \qquad (6)$$

p denoting the length of the perpendicular drawn in the datum section from the axis of the cone to the tangent at ξ, η. The integrals are purely numerical, depending on the geometry of the datum section, and we have seen (§ 4) that $q_r t_r$ is inversely proportional to r^2. Therefore according to (3) each component couple has a constant value for all sections: this result was to be expected on statical grounds.

For tubes of small taper ξ and η will be small in relation to unity. M_x, M_y will then be very small, and the torque will be given to a close approximation by

$$T = q_r t_r r^2\int_c p\,d\sigma = 2q_r t_r r^2 A_d = 2q_r t_r A_r, \qquad (7)$$

A_d denoting the area enclosed within the perimeter of the datum section, and A_r the corresponding area for the cross-section considered (i.e., very approximately, the section made by the plane $z = r$). When the taper is considerable, the Bredt-Batho formula must be replaced by (3) and (6), from which we see that the axis of the resultant couple will in general not be parallel with the axis of the cone.

The Relation of Torque to Twist

6—The twist may be calculated by appeal to energy principles, as in § 162 of my book. Let two "cross-sections", defined by values r and $r+\delta r$, be rotated relatively to one another about the z-axis through an angle $\delta\theta$, so that work is done against the twisting couple at the expense of the strain-energy stored initially. Then we have (C denoting the modulus of rigidity)

$$\tfrac{1}{2}T\delta\theta = \frac{1}{2C}\delta r\int_c q_r^2 t_r\,ds,$$

when the integral is taken round the whole of the cross-section,

$$= \frac{1}{2C}q_r^2 t_r^2\,\delta r\int_c \frac{ds}{t_r}, \qquad (8)$$

since $q_r t_r$ has a constant value on this curve. Using the third of equations (3) to eliminate q_r from (8), we have

$$\tau = \operatorname{Lim}\,(\delta\theta/\delta r) = \frac{T}{4CA_z^2}\int_c \frac{ds}{t_r}, \tag{9}$$

and from (8) again, now using the third of (3) to eliminate T, we have

$$2C\tau = q_r \times \frac{t_r}{A_z}\int_c \frac{ds}{t_r}. \tag{10}$$

When (as was assumed in § 4) t_r is a function of r only and therefore constant along the path of integration, (9) reduces to

$$\left.\begin{aligned} T &= C\tau \times \frac{4A_z^2 t_r}{\bar{s}}, \\ \text{and (10) to} \qquad q_r &= 2C\tau \frac{A_z}{\bar{s}}, \end{aligned}\right\} \tag{11}$$

$\bar{s}$ denoting the perimeter of the "cross-section". Relations equivalent to (11) are given, for a cylindrical tube of uniform thickness, in § 162 of my book: equations (9) and (10) give the modifications which are required in order to take account of thickness varying round the cross-section.

We observe that τ is defined in (9) as *twist per unit length of generator.* This definition is imposed by the consideration that only along a curve of constant r can the stress be taken to be a pure shear, and for such curves there is no appropriate value of z. In the special case of a cylinder ($\delta r = \delta z$) it accords with the customary definition.

A formula whereby A_z can be calculated for a tube of large taper is given in the third of (6). Substituting in (11) we have the required relations between T, τ and q for a conical shell of uniform thickness.

Warping of Cross-Sections

1—*Cylindrical Tube.*

7—The warping of cross-sections is not discussed in my book, and it will therefore be convenient to deal with this matter first in relation to cylindrical tubes.

We have at each point of the cross-section a shear strain in the plate of amount

$$\gamma = q/C, \tag{12}$$

where q is given by (1) or by the corresponding formula for a tube of non-uniform thickness. ***Such part of this strain as is not due to the twist*** **(τ)** ***must be supplied by warping of the cross-section.***

In fig. 4, let Ox, Oy be axes taken in the plane of the paper through O the centre of rotation in twist. (It will be shown later that the position of O is immaterial.) Let $A\nu$ be the normal at P, OA perpendicular to $A\nu$; and let p stand for the length of AP. Consider the relative movement of P and P_0, P_0 being initially at a distance d below P.

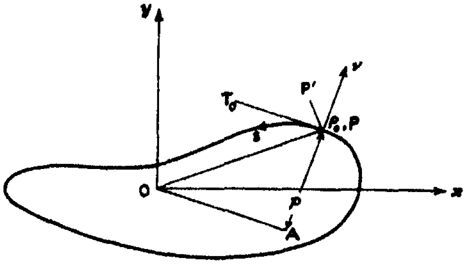

FIG. 4

P_0 being fixed, a *small* twist τ will involve a rotation τd about O, whereby P moves to P', PP' being perpendicular to OP and of length $\tau d . OP$. In consequence, if the co-ordinates of P_0 are $(x, y, 0)$, those of P' will become

$$x - y\tau d, \quad y + x\tau d, \quad d,$$

and the direction-cosines of the line $P_0 P'$ will be (to the first order of small quantities)

$$l = -y\tau, \quad m = x\tau, \quad n = 1. \tag{i}$$

Now the direction-cosines of $P_0 T_0$, the tangent in the cross-section to the tube wall at P_0, are

$$l' = -\cos(y, \nu), \quad m' = \cos(x, \nu), \quad n' = 0, \tag{ii}$$

and from (i) and (ii) we deduce that the cosine of the angle, *after strain*, between $P'P_0$ and $P_0 T_0$ will be

$$ll' + mm' + nn' = \tau\{x\cos(x, \nu) + y\cos(y, \nu)\}. \tag{iii}$$

Hence, if the sections did not warp, the shear strain (wholly due to twist) would be

$$\tau\{x\cos(x, \nu) + y\cos(y, \nu)\} = \tau p \quad \text{(fig. 4)}. \tag{13}$$

Actually the shear strain is given by (12) and (as stated earlier) the difference must be supplied by warping. Therefore, writing

$$w = \tau\phi. \tag{14}$$

for the distance through which a point on the cross-section moves perpendicularly to its original plane (i.e. in the direction Oz), we have

$$\frac{\partial w}{\partial s} = \tau \frac{\partial \phi}{\partial s} = \frac{q}{C} - \tau . p. \tag{15}$$

Excepting terms in w which represent a rigid-body displacement of the cross-section as a whole, this formula does not depend upon the position selected for the origin of co-ordinates, which is therefore immaterial.

Equation (15) makes w single-valued at every point. For on substituting for q/C its value according to (10), and then integrating the right-hand expression round the whole contour, we obtain*

$$\tau(2A - \int_c p ds), \quad \text{which is zero.}$$

It also accords with the exact theory of torsion. For on introducing the complementary torsion function ψ, related with ϕ by the equations (Love 1927, § 217)

$$\frac{\partial \phi}{\partial x} = \frac{\partial \psi}{\partial y}, \quad \frac{\partial \phi}{\partial y} = -\frac{\partial \psi}{\partial x}, \tag{16}$$

and using the formula for shear stress†

$$q = -C\tau \frac{\partial}{\partial \nu}\{\psi - \tfrac{1}{2}(x^2 + y^2)\},$$

we have according to the exact theory

$$q = C\tau \left\{ \cos(x, \nu) \left(\frac{\partial \phi}{\partial y} + x \right) - \cos(y, \nu) \left(\frac{\partial \phi}{\partial x} - y \right) \right\},$$

or

$$\frac{q}{C} = \tau \left(\frac{\partial \phi}{\partial s} + p \right), \quad \text{according to (13).}$$

This equation is identical with (15).

2—*Conical Shell.*

8—The more difficult case of a tapered tube may be treated on similar lines. As in § 7, to find the shear strain which is entailed by twist we consider the relative movement of the line joining two neighbouring points P_0, P of a generator, and of the tangent at P to the tube wall; but now the tangent must be taken along a cross-section (r = const.) instead of in a plane section (z = const.). Moreover, because cross-sections do not (unless the cone is circular) lie in one plane, purely axial displacements would not satisfy the condition that warping must involve no extension of any part of their lengths. Equally, no extension can occur in any part of a generator. Thus our problem is more difficult than it was in § 7, because no single component of displacement will satisfy the double condition, whereas there we could assume that cross-sections did not distort in their own planes.

---

* We suppress the suffix of A, which now has the same value for all cross-sections.

† Love 1927, § 219. A negative sign has been introduced, because q is measured in the direction of s (fig. 4); and C has been substituted for μ.

Let P_0, P lie on the generator through $(\xi, \eta, 1)$ and at distances $r-\delta r$, r from the vertex of the cone, and let Q be a neighbouring point on the tangent at P, so that Q lies on the generator through $(\xi+\delta\xi, \eta+\partial\eta, 1)$ and at a distance r from the vertex. Then the Cartesian co-ordinates of P will be given by (4) of § 5, those of P_0 will be given by (4) with r replaced by $r-\delta r$, and those of Q will be given by

$$x+\delta x, \quad y+\delta y, \quad z+\delta z,$$

where x, y, z have the expressions given in (4) and δx, δy, δz the expressions given by (5) of § 5. Let θ stand for the rotation about Oz of the curve defined by r, so that (as in § 6) $\tau = d\theta/dr$. Then on account of twist P and Q will rotate about Oz through an angle θ, P_0 through an angle

$$\theta-\delta r\frac{d\theta}{dr} = \theta-\tau . \delta r.$$

Without altering the strains we may impose a rotation $(\tau . \delta r-\theta)$ on the whole tube, thus bringing P_0 to its original position and imposing, as the effect of the twist, a rotation $\tau . \delta r$ on P and Q. The consequent changes in the co-ordinates will be:

$$\text{increases } -y\tau\delta r, \quad x\tau\delta r, \quad 0 \text{ in } x_P, y_P, z_P$$

$$\text{increases } -(y+\delta y)\tau\delta r, \quad (x+\delta x)\tau\delta r, \quad 0 \text{ in } x_Q, y_Q, z_Q;$$

so the direction-cosines of P, P_0 will be altered from

$$l_1, m_1, n_1 = -(x, y, z)/r$$

to $$l_2, m_2, n_2 = \left(-\frac{x}{r}+y\tau\right), \quad -\left(\frac{y}{r}+x\tau\right), \quad -(z/r)/\sqrt{\{1+(x^2+y^2)\tau^2\}},$$

where x, y, z are given by (4) of § 5; and the direction-cosines of PQ will be altered from

$$l_1', m_1', n_1' = (\delta x, \delta y, \delta z)/\sqrt{(\delta x^2+\delta y^2+\delta z^2)}$$

to $$l_2', m_2', n_2' = (\delta x_2, \delta y_2, \delta z)/\sqrt{(\delta x_2^2+\delta y_2^2+\delta z^2)},$$

where
$$\delta x_2 = \delta x - \delta y\, \tau \delta r,$$
$$\delta y_2 = \delta y + \delta x\, \tau \delta r,$$

and δx, δy, δz are given by (5) of § 5.

The cosine of the angle between PP_0 and PQ will thus be altered from

$$l_1 l_1' + m_1 m_1' + n_1 n_1' = 0,$$

by (4) and (5), to

$$l_2 l_2' + m_2 m_2' + n_2 n_2' = \frac{\tau(y\,\delta x - x\,\delta y)}{\sqrt{(\delta x^2 + \delta y^2 + \delta z^2)}} = \frac{\tau(y\,\delta x - x\,\delta y)}{\delta s},$$

in the limit, if we neglect terms of the second and higher orders in τ. That is to say, that part of the total shear strain which comes from the twist τ is given by

$$\tau\left(x\frac{dy}{ds} - y\frac{dx}{ds}\right), \tag{17}$$

when s is taken along the "cross-section", so that δs is given by (2).

In a cylindrical tube the cross-sections will be plane, and the quantity (17) has the significance given in (13) of § 7; so we have confirmed the result of that section. In a conical shell the quantity (17) will measure $2\tau\frac{dA_z}{ds}$, where A_z (as in § 4) stands for the area enclosed by the projection of the "cross section" upon the (x, y) plane. The remainder of the shear strain—that is, the quantity

$$\frac{q_r}{C} - 2\tau\frac{dA_z}{ds} \tag{18}$$

which corresponds with $(q/C - \tau p)$ in (15) of § 7—must be supplied by warping.

9—Observing that both terms in (18) vary with r like $(r^2 t)^{-1}$, we see that this warping cannot now be contributed by a displacement w along the generator, because then $\partial w/\partial r$ would be finite and accordingly the plate would suffer extension, thus invalidating our solution for the stresses. In contrast to the type of displacement (w) which we postulated in § 7, we have now to find a type of warping which entails no displacement along the generator.

The problem is simple if we observe that any strip of the shell lying between adjacent generators may be regarded as forming part of a *circular* cone, to which polar co-ordinates are appropriate. The expression for the relevant shear strain is (Love 1927, § 22)

$$e_{r\phi} = \frac{1}{r\sin\theta}\frac{\partial u_r}{\partial\phi} + \frac{\partial u_\phi}{\partial r} - \frac{u_\phi}{r},$$

and the extension of the surface in a direction at right angles to the generator is given by

$$e_{\phi\phi} = \frac{1}{r\sin\theta}\frac{\partial u_\phi}{\partial\phi} + \frac{u_\theta}{r}\cot\theta + \frac{u_r}{r},$$

u_r being the displacement along the generator, u_ϕ the displacement in the conical surface and perpendicular to u_r, and u_θ the displacement normal to the surface. In our notation u_r is w, *and is zero*; $1/r\sin\theta$ is the curvature of the cross-section $= 1/\rho$ (say), so that $\theta = \sin^{-1}(\rho/r)$; $r\sin\theta\, d\phi = ds$: therefore we may write

$$\left.\begin{aligned} e_{\phi\phi} &= \frac{\partial u_\phi}{\partial s} + \frac{u_\theta\cos\theta}{\rho}, \\ e_{r\phi} &= \frac{\partial u_\phi}{\partial r} - \frac{u_\phi}{r} = r\frac{\partial}{\partial r}\left(\frac{u_\phi}{r}\right). \end{aligned}\right\} \tag{19}$$

The first of (19) shows that we shall keep the strain inextensional if with u_r zero we associate u_ϕ and u_θ in suitable proportions. The second permits us to dispose of the remainder (18) of the shear strain by a proportionate displacement (u_ϕ) directed everywhere along the "cross-section". No work (on the whole) is entailed by this displacement: for the shear stress has a uniform line-intensity $q_r t_r$, and $\int_c u_\phi\, ds$ is proportional to

$$\int_c \left(\frac{q_r}{C} - 2\frac{dA_z}{ds}\right) ds = \frac{q_r t_r}{C}\int_c \frac{ds}{t_r} - 2\tau A_z,$$
$$= 0, \text{ by } (10).$$

10—The result of this investigation—that whereas in a cylindrical tube cross-sections warp in an axial direction without change of form in their own planes, cross-sections of the cone will be changed in shape but will not undergo displacement along the generators—is at first sight surprising; but it must be remembered that we have postulated an inextensional type of distortion, on the ground that we are assuming the plating to be infinitesimally thin. Displacements of the type u_ϕ will entail changes in the curvature cross-sections, and in plating of finite thickness these will be resisted by flexural stresses, which are here neglected. In consequence *some* extension will occur in accordance with the principle of minimum strain-energy; but its magnitude will decrease as the thickness is reduced, and our solution may be expected to be correct as regards the main features of the distortion which will occur in practice.*

In the case of the cylindrical tube (§ 7), by neglecting flexural stresses we could have arrived at an alternative type of strain, similarly involving no displacement along a generator. The relevant shear strain is measured by

$$\frac{\partial w}{\partial s} + \frac{\partial u_s}{\partial z}, \tag{20}$$

and the local extension of the cross-section by

$$\frac{\partial u_s}{\partial s} + \frac{u_\nu}{\rho}, \tag{21}$$

u_ν denoting the displacement along the normal to the cross-section, and u_s the displacement along the tangent, at a place when the local curvature is $1/\rho$. According to (20) and (21) we can obtain any value for the shear strain by keeping w zero and giving a suitable distribution to u_s, which must now be proportional to z, and we can eliminate extension by associating with u_s a suitable displacement u_ν. But in so doing we shall alter the curvature of the cross-section and thus introduce flexural stresses, whereas no unwanted stress is entailed by warping of the kind considered in § 7. Therefore, in a cylindrical tube of sensible thickness, the principle of minimum strain-energy prohibits a strain of this alternative type.

PART II—THE TORSION OF NON-CIRCULAR CONES OR OF THICK TUBES WITH TAPER

11—Part I suggests the question, whether any practicable generalization of the well-known theory of torsion for isotropic prisms can be made to cover the effects of taper in thick tubes or rods of non-circular cross-section.

In order to construct an approximate theory in the manner of Saint-Venant, we reduce the boundary conditions to one by assuming that

$$\widehat{\theta\theta} = \widehat{\phi\phi} = \widehat{\theta\phi} = 0, \tag{22}$$

---

* Cf. footnote, †, p. 339.

and then the conditions of equilibrium (Love 1927, § 59 (iv)) simplify at once to

$$\left.\begin{aligned} \frac{1}{r}\frac{\partial}{\partial r}(r^2.\widehat{rr})+\frac{1}{\sin\theta}\left\{\frac{\partial}{\partial\theta}(\sin\theta.\widehat{r\theta})+\frac{\partial}{\partial\phi}\widehat{r\phi}\right\} &= 0,\\ \frac{\partial}{\partial r}(r^3.\widehat{r\theta}) &= 0,\\ \frac{\partial}{\partial r}(r^3.\widehat{r\phi}) &= 0, \end{aligned}\right\} \tag{23}$$

the last two showing that $\widehat{r\theta}$, $\widehat{r\phi}$ (as we should expect on our assumptions) must vary with r as r^{-3}. On this understanding the first of (23) is satisfied by the expression

$$\widehat{rr}=\frac{1}{\sin\theta}\left\{\frac{\partial}{\partial\theta}(\sin\theta.\widehat{r\theta})+\frac{\partial}{\partial\phi}\widehat{r\phi}\right\} \tag{24}$$

(which makes $\widehat{rr}$ vary with r as r^{-3}); and any further term in $\widehat{rr}$ (the complementary function) must vary with r as r^{-2}, thus demanding no other stresses for equilibrium in the direction of r.

We are interested in $\widehat{rr}$ only as this stress-component may be necessary for compatibility of strains. So we may neglect the complementary function and assume that $\widehat{rr}$ is in fact given by (24); also that e_{rr}, $e_{\theta\theta}$, $e_{\phi\phi}$ (which are proportional to $\widehat{rr}$) vary with r as r^{-3},—i.e. that u_r, u_θ, u_ϕ all vary with r as r^{-2}.

12—Because $\widehat{\theta\phi}$ vanishes everywhere we have (Love 1927, § 22)

$$0=e_{\theta\phi}=\frac{\sin\theta}{r}\left\{\frac{\partial}{\partial\theta}\left(\frac{u_\phi}{\sin\theta}\right)+\frac{\partial}{\partial\phi}\left(\frac{u_\theta}{\sin^2\theta}\right)\right\},$$

showing that we may write

$$u_\theta=\frac{\sin^2\theta}{r^2}\frac{\partial\psi}{\partial\theta},\quad u_\phi=-\frac{\sin\theta}{r^2}\frac{\partial\psi}{\partial\phi}, \tag{25}$$

where ψ is some function of θ and ϕ at present undefined; and because $\widehat{\theta\theta}-\widehat{\phi\phi}=0$, we have

$$0=e_{\theta\theta}-e_{\phi\phi}=\frac{\sin\theta}{r}\left\{\frac{\partial}{\partial\theta}\left(\frac{u_\theta}{\sin\theta}\right)-\frac{\partial}{\partial\phi}\left(\frac{u_\phi}{\sin^2\theta}\right)\right\},$$

whence, on substitution from (25), we find that

$$\left[\left(\sin\theta\frac{\partial}{\partial\theta}\right)^2+\frac{\partial^2}{\partial\phi^2}\right]\psi=0. \tag{26}$$

13—In the first place we examine the possibility of equivoluminal solutions, in which $\widehat{rr}$ vanishes everywhere as well as $\widehat{\theta\theta}$, $\widehat{\phi\phi}$. Since $\partial u_r/\partial r$ must be zero, u_r will be independent of r and as such cannot contribute to $e_{r\theta}$, $e_{r\phi}$, which (like $\widehat{r\theta}$, $\widehat{r\phi}$) must be of order r^{-3}. Therefore without loss of generality we may take u_r to vanish, and then it will follow (since $e_{\theta\theta}$, $e_{\phi\phi}$ must vanish) that

$$\frac{\partial u_\theta}{\partial \theta} = \frac{\partial u_\phi}{\partial \phi} + u_\theta \cos\theta = 0, \quad \text{identically.}$$

From the first of these conditions, combined with (25), we deduce that the form of ψ is given by

$$\psi = f_1(\phi)\cot\theta + f_2(\phi),$$

and from the second, that

$$f_1''(\phi) + f_1(\phi) = 0, \quad f_2''(\phi) = 0.$$

Therefore, in any distortion such that e_{rr}, $e_{\theta\theta}$, $e_{\phi\phi}$ are zero, the most general expression for ψ is

$$A + B\phi + C\cot\theta\sin(\phi - \epsilon), \tag{27}$$

A, B, C, ϵ being arbitrary constants; and hence (u_r being zero) we have by (25)

$$e_{r\theta} = \frac{\partial u_\theta}{\partial r} - \frac{u_\theta}{r} = -\frac{3}{r^3}\sin^2\theta\frac{\partial \psi}{\partial \theta} = \frac{3C}{r^3}\sin(\phi - \epsilon),$$

$$e_{r\phi} = \frac{\partial u_\phi}{\partial r} - \frac{u_\phi}{r} = \frac{3}{r^3}\sin\theta\frac{\partial \psi}{\partial \phi} = \frac{3}{r^3}[B\sin\theta + C\cos\theta\cos(\phi - \epsilon)]. \tag{28}$$

These expressions give a zero value for

$$\frac{\partial}{\partial \theta}(\sin\theta \,.\, e_{r\theta}) + \frac{\partial}{\partial \phi}e_{r\phi},$$

and are therefore compatible with a zero value of $\widehat{rr}$ according to (24). We have thus obtained an equivoluminal solution which satisfies all of the imposed conditions.

Its range, however, is not wide. For the condition at the boundary of a cross-section is

$$\sin(s, \phi)\,\widehat{r\phi} - \cos(s, \phi)\,\widehat{r\theta} = 0, \tag{29}$$

and in this equation, according to (28), we have only two constants at our disposal. If, for example, $C = 0$, the condition (29) becomes

$$\tan(s, \phi) = 0$$

and requires that the cone be *circular*. Retaining C, we have a solution applicable to cones of a particular oval section.

14—Dispensing with any one of the simplifying assumptions (22) we should incur the added complication of a second boundary condition. The only remaining possibility is that these assumptions may be compatible with a finite stress $\widehat{rr}$, whereby u_r will be finite and will vary with r like r^{-2}.

By (26) we have ensured that $e_{\theta\theta} = e_{\phi\phi}$, but we have not hitherto made use of the condition

$$0 = \sigma e_{rr} + e_{\theta\theta} = \frac{1}{r}\left\{\frac{\partial u_\theta}{\partial \theta} + u_r + \sigma r \frac{\partial u_r}{\partial r}\right\},$$

$$= \frac{1}{r}\left\{\frac{\partial u_\theta}{\partial \theta} + (1-2\sigma)\, u_r\right\}, \quad \text{since } u_r \propto r^{-2}.$$

Writing

$$(1-2\sigma)\, u_r = -\frac{\partial u_\theta}{\partial \theta} \tag{30}$$

in the expressions for $e_{r\theta}$, $e_{r\phi}$, we have (Love 1927, § 22)

$$(1-2\sigma)\, e_{r\theta} = -\frac{1}{r}\left[\frac{\partial^2}{\partial \theta^2} + 3(1-2\sigma)\right] u_\theta,$$

$$(1-2\sigma)\, e_{r\phi} = -\frac{1}{r}\left[\frac{1}{\sin\theta}\cdot\frac{\partial^2 u_\theta}{\partial\theta\,\partial\phi} + 3(1-2\sigma)\, u_\phi\right],$$

and hence

$$\frac{1-2\sigma}{C}\left\{\frac{\partial}{\partial\theta}(\sin\theta\,.\,\widehat{r\theta}) + \frac{\partial}{\partial\phi}\widehat{r\phi}\right\}$$
$$= -\frac{1}{r}\left[\frac{\partial}{\partial\theta}\left\{\sin\theta\left(\frac{\partial^2 u_\theta}{\partial\theta^2} + 3(1-2\sigma)\, u_\theta\right)\right\} + \frac{1}{\sin\theta}\frac{\partial^3 u_\theta}{\partial\theta\,\partial\phi^2} + 3(1-2\sigma)\frac{\partial u_\phi}{\partial\phi}\right].$$

Now according to (24) this quantity must be equated to

$$\frac{1-2\sigma}{C}\sin\theta\,\widehat{rr} = 2(1+\sigma)(1-2\sigma)\sin\theta\frac{\partial u_r}{\partial r}$$

$$= -4(1+\sigma)(1-2\sigma)\sin\theta\frac{u_r}{r} \quad (\text{since } u_r \propto r^{-2})$$

$$= 4(1+\sigma)\frac{1}{r}\sin\theta\frac{\partial u_\theta}{\partial\theta}, \quad \text{by (30).}$$

Hence we have the condition

$$\left[4(1+\sigma)\sin\theta\frac{\partial}{\partial\theta}+\frac{\partial}{\partial\theta}\left\{\sin\theta\left[\frac{\partial^2}{\partial\theta^2}+3(1-2\sigma)\right]\right\}+\frac{1}{\sin\theta}\frac{\partial^3}{\partial\theta\,\partial\phi^2}\right]u_\theta$$

$$=-3(1-2\sigma)\frac{\partial u_\phi}{\partial\phi}$$

$$=-3(1-2\sigma)\left(\sin\theta\frac{\partial u_\theta}{\partial\theta}-\cos\theta\right)(u_\theta),$$

according to (25) and (26). Rearranging, we deduce that

$$\left[\sin\theta\frac{\partial^3}{\partial\theta^3}+\cos\theta\frac{\partial^2}{\partial\theta^2}+(10-8\sigma)\sin\theta\frac{\partial}{\partial\theta}\right]u_\theta$$

$$=-\frac{1}{\sin\theta}\frac{\partial^3 u_\theta}{\partial\theta\,\partial\phi^2}$$

$$=\left[\sin\theta\frac{\partial^3}{\partial\theta^3}+\cos\theta\frac{\partial^2}{\partial\theta^2}+2\sin\theta\frac{\partial}{\partial\theta}\right]u_\theta,$$

by (25) and (26) again. That is to say, we have the condition

$$8(1-\sigma)\sin\theta\frac{\partial u_\theta}{\partial\theta}=0,$$

and therefore, according to (30), u_r must vanish in virtue of (24) when we take account of the relations (25) and (26) found previously. We are thus brought back to the equivoluminal solution of § 13.

APPENDIX

The Conditions for Axially-Symmetrical Shear Strain in a Flat Circular Plate

In cylindrical co-ordinates, in order that equilibrium may be possible under a purely shearing stress of line intensity $Q = qt$, we must have (cf. Love 1927, § 59)

$$\frac{\partial Q}{\partial\theta}=0=\frac{\partial}{\partial r}(r^2Q);\quad \text{i.e., } r^2Q=\text{const.} \qquad \text{(i)}$$

Also, since the radial and circumferential displacements u_r, u_θ must entail no radial or circumferential stretching, we must have (Love 1927, § 22)

$$\frac{\partial u_r}{\partial r} = 0 = u_r + \frac{\partial u_\theta}{\partial \theta},$$

i.e.

$$u_r = F'(\theta), \quad u_\theta = \Phi(r) - F(\theta).$$

Accordingly

$$\frac{Q}{t} = q = Ce_{r\theta} = \frac{C}{r}\{r\Phi'(r) - \Phi(r) + F(\theta) + F''(\theta)\}$$

$$= f_1(r) + \frac{1}{r} f_2(\theta), \quad \text{say.} \tag{ii}$$

From (i) and (ii), eliminating Q, we find that the thickness is restricted by the condition

$$\frac{1}{t} \propto r^2 f_1(r) + r f_2(\theta). \tag{iii}$$

Particular cases are (*a*) $f_1(r) = 0$, $t \propto \frac{1}{r} f(\theta)$, and

(*b*) $f_2(\theta) = 0$, $t = \phi(r)$,—the case considered here.

References

Love, A. E. H. 1927 "The Mathematical Theory of Elasticity", 4th ed. Camb. Univ. Press.

Southwell, R. V. 1936 "Introduction to the Theory of Elasticity." Oxford Univ. Press.

Refractive Dispersion of Organic Compounds
IX—Optical Exaltation in Unsaturated Hydrocarbons containing Conjugated Double Bonds

By (the late) T. M. Lowry, F.R.S. and C. B. Allsopp, M.A., Ph.D.
Laboratory of Physical Chemistry, The University, Cambridge

(*Communicated by R. G. W. Norrish, F.R.S.—Received* 21 *August* 1937)

One of the ultimate aims of the present investigations of refractive dispersion is to elucidate the phenomenon of "optical exaltation" in organic compounds containing conjugated systems of alternate single and double bonds, as observed by Gladstone in 1881 and defined by Brühl in 1907. A first step was taken in Part IV (Allsopp 1934*a*) when dispersion curves were plotted over a wide range of wave-lengths for two compounds of the *cyclo*hexane series, viz. *cyclo*hexene (I), which contains a single olefinic double bond, and *cyclo*hexadiene (II), with two conjugated olefinic double bonds:

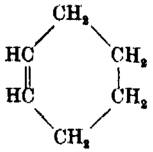
I. *Cyclo*hexene

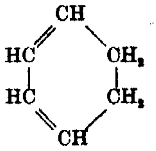
II. 1 : 3-*Cyclo*hexadiene

Actual and Neutral Conjugation

The alternation of single and double bonds, which is shown in (II), produces a very marked optical exaltation in 2 : 4-hexadiene (III), the molecular refraction of which, $M_D = 30{\cdot}64$ (Eykman 1892), is 1·65 units higher than the value $M_D = 28{\cdot}99$, observed in diallyl (IV) (Brühl 1880), where the two double bonds are isolated and the molecular refraction is

$CH_3.CH{=}CH{-}CH{=}CH.CH_3$
III. 2 : 4-Hexadiene

$CH_2{=}CH.CH_2.CH_2.CH{=}CH_2$
IV. Diallyl

almost identical with the value $M_D = 28{\cdot}97$, calculated by Eisenlohr (1912, p. 101). The alternate single and double bonds shown in Kekulé's formula for benzene give rise, however, to a molecular refraction $M_D = 26{\cdot}19$, which approximates closely to the value $M_D = 26{\cdot}30$, calculated for three independent double bonds (Eisenlohr 1912, p. 105). This fact was at first used as evidence in favour of Kekulé's formula (Brühl 1880), but when the phenomenon of optical exaltation was discovered, it was used with equal felicity against it.

In two papers published in 1907, Brühl attributed this anomaly to the presence in the benzene ring of "six absolutely equivalent carbon atoms" or of "three completely symmetrically arranged and identical ethenoid groups". He therefore drew a distinction between "actual" conjugated systems, which give rise to optical exaltation, and "neutral" conjugated systems, which resemble the isolated double bonds of ethylene, diallyl, etc., in that they give approximately normal molecular refractions.

An observation which affords a striking parallel to the absence of optical exaltation in benzene was made by Willstätter and Waser in 1911, when they discovered that the molecular refraction $M_D = 35{\cdot}20$ of *cyclo*octatetrene (V), which contains *four* pairs of alternate single and double bonds in a closed ring, also agrees closely with the calculated value, $M_D = 35{\cdot}24$.

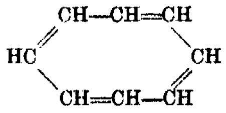
V. *Cyclo*octatetrene

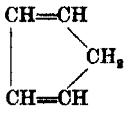
VI. *Cyclo*pentadiene

It was therefore supposed that the normal refractive power of these two hydrocarbons depends on the formation of a "closed circuit" of single and double bonds in the closed ring, in which the double bonds could not be localized, as compared with the more rigid "open circuit" of a conjugated chain; but this explanation was shown to be incomplete by the observations recorded in Part IV, since these provide conclusive evidence that 1 : 3-*cyclo*hexadiene (II), does not give rise to optical exaltation in the visible region of the spectrum.

This property of 1 : 3-*cyclo*hexadiene has already been recorded. Harries (1912) gives the value $M_D = 26{\cdot}85$, and Willstätter (1912) the value $M_D = 26{\cdot}79$, as compared with our own value, $M_D = 26{\cdot}84$, and the calculated value, $M_D = 26{\cdot}77$. Zelinsky and Gorsky (1908) found similar refractivities for both 1 : 3-*cyclo*hexadiene (II), and the 1 : 4-compound (VII), and they also recorded normal refractivity for the conjugated methyl-1-*cyclo*hexadiene-2 : 4 (VIII). Moreover, it has been observed that *cyclo*-

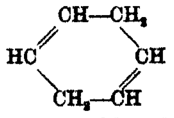
VII. 1 : 4-*Cyclo*hexadiene

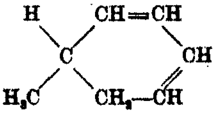
VIII. Methyl-1-*cyclo*hexadiene-2 : 4

pentadiene (VI), actually gives a small *negative* exaltation, $M_D = 21{\cdot}80$ (obs.), 22·23 (calc.) (Auwers and Eisenlohr 1910). On the other hand, the molecular refraction, $M_\alpha = 31{\cdot}57$, of tropilidene (IX), an isomer of toluene (X), containing a 7-atom ring, is 0·78 unit larger than the calculated value,

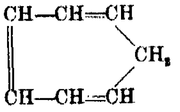

IX. Tropilidene

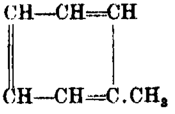

X. Toluene

$M_\alpha = 30{\cdot}89$, so that the conjugation was described as "actual" (Eykman 1892). The molecular refraction of toluene, however, $M_\alpha = 30{\cdot}79$, agrees closely with the calculated value, and the conjugation is obviously "neutral".

The absence of optical exaltation in compounds where the conjugated system forms part of a closed ring is unexpected. It is in direct contradiction to a prediction made by Brühl in 1907 *a*, *b*, which appears to have been widely accepted as an established fact, that 1 : 3-*cyclo*hexadiene, unlike the 1 : 4-diene, "would exercise an increased optical effect", and, indeed, attempts were made to explain away the observations. Thus, Eisenlohr (1912, p. 172) suggested that they might be due to an increase in density resulting from oxidation or polymerization of the very reactive hydrocarbons, and such an increase of density actually occurs in *cyclo*pentadiene (Auwers 1911; Brühl 1908). The new observations in the case of 1 : 3-*cyclo*hexadiene, however, completely rule out such an explanation, since the changes in density and corresponding changes in refraction only became measurable *after* the recorded readings had been made with freshly distilled pure material.

INFLUENCE OF WAVE-LENGTH ON OPTICAL EXALTATION

In view of the conclusion reached in a preceding paper (Allsopp and Willis 1936) that the refractivity of a molecule may be expected to be the sum of the refractivities of its component atoms only when its refractive indices can be represented by a dispersion equation containing a single variable term with a characteristic frequency in the Schumann region, it is desirable at this point to examine the refractivities of benzene and of 1 : 3-*cyclo*hexadiene at a wave-length nearer to the ultra-violet absorption bands of these compounds. Thus, it has already been shown that their dispersion curves rise steeply on passing from the visible into the ultra-violet, and actually intersect at a wave-length of 3030 A (Allsopp 1934 *a*, *b*; Lowry and Allsopp 1931). The respective molecular refractivities at this wave-length can either be calculated from the accurate atomic refractivities of carbon and hydrogen and the C=C double bond which are now available (Allsopp and Willis 1936), or directly from the data set out in Table I by direct extrapolation from the molecular refractions of C_6H_{10} and C_6H_{12}. For the present purpose the latter process is probably preferable, since it automatically corrects for effects due to ring formation which may perhaps have been inherent in the value for H_2 deduced from the difference between the molecular refractions of C_6H_{12} and C_6H_{14}. On this basis the observed molecular refraction for benzene is seen to be 1·21 units higher than the extrapolated value, $M_{3030} = 28{\cdot}79$, for a ring containing *three* double bonds, whilst that of 1 : 3-*cyclo*hexadiene is no less than 3·24 units higher than the extrapolated value, $M_{3030} = 29{\cdot}03$, for a ring with *two* double bonds.

TABLE I—MOLECULAR REFRACTIONS OF HYDROCARBONS AT $\lambda = 3030$ A

	C_6H_6	C_6H_8	C_6H_{10}	C_6H_{12}
M_{3030} (obs.)	30·10	32·27	29·27	29·51
M_{3030} (calc.)	28·79	29·03	29·27	29·51
Exaltation	+1·21	+3·24	—	—

These results can be correlated immediately with the absorption spectra of the two compounds. Thus, (i) in addition to strong bands in the Schumann region, which dominate the curve of refractive dispersion in the visible spectrum, benzene gives a complex group of bands in the ultra-violet rising to a maximum intensity $\log\epsilon = 2{\cdot}3$ at about 2550 A (Henri 1919, p. 112). This weaker absorption only affects the refractive index at wave-lengths near to it (Lowry and Allsopp 1931), but may be considered chiefly responsible for the development of the optical exaltation at short wave-lengths. (ii) 1 : 3-*Cyclo*hexadiene, on the other hand, gives a strong absorption band with twin maxima, $\log\epsilon = 3{\cdot}8$ at 2680 A and 4·0 at 2570 A. This band again makes a much smaller contribution to the refraction than do intense bands in the Schumann region, which quite control the refractive indices in the visible region. The absorption in the ultra-violet is, however, much stronger than that of benzene, and the maxima occur at slightly longer wave-lengths; it therefore produces a much larger partial refraction and an optical exaltation at ultra-violet wave-lengths adjacent to it.

DISCUSSION

In the light of these facts, the optical exaltation exhibited by hydrocarbons containing conjugated systems of olefinic double bonds might be explained as follows:

(i) The refraction of saturated hydrocarbons is controlled by very intense absorption frequencies in the Schumann region at about 1100 A. The molecular refraction of these hydrocarbons is then an additive function of the atomic refractivities of carbon and hydrogen, i.e. of the refractions of the electrons of the single bonds between carbon and carbon and between carbon and hydrogen.

(ii) The refraction of unsaturated hydrocarbons contains an extra term due to an absorption band at the limits of the "quartz" ultra-violet, which may be attributed to the shared electrons of the double bond (Snow and Allsopp 1934). In practice, this extra partial refraction may be represented by the addition to the molecular refraction of a constant amount for each olefinic double bond.

(iii) Conjugated hydrocarbons exhibit absorption bands which are more intense and at lower frequencies than those of unconjugated hydrocarbons. Thus, when two or three double bonds are present in the molecule, these bands are readily observed in an easily accessible region in the ultra-violet; and in systems containing more than four conjugated ethylenic bonds, they may give rise to visible colour (Kuhn and Winterstein 1929). The phenomenon of optical exaltation might therefore be attributed to an additional partial refraction associated with absorption bands in the ultra-violet or visible spectrum which are carried by the electrons of the conjugated system. The magnitude of the exaltation would then depend on the position and intensity of these bands.

More careful examination of the data, however, reveals that this simple description is not complete. Thus, whilst it is in harmony with the fact that exaltation is observed at visual wave-lengths in hexatriene (XI), but not

$$CH_2{=}CH{-}CH{=}CH{-}CH{=}CH_2$$

XI. Hexatriene

in benzene, since the absorption of the open-chain compound is already ten times more intense at 3350 A than that of benzene at its maximum at 2550 A (Baly and Tuck 1908), the same explanation will not account for the appearance of the phenomenon in 2 : 4-hexadiene, for which $\log \epsilon_{max} = 4{\cdot}4$ at 2275 A (Scheibe and Pummerer 1927), and its non-appearance in 1 : 3-*cyclo*hexadiene, with $\log \epsilon_{max} = 3{\cdot}98$ at 2560 A, i.e. with its absorption band nearly 300 A *nearer* the visible spectrum. The wave-lengths of the maxima of intensity of the ultra-violet absorption bands of the few molecules containing conjugated ethylenic bonds for which reliable data have been recorded are collected in Table II, in which the compounds which show optical exaltation at visual wave-lengths are separated from those which do not, but which does not include dienes containing substituted phenyl groups, which are mentioned below. The table reveals the striking fact that, for these simpler structures, exaltation is exhibited by the open-chain compounds, but is entirely or almost completely absent in the corresponding ring compounds, *irrespective of the position of the absorption bands.* In the case of benzene or of toluene, this apparently exceptional behaviour of the ring compound may be attributed to its peculiarly symmetrical electronic configuration, to which the diminished intensity of absorption—ten to fifty times less than for any of the dienes—can also be ascribed; but this configuration cannot be repeated in ring molecules the conventional formulae of which contain only two double bonds, and which possess quite different chemical properties.

TABLE II—ULTRA-VIOLET ABSORPTION BANDS OF HYDROCARBONS CONTAINING CONJUGATED DOUBLE BONDS

Substance	Formula	$\lambda_{\max}$ A	$\epsilon_{\max}$	Observer
	a—Compounds Exhibiting Marked Optical Exaltation			
Butadiene	$H_2C{=}CH{-}CH{=}CH_2$	2170	48,000	Smakula (1934)
Isoprene	$H_2C{=}C(CH_3){-}CH{=}CH_2$	2200	55,000	,, ,,
Dimethyl butadiene	$H_2C{=}C(CH_3){-}C(CH_3){=}CH_2$	2250	47,000	,, ,,
Hexadiene (2 : 4)	$H_3C{-}CH{=}CH{-}CH{=}CH{-}CH_3$	2265	25,000	Scheibe (1927)
Hexatriene	$H_2C{=}CH{-}CH{=}CH{-}CH{=}CH_2$	> Benzene	> Benzene	Baly and Tuck (1908)
	b—Compounds Exhibiting No or Very Little Exaltation			
*Cyclo*pentadiene	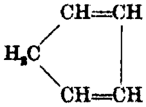	2400	2,850	Ley (1918)
1 : 3-*Cyclo*hexadiene	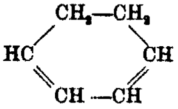	2560	9,900	Allsopp (1934 *a*, *b*)
Benzene	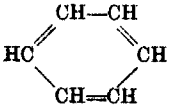	2550	240	Henri (1919)
Toluene	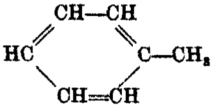	2630	210	Ramart-Lucas (1934)

It appears therefore that the optical properties of systems such as these may be affected strongly by the *configuration* of the double bonds (Allsopp 1934*b*; W. Hückel 1934, p. 102). Such an effect is, indeed, beyond dispute in the crystals of conjugated compounds. Thus, the crystals of quinhydrone, which contain a conjugated system indefinitely extended in one direction (Hengstenberg 1932), have very low refractive indices for vibrations in either of the principal planes perpendicular to this axis; but they are almost opaque to light vibrating in the direction of the parallel double bonds, for which the refractive index rises above 2 (Bernal). It is also known, from the work of R. Kuhn on bixin and on crocetin (1932, 1933), that conjugated systems with a *cis*-configuration are relatively unstable and are readily converted (e.g. under the influence of iodine or of visible light) into the more stable *trans*-compounds, in which all the double bonds are written in a parallel position.

A further paragraph must therefore be added to the description of optical exaltation which was given above, viz. (iv) The intensity and position of the absorption bands, and the magnitude of the optical exaltation produced, may be influenced by many factors, one of which is the configuration of the conjugated hydrocarbon chain. Thus, optical exaltation would be likely to be developed most readily when the double bonds of the C=C—C=C grouping are free to assume a *parallel* configuration, as in 2 : 4-hexadiene (XII), but not so easily when they are held in a *cis*-configuration by the formation of a ring, 1 : 3-*cyclo*hexadiene (XIII). This deduction is in harmony with the existence of optical exaltation (0·9 unit) in methene-*cyclo*hexene (XIV) (Romburgh and Dorssen 1906; Perkin 1907), and in *p*-dimethyl-semi-benzene (XV), for which the value (2·49 units) is almost exactly equal to that observed in hexatriene, M_D = 31·03 (obs.), 28·54 (calc.) (Eisenlohr 1912, p. 147). The "neutralizing" effect of ring formation, so marked in *cyclo*pentadiene, *cyclo*hexadiene, benzene, toluene, *cyclo*-octatetrene, etc., is therefore removed when the double bonds are again free to assume the "parallel" configuration shown in formulae (XIV) and

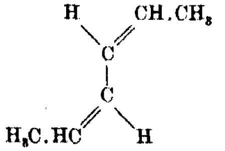

XII. 2 : 4-Hexadiene

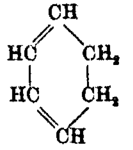

XIII. 1 : 3-*Cyclo*hexadiene

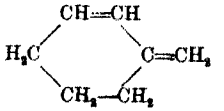

XIV. Methene*cyclo*hexene

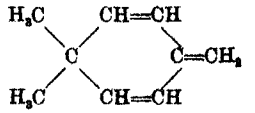

XV. *p*-Dimethyl-semi-benzene

(XV). A similar explanation could perhaps be given of the much enhanced exaltations which are produced when phenyl groups are substituted at the ends of conjugated open chains, e.g. in diphenyl butadiene (XVI) (exaltation = 15 units) (Klages 1907), or in diphenyl hexatriene (XVII), (24 units)

$C_6H_5—CH{=}CH—CH{=}CH—C_6H_5$

XVI. Diphenyl butadiene

$C_6H_5—CH{=}CH—CH{=}CH—CH{=}CH—C_6H_5$

XVII. Diphenyl hexatriene

(Smedley 1908), the absorption bands of these compounds also being markedly displaced towards longer wave-lengths (Smakula 1934). It is also interesting to note that exaltation is observed in styrene (XVIII), for which $\lambda_{max} = 2900$ A, exaltation = 0·6 unit, and in propenyl benzene (XIX), but not in allyl benzene (XX) (Eisenlohr 1912, p. 105).

$C_6H_5—CH{=}CH_2$

XVIII. Styrene

$C_6H_5—CH{=}CH—CH_3$

XIX. Propenyl benzene

$C_6H_5—CH_2—CH{=}CH_2$

XX. Allyl benzene

It must, however, be borne in mind that the conventional formulae for these conjugated systems do not necessarily reproduce their electronic configurations. Thus, if the non-bonding electrons of the carbon atoms in benzene are distributed symmetrically above and below the plane of the ring (Hückel 1931), which may be represented schematically by (XXI), butadiene could be written as in (XXII), in which the thicker lines represent the shorter carbon to carbon distances of the double bonds (Lennard-Jones 1937). The *cis*- and *trans*-configurations in conjugated systems as described above would then become those of (XXIII) and (XXIV) respectively.

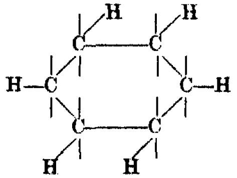

XXI. Benzene

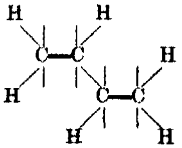

XXII. Butadiene

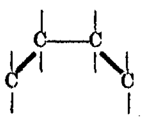

XXIII. *cis*-Double bonds

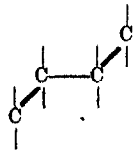

XXIV. *trans*-Double bonds

An attempt to account for some of the properties of conjugated compounds on the basis of resonance has been made by Pauling (1933), who calculated a number of heats of hydrogenation; but the values so obtained are not in agreement with recent measurements by Kistiakowsky (1936), who finds, for instance, that whereas the hydrogenation of many unsaturated systems (e.g. *cyclo*hexene, *cyclo*pentadiene, butadiene) proceeds exothermically, the formation of 1 : 3-*cyclo*hexadiene by hydrogenation of benzene is endothermic. Kistiakowsky concludes that resonance will not account for all the observed facts. In the case of 1 : 3-*cyclo*hexadiene, it seems probable that the endothermic nature of the reaction arises from the existence of a dipole in the product, and that this dipole must also be taken into account in the calculations. It would also explain the displacement of the ultra-violet absorption bands of the ring compound towards lower frequencies as compared with those of (presumably) non-polar butadiene.

This paper was originally written, but left unpublished, by the late Professor T. M. Lowry, F.R.S. It has now been revised and rewritten, at his request, by the junior author, who expresses his indebtedness to his late teacher, and also thanks Professor J. E. Lennard-Jones, F.R.S., and fellow-workers in the Department of Physical Chemistry, Cambridge University, for their friendly advice and criticism.

SUMMARY

Optical exaltation appears to be exhibited by a system of two conjugated ethylenic double bonds when these form part of an open chain (e.g. 2 : 4-hexadiene) but not when they are built into a ring (e.g. 1 : 3-*cyclo*hexadiene). The ultra-violet absorption bands of conjugated ring systems are displaced towards lower frequencies relative to those of the corresponding open-chain systems. These effects of configuration on the optical properties of a conjugated system are discussed.

REFERENCES

Allsopp, C. B. 1934*a* *Proc. Roy. Soc.* A, **143**, 618–30.
— 1934*b* *Rep. Brit. Ass.* p. 291.
Allsopp, C. B. and Willis, H. F. 1936 *Proc. Roy. Soc.* A, **153**, 379–406.
Auwers, K. v. 1911 *Ber. dtsch. chem. Ges.* **44**, 3679–92.
Auwers, K. v. and Eisenlohr, F. 1910 *Ber. dtsch. chem. Ges.* **43**, 806–26 and 1545.
Baly, E. C. C. and Tuck, W. B. 1908 *J. Chem. Soc.* pp. 1902–14.
Bernal, J. D. Private Communication.
Brühl, J. W. 1880 *Liebig's Ann.* **200**, 139–231.
— 1907*a* *J. Chem. Soc.* **91**, 115–22.
— 1907*b* *Ber. dtsch. chem. Ges.* **40**, 878–902, 1153–62.
— 1908 *Ber. dtsch. chem. Ges.* **41**, 3712–20.

Eisenlohr, F. 1912 "Spektrochemie Organischer Verbindungen." Stuttgart: Enke.
Eykman, J. F. 1892 *Ber. dtsch. chem. Ges.* **25**, 3069–79.
Gladstone, J. H. 1881 *Proc. Roy. Soc.* **31**, 327–30.
Harries, C. D. 1912 *Ber. dtsch. chem. Ges.* **45**, 809–16.
Hengstenberg, J. and Mark, H. 1932 *Naturwissenschaften*, **20**, 539–44.
Henri, V. 1919 "Etudes de Photochimie." Paris: Gauthiers-Villars.
Hückel, E. 1931 *Z. Phys.* **70**, 204–86.
Hückel, W. 1934 "Theoretische Grundlagen der Organischen Chemie", **2**. Leipzig: Akademische Verlag.
Kistiakowsky, G. B., Ruhoff, J. R., Smith, H. A. and Vaughan, W. E. 1936 *J. Amer. Chem. Soc.* **58**, 146–53.
Klages, W. A. H. 1907 *Ber. dtsch. chem. Ges.* **40**, 1768–72.
Kuhn, R. and Winterstein, A. 1929 *Helv. chim. Acta*, **12**, 899–903.
— — 1932 *Ber. dtsch. chem. Ges.* **65**, 646–51.
— — 1933 *Ber. dtsch. chem. Ges.* **66**, 209–14.
Lennard-Jones, J. E., Turkevich, J. and Penney, W. G. 1937 *Proc. Roy. Soc.* A, **158**, 280–324.
Ley, H. 1918 *Ber. dtsch. chem. Ges.* **51**, 1808–19.
Lowry, T. M. and Allsopp, C. B. 1931 *Proc. Roy. Soc.* A, **133**, 48–59.
Pauling, L. and Sherman, J. 1933 *J. Chem. Phys.* **1**, 606–17.
Perkin, W. 1907 *J. Chem. Soc.* **91**, 806–16.
Ramart-Lucas, Mme P. 1934 "Structure des Molécules et Spectres d'Absorption." Grignard's "Traité de Chimie Organique", **2**. Paris: Masson.
Romburgh, P. v. and Dorssen, W. v. 1906 *Proc. K. Akad. Wet. Amst.* **8**, 565–8.
Scheibe, G. and Pummerer, R. 1927 *Ber. dtsch. chem. Ges.* **60**, 2163–7.
Smakula, A. 1934 *Z. angew. Chem.* **47**, 657–65.
Smedley, Miss I. 1908 *J. Chem. Soc.* pp. 372–84.
Snow, C. P. and Allsopp, C. B. 1934 *Trans. Faraday Soc.* **30**, 93–9.
Willstätter, R. and Hatt, D. 1912 *Ber. dtsch. chem. Ges.* **45**, 1464–71.
Willstätter, R. and Waser, E. 1911 *Ber. dtsch. chem. Ges.* **44**, 3423–45.
Zelinsky, N. D. and Gorsky, A. 1908 *Ber. dtsch. chem. Ges.* **41**, 2479–87.

Measurements of Range and Angle of Projection for the Protons produced in the Photo-Disintegration of Deuterium

By J. Chadwick, F.R.S., N. Feather and E. Bretscher*

(*Received* 8 *September* 1937)

Introduction

The disintegration of a nucleus by the action of γ-rays—the nuclear photo-effect—was first observed by Chadwick and Goldhaber (1934) in the case of deuterium. The products of the disintegration are of course a proton and a neutron. In the first experiments only the protons liberated in the transformation were detected. This was done by means of an ionization chamber and "proportional" valve amplifier, and in this way a rough estimate was obtained of the mean kinetic energy with which the protons were ejected. Later the same authors (1935) supplemented the earlier evidence by detecting the neutrons liberated in the disintegration.† For this purpose a boron-lined ionization chamber embedded in paraffin wax was used. They were further able to show that, per unit solid angle, the number of neutrons emitted in the direction of the γ-ray quanta was roughly about half the number emitted at right angles to that direction.

The present paper describes an attempt to obtain more detailed information concerning the angular distribution of the disintegration particles and their binding energy in the deuterium nucleus. As was pointed out in each of the earlier discussions, such information can be obtained easily only by use of the expansion chamber. With the expansion chamber it is merely necessary to employ a deuterium-rich gas as filling and to be able to take satisfactory photographs of heavy particle tracks in the presence of the relatively intense background of cloud arising from the general γ-ray ionization in the chamber. These two conditions were successfully realized in the early summer of 1935, and a large number of photographs was taken with various arrangements. This work was carried out in the Cavendish Laboratory. Before all the photographs had been measured a preliminary report was made to the Norwich meeting of the British Association in

---

* Rockefeller Foundation Fellow.

† A successful attempt to detect the production of neutrons was also made independently by Banks, Chalmers and Hopwood (1935).

September 1935.* About the same time all three authors left Cambridge, and the task of completing the measurements and writing the final account of the research was considerably delayed in consequence. Two of us (J. C. and N. F.), however, made an entirely new set of measurements on all the photographs in March and April 1936. The results of these observations, carried out in the Physics Laboratory of the University of Liverpool, showed good agreement with the earlier incomplete data, and the final range and angular distributions have been based upon them exclusively.

Since discussion of these results will be greatly facilitated by a clear appreciation of the dynamics of the disintegration process, we shall begin by a general consideration of this question.

THE DYNAMICS OF THE PROCESS

In a particular case of disintegration, let θ and ϕ be the angles of projection (with respect to the direction of incidence of a γ-ray quantum of energy $h\nu$) of the proton and neutron produced from a deuteron initially at rest. Let M_1, M_2 be the masses of the proton and the neutron, respectively, and E/c^2 (mass units) be the binding energy of the deuteron. Then, from Einstein's law, the mass of the deuteron is simply M_1+M_2-E/c^2. Let the velocity of ejection of the proton be u and that of the neutron be v cm./sec. The equations of conservation of energy and momentum for this disintegration are then as follows:

$$\left.\begin{aligned} M_1u^2+M_2v^2 &= 2(h\nu-E),\\ M_1u\cos\theta+M_2v\cos\phi &= h\nu/c,\\ M_1u\sin\theta-M_2v\sin\phi &= 0.\end{aligned}\right\}\qquad(1)$$

Writing, with sufficient accuracy for present purposes, $M_1=M_2=M$, and introducing new variables s, α and β defined by the relations

$$s=h\nu/Mc\dagger,\quad \alpha=h\nu/Mc^2,\quad \beta=1-E/h\nu,$$

we then have

$$\left.\begin{aligned} u^2+v^2 &= 2c^2\alpha\beta,\\ u\cos\theta+v\cos\phi &= s,\\ u\sin\theta-v\sin\phi &= 0.\end{aligned}\right\}\qquad(2)$$

From these equations a relation between u and θ (the only observables in the present experiment) may be derived by elimination of v and ϕ. After some simplification we obtain

---

* Already frequently quoted in the literature, following the general report on papers in Nuclear Physics, *Nature*, **136**, 467 (1935). See also *Report of the British Association for the Advancement of Science* (1935), p. 346.

† s cm./sec. is then the velocity of a proton (or neutron) with momentum equal to the momentum of the original quantum.

$$2u/c = \alpha\cos\theta + \{4\alpha\beta - \alpha^2(1+\sin^2\theta)\}^{\frac{1}{2}}. \tag{3}$$

We shall find it useful to know, first of all, the difference between the maximum and minimum values of u predicted by this result and, secondly, the value of θ for which the kinetic energies of neutron and proton are equal. Taking $2(u_0-u_\pi)/(u_0+u_\pi)$ as indicating the relative spread in velocity amongst the protons, we have from (3)

$$2(u_0-u_\pi)/(u_0+u_\pi) = (\beta/\alpha - 1/4)^{-\frac{1}{2}}. \tag{4}$$

Again, if neutron and proton have equal energies for $\theta = \phi = \theta_m$, equations (2) reduce to

$$u_m^2 = c^2\alpha\beta,$$

$$2u_m\cos\theta_m = s,$$

giving

$$2\cos\theta_m = (\alpha/\beta)^{\frac{1}{2}}. \tag{5}$$

In our experiments we used a radiothorium source, and the effective γ-rays were those of thorium C″ for which $h\nu = 2{\cdot}623\times10^6\times1{\cdot}591\times10^{-12}$ ergs. This, with the known values of M and c, gives $s = 8{\cdot}38\times10^7$ cm./sec., $\alpha = 2{\cdot}796\times10^{-3}$. For this case the following table shows how the spread in velocity and the angle θ_m depend upon the value of β (or upon the binding energy of the deuteron) in the range of values in question:

β	0·1	0·15	0·2
$2(u_0-u_\pi)/(u_0+u_\pi)$	0·168	0·137	0·118
θ_m	85·2°	86·1°	86·6°

We may sum up by saying that for this range of values of β the effect of the finite momentum of the incident quantum is a difference between forward and backward velocities of the photo-protons (or neutrons) of about 15 % of the mean velocity and the occurrence of the symmetrical mode of disintegration (as seen in the observer's space) with proton and neutron each projected at an angle of about 86° with the direction of incidence of the γ-ray quantum.

ARRANGEMENT OF APPARATUS AND EXPERIMENTAL RESULTS

The mode of operation of the piston-type expansion chamber and stereoscopic film camera which were used throughout this experiment has already been described (Feather 1932, 1933*a*). By comparison with the original arrangement of the apparatus the chief improvement introduced was a reduction of the period of the expansion cycle from about 30 to 22 sec., obtained by replacing the previous driving mechanism and automatic apparatus by one of more robust design. With this apparatus preliminary experiments were made in order to discover the most suitable position and screening for the γ-ray source which was to be used. This source consisted of radiothorium, of about 8 mg. γ-ray activity, sealed in a small cylindrical glass bulb and occupying a total volume of rather less than 1 c.c. It was finally decided to place the source in a cylinder of lead (thus providing about 8 mm. absorbing thickness in every direction) and to fix this source container to the glass roof of the expansion chamber, in the centre and above. Although in this way an appreciable fraction of the chamber in the neighbourhood of the source was obscured, the appearance of a shadow image of the lead cylinder on the film simplified the process of defining the position of the source in the stereoscopic reprojection of the photographs for purposes of measurement. In the final position the centre of the source was 1·3 cm. above the top of the glass roof of the chamber and about 4 and 9 cm., respectively, from the nearest and farthest points in the effective volume of the chamber. A gas mixture of roughly 60 % helium and 40 % "heavy" methane was employed. Such a mixture is characterized by a reasonably small α-particle stopping power and a small γ-ray absorption coefficient and is convenient in that an expansion ratio of about 1·30—somewhat less than the normal "diatomic" value—is appropriate. Moreover, in previous experiments a mixture of hydrocarbon and inert gas had proved entirely satisfactory (Feather 1933*b*; Chadwick, Feather and Davies 1934).

The heavy methane for the present experiment was prepared by the action of 98 % heavy water on aluminium carbide. About 700 c.c. of gas was obtained, using 5 c.c. of water. After being washed with concentrated sulphuric acid (to remove ammonia formed from an impurity in the carbide), this gas was stored over mercury. When required for use the desired amount of gas was passed from the reservoir into the expansion chamber which had previously been filled with helium to an appropriate pressure. Very little further adjustment was then necessary before optimum working conditions were realized.

In the main experiments about 2100 pairs of photographs were taken. From time to time in the course of this work the α-particle stopping power of the gas was investigated by placing a weak source of thorium (B + C) outside a mica window in the side of the chamber and taking photographs with and without an additional mica screen of known air equivalent interposed between the source and the window. At a later stage we shall consider in more detail the method of utilizing these photographs for the calculation of the stopping power. In these experiments 62 measurable tracks of photo-protons were obtained*—of mean length about 6 mm. in the gas.

As previously stated, two different methods of measurement were adopted. For the earlier incomplete measurements the method of stereoscopic reprojection of Nuttall and Williams was used (cf. Feather 1932); later an adjustable projection table of the type constructed by Dee and Gilbert (1936) was employed. The lengths of 46 and the directions of projection of 43 tracks were measured with both arrangements. For 22 tracks the two determinations of length agreed to within 0·2 mm.; for 19 the corresponding determinations of angle did not differ by more than 5°. This degree of agreement is probably as good as could be expected.† Chiefly because a complete set of measurements was possible with the second arrangement, which had not been the case with the first, all the data tabulated below belong entirely to the second set of measurements.

Figs. 1 and 2 (full line) show the observed distributions of the lengths and directions of the tracks of the photo-protons. In fig. 1 no correction has been made for the small variations in the stopping power of the gas in the chamber during the course of the experiments. The directly measured track lengths are given without reduction to a standard condition.

In fig. 2 the angles θ' plotted as abscissae represent angles of projection θ equal to θ' or $\pi-\theta'$, so that θ' ranges up to 90° only. One is compelled to combine these two values of θ because in the present experiments it is frequently impossible to decide which is the "beginning" and which the "end" of a track, owing to the short length of the tracks and the heavy background of cloud. If we denote by $F(\theta)$ the distribution of θ then the distribution of θ' is $G(\theta') = F(\theta')+F(\pi-\theta')$.

In the measurement of θ' it is necessary to determine not only the direction of the track but also the direction of the γ-ray quantum responsible for the disintegration. The latter is the join of the "source" to the beginning of the proton track, and in these experiments it is subject to uncertainties arising from the finite size of the source (about 1 cm. maximum diameter), and, in the cases of those tracks whose beginning and end are not distinguishable, from the finite length of the tracks (about 6 mm.). In compiling the present data, the geometrical centre of the source was for all cases taken as the origin of the γ-ray quantum, and that extremity of a track was chosen as "beginning" which made the angle of projection the smaller of the two possible values. The probable error in θ' due to the finite size of the source ranges from about 3 to 7° according to the position of the track in the chamber, and the error due to the uncertainty about the point of origin of the tracks varies from 0 to about 5° according to the actual value of θ'.

---

* This yield is in satisfactory agreement with the accepted value of about 10^{-27} sq. cm. for the cross-section for the disintegration, assuming reasonable values for the effective volume of the chamber and its time of action.

† The discrepancies in the remaining cases were distributed in a way consistent with probable errors of 0·2 mm. and 5° in the length and angular measurements, respectively.

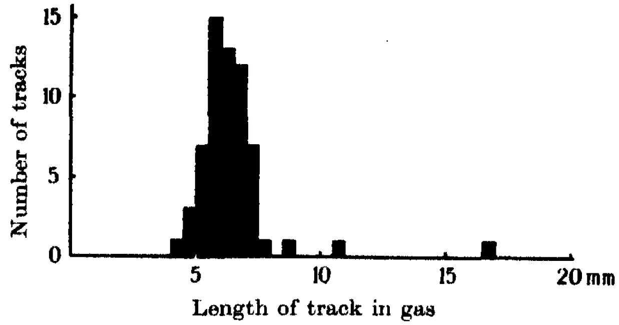

FIG. 1

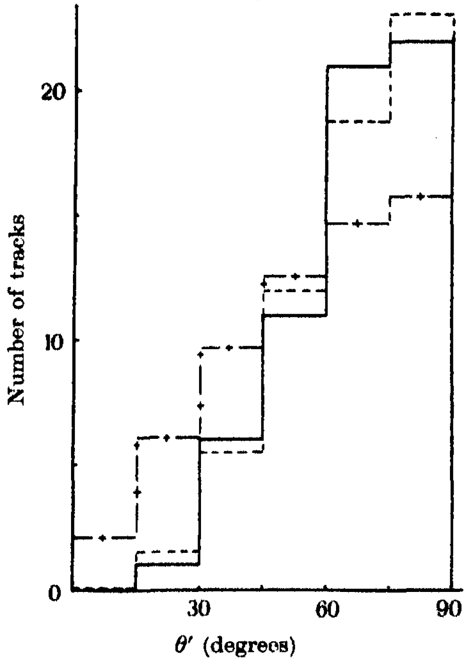

FIG. 2

The error in the general plot of fig. 2 due to these errors in θ' is small compared with the statistical error corresponding to the number of tracks available for measurement.

DISCUSSION

According to the calculations which have already been given the photo-protons from deuterium irradiated by the homogeneous γ-radiation of thorium C″ should possess velocities comprised within a range of roughly ± 7 % about the mean. Qualitatively this is substantiated by the form of the range distribution curve of fig. 1, where a fairly compact group of particles is clearly represented.

To obtain the energies of the photo-protons the observed range has first been reduced to the equivalent range in standard hydrogen, and this deduced range must then be converted into energy by using the data of Blackett and Lees (1932) for the relation between range and energy of slow protons in hydrogen. The initial step depends in the first place on our measurement of the decrease (x cm.) in length of the tracks of α-particles from a source of thorium C′ outside the chamber when a certain mica screen was interposed in the path of the particles between the source and the chamber window (also of mica). The stopping power of the mica screen for α-particles was 0·902 cm. of air, and that of the mica window was about 4·5 cm. of air. The actual residual ranges of the tracks in the chamber with and without the screen were equivalent to about 1·6 and 2·5 cm. of air respectively. This means that the calibration of the stopping power of the chamber gas referred to α-particles of about 2 cm. range, corresponding to a velocity of about $1 \cdot 3 \times 10^9$ cm./sec. According to measurements of Gurney (1925) the relative stopping powers of hydrogen and air for such α-particles are 0·217 : 1. It follows that the ratio of the stopping power of the gas in the chamber to that of hydrogen is $0 \cdot 902/0 \cdot 217x$, for α-particles of velocity 13×10^8 cm./sec. According to existing evidence the ratio will be the same for protons of this velocity but in the present investigation we require this ratio for protons of velocity about 5×10^8 cm./sec. Now in general the ratio of the stopping powers of two gases depends on the velocity* of the particles, but the variation of this ratio with velocity is small unless there is a big difference in the binding energies of the electrons in the two gases. In our case the two gases to be compared are hydrogen and the mixture of 40 % methane and 60 % helium in the chamber. The mixture is in respect of binding energies of the electrons intermediate between air and hydrogen, and is much more like hydrogen than air. Assuming it to behave like hydrogen, a proton with an observed range of l cm. in the chamber would have a range of $0{\cdot}902l/0{\cdot}217x$ cm. in hydrogen. Using the results $x = 2{\cdot}91$ cm., $l = 0{\cdot}613$, we find that the photo-protons would have an average range of 8·8 mm. in hydrogen.

---

* In the limit of large velocities the ratio approaches a constant value equal to the ratio of the numbers of electrons per c.c. in the two gases.

According to the data of Blackett and Lees a proton of this range in hydrogen would have an initial velocity of $5{\cdot}98 \times 10^8$ cm./sec., or an initial energy of $1{\cdot}85 \times 10^5$ e-volts. This therefore is the average energy of the photo-protons.* Now unless there is a considerable excess of forward over backward emission, or vice versa, of the protons, this will also be the average energy of the neutrons. No such excess was found. Out of 22 tracks for which "beginning" and "end" could be distinguished with confidence, 11 were projected forwards and 11 backwards. We therefore conclude that the total kinetic energy appearing in the disintegration particles is $2 \times 1{\cdot}85 \times 10^5$ e-volts. The binding energy of the deuteron is therefore $(2{\cdot}62 - 0{\cdot}37) \times 10^6$, or $2{\cdot}25 \times 10^6$ e-volts. It is not easy to estimate the probable error of this determination with any precision. Our assumption that the chamber gas was effectively pure hydrogen may tend to give too high a value for the kinetic energy of the proton. Had we assumed that the gas mixture in the expansion chamber resembled air in respect to variation of stopping power with velocity and with the nature of the particle we should have arrived at a value of $1{\cdot}40 \times 10^5$ e-volts for the energy of the protons. On the other hand, if we extrapolate the measurements of Parkinson and others (1937) we get a value of $2{\cdot}0 \times 10^5$ e-volts for the proton energy. Taking all these things into consideration we shall write $E = 2{\cdot}25 \pm 0{\cdot}05 \times 10^6$ e-volts, as indicating a liberal margin of uncertainty. Within the assigned limits there is then satisfactory agreement with the earlier result $(2{\cdot}14 \pm 0{\cdot}16 \times 10^6$ e-volts) of Chadwick and Goldhaber. The mass equivalent of our binding energy is $2{\cdot}42 \times 10^{-3}$ atomic units, giving a value of 1·0090 for the mass of the neutron.

We shall now consider the angular distribution of the photo-protons with reference to theoretical predictions. The latter are most conveniently expressed as the distribution of particles in a space in which the centre of gravity of proton and neutron (after disintegration) is at rest. On the basis of our previous calculations we shall neglect the distinction between this space and that in which the deuteron, before disintegration, is at rest, for we have seen (p. 368) that the distinction between backwards and forwards in the moving space corresponds approximately to the distinction $\theta \gtrless 86^\circ$ in that of the observer—and a discrepancy of 4° is within the limits of error in our determination of angles. The theoretical predictions have been given by Bethe and Bacher (1936) and by Breit and Condon (1936) in recent publications. Very briefly they may be summarized as follows. Adopting the usual spectroscopic notation, we assume that the ground state of the deuteron is a ^{3}S state, and we consider transitions between this state and the continuum of ^{3}P and ^{1}S states of the dissociated system. (Because the radiations emitted in the reverse capture transitions are described, respectively, by electric and magnetic dipole fields, it is customary to refer loosely to these dissociative transitions, also, as produced by the electric and magnetic components of the incident radiation.) Then the angular distributions corresponding to the two types of transition—the electric and magnetic effects—are $F_e(\theta) = \frac{3}{4}\sin^3\theta$ and $F_m(\theta) = \frac{1}{2}\sin\theta$ respectively,* the partial cross-sections for these effects increasing and decreasing functions of the quantum energy of the radiation, at least in the range of energies immediately above the threshold.

---

* The average energy of the protons is not strictly equal to the energy of the proton of average range but the difference is quite insignificant.

Referring to fig. 2, the full line represents the experimental results. The dotted lines have been calculated with $F(\theta) = \frac{1}{2}\sin\theta(-+-+-)$ and $F(\theta) = \frac{3}{4}\sin^3\theta(---)$. It is clear that the latter distribution is sufficient alone to represent the experimental results. We conclude that the cross-section for the magnetic effect is already small compared with that for the electric effect for quanta of energy $h\nu = 2{\cdot}62 \times 10^6$ e-volts. Bearing in mind the small number of tracks examined, we may say that the "electric cross-section" is at least three times as great as the "magnetic cross-section" for this quantum energy. Theoretically, the ratio of these partial cross-sections depends upon whether or not the ^{1}S state of the deuteron (assumed of small positive or negative energy in order to explain the large scattering of slow neutrons in hydrogen) is in fact stable or unstable, and—though not critically—upon assumptions concerning the nature and range of action of the forces between proton and neutron. According to the calculations the magnetic effect is relatively less important, compared with the electric effect, if the ^{1}S state is stable than if it is unstable. Our results suggest such a preponderance of the electric effect that one might be tempted to conclude definitely that the ^{1}S state is stable, in spite of the lack of precise knowledge concerning the proton-neutron interaction. However, information about the ^{1}S state has been obtained from the comparison of the elastic scattering with the radiative capture of thermal neutrons in hydrogen (cf. Amaldi and Fermi 1936), assuming as a basis of interpretation that the radiative capture of neutrons of thermal energies takes place almost entirely "magnetically", that is, from the continuum of ^{1}S states of the system. From a consideration of the evidence in such experiments Fermi (1936) has assumed tentatively that the singlet state is unstable. As has been seen, our results suggest that this state is actually stable. We note this disagreement, but we think it would be unwise to stress it, in view of the rather meagre results on which our conclusion is based.

---

* Of these distributions, $F_m(\theta)$, of course, is isotropic; $F_e(\theta)$ is deduced for unpolarized radiation from the result for plane polarized radiation that the intensity per unit solid angle is proportional to $\cos^2\phi$, where ϕ is the angle between the direction of emission of the particle and the direction of the electric field of the radiation.

SUMMARY

Measurements of range and angle have been made on the tracks of 62 protons produced in an expansion chamber containing a deuterium-rich gas and irradiated by the γ-rays from a radiothorium source. These measurements have been analysed in detail and critically discussed. It is concluded that the determinations of range indicate a binding energy of $2{\cdot}25 \pm 0{\cdot}05 \times 10^6$ e-volts for the deuteron and that the angular distribution implies a considerable preponderance of the photoelectric over the photomagnetic type of disintegration with the radiation employed ($h\nu = 2{\cdot}62 \times 10^6$ e-volts). This binding energy gives a value of 1·0090 for the mass of the neutron.

REFERENCES

Amaldi and Fermi 1936 *Phys. Rev.* **50**, 899–928.
Banks, Chalmers and Hopwood 1935 *Nature, Lond.*, **135**, 99.
Bethe and Bacher 1936 *Rev. Mod. Phys.* **8**, 82–229.
Blackett and Lees 1932 *Proc. Roy. Soc.* A, **134**, 658–71.
Breit and Condon 1936 *Phys. Rev.* **49**, 904–11.
Breit, Stehn and Condon 1937 *Phys. Rev.* **51**, 56.
Chadwick, Feather and Davies 1934 *Proc. Camb. Phil. Soc.* **30**, 357–64.
Chadwick and Goldhaber 1934 *Nature, Lond.*, **134**, 237–8.
— — 1935 *Proc. Roy. Soc.* A, **151**, 479–93.
Dee and Gilbert 1936 *Proc. Roy. Soc.* A, **154**, 279–96.
Feather 1932 *Proc. Roy. Soc.* A, **136**, 709–27.
— 1933*a* *Proc. Roy. Soc.* A, **141**, 194–209.
— 1933*b* *Proc. Roy. Soc.* A, **142**, 689–709.
Fermi 1936 *La Ricerca Scientifica*, **7** (2), 13–52.
Gurney 1925 *Proc. Roy. Soc.* A, **107**, 340–9.
Parkinson, Herb, Bellamy and Hudson 1937 *Phys. Rev.* **52**, 75–79.

An Attempt to Detect the Passage of Helium through a Crystal Lattice at High Temperatures

By Lord Rayleigh, F.R.S.

(*Received* 20 *September* 1937)

In a previous paper (Rayleigh 1936), comparative studies were made of the passage of helium through various kinds of glass at the ordinary temperature. Silica glass, pyrex glass, and boron trioxide glass all allow helium to pass through. Ordinary soda glass or flint glass do not pass measurable quantities of helium unless the temperature is raised.

Tests were made at the ordinary temperature on various single crystals, including quartz, mica, beryl, and some others. No passage of helium could be detected.

I was anxious to extend the investigation to single crystals at high temperatures. In the case of glasses, we must probably refer the passage of helium to something in the nature of cracks: and since we have no independent evidence of the existence of these cracks,* and still less any independent evidence of their dimensions, the passage of helium does not throw any very definite light on interatomic and intermolecular forces. With the definite knowledge we now have of the structure of crystals, it is clear that the passage of helium atoms of definite translational energy through the interstices would afford data of precision.

For this reason I was anxious to look for the passage of helium through crystals at temperatures as high as might be practicable.

One difficulty of the investigation is that of the few large crystals which are available, most will not stand a high temperature without cracking or chemical decomposition. Mica appeared to be the most promising in this respect, and my experiments, which have cost an amount of time and trouble which has hardly been rewarded, were made exclusively with this crystal.

To determine whether helium can pass through a layer of a single crystal at high temperature is not technically easy. In the case of silica glass or the ordinary glasses, the material can be obtained in the form of a tube, and this can be tested almost as easily when hot as when cold. But with a material like mica which has to be tested in the form of a plate this is not the case, for there are obvious difficulties in cementing the edges airtight while the plate is hot. After one or two trials with cements supposed to be effective at fairly high temperatures I came to the conclusion that the only feasible plan was to keep the cemented edges of the plate cold while the middle was hot. The arrangement used for this purpose is shown in fig. 1 (one-third actual size).

---

* I have looked for evidence by dark ground microscopic illumination, but without result.

The mica plate *MM* in the middle is confined between two mild steel disks. These disks are made as in the inset, with a central area (hot) and an outside ring (water cooled). The cold annulus and the hot centre are separated by a gap, with eight small bridges left to keep them in relative position. These bridges were made 1 mm. wide and 1 mm. thick. This was about the minimum that was judged safe in respect of mechanical strength. It is important to keep the thermal conductivity of the bridges as low as possible, and it was attempted to construct the apparatus of german silver, which was silver soldered. This failed at the higher temperatures and was abandoned in favour of mild steel, acetylene welded. The difficult welding involved was carried out for me by Messrs. Negretti and Zambra, under the supervision of their Works Manager, Mr. Short, and the assistant Manager, Mr. Harrison, whom I wish to thank for their kind help.

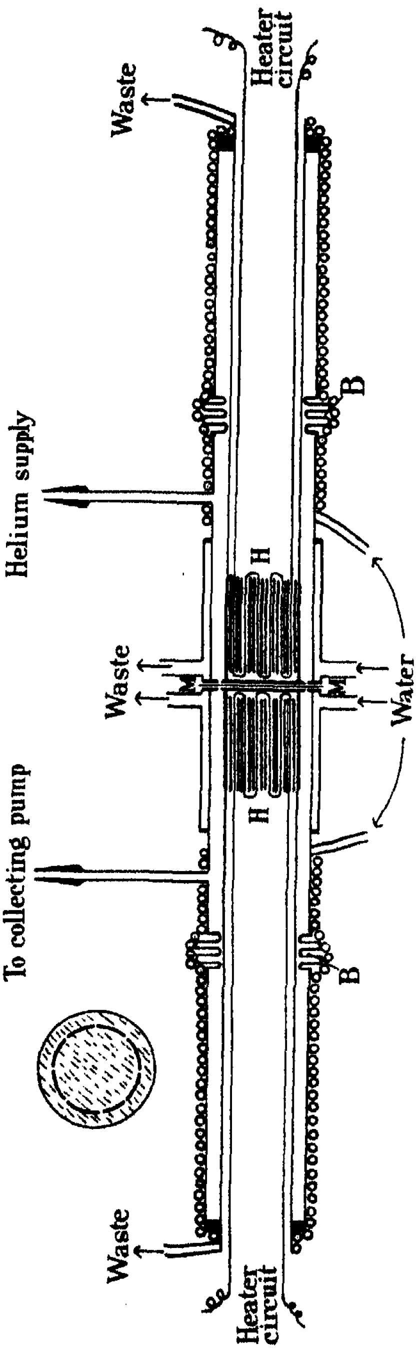

Fig. 1

The mica disk may be trusted not to lie so close against the metal disks that there would be any difficulty in the passage of helium between, and it was assumed that the whole central area of the mica disk was effectively situated for the slow passage of gas through it, when there was helium in the separating gap on one side and vacuum in the other separating gap.

It remains to be explained how the centres of the metal disks were kept hot and the outside annuli cold. The main diagram shows this, the disks being seen in section with the mica plate between them, central to the whole arrangement. The mica plate is cemented with soft red wax to the water-cooled annuli on either side of it, the whole being drawn together by means of a pair of metal collars with bolts and nuts, not shown.

The interior part of each disk is welded to a steel tube. This tube as purchased was 1 mm. thick, but at a distance of 5 cm. from the joint it was filed down to about half this thickness, so as to diminish the longitudinal thermal conduction.

Inside these steel tubes are placed the electrical heaters *HH*. It was found a matter of some difficulty to design these so that the necessary resistance could be got into the small space. This would be most easily done with a low-tension supply, but only direct current at 110 V was available. Eventually nichrome wires were used, threaded through silica tubes 5 cm. long, and doubled to and fro as indicated. A mica disk at the inner end of each steel tube (i.e. against the outer side of each steel disk) prevented any short-circuiting across the ends.

Outside the steel tubes are brass tubes, soft soldered in each case to the external annulus of the steel disk. These brass tubes, as well as the two annuli, are kept cold by external water jackets; but these jackets only extend about 8 cm. from the end, and most of the length is kept cold by a water flow in small "compo" pipe wound over them as shown.

The annular space between the brass and steel silver tubes is closed off airtight as shown, and it was found necessary to use metallic bellows, *BB*, in continuation of the brass tubes to allow for expansion of the steel tubes on heating. Helium at atmospheric pressure was admitted to the annular space on the right, and the annular space on the left was connected to a Töepler pump, to collect helium which might pass through the mica, if any.

The power dissipated in the heaters was measured electrically, so that if a heater burnt out it could be replaced by another without essential change of conditions.

To determine the temperature of the mica under working conditions a special experiment is necessary. The mica is temporarily replaced by two disks of thin asbestos paper with a thermocouple of fine wire between them. This thermocouple is in circuit with a similar one outside which is in opposition to it, and a galvanometer. The outside thermocouple is in contact with a high-temperature thermometer, in an air-bath. The outside couple is heated to the temperature at which it neutralizes the inside one, and this is taken as the actual temperature under the working conditions of electrical power dissipated.

In carrying out the tests, helium at atmospheric pressure was admitted to the right-hand side of the mica, and gas was pumped away from the left-hand side for analysis, to see whether it contained helium. The pumping system for the right-hand side, which was to handle large quantities of helium, was of course entirely independent of that for the left-hand side, where minute quantities of helium were in question. The heat liberated enough gas from the mica and from the hot metal to allow of collection and transference. It was purified by sparking with oxygen, the excess being removed by phosphorus. It was then admitted to contact with cooled charcoal, and the residue (neon or helium) measured with the MacLeod gauge, the spectrum being examined in the gauge tube in the usual way.

It had been hoped either to detect the passage of helium, or, in the alternative, to carry the negative tests up to the point when the mica crystal was disintegrated and destroyed by the heat. This I did not succeed in doing. The design of the apparatus, which was the best I could devise, makes it unavoidable that there should be a great loss of heat by metallic conduction and otherwise from the metal disks in contact with the mica: and I was not able to maintain a temperature of more than 415° C. for 24 hr. without a breakdown of the heaters. No doubt with low-voltage heaters such as could readily be used with an alternating electric supply it would be possible to do better. Considerations of time and expense discouraged me from proceeding further, as the experiments actually carried out gave no indication of a positive result.

In the most significant of the tests made, the temperature was 415° C., the mica disk being 4·5 cm. diameter and 0·2 mm. thick.

After 22 hr. the volume of residual gas from charcoal absorption was measured as $5{\cdot}45 \times 10^{-3}$ cu. mm. The spectrum was that of neon, derived no doubt from atmospheric contamination. It will be safe to say that the helium which passed the mica was less than the volume measured. In all probability it was very much less. Assuming that the rate is inversely proportional to thickness, we find that the volume passed by mica at 415° C./day/sq. cm. area, thickness 1 mm., is less than $\frac{5{\cdot}7 \times 10^{-3} \times 0{\cdot}2}{16}$ or less than 7×10^{-5} cu. mm.

For comparison, it may be mentioned that the transmission for fused quartz at the ordinary temperature/day/sq. cm., thickness 1 mm. is about $2 \cdot 5 \times 10^{-1}$ cu. mm., varying somewhat in different specimens.

ABSTRACT

It is known that helium will pass through silica glass, even at ordinary temperatures. A plate 1 mm. thick and 1 sq. cm. area will pass about $2 \cdot 5 \times 10^{-1}$ cu. mm./day. In this case the helium probably passes through submicroscopic channels or cracks in the material. No single crystal, so far as has been ascertained, will pass measurable quantities of helium through the lattice at ordinary temperatures.

Mica has now been tested up to a temperature of 415° C. The amount of helium passed, by a plate 1 mm. thick and 1 sq. cm. area, if any, is certainly less than 7×10^{-5} cu. mm./day.

REFERENCE

Rayleigh, 1936 *Proc. Roy. Soc.* A, **156**, 350–357.

The Behaviour of an Osglim Lamp

III—Osglims in parallel, forming Models of Reciprocal Inhibition

BY LEWIS F. RICHARDSON, F.R.S.

(*Received* 21 *September* 1937)

INTRODUCTION

The interest of these experiments is twofold. First, they provide sensitive tests of the results of the study of a single osglim (Richardson 1937). Secondly, they have analogies with the psychological phenomenon of concentration and change of attention. In view of the great number and variety of stimuli to which we are usually subjected, concentration is surprisingly easy; and so is change of attention. As soon as the new subject of discourse receives attention, the former subject passes rapidly from our thoughts. Usually no effort is required to reject the old subject; for the new displaces the old automatically. This phenomenon is so familiar that the need for an explanation of it is apt to be overlooked.

Reciprocal inhibition in physiology appears to be broadly similar to mental distraction. Whether the excitation in nerves is propagated electrically or chemically, it has characteristic time relations, which alone are in question here. A model made of neon lamps obtrudes its irrelevant materiality. We shall use it until it has suggested interesting abstract time relations, namely, the equations mentioned in the Conclusion. Then the model may be allowed to be forgotten while the equations are preserved.

VARIOUS DISTRACTION CIRCUITS

The essential feature of all these circuits is a pair of neon lamps wired in parallel. The glowing of either lamp inhibits the other, if the associated battery and resistances are suitably adjusted. The extinct lamp is made to glow by some temporary stimulus. On removal of the stimulus the other lamp is extinguished, although it is permanently connected to the same battery.

In the original experiment (Richardson 1930) the temporary stimulus was provided by an extra battery, which was likened to the Will in psychology. This extra battery brightened the glow in the glowing lamp while causing a still brighter glow in the lamp formerly extinct. This type of stimulation causes too violent and too widespread a disturbance for a good model of reciprocal inhibition.

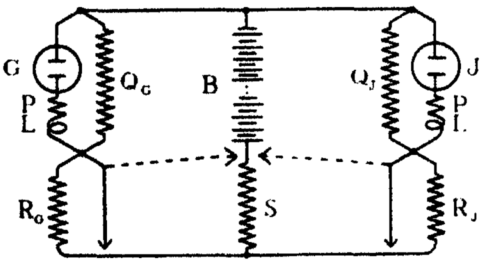

FIG. 1—Apparatus with matching circuits and tapping contacts.

The pair of neon lamps, which were originally tried, happened to be fairly well matched. But with other specimens it has been found desirable to arrange resistances so that the potentials applied to the lamps, when both extinct, can be made unequal.

Both these improvements are incorporated in the following arrangement (fig. 1), which worked particularly smoothly (7 Jan. 1932) after careful trial and adjustment of the resistances. When osglim G was lit and J extinct, a brief short circuit of R_J caused J to light and extinguished G. Then a brief short circuit of R_G restored the original glow in G and extinguished J. The coils P, L are those inserted for protection by the manufacturers in the lamp-stem. A sample coil from the stem of a similar lamp was found to have $P = 3{\cdot}55$ kilohms, L negligible at frequencies up to 50 kc./sec. The setting was $B = 176$ V, $Q_G = Q_J = 1{\cdot}_5$ megohms, $R_G = 108$ kΩ, $R_J = 104$ kΩ, $S = 30$ kΩ. Drift soon put the osglims beyond the range of the weak control exerted by the short circuit of only an R.

In a more robust arrangement S is temporarily short-circuited together with the R on either side as shown by the dotted arrows in fig. 1. This does not provide so good an analogy, because the shorting of S causes the glowing osglim to glow more brightly. It has in fact the same defect as the original arrangement with the extra battery, though not to nearly the same extent. But this model has remained in working order during public demonstrations,* and has repeated its performance with a new battery after a year's storage. For reliability and convenience in such an exhibit, various experiments showed that the resistance S should be at least as large as either of the resistances R; and that both R and S should be of the order of 10^4 or 10^5 Ω. The demonstration apparatus had three lamps, any one of which would inhibit the other two. The values were in megohms $R = 0{\cdot}06$, $S = 0{\cdot}11$, $Q = 1{\cdot}_5$ or ∞. The battery current when the temporary contacts were broken was $0{\cdot}2_6$ mA, for satisfactory working.

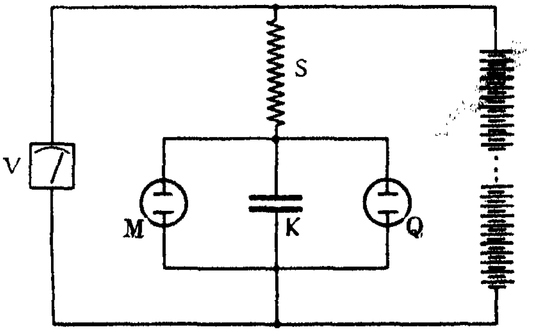

FIG. 2—Automatic apparatus.

A combination of the distraction circuit with the Anson-Pearson circuit was arranged (27 Dec. 1930) as shown in fig. 2. The two osglims (labelled M and Q) were irradiated by dim daylight. K was $3{\cdot}41$ μF, S was greater than a megohm. The battery exerted 253 V. The voltmeter V is convenient but unnecessary. Flashes occurred at the rate of 10 in 80 sec., sometimes on M sometimes on Q, in a quite irregular sequence; but never on both M and Q together. The following is a sample:

---

* (i) Annual exhibition of Physical and Optical Societies Jan. 1932. (ii) Brit. Association, Section of Physiology, 7 Sept. 1937.

$$MQQMMMQMMMMQQMMMMMQQQMQQMQQQMQQMMQQMQ$$
$$QQQQQMQQQQQQQQMQMQQQQMMQQMQQQQQMQQQQQQQ\ldots$$

to more than 45 repetitions of Q.

This automatic apparatus should now take the place of a less satisfactory arrangement mentioned in an earlier paper (Richardson 1930, fig. 2) as a model of reverie in a mind capable of only two ideas. Dr. S. J. F. Philpott has suggested that there is analogy to the automatic reversals of the perspective when certain line diagrams are regarded intermittently.

THE DISTRACTION EXPERIMENT AS AN ARBITER OF THEORIES

In the original paper (Richardson 1930) there were some brief suggestions as to what intrinsic properties of the osglim would explain distraction. Those suggestions must now be replaced by much more definite information. For theoretical discussion let us take a very simple experiment, shown in fig. 3. The two osglims are supposed to be perfectly matched. The crucial phenomena occur just after the stimulation by a temporary contact has ceased. Let R, R, S be resistances, V the voltage of the battery and ϕ and u respectively the voltage and current in the osglim; and let the two osglim branches be distinguished by suffixes 1 and 2. By Kirchhoff's laws,

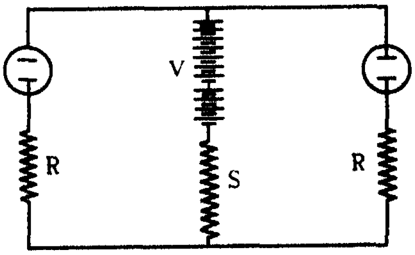

FIG. 3—Apparatus for testing theories.

$$\phi_1 + u_1 R + (u_1 + u_2) S = V, \tag{1}$$

$$\phi_2 + u_2 R + (u_1 + u_2) S = V. \tag{2}$$

By elimination of S and V

$$\phi_1 + u_1 R = \phi_2 + u_2 R. \tag{3}$$

We should indeed obtain (3) even if the S branch contained an inductive ammeter or a capacitative battery. Now suppose that each osglim satisfies the approximate intrinsic equation which sufficed for the explanation of small oscillations at low frequencies, and of relaxational oscillations. That is to say,

$$\phi = \phi_e(u) + b\frac{d\log u}{dt}, \tag{4}$$

with suffixes 1 and 2.

A thorough mathematical treatment would proceed by separation of the variable u_1 from u_2 in (1) and (2) and subsequent integration. That course is difficult. Instead let us bring in experimental evidence, from the size of the glow and from milliammeter readings, to show that u_1 and u_2 are confined to specified ranges. This enables a simple mathematical device to be used. Let ϕ_1, ϕ_2 be eliminated between (3) and the two equations of type (4) with the result,

$$b\frac{d\log(u_1/u_2)}{dt} = R(u_2-u_1)+\phi_e(u_2)-\phi_e(u_1). \tag{5}$$

A solution of (5) is $u_1 = u_2 =$ constant; and this represents an equilibrium. But the question is about stability. If, as $t \to \infty$, $\log(u_1/u_2) \to \pm\infty$ we shall say that distraction has occurred. But if $\log(u_1/u_2) \to 0$ the final state will be $u_1 = u_2$: that is co-existence not distraction.

It is convenient to rearrange (5) thus,

$$\begin{aligned} b\frac{d\log(u_1/u_2)}{dt} &= (u_2-u_1)\left\{R+\frac{\phi_e(u_2)-\phi_e(u_1)}{u_2-u_1}\right\} \\ &= (u_1+u_2)(-R-z), \end{aligned} \tag{6}$$

where

$$z = \frac{\phi_e(u_2)-\phi_e(u_1)}{u_2-u_1}. \tag{7}$$

For, whether u_1 be greater or less than u_2, (6) shows that the motion of $\log(u_1/u_2)$ is towards or away from zero according as the second member of (6) is negative or positive. That is to say, distraction is in progress if $(-R-z)$ is positive. If the two osglims are alike, the quantity z is the slope of the straight line joining the points at u_1, u_2 on their common $\phi_e(u)$ graph. Accordingly z may be called the "difference-resistance of the two osglims".

On this approximate theory complete distraction will occur if and only if $-z > R$ throughout the progress of $\log(u_1/u_2)$ to $\pm\infty$. (8)

Much depends on the relation of u_1, u_2 to u_m the current at which $\phi_e(u)$ is a minimum.

The *experiments for comparison with the foregoing theory* were made in 1937 with two osglims labelled P and L. Of these P was the specimen studied in Parts I and II. The characteristics of L were closely similar, but unfortunately not quite identical, L being easier to light. The glow in L, when covering only part of the disk, sometimes fidgetted from place to place in the manner described by Leyshon (1932). These osglims were so joined that in each the glow occurred nearer to the disk than to the spiral electrode. The resistances R were of types which are practically pure at 10^4 c./sec., namely Dubilier metalized glass rods, Ferranti slot-wound wire and Lewcos toroids. The slight inequality between R_L, R_R, adjacent respectively to osglims L and P, was rendered harmless by trying distraction both ways. A milliammeter was inserted in the V, S branch. The battery, milliammeter, resistances and osglims were separately insulated on paraffin wax, sealing wax or ebonite, and the wires by thick india rubber. The osglims were irradiated by light from a tungsten lamp so as to prevent $\phi_e(0)$ exceeding $\lim_{u \to 0} \phi_e(u)$ (see Part I, p. 303).

Exp. 1—*Currents both greater than u_m*

Set $V = 184$ V, $R_L = 14{,}570\,\Omega$, $R_P = 15{,}080\,\Omega$, $S = 10^4\,\Omega$. On making the battery contact, osglim L alone lit. So R_L was first made infinite and then reduced to its aforesaid value. This manoeuvre left both P and L glowing steadily. The value of S was reduced by a rolling contact on the Lewcos toroid with the following results.

S in kΩ	Joint current mA	Equal steady glows
8	1·71	On pip side of disk
3	2·5	On both sides of disk

Here z, the "difference-resistance", is positive, so $(-R-z)<0$. Theory and experiment agree in showing no distraction.

Exp. 2—*Currents both less than u_m. Zero R*

$V = 184$ V, $R_L = R_P = 0$, $S = 4 \times 10^5\,\Omega$. On repeatedly making the battery contact osglim L usually lit, sometimes osglim P, but never both together. The single current was 0·08 mA. The value of z between 0·08 mA and zero current is $-2{\cdot}3 \times 10^5\,\Omega$. So $(-R-z)$ is very positive. Theory and experiment agree in showing distraction.

Exp. 3—*Currents both less than u_m. Large R, small S*

$V = 184$ V. The steepest part of the $\phi_e(u)$ curve corresponds to $-z = 0{\cdot}3$ MΩ. Here R_L, $R_P = 0{\cdot}677$, $0{\cdot}680$ MΩ, so that $(-R-z)$ was negative for all possible currents u_1, u_2 less than u_m. When S was not too large both osglims were observed to stay alight together at a joint current of 0·04 mA. This agrees with the theoretical expectation (8).

Exp. 4—*Currents both less than* u_m. *Large R, large S*

$V = 184$ V, R_L, $R_P = 0{\cdot}677$, $0{\cdot}680$ MΩ. When S had been increased to 5·2 MΩ, the battery contact was made repeatedly. Usually osglim L lit, but sometimes P instead. In the latter event P soon ceased to glow while L began. The single current was $0{\cdot}0_1$ mA. Both P and L were never steadily alight together. This observation disagrees with the theory, in which S plays no part. The actual circuit is more liable to distraction than the theory indicates. A border-line value of S, at which distraction sometimes did and sometimes did not occur was 0·7 MΩ.

Exp. 4 was repeated with a kathode-ray oscillograph attached to the circuit so that one co-ordinate measured the voltage ϕ across osglim P while the other measured χ across R_P. The resistances were in megohms, $S = 5{\cdot}2$, $R_P = 0{\cdot}67_9$, $R_L = 0{\cdot}67_5$. The battery gave 189 V. The main switch of the house was put off to prevent stray oscillations of 50 c./sec. The filament current of the oscillograph had to be reduced from its normal 0·93 amp. to 0·78 in order to decrease the leak between the plates. Distraction occurred, osglim P lighting and L going out automatically. When osglim L was glowing $\phi = 174$, $\chi = 0$ V. Automatically this changed to $\phi = 165$, $\chi = 2$; corresponding to 3 μA. These end-states were equilibria not oscillations. Apparently the motion from one end-state to the other was along a straight line in the (ϕ, u) plane. But that appearance may have been a stroboscopic illusion. To investigate the changes it would be desirable to use an oscillograph capable of recording a single pulse and having a resistance far exceeding a megohm.

[*Note added* 25 *October* 1937. In this experiment $\log(u_1/u_2)$ passed automatically from ∞ through 0 to $-\infty$, thus performing in rapid succession both the motions that according to the theory (6) are alternative.]

Exp. 5—*One current zero, the other greater than* u_m. *Zero R*

$V = 184$ V, $R_L = R_P = 0$. Only one osglim stayed alight at a time; but each did this. The single current was 1·8 mA. The corresponding ϕ_e is about 142 V, whereas $\lim\limits_{u\to 0} \phi_e(u) = 164$ V or thereabouts. So $z = -12$ kΩ. The observed distraction agrees with the theory (8). The value of S was about 2×10^4 Ω.

Exp. 6—*One current zero, the other greater than u_m. Considerable R, larger S*

$V = 184$ V, $R_L = 14{,}570\ \Omega$, $R_P = 15{,}080\ \Omega$, $S = 2 \times 10^4\ \Omega$. On connexion to the battery, osglim P lit at 0·90 mA. By decreasing R_P from ∞ to 15,080 Ω osglim L was left alight at 0·68 mA. Only one lit at a time. The mean value of z is of the order of $-3 \times 10^4\ \Omega$, so that $(-R-z) > 0$ and the theory (8) predicts the observed distraction.

Exp. 7—*One current zero, the other greater than u_m. Considerable R, smaller S*

Without altering any other condition in Exp. 6 the resistance S was decreased by a rolling contact to $1 \cdot 1 \times 10^4\ \Omega$. The osglim L which had been alight remained so while P lit also. The joint current was 1·4 mA. This effect of S is contrary to the theory (8).

DISCUSSION

Exps. 1, 2, 3, 5, 6 agree with the deduction from the approximation (4); but Exps. 4 and 7 disagree, for they show that a resistance S, when greater than R, increases the tendency to distraction. We have here a dilemma. For whatever more accurate expression of the intrinsic equation we take instead of equations (4) there will still be, in view of equations (1), (2), a strong tendency for S to be eliminated as in (3). Yet S affects the experiments. We can escape from this dilemma by supposing that the intrinsic equation is of such a type that the elimination of S must prevent us from deducing any definite conclusion as to whether or not distraction will occur in the circumstances of Exps. 4 and 7. Here we have a clue, though indeed of a peculiarly abstract kind, towards finding the form of the intrinsic equation. Several forms will now be put to the test, which will be shown to be remarkably critical.

Hypothesis I—Instead of (4) we assume

$$\phi(u) = \phi_e(u) + \lambda(u) \,.\, \frac{du}{dt},$$

where $\lambda(u)$ is a positive slope inductance not restricted to the special form b/u. Any residual inductance associated with R may be included in λ.

Let $$\lambda(u).du = d\chi(u),$$

then $\chi(u)$ must be a monotonic increasing function of u. It follows in the same manner as for (5) that

$$\frac{d}{dt}\{\chi(u_1)-\chi(u_2)\} = -(R+z)(u_1-u_2),$$

whence $|\chi(u_1)-\chi(u_2)|$ is increasing or decreasing according as $(R+z)$ is negative or positive. This is a definite conclusion. Therefore Hypothesis I is inadequate. It explains a kind of distraction that depends on $(R+z)$ but not on S.

Hypothesis II—We generalize the intrinsic equation by inserting a constant resistance σ different in kind from the $\rho(u)$ of the small oscillations (Part I, p. 306).

$$\phi = \phi_e(u)+\lambda(u)\frac{du}{dt}+\sigma.$$

It follows, with χ as defined for the previous hypothesis, that

$$\frac{d}{dt}\{\chi(u_1)-\chi(u_2)\} = (u_2-u_1)(R+z+\sigma).$$

This again would lead, if σ were known, to a definite conclusion not involving S. Therefore Hypothesis II is inadequate. It explains a more general kind of distraction that depends on $(R+z)$ but not on S.

Hypothesis III—Let us instead try a term in $d\phi/dt$ which might have escaped notice at low frequencies of oscillation. We assume that

$$\phi = \phi_e(u)+b\frac{d\log u}{dt}+k\frac{d\phi}{dt},$$

where k is a constant, of the dimensions of time. Both ϕ and $d\phi/dt$ can be eliminated by operating with $(1-kd/dt)$ on equation (3). The result is

$$\left(\frac{b}{u_1}-Rk\right)\frac{du_1}{dt}-\left(\frac{b}{u_2}-Rk\right)\frac{du_2}{dt} = (u_2-u_1)(R+z).$$

If k is negative then $(b/u-Rk)$ is positive everywhere and is equivalent to the positive $\lambda(u)$ of Hypothesis I; and the deduction leads to the same definite conclusion. So Hypothesis III must be rejected as inadequate for $k<0$. But if $k>0$ then $(b/u-Rk)$ may have different signs within the range of u in the experiment; so as S indirectly affects u, it is possible that Hypothesis III may explain the effects of S, provided $k>0$. In Exp. 4

the least value of b/u was of the order of 28 H. As $R = 0{\cdot}7 \times 10^6\,\Omega$ it follows that $k \geqslant 4 \times 10^{-5}$ sec. Even if k were somewhat greater than 4×10^{-5} sec., the effects of k would hardly be noticeable at frequencies below 1000 c./sec. Thus Hypothesis III is promising.

Hypothesis IV—Another term which might escape notice at low frequencies is $cd^2 \log u/dt^2$. We now take the intrinsic equation to be

$$\phi = \phi_e(u) + \left(b\frac{d}{dt} + c\frac{d^2}{dt^2}\right)\log u,$$

in which b and c are independent of u and t. It follows that

$$\left(b\frac{d}{dt} + c\frac{d^2}{dt^2}\right)\log\frac{u_1}{u_2} = (u_2 - u_1)(R+z) = p, \text{ say.}$$

To fix ideas let us suppose that $u_1 > u_2$ and $R+z < 0$ so that p is positive, as in Exp. 4. The sign of $d\log(u_1/u_2)/dt$ cannot be decided, because of the term in c. We reach no definite conclusion; and therefore there is, so far, no objection concerning S to Hypothesis IV. But we are left in doubt as to whether it will explain any kind of distraction, if c is not small.

CONCLUSION ON THEORIES OF DISTRACTION

If our goal has been to find merely some possible mathematical description of reciprocal inhibition we have now achieved it in the statements

$$\phi_1 + Ru_1 = \phi_2 + Ru_2;$$

$$\phi = \phi_e(u) + b\frac{d\log u}{dt}; \quad d\phi_e(u)/du < 0; \quad b > 0;$$

which are to be understood in connexion with the circuit diagram, fig. 3, suffixes being inserted where necessary. Hypothesis II provides a more general theory, not restricted to the neon lamp.

If, however, we have been seeking a description of all the forms of reciprocal inhibition which can occur between a pair of osglim lamps wired in parallel, then the above forms of the intrinsic equation are inadequate. As the same equations fail also for very large oscillations and for small oscillations at frequencies above 1000 c./sec., we may expect that the investigation of the latter two phenomena will clear up the obscurities of the distraction circuit. By the distraction experiments several hypotheses concerning the osglim lamp have been definitely rejected, but so far no objection has been found to the following simple form,

$$\phi = \phi_e(u) + b\frac{d\log u}{dt} + c\frac{d^2\log u}{dt^2} \quad \text{when } c \text{ is near zero,}$$

nor to
$$\phi = \phi_e(u) + b\frac{d\log u}{dt} + k\frac{d\phi}{dt} \quad \text{if} \quad k \geqslant 4\times 10^{-5}\,\text{sec.}$$

Time constants of the same order of magnitude have occurred in unpublished experiments at frequencies above 1000 c./sec.

A loan of apparatus from the Government Grant Committee is gratefully acknowledged.

SUMMARY

Two osglim lamps wired in parallel with one another can be so arranged that the glowing of either inhibits the other. This arrangement is called a "distraction circuit". The lamps are connected through suitable resistances to a battery. An extra stimulus is required to start the extinct lamp. But if a condenser is suitably connected, the apparatus becomes entirely automatic, one or other lamp flashing in a random sequence, but never both lamps together. Although the glowing gas is quite unlike anything in the nervous system, it seems probable that the abstract time relations of the distraction circuit may be similar to those of a number of psychological and physiological phenomena, such as distraction, or alternations of perspective in line drawings, or reciprocal inhibition.

Experiments with these distraction circuits provide many delicate tests of theories of the osglim lamp. It is shown that the negative slope of the equilibrium potential $\phi_e(u)$ taken in conjunction with the approximate intrinsic equation

$$\phi = \phi_e(u) + b\frac{d\log u}{dt},$$

in which u is current, t time and b is a positive constant, together suffice to explain many of the observed effects. But that these hypotheses are inadequate to account for other observations; which, however, could be explained by the presence of a term of higher order, such as $kd\phi/dt$, where $k \geqslant 4\times 10^{-5}$ sec.

REFERENCES

Leyshon, W. A. 1932 *Proc. Phys. Soc.* **42**, 159–69.
Richardson, L. F. 1930 *Psychol. Rev.* **37**, 214–27.
— 1937 *Proc. Roy. Soc.* A, **162**, 293–335.

A Second-Order Focusing Mass Spectrograph and Isotopic Weights by the Doublet Method

By F. W. Aston, F.R.S.

(*Received* 29 *September* 1937)

[Plate 17]

The first survey of the masses of atoms, now called isotopic weights, made with an accuracy high enough to measure their deviations from whole numbers, was published ten years ago (Aston 1927). The instrument used, my second mass spectrograph, had a resolving power of about 1 in 600 and an accuracy approaching 1 in 10,000; with it work was further extended with results later reported in a series of communications to this journal. After the work described in the last of these (Aston 1935*a*), methods of obtaining higher resolving power and accuracy were investigated, and the most hopeful appeared to be: first, stricter collimation of the rays by finer, and preferably adjustable, slits; and secondly, the use of second-order focusing. For the solution of the latter theoretical problem I have been indebted to Mr. W. W. Sawyer of St. John's College, Cambridge, who analysed the conditions and determined the dimensions of the apparatus required to give the best conditions of focus (Sawyer 1936).

APPARATUS

It was found that these conditions could be well satisfied by the use of pole pieces virtually identical with those in the existing magnet, so this was retained, and Messrs. W. G. Pye and Co., of Cambridge, carried out the necessary alterations and constructed the other parts of the apparatus here described. The appearance of the complete mass spectrograph is shown in the photograph, fig. 1, and the main details of its construction in the diagram, fig. 2.

The Discharge Tube—As before two types of discharge were used of the forms fully described in my book (Aston 1933). The cylindrical one was used only for preliminary testing, and any experiments requiring lines, such as D_3, which are best developed at high pressures. Most of the work was done with large 8 in. bulbs which work more steadily and give stronger lines of multiply charged particles. The effects of these two different types of discharge on mass spectra yielded by hydrocarbons such as propane and pentane is striking and raises some interesting chemical problems. With a cylinder the lines of the C_3 group of hydrocarbons virtually cease at 39, C_3H_3, as is well shown in the spectra used for chlorine (IV in Plate 17). On the other hand, with the bulb they are well developed up to 44, C_3H_8, though the even members tend to be weaker than the odd, as is shown in V, VI and VII. The lines of such hydrocarbon groups are of the greatest value in providing suitable doublets with other particles, and it is unfortunate that though every effort has been made to find conditions giving measurably strong lines of molecules containing more than three atoms of carbon so far these have had little success.

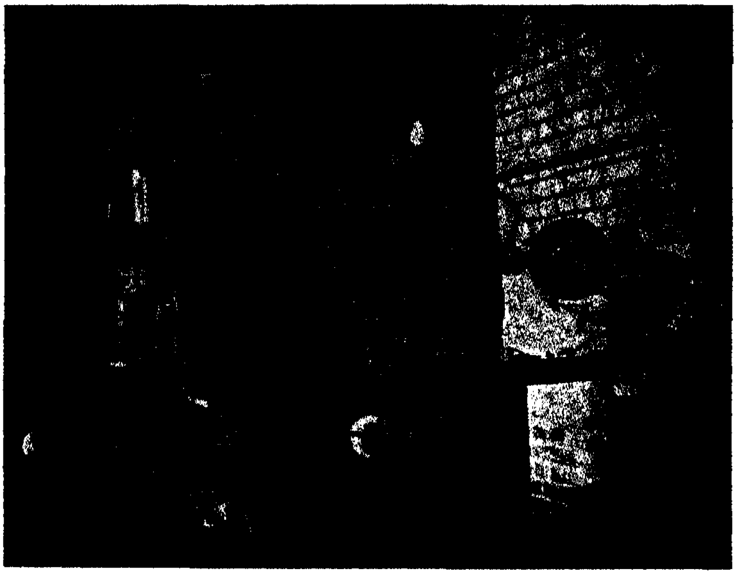

Fig. 1

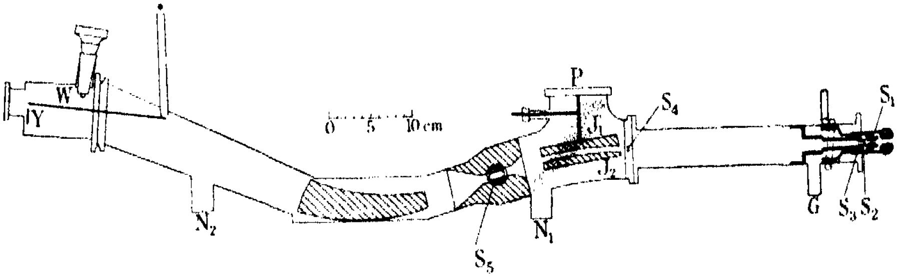

Fig. 2

The Collimator—The first part of the new apparatus to be built was the collimator. This was formed of a stout brass tube, at the ends of the axis of which were mounted the fine slits, which for the first time were adjustable from the outside as regards their effective aperture. They are of identical structure, which is well shown in the photograph, fig. 3. Two cylindrical metal wires, 1 mm. in diameter, are mounted exactly parallel and 0·05 mm. apart in such a manner that they can be tilted with great delicacy about their midpoint by a long arm actuated through a ground joint by means of a divided head. So far as rays directed along the axis of the collimator are concerned this device forms a slit whose aperture can be varied from 0·05 mm. to zero. The fact that, as it closes, its jaws are not in the same plane as they approach the axial line should not be a serious objection, as atomic diffraction is quite negligible. As shown in fig. 4 the front one of these tilting slits S_2 is mounted immediately behind a fixed aluminium slit S_1 of the form used in my original mass spectrograph (Aston 1919), and in front of another fixed narrow opening S_3 admitting the rays to the collimator and camera. S_1 has an extremely high resistance in gaseous diffusion, and the chamber containing the tilting slit S_2 is connected through G to the pumping system so that the very small amount of gas diffusing from the discharge tube is immediately removed. The jaws of the tilting slits were made of bronze, but as work progressed the front one S_2 was so badly eroded by the rays that in this they were replaced by steel piano wire which has so far proved satisfactory.

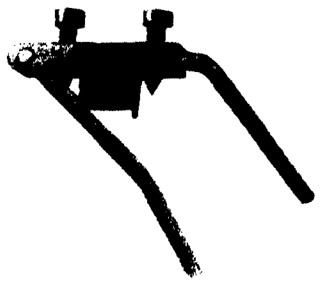

FIG. 3

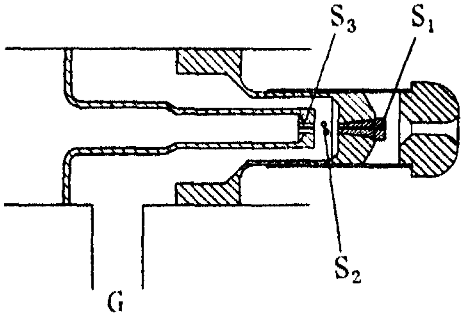

FIG. 4

The new collimator was tested by attaching it to the existing mass spectrograph. By its means the first resolution of the close doublet D–H_2 was achieved (Aston 1935*b*), and its performance was considered good enough to justify the construction of a new analyser embodying the improvements suggested by theory and experience.

The Electric Field—To deflect the rays concentric cylindrical plates were used as before, and since it was regarded as hopeless to attempt to eliminate the surface polarizing effects of the rays entirely the effects of these were mitigated in several ways. The plates were set farther apart, they were mounted in such a way that they could be resurfaced and replaced without disturbing any other part of the apparatus, the intensity of the beam was less than before owing to the finer slits and more sensitive photographic plates, and finally the doublet method employed reduces error due to curvature of the lines to a minimum.

The plates J_1, J_2 are of brass. They are 2 cm. wide and 10 cm. long, curved to a radius of 40 cm. and kept 2 mm. apart by glass distance pieces. The actual form of plane, hole and groove mounting is somewhat complicated and is not shown in detail; by its means it was possible, after removing the cover P, to take out the plates, give them a new surface by polishing with rouge and replace them *exactly* in the same position as before. As a precaution this was done frequently during the research, though at no time was any serious curvature of the lines detected. Simple calculation shows that the energy of the median ray travelling between the plates will be 100 times the voltage applied to them. Voltages ranging from 240 to 400 were used, most frequently 320 corresponding to 32 kV rays. The lower plate J_2 was earthed to the body of the apparatus, and the potential applied to J_1 was obtained from the battery of small accumulators already described (Aston 1927, p. 491). These are still highly satisfactory after 15 years' service with few repairs and replacements. The range of energy of the electric spectrum of the rays is controlled as before by a variable diaphragm S_5 mounted in the bore of a massive and carefully ground brass stopcock. The effective aperture of this can be varied from 2 mm. to zero.

The Magnetic Field—The large ring magnet is that used in the previous instrument which has been fully described (Aston 1927, p. 492). The pole faces are sickle-shaped sections of a circle 15 cm. in diameter as calculated by Sawyer (1936). As tests had shown that constancy of exciting current did not ensure absolute constancy of field it was decided to control the latter directly. For this purpose only the two upper quadrants of the magnet windings were excited, and the lower half, containing over 3000 turns, was used as a search coil. The current was derived from a set of large accumulators, and when it had settled down to the state required the search coil was connected to a delicate fluxmeter made by the Cambridge Instrument Co. easily capable of detecting changes of the order of 10^{-5}. The field was stabilized by a spiral mercury resistance controlled by hand during the exposure.

The Camera—The general design of this can be seen in the diagram. The part containing the photographic plate W and the willemite screen Y is the same as that used before, and this and the collimator are joined to the central part containing the electric and magnetic fields by demountable wax joints. For convenience of construction this central part was made of thick brass plates soldered together. This type of construction is not very satisfactory owing to the inevitable occurrence of small pockets in the joints which simulate air leaks and make any real ones difficult to identify.

Vacuum Technique—The method of maintaining the lowest pressure in the analysing apparatus is the one which experience has shown to be the most satisfactory, that is, a combination of cooled charcoal and a diffusion pump. Where liquid air, or better liquid nitrogen, is easily available the former has still much to recommend it, for it is the only high vacuum device which can be left for indefinite periods with no attention whatever. The charcoal tubes, which are made very much more effective by a septum of coarse iron wire grid so fitted as to increase the effective area of the charcoal, are cooled with liquid nitrogen. They are of pyrex glass 2 cm. wide and are attached at N_1, N_2. The diffusion pump is a Gaede two-stage type G. It is fitted with a liquid air trap and can be cut off by a 1·5 cm. glass stopcock to prevent diffusion of mercury vapour into the apparatus when not in use. It is connected by ½ in. tombac tubing through aperture G to the space behind S_1 to exhaust gases diffusing from the discharge tube, and to the main part of the camera at a point near N_1 to remove any gases not absorbed by the charcoal. The pressure in the camera is measured with a Dushman ionization gauge, and is usually below 10^{-5} mm. of mercury under working conditions.

PHOTOGRAPHIC PLATES

The great improvement in the technique of mass-spectrum analysis in the last few years is due in a large degree to the excellence of the photographic plates now available. In January 1932 when the original batch of Q plates (Aston 1931) was exhausted, Messrs. Ilford, Ltd., kindly permitted their expert, Dr. Olaf Bloch, to collaborate with me in experiments to obtain still better and more sensitive ones. Plates were coated with experimental emulsions in the Ilford Research Laboratory and then tested by me in a parabola apparatus set up in the Cavendish Laboratory for that particular purpose. The research proved long and laborious, and it was only in September 1934, after scores of emulsions had been tested, that a great step forward was made and a plate produced which I estimated to be about 20 times as sensitive as the original batch for heavy rays of about 30 kV energy. A second batch was made, coated on plate glass with the same emulsion, which was, however, not quite so sensitive, and it is with these two types of plates that the results described here were obtained. Whenever intense doublets could be easily produced the plate glass ones were used to eliminate photometric error, but the glass used on the ordinary ones was of so good a quality that no serious difference has been observed. These new Q plates are now on the market and are not only by far the best for mass spectrum analysis (e.g. Bainbridge and Jordan 1936*b*), but have already been put to good use by Skinner and Johnston (1937) in their work in the extreme ultra-violet.

PERFORMANCE OF THE INSTRUMENT

This can be best judged by the actual spectra reproduced in Plate 17. The focusing is well up to expectation, as is shown in the spectrum of hydrocarbon lines (V) which was taken with the slits S_2, S_4, S_5 all wide open. The action of the tilting slits as their effective apertures were reduced was not so satisfactory. For some reason, still obscure but probably connected with minute irregularities in the surface of the wires, the lines were apt to show evidence of structure, as seen in the S–O_2 doublets reproduced (VIII), and their sharpening showed no really practical improvement when the effective aperture of the slit was reduced much below 0·01 mm. As a result the resolving power is only sufficient to separate clearly lines differing by 1 in 2000. This is considerably less than that of the double-focusing mass spectrograph of Bainbridge and Jordan (1936*b*). The dispersion 3–6 mm. for 1 % difference of mass, and the exposures necessary, a few seconds for the D–H_2 doublet and about a minute for the O–CH_4 doublet, are much the same as theirs.

For doublets of favourable width, about 10 units of packing fraction, that is 0·1 % difference of mass, the accuracy of measurement hoped for was 1 in 10^5, but it was soon evident from observations on the D–H_2 doublet that measurements of individual samples of the same doublet at different positions on the plate might vary by 3–4 times that amount. These variations appeared to be completely random and they may possibly be due to minute dust particles on the earthed metal surfaces near the beam. The effect of this source of error seems best reduced by many observations at different parts of the plate. In cases where no other lines could interfere exposures were often made in triplicate by a suitable small voltage being added to and then subtracted from the first applied to the deflecting plates (III, IV and VIII).

MEASUREMENT OF THE DOUBLETS

Lines well matched in intensity were used whenever possible, and their distance apart was estimated by means of the Cambridge micro-photometer previously used for measuring intensities of lines on mass spectra (Aston 1930, p. 514). For this purpose the wedges were not used, but the reading of the Lindemann electrometer was read against 0·05 mm. movements of the screw. The curves were plotted on square paper and the distance apart of the peaks was estimated by eye to 0·005 mm. which corresponds to about 10^{-5} in mass, that is, one-tenth of a unit of packing fraction.

Calibration of the Plate—The scale of the spectrum, as can be seen from the results reproduced, is almost exactly linear. In order to determine the dispersion coefficient at different distances from the fiducial spot I decided to use the lines of bromine. These are particularly suited to the purpose, being equal in intensity, a convenient distance—250 units of packing fraction—apart and fairly easy to produce by the discharge in methyl bromide. A very large number of spectra were taken and measured by means of a travelling microscope. The intervals between the lines were plotted against the displacements of their mid-points from the fiducial spot. This curve, which is nearly a straight line, gives the dispersion coefficient required in terms of the difference of mass of the two bromine isotopes. This I had measured 10 years ago to be 1·997 units (Aston 1927), but in order to make more certain the comparison by series shift of 1 unit was made again with the new apparatus. Enlargements of the results are shown in the Plate (II). The top spectrum is obtained by exposing the bromine group for a time sufficient to bring up the BrH lines to their optimum intensity for measurement and then repeating with the electric field reduced so as to bring the Br lines nearly, but not quite, into coincidence with the BrH lines on the same spectrum, this time with the much shorter exposure necessary for the stronger Br lines. This provides the two outer artificial doublets ^{79}Br–^{79}BrH and ^{81}Br–^{81}BrH. The lower spectrum is then made by repeating the same process with the times of exposure reversed, giving the third inner artificial doublet ^{79}BrH–^{81}Br. It is clear that the difference between the inner doublet and the mean of the outer ones is a measure of the difference between the sum of the masses of two hydrogen atoms and the difference of mass between the two bromine isotopes. The mean of the results from several plates is 0·0179, so taking H as 1·0081 the difference between the masses of the Br isotopes is 1·9983 ± 0·0015, and from the known value of their packing fractions it is safe to assume this is 250·0 units of packing fraction. From the calibration curve the dispersion coefficient could be read off with an accuracy of 0·2 %, which is ample for any but abnormally wide doublets.

THE FUNDAMENTAL DOUBLETS LINKING H, D, C AND O

In my first survey of the packing fractions the comparison of H with the standard ^{16}O could be made only through the intermediate He, and then only indirectly by artificial doublets. The ratio of He to O was particularly difficult to measure and led to a result which is now known to be badly in error. By a most remarkably fortunate chance the mistake was in the direction to give the mass of H too low, which was of the utmost value in encouraging the search for heavy hydrogen. As soon as this remarkable substance was available it became possible to compare the masses of H, D, C and O much more certainly by their natural doublets. The first of these, the D–H_2 doublet at mass 2, is very easy to produce when deuterium gas is used in the discharge. It requires only a few seconds' exposure and was used to test the performance of the tilting slits, so that a large number of doublets obtained over a wide range of conditions were available for measurement, some of which are reproduced in the Plate (I). The mean of all of these is given in the Table and is virtually identical with that given by Bainbridge and Jordan (1936*a*).

The next connecting link, the doublet formed by the doubly charged carbon atom and the triatomic deuterium molecule C^{++}–D_3, was much more difficult to produce. Nearly pure deuterium gas was used in a cylindrical discharge tube, and exposures as long as 20 min. were necessary to obtain good lines. The doublet is also a very wide one, so that the probable error in terms of packing fraction is given in the Table as higher than any of the other doublets measured. While the work on deuterium was in progress a search was made for the possible third isotope of hydrogen of mass 3. The result was completely negative and has been recently published by Lord Rutherford (1937).

The last doublet necessary to connect these results with the standard oxygen, O–CH_4 at mass 16, was easily obtained from a mixture of oxygen and methane, the only precaution to be taken being the absence of any deuterium or its compounds. Specimens of this doublet are reproduced (III in the Plate). A number of very consistent results were obtained, and

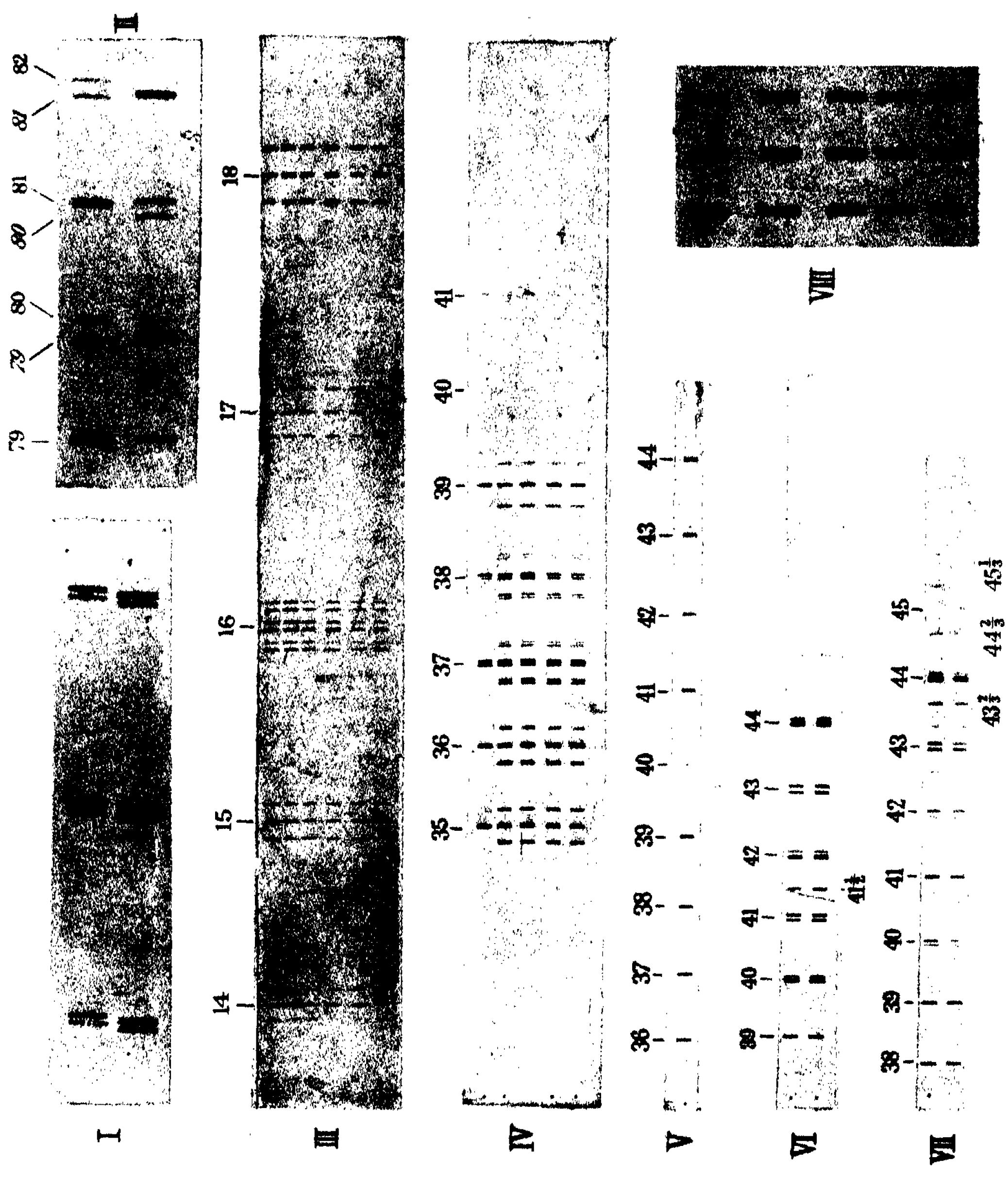

I—Doublets of D–H_2 enlarged. × 3.

II—Lines of the bromine isotopes and their hydrides photographed with a series shift of one unit. × 3. The lines of the second exposure are indicated by italics.

III—One of the plates used in the work on the O–CH_4 doublet.

IV—One of the plates used to measure the isotopes of chlorine by comparison with hydrocarbon molecules of the C_3 group.

V—Lines of the C_3 group obtained from the low pressure discharge in pentane. Most of the effect at 44 is due to CO_2.

VI—Two spectra of the C_3 group of lines and those of doubly charged krypton.

VII—Two spectra of the C_3 group of lines and those of triply charged xenon.

VIII—Doublets of ^{32}S–O_2 enlarged. × 3, showing curious structure.

these combined with those of the other two doublets to give the isotopic weights of H, D and O given in the Table. These were published (Aston 1936) and adopted for calculation of isotopic weights of other elements with which they and their compounds could be compared. Later, Bainbridge and Jordan (1936*a*) published a value for the O–CH_4 doublet greater than mine leading to a discrepancy in the isotopic weight of C of about 1 in 20,000. As this is the most important substandard in work of this kind, I repeated my measurements of the O–CH_4 doublet with another form of discharge and made independent investigations on the mass of C by as many methods as possible. The results of these published in *Nature* (Aston 1937) supported my value for C and justified a reduction in its estimated probable error. They have been since further supported by more accurate measurements of the A–C_3H_4 doublet.

Helium—The wide doublet He–D_2 was quite easy to obtain. The isotopic weight of He deduced from it is in good agreement with that calculated from disintegration experiments.

Boron—A value for the lighter isotope of boron was obtained by means of the discharge in boron trifluoride containing neon. This gives a fairly wide doublet at mass 10 with doubly charged ^{20}Ne. The mass of the latter had already been obtained as will be described.

Nitrogen—The more abundant isotope was compared at mass 14 with CH_2 with a discharge in nitrogen and methane. Very sharp lines were obtained and the values were particularly consistent.

Oxygen—During the work on carbon in which the line of ^{36}A was used as a reference point, and on another occasion when the intensity of the OH_2 line had been sufficiently reduced, a faint doublet ^{18}O–OH_2 could be seen. Three doublets were measured giving very consistent results, from which a provisional value for the isotopic weight of ^{18}O could be calculated. This is in fairly good agreement with that calculated from optical spectra by Birge (1931).

Fluorine—The discharge in heavy water vapour gives a good line at 19 due to ODH. On introducing a little CF_4 well-matched doublets could be obtained with the F atom. This is found to have a small positive packing fraction and a mass slightly higher than that first estimated.

Neon—The most abundant isotope was compared directly with the line OD_2 which was obtained by running the discharge for a long time with the vapour of heavy water mixed with a little neon.

Aluminium—This element has not yet been systematically examined, but two measurable doublets at mass 27 were obtained when ethane was present. The heavier member must be C_2H_3, and it is reasonably certain that the lighter is due to ^{27}Al derived from the cathode. This enables a provisional value of its isotopic weight to be included in the Table.

Silicon—The intensities of the lines of this element, produced by the action of halogens on the walls of the discharge tube, are outside ordinary means of control. It was therefore a matter of good fortune that during the work on P when CF_4 was present a large number of well-matched doublets at mass 28 appeared. These were due to ^{28}Si–CO and enabled a reliable value of the isotopic weight of ^{28}Si to be calculated.

Measurements of the weaker isotope ^{29}Si, the first to be made, were obtained by means of the doublet ^{29}Si–^{10}BF which appeared when BF_3 was used. These indicate that the isotopes of silicon differ in mass by one atomic unit very closely.

Phosphorus—A mixture of phosphine, carbon tetrafluoride and helium in the discharge tube gave a doublet at mass 31 formed by P–CF. The value of the packing fraction of phosphorus is virtually identical with the one obtained by entirely different methods 10 years ago (Aston 1927).

Sulphur—The first accurate measurements have now been made on this element by means of the close doublet ^{32}S–O_2, some examples of which are shown enlarged in the Plate (VIII) and exhibit the curious structure sometimes seen in the lines. The results were very consistent, and since the comparison with the standard is direct the value of the isotopic weight is probably the most accurate in the Table.

Chlorine—The first experiments with this element were done with a mixture of heavy phosphine PD_3 mixed with a little CCl_4. This mixture behaved very badly in the discharge tube, and much better results were obtained later by the use of propane and methyl chloride. By suitable variation of the proportions of this mixture three doublets can be obtained: 36, $H^{35}Cl$–C_3; 37, ^{37}Cl–C_3H; and 38, $H^{37}Cl$–C_3H_2. All of these are seen in Plate (IV), in which one of the plates used is reproduced. The masses of the chlorine isotopes were calculated from measurements of the first two doublets, and the value for ^{37}Cl was checked by measurements of the third.

Argon—The abundant heaviest isotope ^{40}A was measured by means of its second-order line, which gives a very close doublet with ^{20}Ne. The mass deduced 39·9754 has since been confirmed closely by further recent measurements of the doublet $^{40}A–C_3H_4$ which gives 39·9752. This agreement is a very valuable check on the mass of carbon.

The low abundance of ^{36}A makes it difficult to deal with, and it is hoped that samples of gas enriched by diffusion in this constituent may be available in the future. In the meanwhile a few doublets, $^{36}A–C_3$ and $^{36}A^{++}–OH_2$, have been obtained by long exposures. These give further support to my value for ^{12}C and enable a fairly reliable value of the mass of ^{36}A to be deduced.

Krypton—By the use of suitable proportions of krypton mixed with propane in a low-pressure bulb discharge doublets of the doubly charged isotopes and the higher members of the C_3 group are formed as shown (VI) in the Plate. ^{80}Kr cannot be measured in this way owing to the presence of traces of ^{40}A and, on account of its rarity, only a few results were obtained from ^{78}Kr. The other even-numbered isotopes gave very satisfactory and reliable results, which show that the original estimates of their isotopic weights were too low.

Tin—As before, this complex element was studied by comparing the lines of its methyl $SnCH_3$ with those of xenon. The sequence of lines 132 ... 136 was measured up on several plates. Those due to Xe, 132, 134, 136, appeared exactly 2 units of atomic weight apart, while those at 133, 135 appeared equally out of step, 0·016 of a unit too heavy. Assuming the value of Xe given below, values for ^{118}Sn and ^{120}Sn can be calculated which, though provisional, are certainly more accurate than those originally given.

Xenon—Theoretically, three of the isotopes of this element should give, when triply charged, doublets with lines of the C_3 group. The abundant ^{129}Xe is the most convenient for this purpose, and very satisfactory results have been obtained from its doublet at 43 with C_3H_7, specimens of which are reproduced (VII) in the Plate. The inevitable presence of CO_2 interferes with the measurement of the similar doublet at 44 formed by $^{132}Xe^{+++}$ and C_3H_8, but the results so far indicate that ^{132}Xe has a packing fraction nearly identical with that of ^{129}Xe. Measurements of ^{126}Xe have not been attempted owing to its rarity and the difficulty of excluding every trace of krypton.

Mercury—The only data available on this element were obtained from a comparison of its triply charged lines with those of doubly charged xenon. The close doublet $^{134}Xe^{++}–^{201}Hg^{+++}$ was actually photographed though with extreme difficulty owing to the weakness of the mercury line. More reliable results were obtained by raising the intensity of line $^{134}Xe^{++}$ and estimating its position between the lines of more abundant $^{200}Hg^{+++}$ and $^{202}Hg^{+++}$. The difference in packing fraction so measured is 5·8, in very good agreement with 6·1 estimated by the same method in the original survey (Aston 1927). If we combine this result with those now available on Xe we obtain a rather higher positive value of 1·4 for the packing fraction of mercury.

The numerical results of the measurements described in this paper are collected in the two following Tables. Provisional values are given in brackets. If one compares the packing fractions with those given originally, it will be seen that the only change in the packing fraction curve of note is that it is slightly higher in the region of large mass numbers.

TABLE OF NATURAL DOUBLETS MEASURED

Mass no.	Doublet	Number of doublets measured	Difference in packing fraction	Difference in mass
2	$^{2}D-^{1}H_2$	53	7·54 ± 0·2	0·00152
4	$^{4}He-^{2}D_2$	12	63·5 ± 0·2	0·02551
6	$^{12}C^{++}-^{2}D_3$	10	70·3 ± 0·3	0·04236
10	$^{20}Ne^{++}-^{10}B$	14	16·83 ± 0·15	0·01684
14	$^{14}N-^{12}C\,^{1}H_2$	17	8·89 ± 0·05	0·01245
16	$^{16}O-^{12}C\,^{1}H_4$	27	22·48 ± 0·1	0·03601
(18	$^{36}A^{++}-^{16}O\,^{1}H_2$	3	15·09 ± 0·2	0·0271)
(18	$^{18}O-^{16}O\,^{1}H_2$	3	5·80 ± 0·1	0·01044)
19	$^{19}F-^{16}O\,^{2}D\,^{1}H$	10	9·64 ± 0·15	0·01833
20	$^{20}Ne-^{16}O\,^{2}D_2$	14	15·41 ± 0·2	0·03083
20	$^{40}A^{++}-^{20}Ne$	11	5·44 ± 0·15	0·01088
(27	$^{27}Al-^{12}C_2\,^{1}H_3$	2	15·0	0·0405)
28	$^{28}Si-^{12}C\,^{16}O$	11	6·15 ± 0·2	0·0172
29	$^{29}Si-^{10}B\,^{19}F$	7	11·8 ± 0·2	0·0342
31	$^{31}P-^{12}C\,^{19}F$	18	7·88 ± 0·15	0·0244
32	$^{32}S-^{16}O_2$	18	5·53 ± 0·1	0·0177
36	$^{36}A-^{12}C_3$	6	9·06 ± 0·2	0·0326
36	$^{1}H\,^{35}Cl-^{12}C_3$	8	6·25 ± 0·2	0·0225
37	$^{37}Cl-^{12}C_3\,^{1}H$	22	11·14 ± 0·2	0·0412
39	$^{78}Kr^{++}-^{12}C_3\,^{1}H_3$	4	16·28 ± 0·2	0·0635
40	$^{40}A-^{12}C_3\,^{1}H_4$	10	16·98 ± 0·15	0·0679
41	$^{82}Kr^{++}-^{12}C_3\,^{1}H_5$	19	20·20 ± 0·15	0·0828
42	$^{84}Kr^{++}-^{12}C_3\,^{1}H_6$	20	21·73 ± 0·15	0·0913
43	$^{86}Kr^{++}-^{12}C_3\,^{1}H_7$	18	23·10 ± 0·15	0·0993
43	$^{129}Xe^{+++}-^{12}C_3\,^{1}H_7$	14	20·16 ± 0·1	0·0867

TABLE OF PACKING FRACTIONS AND ISOTOPIC WEIGHTS

Symbol	Packing fraction	Isotopic weight
^{1}H	+ 81·2	1·00812 ± 0·00004
^{2}D	+ 73·55	2·01471 ± 0·00007
^{4}He	+ 9·77	4·00391 ± 0·00016
^{10}B	+ 16·1	10·0161 ± 0·0003
^{12}C	+ 2·96	12·00355 ± 0·00015
^{14}N	+ 5·28	14·0073 ± 0·0004
(^{18}O	+ 3·2	18·0057 ± 0·0002)
^{19}F	+ 2·36	19·0045 ± 0·0005
^{20}Ne	− 0·70	19·9986 ± 0·0006
(^{27}Al	− 3·3	26·9909)
^{28}Si	− 4·90	27·9863 ± 0·0007
^{29}Si	− 4·7	28·9864 ± 0·0008
^{31}P	− 5·30	30·9836 ± 0·0005
^{32}S	− 5·53	31·9823 ± 0·0003
^{35}Cl	− 5·71	34·9800 ± 0·0008
^{37}Cl	− 6·10	36·9775 ± 0·0008
^{36}A	− 6·10	35·9780 ± 0·0010
^{40}A	− 6·15	39·9754 ± 0·0014
^{78}Kr	− 7·30	77·9430 ± 0·0020
^{82}Kr	− 7·70	81·9369 ± 0·0015
^{84}Kr	− 7·60	83·9362 ± 0·0015
^{86}Kr	− 7·40	85·9363 ± 0·0015
(^{118}Sn	− 5·8	117·930)
(^{120}Sn	− 5·8	119·930)
^{129}Xe	− 4·46	128·9424 ± 0·0020
(^{132}Xe	− 4·4	131·942)
(^{200}Hg	+ 1·4	200·028)

SUMMARY

A form of mass-spectrograph in which several improvements are embodied, including adjustable slits and second-order focusing. The instrument has a resolving power of 2000 and an accuracy of measurement approaching 1 in 10^{5}. By its means a large number of natural doublets have been measured. In many of these one member is a hydrocarbon molecule, hence the isotopic weight of ^{12}C has been ascertained with particular care. From the results obtained the packing fractions and isotopic weights of over twenty atomic species are tabulated, some for the first time.

REFERENCES

Aston, F. W. 1919 *Phil. Mag.* **38**, 707–14.
— 1927 *Proc. Roy. Soc.* A, **115**, 487–514.
— 1930 *Proc. Roy. Soc.* A, **126**, 511–25.
— 1931 *Proc. Roy. Soc.* A, **132**, 487–98.
— 1933 "Mass Spectra and Isotopes." London: Arnold.
— 1935*a* *Proc. Roy. Soc.* A, **149**, 396–405.
— 1935*b* *Nature, Lond.*, **135**, 541.
— 1936 *Nature, Lond.*, **137**, 357.
— 1937 *Nature, Lond.*, **139**, 922.
Bainbridge, K. T. and Jordan, E. B. 1936*a* *Phys. Rev.* **49**, 883.
— — 1936*b* *Phys. Rev.* **50**, 282–94.
Birge, R. T. 1931 *Phys. Rev.* **37**, 841.
Rutherford, Lord 1937 *Nature, Lond.*, **140**, 303.
Sawyer, W. W. 1936 *Proc. Camb. Phil. Soc.* **32**, 453–60.
Skinner, H. W. B. and Johnston, J. E. 1937 *Proc. Roy. Soc.* A, **161**, 420–40.

Atomic Hydrogen

I—The Calorimetry of Hydrogen Atoms

By H. G. Poole

University College, London

(*Communicated by C. K. Ingold, F.R.S.—Received* 6 *July* 1937)

Since the discovery of Wood (1920, 1921, 1922*a*, *b*) that hydrogen can be dissociated to a considerable extent into free atoms in the glow discharge, many workers have used this method of production of atomic hydrogen for the study of its chemistry. Few attempts have been made, however, to determine the optimum discharge conditions for large yields of atoms, although the consensus of opinion has favoured the use of long discharge tubes, operated with fairly heavy currents at gas pressures of about 0·3–1 mm. The work described in this series of papers was undertaken to determine and explain the factors controlling yield.

Atomic hydrogen has been estimated by several different methods. The calorimetry of the heterogeneous catalysis reaction, $H + H + M \rightarrow H_2 + Q + M$ (Q being the dissociation energy of the hydrogen molecule, and M a suitable catalyst) has been the method employed by a number of workers. Bonhoeffer (1924), Bichowsky and Copeland (1928), v. Wartenberg and Schultze (1930), Dixon (1932), and Smallwood (1929) have all devised calorimeters based on this equation. But with none of these has it been possible to obtain a good degree of accuracy, coupled with reasonably rapid operation and the possibility of making consecutive readings. Probably the method of Smallwood, also used by Amdur and Robinson (1933), is the best of those cited; but this involved corrections for conduction losses amounting to 40 or 45 % of the observed rise of temperature; also about 20 min. were required for each determination, and consecutive readings were not possible owing to the increasing temperature.

Exception has been taken to the calorimetric method for the determination of atom concentrations (Steiner and Wicke 1931; v. Wartenberg and Schultze 1930) on the grounds that the introduction of a powerful catalyst, causing complete removal of the atoms, sets up a diffusion of atoms towards the catalyst and thus changes the local atom concentrations throughout the tube. This objection is obviously valid in spite of Amdur and Robinson's attempted refutation (1933). They found no appreciable difference in the pressure at any point, whatever the position of the catalyst or even if it was removed, and they concluded that "the large linear velocities (9 to 12 metres per second) seem to overcome the pressure drops due to diffusion." But Steiner (1935) has pointed out the concurrent back-diffusion of molecules, on account of which one should not expect that any appreciable change of *total* pressure would result from the introduction of the catalyst. Steiner (private communication) has found that in some circumstances the calculated degree of dissociation may have the absurd value of 120 % if this diffusion is neglected.

Nevertheless the calorimetric method has been adopted in the present work, as the main purpose of the investigation (see Part III) has been to study the connexion between the discharge conditions and the *number of atoms produced per unit time*: the calorimetric method certainly measures this quantity correctly. A new type of calorimeter has been designed, capable of high accuracy, with sensitivity adjustable over a wide range, and with easily estimated corrections for conduction losses, of the order 1–3 %. A high speed of operation has been achieved, equilibrium being attained usually in about ½–1 min., and continuous readings may be made over any length of time.

THE CONTINUOUS-FLOW CALORIMETER

The calorimeter is as shown in fig. 1. The partially dissociated hydrogen, leaving the discharge tube at a point midway between the electrodes, enters a long, wide, glass tube *B* at its midpoint, and is pumped off at one end *D*. A platinum-plated copper tube *C* passes axially through the tube *B*, being cemented with Apiezon wax at the two sleeves *E* and *F*. A steady, measured flow of water is maintained through the copper tube from *E* to *F*, the difference in temperature between the entering and issuing water being determined by the rate of heat production due to catalytic recombination on the platinum surface. The rise of temperature of the water is measured by means of a pair of thermocouples *G*, *G* (copper-constantan) inserted in the copper tube. The lag in attainment of equilibrium depends on the position of the hotter couple, and may be reduced by sliding this couple inside the tube, since it is necessary to ensure only that the couple is still outside the region of heat production. The only other variable factor affecting the lag is the rate of flow of water, but a more important effect of this is the possibility of varying the range and sensitivity of the instrument; rates of water flow of 4–55 c.c./min. have been used, the linear velocities being from about 2–30 cm./sec. Starting with a cold calorimeter, the steady state is reached in about ½ min. with rates of flow above about 16 c.c./min., and in about 1–2 min. with the lower rates; only in extreme cases is as much as 3 min. required. Even low rates of heat production could be measured with high rates of flow if two or three pairs of couples were used in series, and this could easily be done by employing fine wires. There is another important advantage in using a large water flow, namely, the diminution of the correction for loss of heat by conduction, since this depends on the actual rise of temperature.

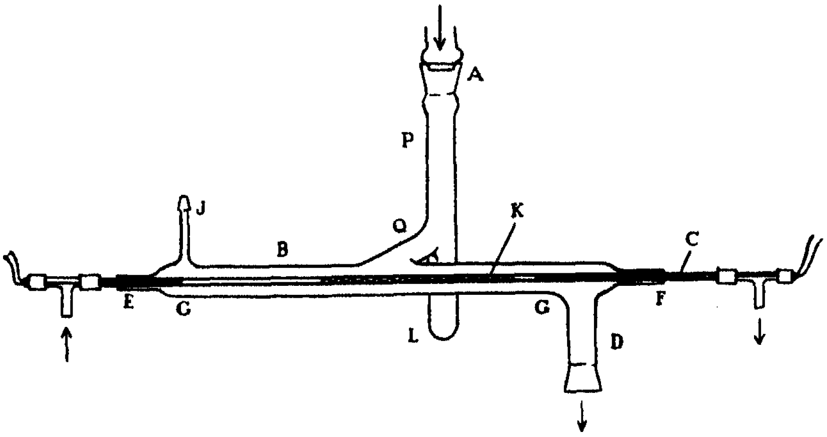

FIG. 1—The continuous-flow calorimeter.

The dimensions of the calorimeter are as follows. The outer glass tube *B* is of 25 mm. bore (as are all the other tubes used in the vacuum system, with the exception of one of the discharge tubes, *S* II, to be described in Part II), and is 42 cm. in length. Experience has shown that the length could probably be reduced to about 20 cm. without any adverse effect. The external diameter of the catalyst tube *C* is 5·5 mm., and its internal diameter 3 mm.; its length is about 65 cm. By using a thinner walled catalyst tube or one of smaller diameter, the lag could easily be made less than that of the system used to measure the thermo-e.m.f. The tube *P* has been extended to *L*, to prevent direct entry of radiation from the discharge tube into the calorimeter. The length of $P+Q$ is 21 cm., and in all of the experiments described there was also an additional length of 5 cm. of tube from the joint at *A* to the discharge tube, the junction being cemented with meta-phosphoric acid. Connexion to a McLeod gauge is made through the joint *J*; owing to the length of catalyst tube, no free atoms can reach this joint.

The thermocouples are enclosed in glass capillary sheaths of about 1 mm. external diameter, and of length up to 80 cm.; their sensitivity is about $40\,\mu$V/degree. Direct deflexion of a galvanometer was abandoned in favour of a null method using a metre bridge (manganin) as potentiometer. The current through the potentiometer was adjusted so that the potential drop along the wire corresponded to 1·00 or 2·00° C./cm. Temperature readings up to 10 or 20° C. could thus be read directly to within 0·02° with only one pair of thermojunctions. The sensitivity of the calorimeter therefore varied from about 0·1 to 1·0 cal./min. with the range of water flow indicated above; the rates of heat production have ranged from 4 to 300 cal./min.

In order to localize the recombination on the catalyst tube, the glass walls of the calorimeter and connecting tube were poisoned with meta-phosphoric acid. This was the case in all of the work to be described in Parts I, II, and III of this series, even when uncoated discharge tubes were used. v. Wartenberg and Schultze recommended the use of syrupy phosphoric acid for this purpose, but in the present work solid meta-phosphoric acid was melted on to the surface of the tube. This forms an internal glassy sheath, which may develop fine cracks on standing, but is nevertheless perfectly safe and stable for indefinite periods. In order to maintain the surface in a condition only weakly catalytic towards the recombination of atoms, the hydrogen used was bubbled through water at atmospheric pressure and room temperature; in this way about 2·5 % of water vapour was added to the hydrogen, the desirability of this procedure having been indicated by Wood and confirmed by v. Wartenberg and Schultze.

It was found necessary to promote rapid mixing of the water inside the catalyst tube by means of a closely fitting rod of twisted copper wires, *K*, as otherwise the temperature registered depended on the (uncontrollable) eccentricity of the end of the thermocouple sheath. In the absence of stirring, the stream-line motion of the water, coupled with its greatly reduced velocity very near the surface of the sheath, leads to the registration of abnormally high temperatures, which may indeed indicate rates of heat production up to 30 % too high. This was shown by using the 80 cm. couple for the longitudinal exploration of both the atom calorimeter and an electrically heated dummy calorimeter of similar construction; the latter gave exact results after insertion of the mixing device in the region of heat production. For example, when the electrical input to the dummy calorimeter, without mixer, was 6·05 W, i.e. 86·8 cal./min., the apparent heat production derived from the maximum of the longitudinal temperature curve was 107 cal./min., this value falling, when the couple was moved farther from the heat source, much more rapidly than can be explained by conduction loss; but after the insertion of the mixer, an input of 3·04 W, i.e. 43·6 cal./min., gave a temperature curve which was practically horizontal and corresponded to 43·4 cal./min., the sensitivity of the calorimeter being about 0·4 cal./min. Accordingly the mixing device was inserted in the atom calorimeter from about 4 cm. before the point of entry of the atomic hydrogen, to about 14 cm. beyond it. This length exceeds considerably the length of the reaction zone, the longitudinal temperature distribution obtained as described above having indicated that reaction occurs only within a few centimetres close to the point of entry of the atoms; this has been confirmed for large atom outputs by the fact that the only change on moving the hot couple several centimetres outwards from its normal position 1 cm. beyond the mixer is a very small drop in temperature corresponding exactly to the additional conduction loss. For example, in one experiment the following results were obtained: hydrogen flow, 314 c.c./min. at N.T.P.; pressure, 0·82 mm.; discharge current, 73 mA; water flow, 11·2 c.c./min.; temperature rise for couple at normal position 15 cm. from point of entry of hydrogen, 12·1°; temperature rise for couple at 19 cm., 12·0°; total heat production registered in the two positions, 135·5 and 134·4 cal./min., the difference being 1·1 cal./min.; conduction loss from 4 cm. of tube at 12° C. and 0·82 mm. pressure, 1·4 cal./min. (next section); sensitivity of calorimeter for the above flow of water, 0·3 cal./min.

CORRECTION FOR CONDUCTION LOSS

The correction to be applied for the radiation and conduction loss in any given circumstances was obtained by passing warm water through the catalyst tube for various pressures and rates of flow of hydrogen, no discharge being used. Hence L, the loss of heat per minute, per cm. length, per degree difference of temperature between catalyst tube and outer glass tube (room temperature), was obtained. For any given pressure, variation of the rate of hydrogen flow was found to have no sensible effect on the loss, as would be expected from the small heat capacity of the gas. The effect of change of pressure was considerable, the curve of L against pressure resembling the conductivity-pressure curves obtained by Senftleben and Riechemeier (1930) for a number of gases. This curve was used to determine the correction to be applied to the indicated heat per minute in any given circumstances, the length, a, of tube giving rise to the loss being taken to extend from 1 cm. before the point of entry of the gas to the position of the hot couple, 1 cm. beyond the mixing device, i.e. 16 cm. If the water flow is f c.c./min., the percentage correction is $100aL/f$. In a few of the earlier experiments this correction was as high as 10 % of the heat produced, but in all the later work it was reduced to less than 3 % by adopting a suitable rate of water flow. The loss at zero pressure would be the radiation loss, which should be insignificant for a bright platinum surface. The observed loss at the lowest pressure used, 0·05 mm., was quite negligible, and hence the measured losses are essentially due to gaseous conduction.

MECHANICAL TRANSFER OF HEAT

Since much heat is produced in the discharge tube, due to the large initial kinetic energies of the atoms produced by the dissociative process (3 e-volts/atom*), to the recombination of atoms in the discharge tube, and to other electronic processes, it seemed possible that the gas reaching the calorimeter might itself be hot, and hence cause calorimeter readings greater than those corresponding to the atom output. The walls of the discharge tube itself were usually less than 50° C. above the room temperature, and were cooler for higher rates of hydrogen flow owing to the smaller degree of dissociation and consequent smaller amount of recombination. The heat transfer, calculated from the specific heats of hydrogen atoms and molecules, for the maximum rate of hydrogen flow and highest current intensity used in the quantitative work of Part III, would be about 8 cal./min. if no cooling at all occurred in the connecting tube. The range of hydrogen flow rates, from

---

* The dissociation energy of H_2 is 4·5 e-volts, and the average energy required for the excitation of the molecule in the step preceding dissociation is about 10 e-volts (see Part III). The two atoms produced therefore share nearly 6 e-volts in the form of kinetic energy.

400 to 5000 c.c./sec., was such that each molecule collides with the walls of the connecting tube (26 cm. from discharge tube to calorimeter) from 1300 to 16,000 times before reaching the calorimeter, so that temperature equilibrium with these walls is to be expected. Since not more than the first 5 cm. of connecting tube showed any signs of perceptible warmth, the amount of heat reaching the calorimeter in this way must have been exceedingly small, in fact less than one-hundredth of the above figure and therefore less than any actual value of calorimeter sensitivity. In the experiments on surface effects, in Part II, temperatures were somewhat higher for the very intense discharges, so that some mechanical heat transfer may have occurred; if accurate readings at high current intensities are needed, water-cooling of the connecting tube, and possibly of the discharge tube, would prevent disturbance from this cause. The point was further checked roughly by replacing the hydrogen by dry argon, at a pressure of 0·55 mm. With an argon flow of 96 c.c./min. at N.T.P., there was no detectable heat registered by the calorimeter (sensitivity 0·3 cal./min.), even when the discharge current was as high as 850 mA, the energy consumption in the positive column being about 300 W. The maximum current and positive column power used in the experiments on wall effects with hydrogen were 630 mA and 300 W, while in the accurate measurements of Part III the corresponding maxima were about 100 mA and 80 W. Therefore it is clear that the calorimeter reading, corrected for conduction loss, accurately corresponds to the number of hydrogen atoms received.

RAPIDITY OF RESPONSE

In order to illustrate the rapidity of response of the instrument, the following experiment was carried out with the discharge tube *P* IV described in Part II. Calorimeter readings were made at intervals of 20 sec. from the commencement of the discharge. The conditions were adjusted for a rather rapid production of atomic hydrogen. The rate of flow of water was 22 c.c./min., the corresponding sensitivity being 0·4 cal./min. Fig. 2 shows that even after the first 20 sec. the calorimeter registered a figure only 4 % below the final value, which was reached within 40 sec. Experience has shown that the steady value attained in this short time is maintained within ½ % for long periods of time with a suitably poisoned discharge tube and in the absence of fluctuations in the supply of electric current.

The conditions in which the above result was obtained are worthy of note. A rapid flow of hydrogen was used, 334 c.c./min. at N.T.P., or 0·90 g.-mol./hr., the pressure in the discharge tube and calorimeter being 0·85 mm. The atom output corresponded to 0·15 g.-atom of hydrogen/hr., the discharge current being only 42 mA. Conclusive evidence will be produced in Part III showing that the condition for high efficiency and easy control in the production of large amounts of atomic hydrogen is the use of a large excess of molecular hydrogen, at a suitable pressure so that the degree of dissociation is relatively small.

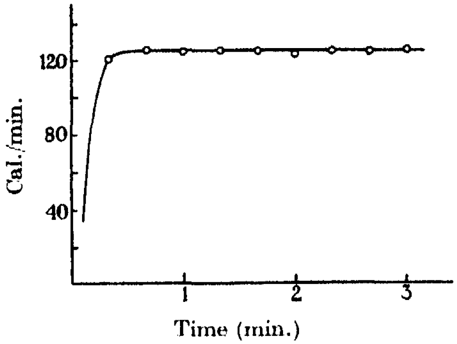

FIG. 2

THE DISSOCIATION ENERGY OF HYDROGEN

In order to convert the calorimeter measurements into values of the atom output, a knowledge of the dissociation energy of the hydrogen molecule is required. This quantity has been determined by a wide variety of methods, and because of its importance a summary seems desirable.

Approximate determinations were made by Langmuir (1926; and a number of papers between 1912 and 1926), Isnardi (1915), Wohl (1924), Bodenstein and Jung (1926), and Bichowsky and Copeland (1928) by consideration of various thermal data; and by Franck (1921) and Olsen and Glockler (1923) using the electron bombardment method. More accurate evaluation has been carried out by Lozier (1933) by electron bombardment; by Witmer (1926), Dieke and Hopfield (1927), Dieke and Blue (1935) and Beutler (1935) from the ultra-violet absorption and rotational-vibrational band spectra of hydrogen; and by Richardson and Davidson (1929) and Richardson (Pauling and Wilson 1935, p. 353) by consideration of spectroscopically determined ionization potentials. Finally, a number of quantum-mechanical calculations have been made, culminating in that of James and Coolidge (1935); these are reviewed by Pauling and Wilson (1935).

Undoubtedly the most accurate experimental determination is that of Beutler, viz. 4·4554 ± 0·0009 e-volt/molecule or 102,720 ± 20 cal./g.-mol. for the lowest state of para-hydrogen; in good agreement with this figure are the values of Lozier, 4·43 ± 0·03; Richardson, 4·448 ± 0·005; and James and Coolidge, 4·454 ± 0·013 e-volt/molecule.

*Measurement of Hydrogen Atoms by Molecular Flow Gauges.**

Bichowsky and Copeland's determination of the dissociation energy is the only direct measurement of the heat produced by recombination of a measured number of atoms, and the discussion of their method raises a question of general importance in relation to previous work on the measurement of atomic hydrogen. The method consisted in letting partly dissociated hydrogen effuse through a set of orifices and impinge on a platinum-coated thermometer bulb, the rate of effusion of atoms being calculated from pressure measurements by means of the theory of molecular flow. It must be pointed out, first, that the authors, by assuming the ratio of the rates of effusion of atoms and molecules to be equal to the ratio of their concentrations before effusion, lost a factor of $\sqrt{2}$, and correction of this error reduces their result of 105,000 cal./g.-mol. to 83,000 cal./g.-mol.; and, second, that they seem not to have appreciated the limitations of the McLeod gauge, a 1 % uncertainty in the reading of which would have caused a 15 % uncertainty in the dissociation energy. The main point, however, is that Knudsen (1909) has proved that molecular flow occurs only if the diameter of the effusion (or diffusion) orifice is less than one-tenth of the molecular mean free path, whereas Bichowsky and Copeland's orifices were much larger than this limit.

The importance of Knudsen's experimental criterion for molecular flow appears to have been overlooked in work on atomic hydrogen. The atom gauges of Wrede (1929) and of Harteck (1928), which depend on molecular flow, have been used by a number of workers, but no adequate evidence has been produced that the molecular flow condition has been satisfied. In some cases the dimensions of the orifice are not stated, reference merely being made to a "Wrede gauge"; in all other cases, including Wrede's own paper, the diameter of the equivalent circular orifice is greater than one-tenth of the molecular mean free path. It seems, therefore, that there is no certain recorded example of the use of a Wrede or Harteck gauge under the correct conditions, and in consequence some uncertainty attaches to all of the concentration measurements so far obtained.

Moreover, although these gauges have been used as "absolute" gauges, e.g. by Steiner and Wicke (1931) for calibration in their spectroscopic method of measuring atom concentrations, the serious effect of small errors in the measurement of pressure, referred to above, has not been generally appreciated. The percentage, A, of atoms in the mixture of atoms and molecules is given, according to molecular flow theory, by the equation $A = 341\,[1-(p/p_1)]$ for both effusion and diffusion gauges, p_1 and p being the measured pressures corresponding to equal mass rates of flow of partially dissociated gas and undissociated gas respectively. It is easily shown that the uncertainty, y %, in A caused by an uncertainty of x % in the values of p and p_1 is given by $y/x = 2(341-A)/A$. The possible percentage error in A is therefore much larger than that in the measurement of pressure: the values of the ratio y/x for various values of A are as follows:

---

* The author is indebted to Dr. B. S. V. R. Rao for the material of this section.

A	7	10	15	30	60	100
y/x	100	66	44	21	9	5

Translational, Rotational and Vibrational Energy.

The above values of the dissociation energy, D, refer to the lowest state of the hydrogen molecule, viz. para-hydrogen without translational or rotational energy and with only zero-point energy of vibration. In "equilibrium hydrogen" at 300° K., vibrational energy is practically limited to the zero-point level, but the rotational energy E_R amounts to 540 cal./g.-mol. The fission of a molecule into two atoms involves the production of an additional $3RT/2$ of translational energy per g.-mol., and, under the constant-pressure conditions of calorimetric experiments, the performance of external work equal to RT. The heat of dissociation at constant pressure is, therefore, $Q = D - E_R + 5RT/2$, and adopting Beutler's value for D this amounts at 300° K. to $102{,}720 - 540 + 1500 = 103{,}680$ cal./g.-mol. This is the value which has been adopted throughout the present experiments in which recombination has occurred always within about 10° of 300° K.

SUMMARY

A new type of calorimeter for the measurement of hydrogen atoms is described, depending on the continuous-flow principle. Considerable accuracy is possible, and the sensitivity of the calorimeter is easily varied as required; sensitivities of 0·1–1·0 cal./min. have been used, the range of rates of heat production so far studied being 4–300 cal./min. Continuous operation and reading over indefinite periods of time are possible, very small corrections due to losses are required, and the lag in attaining equilibrium after large changes in the rate of supply of atomic hydrogen is of the order of 1–2 min.

The spectroscopic value of Beutler for the dissociation energy of hydrogen is adopted; after allowance for the heat capacities of the molecules and atoms, this leads to 103,680 cal./g.-mol. for the heat of dissociation at 300° K. and constant pressure.

The determination of hydrogen atoms by molecular flow gauges is discussed, and sources of error which have hitherto been overlooked are pointed out.

REFERENCES

Amdur and Robinson 1933 *J. Amer. Chem. Soc.* **55**, 1395.
Beutler 1935 *Z. phys. Chem.* B, **29**, 315.
Bichowsky and Copeland 1928 *J. Amer. Chem. Soc.* **50**, 1315.
Bodenstein and Jung 1926 *Z. phys. Chem.* A, **121**, 127.
Bonhoeffer 1924 *Z. phys. Chem.* A, **113**, 199.
Dieke and Blue 1935 *Phys. Rev.* **47**, 261.
Dieke and Hopfield 1927 *Z. Phys.* **40**, 299.
Dixon 1932 *J. Amer. Chem. Soc.* **54**, 4262.
Franck 1921 *Phys. Z.* **22**, 467.
Harteck 1928 *Z. phys. Chem.* A, **139**, 98.
Isnardi 1915 *Z. Elektrochem.* **21**, 405.
James and Coolidge 1935 *J. Chem. Phys.* **3**, 129.
Knudsen 1909 *Ann. Phys., Lpz.*, **28**, 75.
Langmuir 1926 *Gen. Elect. Rev.* **29**, 153.
Lozier 1933 *Phys. Rev.* **44**, 575.
Olsen and Glockler 1923 *Proc. Nat. Acad. Sci., Wash.*, **9**, 122.
Pauling and Wilson 1935 "Introduction to Quantum Mechanics." McGraw-Hill.
Richardson and Davidson 1929 *Proc. Roy. Soc.* A, **123**, 466.
Senftleben and Riechemeier 1930 *Ann. Phys., Lpz.*, **6**, 105.
Smallwood 1929 *J. Amer. Chem. Soc.* **51**, 1985.
Steiner 1935 *Trans. Faraday Soc.* **31**, 623.
Steiner and Wicke 1931 *Z. phys. Chem.*, Bodenstein Festb., p. 821.
v. Wartenberg and Schultze 1930 *Z. phys. Chem.* B, **6**, 261.
Witmer 1926 *Proc. Nat. Acad. Sci., Wash.*, **12**, 238.
— 1926 *Phys. Rev.* **28**, 1223.
Wohl 1924 *Z. Elektrochem.* **30**, 49.
Wood 1920 *Proc. Roy. Soc.* A, **97**, 455.
— 1921 *Phil. Mag.* **42**, 729.
— 1922 *a* *Phil. Mag.* **44**, 538.
— 1922 *b* *Proc. Roy. Soc.* A, **102**, 1.
Wrede 1929 *Z. Phys.* **54**, 53.

Atomic Hydrogen
II—Surface Effects in the Discharge Tube

By H. G. Poole

University College, London

(*Communicated by C. K. Ingold, F.R.S.—Received* 6 *July* 1937)

In the production of atomic hydrogen by means of the glow discharge, Wood (1921) found that a long discharge tube, e.g. 2 m., was desirable, and that a trace of water vapour (or oxygen) in the hydrogen was necessary in order to obtain appreciable yields. Langmuir (Wood 1922) suggested that the effect of water vapour was to form on the walls of the tube a film very much less active than the glass surface as a catalyst for the recombination reaction $H + H \rightarrow H_2$. Wood also suggested that the beneficial effect of using a long tube was due to the removal of the catalytically active electrodes to a considerable distance from the point of emergence of the gas (usually near the middle of the tube).

Bonhoeffer (1925) recommended a long preliminary discharge to "burn out" active areas of the glass surface. Wrede (1929) found that preliminary cleaning of the tube with chromic acid and hydrofluoric acid was desirable. v. Wartenberg and Schultze (1930) showed that a coating of meta-phosphoric acid inside the discharge tube, if used in conjunction with moist hydrogen, resulted in a great improvement in yield, presumably owing to the hygroscopic character of the acid. The latter workers also studied quantitatively the effect of increasing the amount of added water vapour, and showed that the atom output for a constant current rose rapidly from a very low value until about 2 % of water vapour had been added, after which the yield was practically constant. It has been customary, therefore, to introduce about 2·5 % of water vapour, and this is very easily done by bubbling the hydrogen through water at atmospheric temperature and pressure.

The present study of surface effects arose from the following observations. In preliminary attempts to calibrate the discharge system as a source of hydrogen atoms, boiling of the phosphoric acid coating of the discharge tube was found to occur at very high current intensity (about 800–1000 mA). As a result, inactivation of the platinum catalyst of the calorimeter (an earlier design than that described in the preceding paper) was observed, as evidenced by the glowing of a tungsten wire beyond the calorimeter. On the other hand, if the discharge tube was not coated with phosphoric acid, irreproducibility of the results occurred, even after quite short intervals. It therefore appeared necessary to study the variability of output when coated and uncoated tubes were used.

For the investigation of the effect of the condition of the wall surface on the atom output, several discharge tubes have been used, both of glass and silica, with the calorimeter described in Part I. The following experiments relate to a silica discharge tube *S* II and a pyrex tube *P* IV, the behaviour of the other tubes used being similar.

The tube *S* II was nearly 1 m. long, and of diameter 20 mm.; *P* IV consisted of a tube 25 mm. in diameter, 53·5 cm. in length, to which were attached two large electrode chambers of diameter 4·4 cm. and length 23 cm. The electrodes in both cases were of 19 mm. electron metal rod, drilled out to permit of water cooling, and cemented with Apiezon wax directly into the ends of the silica tube, and into closely fitting glass sleeves in the case of the pyrex tube. The wax seals were thus protected from attack by atomic hydrogen. The effective area of the electrodes in the silica tube was merely their cross-section, about 2·8 cm.^{2}; in the pyrex tube it was about 75 cm.^{2}.

The tube *P* IV, together with the remainder of the gas train, is illustrated in fig. 1 of the following paper (p. 427), the only difference being that for the present work the hydrogen was admitted to the discharge tube close to one electrode only. Cylinder hydrogen was used; oxygen was removed by contact with a hot platinum wire, followed by drying. The gas passed through a capillary flowmeter, and was then saturated at room temperature and pressure with water vapour before admission through a needle valve, *N* in the figure, to the low-pressure system. Leaving the discharge tube at its centre, the hydrogen passed through the calorimeter to a rotary oil pump, which had a speed of 7 l./sec.; the importance of using high pumping speeds will be apparent in the next paper.

The discharge tube exit was connected to the calorimeter by a loosely fitting plug joint *A*, cemented with meta-phosphoric acid. This has proved a completely satisfactory vacuum-tight cement, and a junction so made will last several months at least, if protected from atmospheric moisture by means of insulation tape. Such a plug joint can be rapidly connected or dismantled, without the danger of breakage as when a large ground joint is used in this position.

For the present experiments the discharge was produced by an alternating current from a 2 kVA transformer giving up to 5000 V, the electrode voltage being of the order of 1400–2000 V; the discharge current was measured by a thermal milliammeter. For the acid-coated discharge tube, a 5000 V direct current generator was also used.

EXPERIMENTS WITH UNCOATED AND COATED DISCHARGE TUBES

Using the continuous-flow calorimeter with the above apparatus, it is possible to follow quite rapid changes in the atom output of the discharge. It has now been shown that the introduction of water vapour with the hydrogen supplied to the discharge is not sufficient to maintain in a non-catalytic condition the glass or silica walls of the tube (previously cleaned with chromic acid and hydrofluoric acid after the directions of Wrede).

a—Uncoated Silica Tubes—The curves of fig. 1 obtained with the tube *S* II illustrate this. The atomic hydrogen output, measured in calories per minute, is plotted against the time after switching on the current. Calorimeter and

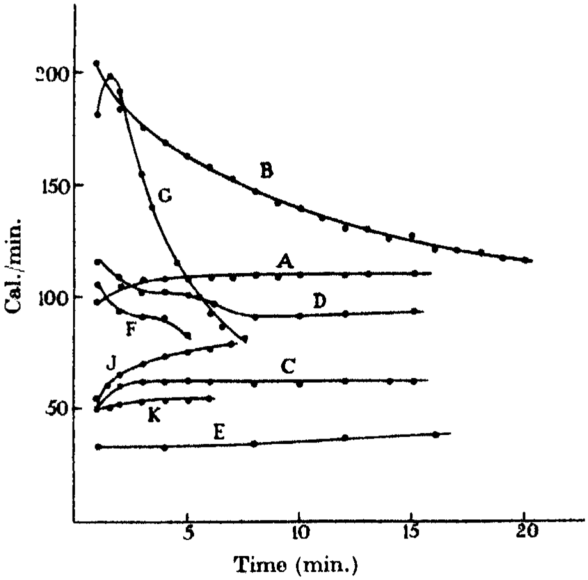

FIG. 1—Output of uncoated silica tube.

Tube History

$p = 0{\cdot}58$ mm.; H_2 flow = 43 c.c./min. at N.T.P.

A, 136 mA (followed by 5 min. rest). *B*, 600 mA (followed by ½ min. rest).
C, 139 mA (followed by ½ min. rest). *D*, 600 mA (followed by 1 min. rest).
E, 80 mA (followed by 2 min. rest). *F*, 600 mA (followed by 25 min. rest).
G, 631–600 mA (followed by 8 min. rest).
J, 75 mA (followed by 1 min. at 600 mA; 40 sec. rest). *K*, 75 mA.

milliammeter readings were made at one minute, or occasionally half-minute, intervals. The tube history is given under the figure; alternate high and low intensity runs were made, separated by short intervals without discharge. It will be seen that a high current run, e.g. *B*, *G*, produces an initially high output, very rapidly decaying to much lower values. It seems most probable that this is due to rapid heating of the tube surface, causing partial stripping of the protective water film; more rapid recombination catalysed by the stripped silica surface then ensues. This suggestion is borne out by the marked difference in efficiency between two low intensity runs, e.g., *A*, *C*, separated by a high intensity run, *B*. This difference occurs even if the high intensity run is of very short duration, as for instance between *J* and *K* at 75 mA, separated by a 1 min. run at 600 mA.

The stripping of water from the walls may be very slight or negligible for lower currents, where the heating of the walls is less intense, as in *A* at 136 mA.* This current seems to be just sufficient to prevent adsorption of water without causing further stripping, for in *C*, with almost the same current, we have a similar constancy of yield, although the actual yield is much lower than in *A* owing to the stripping effect of the intervening run *B* at 600 mA. This is confirmed by the fact that the curve *D*, at 600 mA, obtained after the "stationary" run *C* of 15 min. at 139 mA, appears to be merely an extension of curve *B*, also at 600 mA, just as though run *C* had not intervened.

At still lower currents partial recovery of the previously stripped walls may occur during the run; evidently water adsorption may continue during a run of sufficiently low intensity. Curves *E*, *J*, and *K* show this, though the recovery during *J* (after the rest period of 8 min.) is more rapid than during *K* (immediately following the high intensity run of 1 min. at 600 mA).

Recovery is considerable during rest periods, the stream of moist hydrogen being continued at the same pressure. The effect of the 25 min. rest period between *F* and *G*, at 600 and 631 mA respectively, has been almost complete recovery of the tube for the commencement of *G*, but the decay is now very much more rapid than in the first run, *B*, at this intensity. Apparently the adsorbed water is anti-catalytic whether it has been recently adsorbed or not, but in the former case it appears to be much more loosely held by the wall than in the latter.

The magnitude of the decay in efficiency is large, e.g. from 105 to 60 cal./min. in 20 min. in run *B*, and from 100 to 41 cal./min. in 7 min. in run *G*. A striking feature of the curves is that in *G* at 600 mA the yield after 7 min.

---

* Wrede obtained reproducible results with a discharge tube of diameter 2·5 cm. provided that the current was never allowed to exceed 150 mA.

(still falling rapidly) is the same as the yield after 7 min. (still increasing) in *J* at 75 mA. It must be borne in mind that the effect of the small calorimeter lag (preceding paper) is to reduce the apparent height of the initial portions of the higher curves, and to increase (slightly) their height when the temperature is falling, so that the real decay is greater than appears.

This series of curves was continued after two days' rest, the tube being filled with air during this period. The new curves (not shown in the figure) exhibit the same characteristics as the old. In the resting time some recovery had occurred, presumably due to atmospheric moisture, so that the previous curve *K* at 75 mA, with a yield of about 27 cal./min., had given place to a slowly rising curve at 76 mA, with a yield of about 40 cal./min. This recovery had the non-permanent character already noted, however; new high intensity runs gave high initial yields, e.g. 112 cal./min. at 560 mA, but the decay was even more rapid than in the cases already quoted. In one of the new runs at 560 mA, the decay in 9 min. was from 93 to 27 cal./min. (70 % loss of efficiency), the latter value being below the 40 cal./min. obtained at 76 mA both in the last run *J* of the previous series and in the first run after the tube's 2-day rest.

b—Uncoated Pyrex Tubes—Essentially similar series of curves were obtained with two different pyrex tubes, the high intensity curves for tube *P* IV being shown in fig. 2. (The low intensity curves exhibited exactly the same type of difference as those in fig. 1.) In comparison with the curves for the silica tubes, the following points may be noted: (*a*) the somewhat slower decay for the *first* high intensity run *B* (the current being only 470 mA in this case, however, instead of 600 mA as for the silica tube); this possibly indicates firmer attachment of water molecules on pyrex than on silica; (*b*) the even more rapid decay for subsequent high intensity runs, e.g. *H* and *L*; which appears to indicate looser attachment of the *newly adsorbed* water on pyrex than on silica; (*c*) the slower recovery of the walls on resting; the pyrex curve *H* (fig. 2), after 30 min. rest, shows less marked recovery than the silica curve *G* (fig. 1) after 25 min. rest; and hardly any recovery occurs between *H* and *J* (fig. 2), despite the fact that in the 17 min. rest the pump was stopped and the moist hydrogen allowed to reach atmospheric pressure inside the tube.

Curve *D* (fig. 2) is interesting; it appears to indicate that the initial rapid loss of the newly adsorbed water is followed (after 8 min.) by the slower loss of the residual water of the old surface, the latter loss corresponding to a continuation of curve *B* after the intervening 25 min. "stationary" run *C* at 120 mA. (Curves *B* and *D* are not quite comparable, however, since *B* was at 470 and *D* at 600–628 mA.) The rapidity of the decay in *K*, after the tube had been filled with air for 18 hr., and in *L* after a further 2 hr. with moist hydrogen flowing, shows that, as in the case of the silica tube, the past history of the tube still affects its behaviour after a long period.

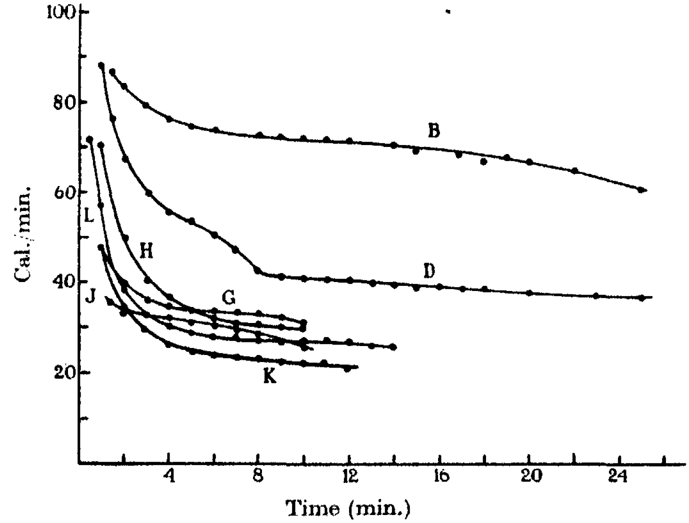

FIG. 2—Output of uncoated pyrex tube.

Tube History

$p = 0{\cdot}46$ mm.; H_2 flow = 43 c.c./min. at N.T.P.

A,* 125–120 mA for 25 min. (followed by 1 min. rest).
B, 470 mA for 25 min. (followed by 1 min. rest).
C,* 124–120 mA for 25 min. (followed by 1 min. rest).
D, 600–630 mA for 25 min. (followed by 1 min. rest).
E,* 125 mA for 30 min. (followed by 1 min. at 660 mA; ½ min. rest).
F,* 124 mA for 10 min. (followed by 1 min. rest).
G, 520 mA for 10 min. (followed by 30 min. rest).
H, 520–536 mA for 10 min. (followed by 17 min. rest; gas allowed to reach atmos. pressure).
J, 560–540 mA for 10 min. (followed by 18 hr. rest; filled with air at atmos. pressure).
K, 550–540 mA for 12 min. (followed by 2 hr. rest; with hydrogen flowing at low pressure).
L, 530 mA for 14 min.

* Not shown.

As an indication of the presence of hydrogen atoms, the glowing of a tungsten wire, due to the surface catalysis of atom recombination, has sometimes been used. Wood remarked that the catalyst appeared to become fatigued after a short period of incandescence, the observed effect being a reduction of its temperature, but that recovery occurred on resting with no discharge passing; these phenomena were observed early in the present experiments also. In view of the curves of figs. 1 and 2, this apparent fatiguing of the catalyst seems to be attributable to the decay of the efficiency of the discharge tube rather than to actual fatigue of the catalyst.

c—Coated Pyrex Tube—The same tube *P* IV was now coated internally with meta-phosphoric acid by melting the acid on the surface. A series of curves was again obtained for runs at low and high intensities. These exhibited none of the behaviour previously described; instead, both high and low intensity curves showed small but appreciable increases with time, with one exception—a low-intensity curve which decreased slightly with time. In explanation of this, the 1-min. readings of the discharge current showed drifts corresponding fairly closely with those of the atom output: control of the alternating current used so far had been difficult, though the fluctuations of current were not in the least comparable with the changes in atom output shown in figs. 1 and 2. The transformer was now replaced by a high tension direct current generator, and, since the current so obtained proved much easier to control, a further series of measurements was made with direct current in order to detect output variations with the coated discharge tube. The corresponding curves (*B*–*J*), with the tube history indicated, are shown in fig. 3, in which a typical curve, *A*, for alternating current is included in order to illustrate the drift referred to. There were still some slight fluctuations of the direct current, but corrections to constant current have been made by assuming that the output is proportional to the current for variations of the order of a few units per cent; this approximation is justified for the present purpose by the results given in Part III. (It was not practicable to use direct current discharges greater than about 250 mA, owing to the occurrence of stray discharges to the calorimeter.) It will be seen that remarkable constancy of output has been attained, together with a high degree of reproducibility, i.e. independence of past history. The 1–4 % discrepancy between *D* and *B*, both at 54 mA but separated by the high intensity run *C* at 214 mA, the 2½ % difference between the curves *E* and *H*, and the small separation of curves *F*, *G* and *J*, are hardly significant in view of the errors of reading the calorimeter and of setting the pressure and rate of flow of hydrogen, all of the order of 1 %.

Further evidence of the reliability of an acid-coated discharge tube is provided by the curves connecting efficiency of atom production with electrical input (Part III); these were found to be reproducible after an interval of two months, and also after stripping and renewal of the meta-phosphoric acid coating.

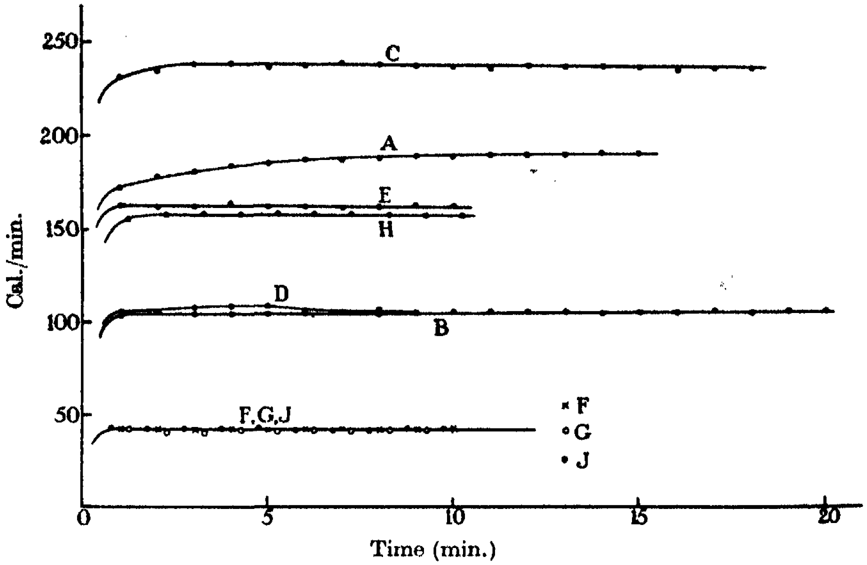

Fig. 3—Output of coated pyrex tube.

Tube History

(A.C.); $p = 0{\cdot}50$ mm.; H_2 flow = 63 c.c./min. at N.T.P.
A, 460–490 mA; sensitivity, 0·3 cal./min.
(D.C.); $p = 0{\cdot}465$ mm.; H_2 flow = 140 c.c./min. at N.T.P.
B, 54 mA (followed by 2 min. rest); sensitivity, 1·0 cal./min.
C, 214 mA (followed by 25 min. rest); sensitivity 1·0 cal./min.
D, 54 mA (followed by 11 min. rest); sensitivity 1·0 cal./min.
E, 112 mA (followed by 6 min. rest); sensitivity 1·0 cal./min.
F, 19 mA (followed by 22 hr. rest); sensitivity 0·4 cal./min.
G, 19 mA (followed by no rest); sensitivity 0·4 cal./min.
H, 112 mA (followed by 1 min. rest); sensitivity 0·4 cal./min.
J, 19 mA; sensitivity 0·4 cal./min.

Conclusion

It is evident from the above that a discharge tube depending solely on a water-on-glass or water-on-silica film for the poisoning of its walls is exceedingly unreliable as a source of atomic hydrogen, since its behaviour not only is not constant even during a single run, but also may reflect its past history for a long period probably extending over several days. Wrede's preliminary treatment of the tube with hydrofluoric acid undoubtedly helps to remove catalytically active patches of foreign substances, but the instability of the resultant water film is not thereby affected. The effect of using a long preliminary discharge as suggested by Bonhoeffer's experiments (p. 415) is now seen to be merely to approach the final flat regions to which the curves of figs. 1 and 2 are tending, although unduly catalytic areas are probably destroyed in the process. But although a sufficiently protracted preliminary run may result in some approach to constancy during a particular discharge, the actual level of output will clearly not be reproducible after a period of rest, or after other runs at different intensities.

On the other hand, it is clear that an acid-coated discharge tube exhibits constant and reproducible behaviour as a source of atomic hydrogen; and the theoretical consideration of the results of Part III will provide strong reason for believing that the walls remain in the same condition for different discharge intensities.

SUMMARY

The output of atomic hydrogen from several different discharge tubes has been measured calorimetrically at 1-min. intervals. Curves were obtained showing that very large changes of atom output with time, even in a few minutes, may occur with discharge tubes depending only on a water-on-glass or water-on-silica film for deactivation of the tube wall as catalyst for the recombination of atoms, and that the behaviour of such tubes depends on their past history. Constant and reproducible output is obtained by the use of a meta-phosphoric acid lining inside the discharge tube.

REFERENCES

Bonhoeffer 1925 *Z. phys. Chem.* A, **116**, 391.
v. Wartenberg and Schultze 1930 *Z. phys. Chem.* B, **6**, 261.
Wood 1921 *Phil. Mag.* **42**, 729.
Wood 1922 *Phil. Mag.* **44**, 541.
Wrede 1929 *Z. Phys.* **54**, 53.

Atomic Hydrogen
III—The Energy Efficiency of Atom Production in a Glow Discharge

By H. G. Poole

University College, London

(*Communicated by C. K. Ingold, F.R.S.—Received* 6 *July* 1937)

A—Introduction

There seems to have been a tendency amongst workers on the use of the glow discharge as a source of atomic hydrogen to regard the current or power as determining the degree of dissociation of the gas, i.e. the equilibrium $H_2 \rightleftarrows 2H$. It is clear, however, that the discharge itself determines only the rate of production of atoms, whereas the degree of dissociation depends also on the rate of removal of atoms by pumping and by recombination processes which are independent of the discharge. The two homogeneous recombination processes are those resulting from three-body collisions between three atoms and between two atoms and a molecule; in addition, there is a heterogeneously catalysed reaction in which the walls of the tube act as the energy acceptor.

Attempts to connect electrical conditions with degree of dissociation have been made by Crew and Hulburt (1927) and by Wrede (1929), but the above remarks show that only empirical relationships can be hoped for. In Crew and Hulburt's experiments, the degree of dissociation was estimated by measuring the change of pressure in a closed system on passing a discharge. A correction for temperature was applied, which was based on the erroneous idea that the rise of temperature due to discharge in helium is about the same as that in hydrogen at the same pressure and power input. The method of determining the pressure depended on an empirical relation between pressure and the length of the cathode dark space in an auxiliary discharge connected to the main system; but since the cathode dark space has not a sharply defined boundary, and the degree of dissociation is calculated from the difference of two pressures measured in this way, considerable error is possible. Furthermore, in a closed system, the rate of production of atoms is equal to the rate of recombination; and since these workers relied on a water-on-glass film to inhibit heterogeneous recombination, and as the power input was 200–1000 W, the catalytic activity of the walls must have been very variable and large (Part II). Crew and Hulburt's curves connecting degree of dissociation with pressure and power input cannot, therefore, be credited with quantitative significance.

In Wrede's experiments also a nearly closed system was used, the only flow of gas being that through the slit of a molecular-flow gauge. Again the rate of atom production is practically equal to the recombination rate, but the protective water-on-glass film was apparently stable under the milder conditions of these experiments; in the pressure range 0·125–0·175 mm. reproducible results were obtained in a tube of diameter 2·5 cm. for currents up to 150 mA. Nevertheless, the use of diffusion and effusion slits of width 0·02 mm. and length 3–4 mm. for the measurement of atom concentrations at the pressures named is open to the criticism (Part I, p. 412) that the orifice is far too large to satisfy the conditions for molecular flow. Considerable systematic error is thus probable, and it would appear that from Wrede's experiments also only qualitative conclusions can be drawn about the connexion between electrical input and atom production.

Practically all the atoms, which are produced by dissociation on electron impact, originate in the positive column, since this is the only region of the discharge in which electrons of the requisite energy are present in appreciable number. Therefore we should measure the energy supply, not to the whole tube, but to the positive column in order to obtain any useful relation between power input and atom output. This precaution (not observed, e.g. in Crew and Hulburt's work) is the more necessary because the discharges which are used for the production of atomic hydrogen are always of the so-called "abnormal" type, for which large and variable cathode potential falls occur: it follows that no simple relationship between the total power and the power supplied to the positive column can be assumed.

The widespread use of alternating current discharges has introduced further difficulties connected with the cathode fall. As the potential drop in the positive column is probably almost constant throughout that part of each half-cycle in which the discharge is passing, the current must be far from sinusoidal; and likewise the cathode fall and electrode voltage must have a quite complicated wave-form. It is, therefore, difficult to know what possible significance to attach to any measurements of potential which have been, or might have been, carried out; as, indeed, the present author found during some preliminary work with alternating current.

B—Experimental

In the work now to be described, a relation has been sought between *the number of atoms produced per second and the electrical energy supplied per second to the positive column.*

Apparatus—The gas system used is shown in fig. 1. As in the work described in Part II, cylinder hydrogen freed from oxygen was used; after being passed through the capillary flowmeter, F, it was saturated at room temperature and pressure with water vapour before being introduced through a needle valve, N, into the vacuum system. The flowmeter was carefully calibrated, alternative ranges being provided by means of two capillaries, both of which were immersed in a mixture of ice and water. Fluctuation of the manometer level was avoided by lowering the level of the water in the safety valve, V, so that the excess hydrogen escaped to the atmosphere without bubbling. With these two precautions, accurately reproducible flow rates, from 5–640 c.c./min. at N.T.P., could be measured on the 35 cm. manometer scale; the calibration curves were practically linear. The discharge tube employed was the tube P IV coated with melted phosphoric acid (Part II, p. 416), the only special feature of the present arrangement being the division of the hydrogen stream into two parts, one entering the discharge tube close to each electrode. The arrangement commonly used is that in which entry occurs near one electrode only; between the other electrode and the point of exit near the centre of the discharge tube there is thus a "dead-end" from which hydrogen atoms can emerge only by diffusion. Even approximate mathematical treatment of this system is out of the question, and so the simpler system with two inlets was adopted in order to ensure a flow of hydrogen throughout the region in which atoms are produced. A first set of results was obtained with a single inlet, however, and these will be referred to later. The atom output was measured by means of the continuous-flow calorimeter coated as before with melted phosphoric acid (Part I, p. 405).

In order to obtain unambiguous electrical measurements, the discharge was operated from the 5000 volt D.C. generator (Part II); and it was controlled by means of a rheostat in the field circuit, a stabilizing resistance of 60,000, 30,000, or occasionally 2000 ohms being included in series with the discharge tube. The current was measured by means of a shunted 0–50 mA moving-coil meter, and the electrode voltage by means of an electrostatic voltmeter. The potential drop along the positive column was estimated by subtracting from the electrode voltage the appropriate value of the cathode fall, obtained as indicated in the next section. The power consumption in the positive column was then determined as the product of the current and the potential fall along the column. The positive column extended from the anode, through the anode chamber and main discharge tube to the lower end of the cathode chamber, occasionally expanding a few centimetres into the latter. From the observed length of the column and the potential drop along it, the average field strength in the column was calculated.

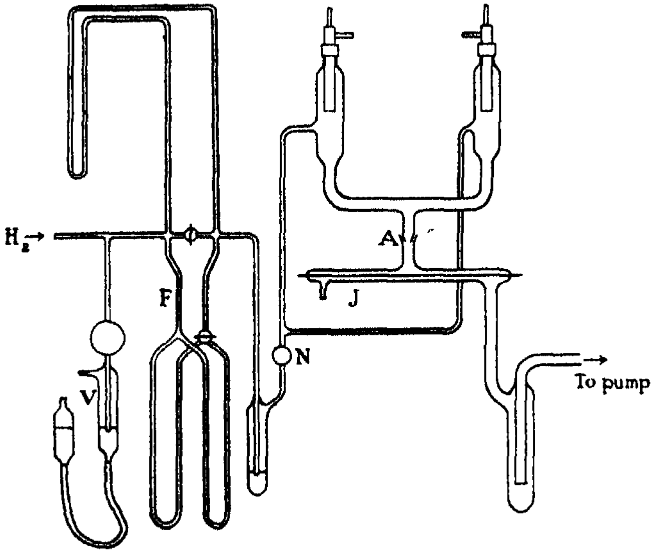

FIG. 1

As it was discovered that the output efficiency of the tube depended on the rate of flow of hydrogen, a device was adopted for varying the flow rate while maintaining constant the pressure in the discharge; this consisted of a variable leak (a second needle valve) fitted close to the pump. By this means air could be admitted about 1 m. beyond the calorimeter so that the effective pumping speed for hydrogen could be varied widely. (Calculation (Hertz 1923) shows that diffusion of air to the calorimeter against the hydrogen stream is quite negligible.) A large range of flow rates of hydrogen could be thus obtained at each pressure. The pressure was measured by a McLeod gauge attached at *J* (fig. 1). The use of wide-bore (25 mm.) tubing throughout has rendered it possible to neglect the pressure drop between the electrodes and the calorimeter, due to the gas flow; direct determination of this drop has shown that, even at the highest streaming velocities, about 14 m./sec., for any pressure between 0·40 and 1·4 mm., the total drop is less than 1 % of the initial pressure, with or without the passage of a discharge.

The Cathode Fall—In the "abnormal" discharge the cathode fall increases with the current, and is also dependent on the pressure. If there is only a small clearance between the cathode and the surrounding discharge tube, then at some pressures the effective area of the cathode becomes limited to the area of cross-section of the tube in front of the cathode, with consequent very rapid increase of the cathode fall with increasing current, and therefore large waste of power. For the pressure range in which the glow discharge is useful as a source of hydrogen atoms, the dimensions of the cathode chamber of the tube *P* IV appear to be about the minimum desirable with the cathode dimensions specified; for pressures below about 0·4 mm. a larger cathode chamber would be better. A large anode chamber is not essential, although when alternating current is used, both chambers should be large.

The cathode fall was determined in a separate series of experiments for a wide range of conditions, by connecting the electrostatic voltmeter between the cathode and a small probe electrode of fine tungsten wire inserted in the Faraday dark space. Several values of the current between 0 and 100 mA were used, at each of several pressures between 0·18 and 1·95 mm.; interpolation enabled curves to be drawn from which the cathode fall for any given conditions could be found. The use of a probe electrode in this manner is open to criticism, since it can be shown that, with zero current through the probe, its potential cannot be the same as that of the surrounding discharge. In view of the length of the positive column, however, it is probable that the error thus caused in the estimation of the potential drop along the positive column is of the order of only 5–10 V in 700–1500 V. The probe electrode was removed before any atom measurements were made.

Measurements—With the above arrangements it was possible to estimate the following quantities:

H c.c./min., the volume rate of flow of hydrogen into the system, measured at N.T.P.

p mm., the pressure at the calorimeter.

$U_0 = 760\text{H}/60p$ c.c./sec., the volume rate of flow into the discharge, measured at 0° C. and pressure p.

MpU_0, the number of molecules per second entering the system. ($M = 3{\cdot}56 \times 10^{16}$ represents the number of molecules per c.c. of a gas at 0° C. and 1 mm.)

q calories per minute, the calorimeter reading, after correction for conduction loss (see Part I).

$2qN/60Q$, the number of atoms per second reaching the calorimeter. (N = Avogadro's number, Q = dissociation energy per g.-mol. of hydrogen.)

i amperes, the discharge current.

v_e volts, the potential difference between the electrodes.

v_c volts, the cathode fall.

$v_p = v_e - v_c$ volts, the potential drop along the positive column.

$W = 6{\cdot}30 \times 10^{18} iv_p$ e-volts/sec., the positive-column power consumption ($= iv_p$ watts).

X volts/cm., the average field in the positive column.

From these data we can determine the *efficiency* of the discharge system, expressed as *the number of dissociated molecules received as atoms at the calorimeter per unit of energy (electron-volt) supplied to the positive column.* This quantity will be represented by μ_c molecules per electron-volt; thus

$$\mu_c = \frac{qN}{60QW} = \frac{1}{64{\cdot}7} \cdot \frac{q}{iv_p}$$

after the substitutions $N = 6{\cdot}06 \times 10^{23}$ molecules/g.-mol. and Q = 103,680 cal./g.-mol. (Part I, p. 413).

The actual volume rate of flow into the discharge differs from U_0 by a temperature factor of about 290/273; in the next section it will be seen that the quantity U_0 has theoretical significance only as part of the expression MpU_0, which defines the number of molecules entering the system before dissociation. In consequence, the volume rate of flow measured at 0° C., U_0, is a more suitable parameter than the actual volume rate of flow.

Experimental Results—The first point to be noticed is that there may be large changes in the value of the efficiency μ_c as the current is varied, other conditions being maintained constant; in almost all circumstances μ_c decreases with increasing current. The relevant data for a specimen series at $p = 0{\cdot}75$ mm. are given in Table I. If the "reciprocal efficiency" $1/\mu_c$, i.e. *the number of electron-volts required per dissociated molecule*, is plotted as a function of the positive-column power input, W or iv_p, a straight line is obtained, which can be expressed by the equation

$$\frac{1}{\mu_c} = P + SW \tag{I}$$

in terms of the gradient S and the intercept P on the $1/\mu_c$ axis: P is the limit of the reciprocal efficiency as the power input approaches zero. If a different rate of flow of hydrogen U_0 is used, the pressure being maintained at the original value by the arrangement already described, a new series of points is obtained, lying on another straight line, for which both P and S are different from those of the first line. The family of such straight lines shown in fig. 2 represents the behaviour of the system for various values of U_0 at

TABLE I

H = 99 c.c. min.$^{-1}$ $p = 0{\cdot}75$ mm.
$U_0 = 1670$ c.c. sec.$^{-1}$ $U_0^{-1} = 6{\cdot}00 \times 10^{-4}$ sec. c.c.$^{-1}$

$10^3 i$	v_p	iv_p	X	q Obs.	 Cond. loss	 Corr.	$10^2\mu_c$	$1/\mu_c$
12·2	1020	12·4	16·5	24·1	0·6	24·7	3·08	32·5
20·0	1000	20·0	15·9	35·3	0·9	36·2	2·80	35·8
32·0	970	31·0	15·2	50·2	1·2	51·4	2·56	39·1
41·6	930	38·7	14·5	61·0	1·5	62·5	2·50	40·0
53·5	890	47·5	13·7	69·1	1·7	70·8	2·30	43·5
64·0	850	54·5	13·1	77·0	1·9	78·9	2·24	44·7
75·0	810	60·5	12·5	83·5	2·1	85·6	2·19	45·7
82·6	790	65·0	12·2	88·5	2·2	90·7	2·16	46·4
91·2	760	69·5	11·7	91·0	2·3	93·3	2·07	48·2

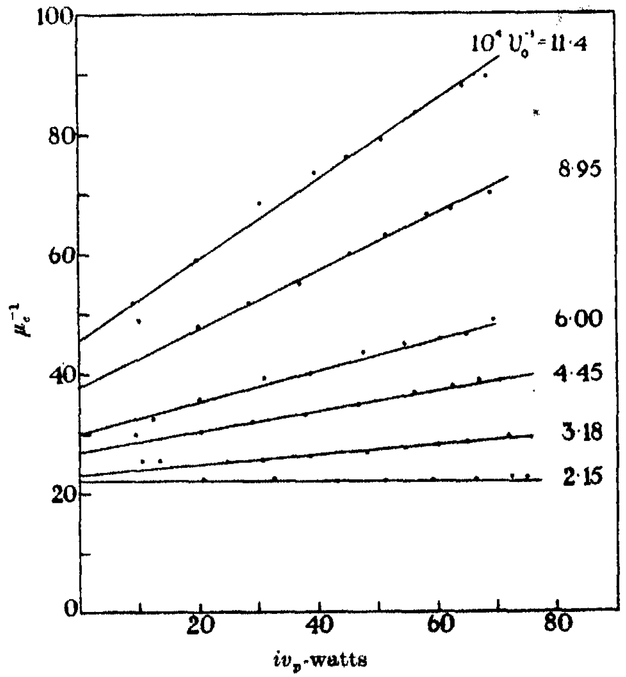

FIG. 2

the same pressure 0·75 mm. It is evident that both P and S are functions of U_0. It has been found that for any given pressure they are both linear functions of U_0^{-1}, this relation having been suggested by a preliminary theoretical investigation; these functions can be written

$$P = \frac{1}{\mu_0}\left(1 + \frac{k}{U_0}\right), \tag{IIa}$$

$$S = \frac{a}{U_0} - b, \tag{IIb}$$

and consequently
$$\frac{1}{\mu_c} = \frac{1}{\mu_0}\left(1 + \frac{k}{U_0}\right) + \left(\frac{a}{U_0} - b\right) W. \tag{III}$$

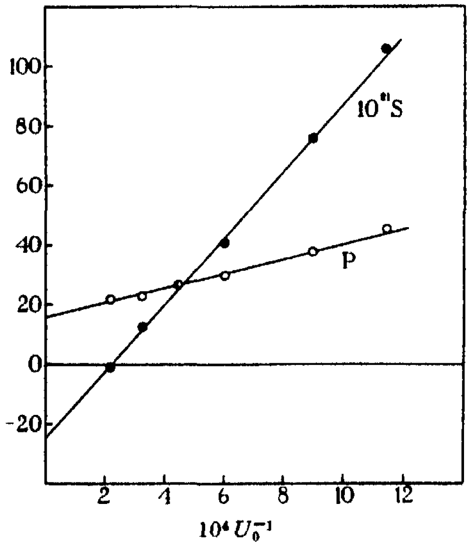

FIG. 3

In these equations $1/\mu_0$ represents the limit of $1/\mu_c$ when extrapolated both to zero power and to infinite flow rate; k, a and b are constants. The quantities μ_0, k, and S will be discussed later from the theoretical standpoint, but although a first approximate analysis led to an expression for $1/\mu_c$ differing from (III) only in the absence of the constant b, more exact treatment gave a less simple form (cf. (XIII), p. 442); the observed relation must therefore be regarded as purely empirical. The curves corresponding to equations (IIa) and (IIb) for p = 0·75 mm. are drawn in fig. 3.

Similar families of curves were obtained for each of several pressures between 0·42 and 1·35 mm.: in tracing these the reciprocal flow rate has been varied over the range $1·7 \times 10^{-4} - 14 \times 10^{-4}$ sec. c.c.$^{-1}$, whilst currents up to 100 mA have been employed. The results are collected in Tables II–VII. The values of P and S are related to U_0^{-1} for each pressure in Table VIII, and the constants μ_0^{-1}, μ_0, k, a, and b to the pressure p in Table IX; in the latter, an estimate has been made of the uncertainty in μ_0^{-1} due to the double extrapolation.

TABLE II—$p = 0·42$ mm.

$10^4U_0^{-1} = 2·60$		3·85		6·05		8·05		10·9		14·1	
iv_p	$1/\mu_c$	iv_p	$1/\mu_c$	iv_p	$1/\mu_c$	iv_p	$1/\mu_c$	iv_p	$1/\mu_c$	iv_p	$1/\mu_c$
11·9	25	10·1	31	10·4	34	10·9	42	5·8	60	12·2	65
15·2	24·4	14·0	29·0	13·5	36·5	14·1	43	8·0	57	16·4	65·5
17·8	24·6	20·8	28·8	15·9	35·5	16·9	43	10·2	57·5	20·9	66
22·5	24·8	25·5	28·3	19·1	36·2	20·5	44·5	13·1	57	27·1	72
29·4	25·0	30·2	29·2	23·6	36·2	24·6	46	17·5	58	31·9	69·5
33·4	23·0	34·8	29·2	28·5	38·2	29·4	49	20·7	58	36·2	73
39·0	23·8	39·2	29·8	32·4	38·9	34·8	50·5	24·6	61	40·0	70
42·1	23·3	42·6	29·7	37·5	39·8	41·1	55	27·1	63	44·0	73
46·4	23·8	45·6	29·7	42·1	39·8	46·9	57·5	30·5	66	45·5	72·5
49·5	23·5	48·5	29·0	45·6	40·6	49·7	58	35·0	65	—	—
—	—	—	—	48·7	40·5	52·0	56·5	40·8	69	—	—
—	—	—	—	—	—	—	—	44·5	71	—	—
—	—	—	—	—	—	—	—	48·0	73	—	—
—	—	—	—	—	—	—	—	51·5	75	—	—

TABLE III—$p = 0·62$ mm.

$10^4U_0^{-1} = 2·25$		2·90		3·85		5·95		7·65		10·0		12·4	
iv_p	$1/\mu_c$	iv_p	$1/\mu_c$	iv_p	$1/\mu_c$	iv_p	$1/\mu_c$	iv_p	$1/\mu_c$	iv_p	$1/\mu_c$	iv_p	$1/\mu_c$
9·7	22·1	9·7	23	12·4	26·5	11·6	35	14·0	44	11·3	46	13·8	64
19·2	22·0	18·9	24·2	20·0	27·2	17·2	36·5	19·4	43·5	16·5	50	20·4	69
29·3	22·2	27·8	24·5	27·0	27·6	24·4	37·8	24·9	45	23·1	53·5	28·8	71
36·6	22·2	34·0	24·9	35·5	28·0	33·0	40·9	35·4	51·5	31·8	58·5	36·8	76
45·8	22·6	43·0	25·3	43·0	29·6	40·0	42·1	40·5	53	39·0	62	42·6	78
51·0	22·9	50·5	26·4	48·5	30·4	45·7	43·2	48·0	56	44·5	64·5	50·5	84
57·0	23·1	56·0	27·1	54·0	31·5	52·0	46·0	54·0	59	51·5	68	57·0	90
64·5	23·9	62·5	27·9	59·5	31·8	59·5	48·5	60·0	60·5	58·0	72	62·5	93
70·0	24·3	66·0	28·2	64·0	32·9	63·5	49·0	65·0	62	62·0	72·5	66·5	94
78·0	26·2	—	—	68·5	32·8	68·0	50·0	68·5	63	66·0	72	—	—

TABLE IV—p = 0·75 mm.

$10^4U_0^{-1}$ = 2·15		3·18		4·45		6·00		8·95		11·4	
iv_p	$1/\mu_c$	iv_p	$1/\mu_c$	iv_p	$1/\mu_c$	iv_p	$1/\mu_c$	iv_p	$1/\mu_c$	iv_p	$1/\mu_c$
10·4	25·4	13·4	25·5	9·4	30	12·4	32·5	10·0	49	9·1	52
20·6	22·4	24·7	25·2	20·2	30·5	20·0	35·8	20·0	48	19·8	59
32·6	22·4	30·6	25·5	28·9	32·0	31·0	39·1	28·4	52	30·4	68·5
43·0	21·7	38·5	26·1	37·8	33·0	38·7	40·0	37·0	55	39·5	73·5
51·2	21·7	48·0	26·6	46·6	34·7	47·5	43·5	45·2	60	45·0	76
59·1	22·0	54·5	27·4	56·1	36·7	54·5	44·7	51·5	63	50·9	79
66·5	22·1	60·0	28·0	62·5	37·8	60·5	45·7	58·5	66·5	56·6	83·5
72·5	22·4	65·0	28·3	67·0	38·7	65·0	46·4	62·5	67·5	64·5	88
75·0	22·4	72·0	29·3	70·5	38·6	69·5	48·2	69·0	70	68·5	89·5

TABLE V—p = 0·85 mm.

$10^4U_0^{-1}$ = 2·00		2·74		4·85		7·65		9·9	
iv_p	$1/\mu_c$	iv_p	$1/\mu_c$	iv_p	$1/\mu_c$	iv_p	$1/\mu_c$	iv_p	$1/\mu_c$
14·8	26	14·3	27·5	13·8	34·5	11·3	49	11·9	56
21·8	24·5	18·9	25·9	18·9	34·5	13·6	47·5	13·8	56·5
27·9	23·8	27·5	25·8	22·0	35·0	16·7	49	16·2	60
40·0	23·3	35·5	25·5	28·1	36·5	21·2	48	18·6	61
46·5	23·0	41·9	26·6	34·8	37·0	26·4	51·5	23·8	64
51·5	22·8	46·7	26·1	39·5	37·5	29·6	53	29·1	65
—	—	—	—	46·0	39·0	34·3	54·5	35·1	71
—	—	—	—	—	—	39·9	56	41·0	74·5
—	—	—	—	—	—	44·9	58·5	46·2	78

TABLE VI—p = 0·97 mm.

$10^4U_0^{-1}$ = 2·05		3·10		4·10		6·35		8·00		10·2	
iv_p	$1/\mu_c$	iv_p	$1/\mu_c$	iv_p	$1/\mu_c$	iv_p	$1/\mu_c$	iv_p	$1/\mu_c$	iv_p	$1/\mu_c$
15·1	27·6	11·7	32	17·5	33	15·6	42	11·2	51	12·1	59
27·8	25·0	22·8	29·0	27·2	32·8	22·2	46·5	24·4	56	22·2	63
41·3	23·8	37·7	29·8	39·0	35·4	32·8	50	37·2	61·5	34·0	73·5
51·0	24·0	46·0	29·5	48·7	35·9	43·1	53·5	45·0	64	45·0	79·5
60·2	23·8	56·3	30·1	58·3	36·6	51·5	54·5	51·5	66	52·8	82·5
65·2	23·1	65·0	30·4	63·4	37·4	60·0	57	59·5	69·5	59·0	86
—	—	72·8	30·6	70·5	38·7	65·0	57	65·0	72	65·8	91
—	—	76·0	29·8	77·0	39·2	71·5	59·5	71·0	73	72·5	94
—	—	83·0	30·4	82·0	39·3	76·0	61·5	77·5	76·5	78·0	97
—	—	—	—	—	—	81·5	62	80·5	76·5	—	—

TABLE VII—$p = 1{\cdot}35$ mm.

$10^4U_0^{-1} = 1{\cdot}70$		$3{\cdot}40$		$6{\cdot}80$	
iv_p	$1/\mu_c$	iv_p	$1/\mu_c$	iv_p	$1/\mu_c$
30·2	29·5	27·5	45	27·0	70
30·5	28·0	50·5	49	41·0	80
49·7	33·0	65·5	49	57·5	89
61·2	32·0	84	51	77·5	101
80·5	29·0	94	49	91	107
—	—	111	53	109	119

TABLE VIII

$p = 0{\cdot}42$ mm.

$10^4U_0^{-1}$	P	$10^{20}S$
2·60	25	−0·5
3·85	28	+0·5
6·05	33	2·65
8·05	36	6·9
10·9	50	7·4
14·1	62?	3·7?

$p = 0{\cdot}62$ mm.

$10^4U_0^{-1}$	P	$10^{20}S$
2·25	21	+0·7
2·90	22	1·4
3·85	24	2·0
5·95	31	4·5
7·65	36	6·5
10·0	41	8·3
12·4	54	9·7

$p = 0{\cdot}75$ mm.

$10^4U_0^{-1}$	P	$10^{20}S$
2·15	22	−0·1
3·18	23	+1·3
4·45	27	2·7
6·00	30	4·1
8·95	38	7·6
11·4	45·5	10·6

$p = 0{\cdot}85$ mm.

$10^4U_0^{-1}$	P	$10^{20}S$
2·00	25·5	−0·8
2·74	25·5	+0·2
4·85	32	2·4
7·65	43	5·4
9·9	49	9·8

$p = 0{\cdot}97$ mm.

$10^4U_0^{-1}$	P	$10^{20}S$
2·05	26	−0·7
3·10	28·5	+0·3
4·10	31	1·6
6·35	41	4·1
8·00	47	5·9
10·2	52	9·3

$p = 1{\cdot}35$ mm.

$10^4U_0^{-1}$	P	$10^{20}S$
1·70	38?	−1·7?
3·40	44	+1·2
6·80	55	9·4

TABLE IX

p	μ_0^{-1}	$10^2\mu_0$	$10^{-3}k$	$10^{17}a$	$10^{21}b$
0·42	19 ± 1	5·3	1·15	?	?
0·62	14 ± 1	7·1	2·00	11·2	16
0·75	16 ± 1	6·3	1·53	12·2	24
0·85	18 ± 1	5·5	1·75	11·2	30
0·97	18 ± 1	5·5	2·00	11·1	30
1·35	33 ± 2	3·0	1·00	22?	57?

It is at once apparent that as the pressure is increased μ_0 passes through a maximum in the neighbourhood of $p = 0{\cdot}6$ mm. The establishment and location of this maximum are of considerable practical interest.

A further point of importance is that high efficiency of output is obtained only for large flow rates. Indeed, the relationship expressed in equation (III) could not have been discovered with a pump of say 5–10 times smaller speed than that actually employed (7 l./sec.).

We may here mention certain discrepancies. At the lowest pressure used, 0·42 mm., the (S, U_0^{-1}) curve shows marked departure from the linear form: at the largest value of U_0^{-1}, 14×10^{-4} sec. c.c.$^{-1}$, the values of $1/\mu_c$ were more irregular than in any other case, and the slope of the $(1/\mu_c, iv_p)$ curve was such as to indicate that there was some undetected disturbance in its determination. The close linearity of all of the remaining thirty-two $(1/\mu_c, iv_p)$ curves renders it justifiable to regard this single exception as due to some cause absent in the other cases. Apart from this individual curve, however, the derived (S, U_0^{-1}) curve for this pressure is still non-linear. It is possible that at this low pressure diffusion effects are sufficiently marked to account for the disturbance; such effects would be more marked at low flow rates, i.e. high values of U_0^{-1}, as is observed. In all other cases the (P, U_0^{-1}) and (S, U_0^{-1}) relations are well represented by straight lines, a few small divergences occurring only at high values of U_0^{-1}.

Entrance of Hydrogen at One Point Only.—In the foregoing experiments the hydrogen was introduced into the discharge at two points, one near each electrode, and was pumped out at the centre of the discharge. A similarly complete survey has been made with the more usual arrangement in which hydrogen entered near one electrode only. The results will not be described in detail, because they were similar to those already given; in fact, it was with these data that the empirical equation (III) was discovered. A large number of measurements were made at four pressures between 0·23 and 1·8 mm., the flow rates covering a range represented by values of U_0^{-1} between 2×10^{-4} and 25×10^{-4} sec. c.c.$^{-1}$. As might be expected from the "dead-end" character of one half of the tube, the dispersion of the points about the straight lines, in the graphs of $1/\mu_c$ against W, is rather greater than for the data of Tables II to VII; there was some tendency to curvature for the lower values of W, but on the whole the linear character was well marked.

The values of μ_0, k, and a obtained were all somewhat smaller than those of Table IX, but were subject to much larger uncertainty. For any given conditions the values of μ_c calculated from these constants for the two systems do not differ very greatly, but the admission of hydrogen at both electrodes is to be preferred because of the smaller uncertainty in the actual output.

C—THEORETICAL

The Emeléus-Lunt-Meek Theory of Reaction in Discharges—In order to understand the significance of equation (III), it is necessary to refer to the theory of Emeléus, Lunt and Meek (1936) and Lunt and Meek (1936). By considering the probability of occurrence in a uniform positive column of any specified type of electronic excitation as a function of the concentrations of molecules and electrons, the electron energy distribution function, and the probability cross-section of the molecule for the specified type of excitation, they obtained the equation

$$\eta_e = \frac{k_0}{W_D X p^{-1}} \cdot \int_0^\infty Q_e(V) \, . \, V^{\frac{1}{2}} \, . f(V) \, . \, dV. \qquad \text{(IV)}$$

Here η_e is the number of excitations of type e per electron-volt supplied to the positive column, i.e. the energy efficiency of the column for these excitations; W_D is the mean drift velocity of the electrons in cm./sec.; X is the field along the positive column in V/cm.; $Q_e(V)$ is the probability cross-section of the molecule for the excitation e, and is a function of the energy, V e-volts, of the colliding electron; $f(V)$ is the electron energy distribution function, so that $f(V)\,dV$ is the probability that an electron shall have energy between V and $V+dV$; and k_0 has the value $1{\cdot}87 \times 10^8$ when the pressure p is expressed in mm. and $Q_e(V)$ in terms of the unit πa_0^2 (a_0 = atomic length unit = 0·532 A). In addition to describing the behaviour of the uniform positive column as a whole, η_e can, and will in the sequel, be treated as the theoretical efficiency of any selected portion of the column, measured in terms of the energy consumption and number of excitations in that portion.

In the first paper Emeléus, Lunt and Meek considered ionizing collisions; on the assumption of a Maxwellian velocity distribution for the electrons, they obtained satisfactory agreement between the calculated and experimental values for the diatomic gases studied, including hydrogen, whereas the use of Townsend's electron distribution function led to wide divergence. In the second paper Lunt and Meek therefore adopted, for diatomic gases, the form of $f(V)$ corresponding to a Maxwellian velocity distribution, and were thus enabled to express the integral in equation (IV) as a function ϕ of the mean electron energy $\bar{V}$:

$$\eta_e = \frac{k_0 \phi(\bar{V})}{W_D X p^{-1}}. \qquad \text{(IV}\,a\text{)}$$

Townsend and his co-workers had previously shown that both $\bar{V}$ and W_D are functions of Xp^{-1}, which have been experimentally determined for a number of gases, including hydrogen; and hence η_e is expressible as a function solely of Xp^{-1}, or of $\bar{V}$. Lunt and Meek now use equation (IV) to calculate numerical values of η_e for the ${}^1\Sigma_g^+ \rightarrow {}^3\Sigma_u^+$ transition in hydrogen, using the values of $Q_e(V)$ quantum-mechanically calculated for this transition by

Massey and Mohr (corrected by Massey; see Lunt and Meek 1936, p. 164); thus they obtain η_e as a function of Xp^{-1} or $\bar{V}$. This is the principal process leading to the production of atoms in the positive column of the glow discharge; the $^1\Sigma_g^+$ state is the ground state, whilst the $^3\Sigma_u^+$ state is a non-radiating repulsive state, so that the excited molecule dissociates into two normal atoms. The next most important process leading to dissociation is the excitation $^1\Sigma_g^+ \rightarrow {}^3\Sigma_g^+$; the $^3\Sigma_g^+$ state emits the continuous spectrum of hydrogen, falling to the $^3\Sigma_u^+$ state, which then dissociates as before. Lunt, Meek and Smith (1937) calculate the efficiency for this excitation, their curve for the corresponding η_e as a function of Xp^{-1} agreeing well with the experimental data for the intensity of the continuous spectrum.

It is probable that these two types of excitation account for nearly all of the atoms produced, the first being of much greater importance than the second; thus, in effect, the sum of their efficiencies is η_0, the dissociation efficiency of the positive column, i.e. the number of molecules dissociated per electron-volt supplied to the positive column. In fig. 6 (p. 448) the calculated values* of the two η_e's, and also their sum, have been plotted against Xp^{-1}; the vertical scale has been increased by a factor of 2·6, for the reason indicated on p. 448.

We have to seek a relation between η_0, which will be called the Emeléus-Lunt-Meek efficiency, and the experimental μ_c, which refers to the number of dissociated molecules *received at the calorimeter*. Any difference between η_0 and μ_c will undoubtedly be connected with, *inter alia*, the loss of atoms by recombination before reaching the calorimeter. Other causes for difference exist, one of which is considered in the next section.

Effect of Variable Composition of the Gas—In the above theory η_e is calculated for excitations caused by electron collisions in a gas consisting only of H_2 molecules. In practice, the gas consists of a mixture of H atoms and H_2 molecules, whose partial pressures in any selected locality will be written λp and $(1-\lambda)p$ respectively; λ is thus defined as the fraction of the pressure due to atoms. *The factor p in equation (IV) was introduced as a measure of*

---

* Dr. Lunt has informed me that the previously published values of the calculated efficiencies for these two excitations require correction; the new values (calculated by the algebraic method (Lunt and Meek 1936, p. 165) using $Q_e(V) = 0{\cdot}167\,\pi a_0^2$ and $0{\cdot}055\,\pi a_0^2$ for the $^3\Sigma_u^+$ and $^3\Sigma_g^+$ excitations respectively) are as follows:

V	2	2·5	3	3·5	4	5	6	7	8	9	10
Xp^{-1}	13	17	21	25·5	31	42·5	55	67·5	80	93	105
$10^3\eta_e(^3\Sigma_u^+)$	0·44	1·00	1·60	1·83	1·95	1·72	1·36	1·06	0·84	0·67	0·54
$10^3\eta_e(^3\Sigma_g^+)$	0·03	0·14	0·20	0·26	0·33	0·36	0·32	0·28	0·24	0·21	0·18

the concentration of molecules available for excitation, and must therefore be replaced by $(1-\lambda)p$ for a discharge producing finite quantities of atomic hydrogen. The efficiency for a given type of excitation would then be a fraction $(1-\lambda)$ of the value given by equation (IV), or (IV *a*), i.e. $(1-\lambda)\,\eta_e$. The efficiency η_λ for the sum of the dissociation processes for a locality defined by λ would therefore be given by $\eta_\lambda = (1-\lambda)\,\eta_0$. This, however, assumes that the remaining quantities in equation (IV) are unchanged when a mixture of atoms and molecules is substituted for pure molecular hydrogen. It is to be expected that for a given pressure the quantities $\bar{V}$, X and W_D will be dependent on λ, i.e. on the composition of the gas. For this reason, η_λ is most simply expressed as a Taylor expansion about the value η_0, corresponding to $\lambda = 0$: thus, writing $D_0^{(n)}$ for the value of $(d^n\eta_\lambda/d\lambda^n)$ at $\lambda = 0$,

$$\eta_\lambda = \eta_0 + \lambda D_0^{(1)} + \frac{\lambda^2}{2!} D_0^{(2)} + \dots. \tag{V}$$

In the sequel, except where otherwise stated, a single value of the pressure is assumed; $D_0^{(1)}$, etc., are then constants.

Conditions in the Discharge Tube—In any actual discharge, with the apparatus described, there will evidently be a steady increase in λ as the gas streams from the point of entry in each half of the discharge tube to the common point of emergence. If x is the distance along the discharge tube, measured from the point of entry as zero, we can write $\lambda = f_1(x)$. Similarly, in the delivery tube from the discharge tube to the calorimeter catalyst, we have $\lambda = f_2(y)$, the co-ordinate y representing distance along the delivery tube. By definition, the number of dissociations produced per second in a length dx, consuming power dw, is then $\eta_\lambda \, . \, dw$; and the total number of dissociations per second for the whole tube (two halves each of length m) is

$$\int \eta_\lambda \, . \, dw = 2\int_{x=0}^{x=m} \left(\eta_0 + \lambda D_0^{(1)} + \frac{\lambda^2}{2!} D_0^{(2)} + \dots\right) \frac{dw}{dx} \, . \, dx,$$

m being the x co-ordinate of the point of emergence of the gas. For simplicity, we will substitute for dw/dx its mean value $W/2m$; since dw is equal to the product of the potential fall $X \, . \, dx$ and the (constant) current i, this is equivalent to assuming that X is constant throughout the tube. Then the total number of atoms produced per second is twice the number of dissociations, i.e.

$$\frac{2W}{m}\int_0^m \left(\eta_0 + \lambda D_0^{(1)} + \frac{\lambda^2}{2!} D_0^{(2)} + \dots\right) dx.$$

Writing $R_x\,.\,dx$ for the number of atoms per second lost by recombination in the segment dx of the discharge tube, the total recombination loss in atoms per second for the whole tube is $2\int_0^m R_x\,.\,dx$, and the net output of atoms per second at the point $x = m$ (where the gas enters the delivery tube leading to the calorimeter) is

$$\frac{2W}{m}\int_0^m \left(\eta_0 + \lambda D_0^{(1)} + \frac{\lambda^2}{2\,!}D_0^{(2)} + \dots\right) dx - 2\int_0^m R_x\,.\,dx = 2W\mu_m. \qquad \text{(VI)}$$

Here μ_m represents the output efficiency for the whole tube for dissociated molecules, measured at the point $x = m$; μ_m will differ from the efficiency μ_c at the calorimeter owing to further loss of atoms by recombination in the delivery tube. Thus, if $R_y\,.\,dy$ is the quantity for the delivery tube which corresponds to $R_x\,.\,dx$ for the discharge tube, then, integrating from the point $x = m$, which we now take as the origin of the co-ordinate y, to the calorimeter catalyst at $y = c$, we may write

$$\int_{y=0}^{y=c} R_y\,.\,dy = 2W\mu_m - 2W\mu_c. \qquad \text{(VII)}$$

Recombination of atoms may occur by the following processes: (*a*) heterogeneously as a first order reaction; the number of atoms lost per second per cm.^{2} of wall (either by adhesion to the wall or by recombination with an atom already adhering) can be written $K_1[\mathrm{H}]$, the constant K_1 referring to 1 cm.^{2} of wall; (*b*) heterogeneously as a second order reaction, corresponding to a triple collision in which the wall is the third body; the loss of atoms per second per cm.^{2} of wall by this reaction can be written $K_2[\mathrm{H}]^2$; (*c*) homogeneously as a triple collision in which two atoms and a molecule are concerned, the loss per second per c.c. being $K_m[\mathrm{H}]^2[\mathrm{H}_2]$; and (*d*) homogeneously as a triple collision in which three atoms are concerned, the loss per second per c.c. being $K_a[\mathrm{H}]^3$. If we write M' for the number of particles (atoms or molecules) in 1 c.c. of gas at a pressure of 1 mm. and the prevailing temperature, we have $[\mathrm{H}] = M'p\lambda$ and $[\mathrm{H}_2] = M'p(1-\lambda)$; for a temperature of 290° K., $M' = 3{\cdot}34 \times 10^{16}$. Then for a tube of radius r cm.,

$$\begin{aligned} R_x\,.\,dx &= [K_1M'p\lambda + K_2(M'p\lambda)^2]\,2\pi r\,.\,dx \\ &\qquad + [K_m(M'p)^3\lambda^2(1-\lambda) + K_a(M'p)^3\lambda^3]\,\pi r^2\,.\,dx \\ &= \pi r[2K_1M'p\lambda + (M'p)^2(2K_2 + rK_mM'p)\lambda^2 + r(M'p)^3(K_a - K_m)\lambda^3]\,.\,dx \\ &= (A\lambda + B\lambda^2 + C\lambda^3)\,.\,dx, \qquad \text{(VIII)} \end{aligned}$$

where λ must be expressed as $f_1(x)$. The same equation holds for the co-ordinate y if λ is replaced by $f_2(y)$. A, B and C are the indicated functions of the four rate constants, A being simply a function of K_1.

The evaluation of the integrals in equations (VI) and (VII) thus depends only on the form of the functions $f_1(x)$ and $f_2(y)$, which are both dependent on W and U_0. The differential equations corresponding to these functions have been found (Appendix, equations (II A) and (III A), p. 452), but they are not soluble, and approximation must be resorted to. For the discharge tube two hypothetical cases will be considered: (i) the fractional atomic pressure λ increases linearly with the distance x, from 0 at the entry to λ_m at the point of emergence m, i.e. $\lambda = \lambda_m x/m$; (ii) diffusion of atoms is effective in maintaining a practically uniform composition, i.e. $\lambda = \lambda_m$ everywhere. Since the straight line $\lambda = \lambda_m x/m$ is almost certainly below* the curve corresponding to the actual (λ, x) relationship for a given λ_m, (i) and (ii) may be regarded as limiting cases.

Case (i)—Using $\lambda = \lambda_m x/m$ and equation (VIII), equation (VI) can be expressed thus:

$$\eta_0 - \mu_m = \frac{m\lambda_m}{W}\left(\frac{A}{2} + \frac{B}{3}\lambda_m + \frac{C}{4}\lambda_m^2\right) - \lambda_m\left(\frac{D_0^{(1)}}{2} + \lambda_m\frac{D_0^{(2)}}{6} + \ldots\right). \quad \text{(IX)}$$

Since in the actual system λ increases as the gas streams through the discharge to the point $x = m$, thereafter decreasing along the delivery tube owing to recombination and diffusion towards the calorimeter catalyst, λ must pass through a maximum close to the point m. We can consider this maximum as being actually at m, and therefore having the value λ_m. As the concentration gradient is here zero, the net diffusion of atoms past this point is also zero, and the number of atoms per second passing the point m is $2\alpha_m MpU_0$, where α_m is the fraction of dissociation corresponding to λ_m, and MpU_0 is the number of undissociated molecules per second entering the system. The fraction of dissociation is related to the fractional atomic pressure thus: $\lambda = 2\alpha/(1+\alpha)$. But the number of atoms per second emerging at m is also given by $2W\mu_m$, this being the definition of μ_m; hence

$$\lambda_m = \frac{2W\mu_m}{MpU_0(1+\alpha_m)}. \quad \text{(X)}$$

---

* This can be shown by solving equation (II A), Appendix, p. 452, on the assumptions that diffusion is negligible, that recombination does not occur, and that $\eta_\lambda = (1-\lambda)\,\eta_0$. The (λ, x) curve corresponding to this solution is nearly linear, being in fact slightly convex upwards. It is then easily shown qualitatively that, for a given value of λ_m, the effects of diffusion and recombination must be to move the (λ, x) curve farther into the region between limits set by (i) and (ii) above, except on the improbable assumption that there is a very rapid *increase* in η_λ as λ increases.

On this account equation (IX) may be re-written thus:

$$\frac{1}{\mu_m}=\frac{1}{\eta_0}\left(1+\frac{mA}{MpU_0}\right)+\left[\alpha_m\left(\frac{1}{\eta_0}-\frac{1}{\mu_m}\right)+\frac{\lambda_m}{MpU_0}\cdot\frac{2m}{\eta_0}\left(\frac{B}{3}+\frac{C}{4}\lambda_m\right)\right.$$
$$\left.-\frac{\lambda_m(1+\alpha_m)}{\eta_0\mu_m}\left(\frac{D_0^{(1)}}{2}+\lambda_m\frac{D_0^{(2)}}{6}+\ldots\right)\right]. \qquad \text{(XI)}$$

Here the terms which are independent of α_m and λ_m, and accordingly independent of the power input, W, have been segregated from those dependent on the power.

Case (ii)—It is easily shown that the expression for $1/\mu_m$ obtained by using $\lambda = \lambda_m$ will differ from (XI) only in having A, B and C instead of $A/2$, $B/3$ and $C/4$, and $D_0^{(1)}$, $D_0^{(2)}/2$, etc., instead of $D_0^{(1)}/2$, $D_0^{(2)}/6$, etc.

The expression (XI) for $1/\mu_m$, and the corresponding one for Case (ii), resemble the experimentally obtained equation (III) for $1/\mu_c$; the first term (the result of extrapolation to $W = 0$, i.e. to $\lambda_m = 0$ and $\alpha_m = 0$) has exactly the same form in the three equations, the coefficients of U_0^{-1} differing by the factor 2 in the two limiting cases (i) and (ii). This suggests that the Emeléus-Lunt-Meek efficiency η_0 may be identical with the experimental limiting efficiency μ_0, and that the empirical constant k of equation (III) may be used to calculate A, and hence the first-order recombination constant K_1, within a factor 2. Before this is possible, however, the relation between μ_m and μ_c must be found. It will be shown that extrapolation of $1/\mu_c$ to $W = 0$ leads to an equation which is non-linear in U_0^{-1}, and that therefore the final limit, $1/\eta_0$, to which $1/\mu_c$ tends on extrapolation to $U_0^{-1} = 0$, cannot be identified with $1/\mu_0$, this quantity having been derived on the assumption that the extrapolation to U_0^{-1} is linear.

Concerning the expression in the square bracket of equation (XI), it is to be noted that its dependence on W and U_0 cannot be shown necessarily to correspond to the empirical equation (III). However, both λ_m and α_m are roughly proportional to W/U_0, and hence an approximation to the W-variable part of equation (XI) might well have a form resembling the experimental relationship.

Conditions in the Delivery Tube—The relation between μ_m and μ_c is given by equation (VII) with $R_y = A\lambda + B\lambda^2 + C\lambda^3$ and $\lambda = f_2(y)$. As before an approximation for $f_2(y)$ is necessary. Corresponding to Case (i) for the discharge tube, we assume that λ falls linearly from λ_m at $y = 0$ to zero at

$y = c$: $\lambda = \lambda_m - \lambda_m y/c$. Proceeding as in the calculation for loss of atoms in the discharge tube we find

$$\frac{1}{\mu_c}\left(1-\frac{cA}{2MpU_0}\right)=\frac{1}{\mu_m}+\alpha_m\left(\frac{1}{\mu_m}-\frac{1}{\mu_c}\right)+\frac{\lambda_m}{MpU_0}\cdot\frac{c}{\mu_c}\left(\frac{B}{3}+\frac{C}{4}\lambda_m\right). \tag{XII}$$

Combination of equation (XII) with equation (XI) gives

$$\begin{aligned}\frac{1}{\mu_c}\left(1-\frac{cA}{2MpU_0}\right)&=\frac{1}{\eta_0}\left(1+\frac{mA}{MpU_0}\right)\\&\quad+\alpha_m\left(\frac{1}{\eta_0}-\frac{1}{\mu_c}\right)+\frac{\lambda_m}{MpU_0}\left(\frac{2m}{\eta_0}+\frac{c}{\mu_c}\right)\left(\frac{B}{3}+\frac{C}{4}\lambda_m\right)\\&\quad-\frac{\lambda_m}{\mu_c\eta_0}\left(\frac{D_0^{(1)}}{2}+\lambda_m\frac{D_0^{(2)}}{6}+\dots\right)\left\{(1+\alpha_m)-\frac{c}{MpU_0}\left(\frac{A}{2}+\frac{B}{3}\lambda_m+\frac{C}{4}\lambda_m^2\right)\right\}.\end{aligned} \tag{XIII}$$

For the assumed $f_1(x)$ of case (ii), a similar equation is obtained.

The apparent possibility of a negative value of $1/\mu_c$ arises from the assumption of linear fall in λ along the delivery tube. This will obviously be far from valid if the recombination loss exceeds a certain value, and, in particular, if $cA/2MpU_0 > 1$, since in this case the first-order recombination alone would use up all the atoms in less than the distance c. From the value of K_1 given later, it can be calculated that in the experiments reported $cA/2MpU_0$ usually lay between 0·08 and 0·4, and did not exceed 0·57. The linear approximation for $f_2(y)$ cannot, as for the discharge tube, be regarded as a lower limit to the true (λ, y) function; but in the absence of further information no other approximation need be considered.

Extrapolation to Zero Power Input—It is clear that as $W \to 0$, $\lambda_m \to 0$ and $\alpha_m \to 0$; hence for case (i),

$$\lim\left(\frac{1}{\mu_c}\right)_{W\to 0}\left(1-\frac{cA}{2MpU_0}\right)=\frac{1}{\eta_0}\left(1+\frac{mA}{MpU_0}\right). \tag{XIV}$$

The quantity $\lim\,(1/\mu_c)_{W\to 0}$ corresponds to P in equation (I) (p. 430), which was obtained by extrapolation of the experimental values to $W = 0$. Equation (II a), viz. $P = (1/\mu_0)(1 + k/U_0)$, is thus the empirical counterpart of (XIV). The apparently linear character of the (P, U_0^{-1}) curves, illustrated in fig. 3 and expressed in equation (II a), is thus only an approximation. Linear extrapolation of such a curve is therefore not fully justifiable; nevertheless it is evident that the value of μ_0 thereby obtained should be almost equal to the theoretical η_0; and that the experimental constant k is closely related to the quantity A, and therefore to the first-order recombination constant K_1.

Equation (XIV) can be used to determine η_0 and K_1 by successive approximation as follows. From equation (VIII) (p. 439) we have $A = 2\pi r K_1 M'p$. M' is the number of molecules per c.c. of gas at 1 mm. pressure and at the temperature prevailing during recombination; and since equation (XIV) refers to the extrapolated condition $W = 0$, the appropriate temperature is room temperature, about 17° C., and therefore $M' = (273/290)M$. The radius of the glass tube is 1·25 cm., and the layer of phosphoric acid is about 1 mm. thick: r is therefore taken as 1·15 cm. Hence $A/Mp = 6{\cdot}8K_1$. The half-length m of the positive column is about 31·5 cm., and the length c of the delivery tube is 26 cm. From these figures, the left-hand side of equation (XIV) is calculated for each value of U_0^{-1}, using the experimental values of P and an assumed value of K_1. The results are plotted against U_0^{-1}, and this gives a second approximation to K_1 and η_0 deriving from the right-hand expression. The process is repeated until the value of K_1 recurs. This procedure applied to the data for $p = 0{\cdot}75$ mm. led to the values $\eta_0 = 5{\cdot}5 \times 10^{-2}$ and $K_1 = 3{\cdot}1$, the first approximation (equation (II a)) being $\mu_0 = 6{\cdot}2 \times 10^{-2}$ and $K_1 = 7{\cdot}1$ (from $k = mA/Mp$). Slightly different values would be obtained for Case (ii).

Summarizing, the above analysis has demonstrated the origin of the form of equation (III), although it is seen that this equation is only an approximation to one much less simple. In particular, the linearity of the $(1/\mu_c, W)$ curves (fig. 2, and equation (I), p. 430) remains a purely empirical relationship, owing to the uncertainty attaching to the true forms of $f_1(x)$ and $f_2(y)$ and to the unknown quantities $D_0^{(1)}$, $D_0^{(2)}$, etc. However, for the limiting conditions in which $W \rightarrow 0$, and therefore $\lambda \rightarrow 0$ throughout the system, it is possible to calculate accurately the limiting forms of the functions $f_1(x)$ and $f_2(y)$, and hence to deduce in an exact way the values of η_0 and K_1. (The homogeneous recombination constants will be considered in a future paper.)

The Energy Efficiency η_0 and the First-Order Recombination Constant K_1—The limiting form of the relation between λ and x as W approaches 0 is shown in the Appendix (equation (IV A), p. 453) to be

$$\lambda = \frac{\eta_0 M p U_0 \lambda_m}{2Am(\lim \mu_m)}(1 - e^{-2Ax/MpU_0})$$

for each half of the discharge tube. Since $\lambda = \lambda_m$ at $x = m$,

$$\lim\left(\frac{1}{\mu_m}\right) = \frac{2Am}{\eta_0 M p U_0}(1 - e^{-2Am/MpU_0})^{-1}. \qquad \text{(XV)}$$

It is also shown in the Appendix (equation (V A), p. 453) that the relation between λ and y for the delivery tube, under the condition $W \to 0$, is

$$\lambda = \lambda_m e^{-Ay/MpU_0}.$$

Hence, by substituting in R_y and omitting terms in λ of degree higher than the first, we obtain from equation (VII), p. 439,

$$\begin{aligned}\lim(\mu_m - \mu_c) &= \lim\left[\frac{1}{2W}\int_0^c A\lambda_m e^{-Ay/MpU_0}\,.\,dy\right]\\ &= (1 - e^{-Ac/MpU_0})\lim\left[\frac{MpU_0\lambda_m}{2W}\right].\end{aligned}$$

On account of equation (X), this can be re-written

$$\lim\left(\frac{1}{\mu_c}\right) = e^{Ac/MpU_0}\lim\left(\frac{1}{\mu_m}\right). \qquad \text{(XVI)}$$

Finally, by combining (XV) and (XVI), we find

$$P = \lim\left(\frac{1}{\mu_c}\right) = \frac{1}{\eta_0}\,.\,\frac{2Am}{MpU_0}\,.\,e^{Ac/MpU_0}(1 - e^{-2Am/MpU_0})^{-1} \qquad \text{(XVII)}$$

or $P = (1/\eta_0)\,.\,Y(U_0)$, where Y is the explicit function indicated. This is therefore the exact equation which connects U_0 with the extrapolated quantity P, and should replace the empirical equation (II *a*).

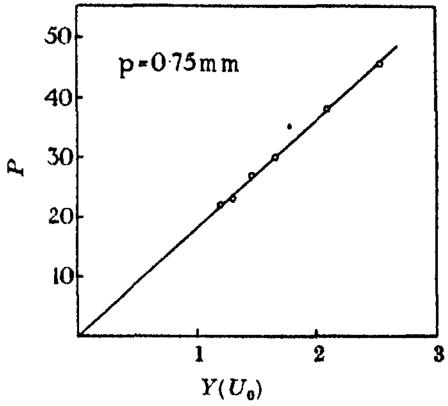

FIG. 4

All the quantities in this equation except A and η_0 are known for each value of U_0 within the experimental range; and as on p. 443, $A/Mp = 6{\cdot}8K_1$. A graphical solution was obtained as follows: P was plotted against $Y(U_0)$ calculated with an assumed value of K_1, a straight line being obtained; this procedure was repeated until a value of K_1 was found for which the straight line passed through the origin. This was the correct value of K_1, and the gradient of the line gave $1/\eta_0$. For the pressure $p = 0{\cdot}75$ mm., fig. 4 shows the final curve of P against $Y(U_0)$, for $K_1 = 2{\cdot}22$ cm. sec.$^{-1}$; η_0 is found to be $5{\cdot}5 \times 10^{-2}$ molecules dissociated per electron-volt. The approximate method involving equation (XIV) gave $K_1 = 3{\cdot}1$ and $\eta_0 = 5{\cdot}5 \times 10^{-2}$, and is thus shown to be inaccurate for the calculation of K_1, although it led to the correct value of η_0.

This procedure has been applied for each of the pressures studied. The values of the efficiency η_0 and the heterogeneous recombination constant K_1 are set out in Table X, in which the values of the empirical μ_0 obtained from equation (II*a*) are included for comparison. The limits of error in these values of η_0 and K_1, having been estimated from the successive graphs, are indicated in the table.

TABLE X

p	$10^2\mu_0$	$10^2\eta_0$	X	Xp^{-1}	K_1	$10^5\gamma$
1·35	3·0	3·05 ± 0·15	25·5	19	2·10 ± 0·24	3·4
0·97	5·5	4·9 ± 0·3	18·0	18·5	2·80 ± 0·24	4·5
0·85	5·5	4·8 ± 0·15	17·0	20	2·34 ± 0·12	3·8
0·75	6·3	5·55 ± 0·15	17·6	23·5	2·22 ± 0·12	3·6
0·62	7·1	5·95 ± 0·3	16·4	26·5	2·57 ± 0·12	4·1
0·42	5·3	5·2 ± 0·2	14·9	35·5	2·34 ± 0·12	3·8
0·24		4·5	9·4	39		
0·10		2·3	6·7	67		
				Mean	2·40 ± 0·15	3·9

In addition to the values derived from the data of Table VIII, values of η_0 for pressures of 0·24 mm. and 0·10 mm. are given in Table X. For the former pressure, η_0 was derived from experiments with two different flow rates U_0 by introducing into equation (XVII) the mean value of K_1 already determined: the same value of η_0 was obtained for each value of U_0. Determinations at 0·10 mm. were difficult owing to the occurrence of stray discharges in the delivery tube, and to the fact that the cathode fall v_c had become very large, the positive column voltage being considerably smaller than v_c and therefore subject to considerable inaccuracy. The value of η_0 recorded for this pressure was obtained, not by extrapolation, but by substituting for the extrapolated quantity P in equation (XVII) the actual experimental value of μ_c at low current ($i = 12$ mA, $iv_p = 5{\cdot}0$ W), again using the mean value of K_1. The value of η_0 obtained in this way is less than the true value, though probably by not more than 25 %.

The Adhesion Coefficient γ—From the definition of K_1, the number of atoms recombining per second per cm.^{2} of wall surface by a first-order mechanism is $K_1[\mathrm{H}]$. If γ is the adhesion coefficient, i.e. the probability of loss of an atom in a collision with the wall, then the number of atoms lost per second per cm.^{2} is given also by $\gamma v[\mathrm{H}]$, where v is one-quarter of the mean thermal velocity of the atoms (Steiner 1935 *b*). Thus $\gamma = K_1/v$; at 290° K., $v = 6{\cdot}2 \times 10^4$ cm. sec.$^{-1}$. The values of γ obtained for different pressures are included in Table X. It will be seen that the figures are remarkably concordant, and indicate that a water film on phosphoric acid is nearly constant in its catalytic behaviour over a very large range of conditions.

By an entirely different experimental method Steiner obtained values of γ between $2{\cdot}2 \times 10^{-6}$ and 9×10^{-6} at pressures between 0·35 and 0·7 mm. for a water film on glass, no phosphoric acid being used;[*] these values are of about the same order of magnitude as those of Table X, but their greater variability, even at a single pressure, is doubtless due to the smaller stability of such films, as indicated by the experiments of Part II. As in Steiner's work, the values of γ now obtained are sufficiently small to justify the neglect of the radial diffusion of atoms due to loss at the walls: the radial concentration gradient in the neighbourhood of the walls was such that in the most unfavourable case the proportionate change of concentration was less than 0·1 % per cm.

The Field X—In order to compare the observed values of η_0 with the values calculated by Lunt and Meek (1936), it is necessary to know the value of Xp^{-1} corresponding to each η_0. The field X has proved somewhat difficult to estimate: the total potential fall along the positive column, v_p, was found, and the length (slightly variable) of the column was noted, for every determination of μ_c; but the values of the field X calculated from these data were not dependent solely on the pressure. This is undoubtedly due to the fact that, as the power input W is increased, the composition of the gas in any locality changes, i.e. λ increases. We should, however, expect that X would be nearly constant for a given *mean* atom concentration in the discharge (at any given total pressure), and that extrapolation of X to $W = 0$ would give values of X appropriate to the observed values of η_0. Actually the (X, W) curves were smooth, but were different for each value of the flow rate (which in part controls atom-concentration), and therefore in order to effect the desired extrapolation it was necessary to arrange a plot of X against some function of W selected to be independent of the flow rate. The function chosen was an approximation to the mean atom concentration, and was obtained as follows. The mean value of λ was assumed proportional to λ_m, and therefore nearly proportional to $2\alpha_m$, i.e. to $2W\mu_m/MpU_0$; the second step is justified if λ_m is not too large. Further, μ_m was taken as proportional to μ_c, so that the mean value of λ became proportional to $2W\mu_c/MpU_0$, which can be replaced by $5{\cdot}48q/pU_0$ if we recall the definition of μ_c in terms of the heat per minute, q, recorded by the calorimeter. The approximations are considerable, but sufficient accuracy is attained for the extrapolation of X to zero power; for if X is plotted against $5{\cdot}48q/pU_0 = \lambda'$ for any fixed pressure, a reasonably well-defined curve is obtained, as is illustrated in fig. 5 for $p = 0{\cdot}75$ mm. Similar curves have been constructed for the other pressures, and have been extrapolated to $\lambda' = 0$, i.e. to $W = 0$. The limiting values of X thus obtained are given in Table X together with the derived values of Xp^{-1}; the figures for the three highest pressures are less accurate than the others owing to uncertainties in the extrapolation.

---

[*] *Note added in proof* 11 *November* 1937. A further series of experiments has now been carried out, in which the discharge tube and the delivery tube were not coated with phosphoric acid. The surfaces were prepared by cleaning with chromic acid followed by hydrofluoric acid, and then washing with distilled water. The discharge current did not exceed 100 mA at any time. The values of μ_c were at first low and erratic, but finally became fairly steady. The plot of $1/\mu_c$ against W were then less regular than in fig. 2, but straight lines could be drawn and the values of P determined. Using the previously established value of η_0, $5{\cdot}95 \times 10^{-2}$, for the pressure used, 0·62 mm., K_1 was then evaluated graphically from the equation (XVII). The values of K_1 found in successive runs were 11·5, 10·6, 9·3, 9·3; corresponding to their mean, γ for a water film on glass is found to be $1{\cdot}6 \times 10^{-4}$, which value differs considerably from that of Steiner.

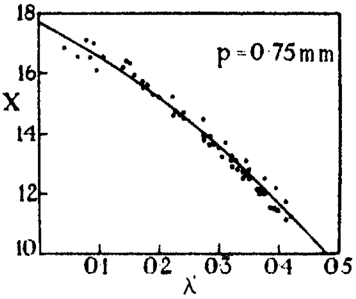

FIG. 5

Comparison of Theoretical and Experimental Values of η_0—The points plotted in fig. 6 represent the observed values* of η_0. As predicted by the theory of Emeléus, Lunt and Meek, η_0 passes through a maximum as Xp^{-1} increases. However, all the calculated efficiencies are smaller than those observed; this is not unexpected, since Massey remarked that there was still some uncertainty about the absolute scale of the amended cross-sections given by him (see Lunt and Meek 1936, p. 159).

---

* The experimental values of η_H quoted by Lunt and Meek (1936, p. 159) were obtained in an earlier attempt at analysis of the present experimental data. They are now to be replaced by the values of η_0 in Table XI. (Note: the units of η_H are *atoms* per e-volt, and hence $\eta_H = 2\eta_0$.)

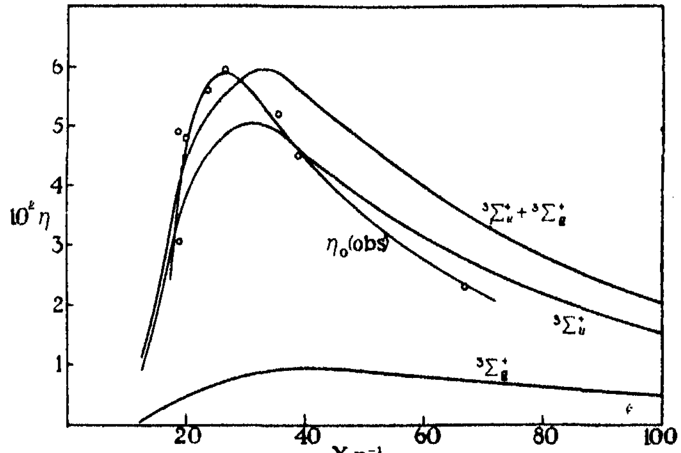

FIG. 6

The curve marked $^3\Sigma_u^+ + {}^3\Sigma_g^+$ in fig. 6 was obtained by arbitrarily increasing the scale of η_0 (calc.) until the maximum of the theoretical (η_0, Xp^{-1}) curve coincided with that of the experimentally found relationship. The maximum having thus been adjusted, general agreement between the calculated curve and the experimental points is good considering the number of extrapolations, and must be regarded as strongly supporting Emeléus, Lunt and Meek's theory. The factor by which the calculated η_0 values have been increased is 2·6; and, from equation (IV), p. 436, this is also the factor by which Massey's probability cross-section $Q_e(V)$ for the $^3\Sigma_u^+$ excitation should be increased, if the uncertainty concerning the cross-section is the cause of the scale discrepancy; Lunt and Meek derived the cross-section for the $^3\Sigma_g^+$ excitation from that for the $^3\Sigma_u^+$ excitation.

Uniform and Striated Positive Columns—A notable difference between the postulated conditions of the theory and those of the present experiments must be pointed out. On p. 436 it was indicated that equation (IV) relates to the efficiency of excitation in a *uniform* positive column, but in all of the experiments herein described the positive column was *striated*. The field X is known to vary largely throughout a single striation, the experimental value of X being merely the average for the whole positive column. The electron energy distribution function $f(V)$ must be different in the two types of discharge, and must vary from place to place throughout each striation; the theoretical calculation of the efficiency of a striated discharge is therefore impossible with our present knowledge of the conditions in such discharges. Nevertheless, the agreement of form between the experimental and calculated curves of fig. 6 suggests that $f(V)$ for the whole striated column does not differ greatly from $f(V)$ in a uniform column with the same average value of Xp^{-1}, at least for energies just above 10 e-volts (the excitation potential for ${}^1\Sigma_g^+ \rightarrow {}^3\Sigma_u^+$ being 9·5 V); and this in turn suggests that for such energies $f(V)$ does not vary much throughout a single striation.

The idea that the properties of the electron population in any locality in a striated discharge should be not very different from the mean for the whole positive column is rendered plausible by the following considerations. The establishment of an energy distribution corresponding to any local value of X can take place only through the occurrence of a considerable number of collisions of each electron during the time in which it remains in the appropriate locality. Owing to the shortness of the distance between striations, of the order of 1 cm., it seems very probable that the electrons do not have sufficient collisions to attain this equilibrium distribution: the "kinetic theory mean free path" of an electron is $4\sqrt{2}$ times the mean free path of a molecule, and is therefore about 2 mm. at $p = 0{\cdot}25$ mm., and 0·6 mm. at $p = 1$ mm., i.e. comparable in all cases with the length of a single striation. It must be remembered that many of the collisions of each electron are elastic, and thus involve no appreciable change of energy.

Some experimental evidence in support of this view was obtained during the experiments with hydrogen entering near one electrode only (p. 435). As the current was increased at $p = 1{\cdot}75$ mm. the discharge changed discontinuously from a rather diffuse striated column to an apparently uniform column. This change was observed at about 25 mA for several rates of gas flow at this pressure. In each case the curve of $1/\mu_c$ against W remained linear, showing no evidence of change in the factors which determine η_0.

The Maxwellian Distribution—The actual magnitude of η_0 is of considerable interest; for the optimum value of Xp^{-1}, 27 V cm.$^{-1}$ mm.$^{-1}$ Hg, η_0 is $6{\cdot}0 \times 10^{-2}$, i.e. each molecule dissociated requires the expenditure of $17 (= 1/\eta_0)$ e-volts *in all the types of electronic processes occurring in the discharge.* Since the excitation potential of the ${}^3\Sigma_u^+$ state is 9·5 V, and for the less important ${}^3\Sigma_g^+$ state is 12 V, it is necessary that an average energy of about 10 e-volts per dissociation should be expended in these two types *of excitation alone. This means that, for this value of Xp^{-1}, about 0·6 of the total electronic energy derived from the field is used for these two types of excitation, mainly for the $^1\Sigma_g^+ \rightarrow {}^3\Sigma_u^+$ process.* This applies to the condition $W \rightarrow 0$, when sensibly only H_2 molecules are present. If, however, we consider the actual, unextrapolated experimental data, the highest observed efficiency of output at the calorimeter was $\mu_c = 4{\cdot}5 \times 10^{-2}$ molecules/e-volt, for $p = 0{\cdot}62$ mm. and 0·75 mm., with $U_0^{-1} = 2{\cdot}2 \times 10^{-4}$ sec. c.c.$^{-1}$ and $iv_p = 20$–70 W; in this case 0·45 of the total positive-column energy was required to produce only those atoms which ultimately reach the calorimeter. The efficiency of the system as a source of atomic hydrogen is thus remarkably high.

The occurrence of such high efficiencies means that the process of excitation of the $^3\Sigma_u^+$ state removes most of the electrons from the energy range just above 9·5 e-volts, owing to the fact that the probability cross-section of the molecules for this (optically disallowed) transition rapidly becomes large once this value of the electron energy is exceeded, passes through a maximum at about 13·5 e-volts, and then rapidly falls to a low value again. This must restrict very considerably the number of electrons which can attain higher energy values; and in such a case it is difficult to see how the velocity distribution of the electrons can conform to the Maxwellian for energies above the excitation potential.

The efficiency η_0 derived from the experimental data, however, refers to that type of electron energy distribution which actually occurs in the striated discharge; and the fact that the experimental (η_0, Xp^{-1}) curve does not, without a scale adjustment, even approximately agree with that calculated by Lunt and Meek may be an effect due to departure from the Maxwellian form in such a discharge. It should be emphasized that the calculation of η_0 and K_1 by means of the analysis given is independent of any assumptions about the nature of the distribution function, and is not affected by the fact that the actual discharges were striated.

D—APPENDIX

The problem of the flow of a mixture of H_2 molecules and H atoms through a tube has been attacked by Steiner (1935 *a*), whose equation gives the total transport of mass past a point, and is not convenient for calculating the flow of one species, e.g. atoms. The evaluation of his quantity v_z, the "average linear velocity of [non-diffusive] flow", is not easy. His method of using the equation involves the assumption that transport of matter by diffusion (atoms in one direction and molecules in the other) is negligibly small in comparison with transport by "flow", a condition which may not always be fulfilled; moreover quite a small ratio of the net transport of matter by diffusion (i.e. the excess diffusive transport of one species) to the total transport may correspond to a much larger ratio of the number of *atoms diffusing* to the *total transport of atoms*. Again, Steiner assumes constancy of pressure in developing his flow-equation; and, although in applying it he makes an allowance for the pressure gradient, this still leaves uncorrected the erroneous equation, $d[\mathrm{H}]/dz = -d[\mathrm{H}_2]/dz$, involved in the assumption of a constant pressure.

The equation for the transport of H atoms and H_2 molecules in mixtures of the two species may be accurately and conveniently expressed in the form derived below, which takes account of the pressure gradient, and is generally applicable, whatever the relative importance of diffusion and "flow", e.g. in the extreme case of diffusion into a closed side-tube.

Let n_0 be the number of undissociated molecules stoichiometrically equivalent to the total amount of hydrogen flowing per second through a tube of radius r; and let n_a and n_m be the respective numbers of atoms and molecules per second passing a cross-section of the tube at z in the direction of flow; then n_0 must be equal to $n_m + \frac{1}{2}n_a$. It will be assumed that surface recombination of atoms does not lead to an appreciable radial concentration gradient, i.e. that throughout a cross-sectional element $\pi r^2 dz$ the composition of the gas is constant. Since there is a drop of total pressure in the direction of flow of the gas, let p_z be the pressure at z. There is also a fall in atom concentration along the tube owing to recombination; this leads to diffusion of atoms forwards and of molecules backwards. Let D_a and D_m be the diffusion coefficients for atoms and molecules respectively at pressure p_z. Then the number of atoms diffusing forwards per second past the cross-section is $-\pi r^2 D_a \,.\, d[\mathrm{H}]/dz$, and of molecules $-\pi r^2 D_m \,.\, d[\mathrm{H}_2]/dz$. The number of atoms per second passing this cross-section by *non-diffusive* flow is then $n_a + \pi r^2 D_a \,.\, d[\mathrm{H}]/dz$, and of molecules $n_m + \pi r^2 D_m \,.\, d[\mathrm{H}_2]/dz$. The ratio of these last two numbers is clearly equal to $[\mathrm{H}]/[\mathrm{H}_2]$, i.e. $\lambda/(1-\lambda)$. Thus

$$(1-\lambda)\left(n_a + \pi r^2 D_a \,.\, \frac{d[\mathrm{H}]}{dz}\right) = \lambda\left(n_m + \pi r^2 D_m \,.\, \frac{d[H_2]}{dz}\right).$$

But $2n_0 = 2n_m + n_a$, so that, eliminating n_m, we have

$$n_a = \left(\frac{2\lambda}{2-\lambda}\right) n_0 + \frac{2\pi r^2}{2-\lambda}\left[\lambda D_m \,.\, \frac{d[\mathrm{H}_2]}{dz} - (1-\lambda)\, D_a \,.\, \frac{d[\mathrm{H}]}{dz}\right].$$

Now $$\frac{d[\mathrm{H}]}{dz} = \frac{d}{dz}\{M'p_z\lambda\} = M'\lambda\,.\,\frac{dp_z}{dz} + M'p_z\,.\,\frac{d\lambda}{dz},$$

and $$\frac{d[\mathrm{H}_2]}{dz} = \frac{d}{dz}\{M'p_z(1-\lambda)\} = M'(1-\lambda)\,.\,\frac{dp_z}{dz} - M'p_z\,.\,\frac{d\lambda}{dz}.$$

(Steiner used $d[\mathrm{H}]/dz = -d[\mathrm{H}_2]/dz$ throughout.) Furthermore, D_a and D_m vary inversely as the pressure, so that we may write $p_z D_a = D_1$ and $p_z D_m = D_2$, where D_1 and D_2 are the diffusion coefficients of atoms and molecules at 1 mm. pressure. Hence

$$n_a = \left(\frac{2\lambda}{2-\lambda}\right)n_0 - \frac{2\pi r^2 M'}{2-\lambda}\left[\left(\frac{d\lambda}{dz}\right)\{\lambda D_2 + (1-\lambda)D_1\} + \frac{1}{p_z}\left(\frac{dp_z}{dz}\right)\lambda(1-\lambda)(D_1 - D_2)\right]. \quad \text{(I A)}$$

For the discharge tube, the difference between the numbers of atoms per second passing cross-sections at x and $x+dx$ is

$$2\eta_\lambda\left(\frac{dw}{dx}\right).\,dx - R_x\,.\,dx = dn_a,$$

and hence

$$2\eta_\lambda\left(\frac{dw}{dx}\right) - (A\lambda + B\lambda^2 + C\lambda^3) = \frac{d}{dx}\left\{\left(\frac{2\lambda}{2-\lambda}\right)n_0 - \frac{2\pi r^2 M'}{2-\lambda}\left[\left(\frac{d\lambda}{dx}\right)\{\lambda D_2 + (1-\lambda)D_1\} + \frac{1}{p_x}\left(\frac{dp_x}{dx}\right)\lambda(1-\lambda)(D_1 - D_2)\right]\right\}. \quad \text{(II A)}$$

Here $n_0 = \frac{1}{2}MpU_0$: the factor $\frac{1}{2}$ arises from the division of the hydrogen stream into two parts, and p is the pressure at which U_0 is measured.

For the delivery tube a similar expression, (III A), may be obtained by putting y instead of x, and $dw = 0$; in this case $n_0 = MpU_0$ (the two streams of gas being reunited in this tube).

Unfortunately these equations are insoluble, even when the term involving $(1/p_x)(dp_x/dx)$ is negligibly small, as in the recorded experiments. We can, however, use them to calculate the *limiting forms* to which the functions $\lambda = f_1(x)$ and $\lambda = f_2(y)$ tend as W approaches zero. In this case λ, $d\lambda/dx$ and $d\lambda/dy$ approach zero everywhere, and therefore in the limit $n_a = \lambda n_0$, $R_x = A\lambda = Af_1(x)$ and $R_y = A\lambda = Af_2(y)$. Also for the discharge tube $dw/dx \to W/2m$ and $\eta_\lambda \to \eta_0$ everywhere, and consequently

$$dn_a = n_0\,.\,d\lambda = (\eta_0 W/m)\,.\,dx - A\lambda\,.\,dx,^*$$

---

[*] A diffusion term involving $d^2\lambda/dx^2$ is here neglected; inclusion of this term leads to equations too complicated for use, but its omission appears to be justified on physical grounds.

i.e.
$$\frac{d\lambda}{(\eta_0 W/mA)-\lambda} = \frac{A\,.\,dx}{n_0}.$$

Since $\lambda = 0$ at $x = 0$, the solution of this is

$$\lambda = \frac{\eta_0 W}{mA}(1-e^{-Ax/n_0}),$$

where $n_0 = \frac{1}{2}MpU_0$. But from equation (X), p. 440, $W/\lambda_m = MpU_0/2(\lim \mu_m)$ in the neighbourhood of $W = 0$, and hence

$$\lambda = f_1(x) = \frac{\eta_0 MpU_0\lambda_m}{2mA\,.\,(\lim \mu_m)}(1-e^{-2Ax/MpU_0}). \qquad \text{(IV A)}$$

For the delivery tube the differential equation is obviously

$$d\lambda/\lambda = -(A/n_0)\,.\,dy,$$

in which $n_0 = MpU_0$. The solution of this, using $\lambda = \lambda_m$ at $y = 0$, is easily seen to be

$$\lambda = f_2(y) = \lambda_m e^{-Ay/MpU_0}. \qquad \text{(V A)}$$

ACKNOWLEDGEMENTS

The author desires to acknowledge his indebtedness to Professor C. K. Ingold for his interest in this work, to the Department of Scientific and Industrial Research for a grant during part of the research, and particularly to Dr. R. W. Lunt for his kindness in communicating the theory of reactions in discharges, prior to its publication.

E—SUMMARY

This investigation shows that the empirical behaviour of the discharge tube for the range of pressure usually employed in hydrogen-atom studies is very satisfactorily represented by equation (III) and the data in Table IX. The importance of high pumping speeds has been demonstrated, and emphasis laid on the desirability of using a large cathode chamber and a wide-bore vacuum system. Analysis of the conditions in the discharge tube and delivery tube has indicated the reasons for the relationship expressed by equation (III); and has led to the determination of the Emeléus-Lunt-Meek efficiency η_0 for the sum of the two dissociative processes involving the $^3\Sigma_u^+$ and $^3\Sigma_g^+$ states of the molecule, over a considerable pressure range. The variation of η_0 as the pressure is changed is in satisfactory agreement with

the theoretical values, provided a correcting factor of 2·6 is applied to the probability cross-section for $^3\Sigma_u^+$ excitations as calculated quantum-mechanically by Massey and Mohr. The velocity constant for the first-order, wall-catalysed recombination of atoms has been found, and hence the adhesion coefficient γ for a water-on-phosphoric acid film, i.e. the fraction of the total number of collisions of atoms with the walls which lead to loss of an atom; γ is found to be $3{\cdot}9 \times 10^{-5}$. In addition, a general equation for the flow of atoms and molecules through a tube has been developed.

REFERENCES

Crew and Hulburt 1927 *Phys. Rev.* **30**, 124.
Emeléus, Lunt and Meek 1936 *Proc. Roy. Soc.* A, **156**, 394.
Hertz 1923 *Z. Phys.* **19**, 35.
Lunt and Meek 1936 *Proc. Roy. Soc.* A, **157**, 146.
Lunt, Meek and Smith 1937 *Proc. Roy. Soc.* A, **158**, 729.
Steiner 1935 *a* *Trans. Faraday Soc.* **31**, 623.
— 1935 *b* *Trans. Faraday Soc.* **31**, 962.
Wrede 1929 *Z. Phys.* **54**, 53.

Address of the President Sir William Bragg, O.M., at the Anniversary Meeting, 30 November 1937

This year the list of those whom death has taken from our Society is very long and heavy.

JOHN THEODORE CASH (1854–1937) was a Fellow of the Society for nearly fifty years. He was very active in research during the eighties and nineties of the last century, and his work helped materially to characterize British pharmacological research of that period. The results of his more important researches were contributed to the Society. They were mainly concerned with the connexion between chemical constitution and pharmacological action and were made in conjunction with the late Sir Lauder Brunton and afterwards with Professor Dunstan. His name will always be associated with the pharmacological action of organic nitrites and of the various aconitines prepared by Dunstan. But his contributions ranged over a wide field, and many were made to other Societies and Associations. All his work was done with enthusiasm and with most painstaking care. These characteristics were shown in his various activities in connexion with the great war. Personally he was of a somewhat retiring disposition but was a charming companion for those who were favoured with his friendship. His chief recreation was salmon and trout fishing, and to a former generation he was widely known as an expert angler.

EDGAR HARTLEY KETTLE, Professor of Pathology at the London Postgraduate School of Medicine, died December 1, 1936 at the age of 54. He was successively, pathologist to the Cancer Hospital, Fulham, Lecturer on Pathology, St. Mary's Hospital, Professor of Pathology at Cardiff, at St. Bartholomew's Hospital, and from 1934 till his death at the London Postgraduate School at Hammersmith. The subjects of his contributions to pathology range from tumours to silicosis. His work on the latter subject and on the effects of noxious dusts, important in industry, are a permanent contribution to knowledge, and the experimental methods he devised for their investigation have improved our resources in the study of this difficult and economically important field. Kettle insisted on the specificity of the lesions produced in the tissues by irritants, whether microbic or inanimate, and showed in his work how these changes could be used as indicators for their presence and causal importance in disease.

In the various schools in which he worked Kettle showed his personal gifts of teaching and administrative ability, and his tact and balanced judgement made him friends everywhere. His election to the Fellowship in May 1936, six months before his death, was welcomed by pathologists throughout the country. His premature death is a loss to the Society as well as to scientific medicine.

Sir HERBERT JACKSON (1863–1937) has been perhaps most widely known for his work, during the great war, on "Chemical and Optical Glasses", the national importance of which has tended to distract attention from his investigations into phosphorescence and phosphorescent materials, the chemistry of photographic processes, his early work in the X-ray field, and so forth.

Primarily, Jackson was an experimenter. Under Bloxam he received a thorough training as an organic chemist, and during his subsequent career he applied his chemical knowledge and his extraordinary energy and experimental skill to the investigation of any problems which came or were brought to his attention.

He was also a microscopist of the first rank, and his microscope was in constant use to assist him in the various investigations which he undertook during a singularly active and varied career.

He published little and kept only the scantiest of notes, but the variety and extent of the work which he did could be gauged by the wealth of knowledge and experience which he could bring to bear on matters of the most diverse character, and by the esteem in which his opinion and advice were held by all who had occasion to call upon him for assistance.

The career of ALFRED ARTHUR ROBB (1873–1937) was entirely devoted to intensive study and investigation. Even at school and College the original trend of his thoughts interfered with his record of success along the normal lines. After graduating at Belfast and later at Cambridge he passed on to Göttingen, where under the influence of W. Voigt he became immersed in the theory of the spectromagnetic effect of Zeeman, then passing from its simple origins into complex developments which are now fundamental, and his degree thesis was for that time a notable analysis of the subject. But his later interests were on the philosophical side. Ever since the days of the great astronomer Bradley, a friend of Newton, there had been a latent discrepancy in the relations of time and space arising from the time required for light to travel, which has only recently been tackled at length, mainly along the impressive lines developed by Alfred Einstein. This, which had become experimentally prominent under Michelson and Rayleigh, was just the kind of subject to excite Robb. His way of probing it to the bottom was from a postulate that the ultimate formative element in the cognition of every observing mind was simply linear succession of impressions in time, named by him the principle of before and after, and he had already advanced and perhaps established the thesis that in order that these impressions of various observers throughout the universe should be mutually consistent, the events to which they relate must be arranged in spatial order not, however, confined to the simple Euclidean space. The mode of argument comes out perhaps most simply in the introductory chapter of the recent second edition of his main book, which he named a "Theory of Space and Time".

Sir GRAFTON ELLIOT SMITH was born in Australia in 1871. After a distinguished early career at the University of Sydney, he entered St. John's College, Cambridge, in 1896. There he obtained a Fellowship in 1899 and was elected an Honorary Fellow in 1931.

In 1900 he was elected to a Chair of Anatomy in the Egyptian School of Medicine in Cairo. From Cairo he was called in 1909 to occupy the Chair of Anatomy in the University of Manchester. After ten fruitful years of work there, he succeeded Sir George Thane in the Professorship of Anatomy in University College, London, where he remained until his retirement in September 1936.

In 1907 he was elected into the Fellowship of this Society, in which he served twice on the Council and also as Vice-President in 1913. He was awarded a Royal Medal in 1912. He received the honour of Knighthood in 1934, and in 1936 the Decoration of Chevalier de l'Ordre National de la Légion d'Honneur.

Elliot Smith's contributions to the subject of brain morphology, both in the way of ascertained fact and in interpretation, were such as to give his work a permanent place in the development of neurological science. He holds a high place for contributions to anthropological science, such as his studies on mummification and on the problem of Egyptian origins: perhaps even more important were his studies in the problem of human ancestry in general. To many of his contemporaries, especially in his later period, he was probably best known as an apostle of what is known as the "diffusionist school" in reference to human cultural origins. Around this phase of his activity controversy has been keen and vocal, his own voice being by no means lacking in resonance.

No account of Elliot Smith, however brief, must fail to take note of his essentially lovable disposition, never quenched by the clamour of the arena.

Nor would any account of him be at all adequate which lost sight of the enthusiasm which he inspired in his pupils and co-workers, for whom he was, and remains, a memorable personality.

On January 13 of this year ROBIN JOHN TILLYARD met an accidental death in Australia. Born in 1881, his early training and career were mathematical. His dominant interest in later years was in animal life, and he became a professional entomologist. After eight years on the staff of the Cawthron Institute, Nelson, New Zealand, he became, in 1928, Commonwealth Entomologist for Australia. He held this post only six years when ill-health forced his retirement. His early biological work was on dragonflies, upon which he wrote many important papers. These researches led him to study the broader problems of wing venation, to the solution of which he made significant contributions. These in turn prepared him for the investigation of the highly interesting fossil insects which were then being disclosed, and his many contributions in this field made him the leading exponent of his day. He also wrote extensively on the more primitive orders of insects living in the Antipodes, and he was the author of a large textbook on the insects of Australia and New Zealand. In economic entomology he achieved notable success in applying biological control to the woolly aphis of the apple in New Zealand. Tillyard became a Fellow of the Royal Society in 1925.

JOHN ALEXANDER MACWILLIAM (1857–1937) studied at the Universities of Aberdeen, Edinburgh and Leipzig, and at University College, London. From 1886 to 1927 he held the Regius Chair of Physiology at Aberdeen. He spent his life investigating the circulatory system, particularly the regulation of the activity of the heart. His early inspiration was drawn from Dr. W. H. Gaskell of Cambridge, and he owed much to his training at the famous school of Ludwig at Leipzig. His researches were at times interrupted by indifferent health, but in spite of that he published important papers which have won him a great reputation. He was a gifted lecturer. He was elected to our Society in 1916.

MAX WEBER, who died last February in his eighty-fifth year, was elected a Foreign Member of our Society in 1935. He was a famous teacher, who taught the whole present generation of Dutch zoologists; and he was himself the last great example of the old school of naturalists who took the whole world for their field of study. As a comparative anatomist he did for our day what Owen did for mammalian anatomy in his; as a student of fishes he set in order the whole rich fauna of the East India Seas; as a traveller and explorer he brought home from the north and the south and the east immense collections for his brother naturalists and himself to study. He was a man of wide culture and great distinction, honoured and beloved throughout the whole brotherhood of zoologists.

FRANCIS SOWERBY MACAULAY, born near Oxford and educated at Bath, graduated from St. John's College, Cambridge, in 1882, and after some time at his old school settled down for many years as chief mathematical master at St. Paul's School. That he was a schoolmaster of novel and quite outstanding ability is shown by the long list of distinguished men whom he sent out. On retirement he settled in Cambridge, was made F.R.S. in 1928, and though hampered by increasing weakness in his last years, continued his interest in his work and in the work of younger men to the end.

He was a man of penetrating logical mind, and was attracted while still a schoolmaster by the algebraical difficulties surrounding a formula, given by Max Noether, for the expression of the equation of a plane curve passing through the intersections of two given curves. This study, to which he devoted many published papers, led him to the study of modular systems, that is, systems of algebraical polynomials which are expressible linearly by means of definite polynomials (with coefficients suitably chosen polynomials). The work had a very living interest in connexion with Hilbert's remarkable proof for the finiteness of the system of invariants of a binary form; this question of finiteness had been a major preoccupation for Cayley and Sylvester and Paul Gordan over many years. Macaulay developed his investigations into a Cambridge Mathematical Tract (1916), which remains a striking contribution to a subject little known in this country. His later writings were for the most part developments of this earlier work.

When WILLIAM TAYLOR, who was elected to our Society in 1934, died in February of this year, the country lost a very great designer and organizer in the realm of fine engineering and optical instruments. As the moving spirit in his firm during the half-century from 1887 to 1937 he developed the design of their precision products, and organized the manufacture of camera lenses of high quality, until Taylor, Taylor and Hobson and their products were known in every country of the world.

But he had more important, though less spectacular, works to his credit. By his work on Government, British Association and other Committees, he materially raised the standard of mechanical and optical manufacture in this country.

As a designer he showed a comprehensive knowledge of engineering practice, an authoritative grasp of the result to be desired, and an untiring patience till his goal was reached.

These qualities were equally brought into play in the running of his factory, which indeed seemed in its arrangements to be characterized by the same accuracy and beauty of design as were displayed in the objects which it produced.

Sir HENRY CAPEL LOFFT HOLDEN was born in 1856, was educated at Ipswich School and the Royal Military Academy. He entered the Royal Artillery in 1875, served in India and was subsequently Superintendent of the Royal Gun and Carriage Factories at Woolwich. As a serving officer he was instrumental in introducing scientific methods into Woolwich Arsenal, particularly in all that concerned the testing of guns and explosives. He possessed a thorough practical knowledge of electricity, and considerable inventive genius. He was a keen experimenter, who was much aided in the design of the various instruments which he invented by his very highly developed skill as an amateur mechanic. The proof butts at Woolwich were first equipped with an efficient modern instrument system as a result of his activities, and the Holden chronograph is still in use for the determination of muzzle velocities. His technical services were also utilized by the War Office in the reorganization and re-equipment of the Royal Gun Factory and the Royal Carriage Factory. The technical excellence of British gunnery during the great war was largely due to his belief in the need for the systematic application of science to technical problems.

SYDNEY YOUNG died on April 9 in his eightieth year. Having worked under Roscoe and Schorlemmer at Owens College he was appointed as Ramsay's assistant in 1882. A long series of papers has linked the names of Ramsay and Young, and set a standard of excellence in physico-chemical determinations. They undertook a systematic investigation of the vapour pressures of solids and liquids, the thermal properties of pure liquids, and the thermodynamical relations involved. Succeeding Ramsay in the Chair at Bristol, Young continued with undiminished energy and, with his pupils, studied the critical constants of pure liquids. The Society's Fellowship, bestowed at the age of 36, was a recognition of the value of this work. The necessity of having liquids of the highest purity led him to study methods of purification by fractional distillation, and it is for this work, purification by means of the formation of binary and ternary mixtures of constant boiling-point, that his name is best known. Along these lines his work found numerous industrial applications. From 1904 to 1928 he held the University Professorship of Chemistry at Trinity College, Dublin. There teaching duties left little time for research, but he published several articles and two important books.

ARTHUR HARRY CHURCH, whose whole life as a working botanist was spent in the Department of Botany at Oxford, combined remarkable distinction of mind with a peculiar mentality, not free from a certain aloofness, which tended to cut him off from his fellow-botanists. He never followed beaten tracks, nor devoted himself to "fashionable" work, but always took his own line, reconsidering many problems in an original way on the basis of patient, long-continued and penetrating investigations. His primary interests were in morphology, and his powers of observation and delineation of plant structures were of the highest order. His theoretical writing was sometimes one-sided, but always valuable and stimulating, and while some of his views have not been and are not likely to be accepted, he illuminated many topics by his fresh treatment and comprehensive outlook. Probably the work least open to criticism is his study of phyllotaxis, which undoubtedly placed the subject on a sound basis. Much of his long paper on "Thalassiophyta", in which he dealt with the condition of evolution of plant life in the sea and its later adaptation to land conditions, is extremely interesting and valuable. Some of Church's best work—notably on the morphology of the flower—was never published, but remains buried in notes for his students. As a teacher he was pre-eminent, and many generations of Oxford undergraduates remember with deep gratitude the stimulus of his teaching, at once critical and constructive. Probably Church had a wider knowledge of the facts and problems of botany—other than the purely physiological—than any teacher of his generation; and he left a deep and lasting impression on the Department in which he laboured continuously and devotedly for more than 30 years.

ARTHUR GEORGE PERKIN was born in 1861, a member of a family devoted to chemical research. He worked under Franklin and Guthrie at the Royal College of Science and subsequently in the Dyeing Department of the Yorkshire College at Leeds. For ten years he was with a Manchester firm, manufacturing alizarin, and had been for some time manager when he left in 1892 to join the Yorkshire College as lecturer and research chemist. In 1916 he succeeded A. G. Green as Professor of Colour Chemistry.

Perkin's fame rests securely on his fine contributions to our knowledge of natural and synthetic colouring matters. He wrote a very large number of papers of importance; he contributed many of the articles on natural dyes in Thorpe's "Dictionary", and with A. E. Everest he published in 1918 a standard work on "The Natural Organic Colouring Matters".

Perkin was an able and inspiring teacher. Though his ways were gentle, his influence was profound. He was very successful in fitting men for industrial work, and the department over which he presided in the University of Leeds acquired a high reputation as a centre both of knowledge and training. His work has been of national importance. He became a member of our Society in 1903, and in 1924 he was given the Davy Medal, which he thoroughly deserved.

The career of THOMAS MATHER illustrates the capacity-catching value of Whitworth Scholarships. One of the first of these was gained by Mather in 1878 after a strenuous five years' engineering apprenticeship combined with regular attendance at evening classes. He was thus enabled at the age of 22 to enter a four-years College course, through which he passed with great distinction. He became an assistant to Professor Ayrton, first at Finsbury and afterwards at South Kensington. On the death of his chief he succeeded him as Professor of Electrical Engineering.

He began to teach when electrical engineering was an entirely new industry. His main life work consisted in the initiation and development of teaching appliances suitable for technical students and also in the help which he gave to laboratory workers of all grades. He was an able pioneer both in the College work which had to precede the commercial production of good instruments and in the equipment of laboratories for industrial testing and research.

The value of his work was recognized by his election as F.R.S. in 1902. Six years later he was joint author with Professor Ayrton and F. E. Smith of three important papers published by the Royal Society and dealing with the establishment of the National Electrical Standards.

The death of HENRY EDWARD ARMSTRONG on July 13, in his ninetieth year, deprives our Society of its senior Fellow (his election dating so far back as 1876), and many scientific institutions and assemblies of a familiar and distinguished figure. When the Davy Medal of the Society was presented to Professor Armstrong in 1911, in recognition of his researches in organic and physiological chemistry, reference was made to the active part he took in the discussion and criticism of current theories in chemistry, and to the fruitful fields of inquiry which he originated or in which he co-operated.

Throughout his scientific life, the spirit of the motto of our Society was manifest in him; and his judgement was never influenced by authority. An example of his departure from orthodox methods was the introduction of crystallography into the course of practical chemistry at the City and

Guilds College, fifty years ago, in association with Sir Henry Miers. This largely determined the character of important later researches by his two assistants, Sir William Pope and Professor T. M. Lowry, both of whom became Fellows of our Society. Four other Fellows who were his colleagues or students, and whose work he inspired, are Professor W. P. Wynne, Professor Stanley Kipping, Professor A. Lapworth, and his son, Dr. E. F. Armstrong. His students occupy leading positions in science and industry in many parts of the world; and in August 1927 they presented to him and Mrs. Armstrong his portrait by Mr. T. C. Dugdale, exhibited at the Royal Academy in that year.

Professor Armstrong was an acute observer and inquirer in many scientific fields other than that of chemistry, such, for example, as agriculture, botany and geology, and he was an untiring advocate of the introduction of research methods into science teaching at all stages.

GEORGE ADOLPHUS SCHOTT (1868–1937) was educated at Bradford Grammar School and Trinity College, Cambridge. He was for a long time Head of the Department of Applied Mathematics at Aberystwyth. The solution of the Hertz-Heaviside form of Maxwell's equations corresponding to the general motion of a point charge is effected by means of the retarded potentials of Liénard. Except in the simplest cases, such as uniform rectilinear motion and in the case of quasi-stationary motion, the evolution of these potentials presents a problem of extreme complexity. Schott was excelled by none in finding out cases capable of explicit expression in elliptic functions and in obtaining Bessel expansions of great generality. His Adams Prize essay, which was published in 1912 under the title "Electromagnetic Radiation", seemed to contain the utmost contribution of the classical theory to the radiation problem. The advent of the Bohr theory, however, turned his attention to the possibility of radiationless orbits, and it is gratifying to know that he crowned his long researches on this subject by actually discovering such orbits within the scope of the classical theory. His last paper containing this discovery was published in the *Proceedings of the Royal Society* in April of this year. In size such orbits were much smaller than the Bohr orbits, and sadly enough in his last paper he speaks of future developments to follow. What possibilities lie in Schott's orbits is a matter for the future.

Among those who drew their inspiration from, and furthered, the pioneer work of Cayley, Sylvester and Salmon in the algebraic invariant theory in the nineteenth century, EDWIN BAILEY ELLIOTT takes a very distinguished place. His peculiar gift of analytical manipulation of complicated mathematical structures was governed by a rare insight and feeling for the natural approach and the appropriate line of enquiry. Continental mathematicians, notably Gordan and Hilbert, had advanced the invariant theory by discoveries of capital importance as to the finiteness of certain apparently infinite systems, this stage being completed in the year 1890. Elliott, who already had shown plain signs of his analytical skill, thereafter became the chief interpreter of these newer concepts in terms of the original operation and theories of Sylvester. His book—the "Algebra of Quantics"—which first appeared in 1895, is a model of its kind, and could not be bettered for lucidity and charm. It is an admirable introduction to his own considerable original writings, and those of his forerunners. His latest published work lay in the field of pure analysis, where he produced a beautiful and simple proof of a theorem on the convergence of positive terms that had taxed the ingenuity of leading analysts. Professor Elliott died on July 21, at the age of 86.

Sir DAVID ORME MASSON (1858–1937) was a son of the Regius Professor of English in the University of Edinburgh. He was a student at the Edinburgh Academy, and afterwards graduated at Edinburgh University. After a short period of research under Crum Brown he became assistant in 1880 to Sir William Ramsay at Bristol. In 1886 he became Professor of Chemistry in the University of Melbourne. A brilliant and inspiring teacher, Masson built up a fine school of chemical research, and thereby exerted a steady influence upon the development of Australian science. He was a leader in the foundation of Australia's scientific institutions. Among these were the Commonwealth Advisory Council of Science and Industry, of which he was deputy-chairman from 1916 to 1920; the Australian National Research Council, of which he was president from 1922 to 1926, and the Australian Chemical Institute, of which he was in 1924 the first president.

Masson's researches were concerned chiefly with physical chemistry, more particularly with the theory of solutions, ionization and chemical dynamics. He had remarkable originality and foresight, so that a long series of important papers came from his laboratory. He was a keen exponent of the ionic theory in its early days, and made many contributions to it. He was the author of important and prescient suggestions respecting the periodic system, the composition of the atom and the laws of electrolysis.

He was a man of great charm, and had a rare gift of lucid exposition. In his long life in Australia he grew to be a loved and venerated leader. He became a Fellow of the Society in 1903.

Lionel Walter, second Baron Rothschild of Tring, who died on August 27 at Tring, aged 68, was greatly devoted to zoology all his life. Before he was thirty he had become in that branch of biology an outstanding figure of world-wide reputation. The cottage he built at Tring in 1889 for the housing of his collections was the small beginning of a museum that has since grown to a great size and contains series of specimens, such as those of anthropoid apes and cassowaries, which are unequalled in any public museum. The greatest asset in the research department is the collection of some two million Lepidoptera providing invaluable material for the study of evolution. All the collections were at the service of specialists, who found the museum an ideal place for working. Lord Rothschild's writings on systematic zoology were very numerous and varied, and his activities were so much appreciated that many foreign scientific societies elected him an honorary member. In 1898 the University of Giessen conferred on him the degree of Dr.Phil. In 1899 he was elected a Trustee of the British Museum; and in 1911 he became a Fellow of the Royal Society. From 1899 to 1910 he represented Mid-Buckinghamshire in Parliament. In a codicil to his will he left his museum to the Trustees of the British Museum on condition that it be continued in some form or other for the benefit of zoological research.

Albert Heim died on August 31 at the age of 88. For sixty years he had been the best known figure among Alpine geologists. His statement of the Glarus "Double Fold", a theory originating with Escher, brought him into prominence in 1878. His eventual recognition in 1902 of the truth of the rival one-way interpretation was a notable event. His "Geologie der Schweiz", 1919–22, furnished an imperishable memorial.

Heim's geological interests were very wide. He made important contributions to stratigraphy, tectonics, metamorphism, glaciology and the study of scenery. He wrote fluently, and had rare skill both as draughtsman and as engraver. With his own hand he engraved many of the illustrations that adorn his text. His delightful personality in its venerable stage will long be remembered both at home and abroad. He was the doyen of the Society's Foreign Members and the last survivor of those elected in the nineteenth century.

Alfred James Ewart was a botanist of varied interests. He was born in Liverpool in 1872 and educated at Liverpool Institute and University College, Liverpool. When only twenty-two he published two contributions to plant physiology, dealing respectively with vitality and germination of seeds and the germination and growth of pollen tubes. At Leipzig under

Pfeffer, he carried out an investigation on assimilatory inhibition in chlorophyllous plants. At Birmingham he occupied a succession of posts ranging from science master at King Edward's School to Deputy-Professor of Botany in the University. During this period Ewart published a number of memoirs on various aspects of plant physiology, including a book on protoplasmic streaming in plants and a paper on the ascent of water in trees which appeared in *Philosophical Transactions*. But, the best known of his botanical achievements during this period of his life is his translation of Pfeffer's "Physiology of Plants" published by the Oxford University Press in three volumes.

In 1906, Ewart was appointed to the Chair of Botany and Plant Physiology in the University of Melbourne. Until 1921 he also held the post of Government Botanist to the Government of Victoria. In Melbourne Ewart maintained his interests in plant physiology and a number of papers dealing with researches on vitality of seeds, ascent of water and photosynthesis appeared from his pen. He wrote also on questions of forestry and mycology. Perhaps his most important publication in the sphere of systematic botany is his "Flora of Victoria".

The gap caused by the death of BARON RUTHERFORD OF NELSON, still in full vigour of mind and body, is one which will be felt far and wide for a very long time. He unravelled the tangled skein of radioactivity with a persistence and acumen rare in the history of science. He modified all our views of atomic theory, and showed that the nucleus of an atom carried most of the mass and all the positive charge. His crowning feat was the first step in the transmutation of matter. He founded schools of able enthusiasts at McGill, Manchester and Cambridge. He combined rare judgment and insight with remarkable manipulative skill and by his genius inspired others to fine achievement. Honours deservedly poured upon him: Order of Merit, Nobel Laureate, President of the Royal Society, a Peerage, but none of these could spoil his friendly, strong and simple character.

I shall not attempt on this occasion to review his scientific achievements, nor to tell the story of his life. So great and wide have been the sense of loss and the desire to pay him tribute that innumerable references have already been made to him. Friends, colleagues, students and many who had never met him but had grasped the value of his work, have recorded their admiration and drawn pictures of him from their different points of view. Already they have constructed for him an imperishable record, though indeed the marvellous advances in scientific knowledge which we owe to him have already given him honour and a name which can never be forgotten. It is only left to me to record here the veneration and affection which in this Society have been his in abundant measure.

Sir HERBERT MAXWELL was born at Edinburgh in 1845 and was educated at Eton and Oxford. He was kin to those who in earlier and doubtless easier days took, or tried to take, all knowledge for their province. In no field did he work intensively, but what he may have lost there he gained in extension, and in a resultant balance of judgment. In the event he achieved a remarkable distinction.

All his life he was a student of the country-side. The Annals of Scottish Natural History, and various horticultural Journals contain short contributions detailing his observations. He was in many ways the Gilbert White of his country and of the neighbouring shires. He was President of the Society of Antiquarians of Scotland for many years and Rhind Lecturer in Archaeology at Edinburgh University on two occasions. He was in 1910 Lecturer on Scottish History in the University of Glasgow. He wrote a number of historical and biographical pieces. For painting and sketching he had both talent and enthusiasm, and their pursuit occupied much of his leisure. He was Member for his county for 26 years, holding his seat in an uninterrupted series of seven general elections. He was a Lord of the Treasury, a Government Whip, Chairman of the Tariff Reform Party in the House of Commons (1903) and Lord Lieutenant of his County. His interest in Scottish History and Literature is reflected in his Chairmanship of the National Library of Scotland. He was an officer in the Ayrshire militia for 21 years. He was a keen fisherman and a good shot.

Diffused as were his interests, his energies were rarely misdirected. North of the Tweed he occupied a very special place in the eyes of his countrymen—a very old and wise Nestor who could give advice to the point on most matters and did not hesitate to tender it.

The sudden death of JAMES RAMSAY MACDONALD from heart failure when on a voyage to South America will be deeply regretted by the Fellows of the Society. In his early days he was a keen student of science, and would no doubt have held to research and teaching all his life had he not become attached to a remarkable group of social reformers in Bristol fifty years ago. Even when he left Bristol to come to London he continued his studies of scientific subjects privately and at Birkbeck College with a view of obtaining a scholarship or exhibition in the old Science and Art Departments examinations. It was impossible, however, for him to find time outside his daily working hours for the intensive study required, and he had to abandon his early hopes.

This is not the occasion for an account of Ramsay MacDonald's great political career. We remind ourselves, however, that when in 1935 he resigned his office as Prime Minister and First Lord of the Treasury, he became Lord President of the Council, and as such was responsible to Parliament for the reports of the Department of Scientific and Industrial Research and of the Medical and the Agricultural Research Councils. He took a particular interest in the work of these Departments. He had indeed maintained his scientific interest throughout his life, and on the ground that he "had rendered conspicuous service to the cause of science" he was elected a Fellow in 1930.

News has just been received in England of the death of Sir JAGADIS CHUNDER BOSE. He was born in 1858, and was educated at Calcutta and Cambridge. In the closing years of last century Bose made a number of ingenious experiments on Hertzian waves. He succeeded in generating waves of such high frequency that it became possible to examine their reflection, refraction and polarisation by means of instruments little more cumbrous than their optical analogues. In later years he was much interested in the response of plants to various forms of stimulus. He founded and directed the Bose Research Institute. He presided over the Indian Science Congress in 1927. He became a Fellow in 1920.

Fellows will have learnt with great pleasure that HIS MAJESTY KING GEORGE VI has graciously consented to be the Patron of the Society, thus continuing a practice which has been, from the foundation of the Royal Society, a source of pride and gratification.

We are grateful also for His Majesty's promise to continue the annual grant of two Royal Medals.

I would like to refer briefly to certain interesting events of our past year.

An informal discussion between the Officers of the Society and an Officer of the National Academy of Washington has led to a very happy result. It was proposed that in alternate years the Society should invite and entertain a distinguished lecturer from the United States, and the Academy should arrange the converse proceeding. The Pilgrim Trust was consulted on the question of providing the money required for the scheme, and most generously offered a sum of 1500 guineas, which in the opinion of the Trust should provide for suitable honoraria to be paid to the lecturers in six successive years. An exchange of communications between the Academy and the Society has resulted in the completion of the necessary arrangements, and the first Pilgrim Trust Lecture will, it is expected, be given in London in the coming summer.

Fellows will, I am sure, feel that no more agreeable way of emphasizing the cordial relations between American and British science could have been devised. Although modern communications are so rapid and complete and views spread so quickly, there is a personal character in the research of each man who breaks into a new field, and this interesting and important character can only be communicated by the man himself. In my opinion these lectures should not be mere summaries of past work, nor general discussions of scientific advance. It might be their special feature that they should transfer from one side of the Atlantic to the other new ideas which had already begun to be fruitful and promised wide expansion in the future. Such lectures would associate workers in a common task, and encourage correspondence and the formation of friendships. The choice of lecturers would not be determined on the same plan as the choice for the awards of medals or other distinctions, but would rather bring into prominence the most important lines of advance of the day. The progress of science would be the object of the Pilgrim Trust Lecture, and not the honouring of scientists.

The provision of funds for six years is sufficient to make trial of the plan. If it is successful, as we may be sure it will be, we hope that means for its continuance will be forthcoming.

I am tempted to further hopes. It may be that the universal wish to promote peaceful relations between the nations of the world may find some who are willing to follow the example of the Pilgrim Trust. Of all the enterprises of mankind the acquisition of Natural Knowledge pays least attention to the divisions of men. We have national industries, national trade, national literature, national art, national characteristics, even national religion, but there is only one Nature for us to know. One could wish that the seasonal interchange of men to show to other nations what new illumination was dawning in this or that subject of enquiry could be firmly established and honoured by the emphatic recognition of the academies and indeed of the State itself. No greater gift could be made by one people to another than an illuminating idea; it would deserve a people's welcome.

In April the delegates to the General Assembly of the International Council of Scientific Unions met for conference in our rooms. Good use was made of the opportunity to discuss some important scientific matters of an international character. The meeting was a particularly pleasant one, largely on account of the personality of the President, Dr. Nörlund, whom many of us are now happy to remember as a friend. Dr. Nörlund conveyed to the General Assembly an invitation from the Royal Danish Academy of Sciences to meet in Copenhagen in 1940, which was accepted.

Last November, I spoke of the large sum which the late Mr. H. B. Gordon Warren had bequeathed to the Society. In the course of the year two Fellows have been appointed under the terms of the bequest. It will be remembered that Mr. Warren desired that the money should be applied to the encouragement of research in metallurgy, engineering, physics and chemistry. One of the new Fellows, Mr. Hartley, proposes to work on oil drops, films and solutions, and the other, Mr. Randall, on the mechanism of fluorescence in pure and impure solids. These subjects have that leaning towards the application of science which was clearly in Mr. Warren's mind; and it is interesting to observe how easily the choice falls into accord with great industrial problems of the day. We associate the study of phosphorescence in the past with but a few enquiring minds, among whom Sir Herbert Jackson, who was so recently with us, was prominent. When C. V. Boys gave the children's Christmas Lectures on soap bubbles at the Royal Institution in 1899, it was generally felt that the subject was redeemed from ultra-childishness only by the exceeding technical skill and the ingenious explanations of the lecturer. In these days the film, and phosphorescence, are very important indeed.

By the addition of these two Warren Fellows the research "staff" of the Society is still further increased. The work which has been accomplished during the year is described in an appendix to the Council Report. Fellows will agree, I am sure, that it makes a fine record.

During the year, four "discussion meetings" have been held, with much success. An attempt has been made on each occasion to collect, even from considerable distances, all who were interested in the subject for discussion, including particularly the younger men who might be working on it. The purpose in view was the encouragement and help that would be expected to follow from personal contact and exchange of information. The Royal Society has some right to look on the young workers of the country as, in a sense, *in statu pupillari*, and has a certain responsibility for their effectiveness. The very considerable sum—more than £30,000 a year—which the Society has undertaken to devote to the improvement of Natural Knowledge gives it power, up to a point, to control the direction of research; and in doing so, to help the workers to do their best. The impression formed at the discussion meetings was certainly one of conviction that they are a help and a pleasure to those who attended them.

The Council Report contains notices of bequests and gifts increasing further the resources of the Society which are to be devoted to research. The reference to Dr. J. H. Stothert will remind Fellows that a lamentable accident on an Austrian river has deprived medical science of an enthusiastic young worker who might have made important contributions to knowledge. Like Moseley, who also was young, he has left his fortune—in his case as a reversionary interest—to the Royal Society. The Society cannot but feel a tenderness in handling such gifts as these.

On a very interesting occasion during the year, a number of letters, which had long remained under seal in the Society's safe, were opened in the presence of Fellows and others. There were no inscriptions governing the manner and time of their opening, and it seemed to the Council that any limits must long have been passed. Several of them were very interesting in their matter, quite apart from the dramatic circumstances of their disclosure so long after their authors had written and sealed them and handed them for safe keeping to the Officers of the Society. The most interesting of all was a letter of Faraday's, written in 1832; it has been published in the Society's *Occasional Notices*, 2. It shows that he was then entertaining the idea that the "diffusion" of magnetic and electric forces was comparable with the spread of waves on water or in air, and had indeed a vibratory character. Perhaps because of preoccupations which hindered the development of the idea, and because of the difficulties of experiment, it was not until 1846 that he made public reference to the matter. In the latter year, Faraday had to take Wheatstone's place on very short notice at a Friday Evening Discourse at the Royal Institution, and found that when he had completed the description of the apparatus which he and Wheatstone had arranged during the afternoon, he had still in hand a portion of the lecture hour. He then went on to speak of his "Thoughts on Ray Vibrations" which afterwards formed the subject of a paper in the *Philosophical Magazine*. It was this paper that led Maxwell (*Phil. Trans.* 1865) to put Faraday's experimental results in a mathematical form, and finally to frame the electromagnetic theory of light. Until this letter was opened at the Royal Society meeting there had been no indication that Faraday's thoughts on ray vibrations had been simmering for so long.

The Report of Council describes alterations of some importance which have been made in the Statutes.

The Report also refers to progress made in the cataloguing, arranging and binding of manuscript letters belonging to the Society. It is well known that the Library contains very valuable material which has never been fully examined. It is surprisingly rich in historical documents, and also in early books and pamphlets. As these are brought into order, the value and interest of the Library will be much increased. The work requires, however, considerable time and labour, and is therefore expensive. The funds provided by the late Sir Arthur Church are at present being devoted to this purpose.

I should like to take this opportunity of welcoming our new Assistant Secretary, Mr. Griffith Davies, who will, I hope, find interesting work with the Society for many years to come. I would like also to thank Mr. Winckworth for his past services as Assistant Secretary, and to express the general satisfaction that he will now occupy himself with the most important task of the Assistant Editor of our publications.

One more matter, which has been mentioned in the *Occasional Notices*, deserves the special attention of the Fellows. Professor Salisbury made a generous donation of £25 towards the decoration of our rooms. The example is excellent. Our rooms are not large, we wish they were much larger. If we are not to enjoy the dignity of spaciousness, we can at any rate make the rooms beautiful; and there can be no doubt that much can be done to that end.

A cursory glance over the research work described in the scientific publications of to-day shows that remarkable interest is concentrated on magnitudes which are too small to be examined in detail under the microscope and too large to be studied conveniently by X-ray methods. Such magnitudes are to be found in all lines of research, medical, industrial, and purely scientific. Their behaviour presents numerous problems of great interest, and also of considerable difficulty. Solutions are of pressing importance, because the want of knowledge is in all cases a considerable hindrance to progress. When in the course of our work we arrive at these magnitudes we realise that we are facing a key position.

The microscope makes it possible to detect objects as small as a few hundred Angstrom units in diameter, but it is far from revealing the details of objects so small as this. There are other optical methods of detecting such magnitudes. Thus Langmuir has recently shown how the polarization effects of films no more than a few dozen A.U. can be made visible: but again this method does not supply a means of examining detail.

The X-rays in a sense go too far. Their wave-lengths are such that the crystalline arrangement of atoms and molecules can be measured with very great accuracy, but their field of view is too narrow to take in the details of larger structures. Thus there is a gap in the means of enquiry, and it is remarkable how consistently the particular deficiency has inconvenient results.

Magnitudes of this order occur for example in the metallurgical field. Their importance is more obvious now that the structures of metals and their alloys are better known. The X-ray methods determine with accuracy the details of the crystal structure of iron and its alloys, but such information is insufficient for a prediction of the behaviour of a specimen of steel. As Smekal has observed there are certain properties which are clearly connected with structure, and are "insensitive" to any treatments to which the steel has been submitted in its previous history. But there are other properties, to be described as "sensitive", which can be modified profoundly by treatment, such as tensile strength, plasticity, and hardness as well as electrical and magnetic properties, and these are most important qualities in practice. Long ago the microscope showed the metal to be an assemblage of grains; and the conditions of the assemblage are clearly connected with the "sensitive" properties. But the exact details of the connexion are difficult to investigate because they fall within the region in which direct illumination fails. Metallurgical theory hovers continually over the idea that a metal or an alloy contains minute groups of atoms or is even a compound of such groups which may be called crystallites since the arrangement of the atoms within each one is perfectly regular. The X-ray diffraction is regular and the lines of a "powder diagram" are clear and sharp. Thus Gough and Wood in their examination of the fatigue of metals due to the cyclic repetition—sometimes to millions of times—of an imposed stress, found that the visible grains gradually broke up to an extent which in any one experiment depended on the magnitude of the stress. Fracture in any one region occurred when the break up into crystallites was complete. It did not imply the disruption of atom from atom resulting in complete disarray, but merely a separation into minute crystals the magnitudes of which were arranged more or less closely about some average. This was shown by the form of the X-ray photograph. A definite stage had been reached in the break up of the material. The existence of such an average would imply that the dimensions of the crystallite are in some way referable to numerical relations between the form or dimensions of the atoms of the metal: analogous to but far more complicated than the formation of the benzene ring of definite form and size from atoms of carbon each of which has tetrahedral qualities.

The discussion as to the specific existence, nature and effect of crystallites has been conducted with great eagerness, very much research on the mosaic structure of crystals in general has been undertaken, and several interesting theories have been put forward. At first theories were suggested which would have provided a super lattice, consisting of a regular arrangement of crystallites, even in the case of a pure metal. But this suggestion could not be maintained, as it evolved a second linear dimension out of a first. Buerger has suggested that the grain-like structure of a metal is due to conditions of growth, various crystalline processes meeting and joining together in irregular fashion during the formation of the whole mass. This however would lead to a casual formation which does not seem to be in accord with metallurgical experiment. G. I. Taylor's ingenious theory of the hardening of a metal by working requires the existence of crystallites of some form. The whole question is still obscure, yet it is extremely important because the properties of metals and alloys depend to a large extent on the grain-like structure which they possess. Whether so-called "crystallites" are formed under some law governing their size or are merely accidental assemblages, they are a centre of interest in the examination of metallic properties.

Similar conditions prevail in other cases where the behaviour of materials is under consideration. In April of this year the International Association for the Testing of Materials met in London. It was attended by about 800 persons, many of whom had come from abroad. The subjects dealt with centred round the use of materials for every kind of engineering design and every kind of manufacture. Under cover of a conference on testing it drew together an imposing assemblage of men engaged in the constructive work of the world. In any constructive work the testing of the material must be a decisive factor in making the design and in building to it. The design of the test itself requires the most careful consideration, because it is always a compromise between what is possible and what is practicable. Knowledge of what is possible depends on scientific research and is related to scientific problems of the greatest interest and the most varied nature. Knowledge of what is practicable is related to other interests but is also founded to a large extent on scientific research. Thus the work of the conference was closely connected with pure scientific research, depending on results already obtained and suggesting numerous opportunities for the increase of knowledge.

It was remarkable that in the case of one material after another the discussion drew attention to the importance of grain-like structure, and showed that the "grain", if I may extend the word widely from its general use in metallurgy, was the object of attack. Thus in the vast variety of fibrous materials, the fibre corresponds to the metal grain, and its study is quite as interesting and important. In all colloidal problems the condition and properties of the minute particle are fundamental. In materials derived from living organisms, the cell and its parts are the centre of interest and of course somewhere in the region of which I am speaking are the outposts of life itself. Even in dielectrics and lubricants, the groupings of atoms and molecules determine the general behaviour.

Moreover, a very considerable change in the use of materials for construction has come about in recent years in consequence of the fact that the gradual changes due to time have become really important. The so-called "creep" of materials is now one of the chief pre-occupations of the engineer. Its new importance is due to two causes. In the first place the development of machinery has necessitated more perfect fitting, and less allowance for clearance than was at one time the case, as for example in modern turbines and internal combustion engines. In such fine adjustments a creep of one part in a thousand is a very serious matter. In the second place the working temperatures have been greatly increased, and creep is thereby encouraged. There is no doubt that in any specimen but a perfect crystal slow changes take place continuously. At every moment molecules are being helped over the barriers which have kept them from positions of greater equilibrium. In this way new crystallizations are set up, or older crystallizations extended. Strain may encourage transfer from one position to another. One might almost say that every portion of a solid is a liquid for a certain fraction of its time, and that the atoms in that portion are capable of a movement which is restricted and guided by the stabilizing action of their surroundings.

The laws which govern these movements are very complicated, and detailed knowledge is scanty though badly wanted. Thus according to Dr. Bailey, a pioneer in these matters, the addition of 1 % chromium to a 0·5 % molybdenum steel increases its initial resistance to creep below a certain temperature and lessens it above. It is probable that the addition of chromium atoms locks the grain structure so long as they stay where they are: but heat facilitates their moving, all the more readily because the complicated alloy has the looser structure. Once they have moved the material would be better without them. But such a rough explanation would be well set aside for a detailed knowledge of the processes involved. Here are very interesting problems of physics and chemistry.

The careful examination of a visible cellulose fibre shows, it is said by some, that it is built up of lesser fibres, fibrillae or fibrils which again consist of ellipsoidal objects of dimensions roughly 1·5 and 1·1 μ. Each such object may contain many millions of cellulose chains, but very little is known of the structure of the contents or of the sheath that encloses them and seems to be the source of their characteristic influence. Chemical analysis and X-ray examination give a satisfactory picture of the cellulose chain-like molecule, and some information also of the details of the molecular assemblages. But information is wanted respecting the larger groups and the fibril formation on which the fibre properties obviously depend. If the fibre belongs to a living organism, change with time may be synonymous with growth. If the fibre is an element of some material in use, it is still subject to change which may seriously affect its quality.

Change may be external or internal. The slow rearrangements of recrystallization or devitrification are due to internal forces: but surface changes due to reactions with surrounding atoms such as corrosion or hydration may also affect behaviour. Naturally such surface changes are the more important the smaller the particle of the substance, as the colloid chemist points out. Thus, for example, it is a much discussed question as to how clay holds the water that is associated with it. The X-ray analysis supplies a very reasonable picture of the clay crystal; the positions of the atoms of oxygen, silicon, aluminium, magnesium, iron and the rest are known with considerable accuracy. But the remarkable properties of clay are dependent on the behaviour of the larger flake-like assemblages of colloidal dimensions, which lie between the direct observation of the X-ray methods and those of the microscope.

In dielectrics the slow changes of time bring about rearrangements, hastened by the electrical tensions to which the material is subjected. The electrical forces look for the weakest point for a break-through, just as a stress discovers the weakest point of a chain or any member of a structure. Changes are therefore important. One would wish that a structure was like the "Deacon's shay" which was so designed that every part was as strong as every other so that when the shay came to its end, it became a heap of dust upon the road. Unfortunately that is not the case with any material in use: and whatever its structure an equal balancing is apt to be destroyed by changes in its grain-like condition.

Perhaps the structure of the huge protein molecules may suggest a way of closing the gap in our knowledge and our means of enquiry. It is a very striking fact that their magnitudes tend definitely to group themselves about certain values, which moreover are simply related to one another. They are not mere groups of atoms thrown together without design. Their definite formation implies obedience to rules which must be in force at the beginning of the assembling, and are in force until an unavoidable result is reached. This would mean, as indeed a vast number of observations already imply, that the junction of carbon atoms is governed by strict geometrical laws of distance and orientation. It has indeed been pointed out by Dr. Wrinch and others that the long chains consisting of two carbons and one nitrogen in regular succession can be formed, under the guidance of the rules mentioned, into space-enclosing sheets presenting an external appearance of linked hexagons, and the number of sizes to which these assemblages can attain is limited. Possibly we have here an example of a form of procedure from the groupings of a few atoms to the larger assemblages of thousands, the process depending on a certain obedience to laws of building which have been shown to hold in the simpler case. We are encouraged to hope that this may be so, by the unexpected strictness and definiteness of the building rules in the cases which fall within the scope of the X-ray methods.

The constitution of the solid body is being examined now as it has never been possible to examine it before. We are not surprised that it is found to possess a grain-like structure, nor that this structure is of first rate importance. It is not only of interest from the purely scientific point of view, but it turns out to be of fundamental importance to all the constructive work of industry and to all the examinations of living constructions within the domain of biology. In the effort to know its details and to understand their significance a host of interesting scientific enquiries make their appearance, so that industry and science more than ever play into each other's hands. It is certainly to be expected that from these tempting labours there will result much improvement of natural knowledge.

Awards of Medals, 1937

Sir HENRY DALE is awarded the COPLEY MEDAL. His most important contributions to physiology and pharmacology lie in two different but closely related fields: (1) the isolation of certain chemical substances, notably histamine and acetylcholine, from animal tissues, and (2) the discovery of the part played by these in a large number of important physiological and pathological processes.

His earlier work (1905–11) on the active principles of ergot led to progress in many allied subjects. The study of histamine, isolated from ergot extract and later found as a normal constituent of certain tissues, has modified profoundly our views of the capillary circulation and of the conditions known as "wound shock" and "anaphylactic shock". In 1914 he became interested in the choline esters and with extraordinary prescience singled out acetylcholine as the most interesting member of the series and pointed out the extreme likeness of its action to that of stimulating the parasympathetic.

In 1924 Loewi demonstrated that a substance indistinguishable from acetylcholine is liberated by the heart when the vagus nerve is stimulated. The researches of others, prominently among them Dale himself and his colleagues, have since shown that acetylcholine is liberated at many other junctions between conducting tissues, and the results with acetylcholine and adrenaline are embodied in the description of nerves as "adrenergic" and "cholinergic". Recently convincing evidence has been given by Dale and his collaborators that acetylcholine plays an important, possibly an essential, role in the transmission of impulse from nerve to voluntary muscle: a discovery which has direct practical bearings on muscular fatigue and in various pathological conditions, and also is of the greatest interest in the theory of the mechanism of the nervous and neuro-muscular systems.

As Director of the National Institute for Medical Research, Dale has inspired and directed a wide variety of investigations outside his special field, and numerous investigators from many countries have worked under his guidance.

A ROYAL MEDAL is awarded to Professor NEVIL VINCENT SIDGWICK. He has always been primarily interested in the causes which determine molecular structure, and his earlier experimental work chiefly dealt with such subjects as tautomerism, and the vapour pressures, boiling-points and solubilities of isomerides. The development of the conception of the nuclear atom, more particularly by Bohr and Moseley, made possible for the first time a quantitative treatment of chemical valency other than purely formal, and the first steps in this direction were taken by Langmuir, G. N. Lewis and Kossel during, or just after, the war. Others followed with theoretical or physical extensions.

Sidgwick's post-war experimental work has all been concerned with particular problems of structure, utilizing to the full available physical methods of attack. To take a few examples, he has shown the existence of co-ordination compounds of the alkali metals, and has demonstrated the co-ordinating properties of the hydrogen atom. In particular, it was he who distinguished clearly the existence of a third and very important type of chemical binding, the so-called co-ordinated covalent link.

In 1927, he published "The Electronic Theory of Valency", in which, for the first time, the most diverse structural phenomena covering the whole field of chemistry were rationally systematized. The book met with immediate and enthusiastic acceptance in all quarters. In 1928, he played a leading part at a conference held at Munich to discuss chemical binding in its relation to atomic structure. In 1931, he lectured in the United States of America. His second book, "The Covalent Link in Chemistry", which appeared in 1933, is based on the course then given and, like the first, has proved effective and stimulating to a high degree. In late years he has continued his work of fruitful interpretation in a series of remarkable contributions made to the Annual Reports of the Chemical Society, and in his recent Presidential Addresses to the same Society on the subject of Resonance Phenomena in Chemistry.

A ROYAL MEDAL is awarded to Dr. ARTHUR HENRY REGINALD BULLER. He was Professor of Botany in the University of Manitoba from 1904 to 1936. His original contributions to science are mainly in the field of Mycology and have been published in his Researches on Fungi. Six volumes of these researches have appeared, the first in 1909, the sixth in 1934, and he is now engaged in the preparation of further volumes.

These researches fall into two groups. The first comprises studies on the morphology, biophysics and physiology of the higher fungi, including the physiology of the mycelium and the organs produced on it, and especially of the production and liberation of spores. The second group deals with sex in the higher fungi, and his studies on this subject rank among the most important that have been made. Particular mention should be made of his observations on the process of diploidization in the higher fungi, and of the discovery, in conjunction with his student Craigie, of heterothallism in the rusts. This work has revolutionized our conception of the life cycle of these forms. Buller's studies have not been confined to one group of fungi, but include researches on Discomycetes and many groups of the Eu-Basidiomycetes, as well as on rusts and smuts. Reference should also be made to his "Essays on Wheat" and to his efforts which made possible the publication of the translation by his friend W. B. Grove of the monumental "Selecta Carpologia Fungorum" of the brothers Tulasne.

During his thirty-two years of occupation of the chair of Botany at Winnipeg, he has been a leading figure in Canadian botany, and was President of the Royal Society of Canada in 1927 and 1928. Since his retirement he has continued his researches in this country.

The DAVY MEDAL is awarded to Professor HANS FISCHER. During the past twenty-five years he has been continuously engaged in the study of the chemistry of the porphyrins, the bile pigment and chlorophyll. Starting from the knowledge that the porphyrin molecule was built up of pyrrole nuclei, variously substituted in the different porphyrins, Fischer developed controlled methods of degradation which extended the possibility of the identification of the pyrroles contained in any given porphyrin.

With the accurate information acquired in this manner as a basis Fischer proceeded, by bold and original synthetic work, artificially to prepare a large number of porphyrins of known structure, many of which proved to be closely related to or identical with natural products; his crowning achievement in this field was the synthesis of protoporphyrin, which, with iron, yielded haematin identical with that derivable from blood haemoglobin.

From the porphyrins Fischer turned his attention to the bile pigments and was able to explain the fundamental chemical features of their relationship to haemoglobin, thus paving the way for the biochemical work which is now proceeding in other laboratories and which promises to explain the actual mechanism of bile pigment formation in the body.

In recent years Fischer has applied his brilliant synthetic technique with outstanding success to the elucidation of the detailed structure of chlorophyll; his work in this field continues at the present time.

The Buchanan Medal is awarded to General Frederick Fuller Russell. He graduated from Columbia College of Physicians and Surgeons in 1893, and began his career as a member of the Medical Corps, U.S. Army, in 1898, advancing through the various grades to that of colonel in 1917. He resigned in 1920. He was curator of the Army Medical Museum, Washington, D.C., from 1907 to 1913, and also instructor in bacteriology and clinical microscopy at the Army Medical School, where he performed distinguished service in developing and producing the typhoid vaccine which the Army has used with great effectiveness since that time. He was professor of pathology and bacteriology at George Washington University School of Medicine from 1909 to 1913 and for the following year lecturer in tropical medicine at the New York Post-Graduate Medical School and Hospital. From 1915 to 1917 General Russell was chief of the Board of Health laboratory in Ancon, C.Z., and during the world war was in charge of the division of infectious diseases and of the laboratory service of the surgeon-general's office, U.S. Army. From 1920 to 1923 he was director of the public health laboratory service of the International Health Board and from 1923 to September 1, 1935 he was general director of the Board. In 1919 he received the Distinguished Service Medal. Recently he was appointed lecturer on preventive medicine and hygiene and epidemiology at Harvard Medical School, Boston.

It was during the period while General Russell was director of the International Health Division of the Rockefeller Foundation that the Foundation gave such material aid towards the establishment of schools of hygiene in various European countries. They also contributed largely to the All India Institute of Hygiene in Calcutta and to the Singapore Medical School. General Russell was also responsible for establishing the yellow fever unit in West Africa. Large grants were given to the Health Section of the League of Nations, and the fellowship scheme under the International Health Division was considerably extended. The policy of the Foundation in these matters was moulded in no small degree by General Russell, whose influence on the development of public health services all over the world has been altogether remarkable.

The SYLVESTER MEDAL is awarded to Professor AUGUSTUS EDWARD HOUGH LOVE. He is most generally known as the author of the "Treatise on the Mathematical Theory of Elasticity" which has attained a universal reputation and remains the standard work of reference on this subject all over the world.

Before the first edition of the treatise was published in 1893 (almost simultaneously with the completion of the publication of Todhunter and Pearson's History of Elasticity), this branch of mathematical physics received little attention and its results were often regarded by engineers with suspicion. During the intervening years it has gradually established itself as one of the most reliable mathematical theories of continuous media and, unlike its sister science of non-viscous hydrodynamics, its results have been increasingly verified in practice. That this has come about is due in great part to the influence of Love's "Treatise", which, indeed, like Lamb's "Hydrodynamics", is far more than a mere treatise and embodies a vast amount of original work.

In other of his published work there is a great volume of research dealing not only with elasticity, but with hydrodynamics and electromagnetism. His earlier work was mostly on hydrodynamics, particularly vortex motion and wave-motion. He returned also at various times to electrical problems, especially those relating to the propagation, scattering and transmission of electric waves. His elastical investigations range over an exceedingly wide field, from the equilibrium of beams and plates of various shapes to the study of vibrations in a variety of difficult cases and to the applications of the theory of elasticity to problems connected with the Earth.

An enumeration of Love's researches, even when restricted to the more important ones, would be too long to attempt in this brief account; but two of them may be explicitly mentioned.

The first of these is the powerful and elegant theory of the support of the continents, of earth-tides and seismic waves and of the elastic stability of the earth, developed in his Adams Prize Essay of 1911, "Some Problems of Geodynamics", where appears for the first time his explanation of the seismic waves vibrating horizontally and transversely to the direction of propagation, waves to which Love's name is now universally attached.

The second is the remarkable paper on biharmonic analysis in a rectangle, published in the Proceedings of the London Mathematical Society in 1929. In this paper Love gives a complete solution of the biharmonic equation subject to given boundary conditions over the perimeter of a rectangle, thus solving at any rate the two-dimensional form of a problem which was described by Lamé as "le plus difficile peut-être de la théorie de l'élasticité", and had till then baffled mathematicians.

The HUGHES MEDAL is awarded to Professor ERNEST O. LAWRENCE, Professor of Physics in the University of California, the inventor (1932) of the cyclotron, the most important instrument of physical research since the C. T. R. Wilson expansion chamber. By its means ions are accelerated in a magnetic field and move within two half-cylinders which change electrical polarity in rhythm with the circulating ions, so that deuterons have been spirally speeded in a vacuum to velocities due to three million volts. These deuterons, impinging on beryllium, have produced neutrons and protons in great number, and some of the protons have been projected through the equivalent of forty centimetres of air. Many elements have been proved to be radioactive when thus bombarded by high-speed protons or deuterons.

Hydrogen molecular ions have been used also as bombarding elements with velocities due to five million volts. Such high-speed ions are available for developing the theory and practice of atomic disintegration, and Professor Lawrence and his co-workers are playing a leading part in this development.

Optical Activity in Ketones. The Rotatory Dispersion and Circular Dichroism of *m*-Methyl *Cyclo*hexanone and of Pulegone in their Ketonic Absorption Bands

By the late T. M. Lowry, F.R.S., Delia M. Simpson
and C. B. Allsopp

Laboratory of Physical Chemistry, The University, Cambridge

(*Communicated by R. G. W. Norrish, F.R.S.—Received* 1 *October* 1937)

Recent investigations of the rotatory dispersions of aldehydes and ketones led to the conclusion that the optical activity of these compounds is due almost entirely to the electrons of the carbonyl group and not directly to the asymmetric carbon atoms. A particularly striking example of this was found in the aldehydic sugar derivative, μ-arabinose pentaacetate, by Hudson, Wolfrom and Lowry (1933), who showed that when the calculated partial rotation contributed by the absorption band between 3000 and 2600 A was subtracted from the observed rotations for the whole molecule, a negligible residual rotation was left at every wave-length at which measurements were made between 6700 and 2300 A. In general, however, absorption frequencies lying in the Schumann region appear to make a small contribution; but the analysis has always been complicated in the cases so far examined by the fact that the molecules contain either two asymmetric carbon atoms, e.g. in camphor (Kuhn and Gore 1931), menthone and carvomenthone (Lowry and Lishmund 1935*a*), or as many as four in the open-chain sugar derivatives (Hudson and others 1933; Baldwin, Wolfrom and Lowry 1935). The absence of any large direct contribution from the asymmetric atoms might therefore be explained in two ways, namely, either that their partial rotations are actually very small, or, as may well be the case in the sugars (cf. Lowry 1935, p. 274), that, though large, they are of opposing signs and tend to annul one another at wave-lengths remote from the region of absorption. It was thus desirable to examine an optically active ketone whose molecule contains only a single asymmetric carbon atom, with no other disturbing factor, and *m*-methyl *cyclo*hexanone (I) was selected for this purpose.

m-Methyl *cyclo*hexanone has the additional advantage that it can easily be prepared in the active form by the hydrolysis, with dilute acid, of pulegone (II), which occurs naturally in peppermint oil. The purification of the product, which is a liquid, proved to be a matter of some difficulty, but it was finally achieved successfully, through the kindness of Professor J. Read, F.R.S., in his laboratory at St. Andrews. Earlier measurements of absorption and rotatory dispersion with less pure samples led to conflicting and extraordinary results, and the observations only became uniformly reproducible when Professor Read's very pure material was available. There is no doubt that the optical properties of the compound are seriously affected by the presence of even small traces of impurity; and it is not surprising therefore that the data now recorded do not agree with those published recently by French and Naps (1936), who describe their specimen only as "purified through its bisulphite addition compound".

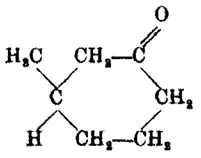
(I) *m*-Methyl *cyclo*hexanone

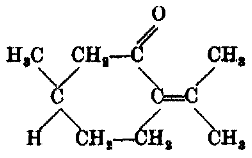
(II) Pulegone

The absorption spectrum, circular dichroism and rotatory dispersion are now recorded for pure methyl *cyclo*hexanone over a long range of ultra-violet wave-lengths, including those covered by the ketonic absorption band. The analysis of the rotatory dispersion on the basis of the observed circular dichroism indicates that the contribution of this band to the rotatory power is considerably larger than the partial rotation due to absorption frequencies in the Schumann region. Since these must include those which are associated with the electrons of the single asymmetric carbon atom, it is concluded that the main function of these electrons is to produce that element of dissymmetry in the molecule the presence of which is necessary for the more easily polarizable electrons of the carbonyl group to become optically active.

Opportunity has been taken during these experiments to examine the parent compound pulegone (II), for which no detailed data were hitherto available, and which is of interest in that it contains an ethylenic bond conjugated with the carbonyl group in the presence of one asymmetric atom, as compared with two in the cases of this type which had previously been studied. The results obtained, however, are very similar to those for methyl *cyclo*hexanone and for the more complex molecules. The optical activity is again largely due to the low-frequency carbonyl band, despite the presence of a second band in the ultra-violet region of the spectrum.

ABSORPTION SPECTRA

*m-Methyl*cyclo*hexanone*—Apart from the work of French and Naps (1936), no accurate quantitative measurements of the absorption of methyl *cyclo*hexanone have previously been attempted. Molecular extinction coefficients for Professor Read's very pure material, in solution in *cyclo*hexane of optical purity (Lowry and Allsopp 1931), are plotted against wave-length in fig. 1, curve I. The absorption curve rises to a maximum value $\epsilon = 14\cdot25$ at 2905 A and is not symmetrical on a scale of wave-lengths, but falls away more steeply on the long wave-length side. It cannot therefore be represented by the simple equation (i) of Lowry and Hudson (1933), curve II, but a good agreement with experiment is obtained by the use of the modified equation (ii) (Hudson 1933; Lowry and Lishmund 1935*b*) when $n = 1\cdot88$, curve III:

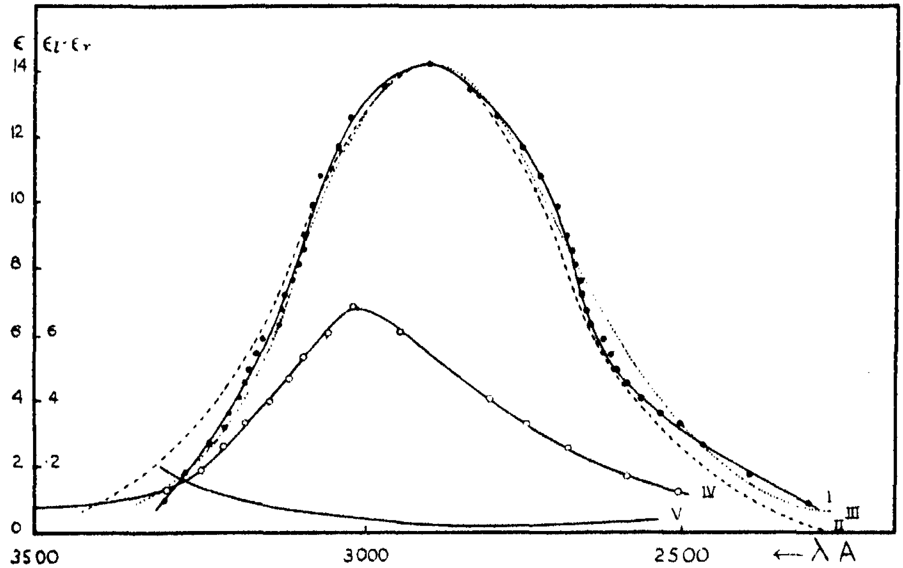

FIG. 1—Absorption and circular dichroism of *m*-methyl *cyclo*hexanone. I, molecular extinction coefficients, ϵ. II, ϵ calculated from equation (i). III, ϵ calculated from equation (ii). IV, circular dichroism, $\epsilon_l - \epsilon_r$. V, dissymmetry factor, g.

$$\epsilon = \epsilon_{\max} . e^{-\left(\frac{\lambda-\lambda_0}{\theta}\right)^2}, \tag{i}$$

$$\epsilon = \epsilon_{\max} . e^{-\left(\frac{\lambda-\lambda_0}{\theta}\right)^2 \left(\frac{\lambda}{\lambda_0}\right)^n} \tag{ii}$$

($\epsilon = \epsilon_{\max}$ at $\lambda = \lambda_0$; $\theta = \lambda'/1\cdot6651$, where λ' = half-width of band; n is an arbitrary parameter).

Methyl *cyclo*hexanone is therefore unlike its lower inactive homologue, *cyclo*hexanone, the absorption band of which—with $\epsilon_{\max} = 16\cdot5$ at 2833 A (Allsopp 1934*b*)—possesses almost perfect symmetry on a wave-length scale, as do those of a number of more complex ketones such as 4-hydroxy-pentan-2-one and acetyl acetone, listed by Lowry and Lishmund (1935*b*); but it resembles the simple aliphatic ketones and their chlorine derivatives, and camphor and piperitone, the bands of which they found to be similarly unsymmetrical.

Pulegone—Molecular extinction coefficients for pulegone, also in *cyclo*hexane, are plotted in fig. 2, curve I. The spectrum consists of two bands, $\epsilon_{\max} = 40$ at 3240 A and $\epsilon_{\max} = 5171\cdot6$ at 2450 A respectively, which are separated by a shallow minimum, and may perhaps be identified with the usual ketonic spectrum displaced towards longer wave-lengths, so that the band which usually falls beyond 1850 A (Scheibe and Grieneisen 1934) can now be observed at ultra-violet wave-lengths. Such a displacement has

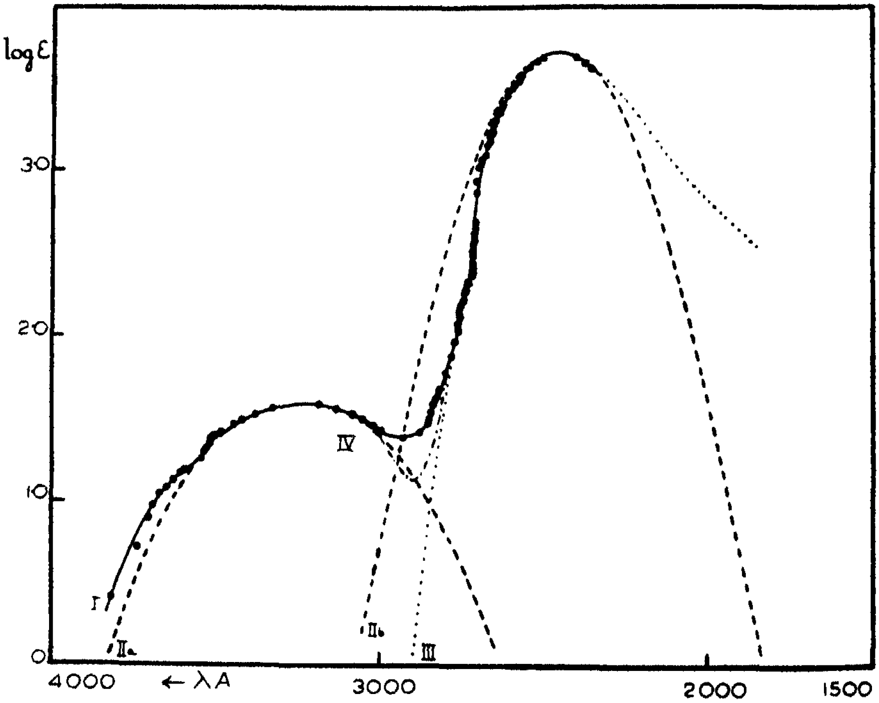

Fig. 2—Absorption spectrum of pulegone. I, log ε, observed values. IIa, IIb, log ε, calculated from equation (i). III, log ε, calculated from equation (ii). IV, curve IIa + curve III.

been attributed to the effect of conjugation, since changes in position and intensity of similar magnitude were recorded by Henri (1919, p. 179) in compounds such as mesityl oxide or citral, and by Lowry and Lishmund (1935*b*) in carvenone and piperitone. The frequency separation of the two maxima now recorded for pulegone, however, is about 10,000 cm.$^{-1}$ and is thus quite different from that of *cyclo*hexanone for which it is about 20,000 cm.$^{-1}$, so that the band of higher frequency, at least, is more probably due to a modified electronic system associated with the conjugated grouping, just as the intense ultra-violet absorption band of 1 : 3-*cyclo*hexadiene is characteristic of the conjugated system of two C=C bonds and bears no resemblance to that of the isolated ethylenic system (Allsopp 1934*a*).

Curve I of fig. 2 reveals the presence, on the long wave-length side of the low-frequency band, of a small "step-out" which is shown in correct proportion on a linear scale in curve I of fig. 3. It may be identified with the weak subsidiary band observed by Schou (1926) in acet- and propionaldehydes. Apart from this "step-out" the band, unlike that of methyl *cyclo*hexanone, is symmetrical on a scale of wave-lengths and can be represented by an equation of type (i). On the other hand, the band of higher frequency is not so symmetrical, but can be represented accurately by equation (ii) when $n = 3{\cdot}96$. The corresponding curves are shown, on a logarithmic scale in fig. 2, curves II*a*, II*b*, III, and on a linear scale in fig. 3, curve II.

Strengths of the Bands—The strength f of an absorption band is given by $f = \frac{n'mc}{\pi e^2} \cdot \frac{1}{N} \int_{-\infty}^{+\infty} \mu \, d\nu$, where m and e are the mass and charge of an electron, c is the velocity of light, N the number of molecules in unit volume, μ is the absorption coefficient at frequency ν, defined by $I/I_0 = e^{-\mu l}$, and n' is the refractive index of the solution at the wave-length of maximum absorption (Born 1933, p. 487). Approximations for this integral, based on equations (i) and (ii), and accurate to about 2 %, as given by Lowry and Lishmund (1935*b*), lead to the following values:

TABLE I—f-VALUES OF ABSORPTION BANDS

Substance	λ_{max} A	Half-width λ' A	f
m-Methyl *cyclo*hexanone	2905	458	$5{\cdot}85 \times 10^{-4}$
Pulegone	3240	580	$1{\cdot}48 \times 10^{-3}$
	2450	350	$2{\cdot}26 \times 10^{-1}$

The strengths of the low-frequency bands are thus comparable with those of *cyclo*hexanone, $f = 9{\cdot}6 \times 10^{-4}$, or of carvomenthone, $f = 7{\cdot}1 \times 10^{-4}$, whilst that of the high-frequency band of pulegone is similar to those for acetyl acetone and diosphenol, $f = 0{\cdot}302$ and $f = 0{\cdot}367$ respectively (Lowry and Lishmund 1935*b*).

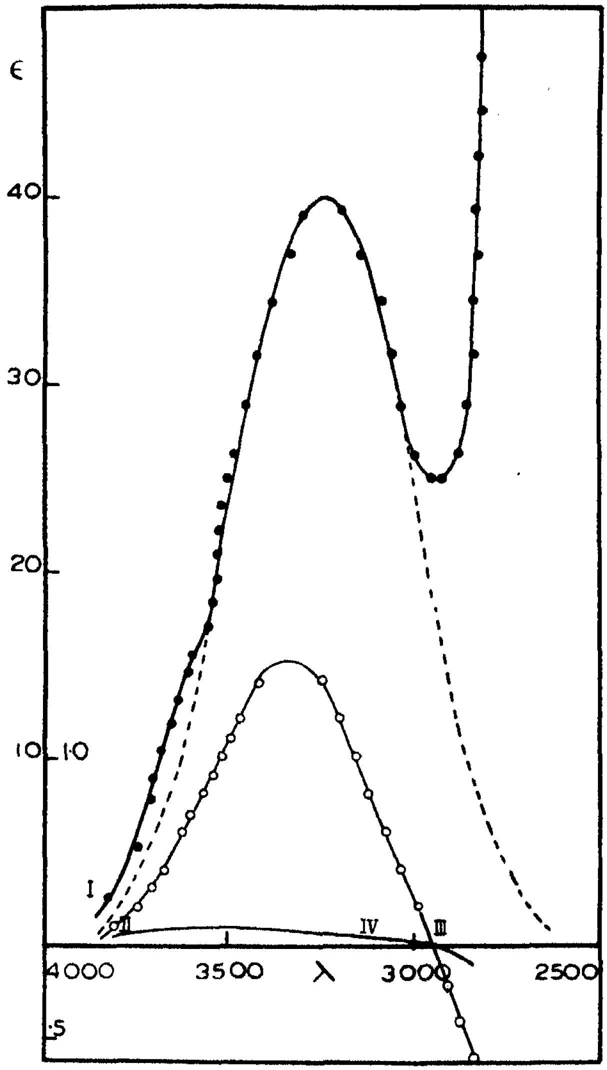

FIG. 3—Absorption and circular dichroism of pulegone. I, ϵ, observed values. II, ϵ, calculated from equation (i). III, $\epsilon_l - \epsilon_r$. IV, g.

CIRCULAR DICHROISM

Measurements of circular dichroism have been made through the band of *m*-methyl *cyclo*hexanone and the corresponding band of pulegone.

m-Methyl cyclo*hexanone*—The results obtained with *m*-methyl *cyclo*hexanone are shown in fig. 1, curve IV. This curve, which has a half-width of 390 A, is unsymmetrical and can be represented best by an equation of type (ii) in which ϵ is replaced by $(\epsilon_l - \epsilon_r)$ and λ_0, λ' and θ now all refer to circular dichroism. The maximum λ_0, $\epsilon_l - \epsilon_r = 0{\cdot}642$, falls at 3020 A and is thus displaced by over 100 A relative to the total absorption, just as in the case of camphor and its derivatives (Kuhn and Gore 1931; Lowry and French 1932) or of camphorquinone (Lowry and Simpson 1936). In consequence of this displacement, the dissymmetry factor, $g = (\epsilon_l - \epsilon_r)/\epsilon$, curve V of fig. 1, is not even approximately constant, as it should be if the absorption band is homogeneous (Kuhn 1930; Lowry and Hudson 1933).

Pulegone—The circular dichroism in the corresponding band of pulegone proved to be of particular interest, since it changes sign and assumes negative values on passing from longer to shorter wave-lengths (fig. 3, curve III), a phenomenon only once observed before, in *d*-bornyl dixanthogenide and xanthates (Lowry and Hudson 1933). The curve rises to a maximum value $\epsilon_l - \epsilon_r = 1{\cdot}53$ at 3300 A, i.e. 60 A from the maximum of absorption. Unlike that of methyl *cyclo*hexanone, the main dichroism curve can be represented quite adequately by an equation of type (i) symmetrical on a wave-length scale, except at the shortest wave-lengths, where it falls steeply to cross the axis at 2950 A. Negative values could be followed as far as $\epsilon_r - \epsilon_l = 0{\cdot}598$ at 2700 A, beyond which the more intense absorption due to the presence of the second band, to which the negative dichroism must be attributed, prevented further readings. In view of this complexity it is not surprising that the dissymmetry factor g is again far from constant, fig. 3, curve IV.

ROTATORY DISPERSION

Measurements of rotatory dispersion could be made at all wave-lengths covered by the absorption band of methyl *cyclo*hexanone and by the low-frequency band of pulegone, and the complete Cotton effect was thus observed in both cases. The characteristics of the rotatory dispersion in the absorption region are set out in Table II.

TABLE II—ROTATORY DISPERSION IN THE REGION OF ABSORPTION

	Positive maximum	Reversal of sign.	Negative maximum
m-Methyl *cyclo*hexanone	$[\alpha] = 1183°$ at 3430 A	3020 A	$[\alpha] = -1115°$ at 2870 A
Pulegone	$[\alpha] = 820°$ at 3550 A	3420 A	$[\alpha] = -2950°$ at 2910 A but still increasing

The partial rotations due to the low-frequency bands, which are in each case opposite in sign to that of the rotation of the asymmetric centre as represented by the contributions from distant Schumann frequencies (cf. Lowry and Lishmund 1935*b*), were calculated from the circular dichroism by means of the Lowry and Hudson formula (1933):

$$\alpha = \frac{10^5 . 9 . 2{\cdot}303}{\pi^{\frac{1}{2}} . M} (\epsilon_r \sim \epsilon_l)_{\max} \left[e^{-\left(\frac{\lambda-\lambda_0}{\theta}\right)^2} \int_0^{\frac{\lambda-\lambda_0}{\theta}} e^{x^2} dx + \frac{\lambda}{2 . 1{\cdot}665(\lambda+\lambda_0)} \right], \quad \text{(iii)}$$

where λ_0 and θ refer to the observed curve of circular dichroism and M is the molecular weight. The results are shown in figs. 4 and 5.

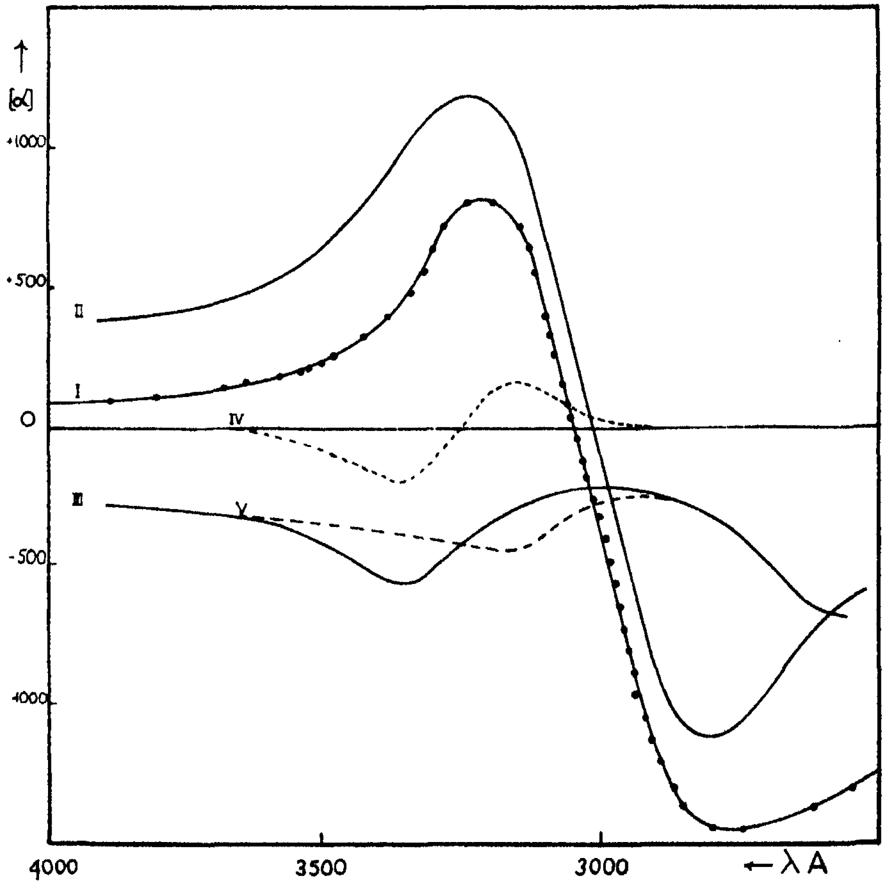

Fig. 4—Rotatory dispersion of *m*-methyl *cyclo*hexanone. I, observed specific rotations. II, partial rotation due to observed circular dichroism. III, curve I–curve II. IV, partial rotation due to subsidiary band. V, curve I–curve II–curve IV.

***m-Methyl** cyclohexanone*—The observed rotatory dispersion of methyl *cyclo*hexanone is drawn in curve I of fig. 4. The positive maximum is sharper than the negative one, and the wave-length at which the rotation is zero is displaced towards longer wave-lengths by 110 A from the maximum of absorption, but only by 25 A from the maximum of circular dichroism. The partial rotation for the band calculated from equation (iii) is drawn in curve II. The difference curve, III, then represents the residual contributions

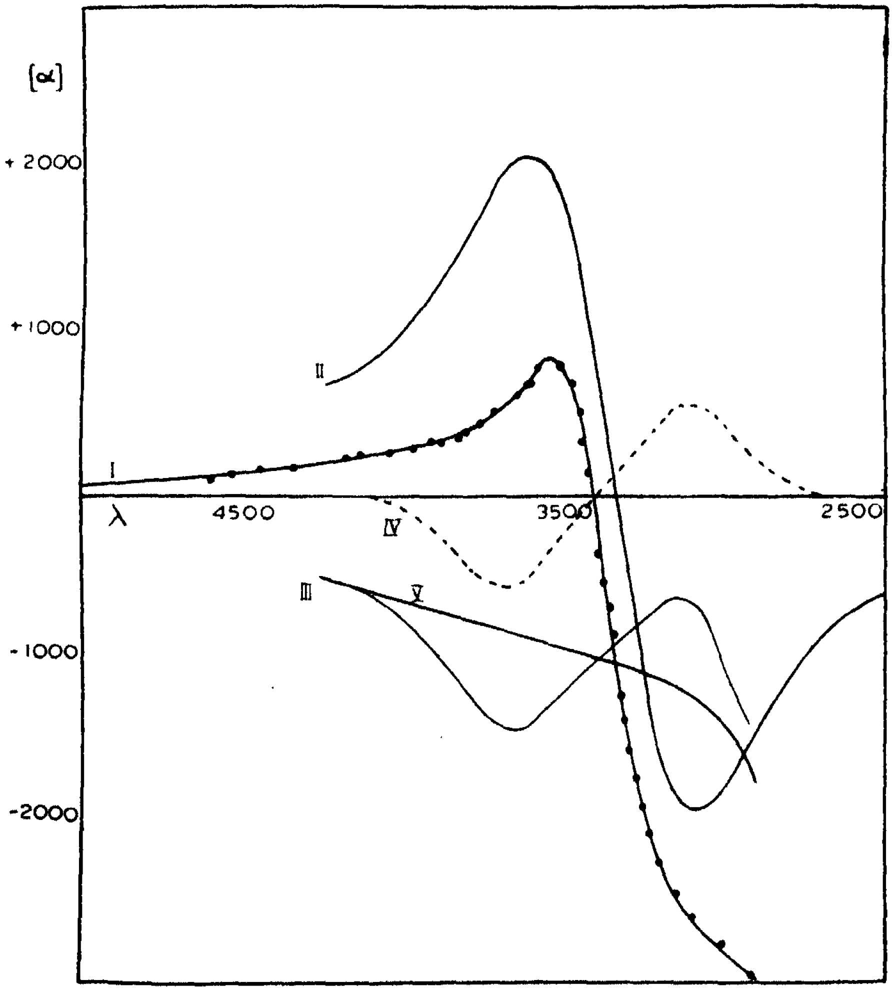

Fig. 5—Rotatory dispersion of pulegone. I, observed specific rotations. II, partial rotation calculated from positive circular dichroism. III, curve I–curve II. IV, partial rotation due to subsidiary band. V, curve I–curve II–curve IV.

from higher frequencies, and should therefore be smooth; but it contains a marked "hump", exactly similar to that obtained for the aldehydic sugar derivatives or for carvenone. In those cases it was accounted for by assuming the presence, at the long wave-length limit of the absorption, of the weak subsidiary band found by Schou in acetaldehyde and now observed in pulegone, giving rise to weak dichroism of opposite sign. The partial rotation which would be produced by such a band with methyl *cyclo*hexanone is drawn in curve IV, and the dotted curve V shows the final residual rotation then obtained. Whilst this result is not entirely satisfactory, it does confirm that all the principal features of the observed rotatory dispersion can be predicted on the basis of an analysis of the circular dichroism of the ketonic absorption band.

Pulegone—The maximum of rotation for pulegone, fig. 5, curve I, is less pronounced, and after reversal of sign the rotation becomes progressively negative, with no indication of a negative maximum before the increasingly intense absorption prevents further readings. The wave-length for zero rotation is displaced by 70 A from the maximum of circular dichroism and by 200 A from the maximum of absorption. The partial rotation, curve II, as calculated from the observed *positive* circular dichroism, leaves a difference, curve III, which has two "humps"; but these disappear completely when a contribution, curve IV, from the negative dichroism of the observed "Schou" band is introduced, and a smooth hyperbolic residue is then obtained, curve V. This curve, however, falls away too sharply at short wave-lengths to be attributed to Schumann frequencies alone, and may therefore be supposed to include also the partial rotation arising from the observed negative dichroism of the second ultra-violet band. Since the three bands overlap, and the circular dichroism could not be measured at the shorter wave-lengths, a more complete analysis can only be made by empirical methods. It has nevertheless been attempted, with some success; but as the results only confirm the conclusions already reached, the very complex details are not reproduced.

ABSORPTION AND ROTATORY DISPERSION OF THE VAPOURS

In order to avoid the serious complications which may be involved in observations made with solutions, the measurements with methyl *cyclo*-hexanone and pulegone were repeated in the vapour state, in the same way as with camphor and camphorquinone (Lowry and Gore 1932). Both compounds, however, were found to undergo thermal decomposition on heating *in vacuo* even at the lowest temperatures (90–100° C.) at which sufficient vapour pressure is developed to enable the rotatory power to be measured. In the case of methyl *cyclo*hexanone, at 100° C. the absorption band changed in shape and was displaced towards shorter wave-lengths; at 150° C. it broadened out, and at 200° C. only a continuum with a sharp long wave-length limit could be observed. The products, after condensation and solution in *cyclo*hexane, gave an absorption spectrum which suggested the presence of aromatic compounds containing an ethylenic bond, but no definite maxima were found. Similar phenomena were observed, at lower temperatures, with pulegone, the band having already vanished at 100° C.

The Origin of Optical Activity in Aldehydes and Ketones

Two significant features have emerged from these and similar detailed analyses of the rotatory dispersions of ketonic compounds, namely, that (i) the rotatory power is mainly a function of electrons associated with the carbonyl group, and (ii) the circular dichroism which is its immediate cause is generally confined to the longer wave-lengths in the carbonyl absorption band. The first of these effects was recognized in 1924 in the analysis, by means of Drude's equation, of the rotatory dispersion of camphor at wave-lengths away from the absorption band (Lowry and Cutter 1925), and the theory of "induced dissymmetry" was put forward to explain it (Lowry and Walker 1924; Lowry 1933). On this view, the unsaturated ketonic group itself acquires an element of dissymmetry under the influence of the asymmetric atoms, so that the two "halves" of the C═O bond are no longer equivalent to one another (cf. Lowry and Allsopp 1934). An alternative view, developed by Kuhn (1930), emphasizes an "induced anisotropy" in the absorption band. These conceptions must now be reviewed in the light of Mulliken's conclusion (1935), based on the analysis of rotational structure in the spectrum of formaldehyde by Dieke and Kistiakowski (1934), that this band of the C═O chromophore originates in the excitation of a non-bonding (lone-pair) electron of the oxygen atom, although the excited orbital is largely localized in the double bond. Dieke and Kistiakowski's analysis does not embrace all the observed rotational bands, but is concerned only with those transitions in which the electric moment is perpendicular to the CO-axis; but it is exactly these transitions which may be expected to be influenced by electrical dissymmetry in the rest of the molecule, so that the optical activity can be attributed to them, i.e. to the non-bonding oxygen electrons. Whilst therefore the phenomenon must no longer be considered to originate in electrons forming the double bond, it is still correct to describe it as "induced in the double bond", since the act of rotation of the plane of polarization takes place when the electron is raised to its excited state, the orbital of which is localized there.

The restriction of circular dichroism to the lower frequencies in the band indicates that in *optically active* ketones, at least, the transitions which are concerned in the activity are displaced relative to the band as a whole; but as the analysis of the rotational structure of the formaldehyde bands was incomplete, and that molecule has much higher symmetry (almost of the symmetrical top type) the inactive transitions cannot definitely be identified. The present analysis shows, however, that it is not correct to identify the active frequencies solely with the bands observed by Schou, leaving the main ketonic band inactive, as was done by Kuhn and Gore (1931).

OPTICAL ACTIVITY AND LONE-PAIRS OF ELECTRONS

This association of the optical activity of the carbonyl radical with the lone-pair of electrons of the oxygen atom was to be expected, since it is reasonable to suppose that they would become "polarized" by the dissymmetric internal field of the molecule more easily than the bound electrons of the bonds. Lone-pairs of electrons may thus be expected to play a part in the activity of other optically active systems, and this is, in fact, observed. Thus, recent work by Baldwin (Lowry and Baldwin 1937; Baldwin 1937) has shown that the rotatory dispersion of amines is controlled by an absorption band which is due to lone-pair electrons on the amino-nitrogen atom, since it disappears, with considerable changes in the rotatory power, when these are saturated, e.g. by salt formation. There is no justification in this case for assuming induced physical dissymmetry in the typically symmetrical NH_2 group, but activity can originate, as in the present case, through the influence of the dissymmetric part of the molecule on the unbound electrons of the nitrogen atom.

An example of another type is provided by the sulphinate and sulphoxides which were resolved by Phillips and his co-workers (Phillips 1925; Harrison, Kenyon and Phillips 1926; Clarke, Kenyon and Phillips 1927; Holloway, Kenyon and Phillips 1928). In these compounds the sulphur-oxygen bond is generally accepted to be semi-polar, $>\overset{+}{\mathrm{S}}—\overset{-}{\mathrm{O}}$. This structure involves the presence of lone-pair electrons on the sulphur atom, and the activity was shown to disappear when these are saturated, as in the corresponding sulphone. Similarly, the resolution of tellurium compounds by Lowry and

Gilbert (1929) and by Lowry and Hüther (1936) is in accordance with the view that in the halides of the type $R_1R_2TeBr_2$ the two halogen atoms are differently bound to the central Te, i.e. by a covalency and an electrovalency respectively. The resulting lone-pair on the central atom might thus be regarded as the fourth radical necessary for its dissymmetry. An asymmetric configuration for these electrons may also provide an explanation of the optical activity of the otherwise completely symmetrical molecule Ph_2TeBr_2, which was resolved by Miss ter Horst (1936) in this laboratory. This would not necessarily be inconsistent with the rhombic bisphenoidal symmetry postulated by Jaeger (1930, p. 50) for the tetrahedra of the sulphur and tellurium atoms, which provides a physical explanation for these cases. It is therefore suggested that lone-pair electrons may play a more prominent part in the production of rotatory power than has hitherto been suspected.

EXPERIMENTAL

Materials—Pulegone, supplied by Drs. Fraenkel and Landau, Berlin, with $[\alpha]_D^{20} = 21{\cdot}9°$, was fractionally distilled, first *in vacuo*, and then very cautiously (since some decomposition is likely to occur) at normal pressures. The final material was kept in sealed tubes, in order to avoid atmospheric oxidation, and had $[\alpha]_D^{20} = 24{\cdot}6°$, which remained constant after further distillations. *m*-Methyl *cyclo*hexanone was prepared from twice-distilled commercial pulegone. This was hydrolysed with dilute sulphuric acid, as described by Rupe (1924, 1927) and the crude product extracted. This material was then treated in Professor Read's laboratory as follows: The ketone was reduced to a mixture of 1-methyl-3-*cyclo*hexanols with moist sodium in ether; a definite 3 : 5-dinitrobenzoate was isolated, and brought to a constant melting point. After hydrolysis, the ketone was reobtained by oxidation with Bechmann's reagent, and finally purified through the semicarbazone (Read and Smith 1922) and by vacuum distillation. The product had $[\alpha]_D^{20} = 13{\cdot}0°$.

Absorption Spectra—The molecular extinction coefficients were measured with a Hilger "Spekker" photometer, in conjunction with a Hilger medium-sized quartz spectrograph, employing a condensed tungsten-steel spark as light-source.

Circular Dichroism and Rotatory Dispersion were measured by methods previously described (Lowry and Hudson 1933).

TABLE III—ROTATORY DISPERSION OF *m*-METHYL *CYCLO*HEXANONE

Temperature = 20° C. Solvent: *cyclo*hexane. Solution A: 10 c.c. contained 0·1244 g., $l = 1$ cm. Solution B: 10 c.c. contained 0·2756 g., $l = 2$ cm.

Specific rotation [α]	Solution	Wave-length		Specific rotation [α]	Solution	Wave-length	
		λ_1	λ_2			λ_1	λ_2
			Positive values				
36·29°	B	4890·77	—	199·56°	B	3542·08	—
40·20	A	4352·76	3053·07	201·00	A	3521·26	3078·02
45·36	B	4383·54	—	217·7	B	3527·79	—
54·42	B	4260·48	—	235·85	B	3506·50	—
72·57	B	4112·12	—	241·15	A	3476·7	3083·74
80·39	A	3945·82	3060·99	321·60	A	3427·12	3091·58
90·71	B	3886·28	—	402·0	A	3383·98	3098·19
108·85	B	3805·34	—	482·4	A	3341·91	3108
120·06	A	3785·71	—	564·8	A	3328·87	3120·44
126·99	B	3767·19	—	643·1	A	3306·26	3125·66
145·13	B	3684·11	—	723·5	A	3280·26	3144·49
161·15	A	3654·92	3075·72	803·9	A	3239·44	3191·66
163·27	B	3640·39	—	884·1	A	3227·81	3205·40
181·42	B	3585·32	—				
			Negative values				
161·15	A	3025·85	—	884·1	A	2940·95	—
241·15	A	3011·49	—	964·6	A	2937·81	—
321·60	A	3000·45	—	1045·0	A	2929·00	—
402·0	A	2987·29	—	1125·0	A	2918·16	—
482·4	A	2980·54	—	1206·0	A	2895·04	2473·18
564·8	A	2973·24	—	1286·0	A	2869·61	2549·61
643·1	A	2965·26	—	1366·0	A	2851·80	2636·45
723·5	A	2956·54	—	1447·0	A	2794·70	2747·55
803·9	A	2975·04	—				

The junior authors acknowledge their indebtedness to the late Professor T. M. Lowry, F.R.S., under whose advice and supervision this work was carried out, and they accept responsibility for the views expressed, which were never discussed with him.

They also thank the Governing Body of Newnham College for a Bathurst Studentship and the Governors of Haberdashers' Aske's Girls' School for a Scholarship held by D. M. S.

SUMMARY

Molecular extinction coefficients, circular dichroism and rotatory dispersion are recorded for *m*-methyl *cyclo*hexanone and for pulegone in the region of their ultra-violet absorption bands. Analysis of the rotatory

dispersion on the basis of the observed circular dichroism shows that the partial rotation due to the ketonic absorption band of methyl *cyclo*hexanone is much greater than that of the single asymmetric carbon atom, and is opposite in sign. A similar result is obtained for pulegone, despite the conjugation of carbonyl and ethylenic double bonds. By comparison with the data for other optically active ketones containing more than one asymmetric carbon atom, it is concluded that in general the direct contribution of each asymmetric centre is itself small relative to that of the chromophoric group. In the light of Mulliken's analysis of the electronic configurations of aldehydes, the optical activity of the carbonyl group is now attributed to the lone-pair electrons of the oxygen atom, and the theory of "induced dissymmetry" is reinterpreted. A possible function of lone-pairs in producing optical activity in other types of compound is discussed.

TABLE IV—ROTATORY DISPERSION OF PULEGONE

Temperature = 20° C. Solvent: *cyclo*hexane. Length of cell = 1 cm. Solution I contained 0·05775 g. in 10 c.c.; solution II contained 0·1511 g. in 10 c.c.

Specific rotation [α]	Solution	Wave-length		Specific rotation [α]	Solution	Wave-length	
		λ_1	λ_2			λ_1	λ_2
			Positive values				
86·6°	I	4592·7	—	347°	I	3922·9	3440°
131	II	4528·6	—	361	II	3800·4	—
169	II	4447·7	—	394	II	3805·0	—
173·1	I	4337·0	3427·0	426	II	3758·2	—
197	II	4325·8	—	434	I	3767·2	—
229	II	4184·9	—	510	I	3727·6	3451
259·7	I	4032·0	—	558	II	3649·5	—
262	II	4045·8	—	607	I	3649·5	3676
295	II	3967·4	—	683	I	3605·5	—
328	II	3888·5	—	780	I	3581·2	3516
			Negative values				
347	I	3392		1736	I	3265	
510	I	3370		1905	I	3230	
683	I	3356		2080	I	3219	
867	I	3340		2250	I	3199	
1040	I	3328		2424	I	3142	
1210	I	3317		2600	I	3100	
1380	I	3306		2870	I	3000	
1560	I	3286		2950	I	2912	

REFERENCES

Allsopp, C. B. 1934*a* *Proc. Roy. Soc.* A, **143**, 618–30.
— 1934*b* *Proc. Roy. Soc.* A, **146**, 300–12,
Baldwin, W. C. G. 1937 *Proc. Roy. Soc.* A, **162**, 215–32; and in publication.
Baldwin, W. C. G., Wolfrom, M. L. and Lowry, T. M. 1935 *J. Chem. Soc.* pp. 696–704.
Born, M. 1933 *Optik.* Berlin: Springer.
Clarke, C. G., Kenyon, J. and Phillips, H. 1927 *J. Chem. Soc.* pp. 188–94.
Dieke, G. H. and Kistiakowski, G. B. 1934 *Phys. Rev.* **45**, 4–28.
French, H. S. and Naps, M. 1936 *J. Amer. Chem. Soc.* **58**, 2303–5.
Harrison, P. W. B., Kenyon, J. and Phillips, H. 1926 *J. Chem. Soc.* pp. 2079–90.
Henri, V. 1919 *Études de Photochimie.* Paris: Gauthiers-Villars.
Holloway, J., Kenyon, J. and Phillips, H. 1928 *J. Chem. Soc.* pp. 3000–6.
ter Horst, M. G. 1936 *Rec. Trav. chim. Pays Bas,* **55**, 697–711.
Hudson, H. 1933 Thesis, Cambridge University.
Hudson, H., Wolfrom, M. L. and Lowry, T. M. 1933 *J. Chem. Soc.* pp. 1179–92.
Jaeger, F. M. 1930 *Cornell Lectures.* London: McGraw-Hill.
Kuhn, W. 1930 *Trans. Faraday Soc.* **26**, 293–308; *Z. phys. Chem.* B, **8**, 281–313.
Kuhn, W. and Gore, H. K. 1931 *Z. phys. Chem.* B, **12**, 389–97.
Lowry, T. M. 1933 *Nature, Lond.*, **113**, 566.
— 1935 *Optical Rotatory Power.* London: Longmans.
Lowry, T. M. and Allsopp, C. B. 1931 *Proc. Roy. Soc.* A, **133**, 36–47.
— — 1934 *Proc. Roy. Soc.* A, **146**, 313–26.
Lowry, T. M. and Baldwin, W. C. G. 1937 *Proc. Roy. Soc.* A, **162**, 204–14.
Lowry, T. M. and Cutter, J. O. 1925 *J. Chem. Soc.* **127**, 604–15.
Lowry, T. M. and French, H. S. 1932 *J. Chem. Soc.* pp. 2654–8.
Lowry, T. M. and Gilbert, F. L. 1929 *J. Chem. Soc.* pp. 2867–76.
Lowry, T. M. and Gore, H. K. 1932 *Proc. Roy. Soc.* A, **135**, 13–22.
Lowry, T. M. and Hudson, H. 1933 *Philos. Trans.* A, **131**, 117–54.
Lowry, T. M. and Hüther, F. 1936 *Rec. Trav. chim. Pays Bas,* **55**, 688–96.
Lowry, T. M. and Lishmund, R. E. 1935*a* *J. Chem. Soc.* pp. 709–13.
— — 1935*b* *J. Chem. Soc.* pp. 1313–19.
Lowry, T. M. and Simpson, D. M. 1936 *J. Chem. Soc.* pp. 1156–9.
Lowry, T. M. and Walker, E. E. 1924 *Nature, Lond.*, **113**, 565–566.
Mulliken, R. S. 1935 *J. Chem. Phys.* **3**, 564–73.
Phillips, H. 1925 *J. Chem. Soc.* **127**, 2552–87.
Read, J. and Smith, H. G. 1922 *J. Chem. Soc.* pp. 1863–72.
Rupe, H. 1924 *Ann. Phys., Lpz.*, **436**, 184–204.
— 1927 *Ann. Phys., Lpz.*, **459**, 195–217.
Scheibe, G. and Grieneisen, H. 1934 *Z. phys. Chem.* B, **25**, 52–6.
Schou, S. A. 1926 *C.R. Acad. Sci., Paris,* **182**, 965–7.

The Temperature Variation of the Work Function of Clean and of Thoriated Tungsten

By A. L. Reimann, Ph.D., D.Sc.

Communication from the Research Staff of the M.O. Valve Co. Ltd., at the G.E.C. Research Laboratories, Wembley, England

(*Communicated by R. H. Fowler, F.R.S.—Received* 3 *June* 1937)

Introduction

It is well known that the relation between the electron emission i from a hot body and its absolute temperature T may be expressed empirically by the equation

$$i = AT^2 e^{-\psi/kT}, \tag{1}$$

in which A and ψ are constants characteristic of the emitting surface, and k is Boltzmann's constant. This is of the same form as the theoretical equation

$$i = A_0 \bar{D} T^2 e^{-\chi/kT}, \tag{2}$$

in which A_0 is a universal constant having the numerical value of 120 amp. cm.$^{-2}$ degree^{-2}, $\bar{D}$ is the mean transmission coefficient, and χ is the work function of the emitter. This quantity is not necessarily constant with temperature, and if we assume its temperature variation to be linear, as we may do within a sufficiently restricted range of temperatures, setting

$$\chi = \omega + \alpha kT, \tag{3}$$

where ω and α are constants, we may rewrite (2) thus:

$$i = A_0 \bar{D} e^{-\alpha} T^2 e^{-\omega/kT}. \tag{4}$$

It may be shown (cf. Reimann 1934*a*, p. 265) that in such cases as occur in nature $\bar{D}$ probably never varies appreciably with temperature, and so, assuming this, and comparing (1) with (4), we may write

$$A = A_0 \bar{D} e^{-\alpha}, \quad \psi = \omega. \tag{5}$$

The values of A for most clean metals lie between about $\frac{1}{4}A_0$ and $\frac{1}{2}A_0$, and it is believed that in these cases the discrepancy between A and A_0 is due almost entirely to variation of χ with T, the transmission being practically perfect (cf. Reimann 1936). The values of A found for strongly electropositively contaminated metals, however, are of a smaller order of magnitude than those for clean metals, and the question arises whether here, too, a temperature variation of the work function is mainly responsible for the discrepancy between A and A_0, or whether the greater part of the discrepancy is due to imperfect transmission.

It was the main purpose of the work described below to try to find the answer to this question in the case of fully activated thoriated tungsten (W-Th). The method adopted was to use infra-saturation thermionic currents to measure the rate at which the contact potential difference (C.P.D.) between a standard source of electrons and a W-Th filament varies with the temperature of the latter. Since the product of C.P.D. and the electronic charge is the same as work function difference (cf. Becker and Brattain 1934), this gives us directly the temperature variation of the work function of W-Th. Incidentally, the same thing was done with the surface of the thoriated tungsten filament clean, information thus being obtained concerning the temperature variation of the work function of clean tungsten.

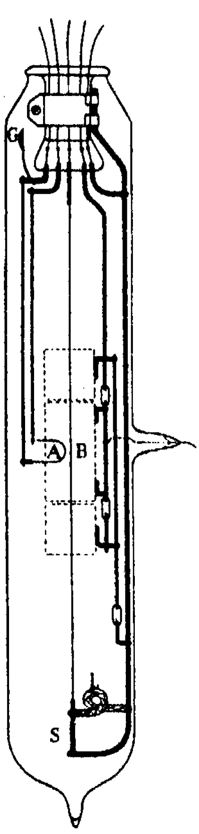

Fig. 1

THE EXPERIMENTAL TUBE

The tube used is shown in fig. 1. A is a U-shaped, stabilized tungsten filament, of 0·1 mm. diameter, which could be used as a constant source of electrons. B is a straight thoriated tungsten filament, coplanar with A, whose centre is about 2 mm. from the tip of A. It is 0·205 mm. in diameter and 20 cm. long, and is kept under tension by the tungsten spring S. Current leads are provided for it, the bulk of the current passing through the flexible multiple-copper-wire lead L. It is in the dependence of the C.P.D. between A and B on the temperature of B that we are interested.

To enable a thermionic test on the surface condition of B to be carried out, this filament is surrounded by three cylindrical electrodes of molybdenum mesh, 2 cm. in diameter and placed end-to-end, being separated from one another by 1 mm. gaps. The length of the central mesh electrode is 4 cm. and that of each of the end ones is 2 cm. When it was wished to test the thermionic emission from B at a given temperature, the filament A, which passes through holes in the mesh of the central molybdenum electrode without touching it, was left electrically floating, the central electrode was held at a potential sufficiently high to saturate the electron current to it, and the two end electrodes were made as much negative relative to the centre of *B* as the central one was positive. Thus the electron current emitted from a length of 4·1 cm. in the centre of *B* was collected by the central cylinder, that emitted from the remainder of the filament being suppressed by an electron-retarding field. To guard against any electrons not emitted from the above-mentioned central part of *B* being collected by the lead to the central cylinder, this lead is taken away laterally through the wall of the tube as shown. Glass beads are provided as insulating supports where required.

G is a pre-degassed nickel disk to which a copper-clad barium getter pellet is held by nickel gauze. The barium could be "dispersed" from this to form an active deposit on the adjacent wall of the tube by heating the disk by means of high-frequency induction.

The treatment of the tube on the pump (a three-stage mercury condensation pump) was as follows: First the tube was baked for 1 hr. at 400° C. Following this the thoriated filament *B* was heated for 1 hr. at 2000° K., and then for 10 min. at 2350° K. The filament *A* was next heated for 5 min. at 2000° K. Then the three molybdenum mesh electrodes were heated to bright redness for about 5 min. by high-frequency induction. Finally, barium was dispersed from the getter disk *G*, and the tube was sealed off from the pump.

It is well known that the vacuum in a sealed-off vessel improves considerably on prolonged "ageing" in which an ionizing electron discharge is passed. The following further treatment was therefore given: First, filament *B* was heated for 114 hr. at 2000° K. Next, *A* was heated for 24 hr. at 2400° K. and for a further 3 hr. at 2600° K. Finally, *B* was again heated, first for 97 hr. at 2350° K. and then for a further 22 hr. at 2400° K. During all this filament heating, all the electrodes other than the heated filament were held at a potential varying between 30 and 50 V positive to it, and collected an electron current (either space-charge-limited or saturated) between 7 and 13 mA.

THE BEHAVIOUR OF CLEAN TUNGSTEN

The filament *B* was now presumed to have a clean surface, but, to make sure of this, its thermionic emission was tested at a series of temperatures ranging from 1624 to 2003° K., the temperatures being calculated from the wire diameter and the currents according to the tables of Jones and Langmuir

(1927). At each temperature the emission was observed at a series of anode potentials (and corresponding negative potentials of the "guard electrodes"). From these data straight Schottky lines were obtained, and these were extrapolated backwards to give zero-field emissions. These were then used to obtain the Richardson line marked W in fig. 2. The corresponding values of the thermionic constants are

$$\rho A = 84 \text{ amp. cm.}^{-2} \text{ deg.}^{-2}, \quad \psi = 4{\cdot}52 \text{ e-volts},$$

where ρ is the "roughness factor" for the filament surface, this being probably of the order of 1·3 (cf. Reimann 1935). These are in good agreement with the accepted values for clean tungsten.

At the two highest temperatures, 1930 and 2003° K., it was found that the emission was not quite stable, increasing slowly with time. Earlier in the ageing process, during which occasional tests were made, the emission was observed to be still less stable (at first much less so). Evidently there was a little reduced thorium present in the wire initially, resulting, possibly, from the inclusion of a few particles of graphite lubricant in wire-drawing. The greater part of the thorium must have been distilled out during the long ageing, although enough remained to give the residual instability. But after the completion of the ageing it was always possible to establish a surface condition of the filament indistinguishable from that of clean tungsten by suitably "flashing" it, and at temperatures up to about 2000° K. the subsequent growth of activity by diffusion of thorium to the surface was sufficiently slow for accurate clean-tungsten emission readings to be obtainable. The flashes actually given were for 1 min. at 2475° K.

The C.P.D. measurements for the clean condition of filament *B* were now carried out. Filament *A* was kept at a constant temperature of 2400° K., and, with the three molybdenum mesh electrodes floating, and *B* either "cold" or at 1070° K., the electron current passing from *A* to *B* noted at various infra-saturation values of the potential difference between them. The reason why the three molybdenum mesh electrodes were left floating was to ensure that they should take up a constant *effective* potential, irrespective of their surface condition. It was also found necessary to shield the whole tube; this was done by wrapping fine copper gauze round it and connecting it to the negative lead of filament *A*.

The current-voltage relationship for filament *B* cold is given by the curve marked W in fig. 3. This curve is drawn so as to best represent the readings, marked by circles. To make sure of the surface condition of *B* it was flashed for 1 min. at 2475° K. and then given 2 min. to cool down before each reading was taken. After 2 min. the filament must, by the combined effects of radiation and conduction to the supports, have reached a temperature sufficiently near to room temperature for the difference (perhaps of the order of 100°) not to matter. The reason for not waiting longer than 2 min. was that a slow decay of the current was observed to occur after somewhat longer times than this, due, probably, to a gradual contamination of the filament surface by electronegative residual gas.

The crosses lying close to the curve W represent readings taken with filament *B* held at 1070° K., again 2 min. after a 1 min. flash at 2475° K. The effective potential of the filament was taken to be that of its centre. To see whether this assumption is justified we have to consider the effects of (1) the potential drop along *A*, (2) the potential drop along *B*, (3) the longitudinal thermal expansion of *B*, and (4) the magnetic field surrounding *B*. A detailed discussion of the first three items shows that their effects are all negligibly small. The effect of the magnetic field due to the 0·83 amp. current flowing along *B* when it was held at 1070° K. is unfortunately more difficult to estimate quantitatively, but from the fact that the curve which would best pass through the crosses appears to be of exactly the same shape as that which passes through the circles—only displaced parallel to the voltage axis—it appears very probable that this effect, also, is negligibly small.

In addition to the question of the effective potential of *B* when heated, there is the effect of the lateral thermal expansion of the filament to be considered. Owing to this its diameter is greater by $\frac{1}{3}$ % at 1070° K. than when it is cold. It would not appear that such a slight geometrical change as this could affect the thermionic current by an appreciable amount, however, since a change in the current could only just be detected when the filament was set in quite violent mechanical vibration, the amplitude near filament *A* being of the order of 1 mm. The mean effect on the current of such a vibration must surely have been considerably greater than that of thermal expansion.

Thus it must be concluded that the displacement of the crosses to the right of the curve marked W is probably a true measure of the change in C.P.D. between the filaments *A* and *B*, and thus of the amount by which the work function of clean tungsten increases when it is heated from somewhere in the region of 300 or 400° K. to 1070° K. The measured mean value of this displacement is 0·05 e-volt. The amount by which the work function should increase for a corresponding temperature rise in the range where the emission was measured, in order to account for the value found for ρA on the assumption that ρ is equal to 1·3 and $\bar{D}$ equal to 1, is 0·04 e-volt. The agreement is as good as could be expected in view of the experimental uncertainty, and also the uncertainty concerning the value of ρ and the constancy of $d\chi/dT$ over the whole range of temperatures.

THE BEHAVIOUR OF W-TH

The filament B was now activated by first flashing it for 3 min. at 2800° K. to reduce thoria to metallic thorium, and then holding it for suitable periods at a succession of activating temperatures, decreasing from 2200 to 1900° K. When the activation was complete the emission was measured at a series of temperatures ranging from 1166 to 1624° K. The Schottky lines obtained were not quite straight, so the emission corresponding to zero field was assumed to be given by the current at which saturation had just been safely attained. The corresponding Richardson plot is the line marked W-Th in fig. 2, and the thermionic constants calculated from it are

$$\rho A = 6{\cdot}5 \text{ amp. cm.}^{-2} \text{ deg.}^{-2}, \quad \psi = 2{\cdot}77 \text{ e-volts.}$$

These are in satisfactory agreement with the data obtained by other observers.

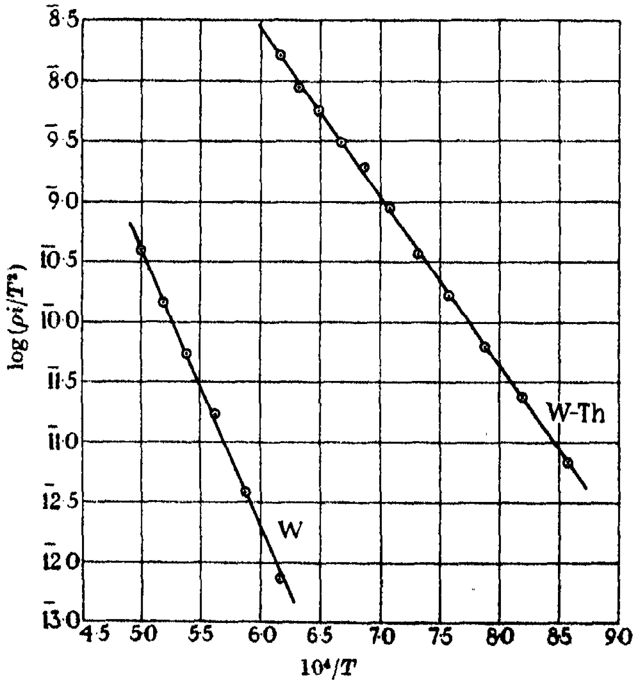

FIG. 2

The C.P.D. measurements taken with the activated filament B "cold" are represented by the circles through which the curve marked W-Th in fig. 3 passes. The two kinds of crosses near this curve represent readings taken with the filament at 970 and at 1070° K. As when the filament was clean, it was found that it slowly became more electronegative when left cold, but a sufficiently long heating at 1960° K. always restored it to its full thermionic activity. The filament was therefore kept running at 1960° K. between readings, and care was taken to space these sufficiently far apart in time. As before, 2 min. were allowed to elapse after the "restorative" heating had been discontinued before each reading was actually taken. This time was not long enough for the condition of the filament to change appreciably.

The curve W-Th was not drawn specially for the W-Th circles, but is simply the curve W moved bodily parallel to the voltage axis until it best represents them. The voltage displacement between the two curves is 1·68 V. This is a measure of the C.P.D., and therefore of the difference between the work functions, of clean and fully activated thoriated tungsten, both cold. On the assumption that $d\chi_{\mathrm{W}}/dT$ and $d\chi_{\mathrm{W\text{-}Th}}/dT$ are both constant with temperature, we have from equation (3)

$$\chi_{\mathrm{W}} - \chi_{\mathrm{W\text{-}Th}} = \psi_{\mathrm{W}} - \psi_{\mathrm{W\text{-}Th}} + (\alpha_{\mathrm{W}} - \alpha_{\mathrm{W\text{-}Th}})\, kT, \tag{6}$$

the subscripts denoting the system to which the symbols refer. Our measured value of $\chi_{\mathrm{W}} - \chi_{\mathrm{W\text{-}Th}}$ is 1·68 e-volts, and that for $\psi_{\mathrm{W}} - \psi_{\mathrm{W\text{-}Th}}$ is $4{\cdot}52 - 2{\cdot}77$, or 1·75 e-volts. Inserting these values in (6), we obtain for $(\alpha_{\mathrm{W}} - \alpha_{\mathrm{W\text{-}Th}})\, kT$ the value of 0·07 e-volt. It is easy to show that on the assumption that the discrepancy between $A_{\mathrm{W\text{-}Th}}$ and A_{W} is due not to internal reflexion in the case of W-Th but to an extra rapid rate of variation of χ with T, $(\alpha_{\mathrm{W}} - \alpha_{\mathrm{W\text{-}Th}})\, kT$ would be 0·066 e-volt at 300° K. and 0·088 e-volt at 400° K. The approximate agreement between these and our 0·07 e-volt is, however, of no real significance, for these quantities are smaller than the combined uncertainties of the experimental data.

There is no certain difference between the displacements of the 970° K. points and those of the 1070° K. points to the right of the cold W-Th curve. But the important thing to note is that these displacements are not appreciably different from those of the 1070° K. clean-tungsten points to the right of the cold W curve. If the difference between $A_{\mathrm{W\text{-}Th}}$ and A_{W} were due solely to a difference between $d\chi_{\mathrm{W\text{-}Th}}/dT$ and $d\chi_{\mathrm{W}}/dT$, the displacement of the 1070° K. points would be about 0·15 V greater in the case of W-Th than in that of W. The actual difference, if any, between the displacements is certainly less than one quarter of this, which is equivalent to a factor of less

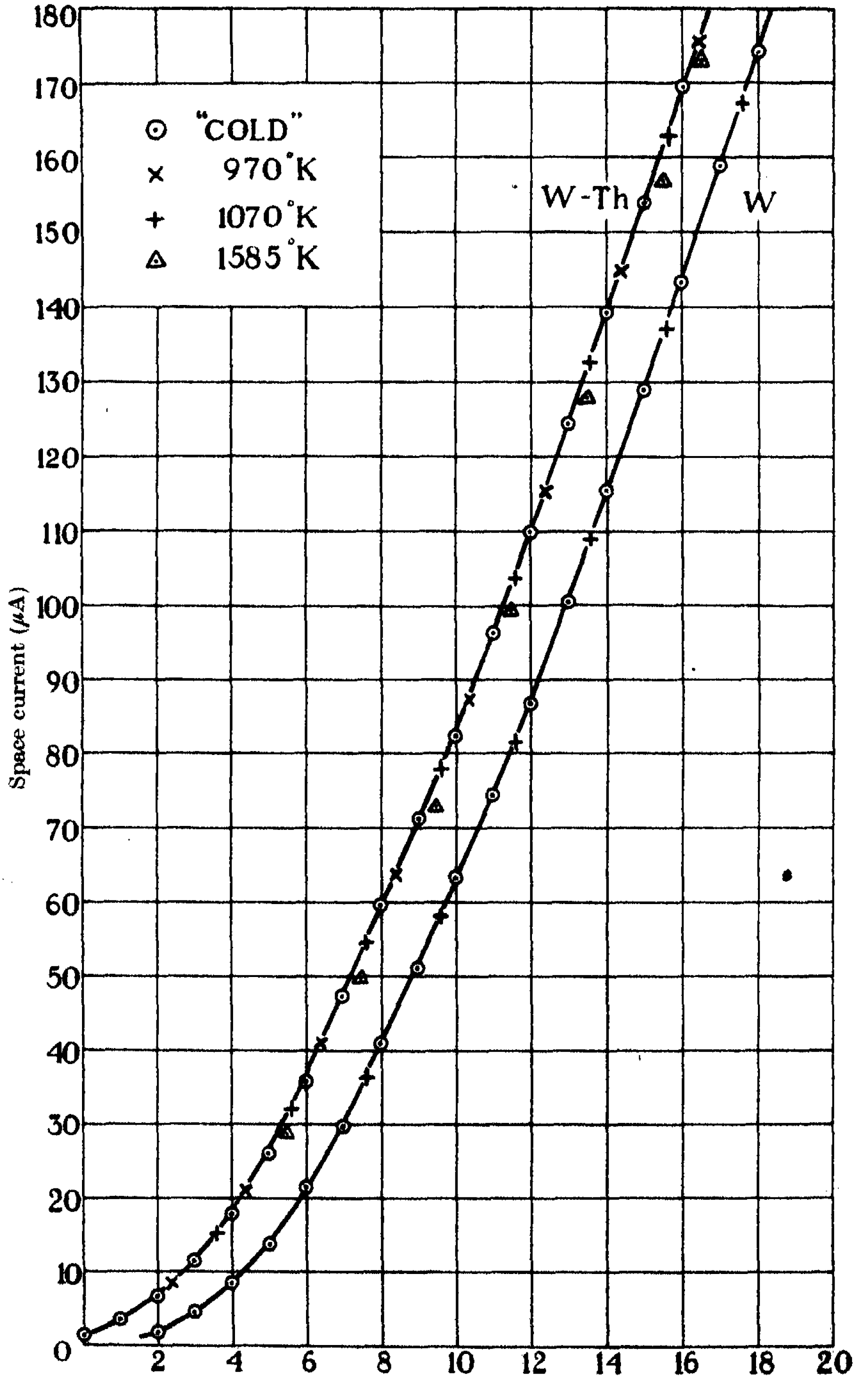
⊙ "COLD"
× 970°K
+ 1070°K
△ 1585°K
W-Th
W
Space current (μA)
0
10
20
30
40
50
60
70
80
90
100
110
120
130
140
150
160
170
180
2
4
6
8
10
12
14
16
18
20
Potential of filamentary anode (volts)

FIG. 3

than 2 in A. In other words, the rate of variation of the work function of W-Th with temperature is insufficient to make its A as low as 30 amp. cm.$^{-2}$ deg.$^{-2}$. Of the total factor by which the A of W-Th is less than A_0 (according to the measurements, about 24) a factor of at least 6 must be due to internal reflexion. It is important to note that the validity of this conclusion is not affected by any uncertainty regarding the effects of magnetic field, etc. on the displacements, since in comparing the displacements for the two conditions of the filament, held at the same temperature in each case, these effects cancel out.

When the work had reached this stage, a paper on the same subject by D. B. Langmuir (1936) appeared, in which the conclusions arrived at differ radically from those drawn here. Langmuir states that between 850 and 1450° K. the value of $\frac{d}{dT}(\chi_{\mathrm{W}} - \chi_{\mathrm{W\text{-}Th}})$ is $3{\cdot}6 \times 10^{-4}$ e-volt/degree. This is about six times the maximum possible value for this quantity for temperatures up to 1070° K. found in the present work, and would account for a factor between A_{W} and $A_{\mathrm{W\text{-}Th}}$ of no less than 70.

In the present work the temperatures at which C.P.D. measurements were made were kept sufficiently low for the thermionic emission from filament B to be negligible. Thus the calculated values of the emission from W-Th at 970 and at 1070° K. are only 2×10^{-8} and 10^{-6} amp. cm.$^{-2}$ respectively. The reason for having done this is that at too high temperatures the emitted electrons, though not allowed permanently to escape, must give rise to a strong space-charge potential minimum in the region of the filament, and so make it behave as if its work function were greater than, in reality, it is. To illustrate this, a further set of readings, taken with filament B at 1585° K., where its emission is $2{\cdot}5 \times 10^{-2}$ amp. cm.$^{-2}$, is shown in fig. 3. Unfortunately it was now too late to restore the clean-tungsten condition of the filament and take comparison readings at the same temperature for this. But if we take the rate of change of voltage for a given thermionic current to give directly $d\chi_{\mathrm{W\text{-}Th}}/dT$, we find between 1070 and 1585° K. a mean value for this quantity of 4×10^{-4} e-volt/degree, which is of the same order as Langmuir's $5{\cdot}2 \times 10^{-4}$ e-volt/degree obtained on the same assumption.

There still remains to be accounted for, however, the discrepancy between our two results in the temperature range 850–1070° K. which we have in common. A clue to this is possibly to be found in the fact that below 850° K. Langmuir found an even higher apparent value of $d\chi_{\mathrm{W\text{-}Th}}/dT$. The cause of this might still have been operative, though to a lesser extent, between 850 and 1070° K.

Langmuir himself does not take his low-temperature results to give the true behaviour of W-Th uncontaminated by gas. While in the present work the filament was subjected to a heat treatment immediately before C.P.D. measurements were made, in order to eliminate gas contaminations, this was not done by Langmuir, who made his observations with the filament in its final, equilibrium condition at the temperature in question. It is a curious fact that whereas in the present work the W-Th filament was observed to become more electronegative with time after cooling from an activating to a relatively low temperature, a time change in the opposite direction was observed by Langmuir. Possibly the residual gases were different in the two cases.

Discussion

We have seen that Langmuir's C.P.D. result for W-Th is only in *apparent* conflict with that obtained here. But in the case of clean tungsten in the approximate temperature range 540–960° K. he finds a slight *negative* temperature coefficient of the work function, the value of which is of the order of 4 or 5×10^{-5} e-volt/degree. As in the present work, the filament was flashed shortly before each reading was taken, so the discrepancy between our two results can hardly be explained in terms of residual gas contaminations. It is possible, however, that the effects of potential drops along the filaments were more important in Langmuir's experimental arrangement than in this. Langmuir himself does not consider the temperature coefficients he obtains to be conclusive.

There remains to be considered a recent exhaustive investigation of the thermionic currents from clean and thorium-contaminated tungsten filaments, at various temperatures and various retarding and accelerating anode potentials, by Nottingham (1936). From the results obtained in this work Nottingham concludes that there is always an important internal reflexion of the slower electrons, and that, surprisingly, this reflexion is *independent of the degree of contamination*. This is quite at variance with what we should expect on the quantum theory of reflexion, and, if substantiated, would require an important elaboration, if not a recasting, of the simple emission theory of Nordheim. The reflexion deduced by Nottingham is sufficiently important to require a negative temperature coefficient of the work function of clean tungsten (actually of the order found by Langmuir) to account for the observed A. For W-Th a positive coefficient is required, which, however, is larger than that found here.

Leaving open the question of how the conflict between Nottingham's conclusions and those arrived at in the present work is to be resolved, let us consider how the latter fit in with the general scheme of thermionic theory. As Reimann has pointed out (1934*b*,* 1936), the more reliable of the experimental determinations of A for clean metals (including tungsten) are in remarkably good agreement with what we should expect on the assumption that the transmission is perfect and the temperature variation of the work function is due almost entirely to the effect of thermal expansion on the critical energy of the Fermi distribution of the internal electrons. In the case of tungsten, experimental data obtained by Copley and Phipps (1934) on the ionization of potassium vapour by a tungsten filament heated in it have been shown by Reimann (1934*c*, 1936) to support the above hypothesis, and the C.P.D. measurements here made constitute independent experimental confirmation that the temperature variation of the work function is, indeed, that which the hypothesis requires. In the case of tantalum, measurements of photoelectric response as a function of exciting frequency and temperature (Cardwell 1931) also indicate a temperature variation of the work function in harmony with our hypothesis (Reimann 1936).

But if, as it appears, the temperature variation of the inner potential is negligibly small in comparison with that of the Fermi critical energy in the case of clean metals, one would naturally expect the same thing to be true in the case of contaminated metals, for in both cases the factors to which the inner potential owes its existence are of the same physical nature. This expectation is borne out by the C.P.D. data for W-Th, there being no measurable difference between $d\chi_{\mathrm{W\text{-}Th}}/dT$ and $d\chi_{\mathrm{W}}/dT$.

In conclusion, the author wishes to tender his acknowledgements to the General Electric Company and the Marconiphone Company, on whose behalf the work was done which has led to this publication.

SUMMARY

Measurements were made of the contact potential difference between a constant source of electrons and a neighbouring tungsten filament collecting space-charge-limited electron current, whose condition was varied. This filament was either clean or covered with a layer of thorium atoms, and, in addition, it was held at various temperatures. In this way direct information was obtained concerning the rates at which the work functions of clean

---

* In this read "A" for "the apparent A", and "$A_0\bar{D}$" for "the true A".

and fully activated thoriated tungsten (W-Th) vary with temperature. Within the limits of experimental uncertainty there is no difference between the temperature coefficients of the two work functions. The temperature coefficient found is about that which would be required to account for the observed value of the thermionic constant *A* of clean tungsten on the assumption of practically perfect transmission. It must be concluded that the factor (of the order of 10–20) by which the *A* of W-Th is less than that of clean tungsten is due to internal reflexion of electrons at the W-Th surface.

REFERENCES

Becker, J. A. and Brattain, W. H. 1934 *Phys. Rev.* **45**, 694.
Cardwell, A. B. 1931 *Phys. Rev.* **38**, 2041.
Copley, M. J. and Phipps, T. E. 1934 *Phys. Rev.* **45**, 344.
Jones, H. A. and Langmuir, I. 1927 *Gen. elect. Rev.* **30**, 310, 354 and 408.
Langmuir, D. B. 1936 *Phys. Rev.* **49**, 428.
Nottingham, W. B. 1936 *Phys. Rev.* **49**, 78.
Reimann, A. L. 1934*a* "Thermionic Emission." Chapman and Hall, Ltd.
— 1934*b* *Nature, Lond.*, **133**, 833.
— 1934*c* *Phys. Rev.* **45**, 898.
— 1935 *Phil. Mag.* **20**, 594.
— 1936 *Sci. J. R. Coll. Sci.* **6**, 104.

The Photochemical Polymerization of Methyl Methacrylate Vapour

By H. W. Melville
Colloid Science Laboratory, Cambridge

(*Communicated by Eric K. Rideal, F.R.S.—Received* 12 *July* 1937)

It is rather a remarkable fact that although the study of polymerization reactions has increased enormously within the past few years, gas-phase polymerization has received scant attention. By performing such experiments in the gas phase all the exact technique of gas kinetics is at once available to unravel the complex sequence of collision types which make up a polymeric reaction. Once the essential features of the reaction are discovered, it is in many cases a comparatively simple matter to control these over wide limits.

It has long been recognized that polymerization processes are chain reactions. If the reaction is initiated thermally, then the observed kinetics of the overall reaction may become rather complicated, so that it is difficult to calculate the absolute velocities of the reactions comprising the whole process. As in ordinary chain reactions, this difficulty can be overcome by adopting photochemical methods of controlling the initiation reaction. Having started the growth of the polymer the velocity of growth is then dependent primarily on the inherent properties of the molecule but may be modified by altering gas pressure and temperature. The termination reaction may be one of a number of types and hence control may or may not be possible. In certain reactions control can often be exercised in one direction, namely, in limiting the growth of the polymer by the introduction of specific inhibitors.

Preliminary observations have indicated that ethylene compounds of the general type 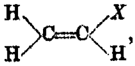 $H_2C{=}CHX$, where X may be halogen $COOCH_3$ etc., can be polymerized by the action of ultra-violet radiation. A systematic survey of the photochemical polymerization of molecules of this type has been started by taking up the study of methyl methacrylate.

The Absorption Spectrum

The absorption spectrum of the molecule was measured by dissolving the ester in spectroscopically pure hexane. The extinction coefficient wave-length curve was measured in the usual way by means of a Hilger rotating sector spectrophotometer. Fig. 1 shows the results obtained. It will be observed that the absorption spectrum consists of two distinct parts on either side of a point at about 2300 A. The absorption on the long wavelength side of the point is certainly due to the $COOCH_3$ group, for it is exhibited by all compounds containing this group. The sudden rise in the coefficient at 2300 A is due to the double bond, as a similar degree of absorption is obtained with trimethylethylene (Snow and Allsopp 1933).

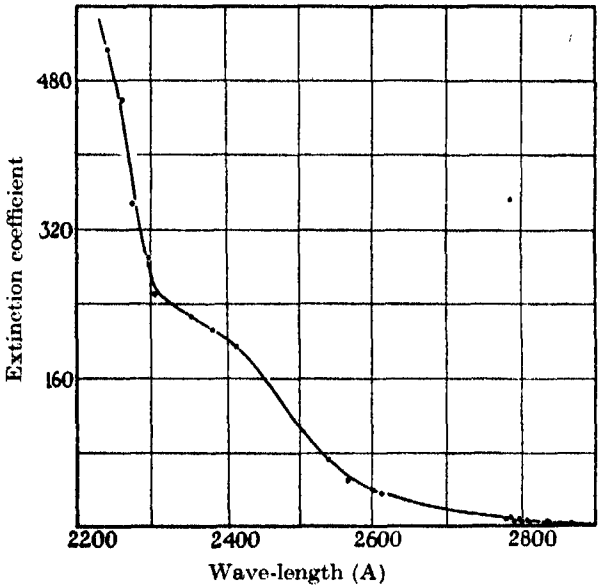

FIG. 1—Extinction coefficient—wave-length curve for methyl methacrylate dissolved in *n*-hexane.

APPARATUS

Methyl methacrylate is readily soluble in tap grease, and hence the reaction system was fitted with mercury cut-offs. For temporary storage of the liquid, greased taps may be employed. There is, however, one difficulty with rubber grease. If the vapour is allowed into contact with it, the unvulcanized rubber apparently acts as a catalyst for the polymerization of the methyl methacrylate, since a glass-like polymer soon effectively seals the barrel of the tap in its socket.

Methyl methacrylate has a comparatively small vapour pressure at room temperatures—*ca.* 30 mm.—and hence the most convenient and also sensitive method of following the course of polymerization is to condense the liquid in a capillary and observe the rate of fall of the liquid meniscus. In this way polymerization could easily be carried out under constant pressure over long periods. In outline the reaction system is shown in fig. 2. The source of light was a water-cooled mercury arc lamp. The light was filtered and focused by a 2 cm. silica tube on to the reaction vessel. A number of different vessels were used. An annular type is shown in fig. 2. The polymerization occurs in the annular space and the inside vessel contains ammonia, the rate of the mercury-sensitized dissociation of this molecule serving as a check on the intensity of the light entering the reaction system. The relationship connecting rate of polymerization and intensity could therefore be easily ascertained. In some experiments the position of the lamp was kept fixed and the intensity altered by interposing suitable perforated screens. The transmission of the latter was calculated and checked by the ammonia photometer. Later it became necessary to measure the mean lifetime of the growing polymer. This was accomplished by a rotating sector interposed between lamp and filter. A two and an eight sector disk (i.e. arranged for equal periods of light and darkness) could be rotated on the spindle of an electric motor up to 2000 r.p.m. The speed of the disk was obtained by driving, through a reduction gear, a commutator which actuated an ordinary telephone call counter.

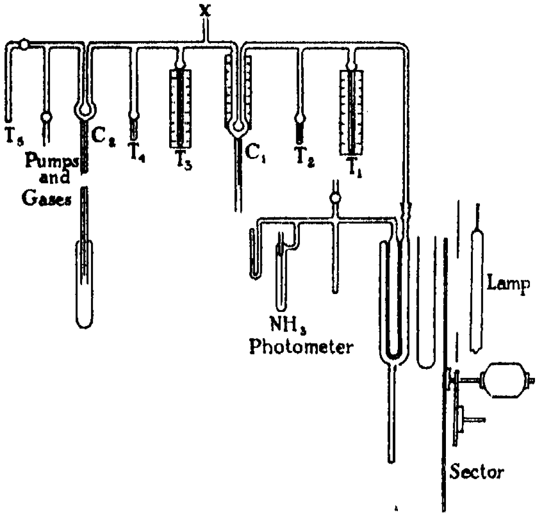

FIG. 2

Before starting the experiments, the ammonia photometer was calibrated against the uranyl oxalate photometer (Forbes and Heidt 1934).

The general procedure in carrying out an experiment was briefly as follows: The intensity of the light was noted by means of the ammonia photometer with the reaction vessel evacuated. Next methyl methacrylate was distilled from T_5 into the graduated capillary T_1 fitted with a millimetre scale which was read to 0·1 mm. by a lens. The mercury in cut-off C_1 was raised and the methacrylate allowed to evaporate until the pressure indicated by C_1 was constant. Another reading was taken on the ammonia photometer to obtain the fraction of the light absorbed by the vapour. Continued exposure was then commenced. During a very long run, the liquid in T_1 sometimes became exhausted. Before this happened T_3 was filled with methacrylate, the mercury in C_1 lowered and the supply of vapour noted from the level of the meniscus in T_3. The combined manometer and cut-off C_1 was also useful in that, if the surroundings changed temperatures during a long run, for example 8 hr., a correction to the level in T_1 was easily made by noting the pressure recorded by C_1. The small traps T_2 and T_4 were attached to the apparatus to enable quick withdrawal of methacrylate vapour from the apparatus and for the measurement of small quantities of the liquid. In addition there were attached to the reaction system a McLeod and a Pirani gauge so that micro-analyses could be made of non-condensable gases produced during polymerization. In some experiments it became necessary to treat the polymer with iodine vapour. Consequently cut-offs C_1 and C_2 were modified by inserting a tap just below the junction of the two limbs of the manometer. A tube containing solid iodine was fused on at X. The polymer was deposited on the reaction vessel, the mercury lowered below the tap in C_1 and C_2, the iodine allowed into contact with the polymer, all mercury surfaces being thus protected. After the requisite period of contact, the iodine was condensed back into the tube and the mercury once more allowed up to its normal level in C_1 and C_2.

RESULTS

Effect of Wave-length of Light

Employing the radiation transmitted by a water filter (i.e. $\lambda > ca.$ 2000 A) from the mercury lamp, the following is a typical run:

INPUT $4\cdot9 \times 10^{17}$ QUANTA/MIN. at λ 2537. VOL. OF SYSTEM 46·6 C.C.

Time (min.)	0	5	10	15	31	40	50	60	180
Press. (mm.)	34·0	34·0	34·0	31·2	25·0	22·0	20·2	19·6	22·0

After 15 hr. in the dark, the pressure of gas non-condensable in liquid air was 9·0 mm. and the pressure of the remaining methacrylate 8·0 mm. The following features of the experiment may be noted. At first there is an induction period before the pressure commences to fall with the simultaneous deposition of visible amounts of polymer. After prolonged illumination, the pressure rises. On leaving the system 15 hr. in the dark, polymerization continues. Finally analysis of the residual gas by condensing in liquid air shows the presence of non-condensable gas, indicating appreciable decomposition of methacrylate, since the polymer is not decomposed to a comparable extent under similar conditions. For example, after 25 mm. illumination only 0·2 mm. of non-condensable gas was produced.

On replacing the water filter by a solution of 50 % acetic acid and illuminating for a similar period, the following run shows that the pressure decreases continuously and that the pressure of non-condensable gas was less than 1 mm.

Time (min.)	0	10	20	30	43	50	61	70	80
Press. (mm.)	25·6	23·0	22·8	20·4	18·0	17·0	15·4	14·0	13·8

This is better shown by the following figures, the pressure of non-condensable gas being measured accurately by a McLeod gauge.

Conditions	Input at 2537 ($h\nu$/min.)	Press. of gas per min.
50 % CH_3COOH 19·4 mm. methacrylate	$1{\cdot}3 \times 10^{17}$	0·021
H_2O filter 26·0 mm. methacrylate	$2{\cdot}2 \times 10^{17}$	0·070

The probable identity of the gas was established by calibrating a Pirani gauge by means of a McLeod gauge with hydrogen and with oxygen. The calibration curve for the gas from the monomer is shown in fig. 3. It lies slightly above the O_2 curve which indicates that it is probably CH_4. There is therefore photo-decomposition of the molecule by light lying in the second region of absorption beyond 2300 A, which is normally eliminated by the acetic acid filter. The photo-dissociation is probably analogous to that undergone by ethylene when it yields acetylene and hydrogen (Mooney and Ludlam 1929). Similar phenomena are observed with methylacrylate where, instead of obtaining methane, hydrogen is the gas non-condensable in liquid air.

As will be seen from the above experiments, even with radiation of λ 2537 A, some decomposition accompanies polymerization, though the quantum yield for the latter process exceeds unity. In fact it is possible to observe the polymer actually growing in the gas as a faint mist which finally deposits on the walls of the reaction vessel. Similarly, when deposited, it is often possible to see the polymer visibly growing along the silica surface. There are therefore two stages in the growth—one in the gas, the other at the surface.

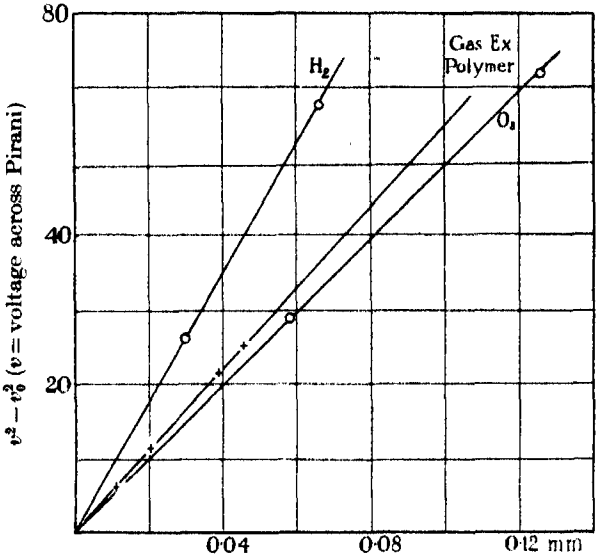

Fig. 3—Calibration curves for Pirani gauge.

Direct or Sensitized Reaction

Direct measurement of the absorption of 2537 radiation by the methacrylate vapour at 30 mm. showed it to be comparable with that of mercury vapour at 0·001 mm. This made it extremely difficult to say whether the reaction was direct or sensitized by mercury vapour. Mercury traps could not be dispensed with and therefore the tube leading to the reaction vessel was packed with gold leaf to trap mercury vapour, but there was no reduction in the velocity of polymerization. Such a trap may not be effective even on slow passage of the vapour through it, and hence for the present it is not possible to decide which type of primary process operates, though indirect evidence points to the direct photo-reaction.

Effect of Time of Illumination on Rate of Polymerization

In order to show the effect of time of illumination on the rate of polymerization, fig. 4 has been constructed from three series of experiments made at constant pressure of methacrylate vapour (31 mm.). The number of molecules polymerized is plotted against time, the periods of illumination being indicated. During the first period the rate gradually increases to a maximum value. This, however, declines, but on switching on the light again attains a steady value slightly greater than that during the previous period. Again, the rate decays on switching off the light, but rises once more to a maximum and remains there whether the light is off or on. Growth was interrupted at 380 min., but continued at exactly the same speed on allowing monomer into contact with the polymer after an interval of 15 hr.

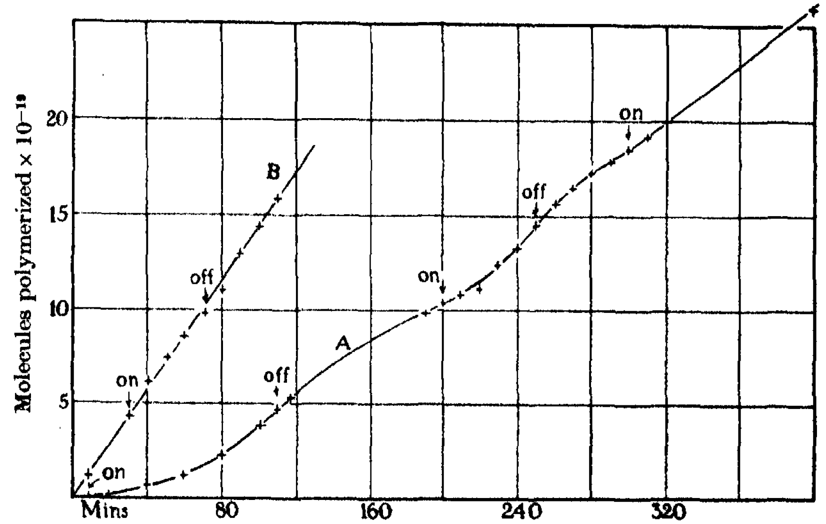

FIG. 4—Rate of polymerization as a function of time of illumination. Curve B is really contiguous with A, but has been transferred to the origin to contract the time scale.

First it may be noted that on switching off the light the rate of polymerization does not immediately drop to zero as do the majority of photochemical reactions. This means that, compared with the steady polymerization, which is not a gas-phase process, there is no measurable amount of polymerization occurring in the gas phase. The centres for the building up of polymers must of course be formed in the gas phase. Moreover, it is probable that polymeric molecules are of considerable size before they settle down on the surface of the reaction vessel from which further growth continues, since they may be seen as a mist diffusing through the gas. The apparent induction period is thus due to the deposition of centres upon the silica surface. There must, however, be a limit to the number of centres which may reside on 1 cm.^{2}. The maximum rate of polymerization is attained when this maximum number is laid down. Assuming then that the rate of gas-phase polymerization can be neglected compared with that occurring on the surface, the variation of rate with time of illumination will be given by an equation of the type

$$R = R_\infty(1-e^{-kt}),$$

where k is a constant proportional to the intensity of illumination and to the area of the reaction vessel illuminated (*vide infra*). From the results in fig. 4 Table I has been constructed. It will be seen that the value of

$$\{\log R_\infty/(R_\infty - R)\}/t$$

increases throughout the induction period; the rate of polymerization is thus increasing faster than can be accounted for by the above assumption. It may also be noted that if the illumination be interrupted, the rate gradually falls off. This phenomenon is repeatedly observed with a clean tube. After continued illumination, or if a tube covered with inactive polymer is employed to start with, there is no decrease in rate on cutting off the illumination. Moreover, the induction period in the latter circumstance is reduced manyfold. Fig. 4 shows a typical experiment to illustrate the effect. These observations indicate that the polymer is in some manner rendered inactive when it is deposited on a silica surface. As polymer accumulates, however, the silica surface is gradually covered up and the activity then persists.

TABLE I—AREA OF ILLUMINATED SURFACE 25 CM.^{2}. PRESS. 31 MM. TEMP. 20° C.

Time (min.)	Rate, molecules/sec. × 10^{-16}	$\{\log R_\infty/(R_\infty - R)\}/t$
35	2·9	0·0021
45	4·2	0·0025
55	6·0	0·0032
65	8·2	0·0040
75	10·6	0·0051
85	12·6	0·0060
95	14·5	0·0073
105	16·3	0·0093

Efficiency of Collisions Leading to Growth—From the above data the apparent collision efficiency of the polymerization reaction may readily be calculated. On an illuminated area of 25 cm.^{2}, the maximum rate of polymerization at 20° is $1\cdot8 \times 10^{17}$ molecules/sec. at 30 mm. pressure. The apparent efficiency is thus $1\cdot0 \times 10^{-7}$. This figure is probably only a maximum, for it is not unlikely that the polymerization is a condensed phase reaction in that the monomeric vapour is first adsorbed by the polymer, the real polymerization occurring thereafter.

Effect of Pressure of Methacrylate on Rate of Polymerization in the Dark—The vapour pressure was simply varied by immersing the capillary containing the liquid methacrylate in a bath at a suitable temperature. In each experiment tests were made by switching on the light to ensure that the maximum number of centres were present on the surface. The data in the following table show that, over the limited range which could be employed, the rate of spontaneous polymerization is approximately directly proportional to the pressure.

AREA OF SURFACE 20 CM.^{2} TEMP. 20° C.

Press. (mm.)	Rate $\times 10^{-16}$ molecules sec.$^{-1}$	Rate/press. $\times 10^{-16}$
11·2	3·1	0·28
20·0	6·3	0·31
28·2	10·4	0·37

Effect of Number of Centres on Rate—Using a tube which had been covered with polymer, the latter having previously been made inactive, the following run was made. Light was switched on for short intervals and the resulting steady rate of polymerization determined. Table II shows the record of one such experiment.

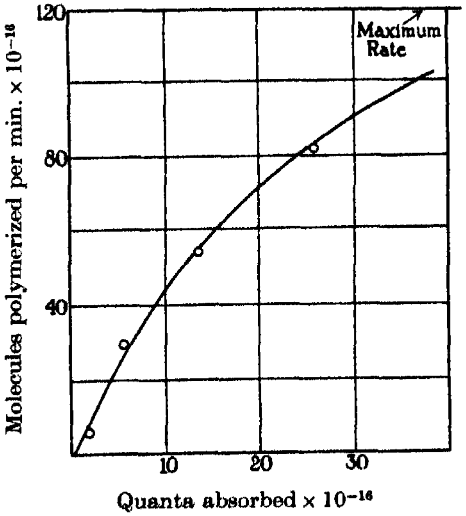

FIG. 5—Rate of steady polymerization as a function of number of quanta absorbed.

From these data, the rate of spontaneous polymerization is plotted against the number of quanta absorbed. The curve in fig. 5 tends to a maximum value. That the maximum is attained is well shown by the result of the last exposure of the system to light: the rate is not increased at all. With such a long dark reaction it is meaningless to define the quantum yield of the reaction. An estimate can, however, be made of the molecular weight of the deposited polymer in the following manner. Assuming that each centre or growing polymeric molecule is as closely packed as possible, it is probable that each centre occupies 20 Å^2, i.e. 5×10^{14} centres/cm.^{2}. On 20 cm.^{2} the maximum rate of polymerization (Table II) is $1 \cdot 1 \times 10^{17}$ molecules/sec. In some experiments polymerization was followed for several hours. In 1 hr., for example, the number of monomeric molecules forming the polymer would amount to 36,000.

TABLE II—NO. OF QUANTA ABSORBED PER SEC. $\times 10^{16}$.
PRESS. 27 MM.

	Time (min.)	No. of molecules polymerized $\times 10^{-18}$	Rate in dark molecules/sec.
	0	0·0	
Light on	10	0·0	
	11	0·0	
	15	0·0	3×10^{15}
	25	0·0	
Light on	30	0·8	
	32	1·3	
	40	2·2	$5 \cdot 1 \times 10^{16}$
	50	3·1	
	60	6·6	
	70	10·0	
Light on	80	12·0	
	85	14·5	
	90	15·4	$6 \cdot 7 \times 10^{16}$
	100	19·0	
	110	23·0	
	120	28·0	
Light on	120	28	
	132	33	
	142·5	40	$1 \cdot 10 \times 10^{17}$
	153	49	
	160	54	
	170	59	
	180	64	
Light on	190	70	
	200	77	

Though the rate of gas-phase polymerization could not be detected with the present experimental arrangement, an upper limit to the quantum yield of the process can be estimated from the data in Table II. Taking the maximum rate of polymerization as $1{\cdot}1 \times 10^{17}$ molecules/sec. and supposing that an increase in velocity of 5 % is indetectable, i.e. $5{\cdot}5 \times 10^{15}$ molecules/sec., then since $1{\cdot}0 \times 10^{16}$ quanta/sec. are absorbed by the methacrylate the quantum yield amounts to 0·5. The active polymer must be of high molecular weight, since it is visible in the gas phase before deposition. The low quantum yield of the total process hence indicates that the primary photo reaction is comparatively inefficient.

The Lifetime of the Growing Polymer—A normal polymerization run was first carried out with a period of illumination long enough to ensure that the surface of the reaction vessel was completely covered with polymer. Thereafter the rate of polymerization in the dark was measured as shown by the line *A* in fig. 6, where the number of molecules polymerized is plotted against time. The monomer was withdrawn after 112 min. and the polymer allowed to stand *in vacuo* for 17 hr. On reintroducing the monomer the speed of polymerization remained unchanged (line *B*). The monomer was once more removed and the polymer allowed to stand for 46 hr. Line *C* shows that a slight decrease in polymerization rate had occurred, since the slope of *C* is less than *A* or *B*. In addition the maximum rate of polymerization was immediately obtained on illuminating the system for only 10 min. It is evident that the half-life for the decay of the activity of the polymer is of the order of a week at least. Introduction of oxygen to a pressure of a few millimetres failed to destroy the active polymer. Even extended exposure to the atmosphere did not impair its activity. Indeed, the active polymer may

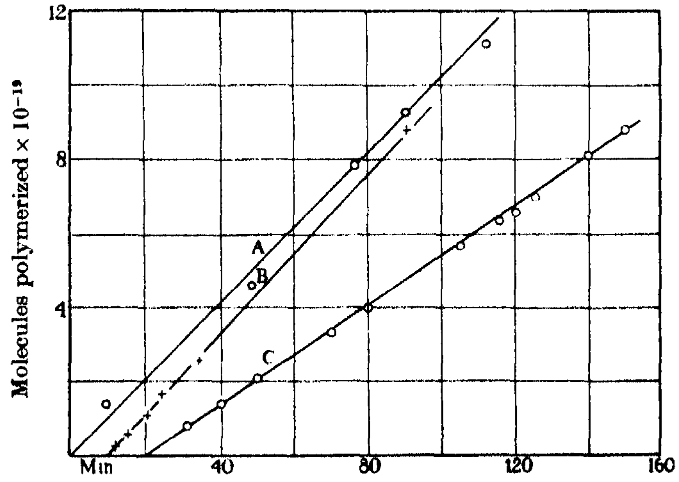

FIG. 6—Pressure of methacrylate 28 mm.

be washed (with alcohol) or scraped out of the reaction vessel and dropped into the monomeric liquid which in turn is polymerized to a glass-like solid. Whether the decay is a natural one or is due to specific inhibitors is a question difficult to answer in view of the long lifetime of the active polymer.

Effect of Continued Illumination on Growth—It has already been shown that the rate of polymerization reaches a maximum on illuminating the system for a sufficiently long time. The next question arises as to what would happen if the light were kept on for prolonged periods. The data in Table III show two experiments carried out under identical conditions; in the first, illumination was switched on for 20 min.; in the second it was kept on for 240 min. There is an appreciable decrease in velocity on prolonged illumination which is probably jointly due to decomposition of deposited polymer and of monomer. At the end of the run no less than 3 mm. of gas non-condensable in liquid air was collected.

TABLE III

Time min.	Molecules polymerized $\times 10^{-18}$ Exp. I	Molecules polymerized $\times 10^{-18}$ Exp. II	Time min.	Molecules polymerized $\times 10^{-18}$ Exp. I	Molecules polymerized $\times 10^{-18}$ Exp. II
20	26	26	140	182	123
40	51	51	160	210	132
60	78	69	180	235	140
80	104	86	200	261	148
100	130	100	220	287	156
120	156	112	240	311	167

Inhibition of Growth—On account of the long life of the active polymer, experiments could be performed on the effect of inhibitors. Whatever the actual nature of the growing polymer, i.e. whether it contains a double bond or has free valencies at either end, it is essentially unsaturated. On addition of any reagent capable of removing such characteristics, the molecule should become inactive. In this way then it will at once become possible to grow the molecule to any desired size and then stop growth.

Experiments were first made by depositing sufficient polymer, then removing monomer, adding hydrogen (+ mercury vapour always present from the mercury cut-offs), illuminating with the unreversed 2537 line of the mercury arc and so obtaining atomic hydrogen which ought to destroy the double bond or saturate the free valencies. Fig. 7 shows one such experiment. Curve *A* shows the dark rate of reaction. Curve *B* shows the effect after the polymer had been treated with 25·6 mm. of H_2 and illuminated for 40 min. If H_2 is merely added to the methacrylate vapour, the inhibiting effect is not observed, possibly because all the hydrogen atoms are removed by the methacrylate before they diffuse to the walls. The rate of production of H atoms in these experiments was about 10^{16}/sec. If each H atom so generated reached the polymer, its activity should be destroyed in a few seconds as the estimated number of active centres is also about 10^{16}. Prolonged illumination is necessary to effect thorough inhibition. This is due to at least two effects, (*a*) a considerable number of H atoms combine in the gas phase, (*b*) another considerable fraction combine on the walls without hydrogenating the polymer. There is no measurable fall of pressure during hydrogenation, nor is there any apparent depolymerization of the polymer.

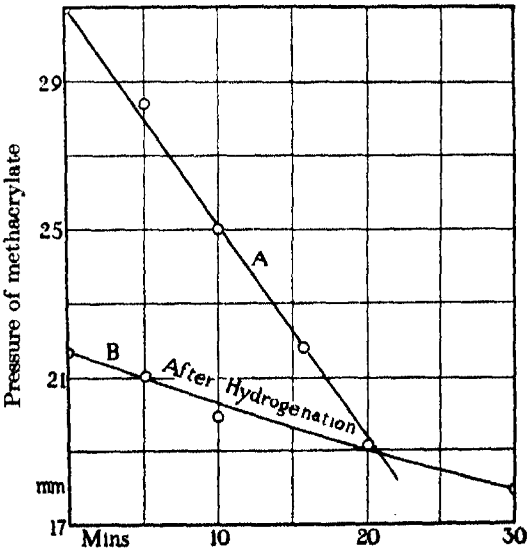

FIG. 7—Inhibition of polymerization by hydrogenation of polymer.

Effect of Iodine—In order to confirm the experiments made with atomic hydrogen, molecular and atomic iodine produced photochemically were employed. Again there was strong inhibition as is shown in Table IV. It will be observed that iodination appears to be a comparatively slow process, for, even after 20 min. treatment, the rate of polymerization is not decreased to zero. On irradiating the monomer once more, the rate of polymerization attains its original velocity and further treatment with iodine reduces it to a small value. In the second series of experiments a considerable amount of polymer had collected on the reaction vessel. This absorbs some monomer which will of course be a competitor for iodine. The reduction in rate of polymerization is therefore not so great as it was at the beginning of the run.

If, however, the iodine vapour is irradiated with light of wave-length $\lambda > 3500$—namely, that transmitted through a soda-glass filter 1 mm. in thickness and therefore capable of dissociating I_2—it will be seen that inhibition is now much more marked. A control experiment in the dark shows that the effect is real. Accordingly the small proportion of iodine atoms produced in this manner must be exceedingly effective in iodinating the polymer.

TABLE IV—INCIDENT INTENSITY *ca.* 10^{16} $h\nu$/SEC. TEMP. 20° C. PRESS. OF MONOMER 26 MM.

Rate of polymerization molecules/sec. × 10^{-15}	Conditions
	Series I
6·4	30 min. illumination, additional illumination of 20 min. to ensure rate a maximum
1·1	After 20 min. exposure to I at 0·1 mm. press.
5·1	40 min. and subsequently 30 min. illumination
1·5	50 min. iodination at 0·1 mm.
	Series II
24·5	Before iodination
20·7	After 8 min. iodination 15 % reduction
21·5	Before iodination
9·4	After 12 min. photoiodination 55 % reduction
23·3	Before iodination
21·0	After 12 min. iodination.

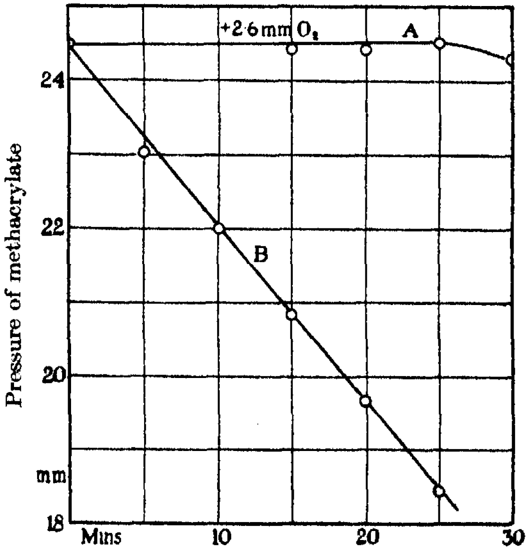

FIG. 8—Effect of oxygen.

Effect of Oxygen—Oxygen at pressures of several hundred millimetres left in contact with the active polymer for several hours did not reduce its activity to any measurable extent. The effect, however, is quite different if the oxygen is present with the methacrylate. Fig. 8 shows the results, a clean tube being used for each experiment. Curve A is that obtained with 2·6 mm. and curve B without oxygen. In absence of oxygen, polymerization starts straightaway, whereas oxygen inhibits the reaction, only a trace of polymerization occurring after 25 min. illumination. Similar results were obtained with the capillary technique. The quantitative effect of oxygen is rather difficult to estimate, since after each run the reaction system has to be taken down, heated to redness in a stream of air and replaced.

Effect of Acetylene and Ethylene—The active polymer does not react at all with acetylene or ethylene as is shown by the following results:

Rate before treatment with 236 mm. C_2H_2 for 15 hr. (no measurable absorption of C_2H_2)	$1{\cdot}72 \times 10^{16}$	molecules/sec.
Rate after contact	$1{\cdot}54 \times 10^{16}$	,,
Rate before treatment with 50 mm. C_2H_4 for 55 min.	$1{\cdot}58 \times 10^{16}$	,,
Rate after treatment	$1{\cdot}62 \times 10^{16}$	,,

During a long series of experiments, the methyl methacrylate in the storage tube usually polymerized to a large extent. To make certain that no active material distilled over from the reservoir when the capillaries attached to the reaction vessel were filled, a clean reaction tube was sealed into position and methacrylate distilled over from the partially polymerized liquid. No trace of polymerization could be detected.

Effect of Temperature—To study the effect of temperature on the activity of the deposited polymer, a small cylindrical furnace was fixed below the reaction tube so that it could be slipped into position when required. Fig. 9 shows the result. At 20° C. the steady rate is quite large. As the furnace temperature increases the rate slows down, but rises again on withdrawing the furnace. On replacing the furnace the rate decreases once more. In another experiment the exact decrease in rate was measured by condensing out the methacrylate vapour with liquid air, raising the furnace temperature to a steady value and readmitting the methacrylate vapour. At 20° the rate was 0·08 mm./min. and at 83°, 0·015 mm./min. An attempt was made to destroy the active polymer by heating *in vacuo* at 90° for 60 min. The rates of polymerization before and after heating, namely, 0·60 and 0·65 mm./min., were identical, showing that although the spontaneous rate has an overall negative temperature coefficient, the inherent activity of the active polymer is not affected.

Next the temperature was increased until appreciable depolymerization became apparent. $1{\cdot}95 \times 10^{20}$ molecules of methacrylate were polymerized

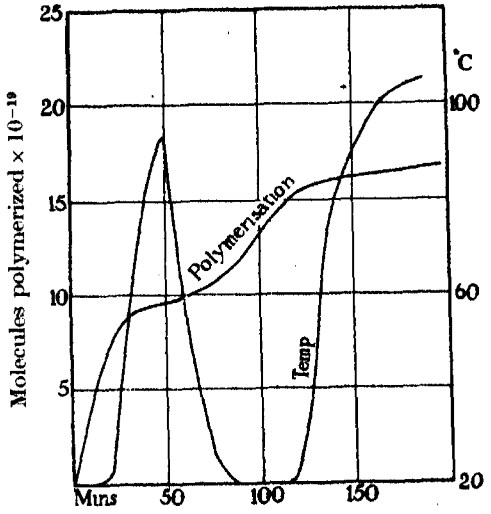

Fig. 9—Effect of temperature on rate of polymerization.

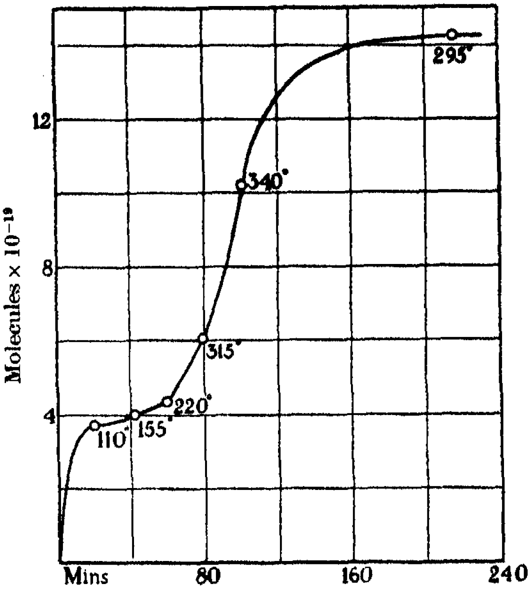

Fig. 10—Thermal depolymerization.

and the polymer heated. The form of the depolymerization curve is shown in fig. 10. There is an apparent rapid depolymerization on heating to about

100° C. This, however, is mostly due to desorption of adsorbed monomer, for this initial steep rise is eliminated if liquid air is applied for about 15 hr. to one of the capillaries attached to the reaction vessel system. The equivalent amount of liquid is collected. As the temperature is increased to 300° C. rapid true depolymerization takes place. This occurs without any charring, and the liquid recovered has exactly the same vapour pressure ($\pm 0{\cdot}2$ mm.) as pure methacrylate, which is conclusive proof that the depolymer is predominantly the monomer. Only $1{\cdot}44 \times 10^{20}$ molecules of the liquid were collected, i.e. about 74 %, since some of the polymer distilled out of the reaction vessel and was deposited on the tubes leading to it.

An experiment was then made to find if the partially depolymerized polymer exhibited any activity. The initial steady rate of polymerization was $9{\cdot}7 \times 10^{18}$ molecules/min. $2{\cdot}5 \times 10^{20}$ molecules were polymerized. On heating to about 300° for 2 hr. $1{\cdot}6 \times 10^{20}$ molecules were recovered. On readmitting monomer at 20° C., the rate of steady polymerization was $1{\cdot}24 \times 10^{19}$ molecules/min., which is approximately the same as that before depolymerization, thus demonstrating that the number of centres remains practically unchanged.

The Hydrogen Sensitized Polymerization

In the polymerization of ethylene derivatives there are only two possible mechanisms whereby the reaction may occur, namely, (*a*) that in which a double bond is formed at the end of the molecule each time the monomer adds on to the polymer, (*b*) that in which the initial step is the formation of a free radical and the subsequent addition of the monomer, a free valency being thereby produced at the end of the growing polymer. An attempt was therefore made to induce methyl methacrylate to polymerize by the second mechanism by producing hydrogen atoms in the system in the hope that free radicals would be produced in sufficient concentration to induce polymerization. By comparing the kinetics of this reaction with those of the direct polymerization it was thought that some light might be thrown on the mechanism of the latter process.

In view of what has been said in the previous section, the addition of molecular hydrogen to methyl methacrylate vapour ought to inhibit polymerization, since (*a*) it will deactivitate a fraction of the excited mercury atoms, (*b*) the atomic hydrogen so produced will hydrogenate the growing polymer. The result is precisely the opposite—hydrogen strongly accelerates the polymerization as is shown by fig. 11. There is no measurable induction period, nor is there any photo after-effect such as is observed in the normal polymerization. The ordinary steady polymerization is also present, and hence the active polymer cannot be appreciably hydrogenated. The hydrogen disappears to a small extent compared with the number of molecules polymerized. For example, in one experiment, 10·4 mm. of hydrogen were added initially, 8·0 mm. remained at the end of the run, i.e. 2·4 mm. disappeared. In this period about 40 mm. of methacrylate were polymerized. The reaction is therefore not the simple hydrogenation of the methacrylate $2H + CH_2:C.(CH_3).COOCH_3 = CH_3.CH_2.(CH_3).COOCH_3$. Visible proof of this was afforded by the deposition of an oil instead of the opaque polymer obtained in the normal polymerization. During the polymerization no trace of any mist in the gas phase was noticed; this pointed to the fact that the polymer was not very large.

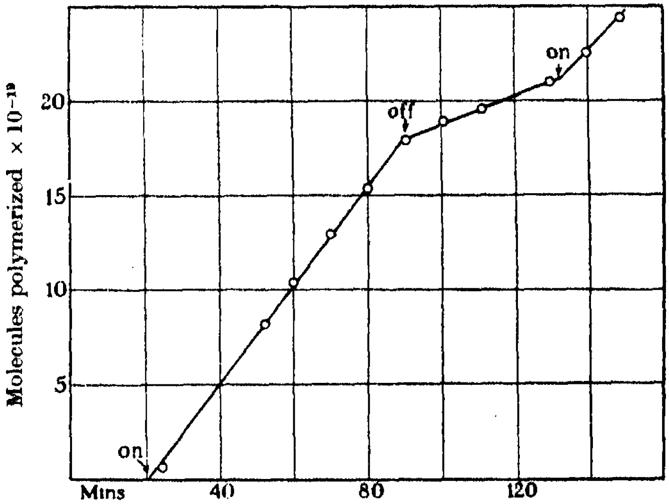

FIG. 11—Hydrogen sensitized polymerization. Pressure of methacrylate 12 mm., pressure of hydrogen 19 mm.

In order to find whether this new polymerization was affected by wall processes, runs were made in the annular reaction vessel—distance between walls 2 mm.—and in the cylindrical vessel, 20 mm. in diameter. Under identical intensities and illuminating the same area of reaction vessel in both experiments, the respective rates were:

20 mm. vessel	$2·6 \times 10^{16}$ molecules/sec.
2 mm. vessel	$3·2 \times 10^{16}$,,

The polymerization is evidently a completely homogeneous reaction.

Mechanism of Initiation of Polymerization—Since the normal polymerization is not affected by molecular hydrogen, and since the only reaction can be the dissociation of H_2 to 2H by the excited Hg atoms, the conclusion is that H atoms initiate polymerization probably by forming a free radical. Since it is known that hydrogen atoms react with unsaturated compounds with a high collision efficiency, the reaction of monomeric molecules with the free radical must occur much more readily than the subsequent addition of another H atom to finally hydrogenate the growing polymer.

Effect of Methacrylate and of Hydrogen Pressure—That the rate of formation of the polymer is independent of methacrylate pressure is shown by fig. 12*a*, where the rate of polymerization is constant within the range 2–25 mm. Below 2 mm. it falls off rapidly. The corresponding experiments with variable hydrogen pressures were carried out manometrically and with the capillary tube method. In the former method the methacrylate vapour is mixed with hydrogen and the initial rate of polymerization determined, whereas in the latter method measurements are made of the dark rate before and after illumination, the mean dark rate being subtracted from the total photo rate in order to get the net rate of the hydrogen sensitized reaction.

TABLE V—CAPILLARY METHOD. TEMP. 20° C.

Dark rates (mm. of liquid per min.)		Gross rate in light	Net rate of H_2 reaction	p_{H_2}	$p_{M.M.}$
Before	After				
0·71	0·71	1·00	0·29	1·4	25
0·10	0·32	0·91	0·70	3·2	26
0·12	0·30	0·97	0·76	11·6	20
0·60	0·60	—	—	0·0	25

Rates are quoted in arbitrary values.

p_{H_2}	$p_{M.M.}$	Initial rate mm./min.	Net photo rate
26·2	25	0·81	0·26
12·8	20·5	0·94	0·39
6·8	20·6	0·90	0·35
0·0	20	0·55	—

In the manometric method (Table V) the net photo rate of the hydrogen sensitized polymerization was computed by subtracting the rate of the normal polymerization for, owing to the variation in methacrylate pressure, the dark rate before and after the photo-reaction could not be measured. The net photo rates may thus be somewhat low, as is shown by a comparison of the absolute rates determined by the two methods. If the absolute rate is plotted against pressure, it will be seen (fig. 12*b*) that it is independent of H_2 pressure above about 4 mm. and the rate has dropped to half the high-pressure value at 1·8 mm. According to the mechanism suggested above, this result would mean a comparatively small value of the quenching radius of methyl methacrylate, namely, $2{\cdot}5 \times 10^{-16}\,\text{cm.}^2$

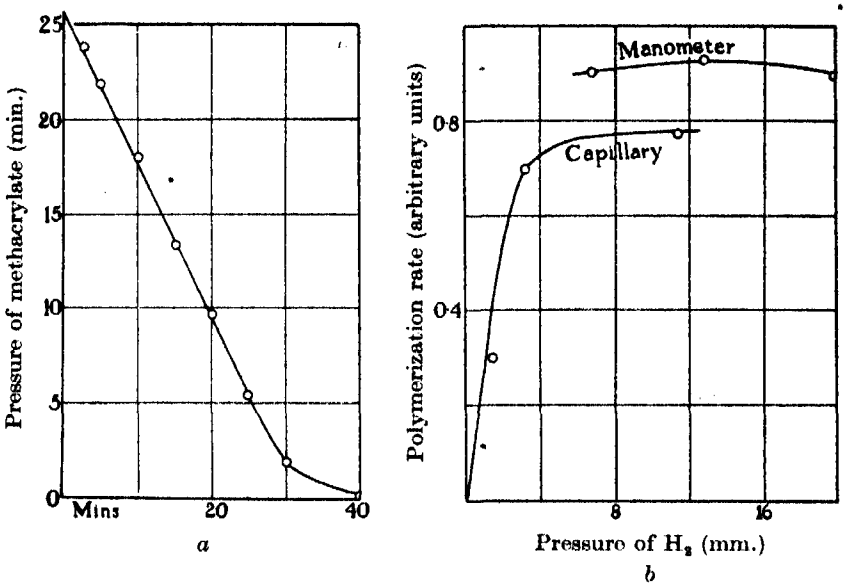

FIG. 12—Variation of polymerization rate with hydrogen and methacrylate pressure.

Mechanism of Cessation of Growth of Polymer

The experiment with the two reaction vessels demonstrates conclusively that the polymer is not deactivated at the walls of the reaction vessel. Termination of growth in the gas can only occur in two ways, if inhibitors are absent from the reaction system. These are: (*a*) mutual destruction of the growing polymers, (*b*) destruction of the growing polymer by collision with monomer. In photochemical polymerizations, whether direct or sensitized, it has been shown (Melville 1936) that it is easy to discriminate between the two by measuring the rate of polymerization as a function of the intensity of the incident light. In case (*a*) rate $\sim I^{\frac{1}{2}}$, in case (*b*), rate $\sim I$.

The procedure was briefly this: The monomer was condensed in the graduated capillary by means of liquid air, the requisite quantity of hydrogen added and the liquid evaporated. With the filter out, the system was illuminated, simultaneous readings of pressure and height being taken so that the number of molecules polymerized could be computed. Next the dark rate was noted, then a further period of illumination, with the filter in position, and finally another measurement of the dark rate. This series of operations was repeated. Measurements of the dark rate before and after each period of illumination were especially necessary when a clean tube was used, since the dark rate in general increased during the run owing to the deposition of active polymer.

The record in Table VI of such a run extending over a period of 5 hr. shows how the results are calculated. The exponent of the intensity factor in the rate equation is thus nearly 0·5, that is, the polymer stops growing by mutual destruction of the growing free radicals. Alternatively, the termination reaction might be the addition of a hydrogen atom, but the method will not distinguish between these mechanisms which are kinetically exactly similar.

TABLE VI—EFFECT OF INTENSITY ON HYDROGEN SENSITIZED POLYMERIZATION

INPUT *ca.* 10^{16} $h\nu$/SEC. PRESS. OF H_2 22·6 MM. PRESS. OF METHACRYLATE 15 MM. TRANSMISSION OF FILTER 35 %

Conditions	Period min.	No. of molecules polymerized $\times 10^{-18}$	Rate of polymerized molecules/sec. $\times 10^{-16}$	Net light-rate molecules/sec. $\times 10^{-16}$	$\frac{\text{Rate filter in}}{\text{Rate filter out}}$	Ratio calc.
Dark	50	—	—			
Light, filter out	20	12·8	1·07	0·94		
Dark	127	19·5	0·255		0·60	0·59
Light, filter in	23	11·1	0·80	0·57		
Dark	25	3·1	0·205			
Dark	25	3·1	0·205			
Light, filter out	21	11·0	0·88	0·59		
Dark	29	6·5	0·375		0·71	0·59
Light, filter in	30	14·4	0·80	0·425		
Dark	29	6·5	0·75			

Fortunately the occurrence of the square-root law permits the determination of the mean lifetime of the growing polymer employing the rotating sector for the purpose. Briefly the theory of the method is as follows. If the sector is rotated so quickly that the interval between successive exposures is less than the lifetime of the polymer, then the rate of reaction is given by $R = \text{const.}\,(I/2)^{\frac{1}{2}}$. On the other hand, if the interval is long compared with the lifetime then $R = \text{const.}\,I^{\frac{1}{2}}/2$, since the exposure time is only half that when the sector is removed completely. The interval at which this change in rate occurs thus gives an approximate estimate of the lifetime.

Owing to the unusual nature of the reaction, the sector speed could not be increased by small increments and the rate of photopolymerization measured at each stage. Two measurements were therefore made during each run.

Then a further two measurements were made, the lower sector speed being equal to or lower than that of the faster speed in the first series of experiments. In this way a rate sector speed curve could be constructed. In order to carry out the two measurements, the following was the schedule of operations. First the spontaneous rate of polymerization was observed, then the photo rate at the lower sector speed, the rate at the higher speed, a second measurement at the lower speed and finally a measurement of the dark rate. The mean of the dark rates was subtracted from the photo rate and the mean of the net photo rates at low speeds of rotation used for comparison with that at high speed. Table VII gives the data obtained in three series of experiments.

Table VII

Conditions	Rate of polymerization molecules/sec. $\times 10^{-16}$	Exposure time sec.	Net light rate molecules/sec. $\times 10^{-16}$
p_{H_2} 23·8 MM. p (METHACRYLATE) 12 MM.			
Dark	0·64		
Light, sector slow	2·83	0·1	2·19
Light, sector fast	3·36	0·005	2·72
Light, sector slow	2·75	0·1	2·11
Dark	0·64		
p_{H_2} 21·8 MM. p (METHACRYLATE) 15 MM.			
Dark	0·48		
Light, sector slow	2·47	0·09	1·99
Light, sector fast	3·05	0·0091	2·57
Light, sector slow	2·64	0·052	2·16
Dark	0·48		
p_{H_2} 21·8 MM. p (METHACRYLATE) 15 MM.			
Dark	0·48		
Light, sector slow	2·05	0·066	1·51
Light, sector fast	2·43	0·023	1·83
Light, sector slow	1·98	0·062	1·44
Dark	0·71		
p_{H_2} 22·8 MM. p (METHACRYLATE) 15 MM.			
Dark	0·51		
Light, sector slow	2·75	0·31	2·24
Light, sector fast	3·00	0·030	2·49
Light, sector slow	2·68	0·31	2·17
Dark	0·51		

If these results are plotted in pairs using the relative velocities at high and at low rates of sector rotation, fig. 13 shows the expected transition at about 10^{-2} sec. It is evident that the mean lifetime of the growing polymer will be of this order of magnitude, but to obtain the exact value it is necessary to compute the average concentration of the growing polymer molecules as a function of the sector speed.

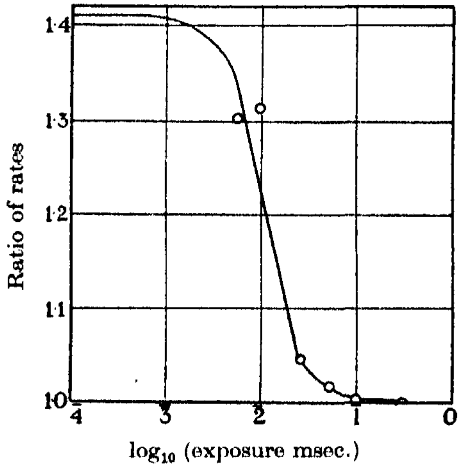

FIG. 13—Variation of reaction rate with sector speed.

The average mean lifetime of the growing polymer, under the conditions of the experiments, is defined by the equation

$$\frac{\text{Conc. of polymer}}{\text{Rate of removal}} = \frac{1}{n}\left\{\frac{[H]}{\{k'_0[H]+k'_1[P_1]+\ldots\}[H]} + \frac{[P_1]}{[P_1]\{k'_0[H]+k'_1[P_1]+\ldots\text{ to } n \text{ terms}\}} + \frac{[P_2]}{[P_2]\{k'_0[H]+\ldots\}} \text{ to } n \text{ terms}\right\},$$

where $[H]$, $[P_1]$, $[P_2]$, etc. refers to the concentrations of the individual molecules. k'_0, k'_1, etc. are the velocity coefficients for the combination of these molecules. Hence T, the lifetime, is given by

$$\begin{aligned} T &= \frac{1}{n}\{(k'_0[H]+k'_1[P_1]+k'_2[P_2]+\ldots)^{-1} \\ &\quad + (k'_0[H]+k'_1[P_1]+k'_2[P_2]+\ldots)^{-1} \text{ to } n \text{ terms}\} \\ &= (k'_0[H]+k'_1[P_1]+k'_2[P_2]+\ldots)^{-1}. \end{aligned}$$

For the present purpose this expression may be reduced to $(k[P])^{-1}$. Then, following the method adopted by Briers, Chapman and Walters (1926), the average mean lifetime is obtained in the following manner. During irradiation, the concentration of the growing polymer is defined by

$$\frac{d[P]}{dt} = f(I) - k[P]^2,$$

and during darkness by $-\frac{d[P]}{dt} = k[P]^2$. Putting $\tau = \{f(I)\,k\}^{\frac{1}{2}}.t$, where τ is the ratio of the time t to the mean life, and $y = k[P]/\{f(I)\,k\}^{\frac{1}{2}}$, where y is the ratio of $k[P]$ at time t to its value under conditions of steady illumination, then with a disk having equal sectors the mean value of y at high rates of rotation, i.e. small τ, is $1/(2)^{\frac{1}{2}} = 0{\cdot}707$. For high values of τ, $y = 0{\cdot}5$. Let this value be y_2. Then it can be shown that y_2 is related to the value (y_1) of y at the commencement of irradiation by

$$\ln\frac{1+y_2}{1-y_2}+\frac{2}{y_2} = \ln\frac{1+y_2}{1-y_1}+\frac{2}{y_1}.$$

During irradiation and darkness, the variation of y with τ is given by

$$y = \tanh\tau \,\text{(in the light)}$$

and $$y = (\tau + 1/y_2)^{-1}\,\text{(in the dark)}.$$

The average value of y when the sector is rotating uniformly is given by

$$y = \frac{\ln\cosh\tau + \ln[2\tau y_2 + 1]}{2\tau},$$

if $\tau = 0$, when $y = y_1$. When $\tau \rightarrow 0$, $y \rightarrow 1/\sqrt{2}$, then

$$\frac{\text{Rate of polymerization for given value of } \tau}{\text{Rate of polymerization as } \tau \rightarrow 0} \quad \frac{\ln\cosh\tau + \ln[2\tau y_2 + 1]}{\sqrt{2}\,\tau}.$$

When the value of the left side of the equation is $\frac{1/\sqrt{2}+1/2}{\sqrt{2}}$, the value of y_2 will be intermediate between the extreme values 0·707 and 1·00, i.e. 0·85. Inserting these values in the above equation, the value of τ required to satisfy the equation is 3·0. From fig. 3 it can be seen that when $\bar{y} = \frac{1/\sqrt{2}+1/2}{\sqrt{2}}$, the exposure time is $1{\cdot}25 \times 10^{-2}$ sec., and therefore the mean life of the polymer is $4{\cdot}2 \times 10^{-3}$ sec. This value will of course depend on the intensity of the light, and hence in virtue of the mechanism of the reaction is not a characteristic property of the sensitized polymerization of methyl methacrylate.

These experiments only indicate that the polymer stops by the mutual interaction of two reactive entities. They do not provide any information about their constitution. Some clue to the nature of the process can, however, be gleaned by investigating the kinetics of the cessation of growth in rather more detail.

Owing to the rather indirect method by which the chains are started, the kinetics are somewhat complicated in spite of their overall simplicity, namely, that the rate is independent of H_2 and of methacrylate pressure and is proportional to the square root of the intensity of the light. As has been pointed out previously, polymerization consists in the addition of unactivated (photochemically) monomer to the growing polymer. Since the rate of polymerization is independent of the hydrogen pressure, the majority of the excited Hg atoms are deactivated by H_2 and hence $\frac{d[H]}{dt} = f(I)$, where I is the intensity of the light, the function being linear. The apparent zero order with respect to the methacrylate concentration is probably due to two compensating factors. The methacrylate vapour, owing to its absorption coefficient being comparable with that of mercury, will act as an internal filter and therefore, as its pressure increases, limit the amount of 2537 radiation available for exciting the Hg atoms. This would mean that the true rate of polymerization is proportional to the first power of the methacrylate concentration.

The hydrogen atoms may disappear in three possible ways: (1) by combination to molecules in the gas or at the walls, (2) by reaction with methacrylate molecules, (3) by hydrogenation of the active growing polymer thereby stopping growth. The stationary state equation for $[H]$ is therefore

$$\frac{d[H]}{dt} = f(I) - k_T[H]^2[X] - k_W[H] - k[H][M] - [H]\{k_1'[P_1] + k_2'[P_2] + \dots\}.$$

There are two mechanisms for termination of growth, (A) process 3 above and (B) mutual destruction of growing polymers. In a preliminary kinetic analysis of polymerization reactions (Melville 1936) it has been shown that deactivation of the growing polymer on the walls or spontaneous gas deactivation need not be considered, since the rate is proportional to the square root of the intensity. Elsewhere it will be shown that hydrogen atoms are picked up by unsaturated molecules much more quickly than by combination in the gas or at the walls. The second and third terms in the right side of the above equation may be neglected compared with the fourth. Next it is necessary to attempt to establish whether the polymer stops growing by hydrogenation or by mutual interaction of two growing polymers. Case (A) may be worked out first.

The stationary state equations for the several molecules are therefore:

$$\frac{d[H]}{dt} = f(I) - k[H][M] - [H]\{k_1'[P_1] + k_2'[P_2] + \ldots\} = 0,$$

$$\frac{d[P_1]}{dt} = k[H][M] - k_1[P_1][M] - k_1'[P_1][H] = 0,$$

$$\frac{d[P_2]}{dt} = k_1[P_1][M] - k_2[P_2][M] - k_2'[P_2][H] = 0,$$

$$\ldots\ldots\ldots\ldots\ldots\ldots\ldots\ldots\ldots\ldots\ldots\ldots\ldots\ldots$$

$$\frac{d[P_n]}{dt} = k_{n-1}[P_{n-1}][M] - k_n[P_n][M] - k_n'[P_n][H] = 0.$$

Hence

$$f(I) - k_n[P_n][M] = 2[H]\{k_1[P_1] + k_2'[P_2] + \ldots + k_n'[P_n]\}.$$

Starting with the equation for $[H]$, each following equation can be solved for $[P_1]$, $[P_2]$, etc., the general solution having the form

$$[P_n] = \frac{k_{n-1}[M]}{k_n[M] + k_n'f(I)/k[M]} \cdot \frac{k_{n-2}[M]}{\ldots\ldots\ldots} \cdots$$
$$\cdots \frac{k_1[M]}{k_2[M] + k_2'f(I)/k[M]} \cdot \frac{f(I)}{k_1[M] + k_1'f(I)/k[M]}.$$

The rate of polymerization will thus be given by

$$R = [M]\left\{k_1 \frac{f(I)}{k_1[M] + k_1'f(I)/k[M]} + k_2 \frac{k_1[M]}{k_2[M] + k_2'f(I)/k[M]}\right.$$
$$\times \frac{f(I)}{k_1[M] + k_1'f(I)/k[M]} + \ldots + k_n \frac{k_{n-1}[M]}{k_n[M] + k_n'f(I)/k[M]}$$
$$\left.\times \frac{k_{n-2}[M]}{\ldots\ldots\ldots} \cdots \frac{f(I)}{k_1[M] + k_1'f(I)/k[M]}\right\}$$

or

$$R = f(I)\left\{\left(1 + \frac{k_1'}{k_1} \cdot \frac{f(I)}{k} \cdot \frac{1}{[M]^2}\right)^{-1} + \left(1 + \frac{k_1'}{k_1} \cdot \frac{f(I)}{k} \cdot \frac{1}{[M]^2}\right)^{-1}\left(1 + \frac{k_2'}{k_2} \cdot \frac{f(I)}{k} \cdot \frac{1}{[M]^2}\right)^{-1} + \ldots\right.$$
$$\left. + \left(1 + \frac{k_1'}{k_1} \cdot \frac{f(I)}{k} \cdot \frac{1}{[M]^2}\right)^{-1}\left(\ldots\ldots\right)^{-1} \ldots \left(1 + \frac{k_n'}{k_n} \cdot \frac{f(I)}{k} \cdot \frac{1}{[M]^2}\right)^{-1}\right\}.$$

It is reasonable to suppose that $\frac{k_1'}{k_1} = \frac{k_2'}{k_2} = \ldots \frac{K^1}{K}$, since the value of the steric factor in the coefficients k_1, k_2, etc., and k_1', k_2', etc., will decrease at the same rate whatever may be the connexion between steric factor and molecular weight. Hence, summing the above series,

$$R = \frac{K}{K^{1}} . k[M]^2.$$

This is not in agreement with experiment, namely, that $R \sim I^{\frac{1}{2}}[M]$. The polymer therefore does not stop growing by mechanism (A).

Case (B) may be treated in a similar manner; the stationary state equations are

$$\frac{d[H]}{dt} = f(I) - k[H][M] - k''_0[H]\{k'_0[H] + k'_1[P_1] + k'_2[P_2] + \ldots + k'_n[P_n]\} = 0,$$

$$\frac{d[P_1]}{dt} = k[H][M] - k_1[P_1][M] - k''_1[P_1]\{k'_0[H] + k'_1[P_1] + k'_2[P_2] + \ldots + k'_n[P_n]\} = 0,$$

$$\frac{d[P_2]}{dt} = k_1[P_1][M] - k_2[P_2][M] - k''_2[P_2]\{k'_0[H] + k'_1[P_1] + \ldots + k'_n[P_n]\} = 0,$$

……………………………………………………………………………………

$$\frac{d[P_n]}{dt} = k_{n-1}[P_{n-1}][M] - k_n[P_n][M] - k''_n[P_n]\{k'_0[H] + k'_1[P_1] + \ldots + k'_n[P_n]\} = 0.$$

Hence

$$f(I) - k_n[P_n][M] = \{k''_0[H] + k''_1[P_1] + \ldots + k''_n[P_n]\}\{k'_0[H] + k'_1[P_1] + \ldots + k'_n[P_n]\},$$

splitting up the combination coefficients to allow for an increasing steric factor in each polymer. This is an important advantage, for, in solving the equations, a series of propagation coefficients may be replaced by a series of termination coefficients or vice versa by means of the introduction of a simple proportionality coefficient. Consequently it is permissible to put $k''_0/k'_0 = k''_1/k'_1 = K$, and therefore

$$\{k'_0[H] + k'_1[P_1] + k'_2[P_2] + \ldots\} = \left(\frac{k[H][M] - k_n[P_n][M]}{K}\right)^{\frac{1}{2}}.$$

If, for simplicity, it is assumed that $k[H][M] \gg k_n[P_n][M]$,

$$[P_1] = \frac{f(I)}{k_1[M] + k''_1\{f(I)/K\}^{\frac{1}{2}}},$$

$$[P_2] = \frac{k_1[M]}{k_2[M] + k''_2\{f(I)/K\}^{\frac{1}{2}}} \cdot \frac{f(I)}{k_1[M] + k''_1\{f(I)/K\}^{\frac{1}{2}}},$$

$$[P_3] = \frac{k_2[M]}{k_3[M] + k''_3\{f(I)/K\}^{\frac{1}{2}}} \cdot \frac{k_1[M]}{k_2[M] + k''_2\{f(I)/K\}^{\frac{1}{2}}} \cdot \frac{f(I)}{k_1[M] + k''_1\{f(I)/K\}^{\frac{1}{2}}},$$

……………………………………………………………………………………

$$[P_n] = \frac{k_{n-1}[M]}{k_n[M] + k''_n\{f(I)/K\}^{\frac{1}{2}}} \cdot \frac{k_{n-2}[M]}{\ldots\ldots\ldots} \cdots \frac{f(I)}{k_1[M] + k''_1\{f(I)/K\}^{\frac{1}{2}}},$$

so that

$$R = f(I)\left\{\left[1+\frac{k_1''}{k_1}\{f(I)/K\}^{\frac{1}{2}}\right]^{-1}+\left[1+\frac{k_1''}{k_1}\{f(I)/K\}^{\frac{1}{2}}\right]^{-1}\left[1+\frac{k_2''}{k_2}\{f(I)/K\}^{\frac{1}{2}}\right]^{-1}+\dots\right.$$
$$\left.+\left[1+\frac{k_1''}{k_1}\{f(I)/K\}^{\frac{1}{2}}\right]^{-1}\left[\dots\dots\right]^{-1}\dots\left[1+\frac{k_n''}{k_n}\{f(I)/K\}^{\frac{1}{2}}\right]^{-1}\right\}.$$

Making again the reasonable assumption that $k_1''/k_1 = k_2''/k_2 = K^1$, then

$$R = f(I)\{[1+K'\{f(I)\}^{\frac{1}{2}}/[M]]^{-1}+[1+K'\{f(I)\}^{\frac{1}{2}}/[M]]^{-2}+\dots\text{to } n \text{ terms}\}$$
$$=\{f(I)\}^{\frac{1}{2}}[M]/K',$$

which is in agreement with the experimental findings, since the rate of polymerization is really proportional to the first power of the methacrylate concentration owing to the internal filter effect of this molecule. The assumption that $k[H][M] \gg k_n[P_n][M]$ is not seriously in error, as both terms are of identical form. If the full expression be used, much complication results without any real advantage being gained in the final equation.

The conclusion to be drawn from this analysis is therefore that the polymer stops growing by interaction with one of a range of growing polymers, present in the reaction system.

Depolymerization Experiments

In order to find whether the hydrogen polymer differed in stability from the normal polymer, thermal depolymerization runs were carried out in exactly the same manner. $21{\cdot}2 \times 10^{18}$ molecules of methacrylate were polymerized of which $8{\cdot}4 \times 10^{18}$ formed the normal polymer. On raising the temperature to 300° C. in 1 hr. and maintaining it there for 6 hr., $17{\cdot}5 \times 10^{18}$ molecules of pure monomer were recovered. The remainder distilled out of the reaction vessel on to the cool connecting tubes. The hydrogen polymer is thus similar in stability to the ordinary polymer.

DISCUSSION OF RESULTS

For the purposes of discussion the principal results are summarized below:

1—Polymerization in light of $\lambda > 2200$ A. Decomposition if $\lambda < 2200$ A.

2—Continuous growth after irradiation—rate proportional to illuminated area, to methacrylate pressure, decreases with increasing temperature.

3—Continuous growth stopped by H atoms, I_2 molecules, unaffected by O_2, C_2H_4, C_2H_2.

4—Deposition of initial centres inhibited by O_2.

5—Quantitative depolymerization to monomer on heating to 300° C. No photo-depolymerization.

Hydrogen sensitized polymerization:

1—Faster than normal polymerization.

2—Rate independent of $[H_2]$, methacrylate pressure and proportional to square root of intensity.

3—Lifetime for growth 10^{-2} sec.

4—Quantitative depolymerization to monomer at 300° C.

Although the activation of the monomer is brought about by a quantum of high energy, namely 120 kg.cal., the comparatively rapid subsequent growth of the polymer indicates that the energy of activation for growth must be fairly small, probably of the order of 5 kg.cal. The question arises as to why there should be such an enormous drop in energy once the dimer is formed. This, however, may be illusory, since the quantum at 2537 A may be far in excess of the minimum requirements for activation. Could a chromophoric group absorbing at a lower wave-length be introduced into the molecule, the smaller amount of energy would probably be adequate to activate the molecule. Alternatively a sensitizing substance might initiate polymerization at a longer wave-length.

Whatever may be the exact mechanism of activation, that is, merely excitation of the double bond so that the molecule may add on another of its kind without further activation, or excitation to the extent of actually producing free valencies at either end of the molecule, there are essentially two mechanisms whereby methyl methacrylate, or any other ethylene derivative, may polymerize, viz.

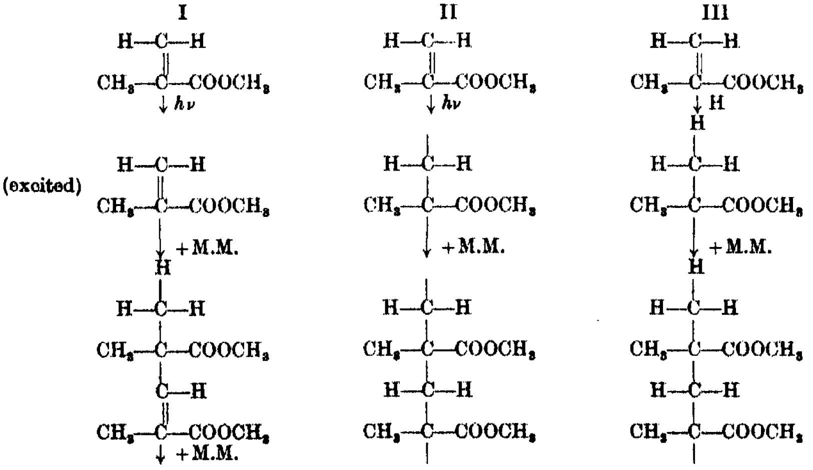

The first scheme involves the migration of a hydrogen atom to the next carbon atom but one of the polymer each time a monomer adds on, with the reproduction of a double bond at the end of the polymer. The second consists in the opening of the double bond of the monomer each time an addition is made. In the first scheme polymerization cannot stop by the mutual saturation of the double bonds and the production of a molecule possessing a double bond in the middle thus:

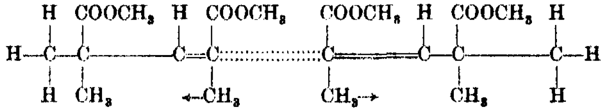

$$H-\overset{H}{\underset{H}{C}}-\overset{COOCH_3}{\underset{CH_3}{C}}-\!\!-\!\!-\overset{H}{C}=\overset{COOCH_3}{\underset{\leftarrow CH_3}{C}}\cdots\cdots\overset{COOCH_3}{\underset{CH_3\rightarrow}{C}}=\overset{H}{C}-\overset{COOCH_3}{\underset{CH_3}{C}}-\!\!-\!\!-\overset{H}{\underset{H}{C}}-H$$

since this would involve the migration of a CH_3 or a $COOCH_3$ group which is exceedingly improbable. The methacrylate on the other hand could not polymerize so that a CH_2 group is produced at the end, since this again would require migration of a CH_3 or $COOCH_3$ group each time a monomeric molecule adds on to the polymer. *The long life of the polymer is therefore primarily due to the fact that there are two relatively immobile groups attached to one carbon atom.*

In the second scheme termination of growth may occur by cyclization of the polymer or by the formation of a cyclic molecule by the mutual interaction of two growing polymers. In the former circumstance, the rate of polymerization would be proportional to the first power of the intensity and to the square root in the latter case. Actually the rate is proportional independent of intensity. Now in the hydrogen sensitized polymerization there is a rapid growth in the gas phase with mutual destruction of the growing polymer, the polymer having a lifetime of the order usually obtained for hydrogen atoms, methyl radicals under comparable conditions. It is evidently a polymerization occurring by means of the free radical mechanism. If both ends of the growing polymer were active, there would not be any significant change in the kinetics. The normal polymerization possesses characteristics which differ in every respect from the free radical mechanism and therefore it may be concluded that the mechanism is depicted by scheme I. This at once accounts for the stability of the growing polymer and its destruction by atomic hydrogen and iodine. In actual practice the two polymers do not differ in their essential structure except that in the hydrogen polymer the structure

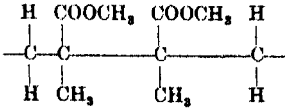

$$-\overset{H}{\underset{H}{C}}-\overset{COOCH_3}{\underset{CH_3}{C}}-\!\!-\!\!-\overset{COOCH_3}{\underset{CH_3}{C}}-\!\!-\!\!-\overset{H}{\underset{H}{C}}-$$

occurs in each molecule as a result of the mutual interaction of growing polymers. This also explains the similarity in behaviour on depolymerization. Moreover the ready solubility in most organic solvents and the ease of thermal depolymerization are strong indications that the molecules are not in any way cross linked.

These remarks apply to the active normal photo polymer adsorbed on the walls. But it must be noted that oxygen is an inhibitor for the deposition of active polymer and therefore the question arises as to whether a small polymer is more susceptible to attack by oxygen than a large, but otherwise exactly similar, polymer. What might be more reasonable to suppose is that two mechanisms operate; for, since the polymer can actually be seen as a faint mist, the molecules, before deposition, must already be comparatively large. This growth occurs before the polymer gets to the walls and hence is extremely rapid compared with the rather slow subsequent polymerization on the walls. In view of the rapidity of the "free radical" mechanism it may be that such a polymerization proceeds according to scheme II. Before cyclization can occur, however, the growing polymer may by the migration of a hydrogen atom revert to the double-bond polymer, after which rapid gas phase growth stops, but growth commences on the walls when the polymer is deposited. Oxygen then retards the formation of centres by preventing reversion to the double-bond polymer.

ACKNOWLEDGMENTS

The writer is greatly indebted to Professor E. K. Rideal for much encouragement and many stimulating discussions during these experiments. He is also indebted to Messrs. Imperial Chemical Industries for a gift of methyl methacrylate.

SUMMARY

The kinetics of the photochemical polymerization of methyl methacrylate vapour have been investigated with the following results. Polymerization occurs nearly quantitatively to a white solid, if the radiation is absorbed by the $COOCH_3$ group in the molecule, i.e. $\lambda > 2200$ A. Light of shorter wavelength absorbed by the double bond leads to decomposition of the molecule.

After a sufficient time of irradiation, the polymer grows continuously in the dark for several days. This steady growth is proportional to the area of the tube illuminated, to the methacrylate pressure and decreases with increasing temperature. It can be stopped by means of H atoms and I_2

molecules; it is unaffected by oxygen, ethylene and acetylene. The polymer is depolymerized to the monomer on heating to 300° C. *in vacuo.*

Polymerization can also be initiated by hydrogen atoms, the velocity of which is faster than the normal polymerization. The rate is independent of methacrylate pressure (above 2 mm.) and hydrogen pressure (above 4 mm.), and is also proportional to the square root of the intensity of the light. The mean life of this polymer is *ca.* 10^{-2} sec. It stops growing when two growing polymers collide in the gas.

The mechanism of the growth of the methacrylate polymer is discussed and reasons advanced to explain why one polymer has a long life and the other a short life. The essential difference is believed to be due to a double-bond polymerization in the former case and a free radical polymerization in the latter case.

REFERENCES

Briers, F., Chapman, D. L. and Walters, E. 1926 *J. Chem. Soc.* pp. 566–70.
Forbes, G. S. and Heidt, L. J. 1934 *J. Amer. Chem. Soc.* **56**, 2363–8.
Melville, H. W. 1936 *Trans. Faraday Soc.* **32**, 258–71.
Mooney, R. B. and Ludlam, E. B. 1929 *Trans. Faraday Soc.* **25**, 442–6.
Snow, C. P. and Allsopp, C. B. 1933 *Trans. Faraday Soc.* **30**, 93–9.

Dissociation, Recombination and Attachment Processes in the Upper Atmosphere—I

By H. S. W. Massey, Ph.D.

Independent Lecturer in Mathematical Physics,
Queen's University, Belfast

(*Communicated by E. V. Appleton, F.R.S.—Received* 13 *July* 1937)

The study of the properties of the earth's upper atmosphere has now progressed so far as to provide what should be a sufficient basis for the development of a detailed theory. Since the state of the upper atmosphere approximates closely to that of the gas in a low-pressure discharge tube (except for the absence of solid boundaries), it is clear that such a theory must deal with the individual collision processes which can occur in such a system. Until the last few years no satisfactory theory of these phenomena was available, but it is now possible to apply quantum mechanical methods with reasonable expectation of results accurate at least as regards order of magnitude. We therefore propose to make use of these methods to obtain a deeper understanding of the physics of the ionosphere. In this paper we confine ourselves particularly to the qualitative study of certain problems associated with the two upper ionized layers (the E and F regions), making use of information already available concerning the probabilities of the various collision reactions which are important. The detailed evaluation of these reaction rates is being carried out, and in later papers it is hoped to deal with the various problems in a more nearly quantitative manner.

1—THE IONIZED LAYERS—PRODUCTION AND LOSS OF IONS

The two main strata of atmospheric ionization are the E region extending roughly from 120 to 160 km. and the F region from 180 to 300 km., at night. During the day each splits into two distinct strata forming the E_1 and E_2 and the F_1 and F_2 regions. The ionization density in each region, as determined from experiments with radio waves, exhibits characteristic annual and diurnal variations besides irregular variations of considerable magnitude. The first problem which arises is the reason for the existence of the stratification. This being understood it is then necessary to account for the observed variations of density, the daytime splitting of the layers, and so on.

When the question of the origin of the layer formation is considered, it is soon found to be closely linked with that of the diurnal variations of ionization density. It has been shown by Chapman (1931) that, if a radiation, entering from without, is absorbed by an atmospheric constituent whose density falls off exponentially with height, the rate of absorption has a sharp maximum at a certain level. This will occur because the rate of absorption at a particular level is proportional to both the gas density and radiation density at that level. The first falls off rapidly with increasing height, the second with decreasing height, giving the sharp maximum at an intermediate level. If the absorption process is one of photo-ionization, there will therefore exist levels at which the rate of ion production is a sharp maximum; this does not necessarily mean, however, that there will also be levels of maximum ionization density, for their position will clearly depend on the variation with height of the rate of disappearance of ions. To answer the primary question of the subject then it is essential to examine the mechanism of loss of ions, and in so doing we can expect to find the explanation of the regular characteristic variations of ionization density in each layer.

If we suppose that the only way in which ions are lost is by recombination of oppositely charged ions, then the stratification and regular variations can be explained in general terms without difficulty. Thus if α is the rate at which ions are being formed by the solar radiation, and n the ionization density, then the time variation of n will satisfy the equation

$$\frac{dn}{dt} = \alpha - \beta n^2, \tag{1}$$

where β is a constant. When equilibrium is attained $n = \left(\frac{\alpha}{\beta}\right)^{\frac{1}{2}}$, and, β being a constant, n is a maximum where α, the rate of ion production, is also a maximum, and the ionization will be concentrated in narrow layers.

Again, at night $\alpha = 0$, and the rate of decrease of density should follow the equation $\frac{dn}{dt} = -\beta n^2$. This seems to be the case for the E region, while for the F region β appears to be so very much smaller that there is no conclusive evidence either for or against the recombination law.

Finally, the seasonal variation in the E region is closely represented by the formula

$$\frac{n_m^w}{n_m^s} = \left(\frac{\alpha^w}{\alpha^s}\right)^{\frac{1}{2}} = \left\{\frac{\sin(\theta+\delta)}{\sin(\theta-\delta)}\right\}^{\frac{1}{2}},$$

where n_m^s, n_m^w are the midsummer and midwinter ionization density maxima, θ is the colatitude of the place of observation and δ the sun's maximum declination. This is just the result that would be derived on the recombination theory (Chapman 1933; Appleton and Naismith 1935).

Despite these successes it is not possible to accept the recombination theory as a complete representation of the facts. The ionization density which is effective in producing dispersion of radio waves, by means of which the experimental measurements are carried out, is not that of all the ions present but only that of the electrons, and it is the variation of electron density which must be considered. Electrons may be removed not only by recombination to positive ions but also by attachment to neutral molecules to form negative ions. If the latter process is at all important, all the conclusions of the recombination theory would seem to require drastic modification. In particular, if loss of electrons by attachment is more important than that by recombination, the equation (1) is replaced by

$$\frac{dn}{dt} = \alpha - \gamma n_0 n,$$

where γ is a constant and n_0 the number of neutral molecules per c.c. At equilibrium

$$n = \frac{\alpha}{\gamma n_0},$$

and n will be a maximum at a level where α/n_0 is a maximum. Since n_0 falls off exponentially with height, it is doubtful if any sharp maximum of n would be expected at all.*

As n_0 is much greater than n, γ would have to be very small compared with β for attachment to be negligible, and we shall show below that it is very unlikely that this is a way out of the difficulty; on the contrary, it appears probable that $\gamma n_0 n$ is much greater than βn^2. However, up to the present we have taken no account of the possibility of detachment of electrons from the negative ions†; when this is done a solution of the difficulty appears. Both attachment and detachment occur so rapidly compared with recombination that a permanent equilibrium ratio of electrons to negative ions is maintained while recombination proceeds. Owing to the maintenance of this dynamical equilibrium between the negatively charged particles, the time variation of the electron density will be independent of attachment and detachment, and the recombination theory can be applied in its original form but with constants depending on the equilibrium ratio of electrons to negative ions.

The considerations on which these conclusions are based will now be given in detail in the following sections.

2—COLLISION REACTIONS IN AN IONIZED LAYER

We can classify the types of collision reaction which occur in an ionized region of the earth's atmosphere as (*a*) dissociation including ionization, (*b*) recombination, either of oppositely charged ions or of molecular fragments to reform a molecule, (*c*) attachment of electrons to neutral molecules, and (*d*) detachment of electrons from negative ions. (*c*) and (*d*) really could be considered as included in (*b*) and (*a*) respectively, but for our purposes it is convenient to deal with them separately. The principal constituents of the upper atmosphere are oxygen and nitrogen in both atomic and molecular states, so the collision reactions which will occur are as follows:

---

* See, however, Martyn and Pulley (1936).

† The necessity for considering detachment was first pointed out by Martyn and Pulley (1936).

a—Dissociation (including ionization)—The following photochemical processes will go on during the daytime:

$$O_2 \rightarrow O + O, \quad (1) \qquad N_2 \rightarrow N + N, \quad (2)$$

$$O_2 \rightarrow O_2^+ + e, \quad (3) \qquad N_2 \rightarrow N_2^+ + e, \quad (4)$$

$$O \rightarrow O^+ + e, \quad (5) \qquad N \rightarrow N^+ + e. \quad (6)$$

These will lead to a supply of atomic oxygen and nitrogen, of electrons and of positive ions. As the sun may be regarded very roughly as a black body of temperature 6000° K., those reactions which require the lowest frequency quanta will be the most important, so we may disregard the formation of atomic nitrogen compared with that of oxygen, and process (6) will be the least important of those leading to ionization.

As we are not concerned in this paper with the rate of initial formation of ions, we shall not further consider the probabilities of the reactions (1)–(6).

b—Recombination—Under this head we shall have

$$O + O \rightarrow O_2 + h\nu, \quad (1) \qquad O + O + X \rightarrow O_2 + X, \quad (2)$$

and similar reactions for nitrogen;

$$O^+ + e \rightarrow O + h\nu, \quad (3)$$

and similar reactions for nitrogen;

$$O_2^+ + e \rightarrow O_2' \rightarrow O' + O'', \quad (4)$$

$$O^+ + O^- \rightarrow O_2 + h\nu, \quad (5)$$

$$O^+ + O^- + X \rightarrow O_2 + X. \quad (6)$$

Processes (1) and (2) need not concern us further except to note that they determine the ratio of atomic to molecular oxygen at any level of the atmosphere at any time of the day. During the night the proportion of atomic oxygen will be less than during the day due to these processes, and this may have important consequences (see § 5). Chapman (1931) has shown from considerations of the equilibrium between atomic and molecular oxygen that, at the height of the E region, one must expect, during the daytime at least, that more than half of the oxygen is in the atomic state, and at greater heights the fraction in the molecular state will be still smaller.

The ion recombination process (3) is probably the most important. Radiative recombination of heavy particles, involved in (5), is always very infrequent, and the three-body recombination (6) is likely to be small because of the low pressure prevailing at the heights concerned. Process (4) does not involve either radiation or a third body, but requires that the excess energy of the captured electron be just sufficient to raise the molecule to an excited state without appreciable change of nuclear separation. Since the dissociation energy of O_2 is less than its ionization energy, this excited state will be unstable and the molecule will dissociate into atoms. It is very unlikely that the electrons in the ionized layers will have energies lying in the narrow range necessary to bring about this type of process, and in any case, as it involves interaction between electronic and nuclear motion within the molecule, its probability will be small.

We are then left to consider (3). In the absence of detailed calculations for recombination to oxygen ions we must make use of the values obtained by Morse and Stueckelberg (1930) for recombination to hydrogen-like ions of nuclear charge Z. They state their results in terms of an effective cross-section which we will call Q^r. For our purposes it is more convenient to have the probability per gas-kinetic collision. This will be given by Q^r/Q_0, where Q_0, the gas-kinetic cross-section, will be about 5×10^{-16} cm.^{2}.

Morse and Stueckelberg find that, if we write

$$Q^r = \Sigma_{nl} Q^r_{nl},$$

where Q^r_{nl} is the effective cross-section for capture of the electron into the state with quantum numbers n, l, then, for low electron energies,

$$Q^r_{nl} = 10^{-20} \frac{Z^2}{V} A_{nl} \text{cm.}^2,$$

where V is the electron energy in e-volts. Numerical values are given for $n = 1$ to 4 and the corresponding l values.

To apply these results to oxygen we suppose that the effective nuclear charge is unity for capture into any of the excited states of the O atom but has the value 3·7 given by Slater's rules (1933) for the ground state. We then find for the cross-section Q^r a value of roughly $2{\cdot}5 \times 10^{-20} V^{-1}$ cm.^{2}, if we allow for capture into the states with total quantum numbers greater than 5 for which no values are given by Morse and Stueckelberg (1930). This gives the chance of recombination per gas-kinetic collision as about $5 \times 10^{-5} V^{-1}$.

c—Attachment—Here we must consider the reactions

$$O + e \rightarrow O^- + h\nu, \quad (1)$$

$$O_2 + e \rightarrow O_2^- + h\nu, \quad (2)$$

if we ignore the possibility of three body processes. We have not included the analogous reactions with nitrogen, as there is still some doubt about the stability of N^- and N_2^- which does not seem to have been observed. Although N^- has been reported by a few investigators (Arnot 1936) it was not observed in the recent experiments of Tüxen (1936), who nevertheless easily detected O^- and O_2^-. There are reasons (see below) for supposing that the binding energy of the additional electron in O_2 is very small, so it is reasonable to expect that N^- is very nearly unstable if not actually so.

Before attempting to estimate the probability per collision of either of the above reactions it is necessary to consider how much knowledge we have of the two ions O^-, O_2^- concerned. Both are definitely stable, and the electron affinity of O^- has been determined by the collision experiments of Lozier (1932) as 2·2 e-volts. The energy necessary to detach an electron from O_2^- has been estimated as between 0·10 and 0·30 e-volt from the experiments of Loeb (1935) and of Bradbury (1933). No theoretical calculations on the structure of either ion have yet been carried out, but we may obtain a reasonable estimate of the attachment probability as follows. The effective cross-section for radiative attachment of an electron to a neutral atom or molecule is

$$Q_a^r = \frac{64\pi^4 e^2 \nu^3}{3hc^3 v} \, |\mathbf{M}|^2,$$

where ν is the frequency of the radiation emitted, v the velocity of the electron before capture and **M** is the mean dipole moment associated with the transition. **M** has been calculated for attachment to chlorine by Massey and Smith (1936), and we can expect that its value will not be very different for oxygen, since in both cases the attached electron will be bound in a p state. The electron affinity of chlorine used in the calculations was 3·6 e-volts, so we can take as a fair approximation for oxygen that

$$Q_a^r(\mathrm{O}) \simeq \left(\frac{2\cdot 2}{3\cdot 6}\right)^3 Q_a^r(\mathrm{Cl})$$

$$= \frac{6 \times 10^{-23}}{V^{\frac{1}{2}}} \text{ cm.}^2 \text{ for low-energy electrons,}$$

where V is again the energy of the electron before capture, in e-volts. For O_2 we are not on such certain ground in supposing that the quantity **M** is roughly the same as that for O; but if it does not differ very much for the two, then

$$Q_a^r(\mathrm{O_2}) \simeq \left(\frac{0\cdot 3}{2\cdot 2}\right)^3 Q_a^r(\mathrm{O})$$

$$= 1\cdot 5 \times 10^{-25} V^{-\frac{1}{2}} \text{ cm.}^2.$$

This comparatively small probability of attachment to the molecule may be important in detailed interpretation of variations of electron density.

We take then for the probability of attachment per collision to oxygen atoms $1{\cdot}2 \times 10^{-7} V^{-\frac{1}{2}}$, and to oxygen molecules $3 \times 10^{-10} V^{-\frac{1}{2}}$.*

d—Detachment—Here we have to consider†

$$O + O^- \rightarrow O_2 + e, \quad (1) \qquad O^- + N \rightarrow NO + e, \quad (2)$$

$$O^- + N_2 \rightarrow N_2O + e, \quad (3) \qquad O^- + h\nu \rightarrow O + e. \quad (4)$$

The photo-ionization process (4) is not important for our present purposes, but it may play a considerable rôle in such phenomena as the daytime splitting of the E level. An estimate of the probability of the type of detachment process represented by (1), (2) and (3), which go on at night as well as in the daytime, is essential for our present argument. Reactions of the reverse type have been investigated in the collision experiments of Lozier (1932) and others. In these experiments a beam of electrons of homogeneous velocity is fired through a gas, such as O_2, at low pressure, and the yield of various types of ion together with their velocity distributions is observed. The reaction

$$O_2 + e \rightarrow O + O^-, \tag{5}$$

which is the reverse of (1), has been extensively examined in this way (Lozier 1932) and, from the yield of O^- ions compared with O_2^+ ions formed by direct ionization, the cross-section for the reaction (5) may be estimated as about 10^{-4} of the gas-kinetic. Thermodynamical arguments show that the cross-section for the reverse process is p_e^2/p_0^2 times this, p_e being the momentum of the electron before attachment (or after detachment in the reverse case) and p_0 that of the relative motion of the atom and ion. In Lozier's experiments (1932), p_e^2/p_0^2 is about 10^{-3}, so for the detachment process in which we are interested the cross-section comes out to be about 10^{-7} of the gas-kinetic. However, we must remember that the experiments refer to oxygen molecules initially in the ground vibrational state, whereas the combination of the ion and atom considered in the detachment process need not result only in formation of molecules in this state but also in excited states. We must therefore allow a factor of, say, 10 for this, giving as a final estimate for the probability of detachment 10^{-6} per gas-kinetic collision.

---

* With this low value of the probability of radiative attachment for O_2, three body processes would lead to greater attachment to O_2 even at the low pressure prevailing in the E region but probably not in the F region.

† The possibility of such reactions as (1), (2) and (3) was first pointed out by Martyn and Pulley (1936).

3—Application to the *E* Layer

Let us consider the rates of recombination, attachment and detachment in the *E* layer, using the values for the various collision probabilities estimated in § 2 above and the information about the physical properties of the region derived from experiment. We take them as rough mean values for the quantities required:

Collision frequency of electrons ...	2×10^5/sec.
Mean energy of electrons	0·10 e-volt
Number of neutral molecules/c.c. ...	5×10^{13}
Number of positive ions/c.c.... ...	10^7
Probability of recombination ...	5×10^{-4}/gas-kinetic collision between an electron and a positive ion
Probability of attachment	$3{\cdot}6 \times 10^{-7}$/gas-kinetic collision between an electron and a neutral molecule
Probability of detachment	10^{-6}/gas-kinetic collision between a negative ion and a neutral molecule

Using these figures we find the following results:*

$$\text{Rate of attachment per electron} = 2 \times 10^5 \times 3{\cdot}6 \times 10^{-7} = 0{\cdot}07/\text{sec.}$$

$$\text{Rate of detachment per negative ion} = 2 \times 10^5 \times (16 \times 1840)^{-\frac{1}{2}} \times 10^{-6} = 10^{-3}/\text{sec.}$$

Here the factor $(16 \times 1840)^{-\frac{1}{2}}$ arises because the high mass of the negative ions decreases their collision frequency in this ratio.

$$\text{Rate of recombination per electron} = 2 \times 10^{-7} \times 2 \times 10^5 \times 5 \times 10^{-4} = 2 \times 10^{-5}/\text{sec.}$$

Here the factor 2×10^{-7} allows for the fact that only this proportion of the total number of collisions made per second by an electron will be with a positive ion.

The important result which emerges from these numerical values is that the rate of recombination is much slower than that of either attachment or detachment. An equilibrium ratio of 100 to 1 or more will be set up between the electrons and negative ions in a time of the order of minutes, and this will be maintained while both are lost much more slowly by recombination. The recombination rate is such that a time of the order of several hours will be necessary to reduce the electron density to a low value during the night. This is in general agreement with observation for the E region. During the daytime decrease of electron density will occur by recombination alone (see, however, § 5), and the important features of the recombination theory may be retained without modification.

---

* These results are only correct as to order of magnitude. Detailed numerical precision is not claimed for them nor is it necessary for the ensuing argument.

It is important to notice that this interpretation requires the density of negative ions to be much greater than (roughly 100 times) that of electrons. This is required also by the "dynamo" theory of the variations of the earth's magnetic field (Chapman 1931). The electron density, determined by radio measurements, is not much greater than 10^4/c.c., whereas the dynamo theory requires about 10^7 free charges/c.c.* This is possible if the number of negative ions exceeds that of electrons in the way our interpretation suggests, and in calculating the rate of recombination we assumed the number of positive ions/c.c. to be 10^7.

4—APPLICATION TO THE F REGION

The collision frequency of an electron in the F region is roughly 6×10^3/sec., 1/30 of that in the E region. This means that the mean gas pressure in the two regions is in this ratio†. Further, the electron density in the upper region is $1{\cdot}2 \times 10^6$/c.c. If we assume the same ratio 10^3 between density of positive ions and density of electrons in both regions, we find for the rate of recombination per electron in the F region

$$6 \times 10^3 \times 5 \times 10^{-4} \times \frac{1{\cdot}2 \times 10^6 \times 10^3 \times 30}{5 \times 10^{-13}} \simeq 216 \times 10^{-5}/\text{sec.},$$

i.e. the recombination rate would be faster than in the E region. This is in contradiction to the observations which indicate very slow recombination indeed. To overcome this difficulty we must suppose that the density of positive ions is not much greater than that of the electrons (so the factor 10^3 may be omitted in the above calculation), and this requires that at the height of the F region the molecules present do not form stable negative ions. It may be for example that the main substance present is nitrogen which, as we remarked in § 2 (*c*), probably does not have an appreciable electron affinity.

---

* Chapman originally considered 10^8 to 10^9/c.c. as necessary, but more recent calculations seem to suggest a considerably lower value.

† Provided that the temperature does not differ too widely between the two layers.

5—CONCLUDING REMARKS

We have shown that it is possible to reconcile the recombination and attachment theories and to obtain a tolerable representation, in very general terms, of the ionic equilibrium in the *E* region. In doing so we have neglected a great number of processes which may have interesting effects. Thus we have pointed out that radiative attachment to oxygen molecules is probably much less probable than that to atoms; so, as the concentration of atoms grows in the daytime by photodissociation, the electron density will tend to diminish by increased attachment. This may give rise to a daytime minimum at which the loss of electrons by this process is balanced by gain from photoionization. In the same way a nighttime maximum could arise. As this paper represents only a preliminary account before detailed evaluation of the various reaction rates has been carried out, we do not propose to pursue the matter further at this stage.

It is a pleasure to acknowledge my indebtedness to Professor T. H. Laby, F.R.S., for drawing my attention to the interesting problems presented in upper atmospheric physics and to Professor E. V. Appleton, F.R.S., Professor S. Chapman, F.R.S., Mr. J. A. Ratcliffe, Professor K. Emeleus and Dr. R. W. Lunt for interesting discussions.

SUMMARY

The probabilities of various collision reactions which occur in the *E* and *F* regions of the ionosphere are considered in general terms. In particular the relative importance of recombination and attachment in effecting electron removal is discussed. As processes in which electrons are detached from negative ions can be expected to go on at a considerable rate (much faster than recombination) and as attachment must also occur very rapidly, the most reasonable representation of the phenomena is to consider the negative ions and electrons as in a dynamical equilibrium adjusting itself rapidly to loss of either by recombination. In this way the usual recombination theory may be retained, even though attachment occurs much more rapidly. A consequence of the theory is that the number of negative ions should considerably exceed the number of electrons in the *E* region as required by the "dynamo" theory of magnetic variations. The low rate of recombination in the *F* region, requiring the density of positive ions to be not much greater than that of the electrons, makes it necessary to suppose that, at these levels, the atmospheric gases present are inert towards electron attachment.

REFERENCES

Appleton and Naismith 1935 *Proc. Roy. Soc.* A, **150**, 685.
Arnot 1936 *Nature, Lond.*, **138**, 162.
Bradbury 1933 *Phys. Rev.* **44**, 883.
Chapman 1931 *Proc. Roy. Soc.* A, **132**, 353.
— 1933 *Proc. Roy. Soc.* A, **141**, 705.
Loeb 1935 *Phys. Rev.* **48**, 684.
Lozier 1932 *Phys. Rev.* **42**, 518.
Martyn and Pulley 1936 *Proc. Roy. Soc.* A, **154**, 455.
Massey and Smith 1936 *Proc. Roy. Soc.* A, **155**, 472.
Morse and Stueckelberg 1930 *Phys. Rev.* **36**, 16.
Slater 1933 *Phys. Rev.* **30**, 57.
Tüxen 1936 *Z. Phys.* **103**, 463.

A Transmutation Function for Deuterons

BY P. L. KAPUR

(*Communicated by R. H. Fowler, F.R.S.—Received* 15 *July* 1937)

I

It has been observed (Lawrence, McMillan and Thornton 1935) that when deuterons are used as bombarding particles, and the reaction involved is of the type

$$^{A}X_{Z} + {}^{2}\mathrm{H}_{1} \rightarrow {}^{A+1}X_{Z} + {}^{1}\mathrm{H}_{1}, \tag{1}$$

the continuous increase of the transmutation function with deuteron energy is not correctly represented by the Gamow factor

$$\exp\left[-\frac{2\pi Ze^{2}}{\hbar}\left(\frac{M}{W}\right)^{\frac{1}{2}}\right], \tag{2}$$

in which $2M$ stands for the mass and W for the kinetic energy of the deuteron.

Oppenheimer and Phillips (1935) explained this by the fact that Gamow's familiar considerations are not applicable in this case, and the deuteron need not penetrate into the nucleus at all. Instead, what actually happens is that the deuteron on account of its large size and low binding energy gets polarized by the field of the bombarded nucleus to such an extent that its neutron is captured by the nucleus, while the proton is repelled. On the basis of these ideas the final formula obtained by them for the cross-section for transmutation differs from Gamow's by having in the exponent of (2) an extra factor

$$f(W/I) = (2/\pi)(W/I)^{\frac{1}{2}}\,\overline{F(W/I)}, \tag{3}$$

where I is the binding energy of the deuteron and $\overline{F(W/I)}$ is the function calculated by Oppenheimer and Phillips (1935).

In obtaining this result they make use of what they call the "adiabatic approximation", which amounts to supposing that the wave function describing the initial state can be expressed as a product

$$\psi(x, y) = u(\zeta, \eta)\,\phi(\zeta), \tag{4}$$

where x, y and ζ refer respectively to the co-ordinates of the proton, neutron, and their centre of mass with respect to the bombarded nucleus (supposed to be fixed), while η denotes the relative co-ordinates of the neutron and the proton; $\phi(\zeta)$ is the wave function for the motion of the centre of mass, and $u(\zeta, \eta)$ that for the relative motion, when the centre of mass ζ is fixed. In other words, they assumed that in the wave equation for u the dependence on ζ may be neglected. In the present paper no such assumption is made, and a solution for ψ is obtained by the method developed in a recent paper (Kapur and Peierls 1937).* This method gives in general an upper limit to the value of the wave function, but in the present case it provides, as we shall see, the correct value. Like Oppenheimer and Phillips (1935) we shall treat the problem as a three-body problem. This involves the neglect of all resonance effects, and it is questionable whether this is justified. (One should remember that resonance would depend on the final energy of the nucleus after the neutron capture, and that, owing to the escape of a proton, this energy can vary even for a given energy of the incident deuteron. Thus it cannot be argued from the smoothness of the transmutation function that resonance must be unimportant.) It will be seen that our results are not greatly different from those of Oppenheimer and Phillips and agree well with the observed variation of yield with incident energy. However, in view of the neglect of the resonance effects, some care should be exercised in interpreting these results.

Publication of these calculations is perhaps justified, because even in a more rigorous theory the transmission coefficient of the potential barrier will be an extremely important factor.

---

* This paper will be referred to as K.P. in the text.

II

On this mechanism of "partial entry" of the deuteron into the nucleus, reaction (1) will take place only after the penetration of the neutron into the nucleus. Once the neutron has penetrated it will have a certain chance of being captured. If we assume that this chance varies less rapidly with the energy of the incident particle than the penetration coefficient, the transmutation function is proportional to the probability of the penetration of the neutron into the nucleus, and it is this that we shall calculate. Further, since the probability for the neutron to be anywhere in the nucleus is approximately constant, we need only calculate the probability of its penetrating to the edge of the nucleus. If we neglect resonance effects, this probability of penetration of the neutron is not influenced by the nuclear forces and we need consider only (i) the coulomb repulsion between the proton and the nucleus, and (ii) the proton-neutron interaction in the deuteron. So that if we consider the bombarded nucleus as fixed, the wave equation to be solved is

$$\left[\nabla_x^2+\nabla_y^2+\frac{2M}{\hbar^2}(E-V)\right]\psi(x, y)=0, \tag{5}$$

V containing the potential energy due to the two above-mentioned forces. Here the origin has been taken at the bombarded nucleus; M denotes, as before, the mass of the proton as well as that of the neutron; $x(\equiv x_1, x_2, x_3)$ and $y(\equiv y_1, y_2, y_3)$ refer to the co-ordinates of the proton and the neutron respectively.

Equation (5) is in six dimensions, but if we define the (1-2) plane as the plane which contains the neutron and the proton, and the 1-axis as the line which joins the proton to the origin, so that the co-ordinates of the proton and the neutron become $(x_1, 0, 0)$ and $(y_1, y_2, 0)$ respectively, and if we confine ourselves to the case of head-on collisions, in which the wave function depends only on the distance between the particles, the dimensions of the equations reduce to three. We treat this problem in the approximation of geometrical optics by the method of K.P. This method uses a path of integration which represents the "easiest path of reaction". It is plausible that this path will be such that the proton, the neutron, and the nucleus always lie on a straight line. This will be verified in §VI. We are then only interested in the variation of the wave function with x and y_1, while y_2 is zero. In addition we shall see that the dependence of the wave function on y_2 is small, so that we can leave out terms in $\partial\psi/\partial y_2$ in the equation. Then omitting the suffixes equation (5) may be written as*

$$\frac{d^2\psi}{dx^2}+\frac{d^2\psi}{dy^2}+\frac{2M}{\hbar^2}(E-V)\psi=0. \tag{6}$$

x and y now denote the distances of the proton and the neutron from the origin, and

$$V=-V(x-y)+Ze^2/x, \tag{7}$$

the last term arising from the coulomb repulsion between the proton and the nucleus.

$V(x-y)$ represents the mutual interaction of proton and neutron and is assumed to be different from zero only when $x-y\approx 0$; if the range of this interaction is short compared with the wave-length and with the radius of the deuteron, its effect is equivalent to imposing upon the wave function the boundary condition (Bethe and Peierls 1935)

$$\left[\frac{1}{\psi}\frac{\partial\psi}{\partial(x-y)}\right]_{x-y=0}=-(MI)^{\frac{1}{2}}/\hbar \tag{8}$$

instead of the usual one, namely that of vanishing of the wave function at $x=y$.

We now apply geometrical optics following the remarks of K.P. For this purpose we write

$$\psi=\exp[-S(x,y)/\hbar] \tag{9}$$

and neglect $(\partial^2S/\partial x^2)$ and $(\partial^2S/\partial y^2)$. We then obtain

$$(\partial S/\partial x)^2+(\partial S/\partial y)^2=2M(V-E). \tag{10}$$

In general S may be complex; so writing $S=\sigma+i\tau$, we get

$$|\operatorname{grad}\sigma|\leqslant(2M)^{\frac{1}{2}}(V-E)^{\frac{1}{2}}.$$

If, however, $\tau=0$, we have $\sigma=S$, and the equality sign holds. We shall see in § IV that for the present problem this indeed is the case.

Thus we have

$$S=\sigma=(2M)^{\frac{1}{2}}\int(V-E)^{\frac{1}{2}}\,ds, \tag{11}$$

---

* Strictly speaking (6) will contain terms like $\frac{\text{const.}}{x}\frac{d\psi}{dx}$; these have, however, been neglected, because they are beyond the accuracy of the method of geometrical optics, which we use.

where ds is the line element in (x, y) space and is given by

$$(ds)^2 = (dx)^2 + (dy)^2,$$

and the integral is taken along a line of steepest gradient of S.

The value of S obtained by requiring the integral (11) to be a minimum provides us in general with a lower limit, because the limits of integration chosen by the minimum condition will not in general select the right set from among the family of curves represented by Euler's equation (11). In the present case, however, we find that the path of integration chosen by the minimum condition is in accord with the boundary condition (8), so that the minimum value of (11) gives us the correct value of S and not a lower limit.

III

Before applying the variation to (11) we must observe that the proton and the neutron enter the field of the nucleus as a deuteron which may be visualized as moving up a "valley"—created by the attractive potential $V(x-y)$—in the "potential mountains" of the bombarded nucleus. This "valley" evidently lies along $x-y = 0$, for it is only in this region that $V(x-y)$ exists. The wave function thus has a ridge along $x-y = 0$, and the line of steepest gradient of S runs along this ridge for some distance and then trails off to the line $y = r$, r being the radius of the nucleus, which means that the neutron has reached the nucleus. To start with we take $r = 0$; its influence will be considered later. We must, therefore, write the integral in (11) as the sum of two integrals, one along the line $x-y = 0$ and the other from some point on $x-y = 0$ (x_1 say) to the point (x, y) at which we want to calculate S, along a path $y = y(x)$; this path is to be determined by the requirement that S is a minimum. Along the line $x = y$ the approximation of geometrical optics, if literally applied, would fail, because the potential $V(x-y)$ varies too rapidly. On the other hand, if we replace this potential by the boundary condition (8), the wave function has a discontinuous slope on the line $x = y$, and this line is no longer a line of steepest gradient of S. Nevertheless, we may integrate along this line, for we know, from (8), the component of grad S normal to this line and thus, by subtraction, also the component along this line. Inserting this we obtain

$$S(x, y) =$$

$$(2M)^{\frac{1}{2}} \operatorname{Min}\left[\int_{x,y}^{x_1} (Ze^2/x - W + I)^{\frac{1}{2}} (1+y'^2)^{\frac{1}{2}}\, dx + \int_{x_1}^{x_0} \sqrt{2}(Ze^2/x - W)^{\frac{1}{2}}\, dx\right], \quad (12)$$

where we have arbitrarily chosen S to be zero at $x = y = x_2$; also $y' = \partial y/\partial x$, x_1, (x, y) are the mobile limits and x_2 is given by $Ze^2/x_2 = W$. We must then find the point ($x = x_0$) on the line $y = 0$, which has the highest probability, i.e. the lowest value of S.

(12) now takes the form

$$S/(2M)^{\frac{1}{2}} = \mathrm{Min}\left[\int_{x_0}^{x_1} f(x, y')\,dx + \int_{x_1}^{x_2} g(x)\,dx\right]. \tag{12'}$$

The variation applied to (12′) gives

$$\frac{\partial f}{\partial y'} = \text{const.} = A \text{ (say)} \tag{13a}$$

as the characteristic curve; the condition

$$f - y'\frac{\partial f}{\partial y'} = 0 \tag{15a}$$

to be satisfied at the limit x_0, which moves along $y = 0$, and

$$f - g - (y' - 1)\frac{\partial f}{\partial y'} = 0 \tag{16a}$$

to be satisfied at the limit x_1, which moves along $x - y = 0$.

Substituting the respective values from (12), we get for the characteristic curve

$$y' = \pm A/(Ze^2/x + \alpha - A^2)^{\frac{1}{2}}. \tag{13}$$

If our solution is to be in conformity with the boundary condition (8), we must choose the lower sign in the above equation. This is shown in § V. So taking the minus sign we get on integration

$$y = \frac{Ax}{A^2 - \alpha}\left(\frac{Ze^2}{x} - A^2 + \alpha\right)^{\frac{1}{2}} + \frac{AZe^2}{(A^2 - \alpha)^{\frac{3}{2}}}\tan^{-1}\left(\frac{Ze^2/x - A^2 + \alpha}{A^2 - \alpha}\right)^{\frac{1}{2}} + B, \tag{14}$$

where $\alpha = I - W$, and A and B are constants of integration to be determined by (15a) and (16a). Further, for the limit x_0, (15a) gives

$$\frac{Ze^2}{Ix_0} = \left(\frac{\beta^2}{2} + \rho - 1\right), \tag{15}$$

and for the limit x_1, (16a) gives

$$\left(\frac{Ze^2}{Ix_1} - \rho\right)^{\frac{1}{2}} = (\beta - 1), \tag{16}$$

where $\rho = W/I$ and
$$\beta = (2A^2/I)^{\frac{1}{2}}. \tag{17}$$

With the help of (15), (16) and (17), equation (14) simplifies to

$$\frac{2-\beta}{(\beta^2+2\rho-2)^{\frac{1}{2}}} = \tan\left[\frac{(\beta^2+2\rho-2)^{\frac{1}{2}}(\beta^2-\beta-1+\rho)}{\beta(\beta^2-2\beta+1+\rho)}\right]. \tag{18}$$

This equation determines in terms of ρ the constant β, and thus the limits x_0 and x_1. From (12′) we now obtain

$$\frac{S}{\surd(2M)} = \pm\int_{x_0}^{x_1}\frac{(Ze^2/x+\alpha)}{(Ze^2/x-A^2+\alpha)^{\frac{1}{2}}}\,dx+\surd 2\int_{x_1}^{x_2}(Ze^2/x-W)^{\frac{1}{2}}\,dx,$$

x_0 and x_1 being now given by (15) and (16) respectively; the double sign corresponds to the two signs in (13); so taking the negative sign in accordance with the remarks after (13) and carrying out the integration, we obtain

$$\frac{S}{\surd(2M)} = -2x_1(Ze^2/x_1-A^2+\alpha)^{\frac{1}{2}}+(2A^2-\alpha)\frac{x_1}{A}$$
$$-\surd 2x_1(Ze^2/x_1-W)^{\frac{1}{2}}+\surd 2\frac{Ze^2}{\surd W}\tan^{-1}\{(Ze^2/x-W)/W\}^{\frac{1}{2}}. \tag{19}$$

If we define a function $F(\rho)$ as

$$F(\rho) = (I/2)^{\frac{1}{2}}Ze^2\{S/\surd(2M)\},$$

it will replace $\overline{F(W/I)}$ in (3), so that (2) becomes

$$\exp\left[-\frac{4Ze^2}{\hbar}(M/I)^{\frac{1}{2}}F(\rho)\right], \tag{20}$$

with
$$F(\rho) = \frac{\beta^2-\beta-1+\rho}{\beta(\beta^2-2\beta+1+\rho)}+\frac{1}{\surd\rho}\tan^{-1}\left(\frac{\beta-1}{\surd\rho}\right), \tag{21}$$

where $\rho = W/I$, and β has the value given by (18). The values of $F(\rho)$ calculated from (21) are shown in fig. 1. The correcting factor (3) has the values given in Table I. In row (3) are given the values of Oppenheimer and Phillips for comparison.

TABLE I

ρ	0·5	0·75	1·0	1·25	1·5	1·60	1·70
$f(\rho)$	0·559	0·484	0·426	0·378	0·338	0·322	0·307
$f(W/I)$	0·507	0·429	0·355	0·295	0·250	0·237	0·224

To compare the results with experiments the excitation curve for copper has been calculated by taking $I = 2{\cdot}25$ mV (Chadwick, Feather and Bretscher 1937), and is shown in fig. 2. The experimental points are taken from Lawrence and others (1935), and we see that for the value of I chosen the calculated curve is in good agreement with the experimental results.

Correction for Radius

In writing (12′) it had been assumed that the neutron reaches the nucleus when $y = 0$, that is to say the radius of the nucleus had been neglected. If we take the radius of the nucleus into consideration, then evidently the neutron will reach the nucleus when $y = r$, where r is the radius of the nucleus.

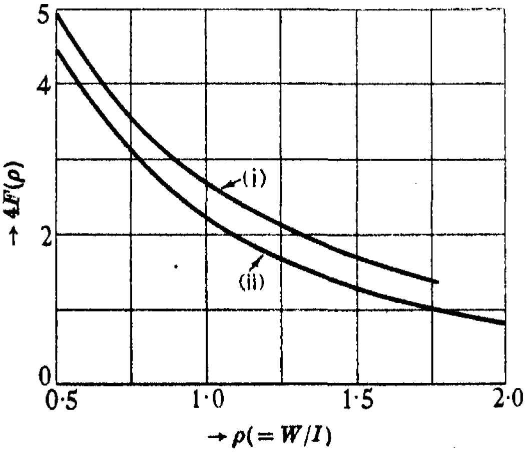

Fig. 1—$4F(\rho)$ as a function of $\rho(= W/I)$. Curve (i) is calculated from equation (21), while (ii) is that obtained by Oppenheimer and Phillips (1935).

As a consequence the limit of integration x_0 in (12′) must be constrained to move along $y = r$. When this is done, the formulae (18) and (21) are slightly modified. β is now determined by

$$\frac{2-\beta}{(\beta^2+2\rho-2)^{\frac{1}{2}}} = \tan\left[\frac{(\beta^2+2\rho-2)^{\frac{1}{2}}(\beta^2-\beta-1+\rho)}{\beta(\beta^2-2\beta+1+\rho)} - \frac{Ir}{Ze^2}\frac{(\beta^2+2\rho-2)^{\frac{1}{2}}}{2\beta}\right] \tag{18′}$$

and $F(\rho)$ is given by

$$F(\rho) = \frac{\beta^2-\beta-1+\rho}{\beta(\beta^2-2\beta+1+\rho)} + \frac{1}{\sqrt{\rho}}\tan^{-1}\left(\frac{\beta-1}{\sqrt{\rho}}\right) - \frac{Ir}{Ze^2}\frac{\beta^2-1+\rho}{\beta}. \tag{21′}$$

Calculations have been carried out for Cu by using (18′) and (21′) as well, but as is evident from fig. 2 the effect of taking the radius into consideration is to make the excitation curve still flatter, and in view of the fact that resonance effects have been neglected this should not be disconcerting.

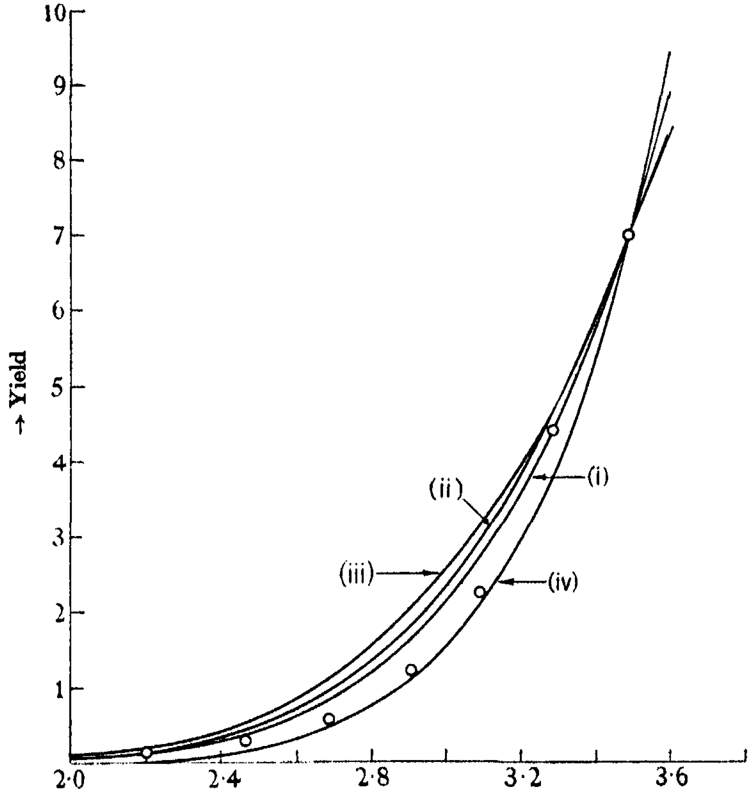

Fig. 2—Excitation curve for copper. The curves are calculated for $I = 2{\cdot}25$ mV. The notation (i) and (ii) is the same as in fig. 1, while the other two curves take the finite radius of the copper nucleus into account; the radius is calculated from the relation $r = r_0 A^{\frac{1}{3}}$, using for r_0 the value obtained on the one-body picture of radioactive nuclei. Curve (iii) is calculated from equations (18′) and (21′), while curve (iv) represents Gamow's function. The experimental points are represented by circles, and the ordinates of the theoretical curves are adjusted to fit the highest experimental point.

IV

All the previous calculations are based on the assumption that S is real in the region A (fig. 3), and on the basis of this, expression (12′) has been obtained for S. In what follows it will be shown that this assumption is justified. For this purpose we observe that the integral (12′) defines a function S which solves the equation (10) with the boundary condition (8) throughout the region A as defined in the figure. If, now, on the basis of (12), we can construct a solution S'[*] in B which fits continuously at the boundary and satisfies (8), and if the real part of this solution nowhere tends to $-\infty$, then we shall have shown that (12) represents the correct solution.

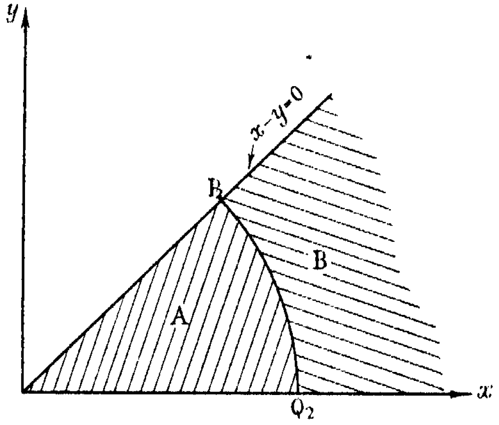

FIG. 3—The point $P_2(x=y=x_2)$ is defined by $Ze^2/x_2-W=0$. P_2Q_2 is the line of steepest gradient of S as given by equation (14) and is the boundary line between regions A and B. The diagram is not drawn to scale.

If, now, such a solution exists, S must obviously be complex in the region B. We may, therefore, in this region, write

$$S' = \sigma + i\tau. \tag{22}$$

It then follows from (10) that

$$(\operatorname{grad}\sigma, \operatorname{grad}\tau) = 0$$

and
$$\sigma = \int\sqrt{(V-E+|\operatorname{grad}\tau|^2)}\,ds. \tag{23}$$

The first of these shows that the lines of steepest gradient of σ are lines of constant τ and vice versa.

Further along the line $x = y$, S' is entirely imaginary, and is given by

$$\tau = \frac{S'}{i} = \int\sqrt{2}(E-V+I)^{\frac{1}{2}}\,dx. \tag{24}$$

The line $x = y$ being a line of constant σ, the lines of steepest gradient of σ meet it at right angles, i.e.

$$\phi(\tau) = [(\partial y/\partial x)_\tau]_{x=y} = -1. \tag{25}$$

---

[*] We write S' to distinguish it from S which is used to denote the solution in the region A only.

This result is in agreement with, and is, in fact, independently deducible from (8).

Further, at the point $P_2(x = y = x_2)$, $\tau = 0$, and therefore

$$\sigma = S' = \int_{P_2} (V-E)^{\frac{1}{2}} ds \tag{26}$$

for all points on the line of steepest gradient of σ passing through P_2, the integral to be taken along this line.

If now we approach the point P_2 from the left, we see that (13) with the the help of (16) gives

$$[y']_{x=y} = -1 \tag{27}$$

and (12) simplifies to
$$S = \int (V-E)^{\frac{1}{2}} ds, \tag{28}$$

both of which are the same as the corresponding values (25) and (26).

Equations (25) and (27) show that the line of steepest gradient of S through P_2 and the line of steepest gradient of σ through P_2 both have the same slope at that point; equations (26) and (28) then establish that these two lines coincide everywhere. We thus see that we obtain the same line of steepest gradient through the point P_2 whether we approach it from the left or from the right, so that S is automatically continuous at the boundary.

Now it remains to enquire if it is possible to construct lines of steepest gradient of σ in the region B satisfying the boundary conditions along $x-y = 0$ and along the boundary with the region A.

Obviously S' is determined if we know grad τ and the lines of constant τ. Since, on the other hand, the value of τ on $x = y$ follows from (24), we need only know the lines of constant τ (lines of steepest gradient of σ). In order to see to what extent these are fixed, we consider the family of curves $y = y(x, \tau)$ with the parameter τ such that for $\tau = 0$, $y(x, 0)$ gives the boundary curve P_2Q_2. Then

$$|\operatorname{grad} \tau| = \frac{\sqrt{\{1+(\partial y/\partial x)_\tau^2\}}}{(\partial y/\partial \tau)_x}. \tag{29}$$

Now $(\partial y/\partial x)_\tau$ is known at all points of the boundary line, being given by (13), whereas $(\partial y/\partial \tau)_x$ is as yet unknown. This, however, is to be chosen subject to the condition that if we pass from one line of constant τ to the next one along the normal, the value of σ remains unchanged. Differentiation along the normal to our family of curves gives

$$-\left(\frac{\partial \sigma}{\partial \tau}\right)_x \left\{\left(\frac{\partial y}{\partial x}\right)_\tau^{-1} + \left(\frac{\partial y}{\partial x}\right)_\tau\right\} + \left(\frac{\partial \sigma}{\partial x}\right)_\tau \left(\frac{\partial y}{\partial \tau}\right)_x = 0. \tag{30}$$

In the above relation, $(\partial\sigma/\partial\tau)_x$ and $(\partial y/\partial\tau)_x$ are as yet unknown. We can, however, eliminate $(\partial\sigma/\partial\tau)_x$ with the help of (23) and (29). Since (29) involves $(\partial y/\partial\tau)_x$ and (23) has to be differentiated with respect to τ, the eliminant will contain $(\partial^2 y/\partial\tau^2)_x$.

Thus if $y(x, \tau)$ and $(\partial y/\partial\tau)_x$ are known for any one value of τ and all x, we can obtain an expression for $(\partial^2 y/\partial\tau^2)_x$ and consequently obtain the values of both y and $(\partial y/\partial\tau)_x$ along a neighbouring line. By repetition of the same procedure it is thus possible to construct step by step the whole family of lines in terms of the values of y and $(\partial y/\partial\tau)_x$ along the first of them, i.e. the boundary line P_2Q_2. We are still left free to choose $(\partial y/\partial\tau)_x$ along P_2Q_2, and this has to be done in such a way as to satisfy (25). In place of (25) we can, however, require the following to be satisfied:

$$\left(\frac{\partial\phi}{\partial\tau}\right)_\eta = 0; \quad \left(\frac{\partial^2\phi}{\partial\tau^2}\right)_\eta = 0, \text{ etc.,} \tag{25'}$$

where η signifies that the differentiation is along $x-y=0$. The first of these conditions may be written as

$$\left(\frac{\partial}{\partial x}\right)_\tau \left(\frac{\partial y}{\partial\tau}\right)_x + \left(\frac{\partial^2 y}{\partial x^2}\right)_\tau \left(\frac{\partial x}{\partial\tau}\right)_\eta = 0,$$

and this we can evidently satisfy by choosing $(\partial y/\partial\tau)_x$ suitably at P_2. Again, if we write down the expression for $(\partial^2\phi/\partial\tau^2)_\eta$, it will contain terms like $(\partial/\partial x)_\tau(\partial^2 y/\partial\tau^2)$ but no higher derivatives. Since, however, at each x, $(\partial^2 y/\partial\tau^2)_x$ can be expressed in terms of $(\partial/\partial x)_\tau(\partial y/\partial\tau)_x$, the term in $(\partial/\partial x)_\tau(\partial^2 y/\partial\tau^2)_x$ depends on $(\partial^2/\partial x^2)_\tau(\partial y/\partial\tau)_x$. This derivative taken at P_2 is arbitrary, since $(\partial y/\partial\tau)_x$ is still arbitrary along P_2Q_2. Similarly, in order to make the nth derivative $(\partial^n\phi/\partial\tau^n)_\eta$ vanish at P_2, we obtain an equation containing $\partial/\partial x(\partial^n y/\partial\tau^n)$ as the term of highest order. From this equation we can obtain another equation containing $(\partial^n/\partial x^n)(\partial y/\partial\tau)$ as the term of highest order. Lower derivatives being already fixed by similar equations, $\left(\frac{\partial^n}{\partial x^n}\right)_\tau\left(\frac{\partial y}{\partial\tau}\right)_x$ can be fixed by the equation $(\partial^n\phi/\partial\tau^n)_\eta = 0$. Thus we can make all derivatives of (25), viz. (25′), vanish, if we choose the function $(\partial y/\partial\tau)_x$ along the line P_2Q_2 suitably, and, subject to the Taylor series converging, there will be only one such solution for $(\partial y/\partial\tau)_x$. Consequently the whole family of lines $y(x, \tau)$ is fixed in conformity with the boundary conditions.

We thus see that starting with a solution of the type (12) we are able to determine its lines of steepest gradient throughout the relevant region of the (x, y) space, and that these lines fit continuously at the boundary between A and B. It is clear, therefore, that the values (12′) for S in A form part of a consistent solution of the problem, and hence the assumption of S being real in A is fully justified.

V

The next point to be investigated is whether the line determined from among the family of curves (14) by the minimum condition (16) is in accord with the boundary condition (8). To see this we write

$$\eta = y - x \quad \text{and} \quad \zeta = x + y. \tag{31}$$

Equation (10) then becomes

$$\left(\frac{\partial S}{\partial \eta}\right)^2 + \left(\frac{\partial S}{\partial \zeta}\right)^2 = M(V-E). \tag{32}$$

With ψ given by (9), the boundary condition (8) becomes

$$\left(\frac{\partial S}{\partial \eta}\right)_{\eta=0} = (MI)^{1/2}. \tag{33}$$

We then get from (32)

$$\left(\frac{\partial S}{\partial \zeta}\right)_{\eta=0} = \sqrt{M}\left(\frac{2Ze^2}{\zeta+\eta} - W\right)^{1/2}_{\eta=0}. \tag{34}$$

It follows from (31), (33) and (34) that the correct line of steepest gradient of S along which the integral is to be evaluated should be such as to satisfy the condition

$$\left(\frac{dy}{dx}\right)_{x=y} = \left[\frac{\partial S/\partial y}{\partial S/\partial x}\right]_{x=y} = \frac{(Ze^2/x - W)^{1/2} + I^{1/2}}{(Ze^2/x - W)^{1/2} - I^{1/2}}. \tag{35}$$

Imposing (35) on (13) we find that, at $x - y = 0$, the desired curve must satisfy the relation

$$(Ze^2/Ix - \rho)^{1/2} = (\beta - 1), \tag{36}$$

which is exactly the same as (16). We thus see that the curve chosen for $y = y(x)$ in (12′) by the variation method, when the negative sign in (13) is taken, is the desired curve and consequently the value obtained for S is the correct value and not a lower limit. If we had chosen the plus sign in (13), equation (16) would have been

$$(Ze^2/Ix_1 - \rho)^{1/2} = (\beta + 1),$$

which is not the same as (36). It was for this reason that the positive sign in (13) was discarded.

VI

Next let us investigate in detail the justification for the neglect of y_2 in § II, which permitted us to treat the problem in two dimensions. When y_2 is taken different from zero, the limit x_0 moves along the surface $y_1 = 0$ and $y_2 = 0$, while the other limit x_1 moves along $x = y_1$ and $y_2 = 0$. These surfaces correspond to the lines $y = 0$ and $y = x$ respectively in the previous discussion in two dimensions. Equation (12′) now becomes

$$S/\surd(2M) = \mathrm{Min}\left[\int_{x_0}^{x_1}(Ze^2/x+\alpha)^{\frac{1}{2}}(1+y_1'^2+y_2'^2)^{\frac{1}{2}}\,dx+\int_{x_1}^{x_2}\surd 2(Ze^2/x-W)^{\frac{1}{2}}\,dx\right]. \tag{37}$$

Applying the variation to (37) we now obtain two equations—one for y_1 and the other for y_2—where before we obtained only one for y. Corresponding to (13) we now get

$$\frac{\partial f}{\partial y_{1,2}'} = \left(\frac{Ze^2}{x}+\alpha\right)^{\frac{1}{2}}\frac{y_{1,2}'}{(1+y_1'^2+y_2'^2)^{\frac{1}{2}}} = A_{1,2}\ (\text{say}).$$

Writing $D^2 = (A_1^2+A_2^2)$, we obtain

$$y_{1,2}' = \pm\frac{A_{1,2}}{\left(\dfrac{Ze^2}{x}-D^2+\alpha\right)^{\frac{1}{2}}}; \tag{38}$$

also

$$y' = (y_1'^2+y_2'^2)^{\frac{1}{2}} = \pm\frac{D}{\left(\dfrac{Ze^2}{x}-D^2+\alpha\right)^{\frac{1}{2}}}. \tag{39}$$

(38) yields on integration

$$y_{1,2}' = \mp\frac{A_{1,2}\,x}{D^2-\alpha}\left(\frac{Ze^2}{x}-D^2+\alpha\right)^{\frac{1}{2}} \mp\frac{A_{1,2}\,Ze^2}{(D^2-\alpha)^{\frac{3}{2}}}\tan^{-1}\surd\left(\frac{Ze^2/x-D^2+\alpha}{D^2-\alpha}\right)+B_{1,2}. \tag{40}$$

Further, the relations to be satisfied at the limits x_0 and x_1 are respectively

$$f-y_1'\frac{\partial f}{\partial y_1'}-y_2'\frac{\partial f}{\partial y_2'} = 0\,*$$

and

$$f-g-(y_1'-1)\frac{\partial f}{\partial y_1'}-y_2'\frac{\partial f}{\partial y_2'} = 0.$$

They yield on substitution $\quad Ze^2/x_0 = D^2-\alpha \qquad (41)$

and

$$(Ze^2/x_1-W)^{\frac{1}{2}} = (I-A_2^2)^{\frac{1}{2}}\pm\surd 2A_1. \tag{42}$$

---

* Here $f=(Ze^2/x+\alpha)^{\frac{1}{2}}(1+y_1'^2+y_2'^2)^{\frac{1}{2}}$, and $g=\surd 2(Ze^2/x-W)^{\frac{1}{2}}$.

Remembering that (41) is to be satisfied at the intersection of (40) with the surface $y_1 = 0$, $y_2 = 0$, and that (42) is to be satisfied at the intersection of (40) with $x = y$, $y_2 = 0$, we get

$$B_1 = B_2 = 0 \quad \text{and} \quad A_2 = 0.$$

We thus see from (40) that the characteristic curve for y_2 is

$$y_2 = 0. \tag{43}$$

Further, with $A_2 = 0$, relations (39), (41) and (42) become identical with (13), (15) and (16) respectively. We thus see that so far as the variation calculation is concerned, the neglect of y_2 is justified.

Let us now examine the condition (35), which is derived from (8), and see how this is affected when y_2 is taken different from zero. Writing again

$$\zeta = x + y \quad \text{and} \quad \eta = y_1 - x,$$

we get from (10)

$$2(\partial S/\partial \zeta)^2 + 2(\partial S/\partial \eta)^2 + (\partial S/\partial y_2)^2 = 2M(V-E),$$

or in terms of the relative distance, r, between proton and neutron

$$(\partial S/\partial \zeta)^2 + (\partial S/\partial r)^2 (1 - y_2^2/2r^2) = M(V-E).$$

We are here considering the deviations of y_2 from the value $y_2 = 0$ so that y_2 is already very small and consequently the ratio $y_2^2/2r^2$ is of second order and may therefore be neglected in comparison with unity. We are then left with

$$\left(\frac{\partial S}{\partial \zeta}\right)^2 + \left(\frac{\partial S}{\partial r}\right)^2 = M(V-E),$$

which is the same as (32). It is now obvious that we shall again get the same condition as (35). Thus we can conclude that the restriction to two dimensions is justified.

In conclusion I wish to express my sincere thanks to Dr. Peierls for his valuable suggestions and discussions throughout.

SUMMARY

A generalization of the method of geometrical optics, commonly known as the Wentzel-Kramers-Brillouin method, is applied to the case of transmutation by deuterons. The treatment of Oppenheimer and Phillips (1935), based on the approximation of a three-body problem, is improved in so

far as the wave equation is not assumed to be separable. The generalization gives, in general, an upper limit to the probability of the process, but in the present case it is shown that it gives the correct value. The results of the calculations are given in Table I and figs. 1 and 2. Formulae ((18′) and (21′)) are also obtained which take into account the finite radius of the nucleus. The results are compared with experiments on copper and are found to be in fair agreement, when the binding energy of the deuteron is taken to be 2·25 mV.

REFERENCES

Bethe, H. and Peierls, R. 1935 *Proc. Roy. Soc.* A, **148**, 146–56.
Chadwick, J., Feather, N. and Bretscher, E. 1937 *Proc. Roy. Soc.* A, 163, 366–375.
Kapur, P. L. and Peierls, R. 1937 *Proc. Roy. Soc.* A, 163, 606–10.
Lawrence, E. O., McMillan, E. and Thornton, R. L. 1935 *Phys. Rev.* **48**, 493–9.
Oppenheimer, J. R. and Phillips, M. 1935 *Phys. Rev.* **48**, 500–2.

A Study of Upper Carboniferous Coals from Western Australia

BY C. R. KENT, PH.D.

(*Communicated by Professor William A. Bone, F.R.S.—*
Received 19 *July* 1937)

In October 1934 the author came to England from Western Australia, bringing with him samples of five representative coals from the Collie Coalfield in that province for the purpose of investigating their chemical properties at the Imperial College, London, under the direction of Professor William A. Bone, having previously had several years' working experience of them, including a survey of the coalfield from which they originated. The investigation was carried out at the Imperial College during the two following years, and the present paper embodies its principal results.

1—THE COLLIE COALFIELD OF WESTERN AUSTRALIA

This coalfield, which lies about 100 miles south of the provincial capital, Perth, covers an area of approximately 50 sq. miles, and comprises estimated reserves within 2000 ft. of 3500 million tons of sub-bituminous coals, the annual output being about 500,000 tons, chiefly for locomotive and power purposes.

It is generally believed that its sedimentary rocks and coal-seams were laid down during Late Carboniferous (formerly called Permo-Carboniferous) and/or Early Permian times upon an eroded surface of pre-Cambrian crystalline rocks, and that originally they extended over a much greater area than now, being continuous with the Wilga coal-measures and Donny Brook sandstones of the near south and with the Irwin River coal-measures some 300 miles to the north. After their deposition faulting occurred, during the course of which the Collie area became a lake, the floor of which consisted of gently tilted and partly eroded sediments and coal-seams upon which were afterwards deposited unconformable lacustrine formations (gravels, sands and clays) some 100 ft. in thickness. Subsequent movements, associated with major disturbances to the west, lifted the area to about 1000 ft. above sea-level, causing the lake water to be drained away. The coal-seams in the area are free from igneous intrusions and exhibit a fairly uniform southerly dip of about 8°, with several major faults, one having a throw of about 250 and others of 70 ft.

Edgworth David classified the Collie and Irwin River Series as belonging to the Permian Section of the Kamilaroi System. The chief interest of the coals is that they originated in the vegetation of Gondwanaland, which was relatively poor in species and dominated by *Gangamopteris* and *Glossopteris*—fern-like in habit though probably pteridosperms—unknown in the contemporary floras north of the Tethys Sea. Hence, while coals of the northern hemisphere originated in a flora rich in heterosporous plants, those of the south were mainly formed from seed-bearing plants and rarely contain more than a low proportion of megaspores. And therefore comparisons of their chemical properties and constitution are of considerable interest.

2—The Coals Investigated

There are three horizons of productive measures in the coalfield, namely, (*a*) the "Co-operative" or "Collie" horizon (oldest), (*b*) the "Collieburn" or "Griffin" horizon, and (*c*) the "Cardiff" horizon (youngest). Of the five coals investigated, those from the "Co-operative" (Co), "Proprietary" (P) and "Stockton" (S) Collieries, respectively, pertained to (*a*), while a fourth came from (*b*) and the fifth from (*c*). They were all sub-bituminous and non-coking with from 15 to 30 % of pit moisture. Representative samples of each coal were put up at the collieries in airtight tins, each holding about 28 lb., and did not suffer any deterioration during subsequent transit to London. Four samples (Co 1, 2, 3 and 4) were taken from the Co-operative Colliery, two (G 1 and 2) from the Griffin Colliery, and one from each of the Proprietary (P), Stockton (S) and Cardiff (Ca) Collieries. Of the four Co-operative samples, Nos. 1 and 2 were from the lower workings, 693 ft. below the surface, and Nos. 3 and 4 were from the upper workings, 48 ft. below the surface; the two "Griffin" samples were from 7 ft. and 6½ ft. seams at 380 and 210 ft., respectively, below the surface. Their proximate and ultimate compositions are shown in Table I.

All the coals are finely banded and have a subconchoidal fracture; and while those of the "Co-operative" and "Cardiff" horizons are usually dull and dirty to handle, those of the intermediate "Griffin" horizon are relatively bright and clean. The former contain unusually large proportions of "fusain" but practically no spores; the latter contain abundant microspores and a few megaspores.

3—Extraction of the Coals by Solvents

A—In preliminary examinations each of the dry coals was extracted Soxhlet-wise at atmospheric pressure successively with (*a*) boiling benzene and (*b*) a boiling mixture of equal volumes of benzene and ethyl alcohol, yielding, in the first case, up to 0·5 % of a brown wax and, in the second, up to about 3·5 % of a brown-black brittle resinous solid which on further successive extractions by boiling light petroleum (60–80°), benzene-alcohol and benzene, respectively, could be resolved into (i) a dark brown brittle substance soluble in light petroleum and amounting to nearly two-thirds of the whole extract, (ii) a soft brown vaseline-like substance, amounting to about another third thereof, and (iii) small amounts of a hard brown brittle wax, m.p. *circa* 80°, resembling the "montan-wax" of brown coals.

B—After the foregoing preliminary extractions, during which about 2·4 % of it was removed, the dry Griffin No. 2 coal was submitted to a further exhaustive Soxhlet-wise benzene pressure extraction in three successive stages at 250, 500 and 750 lb./sq. in. respectively, and the resulting primary extract was subsequently fractionated according to the standard procedure outlined on pp. 171–2 of "Coal, its Constitution and Uses" (1936) by W. A. Bone and G. W. Himus.

Although some water was eliminated at each stage of the extraction, no sign of any gas evolution could be detected in any of them, showing that no

TABLE I—PROXIMATE AND ULTIMATE COMPOSITION OF THE COAL SAMPLES

Sample ...	Co 1	Co 2	Co 3	Co 4	G 1	G 2	P	S	Ca
% Moisture as received	17·9	18·2	21·5	21·1	17·3	20·6	22·7	22·4	23·9
"Volatiles" at 900° in D.A. coal %	31·95	30·35	30·3	29·3	40·45	36·4	31·65	32·0	38·7
Ash in dry coal %	8·05	12·7	8·35	5·5	6·25	6·65	7·25	7·8	5·5
% on dry ashless coal:									
Carbon	79·45	79·45	79·15	80·10	75·60	76·4	78·65	78·35	74·7
Hydrogen	4·25	3·85	4·05	4·00	5·10	4·45	3·95	3·85	4·45
Nitrogen	1·35	1·40	1·50	1·45	1·35	1·50	1·40	1·35	1·35
Sulphur	0·30	0·25	0·40	0·35	0·85	0·65	0·30	0·45	0·45
Oxygen (diff.)	14·65	15·05	14·90	14·10	17·1	17·0	15·70	16·00	19·05
Ratio C/H	18·7	20·65	19·55	20·0	14·8	17·2	19·9	20·35	16·8

breakdown of the fundamental structure of the coal substance had occurred. Most of the primary extract was derived during the second stage. The yields and compositions of the various fractions obtained are shown in Table II.

TABLE II—YIELDS AND COMPOSITIONS OF FRACTIONS FROM THE BENZENE PRESSURE EXTRACTION OF GRIFFIN NO. 2 COAL

Fraction ...	*Ia*	*Ib*	II	III	IV	Residue
Percentage yield on D.A. coal ...	0·85	1·55	1·70	2·5	1·0	92·4
C	81·3	82·4	79·5	77·4	80·7	78·90
H	9·5	10·0	7·3	6·0	5·6	4·05
N	0·8	0·5	1·0	1·5	1·2	1·55
S	0·8	0·6	0·6	0·5	0·7	0·60
O (diff.)	7·6	6·5	11·6	14·6	11·8	14·90
C/H	8·56	8·24	10·9	12·9	14·4	19·5
Description ...	Mobile yellow oil	Brown and vaseline-like	Brittle pitch-like solid	Dark brown resinous solid	Dark brown amorphous powder	

The primary extract also contained about 0·04 % of water-soluble phenolic bodies not included in the above fractions. In general the extraction products resembled those usually yielded by black lignites or sub-bituminous coals save that all the fractions contained material proportions of both nitrogen and sulphur.

4—OXIDATION OF THE COALS BY BOILING ALKALINE PERMANGANATE

a—Carbon Balances—A representative sample of each coal was oxidized by means of boiling alkaline permanganate according to the standard carbon-balance method devised by W. A. Bone and collaborators (*vide* pp. 184–5 of "Coal, its Constitution and Uses") with results as shown in Table III.

TABLE III—CARBON BALANCES OF THE OXIDATIONS

Coal ...	Co	P	S	G 1	G 2	Ca
Percentage original carbon obtained as:						
CO_2	40·5	41·5	42·7	46·3	47·8	53·5
Acetic acid	0·4	0·3	0·2	1·2	0·8	1·2
Oxalic acid	6·1	7·3	4·3	10·5	6·0	5·8
Benzene carboxylic acids	51·0	50·0	50·9	41·2	41·3	35·7
Total	98·0	99·1	98·1	99·2	95·9	96·2

In all cases except P and S a small percentage of the coal was recovered unchanged; but after due allowance for this practically all the carbon was accounted for in the above products. Speaking generally, the observed rates of oxidation were intermediate between those of bituminous coals and lignites. The yields of acetic and oxalic acids were lower and those of benzenoid acids higher than are usually obtained from most of such sub-bituminous coals, indicative of greater maturity.

b—Oxidation of "Fusain" and residual "Anthraxylon" from the Proprietary Coal (P)—Samples of the "fusain" and residual brilliant coal ("Anthraxylon") were hand-picked from a bulk sample of the "Proprietary" Coal (P) and separately submitted to exhaustive alkaline permanganate oxidations according to the "carbon balance" method. At the end thereof about 9·2 % of the "fusain" and 7·1 % of the "anthraxylon" were recovered unchanged. After allowing for such unchanged material in each case, the following carbon balances for the major part actually oxidized were obtained:

Percentage carbon obtained as:	"Fusain"	"Anthraxylon"
CO_2	39·8	46·9
Acetic acid	0·2	1·4
Oxalic acid	5·6	9·9
Benzene carboxylic acids ...	53·5	40·8

c—Detailed Investigation of the Benzenoid Acids from the Bulk Oxidation of the Proprietary Coal—(i) 673 g. of the dry Proprietary Coal (P) were oxidized in two equal portions by means of some 6050 g. of potassium permanganate and 910 g. of caustic potash in 50 l. of water, the total time occupied being about 56 hr. Apart from unavoidable small losses, some 380 g. of crystalline acids were obtained of which about 370 were benzenoid acids of mean ultimate composition,

$$C = 48{\cdot}2,\quad H = 2{\cdot}7 \quad\text{and}\quad O = 49{\cdot}1\ \%,$$

intermediate between those of benzene tri- and tetra-carboxylic acids. (ii) About 228 g. of the crude acids were esterified by refluxing their silver salts with methyl iodide in ethereal solution. The mixed neutral methyl esters were subsequently dissolved in ethyl alcohol and the solution put aside at room temperature for several weeks, during which about 17·5 g. of solid esters crystallized out which subsequent examination proved to be those of mellitic, benzene-pentacarboxylic and mellophanic acids. Finally, after removal of the solvent, some 175 g. of the remaining neutral liquid esters were fractionally distilled under low pressure from a 500 c.c. Claisen flask until incipient decomposition of the residue necessitated stopping the operation at 241° C. under 3 mm. pressure. Subsequently each fraction of the neutral esters was separately hydrolysed and the resulting acids isolated and identified. The results obtained are summarized in Table IV.

TABLE IV—FRACTIONATION OF NEUTRAL METHYL ESTERS

Fraction no.	Range ° C.	Pressure mm.	% by wt.	Acids isolated after hydrolysis
1	28–40	22	0·2	Oxalic and succinic
2	40–60	22	0·7	
3	60–100	20	1·1	Oxalic, succinic, phthalic and *iso*phthalic
4	100–120	20	1·0	
5	60–140	2	2·3	Phthalic, *iso*phthalic, terephthalic and hemimellitic
6	140–170	2	3·3	
7	170–190	2	6·2	Terephthalic, hemimellitic, trimellitic, mellophanic, and pyromellitic
8	187–205	2·5	8·1	
9	200–225	3	6·7	Trimellitic, mellophanic pyromellitic and prehnitic
10	220–241	3	16·1	
11	Residue	—	52·9	Benzenepentacarboxylic and mellitic

It will thus be seen that, apart from quite small proportions of oxalic and succinic acids, the main constituents of the crude crystalline acids were phthalic, *iso*phthalic, terephthalic, trimellitic, hemimellitic, mellophanic, pyromellitic, prehnitic, benzenepentacarboxylic and mellitic acids, the two last named greatly predominating over the rest. Moreover, no less than ten out of the twelve possible benzene carboxylic acids were isolated, and in much the same proportions as were found by Bone and co-workers in the corresponding oxidation products of British bituminous and anthracitic coals. Hence it may be concluded that, notwithstanding considerable differences in the original flora from which they were derived, there is a remarkable similarity in the fundamental benzenoid chemical structure of the main coal substance in both cases.

In conclusion, the author desires to acknowledge his indebtedness to the University of Western Australia for the award of a Hackett Research Studentship which enabled him to carry out the investigation, to the Amalgamated Collieries of Western Australia Limited and the Griffin Coal Mining Company for providing him with the representative coal samples and much information relative thereto, to Messrs. J. M. Limb and J. S. Morrison of the Western Australian Government Railways for the sampling and packing arrangements, and to Professor W. A. Bone and Dr. G. W. Himus for advice and help in regard to the experimental work involved.

Explosion Waves and Shock Waves

V—The Shock Wave and Explosion Products from Detonating Solid Explosives

By W. Payman, D.Sc., Ph.D. and D. W. Woodhead, Ph.D., F.I.C.

(*Communicated by J. F. Thorpe, F.R.S.—Received* 20 *July* 1937)

[Plates 18–23]

Introduction

The methods described in Parts I and II of this series of papers (Payman and Woodhead 1931; Payman, Titman and Woodhead 1935) have been used to obtain photographic records of the atmospheric disturbance produced on detonating a cartridge of explosive when it is freely suspended in air, and at the same time to gain some knowledge of the mode of breakdown of the cartridge during detonation. We have used two coal-mining explosives, Rounkol No. 2, a "low-density" explosive containing ammonium nitrate together with a mixture of nitroglycerine and nitroglycol, and Celmonite, an explosive of normal density of the ammonium nitrate class containing no nitroglycerine. The published compositions of these explosives (parts by weight) are as follows:

	Rounkol No. 2	Celmonite
Nitroglycerine and nitroglycol	14–16	—
Ammonium nitrate	49–52	65·5–68·5
Trinitrotoluene	—	10·5–12·5
Sodium nitrate	8·5–10·5	—
Sodium chloride	6–8	19·5–21·5
Plant fibre	15–17	—
Resin	0–0·5	—
Di-ammonium phosphate	0–0·5	—
Moisture	0·5–2·5	0–2

These explosives have the same weight strength as measured by a ballistic pendulum. Their densities were: Rounkol No. 2 0·66 and Celmonite 1·10; and their rates of detonation Rounkol No. 2 2090 and Celmonite 2950 m./sec. Each explosive was used in cartridges $1\frac{7}{16}$ in. (3·65 cm.) in diameter, wrapped with paper and waxed except when otherwise indicated. No. 6 copper-cased fulminate-chlorate detonators, electrically fired, were used for initiation.

INSTANTANEOUS SPARK PHOTOGRAPHS

The arrangements for instantaneous and continuous photographs were similar to those made previously. Only one instantaneous photograph could be obtained in each experiment, so that to obtain a series showing the progress of the shock wave relative to the cartridge it was necessary to fire a succession of charges. It was found, however, that repeat records had similar characteristics and that a series of records showed a progressive and logical development.

The Development of the Shock Wave—For the first series of experiments one 113 g. (4 oz.) cartridge of Rounkol No. 2, 17·5 cm. long, was suspended across the middle of the Schlieren field, as shown in the scale diagram fig. 1, Plate 18. Fig. 2, Plate 18, is a direct photograph of the luminous effect produced on detonation of this cartridge. The growth of the accompanying disturbance is shown in figs. 3, 4 and 5, Plate 18, the time interval between successive records being approximately 3×10^{-5} sec.

The record in fig. 3, obtained when about one-third of the cartridge had detonated, shows that the disturbance has initially an almost spherical form. Study of the photographic negative shows the shock wave to be about 1·5 mm. in advance of the boundary of the opaque products of detonation. Since we know from the record the volume originally occupied by the air which is compressed into the shell of the "pressure wave" (Payman and Robinson 1926), the mean pressure therein can be calculated. Assuming that the compression is adiabatic, and ignoring heat transfer by radiation and conduction from the products of detonation, we find that at the instant depicted in fig. 3 this mean pressure is about 25 atm.

Neither in fig. 3 nor in the next record, fig. 4, obtained when about two-thirds of the cartridge had detonated, are there any indications as to the precise point within the cartridge reached by the detonation wave at the instant the photograph was taken. From the shape of the atmospheric wave and the way in which it develops, it can be argued that the front of the detonation wave within the cartridge corresponds with the greatest distance travelled by the external disturbance at the periphery of the cartridge.

In fig. 4 the spherical wave has proceeded beyond the end of the cartridge at which detonation is initiated and there is a pronounced deformation growing in this region, showing that the products of detonation from the end expand at a greater rate than those from the side of the cartridge. The remainder of the disturbance is still approximately spherical. The pressure wave is now more clearly visible and has a uniform thickness of 4 mm., which corresponds with a mean pressure due to adiabatic compression within the shell of about 20 atm. Both in front of the shock wave and within the pressure wave there are signs of interference by projected solid material. The record in fig. 5 was obtained shortly after the detonation wave had reached the end of the cartridge; a greater distance now separates the shock wave and the front of the products, which are still spherical except for a distension near the end of the detonated cartridge. In its early stages, therefore, the general form of the growing disturbance is a sphere with a distension at each end of the diameter coinciding with the axis of the cartridge.

Solid Particles Sent Out by the Detonating Explosive—Since it was first shown photographically (Payman 1928) that solid particles are sent out from a detonating cartridge of explosive, and that they pierce and travel in front of the atmospheric shock wave, they have received considerable attention, notably by Audibert (1929) and by Beyling and Schultze-Rhonhof (1933). The method of studying them used by Audibert was simple and effective; their presence was demonstrated and their concentration indicated by the number of perforations made through a sheet of paper placed at a distance from the explosive fired in a cannon. Audibert concluded that the particles were composed of explosive which had escaped decomposition during the detonation, and from other experiments he concluded that the proportion which did so escape could be quite large. Unlike the British coal-mining explosives, the French explosives contained no "cooling salts".

The momentum given to the solid particles must be due to the expansion of the gases, and it would appear surprising at first sight that these particles can distort the front of the shock wave and increase the speed of the gaseous products in certain directions. But the wave and gases expand at rates which from the outset decrease rapidly, whereas the solid particles tend to retain their initial speed because of their greater inertia. Hence particles which at first are behind the wave eventually move ahead, modifying the form of the disturbance in greater or less degree according to their concentration. We shall see that there are more solid particles associated with the wave as it passes from the ends than from the side of the cartridge, for a reason which is best explained with the help of a diagram, fig. 6.

As the detonation wave proceeds along the cartridge, a narrow layer of explosive, such as *e*, fig. 6A, is in process of detonation at any one instant.

The gaseous products arising from this layer are not free to expand with equal facility in all directions. There is considerable resistance to expansion to the rear, where motion is hampered by the presence of gases at high density already produced by the detonation of preceding layers; forward expansion is limited either by the undetonated cartridge or by gases produced by the detonation of subsequent layers, and in no case can it proceed axially at a rate exceeding that of the detonation wave. It is therefore clear that expansion will at first be forward and will be within such a space as shown by the two arrows in broken line in fig. 6A. Since the particles will receive their momentum during the first motion of the gases, the majority will be within the sheaf of projection indicated by the straight arrows in full line on the diagram, and there will therefore be some axial concentration of them.

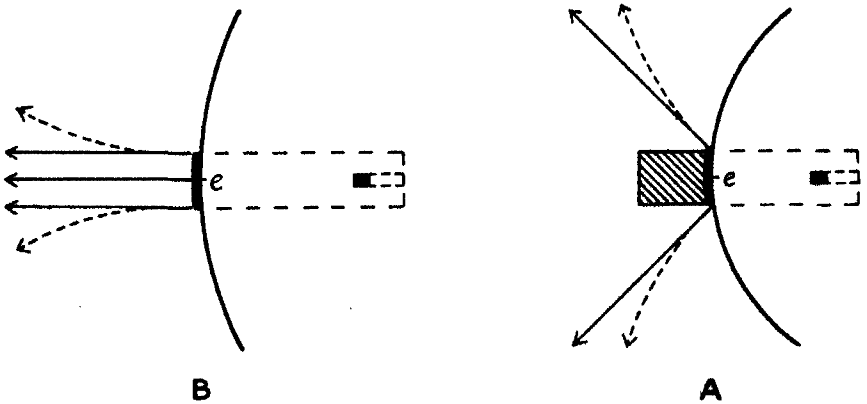

Fig. 6—Expansion of detonation products, A, laterally and, B, axially.

The conditions governing the expansion of the products of the last layers of explosive to be detonated are different. In a long cartridge the wave reaches all points on the flat end at approximately the same time, and there is no solid resistance to the free expansion of the gases, which will proceed initially in a direction normal to the surface, i.e. co-axially with the cartridge, as shown by the continuous arrows in fig. 6B. This directional effect given to the gases does not long persist and spherical expansion at a falling speed soon begins, as indicated by the arrows in broken line in the diagram; but the accompanying particles, having received their initial impulse, will continue to travel axially and will be accompanied or followed by particles produced in preceding stages and concentrated as previously explained.

Later Stages of the Expansion of the Atmospheric Wave—The projection of massed solid particles is shown most clearly by photographs taken when the wave has travelled some distance from the cartridge. The four records shown in fig. 7, Plate 19, were obtained by altering the position of the cartridge relative to the Schlieren field in a manner which will be apparent from the Plate. Figs. 7*a*, *b* and *c* were obtained in three different experiments but were taken as nearly as possible at the same interval of time after initiation of detonation. Fig. 7*d* is an inverted print of fig. 7*c*. The photographs, therefore, show the appearance of the wave all around the cartridge at a particular instant. That the deformation in the atmospheric wave along the axis of the cartridge is associated with swarms of solid particles is evident. In fig. 7*b* numerous prominences in the well-known arrow-head form (see Part II) have appeared near the axis. At the other end of the cartridge, fig. 7*a*, the shower of particles is more concentrated and none has yet broken through the front of the wave. The lateral wave in fig. 7*c* is still expanding spherically, and at this distance, about 25 cm. from the cartridge, it is just beginning to be broken up by solid particles; close behind are the gaseous and solid products of detonation, appearing on the record as a dense black area. The composite record has the general appearance of a spherical wave with deformations at the ends of the cartridge.

Experiments with Celmonite—The earlier experiments were carried out with Rounkol No. 2, because its relatively low rate of detonation facilitated the synchronization of spark records during the development of the "spark switch" described in Part II. Celmonite, which detonates more rapidly, was used later in experiments designed mainly to examine the effect of alteration in the length of the cartridge and to follow the behaviour of the wave, gases and solid particles at greater distances from the explosive. Instantaneous spark photographs were taken of cartridges 5·3 and 10·6 cm. long, the corresponding weights being 57 g. (2 oz.) and 113 g. (4 oz.). Fig. 8, Plate 20, shows the disturbance just emerging from the 5·3 cm. cartridge, taken about 10^{-6} sec. after initiation. Since the detonator is almost as long as the cartridge, its head (containing the fulminate charge) is nearer the left-hand end, although it has been inserted from the right, and the wave first emerges towards the left of the cartridge. Fig. 9, Plate 20, is a similar record with the longer 10·6 cm. cartridge, and it shows that the centre of the disturbance is now nearer the right-hand end of the cartridge. The wave is not so nearly spherical as the wave from Rounkol No. 2, fig. 3, Plate 18; it makes a more acute angle with the edge of the cartridge to the left, indicating that the detonation wave is travelling faster than the atmospheric wave.

The approximately symmetrical projection of the wave with the 10·6 cm. cartridge is evident also in a slightly later stage, fig. 10, which shows the concentration of projected particles from the ends of the cartridge previously noted with Rounkol No. 2. Figs. 11 and 12 show the axial disturbance from the left-hand end of the cartridge after the wave has travelled 20 and 60 cm. respectively. Both records, and particularly fig. 12, show the persistent and directed motion impressed upon the particles from the end of the cartridge.

Prominences in Front of the Wave—Prominences in the front of the wave due to solid particles have been of two types in the records so far described. These have been distinguished in earlier papers as *open* and *cored* prominences and, as exemplified in the disturbance from a charge of explosive fired in a steel cannon, we have described and discussed them in detail (Payman and Woodhead 1934, pp. 12–21).

Briefly, *open* prominences are conical head waves due to isolated particles of inert or non-reacting matter. Travelling at a high speed, which is maintained relatively constant owing to their inertia, they overtake the wave and may travel well in front of it. The fragment of copper sent out from the closed end of a detonator (see Payman and others 1935) produces a prominence of this type. A number of these open prominences may be seen at the extreme right-hand side of fig. 7, Plate 19.

A *cored* prominence we believe to be due to a congregation of individual particles, which may or may not be in a state of active chemical or physical change, with which is associated gas under high pressure. The expansion of this entangled gas is subject to interference and delay due to the presence of the solid material, but it will suddenly become more rapid when it penetrates the shock wave and reaches the external atmosphere, the confining effect of the pressure wave then being no longer operative. Since the production or expansion of this gas must decrease and eventually cease, the speeds of the cored prominences must also decrease, and many of them will be overtaken by the main wave, though the larger individual particles will continue on their journey and will form open prominences.

Another type of secondary disturbance, a modification of a cored prominence, is seen in fig. 13, Plate 20. Here the main spherical wave, which is about 75 cm. from the end of the cartridge, is becoming smooth once more and the axial deformation, hitherto sharply pointed, has taken a spherical form. We term it a "blister prominence". Its formation, as also the development of open and cored prominences, is shown more clearly in records of the propagation of the lateral disturbance from a cartridge of Celmonite.

The Lateral Disturbance—In order to follow the lateral disturbance from cartridges of explosive, they were suspended at different distances above the Schlieren mirror (see, e.g., fig. 14, Plate 21) and these distances are indicated below each record. The value at the side of each figure on Plate 21 shows the distance of the front of the disturbance from the cartridge when the photograph was taken. In fig. 15 the wave front has travelled 12 cm. from the side of the cartridge; it is closely followed by the opaque gaseous products of detonation and is only just beginning to be penetrated by solid particles. In fig. 16, when the wave has travelled 50 cm., there is penetration of the wave by masses of particles as shown by many cored prominences. When the wave front has travelled 70 cm., fig. 17, the region immediately behind it appears mottled. This disrupted appearance of the shock wave and pressure wave is caused by particles, not necessarily more numerous than are shown in fig. 16, but more disseminated, so that there is partial transmission of the Schlieren light. Numerous open prominences due to isolated particles are now apparent in front of the wave.

The acute angle at the arrow-head of the cored prominences in fig. 16 shows that the particles are travelling at a speed much greater than that of the atmospheric wave they produce. In fig. 18, taken when the wave front has travelled 105 cm., the cored prominences have almost disappeared, but the record shows two examples of blister prominences. The spherical form of the blister prominence, in front of the main wave, is evidently due to the fact that it is travelling at approximately the same speed as that at which the associated particles are moving forward. Being no longer maintained, it is soon overtaken by the main wave with which it unites; the life of a blister prominence is therefore brief and for this reason its presence is rarely recorded. The existence of a large number of isolated particles, each giving rise to an open prominence, is shown by the network patterns in figs. 17 and 18.* When the record in fig. 19 was taken, the wave had travelled 135 cm. and all cored prominences had disappeared.

Fig. 20 is a diagram which has been constructed from many instantaneous photographs of the disturbance from Celmonite. It illustrates (A) the three phases in the development of the wave (1) almost spherical, in the short time during which the cartridge is detonating; (2) distorted, particularly

---

* Figs. 18 and 19 are marred by flaws on the mirror, showing as black dots with white edging.

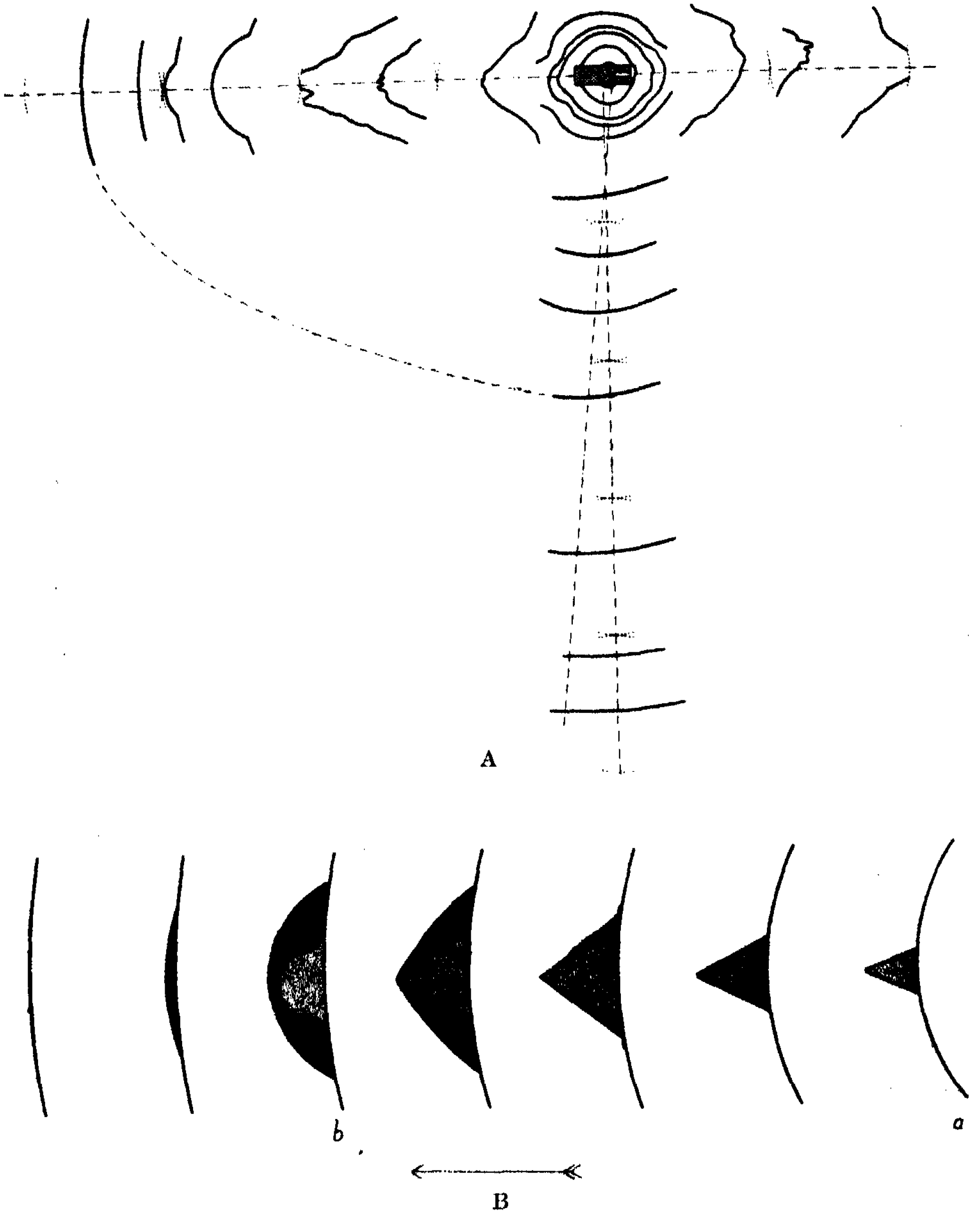

Fig. 20—The wave from 113 g. cartridge of Celmonite.

so along the axis, due to the emergence of congregations of solid particles; and (3) spherical, following the degradation of the end effects and the dissemination of the particles. On the diagram, at B, is also outlined the history of a typical cored prominence. The sharply pointed disturbance (at *a*), developed at high speed, dies down to the slow-moving "blister" (at *b*) shortly before being overtaken by the main wave. There is evidence from the photographs of a minor distension of the main wave, accompanied by a concentration of particles, in a direction inclined to the axis of the cartridge and away from the detonator end. Its direction is shown on the diagram by a straight broken line inclined at a few degrees to the vertical.

The "End Effect"—Conditions at the end of a cartridge exert a specific effect on the shape of the disturbance there. This is clearly shown when alterations are made in either the nature or the shape of the end. Thus the mere removal of the paper wrapper from the flat end of a cartridge has a marked effect, as will be seen from fig. 21, Plate 22, which shows a photograph taken under the same conditions as fig. 7*a*, Plate 19. The axial deformation of the main wave is more pronounced than when the end of the cartridge is covered by paper and a marked luminous effect is apparent. As will be seen later, the wave expands at a higher speed.

In view of the magnitude of the pressure attained during detonation, a paper wrapping would hardly be expected to have an appreciable confining effect, but the fact that it has is in accord with several other observations. The confining effect of the paper wrapping is illustrated by the records reproduced in figs. 23 and 24, Plate 22. The conditions of experiment are indicated in fig. 22; the paper covering one end of the cartridge was cut away and a sleeve of thin cellophane was slipped over it to form an extension tube 15 cm. long. The cartridge was suspended horizontally in such a position that the junction of the cartridge and the extension tube coincided with the right-hand boundary of the field of view. Figs. 23 and 24 were taken at different intervals after firing, and both show clearly an intense luminous effect within the tube but not outside it. The records of the wave and the luminous effect are not synchronized, but it is evident that the wave in fig. 23 has been photographed after the luminous effect has passed almost through the extension tube. The portion of the wave inclined at an angle to the tube can only have escaped after the tube had ruptured. The shape of the conical wave from the tube shows that the latter bursts progressively a short and constant interval of time after the wave inside has passed through it, and that the main spherical wave from the cartridge is expanding outwards at a much lower rate than that at which the axial wave is travelling through the tube. Hence the solid particles are largely concentrated within the extension tube.

The spherical expansion of the main wave and its puncture by the gases blown through the extension tube is shown in fig. 24. The fact that a smooth spherical wave is produced outside the tube shows that the gases are in advance of the particles when the latter begin to emerge. The confinement due to the tube should have little effect on the speed of solid particles but a pronounced effect on the speed of the gases, since for a time the latter are prevented from expanding spherically. In other words, the gas maintains its initial high speed for a longer period than it would have done had the extension tube not been present. Records obtained with the wave-speed camera show that the spherical wave from the extension tube is not overtaken by the main spherical wave, the gap between them still increasing at a distance of 1 m. from the cartridge, so that the effect of the extension tube is to divorce the axial from the lateral expansion.

Munroe (1888) has shown that the "end effect" is intensified considerably by making a conical indentation in the end of a cartridge. A cartridge of Rounkol No. 2 was prepared with such an indentation in one end and a Schlieren record of the resulting wave is shown in fig. 25, Plate 22. The end effect is notably greater than that from the flat-ended cartridge with the end-paper removed, fig. 21.*

"FLAME" PHOTOGRAPHS

On many instantaneous Schlieren records there is superimposed an impression of the fully expanded luminous effect, usually referred to as flame, from the explosive, its position and size as shown in a print bearing no time relation to the particular stage of development of the wave as revealed by the Schlieren record. This image of the luminous effect is unavoidable but its intensity (and hence the degree of its interference with the photographs already described) have been partially controlled by means of the "flame-stop" described in Part II. A number of direct photographs, with full-aperture lens, of suspended cartridges of Celmonite showing large and brightly luminous effects are reproduced on Plate 23. In order to examine the effect of alteration in length, cartridges of three different weights were used: a 57 g. (2 oz.) cartridge, 5·3 cm. long, fig. 26; a 113 g. (4 oz.) cartridge, 10·6 cm. long, fig. 27; and a 227 g. (8 oz.) cartridge, 21·2 cm. long, fig. 28; all 3·65 cm. ($1\frac{7}{16}$ in.) in diameter. A lens of short focal length was used, and the photographs are on approximately half the linear scale of the Schlieren records on the earlier Plates. The length of the cartridge and the position of the detonator are indicated below each photograph. Detonation started at the head of the detonator, and, since this was embedded in the explosive, the wave would always trave some 4 cm. to the right as well as over the greater length to the left-hand end of the cartridge.

---

* The Munroe effect is only operative close to the cartridge; the total explosive effect of the whole cartridge may indeed be reduced by an indentation made in one end of it. A remarkably small indentation in the surface of a gelatinous cartridge reproduces an identical impression on a steel plate with which the explosive is in contact when detonated. This is usually explained as being due to a local intensification of the explosive effect produced by a coalition of shock waves sent out from opposite sides of the indentations. The records obtained in the present work, however, suggest that a concentration of solid particles may play an important part in the production and prolongation of intense local effects.

With the 5·3 cm. cartridge the detonator was nearly as long as the charge, so that the point of initiation was nearer one end of the cartridge. As the diameter of the cartridge was not much less than its length, the detonation wave would nevertheless have only short and not widely differing distances to travel to the ends and sides of the cartridge. The projection of flame from this cartridge, fig. 26, is as a consequence roughly symmetrical about the vertical and horizontal axes, the flame streaks appearing to radiate from a zone near the centre of the cartridge.

The effect of lengthening the cartridge is shown by the record of the 10·6 cm. charge, fig. 27, in which the detonation wave has a longer distance to travel to the left than to the right. The direction of projection of luminous matter corresponds with the theoretical diagram in fig. 6. These features are still more apparent with the longest cartridge, 21·2 cm., fig. 28. Immediately around the detonator the striations toward the side are similar to those shown with the 5·3 cm. cartridge. The apparent concentration towards the left, both laterally and axially, is more pronounced than with the 10·6 cm. cartridge. Although the amount of explosive between the head of the detonator and the right-hand end of the cartridge is the same with all three, there is a more marked axial projection of flame to the right with the 21·2 cm. than with the shorter cartridges.

We believe that the large numbers of meteor-like traces or striations which constitute the "flame" are due to incandescent particles. It will be shown later by moving-film records that the luminous effect arises from a comparatively thin layer of matter moving outwards from the explosive. An instantaneous photograph of the luminous effect would appear at any given stage of its development as a bright distorted ring similar to the outline of a corresponding Schlieren photograph and bearing no apparent relationship to the photographs shown in figs. 26, 27 and 28. Though an instantaneous photograph is not obtainable, its shape at any given instant can be mapped out by the method used by Jones (1928, p. 613), who measured the speed of projection of the luminous effect at different angles to the axis of the cartridge and then plotted the contours of the front of the luminous effect at successive intervals of 10^{-6} sec. These contours, plotted in fig. 6 of his paper (*q.v.*), give the outline of the luminous effects, and their resemblance to the Schlieren records in the present paper is marked.

The striations on the direct flame photographs merely record the travel of luminous matter during the whole time of exposure of the photographic plate, the directions of the striations being those taken by solid matter sent out from the explosive. This luminous matter is not to be confused with the particles which break through the front of the shock wave, since in the several hundreds of instantaneous Schlieren photographs which we have taken of the expanding wave from explosives, either when freely suspended in air or when partially confined in a steel shot-hole (Payman and Woodhead 1934), we have found no correlation between the direct photographic records of the luminous matter and those of the prominences in the wave front. Since they are opaque, the particles causing these prominences may be the cause of the gaps between the striations of the flame photographs.

The identification of the striations with incandescent solid matter shows why their shape agrees with the theoretical diagram of projection in fig. 6 and why there is a greater projection of luminous matter from the ends of the cartridge, more pronounced the longer the cartridge. In explaining the production of these projected luminous particles it is important to remember that the chemical decomposition of the explosive during the detonation is far from complete. Taffanel and Dautriche (1912) estimated that when "safety" explosives are detonated unconfined only 40% of the total theoretical quantity of heat is evolved, whilst Audibert (1929) has produced evidence of the projection in similar circumstances of many particles of unchanged explosive.

WAVE-SPEED CAMERA PHOTOGRAPHS

Revolving-drum cameras have been used by other workers to obtain direct photographic measurements of the rate of detonation in solid explosives and of the speed of projection of luminous matter therefrom.

Only the movement in one direction, that at right angles to the direction of motion of the film, must be photographed or the record will be confused and complicated. Two methods have been used to ensure this. Laffitte (1924) enclosed the explosive in tubes of glass or cellophane, these tubes being longer than the explosive when it was desired to photograph the luminous projection. The measurements were thereby limited to movements along the axis of the explosive, but the tubes usually burst during or soon after the detonation, so that the whole process was not entirely confined within them. In order to overcome this objection, Jones (1928) suspended the cartridge of explosive to be photographed behind a strong steel shield provided with a narrow slit. By altering the inclination of the cartridge relative to the slit, it was possible to measure the speed of projection of luminous matter in any desired direction. The method suffered, however, from the objection that products of detonation which had become non-luminous became luminous again on impinging upon the steel plate. In the wave-speed camera a satisfactory result is obtained by using a diaphragm with a narrow slit immediately in front of the photographic film (Payman and Shepherd 1926). A similar method has been used successfully by Perrott and Gawthrop (1927).

Fig. 29, Plate 23, shows a typical direct photograph obtained by this method with a 227 g. cartridge of Rounkol No. 2. On reference to the explanatory diagram beneath the photograph, the detonation within the cartridge can be distinguished from the luminous projection to 20 cm. beyond its end. It is apparent that the projection travels for some distance after leaving the end of the cartridge at a rate higher than that of the detonation. This enhanced speed of projection of luminous matter was first observed by Comey (1909) and has also been noted by later workers.

A number of measurements have been made of the instantaneous rate of the luminous projection from the 113 g. cartridge of Rounkol No. 2 at the end distant from the detonator. Whereas the rate of detonation of the cartridge was 2090 m./sec., the instantaneous speed of the luminous projection was 3000 m./sec. when the cartridge was completely wrapped in paper as in fig. 29. When the paper was removed from the end of the cartridge the speed increased to 3550 m./sec., and with a conical depression in that end the speed was raised still further to 4800 m./sec.

It was thought probable that, if a conical depression in the end of the cartridge concentrated the stream of gases and of solid particles from the end and caused an increase in their speed, a conical extension would have the opposite effect, spreading the gases and the shower of particles and reducing the speed of projection of the luminous matter. This was found to be correct, the instantaneous speed being 3000 m./sec. with no paper covering the pointed end. These results are included in Table I.

The Speed of the Shock Wave from Rounkol No. 2—Fig. 30, Plate 23, shows a direct photograph of the detonation wave in the cartridge and of the projected luminous matter combined with a Schlieren record of the shock wave sent out axially from the end of the cartridge. This record was obtained with a 113 g. cartridge of Rounkol No. 2 with the end bare and a conical depression made in it. It will be seen that the luminous matter remains near the front of the wave so long as it is visible. In this photograph it is clear that, as has been suggested previously, the luminous matter at any one instant only occupies a thin layer and is not continuous outwards from the explosive. The *mean* axial speeds of the wave from this cartridge with different conditions of its end have been measured over the first 30 cm. distance of travel. The fully wrapped cartridge gave a mean speed of 2010 m./sec.; with the end paper removed the speed was 2250 m./sec.; and with a conical indentation it was 2740 m./sec. The effect of a conical pointed extension, illustrated in fig. 31, is very marked, the mean speed falling to 1590 m./sec. The mean speed in a direction at right angles to the cartridge from the position of the head of the detonator was found also to be 1590 m./sec. These results are also recorded in Table I.

TABLE I—SPEEDS IN METRES PER SECOND OF LUMINOUS MATTER AND SHOCK WAVE FROM A 113 G. (4 OZ.) CARTRIDGE OF ROUNKOL NO. 2

Character of end of cartridge	Instantaneous speed of flame	Speed of wave			Mean speed of wave
		0–10 cm.	10–20 cm.	20–30 cm.	0–30 cm.
With paper folds	3000	2470	2030	1660	2010
Paper removed	3550	2880	2290	1840	2250
Conical extension	3000	2370	1580	1270	1590
Conical depression	4800	3710	3090	2300	2740

The Speed of the Shock Wave from Celmonite—Celmonite was found to give rise to a disturbance generally similar to those from the low-density explosive, i.e. an approximately spherical wave with axial deformations. The expansion of the atmospheric wave from a 113 g. cartridge of Celmonite has however been followed up to a distance of 1·5 m.

Measurements of the speeds of the axial and lateral waves from a 113 g. cartridge of Celmonite, fully wrapped, are given in Table II. Each value is the mean of three determinations. The rates of the lateral wave measured from a point midway along the cartridge agreed very well in repeat experiments; thus the lateral speed recorded at 30–40 cm. as 1260 m./sec. is the mean of three records giving values of 1250, 1260 and 1270 m./sec. The front axial speeds were the least satisfactory, agreement being poor at distances between 30 and 80 cm. The reason for this is apparent from the instantaneous photographs which show that the speed of the wave front is greatly influenced by slight variations in the shape of the wave induced by the solid particles; for when a marked prominence develops in the plane of the photographic slit the recorded speed is considerably greater than if the prominence develops along an axis a few centimetres above or below this plane.

The speed of the products is also recorded in Table II up to 50–60 cm. from the cartridge, at which distance their speed has fallen to about 330 m./sec. and their front has become irregular and ill-defined.

TABLE II—VELOCITIES OF SHOCK WAVES AND PRODUCTS IN METRES PER SECOND FROM A 113 G. CARTRIDGE OF CELMONITE

Distance from cartridge (cm.)	Wave			Products		
	Axial			Axial		
	Front	Rear	Lateral	Front	Rear	Lateral
0– 10	3040	2760	1760	*	*	1820
10– 20	2710	2360	1760	2350	1950	1670
20– 30	2560	1690	1580	2290	1300	1440
30– 40	1670	1220	1260	1450	690	680
40– 50	1390	1040	990	590		330
50– 60	1230	870	840	340		
60– 70	1000	540	740			
70– 80	900	470	640			
80– 90	740	420	560			
90–100	438		505			
100–110	408		482			
110–120	396		458			
120–130	383		430			
130–140	378		427			
140–150	376		421			

* Cannot be distinguished from wave.

The mean value of the speed of the axial wave over the first 10 cm. length both from the front (from right to left in the photographic records) and from the rear (left to right) of the cartridge are of the order of the rate of detonation in the cartridge. As with the 11·3 g. cartridge of Rounkol No. 2, the instantaneous value at the front end, 3560 m./sec., was higher than the rate of detonation. The instantaneous speed was also found to depend on the length of the cartridge, being 4270 m./sec. from a 232 g.

cartridge. The lateral wave begins at a rate considerably less than that of detonation.

It will be seen that, although the axial waves start out at greater speeds than the lateral wave, the lateral wave has the highest speed after travelling about 90 cm. At the instant when the front axial wave has travelled 90 cm., the rear axial wave and the lateral wave have travelled only about 50–60 cm.; the lateral wave, however, reaches a point 1·5 m. from the charge in approximately the same time as the axial wave takes to travel a similar distance, that is the wave has become spherical. When the values for the speeds of the waves are plotted graphically, as in fig. 32, it is seen that the rate of fall in velocity increases suddenly when the wave is about 40 cm. from the cartridge; this is a position similar to that of the wave in fig. 16 on Plate 21. The sudden change thus corresponds with the beginning of the dispersion of the particles in the cored prominences. At this point also the gaseous products, as shown on the graph, begin abruptly to fall behind the wave at a rapid rate.

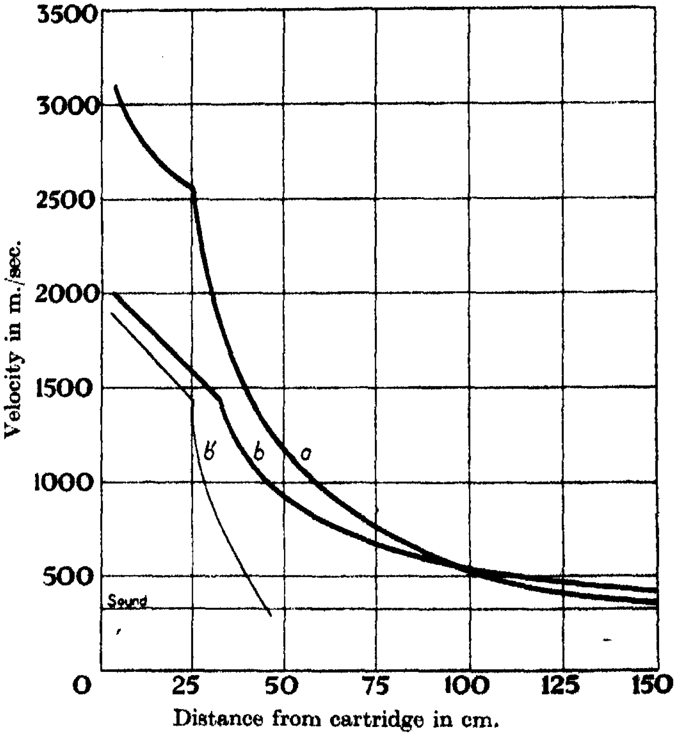

FIG. 32—Speeds of wave and products from 113 g. cartridge of Celmonite. *a*, axial wave; *b*, lateral wave; *b'*, front of lateral products.

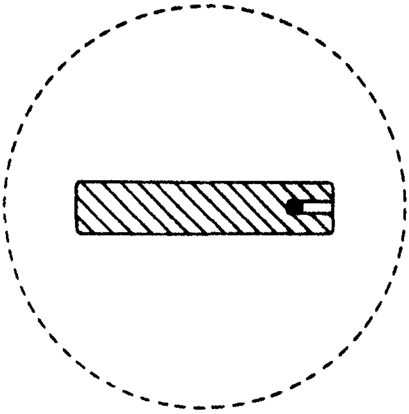

FIG. 1

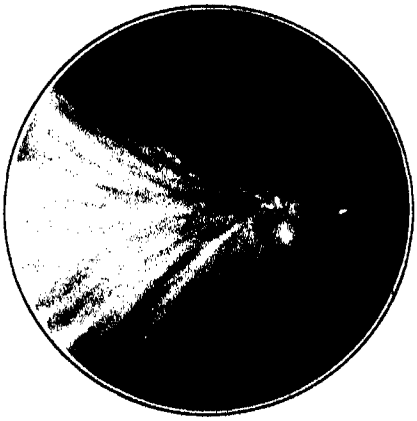

FIG. 2

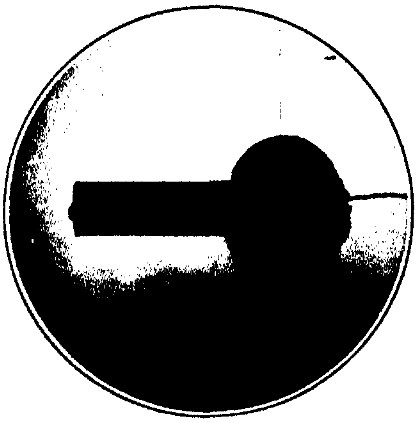

FIG. 3

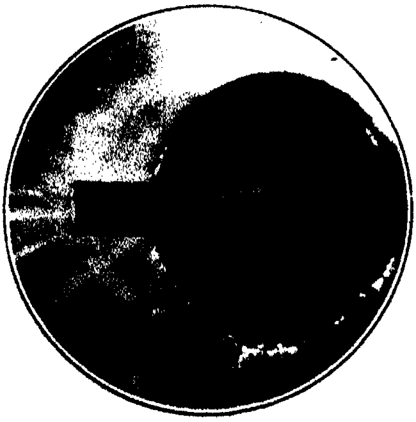

FIG. 4

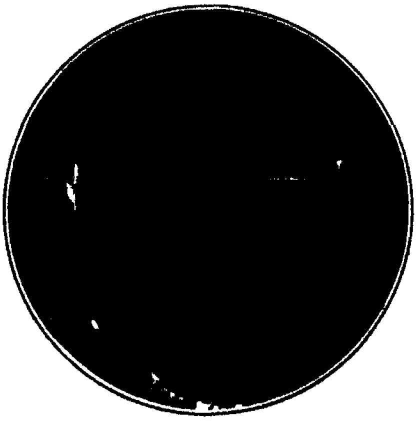

FIG. 5

Rounkol No. 2, 113 g. cartridge

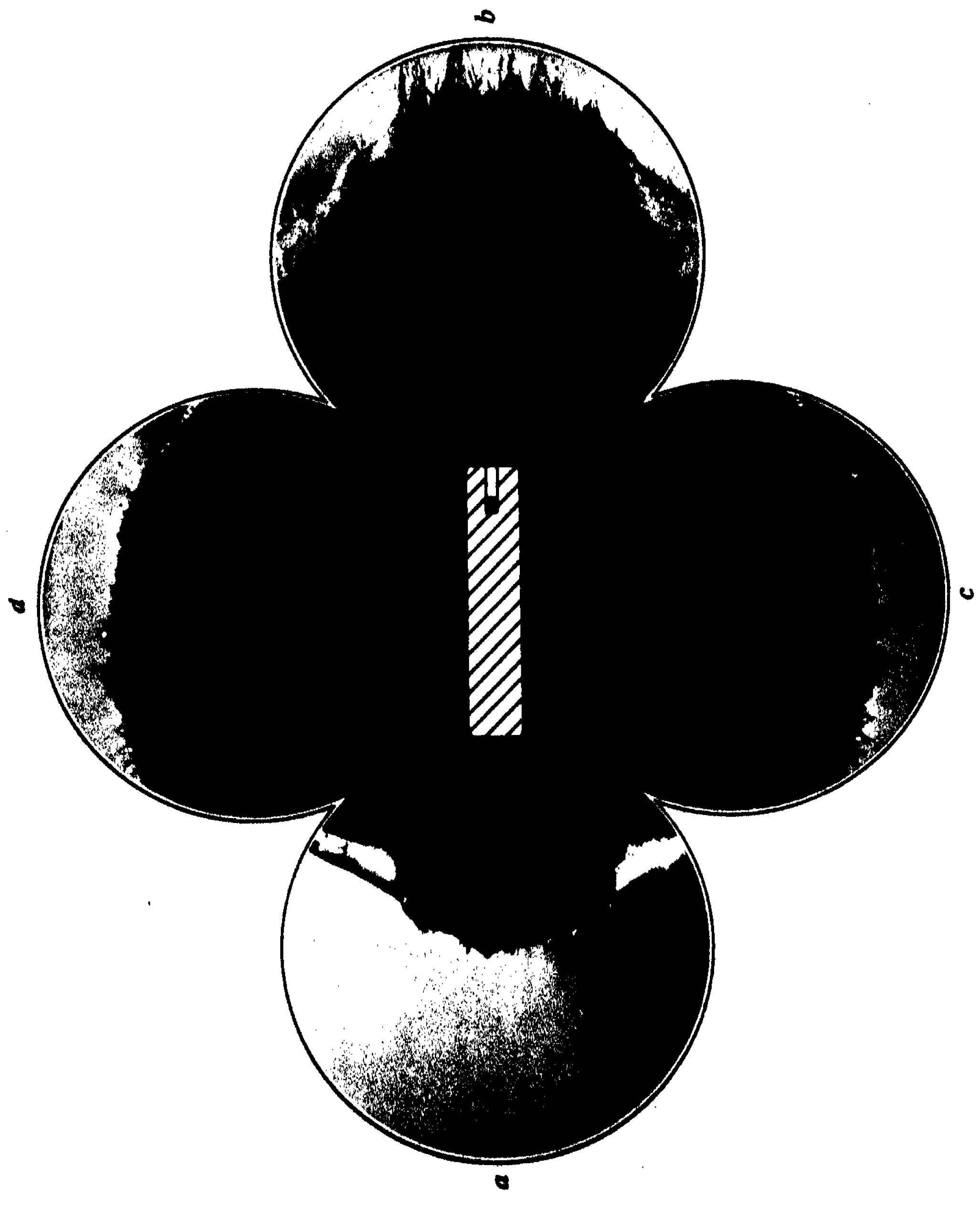

Fig. 7. Rounkol No. 2, 113 g. cartridge

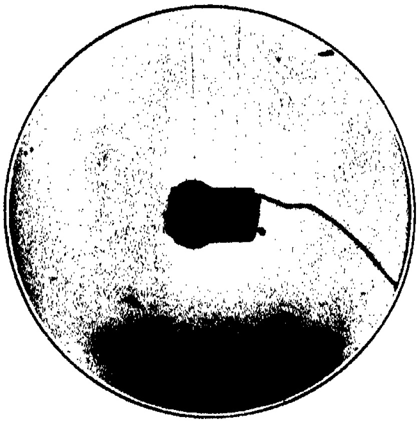

Fig. 8

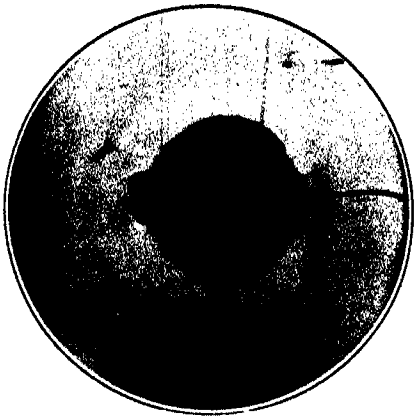

Fig. 9

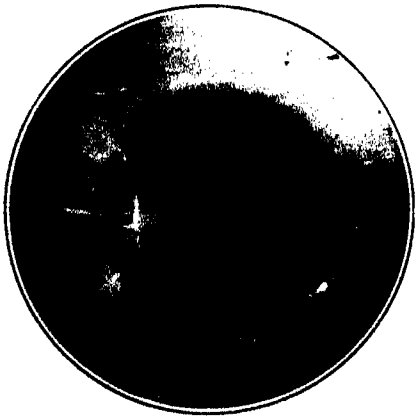

Fig. 10

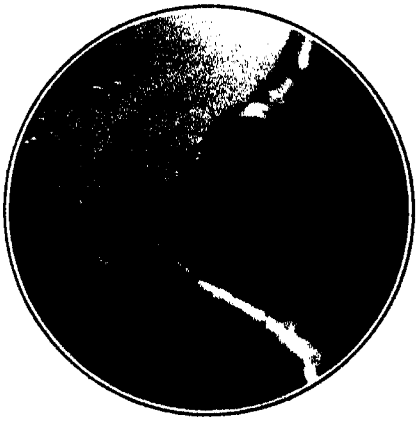

Fig. 11—0–30 cm.

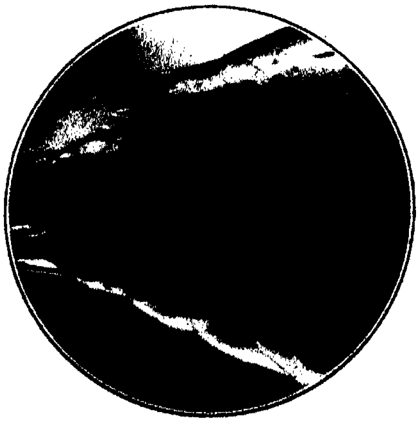

Fig. 12—30–60 cm.

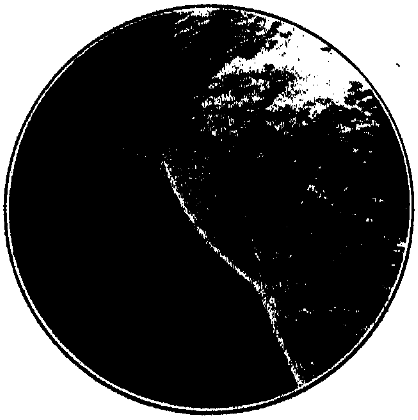

Fig. 13—60–90 cm.

Fig. 8—Celmonite, 5·3 cm. cartridge

Figs. 9–13—Celmonite, 10·6 cm. cartridge

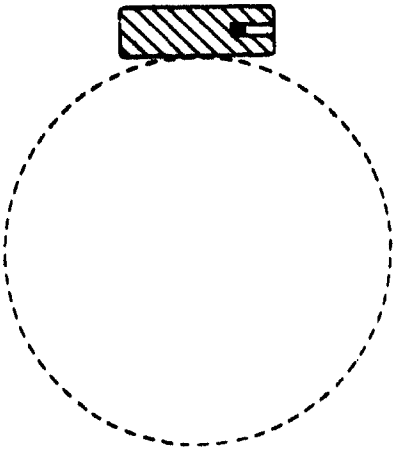

FIG. 14—0-30 cm.

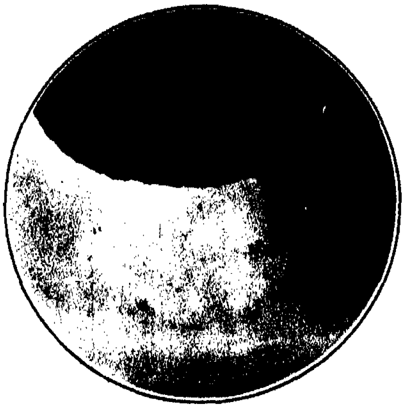

FIG. 15—0-30 cm.

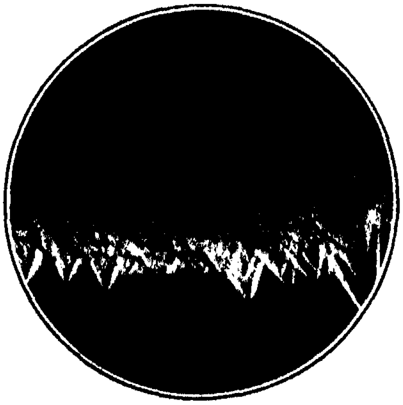

FIG. 16—30-60 cm.

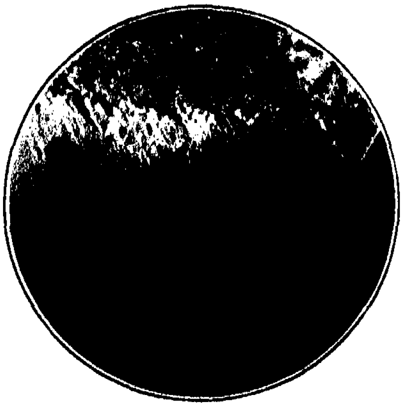

FIG. 17—60-90 cm.

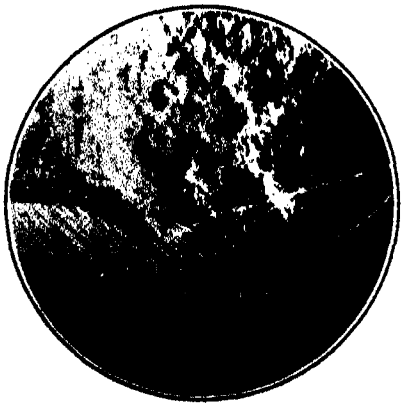

FIG. 18—90-120 cm.

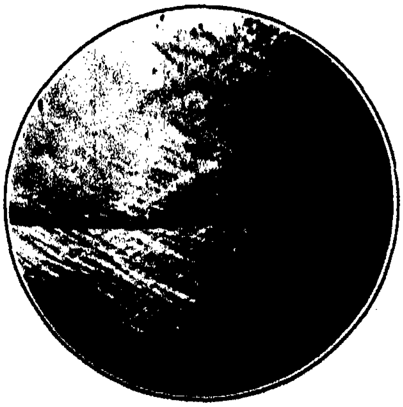

FIG. 19—120-150 cm.

Celmonite, 113 g. cartridge

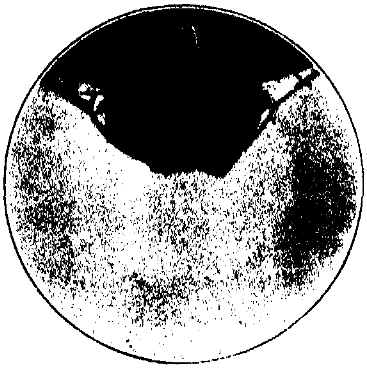
FIG. 21

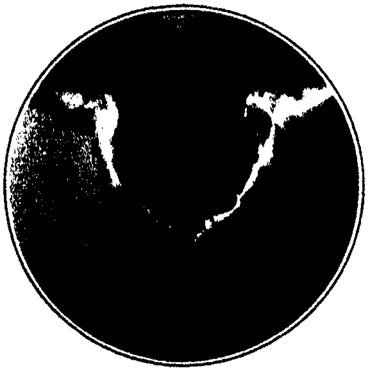
FIG. 25

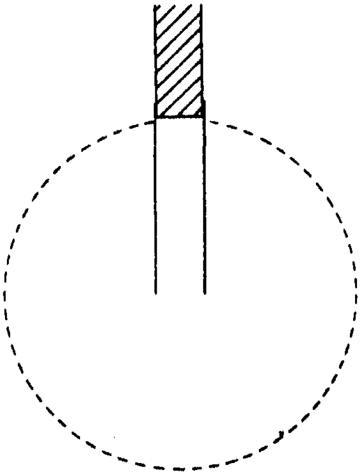
FIG. 22

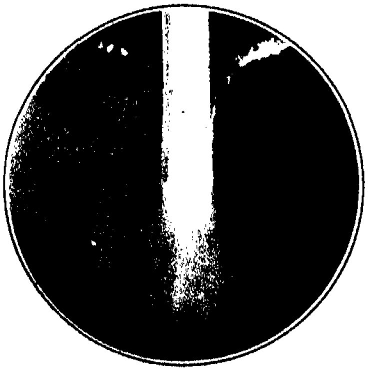
FIG. 23

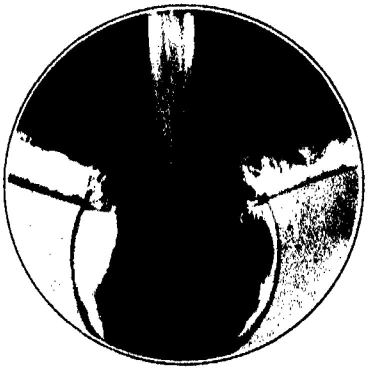
FIG. 24

Rounkol No. 2, 113 g. cartridge

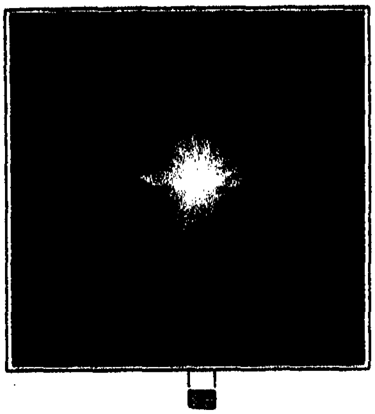

FIG. 26—57 g. Celmonite (5·3 cm.)

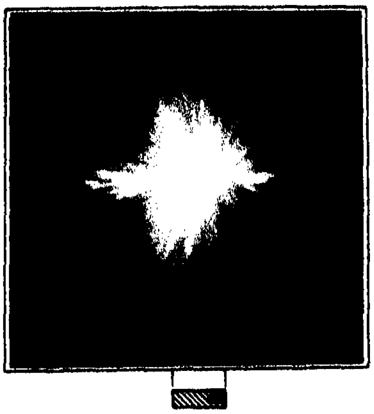

FIG. 27—113 g. Celmonite (10·6 cm.)

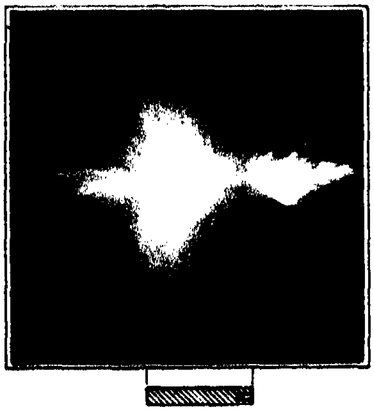

FIG. 28—227 g. Celmonite (21·2 cm.)

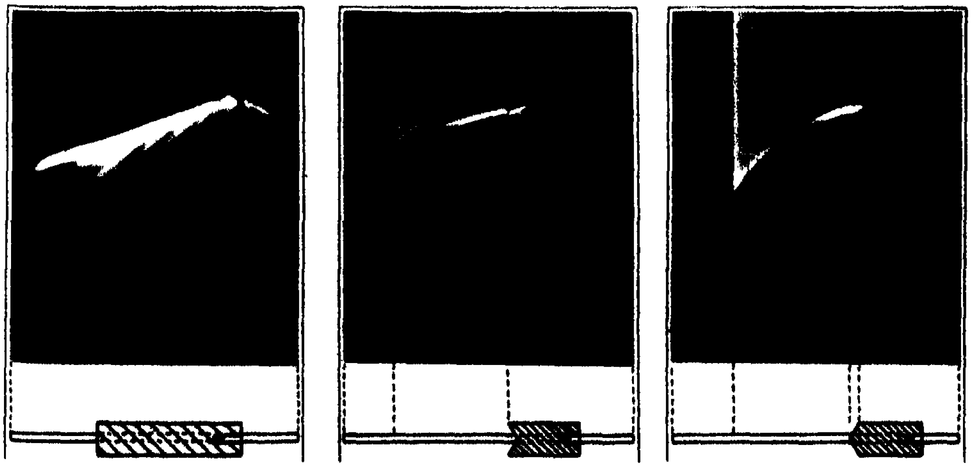

FIG. 29 FIG. 30 FIG. 31

Rounkol No. 2, 113 g. cartridge

The form of the curves in fig. 32 is characteristic of the expansion of the disturbance in all directions. Each curve consists of two distinct portions, the first either linear or logarithmic, and the second logarithmic, contact being made at a more or less sharply defined point about 40 cm. from the cartridge. The disappearance of deformations of the wave form is shown by the crossing of the curves for the axial and the lateral expansions.

SUMMARY

The mode of expansion of the disturbance produced when a cartridge of explosive suspended freely is detonated has been studied by means of Schlieren photography, using cameras of both instantaneous and continuous types. The records show that there are three phases in the life of the disturbance produced.

The first phase is the detonation of the cartridge. This is comparatively short (about 3×10^{-5} sec. in a 113 g. cartridge of Celmonite). The disturbance then may be regarded as arising solely from the side of the cartridge and is very nearly spherical; the shock wave is smooth and precedes the front of the gaseous products by a fraction of a centimetre.

The second phase is longer and may last until the disturbance has travelled 100–125 cm. (6×10^{-4} sec. with a 113 g. cartridge of Celmonite). During the first half of this period the gaseous products are for the most part luminous and follow the shock wave at a gradually increasing distance. The velocities of both wave and products may be greater than the rate of detonation of the cartridge. Many characteristic prominences due to individual solid particles and congregations of particles appear in the wave front. The gaseous expansion from each end of the cartridge is far more vigorous than that from the side, with the result that axial distensions in the form of the wave appear. These deformations from the spherical are accentuated and prolonged by the shower of particles, the density of the shower being clearly greatest axially with the cartridge. In the second half of this period the disturbance is no longer "maintained". The velocity of the gaseous products falls rapidly and the products become mixed with air through turbulence to an increasing extent. Simultaneously, the masses of particles producing the prominences in the wave front become dispersed and, as individual particles, no longer affect materially the progress of the wave.

The third and last phase begins when all prominences have disappeared; the wave becomes smooth again and, when travelling at about 500 m./sec., rapidly assumes the spherical form. The gaseous products are at atmo-

spheric pressure and free to drift. Dispersed particles precede the wave over several metres and sooner or later fall to the ground. The wave spreads with a gradually falling velocity until it ultimately degenerates into a sound wave.

REFERENCES

Audibert, E. 1929 *Ann. Min., Paris*, **15**, 213–87.
Beyling, C. and Schultze-Rhonhof, H. 1933 *Ber. VersGrubenges.* No. 4.
Comey, A. M. 1909 *Seventh Int. Cong. Appl. Chem.* **3b**, 28–37.
Jones, E. 1928 *Proc. Roy. Soc.* A, **120**, 603–20.
Laffitte, P. 1924 *C.R. Acad. Sci., Paris*, **178**, 1277–9.
Munroe, C. E. 1888 *Amer. J. Sci.* **36**, 48–50.
Payman, W. 1928 *Trans. Instn Min. Engrs, Lond.*, **75**, 191–213.
Payman, W. and Robinson, H. 1926 *Pap. Safety Min. Res. Bd, Lond.*, No. 18.
Payman, W. and Shepherd, W. C. F. 1926 *Pap. Safety Min. Res. Bd, Lond.*, No. 29.
Payman, W., Titman, H. and Woodhead, D. W. 1935 *Proc. Roy. Soc.* A, **148**, 604–22.
Payman, W. and Woodhead, D. W. 1931 *Proc. Roy. Soc.* A, **132**, 200–13.
— — 1934 *Pap. Safety Min. Res. Bd, Lond.*, No. 88.
Perrott, G. St. J. and Gawthrop, D. B. 1927 *J. Franklin Inst.* **203**, 103–10.
Taffanel, J. and Dautriche, H. 1912 *Eighth Int. Cong. Appl. Chem.* **4**, 127–45.

The Continuous Absorption Spectrum of Methyl Bromide and its Quantal Interpretation

By Phyllis Fink and C. F. Goodeve

The Sir William Ramsay Laboratories of Inorganic and Physical Chemistry, University College, London

(*Communicated by F. G. Donnan, F.R.S.—Received* 26 *July* 1937)

Of organic compounds exhibiting continuous absorption, methyl bromide is one of the simplest and its spectrum is one most easily analysed quantum mechanically. This communication describes measurements of the extinction coefficients of methyl bromide over a wide range and a calculation from them of the position of the upper potential energy curve. As the absorption band is continuous, this upper potential energy curve is of the repulsive type.

Most of the previous work on methyl bromide deals with the band system in the Schumann region. Herzberg and Scheibe (1930), however, investigated the continuous absorption from 42,000 to 60,000 cm.$^{-1}$ and found a maximum at 50,300 cm.$^{-1}$. Henrici (1932) found a maximum at 51,400 cm.$^{-1}$ and estimated the absorption limit to be at 41,400 cm.$^{-1}$. Hukumoto (1932) also estimated the absorption limit and hence calculated the heat of dissociation, but it is now known that no well-defined absorption limit exists. All the previous workers concluded that methyl bromide dissociates into a methyl radical and a bromine atom, one or both of the products being excited. As will be shown in § 13 below, there is no justification for such a conclusion.

EXPERIMENTAL

The molar extinction coefficient, ϵ, and the absolute extinction coefficient, α, are defined by

$$\epsilon = \log_{10}\frac{I_0}{I_t}\cdot\frac{1}{lc} \tag{1}$$

and

$$\alpha = \log_e\frac{I_0}{I_t}\cdot\frac{1}{ln}, \tag{1a}$$

where I_0 and I_t are the intensities of the incident and transmitted light respectively, l the length of the absorbing column in cm., c the number of g.mol. per litre and n the number of molecules per c.c.

To obtain as wide a range of extinction coefficients as possible, various optical systems were used, as follows:

	Light source	Absorbing column cm.	Range of frequencies cm.$^{-1}$	Methods of photometry	Spectrograph
I	Hydrogen discharge tube	1	53,000 to 41,500	Single cell, rotating sector	Hilger small quartz E. 370
II	Iron tungsten spark	8 and 55	41,500 to 37,000	Spekker divided beam photometer	Hilger E. 3
III	Hydrogen discharge tube	3355	37,000 to 34,500	Single cell, different exposures	Hilger quartz Raman E. 420

All the measurements were made photographically—the intensity of the transmitted light was compared with that of light of the same initial intensity, reduced a known amount by means of a standard device. In the first system, comparison spectra through the empty tube were taken immediately before and after the absorption spectrum of methyl bromide. The "match points", i.e. points of equal blackening on the photographic plate, were determined visually in the systems I and II. In the third system, a series of spectra was taken, with varying exposure times, and compared by means of a Zeiss recording microphotometer. Most of the measurements were made at 20°. With the 3355 cm. tube, the temperature was within the range 17–23°.

The methyl bromide used was obtained from The British Drug Houses, Ltd. It was dried and fractionated before the experiment, only the middle portion being used for the actual measurements. To check the purity of the product, the spectrum of various fractions of the middle portion were examined, but no variation in the extinction coefficient was found.

For certain measurements methyl bromide was prepared from pure methyl alcohol and A.R. potassium bromide in the presence of concentrated sulphuric acid (Bygdén 1910). The gas was washed in water and in A.R. sulphuric acid and further dried over pure calcium chloride. The extinction coefficients obtained with this sample were in good agreement with those obtained with the B.D.H. product. A further test of the purity was made by filling the long tube with the gas. No bands or irregularities were obtained in the spectra, thus excluding the possibility of absorbing substances such as sulphur dioxide being present.

RESULTS

In fig. 1 the extinction coefficients are shown plotted (as logarithms) against the frequencies in wave numbers. The low-frequency side of the curve is almost linear and is steep. The curve rises to a maximum, then falls off, this upper portion being approximately symmetrical. The maximum values of the extinction coefficients are, $\epsilon = 182$, and $\alpha = 6{\cdot}75 \times 10^{-19}$ cm.^{2}, and the maximum lies at 49,000 cm.$^{-1}$. The slope of the log curve increases as the frequency decreases, rising to a value of $6{\cdot}4 \times 10^{-4}$ cm. at 35,000 cm.$^{-1}$.

THEORETICAL

1—*Brief Outline*—The absolute extinction coefficient, which is the probability of absorption of a quantum of radiation by a molecule, is determined largely by the overlapping of the eigenfunctions of the initial and final states of the molecule. These in turn are largely determined by the potential energy-distance curves of the vibratory degree of freedom most closely concerned with the absorbing dipole. From known potential energy curves it is comparatively simple to calculate the extinction coefficients for different frequencies, but *direct* calculation in the reverse direction is impossible in practice. The method used here is one of successive approximations. A calculation of the upper potential energy curve by an approximation used by Goodeve and Taylor (1935) is first made. The resultant curve is sufficiently accurate to permit the calculation of the eigenfunction for any energy level of the upper state, which, when combined with the eigenfunction for a level of the ground state, leads to the probability of transitions between the two

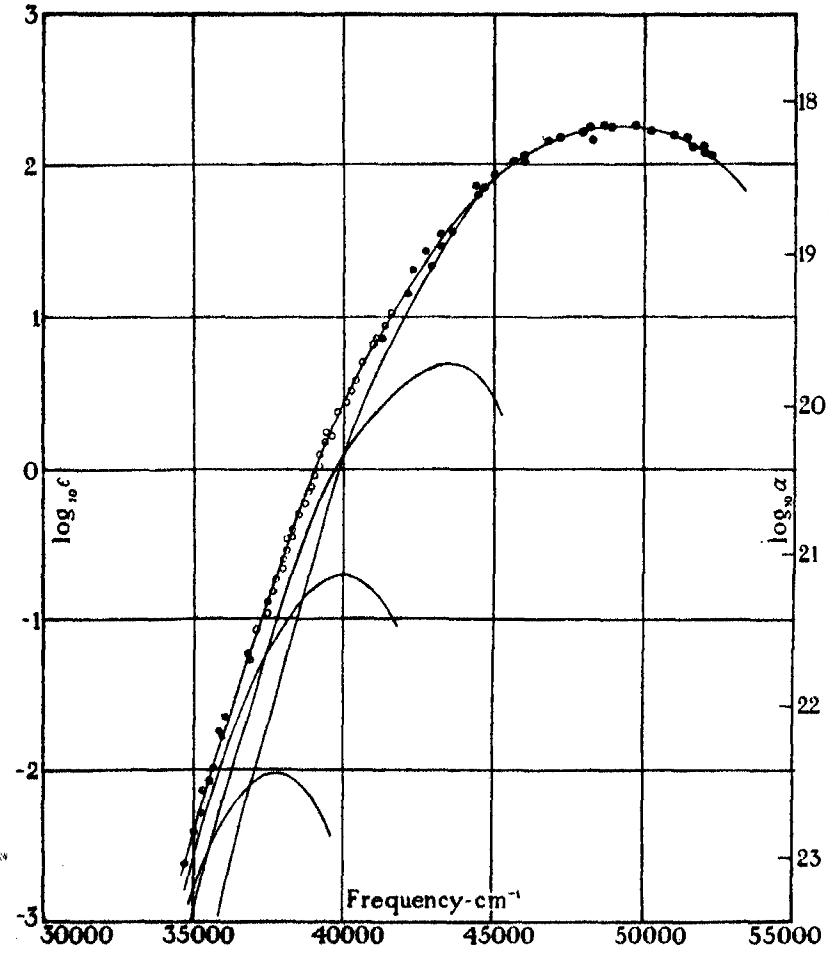

Fig. 1

levels. By considering all levels an extinction coefficient-distance curve is constructed which, when compared with the observed curve, leads to a more correct upper potential energy curve. The procedure is described in detail below.

2—*The Extinction Coefficient*—The relation between the extinction coefficient and the eigenfunctions is as follows (Dirac 1935; see also Gibson, Rice and Bayliss 1933):

$$\alpha = K\nu\left[\int \psi' M \psi''\right]^2, \tag{2}$$

where ν is the frequency, ψ' and ψ'' the eigenfunctions of the upper and lower states, M the dipole moment and K a constant. In most cases the variation in the nuclear eigenfunctions is the determining factor in the value of the above integral as the nuclei are comparatively heavy particles. All of the other terms may, therefore, be assumed constant by comparison and one may write

$$\alpha = K_1\nu\left[\int^{\infty} \psi'_N \psi''_N \, dr\right]^2. \tag{3}$$

This equation forms the basis of the method of analysis used in the present paper. In order to determine ψ'_N, however, resort must be made to a former approximation method.

3—*The Approximate Method of Analysis*—By a further series of approximations, valid for a case in which the slope of the upper potential energy curve is high compared with that of the lower curve, Goodeve and Taylor (1935) simplified equation (3) to the form

$$\alpha = K_2 \psi''^{\,2}_{N,0}. \tag{4}$$

Its application is limited to transitions involving internuclear distances not far from the equilibrium separation, r''_e, and arising from molecules in the zero-point energy level of the ground state.

Equation (4) can be solved by substituting the value of the nuclear eigenfunction, $\psi''_{N,0}$, given by equation (12), § 6, giving

$$\alpha = K_3 e^{-2\beta x^2}, \tag{5}$$

where $x = r - r''_e$, $\beta = \dfrac{2\pi^2\mu\omega}{h}$, μ = reduced mass, and ω = the fundamental frequency of the ground state. From equation (5),

$$\log_e \alpha = \log_e K_3 - 2\beta x^2.$$

$\log_e \alpha$ has a maximum value when $x = 0$ (i.e. $r = r''_e$). Therefore

$$\log_{10}\alpha_{\max} - \log_{10}\alpha = \frac{2\beta x^2}{2{\cdot}3}. \tag{6}$$

By correlating this equation with the observed extinction coefficient-frequency curve, the upper potential energy-distance curve can be determined. The potential energy is expressed here in terms of the frequency interval from the zero-point energy level of the ground state, *plus* the zero-point energy.

In applying this method to methyl bromide it may be treated as a diatomic molecule vibrating along the C—Br link, as vibrations involving movement of the hydrogen atom with respect to the carbon are relatively inactive. The reduced mass is, therefore, $2\cdot08 \times 10^{-23}$ g. The fundamental frequency for this link in the gas, obtained from infra-red data (Barker and Plyler 1935), is 610 cm.$^{-1}$. With these values used in equation (6) the upper potential energy curve was drawn and found to be a straight line with a slope of $-6\cdot25 \times 10^4$ wave-numbers/A, or $-12\cdot4 \times 10^{-4}$ erg/cm. This line is shown by the curve I, in fig. 2.

A more accurate curve is obtained by reintroducing the frequency in equation (4), whereby it becomes

$$\alpha = \nu K_4 \psi''^{2}_{N,0}. \qquad (4a)$$

This gives a slope of $-6\cdot67 \times 10^4$ wave-numbers/A. It has been found, however, that the former value, $-6\cdot25 \times 10^4$ wave-numbers/A, is close to the mean slope of the whole potential energy curve as finally obtained. One calculation of the eigenfunction using this slope is, therefore, sufficient for the whole analysis.

4—*Bayliss's Empirical Rule*—Bayliss (1937) has recently criticized the validity of the assumptions made in deriving equation (4). At the same time he puts forward an empirical rule according to which the reflexion of the $\psi''^{2}_{N,0}$ distance curve from the upper potential energy curve on to a frequency scale gives the variation of extinction coefficient with frequency. This rule is identical with the method used by Goodeve and Taylor as outlined in § 3. Although their method involves assumptions that are difficult to assess, the results obtained by its use are in close agreement, in the region not too far from the maximum, with those obtained by the more accurate method described below (see fig. 2).

5—*The Nuclear Eigenfunctions of the Upper* (*Repulsive*) *State*—From the slope of the upper potential energy curve in the neighbourhood of r''_e the corresponding eigenfunction can be calculated. An accurate solution of the Schrödinger equation

$$\frac{d^2\psi}{dx^2} + \frac{8\pi^2\mu}{h^2} k' x \psi = 0, \qquad (7)$$

where k' is the slope of the upper potential energy curve (assumed linear),

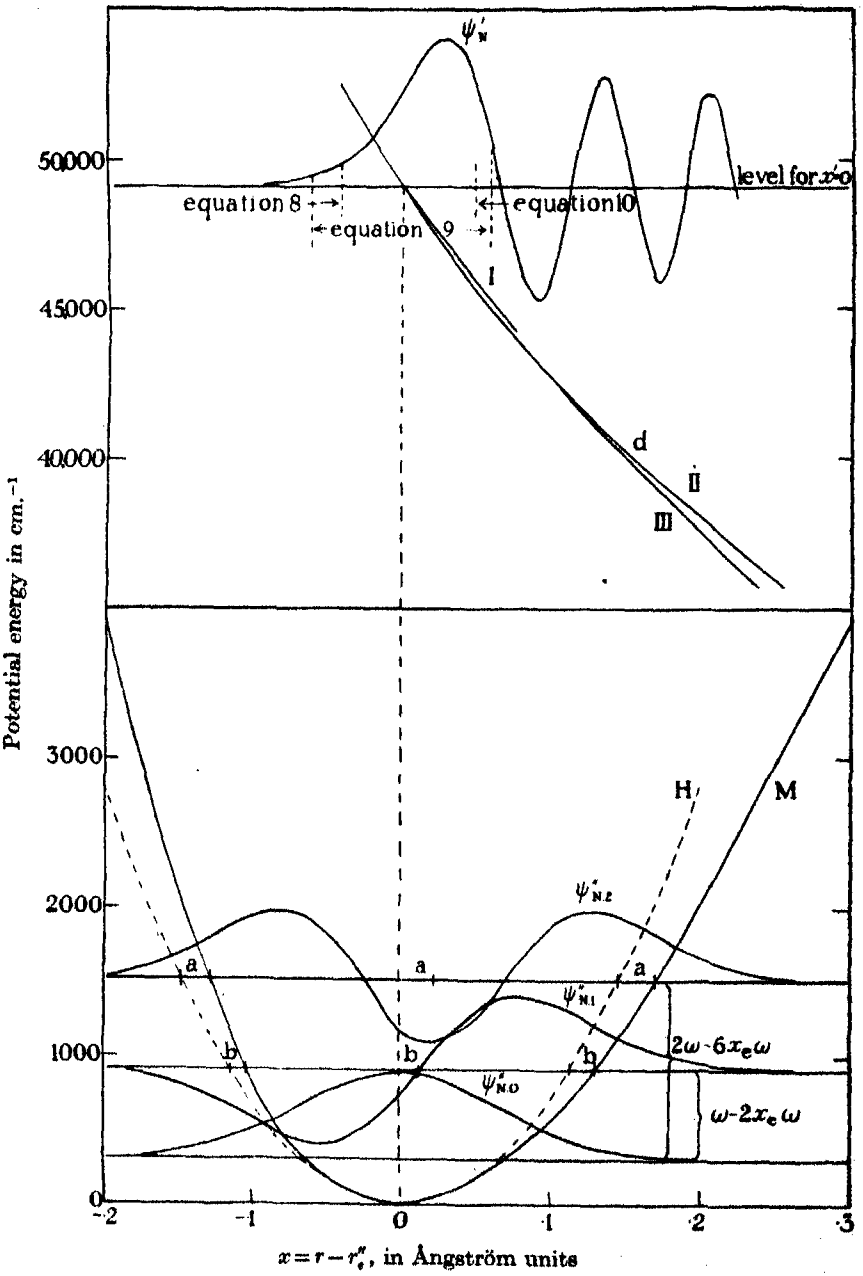
ψ'_N
level for x=0
equation 8
equation 9
equation 10
I
d
II
III
50000
45000
40000
3000
2000
1000
0
Potential energy in cm.^-1
H
M
ψ''_N.2
ψ''_N.1
ψ''_N.0
a
b
2ω-6x_eω
ω-2x_eω
-·2
-·1
0
·1
·2
·3
x = r − r''_e, in Ångström units

FIG. 2

may be obtained in terms of Bessel functions* of order $\pm\frac{1}{3}$. However, equation (7) is simply that encountered in the Wenzel-Kramers-Brillouin (Zwaan 1929) approximation method, the solutions of which are

$$\psi'_N = \frac{1}{2}\frac{1}{(-2\mu k'x)^{\frac{1}{4}}}\exp\left\{-\sqrt{\left(\frac{-8\pi^2\mu k'}{h^2}\right)}\cdot\frac{2}{3}|x|^{\frac{3}{2}}\right\} \tag{8}$$

(for x negative and not near zero),

$$\rightarrow\left(\frac{\pi}{-\mu hk'}\right)^{\frac{1}{6}}\omega\left[\left(\frac{-8\pi^2\mu k'}{h^2}\right)^{\frac{1}{3}}x\right] \tag{9}$$

(for x near zero positive or negative),

$$\rightarrow\frac{1}{(-2\mu k'x)^{\frac{1}{4}}}\cos\left[\sqrt{\left(\frac{-8\pi^2\mu k'}{h^2}\right)}\cdot\frac{2}{3}x^{\frac{3}{2}}-\frac{\pi}{4}\right] \tag{10}$$

(for x positive and not near zero).

The values of ω are tabulated by Kramers (1926) $\left(\frac{-8\pi^2\mu k'}{h^2} = \text{his symbol } \xi\right)$. The first and third of these are asymptotic solutions and, therefore, do not fit exactly on to the second. Regions exist in which the discrepancies are negligible, and a smooth change-over from one equation to the next may be obtained.

The values of this eigenfunction for a repulsive curve of CH_3Br of slope $-6{\cdot}25\times10^4$ wave-numbers/A have been calculated in arbitrary units from the three equations (8)–(10) for their respective regions and are plotted as one curve in fig. 2. The range for which each equation is used is indicated.

While the slope, k', of the upper potential energy curve may vary, only a small effect on the shape and magnitude of the eigenfunction curve is to be expected from the fact that the slope appears only in small powers in equations (8) and (9) and the range involving equation (10) becomes rapidly unimportant. This has been verified by tests using possible extreme values of k'.

6—*The Nuclear Eigenfunctions of the Ground (Molecular) State*—The values of these can be calculated from well-known equations (Pauling and Wilson 1935). For the nth vibrational level of a harmonic oscillator

$$\psi''_{N,n}(x) = N_n \cdot e^{-\frac{\xi^2}{2}} \cdot H_n(\xi), \tag{11}$$

---

* The solution given by Condon and Morse (1929) has a value of $\psi = 0$ for $x = 0$. This is obviously incorrect, as it requires that there be a point of inflexion where neither ψ nor x equals zero, contrary to equation (7).

where $\xi = \sqrt{(2\beta x)}$. The value of N_n which will normalize $\psi''_{N,n}(x)$ is

$$N_n = \left\{\left(\frac{2\beta}{\pi}\right)^{\frac{1}{2}} \frac{1}{2^n n!}\right\}^{\frac{1}{2}}.$$

$H_n(\xi)$, the Hermite polynomial of order "n", is given by

$$H_n(\xi) = (-1)^n e^{\xi^2} \frac{d^n e^{-\xi^2}}{d\xi^n}.$$

This gives the values of the eigenfunction of the first few vibrational levels as

$$\psi''_{N,0} = \left(\frac{2\beta}{\pi}\right)^{\frac{1}{4}} . e^{-\beta x^2}, \tag{12}$$

$$\psi''_{N,1} = \left[\left(\frac{2\beta}{\pi}\right)^{\frac{1}{2}} . \frac{1}{2}\right]^{\frac{1}{2}} e^{-\beta x^2} . 2\sqrt{(2\beta x)}, \tag{13}$$

$$\psi''_{N,2} = \left[\left(\frac{2\beta}{\pi}\right)^{\frac{1}{2}} . \frac{1}{8}\right]^{\frac{1}{2}} e^{-\beta x^2} . (8\beta x^2 - 2). \tag{14}$$

The values of the eigenfunctions for these levels for CH_3Br have been calculated, using the constants given in § 3. They have been plotted in fig. 2 with a correction for anharmonicity described in § 9.

7—*The Probability of Transitions arising from the Zero-Point Level*—As the upper state of methyl bromide is of the repulsive type, there are an infinite number of levels to which transitions can take place. Any particular level cuts the upper potential energy curve at a definite inter-nuclear distance x' from the equilibrium separation in the ground state. The level for $x' = 0$ is shown in fig. 2, together with its eigenfunction curve. For any other energy level the eigenfunction curve is the same (see § 5), except that its origin must be shifted to the value of x' corresponding to the level, i.e. in equations (8)–(10) x is replaced by $(x - x')$.

The probability, α_0, of transitions from the zero level of the ground state, is proportional to $\nu\left[\int_0^\infty \psi'_N \psi''_{N,0} dx\right]^2$ (equation (3)). The value of the integral is markedly dependent on the relative positions of the origins of the two eigenfunction curves ψ'_N and $\psi''_{N,0}$ and has a maximum for the transition to the level where $x' \approx 0$. For any other transition, involving the absorption of light of lower frequency than that corresponding to the maximum extinction, x' is positive.

The values of the integral have been determined by a numerical summation method for successive values of x' differing by 0·01 A. This interval was found to be small enough to avoid the introduction of appreciable errors. The logarithms of the squares of these integrals when plotted against x' have a form similar to the log α-frequency curve, particularly near the maximum. In order to determine the values of the frequencies to be used in equation (3) an approximate correlation of the two curves is made.* This is sufficiently accurate as the variation in the frequency is small compared with the variations in the value of the integral. We finally obtain a curve of $\log \alpha_0$ against x', except for the constant of proportionality, $\log K_1$.

For substances with a high value of the fundamental frequency, ω, most of the molecules are in the zero level and, therefore, transitions from this level only need be considered. For molecules such as CH_3Br at room temperature ($\omega = 610$ cm.$^{-1}$), these transitions are responsible for the extinction curve over a range from $\alpha_{\max}$ to $\frac{1}{10}\alpha_{\max}$. From the vibration partition fraction, f_0 (see equation (16)), 95 % of the molecules are in the zero level, and as the observed molecular extinction coefficient is equal to $f_0\alpha_0$, the value of $\log K_1$ is obtained by equating the maximum value of $\log f_0\alpha_0$ to $\log \alpha_{\max}$. A final correlation gives the upper potential energy curve for small values of x'. The slope of this curve has been found to be the same as that obtained by means of equation (4a).

8—*The Existence of Double Bands*—A continuous absorption band may involve transitions to more than one upper potential energy curve. The analytical method is very sensitive, and double bands produce points of inflexion in the derived upper potential energy curve when treated as single bands. These are particularly marked if the two upper curves are separated by more than 500 cm.$^{-1}$. If the probabilities of transitions to them are equal, the point of inflexion occurs at $x' = 0$; but if unequal, as recently found by Porret and Goodeve for methyl iodide, the point of inflexion occurs at values of x' away from the origin. As no such point of inflexion was found for methyl bromide, it is concluded that its band is single. If other bands exist, they are completely masked by the main band.

9—*Correction for Anharmonicity in the Ground State*—Treatment of the molecule as a harmonic oscillator is a good approximation when dealing with the zero-point energy level, but corrections should be applied for the higher levels. Equations for anharmonic oscillators have been derived (Schrödinger 1926), but as they are very complicated and the anharmonicity for methyl bromide has not been measured, a simple approximate method has been used. An approximate anharmonic constant, $x_e\omega$, is first determined by use of the relation (Jevons 1932)

---

* The analysis can be simplified by using the extinction coefficient divided by the frequency in place of α in the comparisons which follow.

$$D'' = \frac{\omega^2}{4x_e\omega}, \tag{15}$$

where D'' is the heat of dissociation. From the heat of the C—H link (Penney 1935) and the necessary heats of combustion (Landolt and Börnstein Tables, 5th ed.) the value of D'' is equal to 72 ± 10 kg. cal., and the quantity $x_e\omega$ is found to be 3·6 cm.$^{-1}$. (The value calculated in this way is generally lower than the one obtained from the infra-red or Raman data.) It is now possible to plot the lower potential energy curve by use of the Morse equation (1929). This is shown by curve M in fig. 2 in comparison with curve H for a harmonic oscillator of the same frequency. It is seen that for the region considered the anharmonicity produces approximately equal shifts of both sides of the potential energy curve. Since the shapes of the eigenfunction curves are not markedly affected, one can, as an approximation, shift their positions by amounts corresponding to the shifts of the potential energy curve. These are indicated by a's and b's in the figure. This method gives only a partial correction for the anharmonicity and the improvement in the calculation by its use is indicated in § 12.

10—*The Probability of Transitions arising from the First and Higher Vibrational Levels*—In an identical manner to that described in § 7, the probability of a transition to the upper state for a molecule in the first or a higher level has been calculated from equation (3). The value of K_1 is the same for all transitions between the two electronic states so far as the assumptions in equation (3) are valid. In this way values for α_1, α_2 and α_3 have been obtained for a series of values of x'.

The separate contributions of α_0, α_1, etc. to the total extinction depend upon the vibration partition fraction for each of the levels, i.e. upon the fraction of the total number of molecules in each level. The value of this fraction for the nth level is given by

$$f''_n = \frac{e^{-\frac{E_n''}{kT}}}{\sum\limits_n e^{-\frac{E_n''}{kT}}}, \tag{16}$$

where E''_n is the energy of the nth level. The total extinction coefficient is the sum of the values of $f_0\alpha_0$, $f_1\alpha_1$, etc. In order that the sum can be compared with the observed extinction coefficients, attention must be paid to the fact that a transition from the zero level of the ground state to a level of the upper state (characterized by a particular value of x', called x'_i) involves a frequency greater than that from the first level to the same upper level. The difference is equal to $\omega - 2x_e\omega$. It follows (see fig. 2) that a particular frequency interval for a transition from the zero level to that of x'_i appears again for transitions from the first vibration level to a level corresponding to a smaller value of x' equal to $x'_i + \dfrac{\omega - 2x_e\omega}{k'}$ (k', the slope, being negative). Similarly, the same frequency interval is found for transitions from the second vibration level to levels corresponding to $x'_i + \dfrac{2\omega - 6x_e\omega}{k'}$. The total probability of absorption of radiation of the particular frequency equal to this interval is given by

$$f_0\alpha_0(x'_i) + f_1\alpha_1\left(x'_i + \frac{\omega - 2x_e\omega}{k'}\right) + f_2\alpha_2\left(x'_i + \frac{2\omega - 6x_e\omega}{k'}\right) + \dots, \qquad (17)$$

where the brackets indicate "function of".

Values of the total extinction coefficient have been calculated according to equation (17) and plotted against x'. By correlating this curve with the experimental one as in § 7, the relation between x' and ν has been extended to higher values of x', as shown by curve II, fig. 2, up to the point "d".

In the above treatment it has been assumed that the slope, k', of the upper potential energy curve is constant, but from fig. 2 it is seen to decrease as x' increases. As pointed out in § 7, a change of k' makes an inappreciable effect on the values of ψ'_N in the range concerned. The value of k' is, however, of importance in equation (17). The extreme part of curve II has been determined by using changing values of k' as the analysis proceeds. This method of successive approximations, while involving an extrapolation, is valid for methyl bromide as the successive corrections rapidly vanish.

11—*The Extinction Coefficient for Various Temperatures*—By the use of the potential energy curves the extinction coefficient curve for any temperature can be calculated. Increase of temperature affects only the partition fractions. The contributions from the separate vibration levels of the ground state are shown for 20° in fig. 1. The sum of these curves must, of course, agree with the experimental one. The extinction coefficients for certain frequencies for methyl bromide at 100° were calculated, and the values obtained were in good agreement with observations made at this temperature, as shown in the following table:

Frequency cm.$^{-1}$	log α_{20° (obs.)	log α_{100° Calc.	log α_{100° Obs.
35,500	$\overline{23}{\cdot}45$	$\overline{22}{\cdot}23$	$\overline{22}{\cdot}36$
36,000	$\overline{23}{\cdot}77$	$\overline{22}{\cdot}46$	$\overline{22}{\cdot}55$
37,000	$\overline{22}{\cdot}38$	$\overline{22}{\cdot}94$	$\overline{22}{\cdot}99$

The accuracy of the observations at 100° was not as high as those at 20°, the probable error being about ± 0·08 on a logarithm scale.

12—*Discussion*—Errors in the above determination of the upper potential energy curve may arise from various causes. The assumption that the absorption band is associated with the C—Br link is, of course, based on the fact that the band is characteristic of this grouping and not of the alkyl radical. This is supported by measurements made by Porret and Goodeve of the absorption spectra of other alkyl bromides.

The method of correcting for the anharmonicity is a simple one and the difference it makes is seen by comparing in fig. 2, curves II and III—the latter being calculated assuming the vibrations in the ground state to be harmonic. It is probable that the true upper potential energy curve lies slightly higher than curve II at large values of x', as the use of a higher value of the anharmonic constant and of a more accurate unsymmetrical eigenfunction curve would tend to raise the potential energy curve in this region.

The regularity of the upper potential energy curve and the agreement between the calculated and observed temperature coefficients indicate that the errors due to the above approximations are not large or compensate one another.

13—*Conclusions*—It may be seen, from the resolution of the observed extinction coefficient curve into its partial curves, that the slope of the "threshold" of absorption is determined by the curvature of the partial curves and by the influence of the successive vibration levels. The higher the temperature the more important is the influence of the latter. If the pressure and/or tube length be continuously increased, it is obvious that no absorption limit will ever be found. Arguments based upon measurements of the apparent limit have, therefore, no foundation.

Heats of dissociation or the nature of the products arising out of absorption of light in a continuous band may possibly be determined by extrapolation of the upper potential energy curve. In the case of methyl bromide the errors of extrapolation are too large to permit any conclusions to be drawn. The value of 72 kg. cal. for the heat of dissociation would appear, however, to be a reasonable one.

The authors are indebted to Dr. W. G. Penney for his kind advice and criticism.

SUMMARY

The extinction coefficients of methyl bromide have been measured over the range 35,000 to 52,000 cm.$^{-1}$. Quantal methods previously applied to the interpretation of continuous absorption bands of diatomic molecules have been extended to the interpretation of the band of methyl bromide. The upper potential energy curve has been calculated and the extinction coefficient curve resolved into the parts arising from molecules in various vibrational levels. The analytical method shows the construction of thresholds of continuous absorption.

REFERENCES

Barker, E. F. and Plyler, E. K. 1935 *J. Chem. Phys.* **3**, 367–8.
Bayliss, N. S. 1937 *Proc. Roy. Soc.* A, **158**, 551–61.
Bygdén, A. 1910 *J. prakt. Chem.* **83**, 421–4.
Condon, E. U. and Morse, P. M. 1929 "Quantum Mechanics", pp. 44–47. New York: McGraw-Hill Book Co., Inc.
Dirac, P. A. M. 1935 "The Principles of Quantum Mechanics", p. 178. Oxford: Clarendon Press.
Gibson, G. E., Rice, O. K. and Bayliss, N. S. 1933 *Phys. Rev.* **44**, 193–200.
Goodeve, C. F. and Taylor, A. W. C. 1935 *Proc. Roy. Soc.* A, **152**, 221–30.
Henrici, A. 1932 *Z. Phys.* **77**, 35–51.
Herzberg, G. and Scheibe, G. 1930 *Z. phys. Chem.* B, **7**, 390–406.
Hukumoto, Y. 1932 *Sci. Rep. Tôhoku Univ.* **21**, 906–27.
Jevons, W. 1932 "Report on Band Spectra of Diatomic Molecules", p. 27. London: Physical Society.
Kramers, H. A. 1926 *Z. Phys.* **39**, 840.
Morse, P. M. 1929 *Phys. Rev.* **34**, 57–64.
Pauling, L. and Wilson, E. B. 1935 "Introduction to Quantum Mechanics", pp. 77–81. New York and London: McGraw-Hill Book Co., Inc.
Penney, W. G. 1935 *Trans. Faraday Soc.* **31**, 734–46.
Porret, D. and Goodeve, C. F. (not yet published).
Schrödinger, E. 1926 *Ann. Phys., Lpz.*, (4), **80**, 437–490.
Zwaan, H. 1929 *Arch. néerl. Sci.* **12**, 33–40.

Penetration into Potential Barriers in Several Dimensions

By P. L. Kapur and R. Peierls

(*Communicated by R. H. Fowler, F.R.S.—Received* 30 *July* 1937)

It is well known that in regions in which the refractive index varies sufficiently slowly, Schrödinger's equation can be very simply treated by using its connexion with Hamilton-Jacobi's differential equation. It is also known that a similar approximation is possible in regions of slowly varying *imaginary* refractive index (total reflexion). For the latter case the method was developed in papers by Jeffreys (1924), Wentzel (1926), Brillouin (1926) and Kramers (1926). These papers discuss also the behaviour of the wave function in the neighbourhood of the limit between the regions of real and imaginary refractive index.

But although the connexion with the Hamilton-Jacobi equation holds in any number of dimensions, this equation can be solved by elementary means only in one dimension (or for problems that can by separation be reduced to one dimension), and for this reason the practical application of the method has so far been limited to one-dimensional or separable problems. In the present paper we discuss the case of more than one dimension and show that certain very simple inequalities may be obtained.

The problem presents itself usually in the following form: A particle of energy E and mass m moves in a potential field $V(x, y, z)$. We wish to know the probability of it being found at a place P_1, with the co-ordinates x_1, y_1, z_1 at which $V(x_1 y_1 z_1) > E$.

In the neighbourhood of P_1 we may write the wave function ψ of the particle in the form

$$\psi = e^{-S/\hbar}, \tag{1}$$

and obtain from Schrödinger's equation the condition

$$(\text{grad}\, S)^2 - \hbar \nabla^2 S = 2m(V - E). \tag{2}$$

The first term on the left-hand side will as a rule be larger than the second. If $V - E$ is large and varies slowly in space, the same must hold for the magnitude of the vector *grad* S, and except for points at which the vector rapidly alters its direction, each component will vary slowly and hence $\nabla^2 S$ will be small.

Neglecting the second term, we obtain as a first approximation

$$(\operatorname{grad} S)^2 = 2m(V-E), \tag{3}$$

which, apart from its sign, is identical with the Hamilton-Jacobi equation.

It should be kept in mind that S is in general complex. In fact, for a free particle with positive kinetic energy, S is purely imaginary. In the total reflexion of a particle by a plane of potential discontinuity with oblique incidence, *grad* S has a real component at right angles to the plane and an imaginary one parallel to it. We shall be particularly interested in the real part of S, since it determines the modulus of ψ and hence the probability.

Let

$$S = \sigma + i\tau \tag{4}$$

with σ and τ real. Then (3) becomes

$$(\operatorname{grad} \sigma)^2 = 2m(V-E) + (\operatorname{grad} \tau)^2, \tag{5a}$$

$$(\operatorname{grad} \sigma, \operatorname{grad} \tau) = 0. \tag{5b}$$

From (5*a*) it is evident that

$$|\operatorname{grad} \sigma| \geqq \sqrt{\{2m(V-E)\}}. \tag{6}$$

The equality sign holds if, and only if, S is real. This occurs in a number of cases of practical interest.

We want to find the probability density at the point P_1. We have

$$|\psi(P_1)|^2 = e^{-2\sigma(P_1)/\hbar}. \tag{7}$$

$\sigma(P_1)$ may be written as

$$\sigma(P_1) = \sigma(P_0) + \int_{P_0}^{P_1} |\operatorname{grad} \sigma|\, ds, \tag{8}$$

where ds is the line element and the integral is to be taken along a line of steepest gradient of σ. The point P_0 must then be a point on the same line of steepest gradient as P_1, but it is otherwise arbitrary. We may thus follow the line of steepest gradient up to that region in which the approximation (3) breaks down. That is the region which would be accessible to the particle on classical mechanics, and in this region the particle is found with large probability. Hence, unless the point P_1 lies too close to the boundary of this region, the magnitude of $|\psi|^2$ is mainly governed by the decrease from P_0 to P_1, i.e. by the integral in (8).

In order to calculate this integral and in order to find the point P_0 it would be necessary to know the lines of steepest gradient of σ, and that is in general not possible without knowing the function σ itself. However, we may easily find a lower limit for the integral. Consider the same integral, taken along an arbitrary path from P_1 to any point P_0' on the boundary of the classically accessible region.*

There will be one particular path of integration and one particular end-point P_0' which will make the integral a minimum, and we have

$$\sigma(P_1) - \sigma(P_0) = \int_{P_0}^{P_1} |\operatorname{grad} \sigma|\, ds \geqq \operatorname{Min} \int_{P_0'}^{P_1} |\operatorname{grad} \sigma|\, ds, \tag{9}$$

where *Min* means the lowest value of the integral that can be obtained by suitably choosing the path of integration and the end-point. Using (6), we find

$$\sigma(P_1) - \sigma(P_0) \geqq \operatorname{Min} \int_{P_0'}^{P_1} \sqrt{\{2m(V-E)\}}\, ds. \tag{10}$$

The path of integration which yields the minimum value can easily be determined from the variation principle

$$\delta \int \sqrt{\{2m(V-E)\}}\, ds = 0, \tag{11}$$

where the upper limit of integration, P_1, is fixed, while the other, P_0', is to be varied along a given boundary.

(10) provides us with a lower limit of the difference $\sigma(P_1) - \sigma(P_0)$ which we require, but in general we do not know how far this will be from the actual value.

However, in some cases, it is possible to see that the inequality (11) is much closer than would appear from the above derivation. For in some cases one knows that S is real in the region under discussion or at least in its greatest part. In that case the equality sign applies in (6). Moreover, in this particular case the lines of steepest gradient of S are solutions of the variation problem (11) provided only we do *not* vary the end-point P_0'.

This statement is familiar for the imaginary part of S, in the region in which S is purely imaginary, and $V < E$. For there the lines of steepest gradient form the classical orbits of the particles and the variation integral (11) represents the principle of least action. However, in our case the reality conditions are different and we must therefore translate the usual proof of the principle of least action.

The lines of steepest gradient are defined by

$$\frac{dx}{ds} = \frac{\partial \sigma}{\partial x} \Big/ \sqrt{\left\{\left(\frac{\partial \sigma}{\partial x}\right)^2 + \left(\frac{\partial \sigma}{\partial y}\right)^2 + \left(\frac{\partial \sigma}{\partial z}\right)^2\right\}},$$

---

* This boundary itself may depend on the form of σ and the lack of knowledge of its position may necessitate a further under-estimate of the integral.

which, if S is real and hence $\sigma = S$, becomes

$$\frac{dx}{ds} = \frac{\partial\sigma}{\partial x}\bigg/\sqrt{\{2m(V-E)\}} \tag{12}$$

with similar equations for y and z.

Hence
$$\frac{\partial\sigma}{\partial x} = \sqrt{\{2m(V-E)\}}\frac{dx}{ds}$$

and
$$\frac{d}{ds}\left(\frac{\partial\sigma}{\partial x}\right) = \frac{d}{ds}\left\{\sqrt{\{2m(V-E)\}}\frac{dx}{ds}\right\}.$$

The left-hand side may also be written $\frac{\partial}{\partial x}\left(\frac{d\sigma}{ds}\right)$ which, using again (6), becomes

$$\frac{\partial}{\partial x}\sqrt{\{2m(V-E)\}} = \frac{d}{ds}\left\{\sqrt{\{2m(V-E)\}}\frac{dx}{ds}\right\} \tag{13}$$

and two other equations for y and z. On the other hand, the variation integral (11) may be written

$$\delta\int\sqrt{\{2m(V-E)\}}\,.\sqrt{\left\{\left(\frac{dx}{ds}\right)^2+\left(\frac{dy}{ds}\right)^2+\left(\frac{dz}{ds}\right)^2\right\}}\,ds = 0$$

where now x, y, z may be treated as independent functions of s. This leads to the equation

$$\begin{aligned}\int ds\bigg\{\delta x\frac{\partial}{\partial x}\sqrt{\{2m(V-E)\}}+\sqrt{\{2m(V-E)\}}\frac{dx}{ds}\delta\left(\frac{dx}{ds}\right)\\ \delta y\frac{\partial}{\partial y}\sqrt{\{2m(V-E)\}}+\sqrt{\{2m(V-E)\}}\frac{dy}{ds}\delta\left(\frac{dy}{ds}\right)\\ \delta z\frac{\partial}{\partial z}\sqrt{\{2m(V-E)\}}+\sqrt{\{2m(V-E)\}}\frac{dz}{ds}\delta\left(\frac{dz}{ds}\right)\bigg\} = 0.\end{aligned}$$

Integrating by parts and remembering that δx, δy, δz vanish at the end-points, we obtain equations that are identical with (13).

We see thus that, if $\tau = 0$, the lines of steepest gradient of σ are solutions of the variation problem (11) with fixed end-points.

The only unknown variable which is then left is the end-point P_0' of the integration; for there are many solutions of (13) which pass through the point P_1 and only one of them represents a line of steepest gradient of S. If we vary P_0' in (11) we select a particular one of these lines, but in general not the right one. Hence (10) remains an inequality.

There are, however, cases in which (10) supplies the exact solution. This will, for example, occur if the potential field V represents a potential well and if the region in which $V > E$ is of small extension as compared to its distance from the point P_1, at which the probability is wanted. Then the wave function will have its maximum value in the potential well. Unless the potential field is very complicated, there will be no secondary maxima and therefore every line of steepest gradient will eventially lead into the potential well. In this case, the complete variation problem (11) leads to the right solution.

Another application in which (11) provides the complete answer will be discussed in a paper by one of us.

SUMMARY

The method of geometrical optics is discussed in application to the penetration of particles into regions of negative kinetic energy. It is shown that in the case of problems in more than one dimension which cannot be separated, it is generally possible to derive an upper limit for the probability of penetration, and that in special cases the method gives the actual value of this probability.

REFERENCES

Brillouin, L. 1926 *C.R. Acad. Sci., Paris*, **183**, 24.
Jeffreys, H. 1924 *Proc. Lond. Math. Soc.* **23**, 428.
Kramers, H. A. 1926 *Z. Phys.* **39**, 828.
Wentzel, G. 1926 *Z. Phys.* **38**, 518.

INDEX TO VOLUME CLXIII (A)

Absorption spectra of some cyanine dyes (Beilenson, Fisher and Hamer), 138

Alexander (A. E.) and Rideal (E. K.) Reaction kinetics in films. The hydrolysis of long-chain esters, 70.

Allsopp (C. B.) *See* Lowry and Allsopp.

Allsopp (C. B.) *See* Lowry, Simpson and Allsopp.

Andrade (E. N. da C.) Preparation of single crystal wires of metals of high melting point, 16.

Andrade (E. N. da C.) and Tsien (L. C.) The glide of single crystals of sodium and potassium, 1.

Aston (F. W.) A second-order focusing mass spectrograph and isotopic weights by the doublet method, 391.

Atomic constants, paper by von Friesen (Townsend), 188.

Atomic hydrogen (Poole), 404, 415, 424.

Atoms and molecules, interaction with solid surfaces (Lennard-Jones and Goodwin; Lennard-Jones; Devonshire), 101, 127, 132.

Bagnold (R. A.) The size-grading of sand by wind, 250.

Beilenson (B.), Fisher (N. I.) and Hamer (F. M.) A comparison of the absorption spectra of some typical unsymmetrical cyanine dyes, 138.

Bragg (Sir William) Address of the President at the Anniversary Meeting, 30 November 1937, 455.

Bretscher (E.) *See* Chadwick, Feather and Bretscher.

Brookman (E. F.) *See* Norrish and Brookman.

Buckingham (R. A.) *See* Massey and Buckingham.

Chadwick (J.), Feather (N.) and Bretscher (E.) Measurements of range and angle of projection for the protons produced in the photo-disintegration of deuterium, 366.

Chow (Y. S.) *See* Tsien and Chow.

Coals, Upper Carboniferous, from Western Australia (Kent), 568.

Cyanine dyes, absorption spectra (Beilenson, Fisher and Hamer), 138.

Dee (P. I.) and Gilbert (C. W.) The angular distribution of protons projected by fast neutrons, 265.

Deuterons, transmutation function (Kapur), 553.

Devonshire (A. F.) *See* Lennard-Jones and Devonshire.

Devonshire (A. F.) The interaction of atoms and molecules with solid surfaces. XII—Critical phenomena in a two-dimensional gas, 132.

Egerton (A. C.) *See* Hanson and Egerton.

Emulsification, spontaneous (McBain and Ts-Ming Woo), 182.

Explosion waves and shock waves (Payman and Woodhead), 575.

Feather (N.) *See* Chadwick, Feather and Bretscher.

Fink (Phyllis) and Goodeve (C. F.) The continuous absorption spectrum of methyl bromide and its quantal interpretation, 592.

Fisher (N. I.) *See* Beilenson, Fisher and Hamer.

Gases, critical phenomena (Lennard-Jones and Devonshire), 53.
Gilbert (C. W.) *See* Dee and Gilbert.
Godfrey (G. H.) and Price (W. L.) Thermal radiation and absorption in the upper atmosphere, 228
Goodeve (C. F.) *See* Fink and Goodeve.
Goodwin (E. T.) *See* Lennard-Jones and Goodwin.
Greenland (K. M.) Slip bands on mercury single crystals, 28.
Greenland (K. M.) The critical shear stress of mercury single crystals, 34.
Griffiths (Ezer) *See* Powell and Griffiths.

Hamer (F. M.) *See* Beilenson, Fisher and Hamer.
Hanson (T. K.) and Egerton (A. C.) Nitrogen oxides in internal combustion engine gases, 90.
Helium, passage through a crystal lattice (Rayleigh), 376.

Internal combustion engine gases (Hanson and Egerton), 90.
Isotopic weights by the doublet method (Aston), 391.

Kapur (P. L.) A transmutation function for deuterons, 553.
Kapur (P. L.) and Peierls (R.) Penetration into potential barriers in several dimensions, 606.
Kent (C. R.) A study of Upper Carboniferous coals from Western Australia, 568.
Ketones, optical activity (Lowry, Simpson and Allsopp), 483.

Latent energy, emission of (Quinney and Taylor), 157.
Lennard-Jones (J. E.) The interaction of atoms and molecules with solid surfaces. XI—The dispersal of energy from an activated link, 127.
Lennard-Jones (J. E.) and Devonshire (A. F.) Critical phenomena in gases—I, 53.
Lennard-Jones (J. E.) and Goodwin (E. T.) The interaction of atoms and molecules with solid surfaces. X—The activation of adsorbed atoms by metallic electrons, 101.
Lowry (the late T. M.) and Allsopp (C. B.) Refractive dispersion of organic compounds. IX—Optical exaltation in unsaturated hydrocarbons containing conjugated double bonds, 356.
Lowry (the late T. M.), Simpson (Delia M.) and Allsopp (C. B.) Optical activity in ketones. The rotatory dispersion and circular dichroism of *m*-methyl *cyclo*hexanone and of pulegone in their ketonic absorption bands, 483.

McBain (J. W.) and Ts-Ming Woo Spontaneous emulsification, and reactions overshooting equilibrium, 182.
Massey (H. S. W.) Dissociation, recombination and attachment processes in the upper atmosphere—I, 542.
Massey (H. S. W.) and Buckingham (R. A.) The nature of the interaction between neutron and proton from scattering experiments, 281.
Melville (H. W.) The photochemical polymerization of methyl methacrylate vapour, 511.
Mercury single crystals (Greenland), 28, 34.
Methyl methacrylate vapour, photochemical polymerization (Melville), 511.
Miller (J. C. P.) *See* Rosenhead and Miller.

Norrish (R. G. W.) and Brookman (E. F.) The formation and structure of polymers of the insoluble cross-linked type, 205.
Norrish (R. G. W.) and Noyes (W. A.) Photochemical reactions in the fluorite region. II—Photochemical decomposition of formaldehyde vapour, 221.
Noyes (W. A.) *See* Norrish and Noyes.

Osglim lamp, III (Richardson), 380.

Payman (W.) and Woodhead (D. W.) Explosion waves and shock waves. V—The shock wave and explosion products from detonating solid explosives, 575.
Peierls (R.) *See* Kapur and Peierls.
Photochemical reactions in the fluorite region (Norrish and Noyes), 221.
Polymers, formation and structure (Norrish and Brookman), 205.
Poole (H. G.) Atomic hydrogen. I—The calorimetry of hydrogen atoms. II—Surface effects in the discharge tube. III—The energy efficiency of atom production in a glow discharge, 404, 415, 424.
Powell (R. W.) and Griffiths (Ezer) The variation with temperature of the thermal conductivity and the X-ray structure of some micas. I—The thermal conductivity up to 600° C., 189.
Presidential Address (Bragg), 455.
Price (W. L.) *See* Godfrey and Price.
Protons projected by fast neutrons, angular distribution (Dee and Gilbert), 265.

Quinney (H.) and Taylor (G. I.) The emission of the latent energy due to previous cold working when a metal is heated, 157.

Rayleigh (Lord) An attempt to detect the passage of helium through a crystal lattice at high temperatures, 376.
Reaction kinetics in films (Alexander and Rideal), 70.
Reimann (A. L.) The temperature variation of the work function of clean and of thoriated tungsten, 499.
Richardson (L. F.) The behaviour of an osglim lamp. III—Osglims in parallel, forming models of reciprocal inhibition, 380.
Rideal (E. K.) *See* Alexander and Rideal.
Rosenhead (L.) and Miller (J. C. P.) Electrosmosis between plane parallel walls produced by high-frequency alternating currents, 298.

Sand, size-grading by wind (Bagnold), 250.
Scattering experiments, interaction between neutron and proton (Massey and Buckingham), 281.
Simpson (Delia M.) *See* Lowry, Simpson and Allsopp.
Single crystals, glide of (Andrade and Tsien, Tsien and Chow), 1, 19.
Single crystals, mercury (Greenland), 28, 34.
Single crystal wires, preparation (Andrade), 16.
Southwell (R. V.) On the torsion of conical shells, 337.
Spectrum, continuous absorption, of methyl bromide (Fink and Goodeve), 592.

Taylor (G. I.) A discussion on viscosity of liquids, 319.
Taylor (G. I.) *See* Quinney and Taylor.

Thermal conductivity, variation with temperature (Powell and Griffiths), (Wood), 189, 199.
Thermal radiation and absorption in the upper atmosphere (Godfrey and Price), 228.
Torsion of conical shells (Southwell) 337.
Townsend (J. S. E.) A comment on the paper by Sten von Friesen "On the values of fundamental atomic constants", 188.
Tsien (L. C.) *See* Andrade and Tsien.
Tsien (L. C.) and Chow (Y. S.) The glide of single crystals of molybdenum, 19.
Ts-Ming Woo *See* McBain and Ts-Ming.
Tungsten, temperature variation of the work function (Reimann), 499.

Upper atmosphere (Massey), 542.

Viscosity of liquids, discussion (Taylor), 319.

Wood (W. A.) The variation with temperature in the thermal conductivity and the X-ray structure of some micas. II—The X-ray examination of the structure, 199.
Woodhead (D. W.) *See* Payman and Woodhead.

END OF THE ONE HUNDRED AND SIXTY-THIRD VOLUME (SERIES A)

ERRATUM

Proc. Roy. Soc., A, vol. 162, *p.* 423

"average value of 1 for" in second line from bottom of page *should read* "average value of 91 for".

ABSTRACTS

OF PAPERS COMMUNICATED TO THE ROYAL SOCIETY OF LONDON

In accordance with a resolution of Council, summaries or abstracts of papers are to be published as soon as practicable. The publication of such abstracts in no way indicates that the papers have been accepted for publication in any fuller form. These abstracts will be issued for convenience with the "Proceedings of the Royal Society of London" but do not form a part of the "Proceedings".

NOTE.—The pagination of the "Abstracts" will be consecutive through the year and independent of the "Proceedings". To avoid any confusion with the "Proceedings", the page numbers will be preceded by the letter S (*i.e.* Summary).

---

19 November 1937

The Temperature Variation of the Work Function of Clean and of Thoriated Tungsten

By A. L. Reimann

(*Communicated by R. H. Fowler, F.R.S.—Received* 3 *June* 1937)

Measurements were made of the contact potential difference between a constant source of electrons and a neighbouring tungsten filament collecting space-charge-limited electron current, whose condition was varied. This filament was either clean or covered with a layer of thorium atoms, and, in addition, it was held at various temperatures. In this way direct information was obtained concerning the rates at which the work functions of clean and fully activated thoriated tungsten (W-Th) vary with temperature. Within the limits of experimental uncertainty there is no difference between

the temperature coefficients of the two work functions. The temperature coefficient found is about that which would be required to account for the observed value of the thermionic constant A of clean tungsten on the assumption of practically perfect transmission. It must be concluded that the factor (of the order of 10–20) by which the A of W-Th is less than that of clean tungsten is due to internal reflexion of electrons at the W-Th surface.

The Scattering of Wireless Waves in the Ionosphere

By T. L. Eckersley

(*Communicated by W. H. Eccles, F.R.S.—Received* 11 *June* 1937)

Application of the Phase Integral Method to the Analysis of the Diffraction and Refraction of Wireless Waves round the Earth

By T. L. Eckersley and G. Millington

(*Communicated by W. H. Eccles, F.R.S.—Received* 11 *June* 1937)

Relaxation Methods applied to Engineering Problems II—Basic Theory, with applications to Surveying and to Electrical Networks, and an extension to Gyrostatic Systems

By A. N. Black, B.A. and R. V. Southwell, F.R.S.

(*Received* 22 *June* 1937)

The method of systematic relaxation, originally devised for the calculation of stresses in frameworks, has since been extended to other elastic systems. This paper shows that its basis is the principle of minimum potential energy, and thereby demonstrates its convergence as applied not only to elastic problems, but to any problem for which a minimal theorem exists. Examples treated are the adjustment of errors in surveying and the partition of electric current in non-inductive networks.

Finally, networks characterized by self-induction and/or capacity are discussed as examples of "gyrostatic systems", which do not present minimal problems of the standard type. Here too convergence can be demonstrated, and a numerical example shows that no special difficulty is presented.

The Seiches in a Strait connecting Two Seas

By G. R. Goldsbrough, F.R.S.

(*Received* 29 *June* 1937)

The problem studied is that of the natural vibrations of the water in a strait connecting two open seas. The shores of the strait are the two branches of a hyperbola and a certain law of depth is chosen. It is shown that such a system has free modes of four distinct types characterized by symmetry about both axes, asymmetry about the conjugate axis, asymmetry about the transverse axis and asymmetry about both axes, respectively. In each case there is an infinite number of distinct modes. The waves diminish rapidly in amplitude as the channel widens. The nodal

lines are members of the same family of confocal ellipses and hyperbolas of which the shores are a member.

Some of the lower modes are worked out completely for special cases. But simpler approximations are given covering all the forms where the eccentricity of the bounding hyperbola is not too small.

On the Torsion of Conical Shells

By R. V. Southwell, F.R.S.

(*Received* 30 *June* 1937)

By imagining a flat plate to be distorted by shearing stresses in its own plane, and then with shear stresses operative to be bent into the appropriate shape, the Bredt-Batho formula for the stresses produced by torsion in non-circular tubes is obtained and extended to shells having the forms of non-circular cones (tapered tubes). The strains are also deduced, and the results for cylindrical tubes conform with what are given by the classical theory of Saint-Venant, both as regards the twist and the warping of cross-sections out of their planes. In thin conical shells it is shown that warping will be replaced by a strain which alters the shapes of cross-sections, for the reason that it would involve extensions, which occurring in a sheet of negligible thickness would violate the principle of minimum strain-energy. In cylindrical tubes, either type of strain is possible according to a theory in which the thickness is neglected: warping occurs in fact, because unlike the other alternative it involves no flexural stresses.

Part II is concerned with the question, whether Saint-Venant's celebrated theory of torsion can be extended so as to include *thick* tubes and rods having the forms of non-circular cones. It is found (as would be expected from the foregoing results) that except in relation to sections of a special (circular or oval) type no progress can be made by assuming that the shapes of the cross-sections are not altered by torsional strain.

Galvanometer Effects in Bismuth Alloys

BY W. THOMPSON

(*Communicated by A. M. Tyndall, F.R.S.—Received* 3 *July* 1937)

An account is given of experimental observations on the Hall effect and transverse magneto-resistance effect in single crystals of bismuth containing small and known amounts of impurity, up to 1 % of lead and 0·1 % of selenium. Measurements were made at fields up to 22,000 oersted, at temperatures from 20° A. to 290° A., and for three principal crystal orientations. The results are found to be in general agreement with theory, and a hypothesis is advanced to explain the divergencies. It is concluded that the number of free electrons per atom in metallic bismuth is of the order of 3×10^{-5}.

Atomic Hydrogen

BY H. G. POOLE

(*Communicated by C. K. Ingold, F.R.S.—Received* 6 *July* 1937)

I—The Calorimetry of Hydrogen Atoms

A new type of calorimeter for the measurement of hydrogen atoms is described, depending on the continuous flow principle: water flowing through a copper tube is warmed by the catalytic recombination of atoms on the platinum-plated outer surface of the tube, and the rise of temperature of the water then determines the rate of recombination of atoms. Considerable accuracy is possible, and the sensitivity of the calorimeter is easily varied as required; sensitivities of 0·1–1·0 calories per minute have been used, the range of rates of heat production so far studied being 4–300 calories per minute. Continuous operation and reading over indefinite periods of time are possible, very small corrections due to losses are required, and the lag in attaining equilibrium after large changes in the rate of supply of atomic hydrogen is of the order of 1 to 2 min.

The spectroscopic value of Beutler for the dissociation energy of hydrogen (102,720 cals./g.-mol.) is adopted; after allowance for the heat capacities

of the molecules and atoms this leads to 103,680 cals./g.-mol. for the heat of dissociation at 300° K. and constant pressure.

The determination of hydrogen atoms by molecular flow gauges is discussed and sources of error which have hitherto been overlooked are pointed out. In particular, the effect of small errors in the measurement of pressure is shown to be large.

II—Surface Effects in the Discharge Tube

The output of atomic hydrogen from several different discharge tubes of silica and pyrex has been measured calorimetrically at one-minute intervals. The curves obtained show that very large changes in atom output with time, even in a few minutes, may occur with discharge tubes depending only on a water-on-glass or water-on-silica film for de-activation of the tube wall as catalyst for the recombination of atoms, and that the behaviour of such tubes depends on their past history. The conclusion is reached that destruction of the protective water film occurs during intense discharges, and that readsorption of water takes place during rest periods and sometimes during weak discharges; the increasingly rapid decay of output for successive high intensity discharges indicates that a new water film is less firmly held than an old film.

Constant and reproducible output is obtained by the use of a metaphosphoric acid lining inside the discharge tube.

III—The Energy Efficiency of Atom Production in a Glow Discharge

The efficiency of the glow discharge system for the production of hydrogen atoms has been determined as the number of dissociated molecules received at the calorimeter per unit energy (electron-volt) supplied to the positive column. This efficiency, μ_c, has been found to vary with the power input to the positive column, W, with the volume rate of flow of gas, U_0, and with the pressure; for any given pressure, the behaviour of the discharge tube is satisfactorily represented by the empirical equation

$$\frac{1}{\mu_c} = \frac{1}{\mu_0}\left(1+\frac{k}{U_0}\right)+\left(\frac{a}{U_0}-b\right)W$$

in which μ_0, k, a and b are constants depending on the pressure.

Analysis of the conditions in the discharge tube and delivery tube has indicated the reasons for the above relationship; and has led to the determination of the Emeléus-Lunt-Meek efficiency, η_0, i.e. the sum of the efficiencies for the excitation of the two states, ${}^3\Sigma_u^+$ and ${}^3\Sigma_g^+$, leading to dissociation of the molecule, over the pressure range 0·10–1·35 mm. The variation of η_0 as the pressure is changed is in satisfactory agreement with the theoretical values, provided that a theoretically permissible correcting factor of 2·6 is applied to the probability cross-section for ${}^3\Sigma_u^+$ excitations as calculated quantum-mechanically by Massey and Mohr. The velocity constant for the first order, wall-catalysed recombination of atoms has been determined from the same data, and hence the adhesion coefficient γ for a water-on-phosphoric acid film, i.e. the fraction of the total number of collisions of atoms with the walls which lead to the loss of an atom; γ is found to be $3{\cdot}9 \times 10^{-5}$.

In addition, a general equation for the flow of atoms and molecules through a tube has been developed.

Photochemical Polymerization of Methyl Methacrylate Vapour—I

By H. W. Melville

(*Communicated by E. K. Rideal, F.R.S.—Received* 12 *July* 1937)

The kinetics of the photochemical polymerization of methyl methacrylate have been investigated with the following results. Polymerization occurs nearly quantitatively to a white solid, if the radiation is absorbed by the $COOCH_3$ group in the molecule, i.e. $\lambda > 2200$ A. Light of shorter wavelength absorbed by the double bond leads to decomposition of the molecule.

After a sufficient time of illumination, the polymer grows continuously in the dark for several days. This steady growth is proportional to the area of the tube illuminated, to the methacrylate pressure and decreases with increasing temperature. It can be stopped by means of H atoms and I_2 molecules; it is unaffected by oxygen, ethylene and acetylene. The polymer is depolymerized to the monomer on heating to 300° C. *in vacuo.*

Polymerization can also be initiated by hydrogen atoms, the velocity of which is greater than that of the normal polymerization. The rate is independent of methacrylate pressure (above 2 mm.) and hydrogen pressure (above 4 mm.), and is proportional to the square root of the intensity of the light. The mean life of this polymer is *ca.* 10^{-2} sec. It stops growing when two growing polymers collide in the gas.

The mechanism of the growth of the methacrylate polymer is discussed and reasons advanced to explain why one polymer has a long life and the other a short life. The essential difference is believed to be due to a double bond polymerization in the former case and to a free radical polymerization in the latter case.

Photochemical Polymerization of Methyl Methacrylate Vapour—II

By H. W. MELVILLE

(*Communicated by E. K. Rideal, F.R.S.—Received* 12 *July* 1937)

When atomic hydrogen, generated photochemically, is produced in presence of methyl methacrylate vapour, a polymer is formed as a colourless oil, much faster than the normal polymerization mentioned in the previous paper. This polymerization reaction has entirely different characteristics. It occurs wholly in the gas phase and stops immediately the light is cut off. Above pressures of 2 mm. of methacrylate, the rate of polymerization is independent of methacrylate pressure. The rate is also independent of hydrogen pressure above 4 mm. It is proportional to the square root of the intensity of the absorbed light. By using a rotating sector the mean life of the polymer is shown to be less than 10^{-2} sec. A kinetic analysis of the results demonstrates that the polymer stops growing when *two* growing polymer molecules unite.

Considering the above results together with those described in the previous paper, the question of the mechanism of growth of methyl methacrylate polymers is discussed. It is concluded that in the normal photochemical polymerization growth on the surface occurs by the reproduction

of a double bond at the end of a polymeric molecule each time a monomer adds on. This accounts for the stability of the polymer, its behaviour toward solvents and ease of thermal depolymerization. The initial gasphase growth of the polymer may, however, proceed through the medium of a free radical polymerization exactly analogous to that occurring in the hydrogen sensitized polymerization.

Dissociation, Recombination and Attachment Processes in the Upper Atmosphere—I

By H. S. W. Massey, Ph.D.
Independent Lecturer in Mathematical Physics,
Queen's University, Belfast

(*Communicated by E. V. Appleton, F.R.S.—Received* 13 *July* 1937)

The probabilities of various collision reactions which occur in the E and F regions of the ionosphere are considered in general terms. In particular the relative importance of recombination and attachment in effecting electron removal is discussed. As processes in which electrons are detached from negative ions can be expected to go on at a considerable rate (much faster than recombination) and as attachment must also occur very rapidly, the most reasonable representation of the phenomena is to consider the negative ions and electrons as in a dynamical equilibrium adjusting itself rapidly to loss of either by recombination. In this way the usual recombination theory may be retained, even though attachment occurs much more rapidly. A consequence of the theory is that the number of negative ions should considerably exceed the number of electrons in the E region as required by the "dynamo" theory of magnetic variations. The low rate of recombination in the F region, requiring the density of positive ions to be not much greater than that of the electrons, makes it necessary to suppose that, at these levels, the atmospheric gases present are inert towards electron attachment.

A Transmutation Function for Deuterons

By P. L. Kapur

(*Communicated by R. H. Fowler, F.R.S.—Received* 15 *July* 1937)

A generalization of the method of geometrical optics, commonly known as the Wentzel-Kramers-Brillouin method, is applied to the case of transmutation by deuterons. The treatment of Oppenheimer and Phillips (1935), based on the approximation of a three-body problem, is improved in so far as the wave equation is not assumed to be separable. The generalization gives, in general, an upper limit to the probability of the process, but in the present case it is shown that it gives the correct value. The results of the calculations are given in Table I and figs. 1 and 2. Formulae ((18′) and (21′)) are also obtained which take into account the finite radius of the nucleus. The results are compared with experiments on copper and are found to be in fair agreement, when the binding energy of the deuteron is taken to be 2·25 mV.

A Study of Upper Carboniferous Coals from Western Australia

By C. R. Kent, Ph.D.

(*Communicated by Professor William A. Bone, F.R.S.— Received* 19 *July* 1937)

Explosion Waves and Shock Waves

V—The Shock Wave and Explosion Products from Detonating Solid Explosives

By W. Payman, D.Sc., Ph.D. and D. W. Woodhead, Ph.D., F.I.C.

(*Communicated by J. F. Thorpe, F.R.S.—Received* 20 *July* 1937)

The mode of expansion of the disturbance produced when a cartridge of explosive suspended freely is detonated has been studied by means of

Schlieren photography, using cameras of both instantaneous and continuous types. The records show that there are three phases in the life of the disturbance produced.

The first phase is the detonation of the cartridge. This is comparatively short (about 3×10^{-5} sec. in a 113 g. cartridge of celmonite). The disturbance then may be regarded as arising solely from the side of the cartridge and is very nearly spherical; the shock wave is smooth and precedes the front of the gaseous products by a fraction of a centimetre.

The second phase is longer and may last until the disturbance has travelled 100–125 cm. (6×10^{-4} sec. with a 113 g. cartridge of celmonite). During the first half of this period the gaseous products are for the most part luminous and follow the shock wave at a gradually increasing distance. The velocities of both wave and products may be greater than the rate of detonation of the cartridge. Many characteristic prominences due to individual solid particles and congregations of particles appear in the wave front. The gaseous expansion from each end of the cartridge is far more vigorous than that from the side, with the result that axial distensions in the form of the wave appear. These deformations from the spherical are accentuated and prolonged by the shower of particles, the density of the shower being clearly greatest axially with the cartridge. In the second half of this period the disturbance is no longer "maintained". The velocity of the gaseous products falls rapidly and the products become mixed with air through turbulence to an increasing extent. Simultaneously, the masses of particles producing the prominences in the wave front become dispersed and, as individual particles, no longer affect materially the progress of the wave.

The third and last phase begins when all prominences have disappeared; the wave becomes smooth again and, when travelling at about 500 m./sec., rapidly assumes the spherical form. The gaseous products are at atmospheric pressure and free to drift. Dispersed particles precede the wave over several metres and sooner or later fall to the ground. The wave spreads with a gradually falling velocity until it ultimately degenerates into a sound wave.

Some Conditions Governing the Solubility of Iron

By L. H. N. Cooper, Ph.D., F.I.C.

Assistant Chemist at the Plymouth Laboratory of the Marine Biological Association

(*Communicated by W. R. G. Atkins, F.R.S.—Received* 26 *July* 1937)

Existing data on the solubility products of ferrous and ferric hydroxides and on the ion, $FeOH^{++}$, have been used to calculate the maximum activities of Fe^{++}, $FeOH^{++}$ and Fe^{+++} which may exist in sea water.

The maximum activity of ferrous ion is controlled both by the activity of the ferric ion and by the oxidation-reduction potential of the system.

The maximum activity of the three ions at equilibrium in sea water are presented in Table VII. Other tables show equilibrium conditions at a range of oxidation-reduction potentials and hydrogen-ion concentrations.

The total quantity of iron in true solution in water after equilibrium has been attained does not exceed

3×10^{-8}	mg. iron	per cubic metre	at pH	8·5
4×10^{-7}	,,	,,	,,	8·0
4×10^{-5}	,,	,,	,,	7·0
5×10^{-3}	,,	,,	,,	6·0

and of this the greater part consists of ferrous and $FeOH^{++}$ ions. In more acid solutions ferrichloric acids may have to be taken into account.

These values apply to iron in sea water, in natural waters and in many physiological fluids.

On the Equations of Electromagnetism

I—Fundamental Identifications

By E. A. Milne, F.R.S.

(*Received* 26 *July* 1937)

The paper offers a purely kinematic formulation of the phenomena of electromagnetism. It proceeds by first examining the most general type of external force after gravitational forces which are encountered in the study of the dynamics of a particle in the presence of the substratum or smoothed-out universe. Such external forces involve mention of 6-vectors, and the form of the resulting force is obtained in a form holding good for all epochs and for all distances from the observer. For the present epoch and at small distances it reduces to the Larmor-Lorentz formula for the ponderomotive force on a moving charge. A scalar multiplier emerges in the treatment which is afterwards identified as charge. A 6-vector is then derived by appropriate differentiation of an undetermined scalar with regard to the co-ordinates of two events, one being the source of the field and the other the event of the measurement of the field. With this it is possible to obtain the relativistic equations of motion of two charged particles in one another's presence, and to deduce the associated energy equation. By requiring the radiation to vanish when the accelerations vanish, it is found possible to fix all undetermined scalars completely. It is then possible to evaluate the "field" due to a given charge in given motion, at a given external point, as measured by the force on a test-charge in given motion, and by comparing the theoretically derived formulae with the observed experimental laws to identify the various symbols introduced. The inverse square law of Coulomb is obtained in exact relativistic form. But the law expressing the magnetic field at a distance r from a given charge e_2 moving with a given velocity $\mathbf{V}_2$ relative to a fundamental observer O is found to contain mention of the velocity $\mathbf{V}_1$ of the test-charge measuring the field; in detail, the classical Biot and Savart law $\mathbf{H} = (e_2/c)\, \mathbf{V}_2 \wedge \mathbf{r}/|\mathbf{r}|^3$ is found to be replaced by

$$\mathbf{H} = (e_2/c)\, \tfrac{1}{2}(\mathbf{V}_1 + \mathbf{V}_2) \wedge \mathbf{r}/|\mathbf{r}|^3.$$

The two agree for $\mathbf{V}_1 = \mathbf{V}_2$, but the new formula gives half the classically calculated field for $\mathbf{V}_2 = 0$, as required by Uhlenbeck and Goudschmidt and as found by a different method by L. H. Thomas. Our result is of more than mere numerical significance, as it compels the abandonment of the concept of a magnetic field as something independent of the circumstances of its measurement. This will be more fully developed in Part II.

Secular factors in the laws of electromagnetism are considered, and the results applied to the simple Bohr atom and to Dirac's cosmological relation. It is shown that in kinematic measure the radius of an atom is proportional to t, tending to zero as $t \to 0$. It is also shown that Dirac's relation does not require the creation of matter.

On the Equations of Electromagnetism
II—Field Theory

By E. A. Milne, F.R.S.

(*Received* 25 *July* 1937)

Following the mathematical treatment of the preceding paper, a physical discussion is given in which it is shown that the concept of an electromagnetic field (**E**, **H**) as existing in free space independent of the circumstances of the test-charge used to measure it must be abandoned. Instead it is replaced by the concept of a pair (**E**, **H**) which depend on the velocity **V** of the test-charge at the point concerned used to measure it. Nevertheless "field identities" are found which are satisfied at each event by the (**E**, **H**) as measured there; these identities are explicitly independent of the velocity **V** of the test-charge employed. These are stated as equations (12), (13), (29), (30). Two of them coincide with two of Maxwell's equations, namely those expressing the non-existence of isolated magnetic poles and Faraday's law of electromagnetic induction. The remaining two are modifications of Maxwell's other two equations for free space. They imply wave-propagation of **E**, **H**, and admit the existence of a vector-potential.

With the abandonment of the concept of a field as existing in free space independent of the velocity of the test-charge used to measure it, the expression of electromagnetic energy as a volume integral must be abandoned also. Instead we have an expression for the electromagnetic energy associated with the different pairs of charges present in the field, calculated mechanically. The sum of this and the mechanical energies of the moving massive particles varies with the time according to a linear function of the accelerations of the charged particles in one another's presence. The latter vanishes in certain well-defined circumstances, or has a mean value zero, and this gives rise to the phenomenon of non-radiating, i.e. "stationary", states. Radiation occurs in certain cases of accelerated motion, but not for periodic systems. The rôle of the field is then the same as that put forward by Bohr, Kramers and Slater, namely that energy is not located in the field but that the field is the mechanism for conveying energy from one set of charged particles to another.

A unified treatment of gravitational and electromagnetic phenomena is briefly sketched, and the energy formula obtained.

Structure of Stretched Rubber

BY C. J. B. CLEWS AND F. SCHOSZBERGER

(*Communicated by Sir William Bragg, P.R.S.—Received* 26 *July* 1937)

A picture of micellar structure is developed which is intermediate between the two formerly proposed theories. The micelles are of lath-shaped form, and possess, on account of their shape and of their transverse bindings, a definite individuality, even though the "Hauptvalenzketten" themselves extend beyond the sphere of single micelles.

Rubber films, obtained from dilute solutions in various solvents, have been examined to determine a possible influence on "higher orientation". The X-ray photographs were taken on a fibre camera.

All films derived from these solutions show "higher orientation" on extreme extension to 700 %. It is therefore established that the capacity for building up micelles in the way described is an intrinsic property of the "Hauptvalenzketten".

The Continuous Absorption Spectrum of Methyl Bromide and its Quantal Interpretation

BY PHYLLIS FINK AND C. F. GOODEVE

The Sir William Ramsay Laboratories of Inorganic and Physical Chemistry, University College, London

(*Communicated by F. G. Donnan, F.R.S.—Received* 26 *July* 1937)

The extinction coefficients of methyl bromide have been measured over the range 35,000 to 52,000 cm.$^{-1}$. Quantal methods previously applied to the interpretation of continuous absorption bands of diatomic molecules have been extended to the interpretation of the band of methyl bromide. The upper potential energy curve has been calculated and the extinction coefficient curve resolved into the parts arising from molecules in various vibrational levels. The analytical method shows the construction of thresholds of continuous absorption.

Hyperfine Structure and Nuclear Moments of Aluminium

By D. A. Jackson and H. Kuhn
Clarendon Laboratory, Oxford

(*Communicated by F. A. Lindemann, F.R.S.—Received* 28 *July* 1937)

The hyperfine structure of the resonance lines of aluminium was investigated by means of the absorption in an atomic beam of aluminium. The line $3\,{}^2P_{\frac{1}{2}}$–$4S_{\frac{1}{2}}$ was found to possess three components at $-0{\cdot}048$, $0{\cdot}000$ and $+0{\cdot}048$ cm.$^{-1}$ of nearly equal intensity. The line $3\,{}^2P_{\frac{1}{2}}$–$3\,{}^2D_{\frac{3}{2}}$ possessed two components of separation 0·066 cm.$^{-1}$, the intensity ratio of which was measured to a high degree of accuracy; the value found was 1·21 : 1, the component of longer wave-length being the stronger.

From the structure of the line $3\,{}^2P_{\frac{1}{2}}$–$4S_{\frac{1}{2}}$ it follows that the levels $4S_{\frac{1}{2}}$ and $3\,{}^2P_{\frac{1}{2}}$ are both split into two levels, of separation 0·048 cm.$^{-1}$ (the greater splitting of the line $3\,{}^2P_{\frac{1}{2}}$–$3\,{}^2D_{\frac{3}{2}}$ is due to a small unresolved, inverted structure of the level $3\,{}^2D_{\frac{3}{2}}$ which is probably caused by perturbation by the term $3s\,3p^2\,{}^2D_{\frac{3}{2}}$). The observed intensity ratio of the components of the line $3\,{}^2P_{\frac{1}{2}}$–$3\,{}^2D_{\frac{3}{2}}$ gives a value $\frac{9}{2}$ for the nuclear spin, and the splittings of the levels $4S_{\frac{1}{2}}$ and $3\,{}^2P_{\frac{1}{2}}$ give values 4·1 and 3·6 nuclear magnetons respectively for the magnetic moment of the nucleus according to the formulae of Goudsmit.

The lines $4S_{\frac{1}{2}}$–$5\,{}^2P_{\frac{3}{2}}$ and $4S_{\frac{1}{2}}$–$5\,{}^2P_{\frac{1}{2}}$ were observed in emission and were found to be doublets, only just resolvable on account of their Doppler width, of separation about 0·05 cm.$^{-1}$ and of intensity ratio (when corrected for overlapping) about 1·23 : 1, the component of longer wave-length being the stronger. This structure is in complete agreement with the interpretation of that observed in the resonance lines.

This result is in disagreement with the contents of a preliminary note by Ritschl in which, from an observed doublet structure of the arc lines 3057 and 3050 and the spark line 2669, he suggested a nuclear spin of $\frac{1}{2}$; an investigation of the structure of these lines showed that the observed doublet structures do not represent a complete resolution.

Penetration into Potential Barriers in Several Dimensions

By P. L. Kapur and R. Peierls

(*Communicated by R. H. Fowler, F.R.S.—Received* 30 *July* 1937)

The method of geometrical optics is discussed in application to the penetration of particles into regions of negative kinetic energy. It is shown that in the case of problems in more than one dimension which cannot be separated, it is generally possible to derive an upper limit for the probability of penetration, and that in special cases the method gives the actual value of this probability.

The Geometrical Representation of Milne's Kinematical Relativity

By W. H. McCrea

(*Communicated by E. T. Whittaker, F.R.S.—Received* 30 *July* 1937)

It is shown that the assumptions on which Milne's kinematical relativity rests may be translated into the axioms of incidence of projective geometry, together with the usual axioms of order and continuity. The analytical expression of Milne's theory corresponds then to the metrical expression of the geometrical properties achieved in the usual way by the use of an Absolute Quadric. This throws light, in particular, on Milne's introduction of the Lorentz transformation. It also exposes certain restrictions imposed by his assumptions, as compared, for example, with those of general relativity. Further, it makes explicit the degree of arbitrariness allowable in the choice of a "geometry" to represent the properties of the system.

On Anomalous Vibrational Spectra

By M. Blackman, *Trinity College, Cambridge*

(*Communicated by R. H. Fowler, F.R.S.—Received* 4 *August* 1937)

The equation of motion of an elastic continuum is investigated, and it is shown that the continuum becomes unstable when the elastic constants obey certain relations. The vibrational spectrum of lattices for which these relations hold is shown to undergo a characteristic change, the density of normal vibrations going over into the one-dimensional or into the two-dimensional form. The significance of this is considered from the point of view of the specific heat and the vibrational spectrum of actual crystals; it is found that no actual crystals are near enough to the critical regions for the effect of the approach to be apparent in the specific heat, but in some cases this should be noticeable in the vibrational spectrum.

Refractive Dispersion of Organic Compounds

IX—Optical Exaltation in Unsaturated Hydrocarbons containing Conjugated Double Bonds

By (the late) T. M. Lowry, F.R.S. and C. B. Allsopp, M.A., Ph.D.
Laboratory of Physical Chemistry, The University, Cambridge

(*Communicated by R. G. W. Norrish, F.R.S.—Received* 21 *August* 1937)

Optical exaltation appears to be exhibited by a system of two conjugated ethylenic double bonds when these form part of an open chain (e.g. 2 : 4-hexadiene) but not when they are built into a ring (e.g. 1 : 3-*cyclo*hexadiene). The ultra-violet absorption bands of conjugated ring systems are displaced towards lower frequencies relative to those of the corresponding open-chain systems. These effects of configuration on the optical properties of a conjugated system are discussed.

Crystal Growth from Solutions

BY W. F. BERG, PH.D. (BERLIN), PH.D. (MANCHESTER)

(*Communicated by W. L. Bragg, F.R.S.—Received* 21 *August* 1937)

An optical method of measuring the concentration distribution round a growing crystal is described. The flow of molecules at every point of the crystal surface can be determined. The results obtained on sodium chlorate are:

1—The concentration is not constant all over the crystal surface, but is highest at the corners.

2—One has to assume the existence of an adsorbed layer on the crystal surface, and that a lateral flow of molecules takes place in this layer.

3—There is a hitherto unexplained effect influencing the transition of molecules from the solution into the different parts of the adsorbed layer. The influx is smaller at the corners than at the centres of the faces, although the concentration of the solution is higher on the corners.

Measurements of Range and Angle of Projection for the Protons produced in the Photo-Disintegration of Deuterium

BY J. CHADWICK, F.R.S., N. FEATHER AND E. BRETSCHER

(*Received* 8 *September* 1937)

Measurements of range and angle have been made on the tracks of 62 protons produced in an expansion chamber containing a deuterium-rich gas and irradiated by the γ-rays from a radiothorium source. These measurements have been analysed in detail and critically discussed. It is concluded that the determinations of range indicate a binding energy of $2{\cdot}25 \pm 0{\cdot}05 \times 10^6$ e-volts for the deuteron and that the angular distribution implies a considerable preponderance of the photoelectric over the photomagnetic type of disintegration with the radiation employed ($h\nu = 2{\cdot}62 \times 10^6$ e-volts).

Investigations on Magne-crystallic Action V—Para-Magnetic Salts of the Rare Earth and the Iron Groups of Metals

By K. S. Krishnan and A. Mookerji

(*Communicated by Sir Venkata Raman, F.R.S.—Received* 9 *September* 1937)

On the Forces acting between Atoms and Ions and the Physical Properties of Matter in Bulk

By J. A. Wasastjerna

(*Communicated by W. L. Bragg, F.R.S.—Received* 9 *September* 1937)

A method is developed according to which it is possible to analyse, by the aid of accessible experimental data, the question of the dependence of the potential energy on the interatomic distance for atoms and ions with closed shells. The results of the analysis have been made the foundation for a theoretical calculation of a number of physical properties of crystals. In many instances the results of the calculations can be compared with experimental data. In other instances information is obtained concerning data which have previously been entirely unknown or about which great uncertainty has prevailed. Finally, a theoretical interpretation is given to the empirical results. The experimental values of the van der Waals forces both for rare gases and ionic crystals are about twice as large as the theoretical ones, and there is thus a rather serious discrepancy.

Studies of the E Region of the Ionosphere

By J. E. Best, F. T. Farmer and J. A. Ratcliffe

(*Communicated by E. V. Appleton, F.R.S.—Received* 9 *September* 1937)

Statistical Mechanics of the Adsorption of Gases at Solid Surfaces

BY F. J. WILKINS

(*Communicated by R. H. Fowler, F.R.S.—Received* 20 *September* 1937)

The generalized adsorption isotherm is shown to be

$$Cg/Ca = \frac{fg(T)\,B_{Ng}(T)}{fa(T)\,B_{Na}(T)}\,e^{-\phi/RT+\left\{Ng\frac{\partial}{\partial_{Ng}}\log B_{Ng}(T)-Na\frac{\partial}{\partial_{Na}}\log B_{Na}(T)\right\}},$$

where Ca and Cg are the molecular concentrations in the adsorbed and gaseous phases respectively; ϕ is the adsorption potential and $fg(T)$, $fa(T)$, $B_{Ng}(T)$ and $B_{Na}(T)$ are partition functions. These functions have been evaluated for three special cases in which the adsorbed phase is (*a*) a three dimensional gas, (*b*) a gas of two dimensional lateral mobility whose molecules vibrate in a plane perpendicular to the plane of lateral mobility, and (*c*) a group of Planck oscillators with three degrees of freedom.

The relation between ϕ and q, the differential heat of adsorption, is deduced and it is shown that the common practice of calculating from the equation

$$(\partial \log p/\partial T)_x = -q_x/RT^2$$

is erroneous. The correct equation is

$$(\partial \log p/\partial T)_{(x/\alpha d)} = -q/RT^2,$$

where $(x/\alpha d)$ is the concentration in the adsorbed layer.

The Absorption of Argon, Nitrogen and Oxygen on Smooth Platinum Foil at Low Temperatures and Pressures

BY F. J. WILKINS

(*Communicated by R. H. Fowler, F.R.S.—Received* 20 *September* 1937)

The adsorption of argon, nitrogen and oxygen on a smooth platinum foil has been measured at various temperatures between 77 and 193° K. over the pressure range of 5×10^{-3} to 2×10^{-1} mm. It is found that the deviations from the Langmuir adsorption isotherm are greater the lower is the temperature. The values α of the fraction of the apparent surface covered by the gas at saturation is unity only for argon at 77° K. In all other experiments α was much less than unity. Further, the rate of decrease of α with increase of temperature is much more rapid than is given by Zeise's linear equation and can be expressed approximately by

$$\alpha = ce^{-\beta/T},$$

where c and β are constants. After a discussion of the results, using the virial adsorption isotherm, the failure of the Langmuir adsorption isotherm at low temperatures is attributed to the intermolecular forces of attraction which exert a pronounced effect on the amount of gas adsorbed.

The adsorption potentials of argon and nitrogen are calculated to be approximately 5000 and 5500 cal./g. mol. respectively. These compare with the corresponding values calculated from quantum mechanics of 3200 and 1500 cal./g. mol. The possible reasons for the discrepancy are discussed.

An Attempt to Detect the Passage of Helium through a Crystal Lattice at High Temperatures

By Lord Rayleigh, F.R.S.

(*Received* 20 *September* 1937)

It is known that helium will pass through silica glass, even at ordinary temperatures. A plate 1 mm. thick and 1 sq. cm. area will pass about $2{\cdot}5 \times 10^{-1}$ cu. mm./day. In this case the helium probably passes through submicroscopic channels or cracks in the material. No single crystal, so far as has been ascertained, will pass measurable quantities of helium through the lattice at ordinary temperatures.

Mica has now been tested up to a temperature of 415° C. The amount of helium passed, by a plate 1 mm. thick and 1 sq. cm. area, if any, is certainly less than 7×10^{-5} cu. mm./day.

The Behaviour of an Osglim Lamp
III—Osglims in Parallel forming Models of Reciprocal Inhibition

By Lewis F. Richardson, F.R.S.

(*Received* 21 *September* 1937)

Two osglim lamps wired in parallel with one another can be so arranged that the glowing of either inhibits the other. This arrangement is called a "distraction circuit". The lamps are connected through suitable resistances to a battery. An extra stimulus is required to start the extinct lamp. But if a condenser is suitably connected, the apparatus becomes entirely automatic, one or other lamp flashing in a random sequence, but never both lamps together. Although the glowing gas is quite unlike anything in the nervous system, it seems probable that the abstract time-relations of the distraction circuit may be similar to those of a number of psychological and physiological phenomena, such as distraction, or alternations of perspective in line drawings, or reciprocal inhibition.

Experiments with these distraction circuits provide many delicate tests of theories of the osglim lamp. It is shown that the negative slope of the equilibrium potential $\phi_e(u)$ taken in conjunction with the approximate intrinsic equation

$$\phi = \phi_e(u) + b\frac{d\log u}{dt},$$

in which u is current, t time and b is a positive constant, together suffice to explain many of the observed effects; but these hypotheses are inadequate to account for other observations, which however could be explained by the presence of a term of higher order, such as $k\,d\phi/dt$, where $k \geqslant 4 \times 10^{-5}$ sec.

The Production of Neutrons by Bombardment of Beryllium with α-Particles

By T. Bjerge

Institute of Theoretical Physics, Copenhagen

(*Communicated by N. Bohr, For. Mem. R.S.—Received* 21 *September* 1937)

In the energy spectrum of the neutrons from beryllium bombarded with α-particles there are present some groups with energies of several million electron-volts. These are accounted for by the process

$$ {}^{9}_{4}\mathrm{Be} + {}^{4}_{2}\mathrm{He} \rightarrow {}^{12}_{6}\mathrm{C} + {}^{1}_{0}n. \tag{1} $$

The ${}^{12}_{6}\mathrm{C}$ may be left in an excited state and afterwards emit a γ-quantum.

There is also, as shown by Auger and others, a neutron group of energies of the order of *c.* 100,000 e-volts. Auger gave reasons for supposing that these neutrons are created in a process, where the incident α-particle first transfers some energy to the ${}^{9}_{4}\mathrm{Be}$, which then disintegrates in the following way:

$$ {}^{9}_{4}\mathrm{Be} \rightarrow 2\,{}^{4}_{2}\mathrm{He} + {}^{1}_{0}n. \tag{6} $$

This view is supported by the ideas of Bohr on nuclear reactions. The present paper describes experiments which give the yield of the faster and slower neutron group and of the γ-rays as a function of the α-particle energy. It is shown that the slower group is not accompanied by γ-rays, and that it begins to be emitted at the α-particle energy which is just necessary for the process (6) to take place.

Stability of Polyatomic Molecules in Degenerate Electronic States. II—Spin Degeneracy

By H. A. Jahn

(*Communicated by Sir William Bragg, O.M., P.R.S.—*
Received 22 *September* 1937)

It is shown that a polyatomic molecule cannot possess a stable non-linear nuclear configuration in an electronic state having spin degeneracy

unless this degeneracy is the special twofold one which can occur only when the molecule contains an odd number of electrons. Instability caused by the spin alone is shown to be of secondary importance compared with the orbital effects discussed in a previous paper. Table I gives the irreducible two-valued representations of all the point groups and will be useful in discussion of the electronic states of polyatomic molecules containing an odd number of electrons with spin.

Radioactive Nodules from Devonshire

By M. Perutz

(*Communicated by J. D. Bernal, F.R.S.—Received* 28 *September* 1937)

A Second-Order Focusing Mass Spectrograph and Isotopic Weights by the Doublet Method

By F. W. Aston, F.R.S.

(*Received* 29 *September* 1937)

Optical Activity in Ketones. The Rotary Dispersion and Circular Dichroism of *m*-Methyl *Cyclo*hexanone and of Pulegone in their Ketonic Absorption Bands

By the late T. M. Lowry, F.R.S., Delia M. Simpson
and C. B. Allsopp

(*Communicated by R. G. W. Norrish, F.R.S.—Received* 1 *October* 1937)

Molecular extinction coefficients, circular dichroism and rotatory dispersion are recorded for *m*-methyl *cyclo*hexanone and for pulegone in the region of their ultraviolet absorption bands. Analysis of the rotatory dispersion on the basis of the observed circular dichrosim shows that the

partial rotation due to the ketonic absorption band of methyl *cyclo*hexanone is much greater than that of the single asymmetric carbon atom, and is opposite in sign. A similar result is obtained for pulegone, despite the conjugation of carbonyl and ethylenic double bonds. By comparison with the data for other optically active ketones containing more than one asymmetric carbon atom, it is concluded that in general the direct contribution of each asymmetric centre is itself small relative to that of the chromophoric group. In the light of Mulliken's analysis of the electronic configurations of aldehydes, the optical activity of the carbonyl group is now attributed to the lone-pair electrons of the oxygen atom, and the theory of "induced dissymmetry" is reinterpreted. A possible function of lone-pairs in producing optical activity in other types of compound is discussed.

On the Penetrating Component of Cosmic Radiation

BY H. J. BHABHA

(*Communicated by R. H. Fowler, F.R.S.—Received* 4 *October* 1937)

An analysis of the experimental data is carried through to show that a "break down" theory for radiation loss of electrons cannot explain (1) the latitude effect at sea level from latitudes of 35 to 50°, (2) the large number of particles found at sea level in the difference curves of Bowen, Millikan and Neher for charged particles of 10^{10} e-volts, (3) the shape of the transition curve for large bursts. All these facts can be explained by assuming that the penetrating component consists of new particles with masses between those of the electron and proton. But in order to explain the energy loss measurements of Blackett and Wilson, one must then assume that these particles suffer large energy losses in addition to the ordinary Bremstrahlung which must vary in different substances as Z rather than Z^2, as for example a change in the rest mass of the particles.

The radiation loss and the pair-creation cross-sections taking screening into account accurately for "heavy" electrons are calculated. The frequency of the production of showers of different sizes by such heavy electrons as also the intensity of electrons in equilibrium with such particles forming a soft component are also calculated, and it is shown that

though both these are somewhat larger in heavier elements, the variation is much less than a Z^2 law would give.

If such heavy electrons can be created as usual in pairs, then a part of the hard component at sea level could consist of heavy electrons of mass $10m$ created by the soft component in the upper atmosphere.

It is shown that there are reasons to suppose that the uppermost layers of the atmosphere are more absorbing than one should expect from their mass. This may be due to the fact that the atoms in these layers are largely ionized.

On the Diamagnetic Susceptibility of Bismuth

By M. Blackman

(*Communicated by R. H. Fowler, F.R.S.—Received* 4 *October* 1937)

An extension is made of the existing theory of the marked variation of the susceptibility of bismuth with field strength at low temperatures (known as the de Haas-van Alphen effect). The object of the investigation is to explain the finer features of the experiments, to account for the order of magnitude of the effect and for the dependence on the orientation of the binary axes. The extension consists in assuming a more general form for the relevant part of the surface of constant energy of the electrons. It is found possible to account for all the features of the susceptibility curves and also to fit the experimental curves fairly well. For this purpose one has to assume that the motion of the electrons is violently anisotropic and that only a small fraction of the conduction electrons contribute to the de Haas-van Alphen effect.

Production and Dissipation of Vorticity in a Turbulent Fluid

By G. I. Taylor, F.R.S.

(*Received* 6 *October* 1937)

When isotropic turbulence is set up in a fluid, e.g. by moving a grid of regularly spaced particles through it, the average vorticity decreases with time;

this decrease is due to viscosity. Recently von Karman has calculated the rate at which vorticity is destroyed by viscosity. His equation involves only quantities which can be measured in a wind tunnel by means of the hot wire technique. These quantities have now been measured in one case, and the rate of decrease in the mean square of the vorticity has also been measured. In this case it is proved that the rate of destruction of vorticity by viscosity is four times as great as the rate at which vorticity disappears. Vorticity is therefore being produced by extension of vortex filaments three times as fast as it is disappearing.

It seems that the stretching of vortex filaments must be regarded as the principal mechanical cause of the high rate of dissipation which is associated with turbulent motion.

The Buckling of Grids of Stringers and Ribs

By H. L. Cox, B.A. and H. E. Smith, B.Sc.

Both of the Engineering Department, National Physical Laboratory

(*Communicated by H. J. Gough, F.R.S.—Received* 6 *October* 1937)

The paper describes a theoretical analysis of the stability of a plane rectangular grid consisting of two sets of parallel members (stringers and ribs) intersecting at right angles, when loaded in compression parallel to one set of members (the stringers). Both sets are composed of a number of similar members of uniform section, spaced uniformly, and the ends of all the members are held in the original plane of the grid. The exact solution of this problem appropriate to certain special edge conditions is obtained both by consideration of the equations of equilibrium and by the Rayleigh-Ritz energy method, and the results are compared with previous solutions obtained by an approximate method.

The Emission Band Spectrum of Chlorine (Cl_2^+).—II

By A. Elliott and W. H. B. Cameron

(*Communicated by S. R. Milner, F.R.S.—Received* 7 *October* 1937)

The Hydrolysis of the Methyl Halides

By E. A. Moelwyn-Hughes

(*Communicated by E. K. Rideal, F.R.S.—Received* 19 *October* 1937)

For a chemical reaction proceeding with measurable rate, the most significant single constant is the energy of activation, found by the familiar method of Arrhenius. The value obtained is, in the majority of known cases, a true constant over the accessible temperature regions. In the case of the catalysed hydrolysis of some complicated molecules, namely the glykosides, it has, however, been found (1934) that the energy of activation falls markedly with a rise in temperature. As the result carried significant theoretical consequences, it became necessary to give an experimental answer to the question as to whether this fall was specific to the acidic hydrolyses of glykosides, or of a more general character. In the present work, we have investigated the uncatalysed and uncomplicated hydrolysis of some very simple molecules, namely the methyl halides, and have found that in these cases also the Arrhenius constant falls as the temperature is raised.

The fall effect seems to be most pronounced in, if not confined to, reactions involving collisions between solute and solvent molecules, and as far as can be judged is always negative. The conclusion is confirmed by collateral evidence on the mutarotation of glucose and the decomposition of oxalic acid.

At least three causes are recognized as responsible for the total effect. They are (1) the distribution of energy among a number of oscillators, (2) the electrostatic interaction of the polar molecules of solute and solvent, and (3) the frequency of the rotation of a solute molecule in the solvent atmosphere.

On the Solution of the Laminar Boundary Layer Equations

By L. Howarth

(*Communicated by L. Bairstow, F.R.S.—Received* 20 *October* 1937)

Part I. The problem of the flow along a flat plate placed edgewise to a steady stream, when a retarding pressure gradient varying linearly as the distance x from the leading edge of the plate is superposed, is discussed. If y denotes distance measured perpendicular to the plate, a solution is obtained in the form of a power series in x whose coefficients are functions of $y/x^{\frac{1}{2}}$. Differential equations are obtained for these coefficients. Seven of the coefficients have been obtained with reasonable accuracy and the eighth and ninth roughly. Unfortunately it appears that about eight more terms are required to carry the solution to the point of separation; the work involved in their determination is prohibitive. Two approximate methods have been developed for determining the error when the first seven terms of the series are used as an approximation. These methods lead to the determination of the point of separation and are in agreement as to its position. If b_0 is the velocity at the edge of the boundary layer at the leading edge of the plate and b_1 is the velocity gradient, separation is found when $b_1x/b_0 = 0{\cdot}120$.

Part II. A method is developed for the solution of the boundary layer equations in any retarded region. It is obtained by replacing the velocity distribution at the edge of the boundary layer by a circumscribing polygon of infinitesimal sides and applying the preceding solution to each of these sides, making the momentum integral continuous at each vertex. The problem is thereby reduced to the solution of a first order differential equation.

The Theory of the Photolysis of Silver Bromide and the Photographic Latent Image

By R. W. Gurney and N. F. Mott, F.R.S.

(*Received* 21 *October* 1937)

An attempt is made to explain the photolysis of silver halides in terms of the concepts of atomic physics. The mechanism by which the silver atoms formed by the light coagulate to form specks of metallic silver is discussed. The ideas used in this discussion are then turned to the photographic latent image, and are shown to account qualitatively for the variation of developed density with temperature, and, for given exposure, with intensity of light. A brief discussion is given of the Herschel effect, and of sensitization by dyes.

Self-consistent Field, with Exchange, for Calcium

By D. R. Hartree, F.R.S. and W. Hartree

(*Received* 27 *October* 1937)

Calculations of the self-consistent field, with exchange, have been made for Ca^{++}, and the results are given.

Solutions of Fock's equations, without allowance for the perturbation of the core by the series electrons, have also been carried out for the $(4s)$, $(4p)$ and $(3d)$ states of Ca^{+} and $(4s)^2$, $(4s)(4p)$ ^3P and ^1P states of neutral Ca. Energy values for all these states have been calculated and are composed with the observed values; it appears that exchange effects have considerable influence on the relative strengths of binding of a $(4s)$ and a $(3d)$ electron, and so are significant from the point of view of the position of the beginning of the transition group of elements in the periodic table.

Transition probabilities have also been calculated for the $(4s)$–$(4p)$ and $(3d)$–$(4p)$ transitions of Ca^{+} and the $(4s)^2$–$(4s)(4p)$ singlet transition of neutral Ca; these transitions all give lines of astrophysical interest, and absolute values of transition probabilities may have astrophysical applications.

The Continuous Absorption Spectra of Alkyl Iodides and Alkyl Bromides and their Quantal Interpretation

By D. Porret and C. F. Goodeve

(*Communicated by F. G. Donnan, F.R.S.—Received* 27 *October* 1937)

The extinction coefficient curve for methyl iodide has been analysed according to the method used by Fink and Goodeve, and the existence of two bands has been deduced. The upper potential energy curves corresponding to these bands have been determined.

The extinction coefficients of ethyl iodide and of ethyl and butyl bromides have been determined over a wide range. Influence of the carbon chain has been found to be small. The conditions under which chromophoric groupings retain their individuality have been discussed.

The Measurement of Particle Size by the X-ray Method

By F. W. Jones

(*Communicated by W. L. Bragg, F.R.S.—Received* 23 *October* 1937)

Laue's theory of the broadening of the X-ray diffraction lines by small particles has been discussed and a different value of a constant ω is found. New methods applicable to any type of Debye-Scherrer camera are given for correcting the line breadths for the effect of experimental conditions and the separation of the α-doublet. As an example of the use of these methods a specimen of colloidal gold has been examined and the particle size and shape determined, the procedure in the shape determination having been simplified and made of general use by means of "shape-curves". An attempt has been made to estimate the order of the error introduced by the particle size distribution.

Resolution and Interpretation of the Luminescent Spectra of some Solids at Low Temperatures

By J. Ewles

(*Communicated by R. Whiddington, F.R.S.—Received* 23 *October* 1937)

Resolution of the cathode luminescent spectra of some solids has been obtained at the temperature of liquid air. It is suggested that the spectra may be accounted for as electron vibration bands derived from a neutral metallic atom or an ion of the parent lattice still associated with the lattice. This idea is found to account for the luminescent spectra of a number of solids—some investigated under cathode ray excitation by the writer and some under various modes of excitation by other workers. A possible explanation of some types of phosphorescence is outlined—based on the frequent occurrence of metastable levels in the suggested atomic transitions.

The Infra-red Absorption Spectrum of Methylene Chloride

By C. Cain and G. B. B. M. Sutherland

(*Communicated by R. G. W. Norrish, F.R.S.—Received* 24 *October* 1937)

The Infra-red Absorption Spectrum of Methylene Chloride

By C. Cain and G. B. B. M. Sutherland

(*Communicated by R. G. W. Norrish, F.R.S.—Received* 29 *October* 1937)

The infra-red absorption spectrum of methylene chloride has been examined between 2μ and 12μ with a prism spectrometer. Twenty-six bands have been observed of which sixteen are recorded for the first time. The agreement with earlier experimental work on the vibration spectrum of this molecule is satisfactory. In particular, the existence of a very intense absorption band which cannot be accounted for on the current assignment of fundamental frequencies has been confirmed. The explanation of this absorption band has necessitated a reinterpretation of the whole vibrational spectrum. This has been done using (1) the method of semi-independent groups, (2) an application of the isotope effect in polyatomic molecules of the type YX_4. The latter method is a surprisingly successful way of approximating to the "inter-group" frequencies of a polyatomic molecule and should be capable of wide application in this field.

Two New Echinoidea from the Upper Silurian of Girvan

By E. W. MacBride, F.R.S. and W. K. Spencer, F.R.S.

(*Received* 25 *August* 1937)

The communication deals with two new Echinoids from the Ordovician and a new form interpreted as the first known plated Holothurian.

The new Echinoids are important because they prove that typical Palaeozoic Echinoidea, which characteristically differ in many important characters from later Echinoidea, existed in the Ordovician. Previously it had been supposed that a form with very different build, *Bothriocidaris*, was the typical Ordovician Echinoid. The new forms in consequence have important bearing on the Echinoid ancestry and evolution. They are very well preserved, giving views both of the outer portions of the test and the test interior and are easier to study than any of the later Palaeozoic forms. A rather surprising discovery is that one of the Echinoidea is elongated

and bilaterally symmetrical, somewhat like a recent Heart Urchin but with a different plane of symmetry.

At least one Holothurian, *Cucumaria*, is known to have a plated test in an early developmental stage. It is consequently of considerable interest that a plated Holothurian is now known to occur in the early Palaeozoic. The form in most respects has a marked resemblance to an Echinoid and is very good evidence of the view that Echinoids and Holothurians are nearly related. It is suggested that the Echinoids show distinct relationship with the primitive starfish but detailed homologies between starfish, Echinoids and Holothurians are reserved for a later paper.

On Individual Variations in Ability to Acclimatize to High Altitudes

By A. Keys, B. H. C. Matthews, W. H. Forbes,
R. A. McFarland and D. B. Dill

(*Communicated by Sir Joseph Barcroft, F.R.S.—Received* 31 *March* 1937)

1. The International High Altitude Expedition made observations at sea level, 9000, 12,000, 16,000 and 20,000 ft. of the physiological constitution of ten normal subjects. An attempt is now made to correlate these observations with acclimatization.

2. The capability of acclimatization of the members of the party was graded by a questionnaire to which all gave answers as to the deviation in physical and mental performance from their sea level values, of all members of the party. By this classification the members of the party were arranged in order at each altitude.

3. A number of physiological properties were observed at sea level, and at each station. No one of these yielded a good correlation with the classification referred to in paragraph 2 (above), but the whole series taken together with suitable empirical coefficients yield a good correlation with the acclimatization classification. So much so as to encourage the belief that it would thus be possible to predict from sea level measurements whether an individual would acclimatize well or badly.

Electrotonus and Excitation

By H. Rosenberg

(*Communicated by A. V. Hill, Sec.R.S.—Received* 4 *May* 1937)

When an electric current is applied to a nerve a potential difference across the axon membrane is developed. It has previously been suggested that this potential is the intrinsic stimulus, and that the attainment of a certain critical potential beneath the stimulating pole is the threshold condition for excitation. On the basis of the core-conductor theory it is assumed that this potential is measured when the electrotonic potential between the pole and a distant extrapolar point is determined. New experimental evidence with respect to this conception is submitted and related with the physical theory of excitation in nerve (Hill). The main results are:

The voltage-capacity relation for constant subliminal electrotonus fits closely the theoretical curve which represents the data for threshold stimulation with condenser discharges. Similarly the intensity-frequency relation of electrotonus is in agreement with theory and experiment of threshold stimulation by sinusoidal currents within a certain frequency range (300 and 3000 hz.). The time constants derived from observations on electrotonus at the cathode are only about half of those obtained in excitation. If, however, the time constants are determined for catelectrotonus at a short distance from the pole, they are comparable with those found in excitation. Hence the hypothesis is advanced that the establishment of a gradient of critical potential along a finite length of nerve is the threshold condition for excitation. Other possibilities are discussed.

The Effect of Temperature on the Photochemical Bleaching of Visual Purple Solutions

By H. J. A. Dartnall, C. F. Goodeve and R. J. Lythgoe

(*Communicated by Sir John Parsons, F.R.S.—Received* 5 *May* 1937)

Using a new method of extraction, the authors have prepared solutions of visual purple much freer from foreign matter than those obtained

hitherto. Photochemical bleaching curves have been obtained using monochromatic light, with the solutions at various temperatures from 5–60° C. The theoretical treatment of bleaching curves developed in a previous paper (*Proc. Roy. Soc.* A, 1936, **156**, 158) has been extended to allow corrections to be made for the thermal bleaching occurring at the higher temperatures. Anomalous effects were found to occur at 10–15° C. owing to the production of a coloured substance "transient orange" and its decomposition. At lower temperatures this substance was found to be stable and it has been shown that the theoretical equation for the bleaching curve applied also in this range.

The results of 25 experiments showed that the extinction coefficient and the quantum efficiency are both independent of temperature and *p*H. Further arguments are put forward to support the contention that the quantum efficiency of the bleaching process is 1 or not much less than 1. On this basis a value for the molar extinction coefficient is derived which is found to be normal for this type of chromophoric grouping.

The Monaural Threshold

BY J. W. HUGHES

(*Communicated by T. Graham Brown, F.R.S.—Received* 26 *May* 1937)

The change of threshold intensity in one ear when a note of fixed subliminal intensity is sounded in the other has been determined by direct experiment. The results of the investigation show that for two notes in unison, the total energy required in the two ears at the "binaural threshold" is equal to the energy required in one ear at the monaural threshold, independently of the actual division of energy between the two ears. For two notes of different frequencies, the result still holds good in the form

$$\left(\frac{E_1}{E_0}\right)_R + \left(\frac{E_1}{E_0}\right)_L = 1,$$

where E_0 represents the monaural threshold intensity, and E_1 the intensity of the note present in the same ear at the binaural threshold, the subscripts R and L referring to the two ears. The bearing of the results on the theory of hearing is discussed.

The External Mechanics of the Chromosomes
VI—The Behaviour of the Centromere at Meiosis

By Margaret Upcott

(*Communicated by Sir Daniel Hall—Received* 26 *June* 1937)

The Control of Beating and of Micro-fibrillation by Means of Potassium, Calcium and Sodium in the Chick Embryo Heart
I—Calcium Fibrillation and the Control of Beating

By P. D. F. Murray

(*Communicated by Sir Henry Dale, F.R.S.—Received* 12 *July* 1937)

The principal experimental results are summarized in Table VIII. The numbers in square brackets in the summary refer to the numbers of experiments in this table.

(1) The effect of various solutions on the heart was studied [1–5]; in the majority of experiments [7–21] two or three solutions were used with the object of examining the effect of each solution on hearts previously treated with various other solutions.

(2) Hearts which had been treated with media lacking potassium were readily thrown into fibrillation by small quantities of calcium ($CaCl_2$ 0·03 %) [7, 8, 9, 10], but if small quantities of potassium (KCl 0·06 %) were present in the first solution, this protected them against the fibrillating action of small quantities of calcium in the second [5, 14, 15, 16, 17].

(3) When hearts treated with solutions lacking potassium were transferred to solutions containing calcium, but not potassium, fibrillation occurred, and was not transient [10]. But if the second solution contained both potassium and calcium, fibrillation was transient, ceasing in a few minutes [7, 8, 9].

(4) The observations recorded in a separate paper (Watchorn and Murray) show that potassium was lost from hearts when they were treated in solutions lacking potassium. There is indirect evidence that potassium was also lost in $Na+k$ [16].

(5) It is concluded (discussion) that fibrillation in the medium depends upon an abnormally high ratio between calcium at the cell surface and potassium in the cell interior, i.e. on Ca_s/K_i.

(6) Stimulation of the beat (strengthening, or restoration after loss) occurred when the hearts were transferred to a solution containing more or relatively more calcium than was present in the first solution [5, 7, 10, 14, 15, 16], unless the effect was prevented by the presence of large quantities of potassium [8, 9, 17]. If the hearts were not potassium-poor, the improved beating was maintained for long periods [14, 15, 16], but if the hearts were potassium-poor the stimulation was at once followed by stoppage of the beat. If the second solution contained no potassium the stoppage was permanent [10]; but if the second solution contained small quantities of potassium the beat subsequently returned [7].

(7) When hearts were transferred to solutions containing more, or relatively more, potassium than the first solution (but not more calcium unless potassium greatly preponderated over it), the beat was depressed or stopped [4, 8, 9, 11, 12, 13, 17, 18, 19, 21]. The inhibitory effect of potassium appeared much more rapidly if the hearts were potassium-poor than if they were not.

(8) From these and a large number of other facts it is concluded (discussion) that the influence upon beating of potassium and calcium in the medium depends upon the ratio between potassium and calcium at the cell surfaces and potassium in the cell interiors (i.e. upon Ca_s/K_i and K_s/K_i), but not upon the ratio between the two ions at the surface (i.e. Ca_s/K_s) except in so far as this affects Ca_s/K_i and K_s/K_i. Rise of the ratio K_s/K_i is inhibitory of beating, of Ca_s/K_i stimulatory, provided it does not rise too high, when it stops beating and induces fibrillation.

The Royal Society Expedition to Montserrat, B.W.I.
The Volcanic History and Petrology of Montserrat, with Observations on Mt. Pelé in Martinique

By A. G. MacGregor

(*Communicated by E. B. Bailey, F.R.S.—Received* 20 *July* 1937)

Oscillographic Study of Electron Transfer by Yellow Ferment and by Cytochromes during Muscular Contraction

By F. Urban and H. B. Peugnet

(*Communicated by D. Keilin, F.R.S.—Received* 18 *August* 1937)

An apparatus is described which records instantaneous changes in the absorption spectrum of muscle.

By means of this apparatus, it is shown that *yellow ferment* and cytochrome *c* are active during the aerobic contraction phase of a gastrocnemius muscle.

Stimulation of the Corpora Lutea of the Rat by Means of Progesterone and Testosterone

By T. McKeown and S. Zuckerman
Department of Human Anatomy, Oxford

(*Communicated by W. E. Le Gros Clark, F.R.S.—Received* 25 *August* 1937)

Normally cyclic female rats were injected with testosterone propionate or progesterone daily for from 9 to 11 days. At autopsy several recent corpora lutea were seen in the ovaries of all the experimental animals. The activity of these corpora is indicated by progestational changes in the uterus and by the production of a deciduoma in one of the rats that had been injected with testosterone. Similar endometrial changes were not induced in spayed rats that were injected with oestrone followed by testosterone or with testosterone alone. The luteinization observed in the ovaries was either a direct effect of the injections, or an indirect one due to the suppression of follicles.

Loss of Potassium from Embryonic Chick Hearts in Potassium-free Media with and without Calcium

By E. Watchorn and P. D. F. Murray

(*Communicated by Sir Henry Dale, F.R.S.—Received* 26 *August* 1937)

Factors Influencing the Effectiveness of Administered Hormones

By R. Deanesly and A. S. Parkes, F.R.S.

(*Received* 9 *September* 1937)

1. Further work has been carried out on the relation between method of administration and effectiveness of hormone preparations.

2. The response of the capon's comb and of the accessory glands of the castrated rat has been used in the study of androgenic activity and the response of the plumage of the Brown Leghorn capon in that of gynogenic activity.

3. Experiments are described on the degree of subdivision of the total dose, nature of the solvent, addition of fatty acid to the solution, esterification of the hormone, volume of medium and route of administration.

4. The influence of these different variables may be quite different for different substances, and it is concluded that no valid quantitative comparison of two compounds can be made without a careful examination of the conditions necessary for maximum effectiveness.

5. Certain of the free hormones show greatly increased effectiveness when given in dry form by the subcutaneous implantation of tablets or crystals. Recovery of the residue of the tablet from the rat after a ten-day period of experiment has made it possible to estimate the amount of hormone actually absorbed, and successive implantations of the same tablet to successive groups of rats has enabled the maximum effectiveness of a given dose to be determined.

6. The esters lose their increased effectiveness when given by intraperitoneal or intravenous injection and it is concluded that the prolongation of action by esterification is due to delay of absorption from the site of injection rather than to slow hydrolysis of the compound after absorption.

7. In general, it seems that the free hormones lose their inferiority to the esters if the method of administration ensures slow absorption, whereas the esters lose their superiority to the free hormones if absorption is rapid or instantaneous.

Studies on the Onychophora. IV

By S. M. Manton

(*Communicated by W. T. Calman, F.R.S.—Received* 15 *September* 1937)

1. The passage of spermatozoa to the ovarian lumen from the spermatophores attached to the body of the female is described.

2. Following the deposition of a spermatophore, leucocytes invade the subcutaneous region and break through the ectoderm. The cuticle of the body and the lower wall of the spermatophore are ruptured.

3. Spermatozoa swim from the spermatophore through the perforated cuticle and ectoderm and reach the vascular spaces. They pass through the haemocoel by their own activity and reach the ovary.

4. Clumps of spermatozoa force their way through the ovarian wall to reach its lumen.

5. The spermatophore wall remains attached to the cuticle, so closing the wound caused by the entry of the spermatozoa. The ectoderm regenerates and forms a new cuticle which is exposed at the next ecdysis.

6. The earliest oogonia in adult animals lie freely in the ovarian lumen among the spermatozoa. Their cytoplasm is invaded by sperm heads. They divide to form ova which absorb the sperm heads and grow.

7. Each ovum sinks into the germinal ridge epithelium. The formation of the egg follicle and ovarian egg membrane are described.

8. The ripe ovum passes through the follicle stalk back to the ovarian lumen. Here it emerges from the egg membrane. Fertilization takes place and the egg passes down the oviduct. The fertilized egg swells rapidly and a membrane is formed round it, which is probably the fertilization membrane. The oviduct secretes a second very thick membrane outside the first; only this second membrane persists during embryonic life.

9. The spermatozoa in the ovary (1) fertilize the eggs, (2) provide the early ova with nutriment necessary for their growth, and (3) may supply the animal with nourishment or other special substances.

Studies in Stimulation Phenomena in Plants due to *Bacterium solanacearum*

By B. J. Grieve

(*Communicated by A. J. Ewart, F.R.S.—Received* 21 *September* 1937)

1. A detailed study has been made of petiole-epinasty in plants invaded by the vascular parasite, *Bacterium solanacearum* E.F.S. It has been shown to be an irreversible growth reaction and has been demonstrated to occur in infected potato, tomato, castor oil and African Marigold plants.

2. The reaction has been shown to occur mainly when invasion of the petioles is unilateral or apparently unilateral. It may also occur before the invading organisms enter the petiolar bundle.

3. Petiole-epinasty is conditioned by the plant variety, its size, the point of inoculation, and by environmental conditions. A high water content in potentially reactive petioles is a necessary condition for the occurrence of the growth reaction.

4. The growth reaction has been shown to be independent of gravity.

5. Experiments designed to determine the proximate cause of petiole-epinasty showed that the bacterial secretion heteroauxin, while being produced in culture media, was not produced in sufficient amount in the invaded vessels to bring about the growth reaction. Tests to determine whether the alkaline reaction in invaded vessels, or the ammonia to which it is largely due, was a causal factor in petiole-epinasty, gave negative results. It was found, however, that the opposite condition of hyponasty could be induced in plant parts by placing them in certain acid buffer solutions. The evidence points to the conclusion that it is some toxic by-product of bacterial metabolism, as yet unidentified, which acts as the proximate cause of the reaction.

6. A possible mechanism of the growth reaction is suggested and the importance of the water factor in relation to this is discussed.

The Effect of Freezing on Bacteria

By R. B. Haines

(*Communicated by Sir Joseph Barcroft, F.R.S.—*
Received 25 *September* 1937)

1. Rapid freezing of aqueous suspensions of bacteria under defined conditions leads to death of a constant proportion of the cells, varying

from about 80 % with the most sensitive organism, *B. pyocyaneus*, to little or none with spores.

2. The temperature or rate of freezing appears to have little effect on the mortality within specified limits.

3. Storage of aqueous suspensions of bacteria in the frozen state at temperatures from -1 to -20° C. gives a most rapid rate of death near the highest temperature of storage.

4. It is shown that storage at -2° C. of a frozen solution of the native cellular proteins of *B. pyocyaneus*, extracted at low temperature, leads to rapid coagulation of one fraction of the proteins. Such flocculation is negligible at -20° C.

5. It is suggested either that two factors are responsible for the death of the bacterial cell on freezing: one unknown, but apparently not mechanical, and the other, some change leading to flocculation of the cellular proteins; or else that there is in reality one process, leading to coagulation, but with a time-lag, so that coagulation is not found on immediate freezing and thawing.

Dominance in Poultry; Feathered Feet, Rose Comb Internal Pigment and Pile

By R. A. Fisher, F.R.S.

(*Received* 27 *September* 1937)

The Suppression of Oestrus in the Rat during Pregnancy and Lactation

By T. McKeown and S. Zuckerman

From the Department of Human Anatomy, Oxford

(*Communicated by W. E. Le Gros Clark—Received* 5 *October* 1937)

Destruction of the corpora lutea of both ovaries of seven rats by means of a thermocautery at various times between the third and seventh days of pseudopregnancy led to the reappearance of oestrus within 4 days (experimental dioestrus of 7 to 11 days). The control pseudopregnancy in five unoperated animals lasted 12 to 15 days.

The corpora lutea of three pregnant animals were destroyed and the foetuses and placentae were removed on the 6th, 6th and 7th days of gestation respectively. Oestrus occurred 4, 7 and 3 days later respectively. The corpora alone were destroyed in two pregnant animals on the 4th and 5th days of gestation; oestrus reappeared on the 8th and 9th days respectively. In three control operations Caesarian section on the 6th, 7th and 7th days led to the reappearance of oestrus on the 12th, 14th and 14th days respectively.

Oestrus did not follow destruction of the corpora lutea of 12 rats which were operated on at various times between the 11th and 16th days of pregnancy. Two of these animals aborted as the result of the operation and most of the others showed partial resorption of the uterine contents. In only one was pregnancy normal.

Oestrus did not occur in four lactating animals that were left with their litters after destruction of the corpora lutea of both ovaries. Oestrus reappeared within six days in seven of eight lactating animals that were weaned soon after the same operation.

These facts show that the placentae as well as the corpora lutea have the power of suppressing oestrus, and that the progestin-threshold for the inhibition of oestrus in the second half of pregnancy is relatively low. The suppression of oestrus during lactation is probably due to the lack of follicle-stimulating hormone, but both the corpora lutea and the lactogenic hormone of the pituitary are also able to inhibit oestrus.

Progonadotropic sera

By I. W. Rowlands

(*Communicated by A. S. Parkes, F.R.S.—Received* 20 *October* 1937)

The serum of a sheep receiving a course of injections of extract of sheep pituitary did not show antigonadotropic activity, but possessed the power to augment the activity of an extract prepared from the same species on test rats.

The serum of a goat injected with pig pituitary extract augmented the action of pig, sheep and ox pituitary extracts in promoting ovarian growth in the immature rat; at the same time, this serum inhibited the ovulation-producing activity of the same extract of pig pituitary in the oestrous rabbit. The serum also inhibited the gonadotropic action on the rat ovary of extracts of horse pituitary, pregnant mare serum and human urine of pregnancy.

This augmentatory action is perhaps explicable by reference to Evans's pituitary antagonist.

The Specificity of Antigonadotropic Sera

BY I. W. ROWLANDS

(*Communicated by A. S. Parkes, F.R.S.—Received* 20 *October* 1937)

The specificity of various antigonadotropic sera has been investigated, and an attempt has been made to classify the reactions according to "species-specificity" and "source-specificity".

Antisera were obtained to gonadotropic extracts of ox pituitary, horse pituitary, human urine of pregnancy and pregnant mare serum. All were prepared in rabbits, except an additional antiserum to urine of pregnancy extract which was prepared in a goat. The activity of the antisera was tested by their ability to inhibit the effects on immature rats and oestrous rabbits of gonadotropic extracts of horse, ox, sheep, pig and human pituitaries, human and mare pregnancy serum and human urine of pregnancy and placenta.

Complete "species-specificity" is shown by the reaction of the antisera to gonadotropic extracts of human urine of pregnancy and pregnant mare serum, whereas antisera to similar extracts of pituitary origin exhibit only incomplete "species-specificity". Complete "source-specificity", on the other hand, is only found in the reactions of the antiserum to gonadotropic extracts of pregnant mare serum.

The difficulties encountered in the interpretation of these results and their bearing on the probable occurrence in the pituitary of separate follicle-stimulating and luteinizing hormones and of a gonadotropic antagonist is discussed, and it is concluded that much more evidence is required before such specificity as is shown by antigonadotropic sera can be ascribed to immunological factors.

The Effect of Sex Hormones on Lactation in the Rat

By S. J. Folley and S. K. Kon

National Institute for Research in Dairying, University of Reading

(*Communicated by A. S. Parkes, F.R.S.—Received* 20 *October* 1937)

1. Administration of oestradiol monobenzoate (approximately 0·3 mg. per 100 g. body weight daily) to intact lactating rats causes a marked inhibition of lactation.

2. In rats ovariectomized on the day following parturition, the inhibitory effect of similar doses of oestradiol monobenzoate, while definite, was much less marked.

3. Testosterone propionate (approximately 0·4 mg. per 100 g. body weight daily) administered to lactating rats also inhibited lactation, while progesterone and androsterone in doses of approximately 0·3 mg. per 100 g. body weight daily had no effect on lactation.

4. Rats ovariectomized on the day following parturition and then given daily injections of sesame oil lactated satisfactorily.

5. The bearing of these results on the theoretical aspect of lactation is discussed.

The Genetical and Mechanical Properties of the Sex-chromosomes

IV. The Golden Hamster

By P. C. Koller

(*Institute of Animal Genetics, University of Edinburgh*)

(*Communicated by A. S. Parkes, F.R.S.—Received* 20 *October* 1937)

1. The diploid number of chromosomes in the golden hamster (*Cricetus auratus*) is 38. The chromosomes at mitotic metaphase show differences in size and shape.

2. The sex chromosomes are the largest of the complement. The *X* and *Y* chromosomes of the male are morphologically very alike and show no significant size difference. They are approximately 4·5–5 long, and have

a subterminal centromere. The ratio of the length of the two arms is about 1 : 4.

3. During meiotic prophase the sex complex is composed of two regions; one a precociously condensed, the other non-condensed or diffuse. The former is identified as the associated homologous or pairing segments of the *X* and *Y*; the latter gives rise to the differential segment of the *X*.

4. Two types of sex bivalent are formed with unequal frequency at meiotic metaphase; asymmetrical (81·6 %), indicating pre-reduction, and symmetrical (18·4 %) conditioning the post-reductional segregation of the differential segment.

5. The centromere is localized in the pairing segment; consequently chiasmata representing genetical crossing-over between the *X* and *Y* chromosomes, can be formed on both sides of the centromere. At metaphase the chiasma-frequency in the sex bivalent is less than in the autosomal bivalents.

6. The sex chromosomes are unpaired or fail to form chiasmata after pairing in about 8 % of the primary spermatocytes. The failure is brought about by the strong precocity of the pairing segment.

7. Analysis of the morphological structure and behaviour of the differential segment suggests that at meiotic metaphase it has minor relic and interchromatid relational coiling. Coils, which are characteristic of the pairing segment and of the autosomal bivalents, are absent.

8. It is predicted that in hamster there are great numbers of genes, which will exhibit very little sex linkage, though they are borne in the sex chromosomes. These genes are localized in the pairing segment of the *X* and *Y*.

The Geological History of the Lake Rudolf Basin

By V. E. Fuchs, M.A., Ph.D.

(*Communicated by O. T. Jones, F.R.S.—Received* 25 *October* 1937)

This is an account of the geology of an area the greater part of which has not been described. It is important because it includes the northern continuation of the Kenya Rift Valley fractures and because it extends to the Central African region of which the climatic and volcanic history is known.

The first movements which affected the region began in the late Oligocene and continued periodically into the Upper Pleistocene. Particular interest is attached to these movements for not only do they form the northern continuation of the Kenya fractures, but there is some evidence in this region that they were of a compressive nature.

The initial fracture cut off the north extension of the late Oligocene peneplain of Uganda, and upon its downthrow side a series of Miocene sediments and volcanics accumulated. The former are correlated with Gregory's Nyasan (Kamasian) deposits of the Baringo area in the south. The whole Miocene series was then folded from east to west and accompanied by faulting; these Pliocene movements gave rise to the topography of the early Pleistocene lake basin. The deposits formed in the latter were disturbed by still later movements which, accompanied by vulcanicity, completed the lake basin in its present form.

Today the lake does not occupy so large an area as it did because fluctuating but progressive desiccation has lowered its level by more than 300 ft. since Acheulian times. Everywhere its past high-water marks are defined by lake beaches containing mammalian and molluscan remains together with the stone implements of early man. An interpretation of the evidence afforded by these beaches is offered and the events within the Lake Rudolf Basin are correlated with those already known in Kenya and Uganda. Modern conditions indicate that the desiccation of the area still continues.

ABSTRACTS

OF PAPERS COMMUNICATED TO THE ROYAL SOCIETY OF LONDON

In accordance with a resolution of Council, summaries or abstracts of papers are to be published as soon as practicable. The publication of such abstracts in no way indicates that the papers have been accepted for publication in any fuller form. These abstracts will be issued for convenience with the "Proceedings of the Royal Society of London" but do not form a part of the "Proceedings".

---

7 December 1937

Significance Tests for Continuous Departures from Suggested Distributions of Chance

By H. Jeffreys, F.R.S.

(*Received* 1 *November* 1937)

A method is developed for testing whether a set of observed frequencies support a uniform distribution of chance or a suggested departure from it, and is applied to linear and harmonic departures. A modification applicable to grouped data is given, and a possible way of extending the method to test departures from suggested non-uniform laws of chance is described.

The Male Sexual Stage in Salmon parr (*Salmo salar* juv.)

By J. H. Orton, J. W. Jones and G. M. King

(*Communicated by J. Gray, F.R.S.—Received* 2 *November* 1937)

A high proportion, about 40%, of the population of two- and three-year-old salmon parr become sexually mature in October in the River Dee, Wales and Cheshire. There is virtual proof that they spawn on the immigrating adult female salmon redds before migrating to the sea as smolts. Mature and maturing male parr have been observed constituting a large proportion of the population in other rivers in Great Britain, Norway and Finland, whence it is highly probable that most or all of the males of *Salmo salar* normally attain their first sexual maturity and spawn in the river in which they are reared. The phenomenon of early sexual maturity in the salmon is comparable with late paedogenesis.

The Two-dimensional Hydrodynamical Theory of Moving Aerofoils—II

By Rosa M. Morris, B.Sc.

(*Communicated by L. N. G. Filon, F.R.S.—Received* 2 *November* 1937)

The discussion of our solution of the problem of a general cylinder moving in liquids is generalized to include the effect of a vortex sheet wake extending backwards in the liquid from a trailing edge. Assuming the wake to be of any shape and to have associated with it a total circulation which is equal and opposite to that of the main circulation round the cylinder, general formulae are derived for the potential function of the fluid motion and the resultant of the fluid pressures on the cylinder boundary.

As steps in the analysis the solution of the problem of this general cylinder at rest (i) in a uniform stream, (ii) in a stream due to an external line vortex parallel to its axis, are solved in detail.

The general formulae are then examined in their approximate form under conditions analogous to those assumed for the particular problems whose

solutions are already known, with the object (i) of determining the first order effects of camber and thickness, and (ii) of verifying the approximate theoretical results now used in practice. The result that the camber and thickness have no effect on the force (lift or drag) and only a small effect on the couple when there is acceleration, is verified but in a form which shows the precise conditions governing the degree of approximation involved.

The result for the lift arising from the circulations, however, differs from that usually given. It is shown that under the usual conditions assumed for the wake, the lift force produced is greater than that produced by the corresponding simple circulation, and that this greater lift is attained without the drag which accompanies it in the simple circulation.

On the Velocity and Temperature Distributions in the Turbulent Wake behind a Heated Body of Revolution

By S. Tomotika

(*Communicated by G. I. Taylor, F.R.S.—Received* 3 *November* 1937)

In the present paper, Taylor's modified vorticity transport theory of turbulence is applied to the calculation of the velocity and temperature distributions in the turbulent wake behind a solid of revolution which is placed in a uniform stream such that its axis of revolution is parallel to the direction of the undisturbed velocity.

In order to carry out the calculation, it is assumed, with Prandtl, that for sufficiently high Reynolds numbers and at a sufficient distance downstream there is geometrical and mechanical similarity in different sections of the wake and that the values of the mixing length at corresponding points in different sections are proportional to the breadths of the sections. Also, the isotropy in turbulence is assumed.

Assuming the mixing length to be constant over any one section, the distribution of mean velocity is first calculated and the result is compared with the results of Schlichting's and Simmons's observations. The agreement between theory and observations is not quite satisfactory.

Next, the distribution of temperature is calculated. However, the comparison of the theoretical result with observations is not made, because no measurements of the distribution of temperature in the wake behind a heated body of revolution have yet been made.

Application of the Modified Vorticity Transport Theory to the Turbulent Spreading of a Jet of Air

By S. Tomotika

(*Communicated by G. I. Taylor, F.R.S.—Received* 3 *November* 1937)

The turbulent spreading of a jet of air emerging from a small circular aperture is discussed on the basis of Taylor's modified vorticity transport theory of turbulent motion. Assuming the isotropy in turbulence, the distribution of mean axial velocity is calculated for any one section of the jet whose distance from the aperture is great in comparison with the diameter of the aperture. The calculated curve is compared with the Göttingen measurements and the fairly satisfactory agreement between theory and observations is found, as in the case of Tollmien's calculation on the basis of Prandtl's momentum transport theory.

Croonian Lecture—The Transport of Materials in Plants

By H. H. Dixon, F.R.S.

(*Received* 5 *November* 1937)

Movement of water regarded as motion down a vapour-pressure gradient. Need of cohesion. Conditions of aqueous cohesion. Measurement of the tensile strength of sap. Demonstration of the tensile state of the water in the conducting tracts (wood, xylem) of plants. Action of adjacent living cells. "Suction pressure", rarely a lifting force, comes automatically into equilibrium with the vapour pressure in the conducting tracts at the same level. Hence observed "suction-pressure" gradient. Osmotic pressure in cell vacuoles, compared to supporting structures in the conducting capillaries. Correspondence between the osmotic pressures and the resistance experienced by the transpiration stream. Transpiring cells secretory; abstract the solvent from the solution. Transpiration into saturated spaces by means of respiratory energy. Tension in solvent; solutes in compression.

Temperature and cell permeability. Local fluctuations of temperature lead to changes of permeability and reversals in water-movement. Trans-

piration current carries solutes. Wood a channel of transport. Mason and Maskell's work; Bast (phloem) also an effective passage for solutes. Mechanism of movement. Muench's hypothesis. Thermo-electric method demonstrates simultaneous upward and downward movements.

Transport of growth substances.

Movement of virus compared to autocatalytic advance.

On the Motion of a Fluid Heated from below

BY R. J. SCHMIDT AND O. A. SAUNDERS

(*Communicated by S. Chapman, F.R.S.—Received* 11 *November* 1937)

If a horizontal layer of fluid, initially at rest, is heated from below, instability and cellular motion set in when $\lambda\,(\equiv \alpha g c(\theta_1-\theta_2)\,d^3/k\nu)$ is about 1700. Experiments for several layer depths show that on further heating the layer becomes completely turbulent at about $\lambda = 45{,}000$. Observations by an optical method indicate that in the case of water the turbulence develops suddenly, but that in air the transition is more gradual, the first signs of turbulence occurring at about $\lambda = 5000$. The rate of heat transfer is measured at each stage, and the increase at the change from cellular to turbulent motion is found to be less than that at the change from equilibrium to cellular motion.

In the cellular motion the horizontal length of the side of a cell is found to be twice the layer depth. The vertical temperature gradients at positions on the plane midway between the boundary surface decrease to negligible values as the motion develops with increasing λ. The horizontal temperature gradients are greatest at the mid-plane.

In the turbulent motion the fluctuating temperature gradients are very small on the mid-plane. The horizontal gradients are very small on the mid-plane, but have maxima at positions between the mid-plane and either boundary surface.

The Crystal Structure of Insulin—I

BY DOROTHY CROWFOOT

(*Communicated by R. Robinson, F.R.S.—Received* 11 *November* 1937)

X-ray crystallographic measurements show that insulin crystallises in the rhombohedral system, space group $R3$. The dimensions of the unit cell are $a = 44{\cdot}4$ A, $\alpha = 114^\circ\ 28'$ or, giving hexagonal axes, $a = 74{\cdot}8$, $c = 30{\cdot}9$ A correct to about 0·5 %. The densities of three samples of crystalline insulin have been measured in four different immersion media and show small variations between values of 1·292 and 1·314. From these and the cell dimensions the unit cell molecular weight may be calculated as most probably 39,700 (maximum 40,800, minimum 38,200). The crystals contain water which they lose when dried at 104° in a vacuum and this has been estimated at 5·35 %. The molecular weight of protein in the unit cell is hence calculated as 37,600 (33,900–36,000), which is of the order of magnitude though rather less than the molecular weight of insulin found by Svedberg. There is however no crystallographic evidence that this weight constitutes a single molecule.

The intensities of all the X-ray reflexions that could be observed from single crystals of insulin have been estimated visually and are recorded as terms proportional to F_2. From these terms a series of Patterson-Harker Fourier synthesis have been formed which show the distribution of the main interatomic distances within the insulin molecule. The patterns correspond to a fairly large scale structure and as such cannot give information on the placing of individual atoms or as to whether the trigonal symmetry shown is necessarily carried to atomic dimensions. The most important interatomic distances that appear are at 10 and 22 A roughly parallel to the basal plane. It is suggested that these are related to the characteristic X-ray spacings of many proteins both globular and fibrous, and the virus proteins.

The Effect on the Growth of *Lemna minor* of Alternating Periods of Light and Darkness of Equal Length

BY H. DICKSON

(*Communicated by V. H. Blackman, F.R.S.—Received* 12 *November* 1937)

Apparatus has been designed to enable *Lemna* to be grown in controlled conditions and under various equal alternating periods of light and darkness ranging from alternations of 5 sec. to 12 hr.

Sixteen experiments are recorded in which the rate of frond increase and the dry weight per frond were determined continuously under several different lighting conditions for periods of up to 9 weeks duration.

It has been shown that the relative rate of increase of dry weight is at a maximum in continuous light. Under 12 hr. and 5 min. alternating periods the rate was lower, but as the light intensity was the same in all cases, and the plants in continuous light consequently received twice the amount of those in the alternating periods, the efficiency was much higher in alternating light than under continuous illumination. The rate was lowest at 1 min. alternations but with 5 sec. alternating periods it was much higher, being even significantly higher than with 12 hr. illumination.

Curves of the relative rate of increase in frond number and of the average weight per frond were similar to those for rate of dry-weight increase, except that the rate in 5 sec. alternating periods was not significantly different from that in 12 hourly alternations.

Portsmouth (1937) attributed the small growth rate of cucumber plants in one minute alternating periods as probably due in part at least to closure of the stomata. Observation shows that the stomata of *Lemna* are non-functional, so that in view of the fact that decrease in growth-rate at 1 min. alternating periods is as marked in *Lemna* as it is in cucumber plants it appears more likely that stomatal closure is a secondary effect rather than the cause of the drop in growth rate.

The appearance of the plants in 1 min. alternating periods is very different from that under other conditions of illumination. The fronds are small in size and not glossy, and lie at all angles to one another. This change in morphology takes place comparatively suddenly.

An Analysis of the "Pleiotropic" Effects of a New Lethal Mutation in the Rat (*Mus norvegicus*)

By G. Grüneberg

(*Communicated by J. B. S. Haldane, F.R.S.—Received* 12 *November* 1937)

"Pleiotropism" of genes can theoretically arise in three different ways. Two effects *a* and *b* may either be produced by the gene directly by means of two different mechanisms; or they may be produced by the gene directly by means of the same mechanism; or the gene may produce only one effect *a*, which in turn conditions *b* (indirect gene action). In the latter two cases, unity of gene action is maintained (spurious pleiotropism), whereas only the first case would constitute genuine pleiotropism, the gene producing manifold effects in different ways.

The analysis of the manifold effects of a new recessive lethal factor in the rat, which is linked to pink-eye dilution, shows that the most fundamental disturbance so far discovered is an anomaly of the cartilage; this single mechanism affects several structures of the body in a similar way. Hyperplasia of the ribs and of the cartilage rings of the trachea thus produced leads secondarily to the development of an emphysema of the lungs, and the animals ultimately die from more or less remote consequences of this emphysema.

Unity of gene action is therefore maintained in this case, which, despite the complex ramifications of the effects, is only an example of spurious pleiotropism. This seems also to apply to the few other cases which are fully analysed. The existence of genuine pleiotropism has never been conclusively proved. As unity of gene action is the simpler conception, and as it has been shown to explain fully analysed cases, it may be adopted as a general principle unless and until the occurrence of genuine pleiotropism has been conclusively demonstrated.

Resonance in Crystal Beams of Sodium-Ammonium Seignette Salt

By W. Mandell

(*Communicated by O. W. Richardson, F.R.S.—Received* 13 *November* 1937)

Experiments are made with longitudinal oscillations in crystal beams of sodium-ammonium seignette salt. For a square beam a theory is deduced for the interaction of two longitudinal oscillations at right angles. These are considered as analogous to two coupled electrical circuits. If the natural frequencies in the two directions agree to within a small number of cycles per second, the theory requires that resonance shall occur with the production of two new fundamental frequencies. This result is demonstrated experimentally.

Experiments are also made to determine the change in wave-length with change in breadth and thickness. Theoretical calculations are made of the lateral contractions along the breadth and along the thickness, accompanying extensions along the length. The effect of thickness on the wave length is found to be very small, in spite of the fact that the lateral contractions are large in two types of beams used. A change of breadth may change the wave-length by 20 %. The experimental results for two types of beam agree closely with an empirical formula, while one type of beam behaves in an anomalous manner.

On the Mechanism of the Decomposition of Hydrogen Peroxide by Catalase

By D. Keilin, F.R.S. and E. F. Hartree, Ph.D.
The Molteno Institute, University of Cambridge

(*Received* 15 *November* 1937)

1—A new explanation of the mechanism of the decomposition of H_2O_2 by catalase is proposed. According to this explanation the reaction is brought about by the successive reduction of the catalase iron by H_2O_2 and its

reoxidation by molecular oxygen; the reaction proceeding according to the following equation:

$$\begin{array}{c} 4\text{Fe}^{\cdot\cdot\cdot} + 2\text{H}_2\text{O}_2 = 4\text{Fe}^{\cdot\cdot} + 4\text{H}^{\cdot} + 2\text{O}_2 \\ 4\text{Fe}^{\cdot\cdot} + 4\text{H}^{\cdot} + \text{O}_2 = 4\text{Fe}^{\cdot\cdot\cdot} + 2\text{H}_2\text{O} \\ \hline 2\text{H}_2\text{O}_2 = 2\text{H}_2\text{O} + \text{O}_2 \end{array}$$

2—This explanation is supported by the following experiments:

a—It has been shown manometrically that the decomposition of H_2O_2 by catalase does not proceed in absence of molecular oxygen.

b—It has been shown spectroscopically with azide- and hydroxylamine-catalase that H_2O_2 is the only known substance capable of reducing catalase iron, which can then be readily reoxidised by molecular oxygen.

3—The inhibitors of catalase can be separated into two groups, those like KCN, H_2S, C_2H_5OOH which inhibit the reduction of catalase iron by H_2O_2 and those like azide, hydroxylamine and hydrazine which inhibit the reoxidation of the reduced catalase by molecular oxygen (Keilin and Hartree, 1936).

4—The decomposition of H_2O_2 by pure catalase preparations is not inhibited by CO in presence of even a very small concentration of oxygen, which shows that the reduced catalase has a much greater affinity for oxygen than for CO.

5—Some catalase preparations have been obtained which show a more or less marked light sensitive inhibition by CO. Pure catalase preparations become sensitive to CO in presence of a very small concentration of azide, cysteine or glutathione, substances which apparently inhibit the reoxidation of reduced catalase.

Instability of Fluids Heated from below

By Krishna Chandra, M.Sc.

(*Communicated by Sir Gilbert Walker, F.R.S.*
Received 20 *May* 1936—*Revised* 12 *November* 1937)

A layer of air in a shallow chamber was made unstable by heating from below, and the motion which ensued, made visible by smoke, was studied for a range of depths of the chamber, and for a range of differences of temperature between top and bottom of the chamber. It was found that, unless the excess of temperature at the bottom exceeded a certain critical value, no motion took place. In depths of 10 mm. or more, the motion observed when the critical value was exceeded was in the form of polygonal prismatic cells, with descending motion at their centres, and the critical difference of temperature necessary to produce motion was in good agreement with the theoretical formula given by Jeffreys. In depths of less than 10 mm., the motion observed when the critical difference of temperature was first exceeded was of a different character, the ill-defined smoke structures having ascending air at their centres, and the critical difference of temperature was less than that given by Jeffreys' theory. It was found that with still higher differences of temperature the motion in depths of 7–10 mm. took the form of polygonal cells, the change in type of motion occurring at critical differences of temperature which were in agreement with the theoretical expression given by Jeffreys.

When the air in the chamber was subjected to a shear by motion of the top bounding plate, the smoke patterns in the chamber, when the initial conditions were such as to give polygonal cells in the absence of shear, were in the form of transverse rolls, distorted polygonal cells, or longitudinal pairs of roll vortices, according to the rate of shear and the difference of temperature in the chamber. If the motion in the absence of shear were of the other type, the effect of shear was always to give spindle shaped structures, whose length was increased by increase of the rate of shear.

Studies on the Origin of the Larval Kidneys of the Mollusca

I—Pulmonata Stylommatophora

By W. Fernando

(*Communicated by E. W. MacBride, F.R.S.—Received* 16 *November* 1937)

From the mesodermal bands differentiate the rudiments of the larval kidneys in *Achatina*, *Glessula*, and *Opeas*.

In *Achatina* this mesodermal rudiment isolates from the remainder of the mesoderm and develops a lumen inside. An ectodermal invagination later unites with the mesoderm and a tubular larval kidney results, opening

at one end to the exterior. In *Glessula* the isolation of the mesodermal rudiment is less marked than in *Achatina*, but subsequent development is the same. In *Opeas* the mesodermal rudiment of the larval kidney is differentiated at a very early stage while still in contact with the rest of the mesodermal band. The ectodermal invagination also develops very early but the union of the two portions takes place at a later stage.

The larval kidneys of the Stylommatophora are for the greater part mesodermal, only a small portion with the external aperture being formed of ectoderm.

The Reflection Coefficients of Ionospheric Regions

By E. V. Appleton, F.R.S. and J. H. Piddington

(*Received* 17 *November* 1937)

Experiments on the radio sounding of the ionosphere are described which give no support to the supposed existence of permanent highly reflecting regions at heights of 10 km. It is considered possible that the echoes of short delay noted by previous workers are due to scattering from patches of ionisation of very low effective reflexion coefficient. It is found that, after the normally recognized regions of the ionosphere, the radio reflecting centres in the atmosphere next in order of importance as regards wireless echo production are transitory bursts of ionisation which occur at equivalent heights of from 80 to 160 km. Such bursts of ionisation are due to some cosmic agency which is usually effective throughout the whole of the day and night.

ABSTRACTS

OF PAPERS COMMUNICATED TO THE ROYAL SOCIETY OF LONDON

In accordance with a resolution of Council, summaries or abstracts of papers are to be published as soon as practicable. The publication of such abstracts in no way indicates that the papers have been accepted for publication in any fuller form. These abstracts will be issued for convenience with the "Proceedings of the Royal Society of London" but do not form a part of the "Proceedings".

---

22 December 1937

On the Cascade Theory of Electronic Showers

By Dr L. Landau and Dr G. Rumer

(*Communicated by P. Kapitza, F.R.S.—Received* 18 *November* 1937)

1. Starting from the physical idea proposed by Bhabha and Heitler, and Carlson and Oppenheimer on the cascade production of showers, a more rigorous treatment of the problem is given (§§ 1–5).

2. A table is given for the calculation of the number of the shower particles as function of penetrated depth for any given initial energy of the creating particle and also of the energy distribution for shower particles at a given depth (§ 6).

3. The showers possess a definite range (§ 7).

4. The behaviour of shower passing from air to a medium with a different atomic number is studied (§ 9).

5. The consequences arising from the hypothesis of the new "semi-heavy" particles are discussed.

The Crystal Structure of Pentaerythritol Tetracetate

By Thomas H. Goodwin and Rowland Hardy

(*Communicated by W. L. Bragg, F.R.S.—Received* 18 *November* 1937)

The crystal structure of pentaerythritol tetracetate has been determined by the method of X-ray analysis. This is the first ester to be examined in detail and the results show:

(*a*) that the valencies of the central carbon atom are inclined to each other at the tetrahedral angle (109½°);

(*b*) that the acetate group $—\mathrm{O.CO.CH_3}$ has a planar configuration;

(*c*) that the valency angle of oxygen $\overset{\diagdown\ \diagup}{\mathrm{O}}$ is 109½° ± 3° in this compound;

(*d*) that the length of the $\mathrm{C{=}O}$ bond in an ester is $1{\cdot}33 \pm 0{\cdot}03$ A.

The first two of these conclusions are in agreement with stereo-chemical theory. In view of the assertions of Gerstäcker, Möller and Reis (1928) it seems desirable to call attention to (*a*) which indicates that the central carbon atom has a tetrahedral and not a pyramidal distribution of valencies.

The co-ordinates of all the atoms in the unit cell have been determined by means of two- and three-dimensional Fourier syntheses. It is believed that this is the first compound for which three-dimensional syntheses (sections through the unit cell at different heights or along special lines) have been made.

Critical Phenomena in Gases

II—Vapour Pressures and Boiling Points

By J. E. Lennard-Jones, F.R.S. and A. F. Devonshire

(*Received* 24 *November* 1937)

This paper extends to liquids the theory which was given recently by the authors for the equation of state of a gas at high densities. A direct calculation is made of boiling points in terms of interatomic forces and the numerical results for the inert gases are in satisfactory agreement with the

observed values. A theoretical interpretation is given of Trouton's empirical rule connecting the heat of vaporization with the boiling temperature and also of Hildebrand's modified form of it. Calculations are made of the heats of vaporization of the inert gases.

The Electronic Structure of some Polyenes and Aromatic Molecules

IV—The Nature of the Links of certain Free Radicals

By C. A. Coulsdon

(*Communicated by J. E. Lennard-Jones, F.R.S.—*
Received 24 *November* 1937)

General formulae are given for the lengths of the links of free radicals and molecules of chain form $C_{2n+1}H_{2n+3}$. It is shown that in these chains the effect of resonance is to remove some of the characteristic properties of alternate single and double bonds. Calculations have been made of the energies of these radicals in particular cases, and the effect of resonance has been estimated.

The Electronic Structure of some Polyenes and Aromatic Molecules

V—A Comparison of Molecular Orbital and Valence Bond Methods

By G. W. Wheland

(*Communicated by J. E. Lennard-Jones, F.R.S.—*
Received 24 *November* 1937)

The valence-bond and the molecular orbital treatments of cyclobutadiene disagree in two respects. The first treatment predicts that the resonance energy should be about −1·5 e.v. and that the ground state should be a singlet; the second, on the other hand, predicts that the resonance energy should be zero and that the ground state should be a triplet. The first of these discrepancies is found to be a result of the fact that the molecular orbital treatment neglects the resonance between the two Kekulé-like structures. The second discrepancy is found to be due to the effect of ionic structures, which are not taken into account in the valence-bond treatment, but which are made important in the molecular orbital treatment. The resonance among these ionic structures is of such a nature as to stabilize the triplet considerably more than the singlet state. A similar discussion of benzene shows that the ionic structures contribute to the stability of the singlet ground state in essentially the same way as to the lowest triplet state of cyclobutadiene.

The Electronic Structure of some Polyenes and Aromatic Molecules

VI—Phenylethylene, Stilbene, Tolane and the Phenyl Methyl Radical

By W. G. Penney and G. J. Kynch

(*Communicated by J. E. Lennard-Jones, F.R.S.—*
Received 24 *November* 1937)

Calculations are made to find the internuclear distances in molecules containing the system $C{=}C{-}C_6H_5$. The length obtained for the double bond is the same as that in ethylene; the ring distances are the same as those in benzene; but the "single" bond has the peculiarly short length 1·44 A. Similarly, in the system $C{\equiv}C{-}C_6H_5$, the triple bond has a normal length 1·20 A, the ring distances are the same as in benzene, but the "single" bond has a length 1·41 A. Measurements by Robertson and Woodward on stilbene and tolane agree exactly with these results.

The Rotational Energy Levels of a Diatomic Molecule in a Tetrahedral Field

By H. M. Cundy, Trinity College, Cambridge

(*Communicated by J. E. Lennard-Jones, F.R.S.—*
Received 24 *November* 1937)

It is shown by general principles of the theory of groups how the Schrödinger equation may be solved for a diatomic molecule, when the potential energy varies with the angular coordinates in such a manner that it has the symmetry of the regular tetrahedron. Infinite series for the wave-functions are given, and the energy levels and corresponding wave-functions evaluated for a particularly simple potential-energy function of the given type. Three methods of obtaining these levels are described, two of which are asymptotic approximations, and the third involves the use of the Mallock electric calculating machine. A good agreement is obtained between the three, enabling a plot to be made of the energy levels over wide ranges of magnitude of the potential energy term.

The Potato Virus 'X'; its Strains and Reactions

By R. N. Salaman, F.R.S.

(*Received* 27 *November* 1937)

The X virus is a term which should be applied to a group of strains rather than to a single specific pathogen with fixed and constant reactions. It is shown that at least six strains are to be found distributed amongst the diseased potato plants of this country, and that most of them are represented in Germany, Canada and the U.S.A.

In the open field a potato plant is usually infected by two or more strains simultaneously, but in the case of the milder X^H and the more virulent X^N pure single strain infections do occur.

The strains range in respect to their virulence, as judged by their behaviour in tobacco and Datura from the creation of a symptomless carrier

to an intensely virulent necrosis endangering the continued existence of the host. The reaction of the strains is described on a large range of plants.

The strain X^N is shown to be the pathogen responsible for a distinctive morbid condition in the potato, here called "interveinal necrosis". The disease and the reactions of the strain are described for the first time.

Infection by any of the strains brings about the formation of inclusion bodies within the host tissues. Such inclusions do not vary in character or frequency in relation to the virulence of the strain. There is a certain variety in their appearance which may be recognized, whichever strain is infecting the host.

All the strains are made up of similar sized particles and possess certain identical serological reactions.

From plants infected by each strain the same type of nucleoprotein has been recovered, which in solution exhibits anisotropy of flow.

The physical properties of the strains are alike except for the degree of dilution which they will withstand.

The clinical results obtained by mixture of pure strains has been studied, evidence is given that a tenfold excess of a weak over a strong may lead to the clinical masking of the latter in the host plant, a lesser relation of strong to weak has the opposite result.

The double reactions that ensue from mixtures of the different X strains with the Y virus, the A virus and tobacco mosaic respectively, conform to the actual differences in virulence of the different strains themselves.

Conversion of one strain to another has been studied both in material which is relatively pure to strain as well as in that which we have good reason to believe is in reality pure. In both conversions have taken place. Conversions have been effected by passage through certain unrelated plants.

All conversions, whether purposely designed or not, have been from the more to the less virulent strain.

The nature of these conversions is discussed and the conclusion reached that they should be regarded as true mutations.

The phenomenon of acquired immunity as exhibited by the potato and other solanaceous plants in respect to the X virus is described as well as its occurrence in nature, and the possible relation of the same to the occurrence of certain types of carriers.

X-ray analysis of the Dibenzyl Series
V—Tolane and the Triple Bond

By J. Monteath Robertson, M.A., D.Sc. and I. Woodward, M.A.

(*Communicated by Sir William Bragg, O.M., F.R.S.—*
Received 27 *November* 1937)

The crystal dimensions of tolane are very similar to those of stilbene, and this fact has been used in making a very direct X-ray analysis of the tolane structure, without the use of any model based on the chemistry of the compound. The two central atoms linked by the triple bond are found to be collinear with the end atoms of the benzene rings to which they are joined. The carbon-carbon triple bond distance is 1·19A, and for the "single" bond connecting these central atoms to the benzene ring, the unusually small distance of 1·40A is obtained. These results are discussed in relation to acetylene and other compounds.

As in the stilbene structure, there are four molecules in the unit cell, and two of these make independent contributions to the asymmetric unit of the crystal. The orientations of these two molecules are deduced, and the coordinates of the atoms are given. The minimum intermolecular approach distances are between 3·5 and 3·6A for the carbon atoms.

Further Studies on the Relationship between *Hyoscyamus* Virus 3 and the Aphis *Myzus persicae* (Sulz.) with special reference to the Effects of Fasting

By M. A. Watson

(*Communicated by Sir John Russell, F.R.S.—*
Received 29 *November* 1937)

The aphides (*Myzus persicae*) are much more likely to transmit *Hyoscyamus* virus 3 if they are made to fast immediately before feeding on the source of infection. Their efficiency as vectors increases rapidly during the first hour of fasting, but the rate of increase is much slower during the following 12 hours.

The increase in efficiency induced by such preliminary fasting decreases

as the infection feeding period is increased, and after one hour's feeding on the infected plants preliminary fasted aphides give no more infection than do continuously fed aphides.

Infectivity is lost by the aphides after the cessation of infection feeding, and the rate of loss is probably more rapid than the rate at which the virus deteriorates *in vitro.* This loss of infectivity is complete in 1 hour if the aphides do not fast before infection feeding, or if they are fed on an intermediate healthy plant between the infection feeding and the infection trial; but if they fast both before and after the infection feeding, the relative rate of loss of infectivity is slower, and a few insects may remain infective for many hours.

The infectivity of an aphid is greater after two or more successive infection feedings of equal length, unless the treatment given between the feedings is such that all the infectivity is lost. The infectivity actually acquired at the second or third infection feeding is, however, less than that acquired at the first, because the feeding activity of the aphid is decreased by the experimental conditions.

The effect of preliminary fasting appears to be independent of feeding activity or "appetite", and is very much more important.

It is possible to explain these results if it be assumed that, during the process of transmission from one plant to another in the recently fed aphid, the virus comes into contact with some substance which partially or wholly destroys its infectivity. The possible nature of this substance is discussed.

Tides in Oceans bounded by Meridians

III—Ocean bounded by Complete Meridian: Semidiurnal Tides

By A. T. Doodson, F.R.S.

(*Received* 29 *November* 1937)

The first two parts of this series of memoirs have dealt with the general equations for the motion in an ocean bounded by a complete meridian (Proudman 1936) and with their application to the diurnal tide (Doodson 1936). This present memoir is concerned with the semidiurnal tide (K_2).

The investigation, as in Part II, is dependent upon the formulation and numerical solution of the equations from the use of 63 co-ordinates or variables, and the solution has been effected and is illustrated for 20 values of the depth of the ocean, from very large to medium depths. Though a part of the work of solution is common to all cases, in effect 20 sets of equations, each set having 63 equations, have been solved.

The results are of exceedingly great interest in connexion with tidal theory. The genesis and development of amphidromic systems, as the depth is changed, can be fully traced. The possible systems of cotidal lines are of great variety, and the type of amphidromic system changes so rapidly with the depth that a single illustration of the tides for a particular depth is of doubtful value for comparison with an actual ocean but it is hoped that the complete series of illustrations will provide material for the derivation of principles which can be applied to terrestrial oceans.

Thermal Conduction in Hydrogen-deuterium Mixtures

By C. T. Archer, A.R.C.S., M.Sc., Senior Lecturer in Physics,
Royal College of Science, London, S.W. 7

(*Communicated by A. O. Rankine, F.R.S.—Received* 30 *November* 1937)

The paper describes an experimental investigation of thermal conduction in hydrogen, deuterium, and hydrogen-deuterium mixtures of varying concentration. The hot wire method, used by the author and others previously in similar work, was adopted to determine the thermal conductivity at 0° C. of hydrogen, deuterium, and of each mixture, and also the accommodation coefficients of hydrogen and deuterium relative to a platinum surface at 0° C.

The hydrogen was prepared from distilled water, the deuterium from deuterium oxide of 99·95 % guaranteed concentration, and the gaseous mixtures from mixtures of the water and deuterium oxide, by passing the vapour over magnesium heated to about 500° C. in an electric furnace. Deuterium was also prepared from the oxide by reaction with metallic sodium in vacuo. The percentage concentrations of the gaseous mixtures were obtained from observations of the densities of the liquid mixtures, using a flotation method.

The values obtained of the thermal conductivity at 0° C. of hydrogen and deuterium were $0{\cdot}000418_2$ and $0{\cdot}000308_9$ cal. cm.$^{-1}$ sec.$^{-1}$ deg.$^{-1}$ C., and of the accommodation coefficient $0{\cdot}29_6$ and $0{\cdot}37_6$ respectively. The values of the thermal conductivities of all the gases together with the percentage concentrations are shown in a Table, and also represented by means of a graph.

Antiplasmodial Action and Chemical Constitution

I—Cinchona Alkaloidal Derivatives and Allied Substances

By A. Cohen and Harold King, F.R.S.

(*Received* 30 *November* 1937)

Experimental bird malaria is utilized for following the effect of changes of structure in the cinchona alkaloids on the therapeutic activity. It is shown that although antiplasmodial action is not very sensitive to stereochemical changes, it is sensitive to changes of structure. Thus there is apparent loss of activity when the central —CHOH— group is modified in any way. Thus its conversion into —CHCl—, $—CH_2—$ or —CH═ leads in almost all cases to an increase in toxicity and loss of antiplasmodial action. The preparation and properties of a series of allied substances is also described.

Antiplasmodial Action and Chemical Constitution

II—Some Simple Synthetic Analogues of Quinine and Cinchonine

By A. D. Ainley and Harold King, F.R.S.

(*Received* 30 *November* 1937)

Quinicine (quinotoxine), the ketonic isomeride of quinine, is inactive in bird-malaria. Reduction to dihydroquinicinol (2 diastereoisomerides) with re-formation of a carbinol group does not restore activity; neither is activity found in α-*N*-methyldihydroquinicinol. Consideration of these results led the authors to the synthesis of 4-quinolyl-α-piperidylcarbinol and 4-(6-methoxyquinolyl)-α-piperidylcarbinol and their *N*-methyl, *N*-propyl, *N*-allyl, *N*-butyl and *N*-crotyl derivatives. The only compounds

obtained showing antiplasmodial activity were 4-(6-methoxyquinolyl)-α-piperidylcarbinol and its diastereoisomeride *iso*-4-(6-methoxyquinolyl)-α-piperidylcarbinol. These two substances appear to be the first simple substances built on the pattern of the cinchona alkaloid molecule to show antiplasmodial activity.

Propagation of Wave-packets Incident Obliquely upon a Stratified Doubly Refracting Ionosphere

BY K. G. BOOKER, PH.D.

(*Communicated by E. V. Appleton, F.R.S.—Received* 1 *December* 1937)

A study is made of the propagation of wave-packets incident obliquely upon a slowly varying plane-stratified doubly refracting medium with a view to applying the results to the ionosphere. The magneto-ionic theory in the form given by Appleton is only suitable for investigating vertical propagation in the ionosphere. The theory is generalized so as to be capable of describing oblique propagation of a magneto-ionic component through the ionosphere without using a refractive index which depends in a complicated way upon an unknown angle of refraction. The fundamental formula of the oblique-incidence magneto-ionic theory is an algebraic quartic equation for a quantity q which depends upon the prescribed angle of incidence and which at vertical incidence becomes identical with the well-known refractive index. The four roots of the quartic equation for q correspond to the upgoing ordinary wave, the upgoing extraordinary wave, the downcoming ordinary wave and the downcoming extraordinary wave. The level in the ionosphere where the individual wave-crests are moving horizontally across a characteristically polarized wave-packet is given by the condition $q = 0$, which is equivalent to putting the angle of refraction equal to $x/2$ in Snell's Law. But the level of reflexion of the magneto-ionic component is the level where the wave-packet *as a whole* is travelling horizontally and is given by the condition that the root of the quartic equation for q corresponding to the upgoing magneto-ionic component should be equal to a root corresponding to a downcoming magneto-ionic component.

The detailed application of these results to the ionosphere depends on our ability to solve the fundamental quartic equation for q, and the only practical way of achieving this in general is to resort to one of the standard numerical methods. Special cases worked out in this way show that the critical electron density required for reflexion of a magneto-ionic component can easily be as much as 25 % in excess of the erroneous value which would be calculated by putting the angle of refraction equal to $\pi/2$ in Snell's Law.

The analytical solution of the quartic equation for q is sufficiently simple to be of practical value in the case of east-west transmission (including vertical incidence) and in the case of propagation in equatorial regions. Owing to the symmetrical influence of the earth's magnetic field upon the propagation of the upgoing and downcoming waves in these special cases it is legitimate to calculate the critical electron densities of the magneto-ionic components from the condition ($q=0$) that the direction of phase-propagation is horizontal. Representative curves are drawn.

An Experimental Determination of the Spectrum of Turbulence

By L. F. G. Simmons, M.A. and C. Salter, M.A.

With an Appendix: Method of Deducing $F(n)$ from the Measurements

(*Communicated by G. I. Taylor, F.R.S.—Received* 1 *December* 1937)

The time variation of velocity at a fixed point in a turbulent air stream is analysed into a spectrum. The method adopted involves the use of the ordinary hot-wire technique to produce changes of potential in a Wheatstone bridge circuit, which are magnified by a value amplifier. The fluctuating voltage drop generated is then applied, in turn, to electrical filters having different cut-off frequencies. In each case the output current is measured, with and without each filter in circuit, by means of a thermal milliammeter which indicates the mean value of the square of the current supplied to it. From the ratios of the readings taken with and without each filter, the spectrum curve is calculated by a method described in the Appendix.

All measurements were made in a wind tunnel, at a point in the air stream where the turbulence created by a grid of regular mesh was known to be isotropic: the wind speeds used were 15, 20, 25, 30 and 35 ft./sec.

The Spectrum of Turbulence

By G. I. Taylor, F.R.S.

(*Received* 1 *December* 1937)

It is shown that a definite connexion exists between the spectrum of the time variation in wind at a fixed point in a wind stream and the curve correlation between the wind variations at two fixed points. The spectrum curve and the correlation curve are, in fact, Fourier transforms of one another.

As an example of the use of this relationship the spectrum of turbulence in an American wind tunnel was calculated from measurements of correlation by Dryden. In some further experiments Dryden modified this spectrum by inserting a filter circuit and then measured the correlation with this filter in circuit. The modified spectrum is here calculated from the filter characteristics and the Fourier transform theorem is used to calculate the modified correlation curve. The agreement with Dryden's measurements is very good indeed.

The paper ends with some remarks on the bearing of the spectrum measurements on the theory of dissipation of energy in turbulent flow.

The Alkaline Permanganate Oxidation of Organic Substances selected for their bearing on the Chemical Constitution of Coal

By R. B. Randall, Ph.D., M. Benger, Ph.D. and
C. M. Groocock, Ph.D.

(*Communicated by Professor W. A. Bone, F.R.S.—*
Received 3 *December* 1937)

The paper describes the results of systematic qualitative and quantitative investigations of some sixty organic substances, namely, (i) carbohydrates and aliphatic carboxylic acids, (ii) aromatic hydrocarbons, (iii) aromatic substances containing =CO groups, (iv) aromatic carboxylic acids and ethers, and (v) heterocyclic compounds, selected for their bearing on the coal-constitutional problem, and discusses the principal conclusions to be drawn therefrom. Details are also given of the experimental methods employed.

Indicators of Salt Accumulation by Plants; the Absorption of Rubidium Bromide by Potato Discs

BY F. C. STEWARD AND J. A. HARRISON

(*Communicated by V. H. Blackman, F.R.S.—Received* 6 *December* 1937)

The paper describes the results of a quantitative investigation of the absorption of rubidium and bromide from dilute solution by discs of potato tissue. The results contribute to knowledge of the absorption process in plants.

An accurate spectrographic method for the determination of rubidium in plant extracts was devised for this investigation. The method, which is applicable to other biological problems, is described in detail.

The ions rubidium and bromide were used as sensitive indicators of the absorption of cation and anion respectively because they are not normally present in potato tissue, except in negligible amounts, they are both readily absorbed and can be estimated accurately. The experiments which were carried out under rigorously controlled conditions by a technique which has been described elsewhere, concern the effects of oxygen concentration, time and the specific surface of the discs on the absorption of rubidium and bromide.

The results establish the relationship between the metabolism of the cells and the absorption of both bromide and rubidium. The absorption of rubidium is, however, of two kinds, one which is determined by the metabolism of the tissue and the other which is independent of vital activity and may be observed in dead discs. The two types of absorption may be distinguished by their relations to the variables oxygen concentration, time and temperature. The maintained absorption of rubidium and of bromide which is dependent upon vital activity is confined to a surface layer of active cells in the discs whereas that part of the absorption of rubidium which is due merely to a property of the tissue substances occurs throughout the whole of the disc.

Experiments upon the effects of concentration upon absorption, carried out on both living and dead discs, reveal the general nature of the two absorption mechanisms and lead to a new outlook upon the problem of the relative uptake of anion and cation in plants.

The Action of Ultra-violet Radiation on Proteins, I, II

By J. S. Mitchell

(*Communicated by E. K. Rideal, F.R.S.—Received* 8 *December* 1937)

1. A brief review is given of the photochemistry of proteins with especial reference to the process of oxidative photolysis.

2. The photochemical significance of the ultraviolet absorption spectra of proteins is discussed quantitatively, in relation to the hydrolytic analyses. Measurements of the absorption spectra of certain proteins—ovalbumin, gliadin and insulin—and of the tyrosine derivatives—glycyl-tyrosine and *N*-stearyl-tyrosine ethyl ester—are given. For the absorption of radiation of wavelengths 3150–2350 A the only residues of importance, in typical proteins, are those derived from the "aromatic" amino acids—tyrosine, phenylalanine and tryptophane—and also cystine and arginine—further, 85–100% of the total light absorption is due to the three "aromatic" amino acids. Thus the proteins must be regarded as macromolecular polycondensation products in which only a small fraction of the total number of repeating units possess chromophoric groups and can take part in primary photochemical processes.

At *p*H 2 and 7·2 the assumption of linear additivity of the absorption coefficients of the individual amino acids of proteins is a poor approximation, but at *p*H 12 at the wavelength of the absorption maximum, it is possible to calculate the molecular extinction coefficient of insulin with an error of less than 3%.

3. The photochemical decomposition, in aqueous solution, of ovalbumin, insulin, glycyl-tyrosine and l-dihydroxyphenylalanine ("dopa") by the approximately monochromatic radiation, of wavelength 2537 A, given by a mercury-neon discharge tube, has been examined chemically and by observation of the changes in the ultraviolet absorption spectra.

4. Ovalbumin, in solution in the presence of oxygen, undergoes complete photo-oxidative decomposition with production of proteoses as end-products, and disappearance of the reactions characteristic of tyrosine, tryptophane and cystine; the changes in the absorption spectrum emphasise the importance of the aromatic groups.

It appears from the present and previous work that, in general, the end-products of unsensitized photolysis of proteins with light of wavelengths longer than 2350 A are to a large extent fragments of high molecular weight and not the constituent units, thus suggesting selective photochemical attack at localized sites in the molecule.

5. A detailed examination has been made of the photochemistry of glycyltyrosine in solution, to test the hypothesis that the photo-oxidative decomposition of proteins with light of wavelengths longer than 2350 A is due to molecular fragmentation at the sites of attachment of the aromatic chromophors. Ancillary studies of dopa and indol were made. As a result of light absorption in the aromatic nucleus, glycyl-tyrosine undergoes a series of photo-oxidative transformations—involving the formation of dihydroxyphenyl compounds, probably orthoquinones, and indol derivatives—which result in fragmentation of the peptide linkage with production of glycine; this last step is probably one of photochemical hydrolysis.

6. This mechanism of indirect oxidative photolysis of the peptide linkage adjacent to the aromatic chromophor appears applicable to proteins. The changes in the absorption spectrum on ultraviolet irradiation in presence of oxygen have been compared, in the case of insulin—where the only important chromophors are those derived from tyrosine—and of glycyl-tyrosine; it must be concluded that there is no fundamental difference between the photo-oxidative transformations of the tyrosine chromophors in the two cases.

New Bands Ending on the $1s\sigma 2p\sigma\, {}^1\Sigma_4$ State of H_2

By O. W. Richardson, F.R.S.

(*Received* 8 *December* 1937)

This paper describes two new band systems which go down to $1s\sigma\, 2p\sigma\, {}^1\Sigma u$, the state on which the strongest hitherto known systems in the visible end. The systems extend from the yellow to the photographic infra-red limit (8500 A) and probably beyond. The upper states are both ${}^1\Sigma g$ states. They are very close to one another and appear to be perturbing each other as well as the state $1s\sigma\, 2s\sigma\, {}^1\Sigma g$ which is in the same neighbourhood. Their rotational structure resembles closely that of the "abnormal" ${}^1\Sigma g$ states $3\,{}^1K$, ${}^1L$, ${}^1M$ and ${}^1N$. Reasons are given which make it impossible to regard either of the two new states as states with only one electron excited. Two alternative methods of classifying the two new states and the seven other abnormal states which have transitions to $1s\sigma\, 2p\sigma\, {}^1\Sigma u$ and uniting them into a consistent scheme as states with both electrons excited are put forward and their merits discussed.

INDEX TO AUTHORS

NOTE—The letter S is to be understood with all page references

Ainley, A. D. and King, H. 70
Allsopp, *see* Lowry
Appleton, E. V. and Piddington, J. H. 60
Archer, C. T. 69
Aston, F. W. 25

Benger, *see* Randall
Berg, W. F. 19
Best, J. E., Farmer, F. T. and Ratcliffe, J. A. 20
Bhabha, H. J. 26
Bjerge, T. 24
Black, A. N. and Southwell, R. V. 3
Blackman, M. 18, 27
Booker, K. G. 71
Bretscher, *see* Chadwick

Cain, C. and Sutherland, G. B. B. M. 32, 33
Cameron, *see* Elliott
Chadwick, J., Feather, N. and Bretscher, E. 19
Chandra, K. 58
Clews, C. J. B. and Schoszberger, F. 15
Cohen, A. and King, H. 70
Cooper, L. H. N. 12
Coulsdon, C. A. 63
Cox, H. L. and Smith, H. E. 28
Crowfoot, D. 54
Cundy, H. M. 65

Dartnall, H. J. A., Goodeve, C. F. and Lythgoe, R. J. 35
Deanesley, R. and Parkes, A. S. 40
Devonshire, *see* Lennard-Jones
Dickson, H. 55
Dill, *see* Keys
Dixon, H. H. 52
Doodson, A. T. 68

Eckersley, T. L. 2
Eckersley, T. L. and Millington, G. 2
Elliott, A. and Cameron, W. H. B. 28
Ewles, J. 32

Farmer, *see* Best
Feather, *see* Chadwick
Fernando, W. 59
Fink, P. and Goodeve, C. F. 15
Fisher, R. A. 43
Folley, S. J. and Kon, S. K. 46
Forbes, *see* Keys
Fuchs, V. E. 47

Goldsbrough, G. R. 3
Goodeve, *see* Dartnall, Fink, Porret
Goodwin, T. H. and Hardy, R. 62
Grieve, B. J. 42
Groocock, *see* Randall
Grüneberg, G. 56
Gurney, R. W. and Mott, N. F. 30

Haines, R. B. 42
Hardy, *see* Goodwin
Harrison, *see* Steward
Hartree, D. R. and Hartree, W. 31
Hartree, E. F., *see* Keilin
Howarth, L. 29
Hughes, J. W. 36

Jackson, D. A. and Kuhn, H. 16
Jahn, H. A. 24
Jeffreys, H. 49
Jones, F. W. 32
Jones, J. W., *see* Orton

Kapur, P. L. 10
Kapur, P. L. and Peierls, R. 17
Keilin, D. and Hartree, E. F. 57
Kent, C. R. 10
Keys, A., Matthews, B. H. C., Forbes, W. H., McFarland, R. A. and Dill, D. B. 34
King, G. M., *see* Orton
King, H., *see* Ainley, Cohen
Koller, P. C. 46
Kon, *see* Folley
Krishnan, K. S. and Mookerji, A. 20
Kynch, *see* Penney

Landau, L. and Rumer, G. 61
Lennard-Jones, J. E. and Devonshire, A. F. 62
Lowry, T. M. and Allsopp, C. B. 18
Lowry, T. M., Simpson, D. M. and Allsopp, C. B. 25
Lythgoe, *see* Dartnall

MacBride, E. W. and Spencer, W. K. 33
McCrea, W. H. 17
McFarland, *see* Keys
MacGregor, A. G. 38
McKeown, T. and Zuckerman, S. 39, 43
Mandell, W. 57
Manton, S. M. 41
Massey, H. S. W. 9
Matthews, *see* Keys

Melville, H. W. 7, 8
Millington, *see* Eckersley
Milne, E. A. 12, 14
Mitchell, J. S. 75
Moelwyn-Hughes, E. A. 29
Mookerji, *see* Krishnan
Morris, R. M. 50
Mott, *see* Gurney
Murray, P. D. F. 37
—— *see also* Watchorn

Orton, J. H., Jones, J. W. and King, G. M. 50

Parkes, *see* Deanesley
Payman, W. and Woodhead, D. W. 10
Peierls, *see* Kapur
Penney, W. G. and Kynch, G. J. 64
Perutz, M. 25
Peugnet, *see* Urban
Piddington, *see* Appleton
Poole, H. G. 5
Porret, D. and Goodeve, C. F. 31

Randall, R. B., Benger, M. and Groocock, C. M. 73
Ratcliffe, *see* Best
Rayleigh, Lord 22
Reimann, A. L. 1
Richardson, L. F. 23
Richardson, O. W. 76
Robertson, J. M. and Woodward, I. 67
Rosenberg, H. 35
Rowlands, I. W. 44, 45
Rumer, *see* Landau

Salaman, R. N. 65
Salter, *see* Simmons
Saunders, *see* Schmidt
Schmidt, R. J. and Saunders, O. A. 53
Schoszberger, *see* Clews
Simmons, L. F. G. and Salter, C. 72
Simpson, *see* Lowry
Smith, *see* Cox
Southwell, R. V. 4
—— *see also* Black
Spencer, *see* MacBride
Steward, F. C. and Harrison, J. A. 74
Sutherland, *see* Cain

Taylor, G. I. 27, 73
Thompson, W. 5
Tomotika, S. 51, 52

Upcott, M. 37
Urban, F. and Peugnet, H. B. 39

Wasastjerna, J. A. 20
Watchorn, E. and Murray, P. D. F. 39
Watson, M. A. 67
Wheland, G. W. 63
Wilkins, F. J. 21, 22
Woodhead, *see* Payman
Woodward, *see* Robertson

Zuckerman, *see* McKeown

Indian Agricultural Research Institute Library, New Delhi

1 Books are issued for 14 days beyond if for next 7 days a fine of 15 paise & after wards 25 paise per day shall be charged

2 Books may be renewed at the discretion of the head Library Services.

3 Dog-earing of pages of a book, marking of writing there in with ink or pencil, tearing or taking out its pages or otherwise damaging it will constitute an injury to a book.

4. Unless a borrower points out the injury at the time of borrowing the book, he shall be required to replace the book or pay its prise, if detected at the time of return.

HELP US TO KEEP THIS BOOK,
FRESH AND CLEAN

Indian Agricultural Research Institute (Pusa)
LIBRARY, NEW DELHI-110012

This book can be issued on or after________________

Return Date	Return Date